University of Plymouth

PEARL **https://pearl.plymouth.ac.uk**

04 University of Plymouth Research Theses 01 Research Theses Main Collection

2000

SPATIAL VARIATION IN ZOOPLANKTON SIZE AND TAXONOMIC COMMUNITY STRUCTURE ALONG A 50N TO 50S TRANSECT OF THE ATLANTIC

WOODD-WALKER, RACHEL SARAH

http://hdl.handle.net/10026.1/2663

http://dx.doi.org/10.24382/3762
University of Plymouth

All content in PEARL is protected by copyright law. Author manuscripts are made available in accordance with publisher policies. Please cite only the published version using the details provided on the item record or document. In the absence of an open licence (e.g. Creative Commons), permissions for further reuse of content should be sought from the publisher or author.

SPATIAL VARIATION IN ZOOPLANKTON SIZE AND TAXONOMIC COMMUNITY STRUCTURE ALONG A 50 ^{O}N TO 50 ^{O}S TRANSECT OF THE ATLANTIC

By

RACHEL SARAH WOODD-WALKER

A thesis submitted to the University of Plymouth
in partial fulfilment for the degree of

DOCTOR OF PHILOSOPHY

Institute of Marine Studies
Faculty of Science

In collaboration with
CCMS Plymouth Marine Laboratory

April 2000

UNIVERSITY OF PLYMOUTH
Item No. 900426343 5
Date 18 MAY 2000 S
Class No. T 592.09163 WOO
Contl. No. X 704069147
LIBRARY SERVICES

900426343 5

REFERENCE ONLY

LIBRARY STORE

Copyright statement

This copy of the thesis has been supplied on condition that anyone who consults it is understood to recognise that its copyright rests with its author and that no quotation from the thesis and no information derived from it maybe published without the author's prior consent.

Signed

Rachel Woodd-Walker

Spatial variation in zooplankton size and taxonomic community structure along a 50 °N to 50 °S transect of the Atlantic

Rachel Sarah Woodd-Walker

Abstract

Zooplankton play a vital role in the world's oceans in terms of transport of carbon out of the surface layer and providing food for fish. Zooplankton are patchily distributed on all scales, and this has important consequences for both sampling and understanding their role in the ocean. The distribution of zooplankton on different scales forms the focus of this study.

Three Atlantic Meridional Transect (AMT) cruises were carried out and data made available from three previous cruises. Zooplankton data were collected using a combination of vertical nets and using an optical plankton counter (OPC) sampling from the pumped seawater supply. Validation of methods showed that the OPC data could reliably be converted to carbon and numerical abundance estimates for open ocean conditions.

Spectral analysis suggested that surface zooplankton heterogeneity followed a power law relationship over several scales. Over the 30 to 1000 km range this was approximately –1, and for smaller and larger scales the slope was reduced. Chlorophyll was less patchy, following temperature and salinity over the same range with a slope of –1.8.

Analysis of large scale heterogeneity showed clear latitudinal trends in diversity, particularly evident in the copepod genera, with low diversity at high latitudes. The size structure appeared to be more closely related to the productivity of the area, with high zooplankton biomass associated with larger zooplankton. Regions with similar copepod communities were identified. These were found to be similar to other pelagic regions, but less closely related to watermasses or production regimes.

Multiple linear regression of surface zooplankton biomass showed a strong relationship with the physics (temperature and salinity), chlorophyll and the time of day, accounting for 55% of the variability. Use of the regression equations to predict new transects gave R^2=0.34. Improvement could be made by dividing the transect into smaller regions. Neural networks gave enhanced predictability (R^2 = 0.77 for the training set, and R^2= 0.47 for the novel set) with a simpler model, although similar variables were important.

This study has shown that copepods show latitudinal gradient in diversity, associated with seasonality, and form regions of similarity that do not conform to biogeochemical provinces or the watermasses. Neural networks may be used to predict zooplankton abundance from a few readily available parameters.

Contents

Chapter 1: Introduction 1

Community structure 3
Atlantic Meridional Transect 5
Atlantic Ocean 7
Spatial variability 7
Turbulence 9
Small scale turbulence *10*
Turbulent eddies rings *10*
Large scale spatial variability 12
Divisions of the ocean 13
Understanding zooplankton abundance 18
Aims 20

Chapter 2: Methods, intercomparisons and validation 21

Introduction 21

Method 25
L4 station 25
Cruises 26
Net sampling 30
Carbon 30
Effects of thoroughness of sieving *31*
Effects of preservation of carbon samples *31*
Taxonomic analysis 32
The OPC 33
OPC processing of net samples *33*
OPC underway *34*

Comparison of OPC counts with microscope counts for net samples 35
Comparison of OPC counts with microscope counts for underway samples 35
Comparison of OPC biovolume with carbon biomass 36
Comparison of OPC size fractions and sieve size fractions 36
Comparison of OPC sizing and sieve sizing with microscope measurements 36
Estimating coincidence for the OPC 37
Theory predicting coincidence and its effect on mean ESD 38
Maximum count rate 41

Results **42**
Effects of thoroughness of sieving 42
Effects of preservation on carbon samples 44
Comparison of OPC counts with microscope counts for net samples 46
Comparison of OPC counts with microscope counts for underway samples 47
Comparison of OPC biovolume with carbon biomass 49
Comparison of OPC size fractions and sieved size fractions 52
Comparison of OPC sizing and sieve sizing with microscope measurements 53
Coincidence for the OPC 55

Discussion **56**
Effects of thoroughness of sieving 56
Effects of preservation of carbon samples 56
Comparison of OPC counts with microscope counts 57
Comparison of OPC biovolume with carbon biomass 58
Sizing by different methods 59
Test of coincidence for the OPC 61

Conclusion **62**

Chapter 3: Analysis of Scale 64

Introduction **64**

Data Analysis **65**

Spectral analysis 65
Cross-spectral analysis 67

Results **68**
Spectral analysis 68
Cross-spectral analysis 77

Discussion **83**

Conclusion **88**

Chapter 4: Large scale variation 89

Introduction **89**

4.1 Latitudinal trends **90**

Introduction **90**
Diversity 91

Data Analysis **94**
Large scale changes in diversity 94
Large scale changes in size 97
Large scale changes in biomass 97

Results **97**
Diversity 97
Size 103
Biomass 107

Discussion **108**
Diversity 108
Size 115

4.2 Global Provinces **118**

Introduction **118**

Data Analysis **119**
Taxonomic regions *119*
Comparison with published data *120*
OPC groups *120*

Results **121**
Taxonomic regions *121*
Comparison with published data *128*
OPC groups *129*
OPC underway groups *133*

Discussion **138**
Taxonomic regions *138*
Size structure *141*

Conclusion **142**

Chapter 5: Modelling zooplankton **144**

Introduction **144**

Analysis **147**
Data manipulation *147*
Multiple regression *148*
Neural networks *149*

Results **150**
Multiple regression *150*

Neural networks 162
Comparison of neural network with multiple linear regression 166
Analysis of neural network behaviour 167

Discussion 173
Multiple regression 173
Neural networks 175

Conclusion 178

Chapter 6: Discussion 179

Conclusion 188

References 190

Appendices 215

Appendix 1:AMT 1-6 station details 215
Appendix 2: AMT 1-6 200m net carbon and biovolume estimates 221
Appendix 3: AMT 200m net samples, numerical abundance estimated from OPC and microscope for transects 1-6 223
Appendix 4: AMT underway OPC counts compared with microscope counts for the six transects 225
Appendix 5: AMT 1-6 OPC underway mean ESD derived from 30 min bins, with 24 hour moving averages 227
Appendix 6: AMT 1-6 Major groups analysis from deep nets (m^{-3}) 229
Appendix 7: AMT 4-6 Copepod genera from deep nets (m^{-3}) 243

Publications 252

A test model for optical plankton counter (OPC) coincidence and a comparison of OPC-derived and conventional measures of plankton abundance

Spatial distribution of copepod genera along the Atlantic Meridional Transect

Using neural networks to predict surface zooplankton biomass along a 50°N to 50°S transect of the Atlantic

List of figures

Figure 1.1: Zooplankton size categories. 3

Figure 1.2: SeaWiFS image of chlorophyll concentrations in the Atlantic ocean with AMT cruise tracks shown. 6

Figure 1.3: Sources of heterogeneity in the ocean and the scales over which they act. 9

Figure 1.4: A biogeographic division of the world Ocean in 1946. 14

Figure 1.5: A current generalised biogeographic division of the world oceans. 14

Figure 2.1: Station L4: 50° 15'N, 04° 15'W. 25

Figure 2.2: General AMT cruise track. 28

Figure 2.3: AMT 4 – 6 cruise tracks with stations. 29

Figure 2.4: A schematic of the OPC. 33

Figure 2.5: The OPC set up for processing net samples. 34

Figure 2.6: The OPC set up for sampling the uncontaminated seawater supply. 35

Figure 2.7: Estimate of ESD of *Coscinodiscus wailesii*. 38

Figure 2.8: Predictions from the Poisson distribution for coincidence. 40

Figure 2.9: a) The maximum theoretical number of counts per second. calculated for different sized particles, b) The theoretical response of the OPC measured biovolume to the OPC measured count rate for Coscinodiscus spp. 41

Figure 2.10: Comparison of thorough and normal sieving. 42

Figure 2.11: Comparison of preservation techniques for biomass. 45

Figure 2.12: Comparison of half net counts by the OPC and by microscope counts for AMT 1-6. 46

Figure 2.13: Comparison of size counts in each size fraction between OPC and microscope for AMT 5. 47

Figure 2.14: Comparison of underway counts by microscope and OPC. 48

Figure 2.15: Comparison of AMT 1-6 total OPC biovolume and carbon biomass from 200 m net samples. 50

Figure 2.16: Comparison of AMT 1-6 OPC biovolume and carbon biomass from 200 m net samples for the four JGOFs size fractions. 51

Figure 2.17: A comparison of sieve sizing and OPC sizing. 52

Figure 2.18: The OPC calculated mean ESD of sieved size fractions. 53

Figure 2.19: Comparison of the size distribution of copepods from three sieve size classes. 54

Figure 2.20: Comparison of measured and OPC mean ESD for different zooplankton groups. 55

Figure 2.21: The effect of count rate on particle volume for *Coscinodiscus wailesii*, observed compared to predicted. 55

Figure 3.1: The mean spectral density for AMT 1-5 38°S-50°N calculated from 10 min averages, for zooplankton. 69

Figure 3.2: The mean spectral density for AMT 1-5 38°S-50°N calculated from 10 min averages, for size fractionated zooplankton. 71

Figure 3.3 The mean spectral density for AMT 5 38°S-50°N calculated from 2 min averages, for zooplankton. 72

Figure 3.4: The mean spectral density for AMT 1-5 38°S-50°N calculated from 10 min averages, for chlorophyll, temperature, salinity. 73

Figure 3.5: The regression of the mean spectral density for AMT 1-5 38°S-50°N calculated from 10 min averages over spectral range 30 km to 1000 km, for zooplankton measures and other variables. 74

Figure 3.6: The mean spectral density for AMT 1-5 38°S-50°S (Port Stanley – Monteovideo) calculated from 10 min averages, for zooplankton. 75

Figure 3.7: The mean spectral density for AMT 1-5 38°S-50°S (Port Stanley – Monteovideo) calculated from 10 min averages, for chlorophyll, temperature and salinity. 76

Figure 3.8: Coherence and Phase between different measures for zooplankton. 78

Figure 3.9: Coherence and Phase between zooplankton, and chlorophyll temperature and salinity. 79

Figure 3.10: Coherence and Phase between chlorophyll, temperature and salinity. 80

Figure 3.11: Coherence and Phase between different measures for zooplankton. for Montevideo to Port Stanley (nfft=256). 81

Figure 3.12: Coherence between zooplankton biovolume and chlorophyll temperature and salinity, and Phase for temperature with salinity. 82

Figure 4.1: The relationship between Margalef's major group richness (D) and latitude for AMT 1,2, 4-6. 98

Figure 4.2: The relationship between Margalef's genera richness (D) and latitude for AMT 4-6. 98

Figure 4.3: Number of subfamily and families along the AMT transect. 99

Figure 4.4: Number of genera and major groups along the AMT transect, when the samples are grouped by 5^{0} latitude. 100

Figure 4.5: Pielou's evenness along the AMT transects for the major groups. 101

Figure 4.6: Pielou's evenness along the AMT transects for the copepod genera. 101

Figure 4.7: Taxonomic distinctness for copepod genera in 200m net samples (open symbols are samples taken on the shelf). 102

Figure 4.8: Taxonomic diversity for copepod genera in 200m net samples (open symbols are samples taken on the shelf). 102

Figure 4.9: Percentage of the total number of copepods in each size fraction for AMT 4-6. 104

Figure 4.10: The total number of organisms in each size fraction for AMT 4-6. 105

Figure 4.11: Variation in mean carbon per individual along the transect for AMT 4-6. 106

Figure 4.12: The pattern of zooplankton carbon from 200m nets along the AMT. 107

Figure 4.13: The pattern of zooplankton biovolume from 200m nets along the AMT. 108

Figure 4.14: Number of copepod genera for different regions including literature data, showing the pattern for the Atlantic. 109

Figure 4.15: Taxonomic diversity along the transect, extended with unpublished data. 111

Figure 4.16: The relationship between sea surface temperature and species richness for AMT data. 112

Figure 4.17: The relationship between sea surface temperature and taxonomic diversity. 114

Figure 4.18: Total zooplankton carbon from 200m net samples compared to mean carbon content per individual. 116

Figure 4.19: MDS ordination for major groups (AMT1-6). 122

Figure 4.20: MDS ordination for copepod genera (AMT4-6). 123

Figure 4.21: MDS ordination for copepod genera (AMT4-6) for temperate and the Benguela stations. 124

Figure 4.22: MDS ordination for copepod genera (AMT4-6) for the tropical and subtropical stations. 124

Figure 4.23: Principle components analysis on 200 m net samples OPC size fractions, standardised for AMT 4-6. 130

Figure 4.24: PC 2 and PC3 for 200 m net samples OPC size fractions, for AMT4-6. 131

Figure 4.25: MDS of $\log_2$ OPC biovolumes for AMT 4-6 for 200 m net samples. 132

Figure 4.26: Principle components analysis of 24 hour underway $\log_2$ biovolumes, double root transformed and standardised along the latitudinal transect, for AMT 1-6. 135

Figure 4.27: MDS of underway OPC biovolumes in $\log_2$ size classes averaged over 24 hours, for AMT 3-6. 166

Figure 4.28: Inter-comparison of latitudinal groups along the AMT. 140

Figure 5.1: Diagram of the two layer feed forward artificial neural network used. 149

Figure 5.2: Linear regression models of biovolume from the whole transect compared with actual. 153

Figure 5.3: The contribution of the different components to the whole transect model derived from the linear regression equation compared to the actual $\log_e$ transformed biovolume for the AMT 4 transect. 153

Figure 5.4: Linear regression models of biovolume from the separate temperate and warm water regions compared with actual. a)AMT 4, b)AMT 5 155

Figure 5.5: Linear regression models of biovolume from the separate regions compared with actual a)AMT 4, b)AMT 5. 156

Figure 5.6: Linear regression models of biovolume from the separate warm water and north and south temperate regions compared with actual biovolumes. a)AMT 4, b)AMT 5 157

Figure 5.7: Linear regression models of biovolume from the separate warm water and north and south temperate regions compared with actual biovolumes. a)AMT 4, b)AMT 5 158

Figure 5.8: Comparison of predicted biovolume from regression model of the whole transect with actual biovolumes for AMT 2, AMT 3. 159

Figure 5.9: Comparison of predicted biovolume from regression model of the regions with actual biovolumes for AMT 2, AMT 3. 160

Figure 5.10: Comparison of predicted biovolume from regression model of the regions with actual biovolumes for AMT 2, AMT 3. 161

Figure 5.11: Artificial neural network model of biovolume of the original parameter set using the smoothed algorithm, compared with measured biomass. 162

Figure 5.12: Artificial neural network model of biomass of the optimised parameter set compared with measured biomass (R^2= 0.77), for a) AMT 4, b)AMT 5. 164

Figure 5.13: Artificial neural network model of biovolume of the optimised parameter set compared with measured biovolume (R^2= 0.47), for a) AMT 2, b)AMT 3. 165

Figure 5.14: Comparison of residuals between multiple linear regression (MLR) and artificial neural network (ANN) models of zooplankton. 167

Figure 5.15: Sensitivity analysis of latitude, showing the effect on biovolume in the different regions. 168

Figure 5.16: Sensitivity analysis of temperature showing the effect on biovolume in the different regions. 169

Figure 5.17: Sensitivity analysis of salinity, showing the effect on biovolume in the different regions. 170

Figure 5.18: Sensitivity analysis of chlorophyll, showing the effect on biovolume in the different regions. 171

Figure 5.19: Sensitivity analysis of diel time, showing the effect on biovolume in the different regions. 172

Figure 5.20: The neural network model of diel changes in surface zooplankton for the different regions on a standardised day. 172

Figure 5.21: Optimised model comparing the predicted biovolume if sampling was at night, with sampling including diel migration. 177

List of Tables

Table 2.1: Summary of cruises. 27

Table 2.2: Results of three-way ANOVA for sieving thoroughness. 43

Table 2.3: Results of two-way ANOVA of sieving thoroughness for each size fraction. 43

Table 2.4: Total carbon and nitrogen for samples. 43

Table 2.5: Two-way ANOVA of preservation techniques. 44

Table 2.6: Paired T-test of the different preservation methods. 45

Table 2.7: Result of functional regression of Log_e transformed AMT total OPC counts versus microscope counts. 46

Table 2.8: Results of functional regression of size fractionated counts for AMT 5. 47

Table 2.9: Result of functional regression of Log_e transformed AMT total OPC counts verses microscope counts. 48

Table 2.10: Results of functional regression of Log_e transformed size total carbon and biovolume for AMT 1-6. 49

Table 2.11: Results of functional regression of Log_e transformed size fractionated carbon and biovolume for AMT 1-6. 51

Table 2.12: OPC size distribution of sieved size fractions. 52

Table 2.13: Summary of the advantages and disadvantages of different methods. 63

Table 4.1: Summary of taxonomic groups used for calculating taxonomic relatedness. 96

Table 4.2: The number in each size fraction with standard deviation and percentage. 103

Table 4.3: Details of source data used for extended transect. 109

Table 4.4: Analysis of similarity of the genera derived groups. 125

Table 4.5: The rank importance of genera (root transformed) for determining the differences between groups. 126

Table 4.6: The rank importance of genera (double root transformed) for determining the differences between groups. 127

Table 4.7: Mean abundance of the genera important in determining the dissimilarities, for each group and overall (per sample). 127

Table 4.8: Strength of groupings by different schemes for copepod genera. 128

Table 4.9: Pairwise comparison of groups for Backus and Bé schemes from ANOSIM. 128

Table 4.10: The principle components from PCA on the 200 m net $\log_2$ OPC biovolume size classes (standardised). 129

Table 4.11: Analysis of similarity of the genera derived groups (double root transformed), carried out on OPC 200 m nets for AMT 4-6, with 10,000 permutations used. 132

Table 4.12: Analysis of similarity of the Backus' (1986) regions carried out on OPC 200 m net samples, with 10000 permutations used. 133

Table 4.13: Principle components analysis of 24 hour underway $\log_2$ biovolumes, double root transformed and standardised, for AMT 1-6. 134

Table 4.14: Analysis of similarity of the genera derived groups (double root transformed) using 5000 permutations, carried out on OPC 24 hour underway averages for AMT 3-6. 137

Table 4.15: Analysis of similarity of the Backus' (1986) regions carried out on OPC underway 24 hour averages. 137

Table 4.16: Analysis of similarity of the adjusted Backus' (1986) regions carried out on OPC underway 24 hour averages. 138

Table 5.1: Coefficients for variables from multiple regression of $\log_e$ transformed biovolume for AMT 4 and 5 with R^2 of the regression. 152

Table 5.2: Correlation coefficients of multiple regression models for the whole transects made from the component models of the transect sections for AMT 4 and 5. 154

Table 5.3: Correlation coefficients of multiple regression models for the whole transect made from different components compared with AMT 2 and 3 biovolumes. 159

Table 5.4: Summary of neural networks optimising variables for the whole transect, showing the results at each stage of subtraction. 163

Table 5.5: Summary of neural networks optimising for each region, and variables for each region. 166

List of Abbreviations

AMT	Atlantic Meridional Transect
ANOSIM	Analysis of similarity
ANOVA	Analysis of variance
BAS	British Antarctic Survey
C	carbon
CCMS	Centre for Coastal and Marine Science
DVM	Diel vertical migration
ESD	Equivalent spherical diameter
JGOFS	Joint Global Ocean Flux Study
ln	Log_e
MDS	Multidimensional scaling
min	minute
N	nitrogen
OPC	Optical Plankton Counter
PC	Principal component
PCA	Principal component analysis
PML	Plymouth Marine Laboratory
PRIME	Plankton Reactivity in Marine Ecosystems
PRIMER	Plymouth Routine in Multivariate Ecological Research
RRS	Royal Research Ship
SIMPER	Similarity of percentages
TIR	Total incident radiation
UK	United Kingdom
UNESCO	United Nations Educational Scientific and Cultural Organisation
UOR	Undulating oceanographic recorder

Acknowledgements

I would like to take this opportunity to express my thanks to the following people for their help and support during this study.

To my supervisors Dr Derek. Pilgrim (University of Plymouth), Dr Roger Harris (CCMS Plymouth Marine Laboratory) and Dave Robins (CCMS Plymouth Marine Laboratory) for all their help and support throughout this project.

To Plymouth Environmental Research Council for the University of Plymouth studentship, to Plymouth Marine Fund for funds towards attending the 7th International Conference on Copepoda and to PRIME for the grant to support my participation in cruises and consumables for scientific work.

To the AMT steering committee for enabling me to participate on three AMT cruises. To the officers and crew of RRS James Clark Ross for their friendly and professional support, particularly Simon Wright, Deck Engineer. To the other participants of the cruises, notably Inaki Huskin (University of Oviedo) for collaboration with net sampling and major groups analysis of AMT 2 and 5 200m net samples, and Dr Chris Gallienne (CCMS Plymouth Marine Laboratory) for instruction on the OPC and net sampling, and the use of previous cruise data.

To my colleagues at CCMS Plymouth Marine Laboratory and the Institute of Marine Studies for their help and support. To Dave Conway (CCMS Plymouth Marine Laboratory) for instruction and help with the identification of copepod genera, and Bob Head (CCMS Plymouth Marine Laboratory) for assistance with the carbon analysis and technical support. To Ken Kingston (Institute of Marine Studies) for help with the neural network analysis. To Dr Peter Ward (British Antarctic Survey) for allowing me to use his unpublished data in the large scale analysis of diversity.

Last but by no means least to Adrian Nicholas and my family for putting up with and supporting me over this time.

Author's declaration

At no time during the registration of this PhD has the author been registered for any other University award.

This study was financed with the aid of a studentship from the University of Plymouth, and PRIME special topic grant (GST/02/1068), and carried out in collaboration with CCMS Plymouth Marine Laboratory.

A programme of advanced study was taken including Research Techniques module, PRIMER workshop, and Graduate Teach Assistant course. Three major research cruises were undertaken in the course of this work: AMT 4, 5 and 6.

Relevant scientific seminars and conferences were regularly attended at which work was often presented; external institutions were visited for consultation purposes and several papers were prepared for publication.

Publications:

Aiken, J., Cummings, D.G., Gibb, S.W., Rees, N.W., Woodd-Walker, R.S., Woodward, E.M.S., Woolfenden, J., Hooker, S.B., Berthon, J.-F., Dempsey, C.D., Suggett, D.J., Wood, P., Donlon, C., Gonzalez-Benitez, N., Huskin, I., Quevedo, M., Barciela-Fernandez, R., deVargas, C. and McKee, C. Hooker, S.B. and Firestone, E.R. (Eds.) (1998) Volume 2, AMT-5 Cruise Report. NASA/TM-1998-206892v, pp.1-113. Greenbelt, Maryland: Laboratory for Hydrospheric Processes.

Gallienne, C.P., Robins, D.B. and Woodd-Walker, R.S. (In Press) Abundance and distribution of mesozooplankton along a 20° west meridional transect of the north Atlantic Ocean. *Deep Sea Research*

Woodd-Walker, R.S. (in review) Spatial distribution of copepod genera along the Atlantic Meridional Transect. *Hydrobiologia*

Woodd-Walker, R.S., Gallienne, C.P. and Robins, D.B. (2000) A test model for optical plankton counter (OPC) coincidence and a comparison of OPC derived and conventional measures of zooplankton abundance. *Journal of Plankton Research* 22: 473-484

Woodd-Walker, R.S., K.S. Kingston and C.P. Gallienne (submitted): Neural network prediction of surface zooplankton biomass along a 50 °N to 50 °S transect of the Atlantic. *Marine Ecology Progress Series.*

Presentations and conferences attended:

ICES Young Scientist Conference: Marine Ecosystems Perspectives (Nov. 1999)
Woodd-Walker, R.S., K.S. Kingston, C.P. Gallienne: Modelling spatial variation of surface zooplankton biomass along a 50°N to 50°S transect of the Atlantic (Oral Presentation)

7th International conference on Copepoda, Curitiba, Brazil (July 1999)
Woodd-Walker, R.S.: Spatial distribution of copepod genera along the Atlantic Meridional Transect. (Oral presentation)
Woodd-Walker, R.S. and C.P. Gallienne: Spatial variation of zooplankton community size structure along the Atlantic Meridional Transect. (Poster)
Woodd-Walker, R.S. and C.P. Gallienne: Spatial variation in zooplankton community size structure between Montevideo and Port Stanley. (Poster)

PERC workshop, Plymouth, UK (Jan. 1999)
Woodd-Walker, R.S.: Regions analysis of the AMT transect using copepod genera (Oral presentation)

Atlantic Meridional Transect Workshop, Plymouth, UK (Feb. 1997)

External contacts:
Dr. Peter Ward, British Antarctic Survey, Cambridge
Prof. Riccardo Anadon, Inaki Huskin, University of Oviedo, Oviedo, Spain
Prof. Patrick Holligan, Southampton Oceanographic Centre, Southampton

Signed Rachel Woodd-Walker
Date 26 April 2000

Author's declaration

At no time during the registration of this PhD has the author been registered for any other University award.

This study was financed with the aid of a studentship from the University of Plymouth, and PRIME special topic grant (GST/02/1068), and carried out in collaboration with CCMS Plymouth Marine Laboratory.

A programme of advanced study was taken including Research Techniques module, PRIMER workshop, and Graduate Teach Assistant course. Three major research cruises were undertaken in the course of this work: AMT 4, 5 and 6.

Relevant scientific seminars and conferences were regularly attended at which work was often presented; external institutions were visited for consultation purposes and several papers were prepared for publication.

Publications:

Aiken, J., Cummings, D.G., Gibb, S.W., Rees, N.W., Woodd-Walker, R.S., Woodward, E.M.S., Woolfenden, J., Hooker, S.B., Berthon, J.-F., Dempsey, C.D., Suggett, D.J., Wood, P., Donlon, C., Gonzalez-Benitez, N., Huskin, I., Quevedo, M., Barciela-Fernandez, R., deVargas, C. and McKee, C. Hooker, S.B. and Firestone, E.R. (Eds.) (1998) Volume 2, AMT-5 Cruise Report. NASA/TM-1998-206892v, pp.1-113. Greenbelt, Maryland: Laboratory for Hydrospheric Processes.

Gallienne, C.P., Robins, D.B. and Woodd-Walker, R.S. (In Press) Abundance and distribution of mesozooplankton along a 20° west meridional transect of the north Atlantic Ocean. *Deep Sea Research*

Woodd-Walker, R.S. (submitted) Spatial distribution of copepod genera along the Atlantic Meridional Transect. *Hydrobiologia*

Woodd-Walker, R.S., Gallienne, C.P. and Robins, D.B. (2000) A test model for optical plankton counter (OPC) coincidence and a comparison of OPC derived and conventional measures of zooplankton abundance. *Journal of Plankton Research* 22: 473-484

Woodd-Walker, K.S. Kingston and C.P. Gallienne (submitted): Neural network prediction of surface zooplankton biomass along a 50 °N to 50 °S transect of the Atlantic. *Marine Ecology Progress Series.*

Presentations and conferences attended:

ICES Young Scientist Conference: Marine Ecosystems Perspectives (Nov. 1999)
Woodd-Walker, R.S., K.S. Kingston, C.P. Gallienne: Modelling spatial variation of surface zooplankton biomass along a 50°N to 50°S transect of the Atlantic (Oral Presentation)

7th International conference on Copepoda, Curitiba, Brazil (July 1999)
Woodd-Walker, R.S.: Spatial distribution of copepod genera along the Atlantic Meridional Transect. (Oral presentation)
Woodd-Walker, R.S. and C.P. Gallienne: Spatial variation of zooplankton community size structure along the Atlantic Meridional Transect. (Poster)
Woodd-Walker, R.S. and C.P. Gallienne: Spatial variation in zooplankton community size structure between Montevideo and Port Stanley. (Poster)

PERC workshop, Plymouth, UK (Jan. 1999)
Woodd-Walker, R.S.: Regions analysis of the AMT transect using copepod genera (Oral presentation)

Atlantic Meridional Transect Workshop, Plymouth, UK (Feb. 1997)

External contacts:

Dr. Peter Ward, British Antarctic Survey, Cambridge

Prof. Riccardo Anadon, Inaki Huskin, University of Oviedo, Oviedo, Spain

Prof. Patrick Holligan, Southampton Oceanographic Centre, Southampton

Signed

Date

Chapter 1: Introduction

Plankton are organisms which are incapable of making their way against the current and therefore are passively transported with the current (from the Greek *planktos* meaning drifting or wandering). Zooplankton are animal plankton and are heterotrophic, i.e. derive their energy from organic sources. Zooplankters feed on bacterioplankton and phytoplankton as well as smaller members of the zooplankton. Zooplankton in turn are eaten by members of the nekton such as fish. As well as being important in their own right, understanding the role of zooplankton is critical in the interpretation and prediction of carbon flux within the oceans, and hence the role of the oceans in global climate change, and from a commercial perspective, fish stocks. The importance of zooplankton was recognised, as early as 1901. Jenkins (1901 cited from Huntley and Lopez 1992) pointed out that the "plankton undoubtedly forms the sole food supply for many of our important fishes", and also suggested that variation in fish stocks was related to variation in zooplankton, particularly copepods.

Zooplankton affect carbon flux in several ways. Grazing phytoplankton can reduce the standing stock and therefore the primary production. However, nutrients recycled by the zooplankton through excretion support primary production, particularly in oligotrophic regions (Banse 1995). Zooplankton provide food for higher trophic levels such as fish and other members of the nekton. 'Sloppy' feeding by zooplankton has been indicated as a potential source of dissolved organic matter supporting the bacterial food chain and nutrient regeneration (Jumars *et al.* 1989). Faecal pellets from zooplankton have high sinking rates and are important in enhancing transfer of carbon out of the surface layers (Landry *et al.* 1995). Vertical migration of zooplankton may also aid transfer of carbon

from the surface layer through faecal pellet production, respiration and being preyed upon at depth (Longhurst and Harrison 1988, Longhurst *et al.* 1990a, Morales 1999).

The distribution of zooplankton will impact the nature of the oceans in terms of their role in carbon flux and the productivity available for the nekton. Their heterogeneity will influence nutrient regeneration (Paffenhöfer and Knowles 1979, Lehman and Scavia 1982) and feeding activity (e.g. Tessier 1983, Marrase *et al.* 1990, Paffenhofer and Knowles 1980, Williamson and Butler 1986, Landry 1978). Zooplankton patchiness also influences predation rates (Neill and Peacock 1980, Rothchild and Osborn 1988, Davis *et al.* 1991, Noda *et al.* 1992, Williamson 1993). Zooplankton patchiness may also be important for reproductive activity (De Nie *et al.* 1980).

Zooplankton can be sub-divided by size (Figure 1.1). Mesozooplankton are generally considered to be between 200 and 2000 μm. This range is chiefly derived from practical considerations, being zooplankton caught with a WP2 200 μm mesh net. Larger zooplankters are not sampled efficiently. The mesozooplankton is the size spectrum under consideration here. The mesozooplankton consists of a wide range of animals from several phyla including crustaceans (copepods, ostracods, mysids, euphausiids), polychaetes, molluscs, cnidarians, ctenophores, chaetognaths, echinoderms, hemichordates and chordates. Zooplankton have a variety of lifecycles. Holoplankton spend all of their lifecycle as plankton in the pelagic realm, whereas meroplankton do not. The proportion of meroplankton is very variable but is appreciable in coastal areas particularly at certain times of the year (Raymont 1983). Oceanic plankton tend to be dominated by holoplankton.

Category	Size
Ultraplankton	< 2 μm
Nannoplankton	2-20 μm
Microplankton	20-200 μm
Mesozooplankton	200-2000 μm
Macroplankton	2-20 mm
Micronekton	20-200 mm
Megaloplankton	>200 mm

Figure 1.1: Zooplankton size categories (after Dussart 1965)

Community structure

The term 'community' may be defined in a number of ways, with different interpretations as to the nature of the interactions between members of a community (Ricklefs 1990). In this instance, I would like to define a community as an assemblage of populations occurring together in space and time. Traditionally zooplankton community structure has been defined in terms of taxonomic composition. Species assemblages have been described for many parts of the ocean. But what determines the assemblage, the boundaries of the assemblage, and abundance of the species and the variability in the community structure is less well defined and understood.

More recently, another aspect of the zooplankton community has been analysed, the community size structure. In the 1970s and 1980s there was a trend to look at fluxes through systems in terms of carbon, energy and nutrients. This led to the use of bulk measures such as biomass and carbon standing stock. From this approach, theories on the transfer of energy based upon the size structure were developed. Sheldon *et al.* (1972) developed a theory of the distribution of biomass within different size classes. Sheldon *et al.* (1977) also showed that log size to log abundance was approximately proportional across a large size range from bacteria to whales, and that the rate of population doubling was also inversely proportional to size. Kerr (1974) suggested a model to explain this constancy, based on size related predators and prey. Haedrich (1986) looked at the size

spectra for mesopelagic fish assemblages, and found different distributions in different areas. In the sub-arctic, the size distribution had peaks associated with particular size classes. The spectrum for the Sargasso Sea was very smooth, and the central gyre and high latitudes had intermediate spectra. Piontkovski *et al.* (1995) looked at mesoscale variation in the Arabian Sea, and the South and North Sub-Equatorial Divergence of the Indian Ocean. Spatial heterogeneity of biomass increased with organism size (from phytoplankton through to macrozooplankton). Zooplankton size spectra changed with hydrographic regime. Smaller size classes dominated where primary production was high. These smaller zooplankton were associated with greater grazing efficiency (i.e. more zooplankton per unit phytoplankton; Piontkovski et al. 1995). Boudreau and Dickie (1992) suggested that biomass spectra were more closely related to the environment than the taxonomic structure, even though the zooplankton communities may also change. Allometric relationships were discovered between size and processes e.g. metabolic rates (e.g. Peters 1983 and references therein, Ikeda 1985). Zhou and Huntley (1997) used size structure to estimate population dynamics and growth rates.

Size distribution has great advantages over taxonomic analysis of community composition in that it can be carried out quickly and accurately, and it avoids issues of taxonomic ambiguity and misidentification. In addition, size structure allows inter-comparison of communities with different species composition. Recently methods, such as the use of the optical plankton counter (OPC), have allowed fully automated analysis in real time of the size structure (Herman 1992). The taxonomic and community size structure need not be considered separately, and may shed light on different aspects of the functioning of the zooplankton community. As with any community study, zooplankton community structure cannot be understood without reference to the environment that forms the ecosystem.

Atlantic Meridional Transect

The Atlantic Meridional Transect (AMT) is a programme of cruises using RRS James Clarke Ross (JCR) as a ship of opportunity on her journey to and from Antarctica (Robins and Aiken 1996). The programme was set up in 1996 by CCMS Plymouth Marine Laboratory (PML) in collaboration with British Antarctic Survey (BAS) and in association with Southampton Oceanographic Centre (SOC) and University of Plymouth. The JCR journeys to Antarctica in September for the Austral summer in order to carry out scientific research in the southern ocean and resupply the BAS bases, returning in April/May. The AMT utilises the transect between UK and Falklands each spring and autumn, forming a 50 ^{o}N to 50 ^{o}S transect along the Atlantic. The cruise track generally avoids the Exclusive Economic Zones (EEZs) and coastal zones, keeping to the open ocean except at either end of the transect, and sometimes a port of call at Montevideo, Uruguay. Due to the opportunistic nature of the cruises, the exact timing depends on the commitments of BAS, and AMT 6 was from Cape Town to UK. Figure 1.2 shows the generalised cruise track, and AMT 6, which included the Benguela Upwelling System. The AMT provides one of the few basin-scale oceanic transects and provides a unique opportunity for large ocean studies.

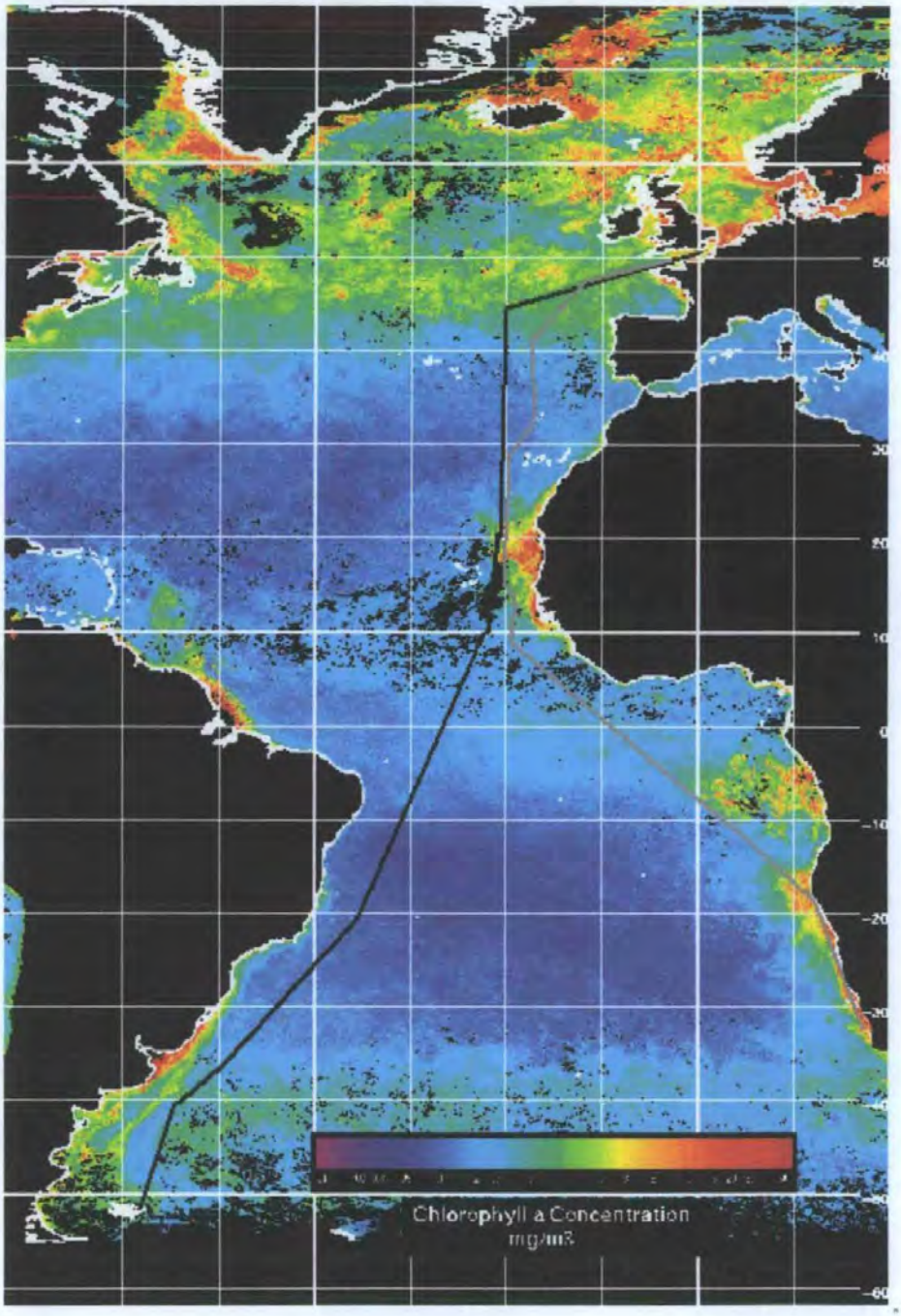

Figure 1.2: SeaWiFS image of chlorophyll concentrations in the Atlantic ocean with AMT cruise tracks shown.(Generalised AMT black, AMT 6 grey; Courtesy of CCMS Plymouth Marine Laboratory remote sensing group)

The overall aim of the AMT is to investigate the basic biological processes in the open Atlantic Ocean over very broad scales. Specific objectives include: acquisition of data for calibration of remotely sensed observations, secondary validation of remotely sensed products, development of models that enable the interpretation of satellite imagery in terms of total water column properties, interpretation of basin scale remote sensing observations,

understanding of the interaction between physical processes and biological production, identifying and quantifying latitudinal changes in the biogeochemical provinces, determination of phytoplankton characteristics and photosynthetic parameters, and identifying nutrient regimes (details can be found at http://www1.npm.ac.uk/amt/).

Atlantic Ocean

The Atlantic Ocean is the youngest of the ocean basins and is still growing from the mid-Atlantic ridge. It is bound to the west by the Americas and to the east by Europe and Africa. Water flow is restricted between the Pacific and Indian Oceans. To the north there is some flow through the Davis Strait to the west and the Faeroe Bank Channel to the east, but both are shallow (600 m and 800 m respectively); to the south the circumpolar current allows transfer between the oceans. Recently the Panama Canal has allowed limited connection between the Pacific and Atlantic at tropical latitudes. However, the Panama Canal opens into the Caribbean Sea that has its own circulation, so invasion of new species into the Atlantic is likely to be low. Other seas that are connected to the Atlantic are the North Sea, Baltic Sea and the Mediterranean Sea. The North Sea has a comparatively open connection with the Atlantic whereas the Mediterranean and Baltic Seas have restricted exchange due to shallow sills. Another notable feature of the Atlantic is the Amazon River plume, which can be detected several 100 km off shore by its high temperatures and low salinities. The AMT does not pass close enough to the coast or these seas to be significantly affected by them.

Spatial variability

For more than 100 years spatial variation in zooplankton abundance and biomass has been researched. Although plankton were initially assumed to be randomly or uniformly distributed (Lussenhop 1974), Haeckel (1891 in Pinel-Alloul 1995) questioned this

assumption of homogeneity. Since the 1960s, spatial heterogeneity has been recognised as a fundamental feature of plankton communities (Cassie 1963, Frontier 1973, Riley 1976, Fasham 1978), defining patterns of population dynamics within ecosystem trophic webs (Lasker 1975, Lasker and Zweifel 1978, LeBrasseur *et al.* 1969). There have been several reviews on spatial heterogeneity (Cassie 1963, Steele 1978, Longhurst *et al.* 1981, Horne and Platt 1984, Mackas *et al.* 1985, Haury and Pieper 1988, Pinel-Alloul 1995). Haury *et al.* (1978) synthesised these ideas of heterogeneity on different temporal and spatial scales into a Stommel diagram. Generally as increasing spatial scales are considered, relevant time scales also increase. There have been two approaches to the analysis of zooplankton patchiness: reductionist and holistic. The reductionist approach has involved studies on the morphology of patches, their form, dimensions and density in space in relation to various environmental factors (e.g. Boyd 1973, Omori and Hamner 1982, Alldredge *et al.* 1984). The sources of variability are dependent on scales and are a combination of the physical and biological environment, as well as from within the zooplankton community. Figure 1.3 summarises the main sources and the scales on which they act.

Spatial Scale	Physical Process	Biological Processes	Persistence (days)
1000+ km	Gyres Continental upwelling Water mass boundaries	Evolution	1000+
100 km	Warm and cold rings Tidal fronts Seasonal coastal upwelling	Seasonal growth (e.g. spring blooms) Differential growth of phyto- and zooplankton Lunar cycles (e.g. fish spawning)	100
10 km	Turbulence (e.g. estuarine mixing, island wake effect)	Reproductive cycles Grazing/predation Diel migration	10 1
100 m		Physiological adaptation (e.g. buoyancy, light)	0.1
10 m	Langmuir circulation Wave action	Behavioural adaptation	0.01

Figure 1.3: Sources of heterogeneity in the ocean and the scales over which they act (from Lalli and Parsons 1997)

The holistic approach involves treating patchiness as a continuum on all scales using spectral analysis, and correlation functions (e.g. Platt and Denman 1975, Fasham and Pugh 1976, Herman *et al.* 1981). Analysis of scale has mainly utilised data from coastal regions due to ease of sampling (e.g. Denman 1976, Fasham and Pugh 1976, Mackas and Boyd 1979). The range of scales which have been analysed tend to be limited due to logistical constraints. There has been a great deal of theory derived from understanding of turbulence. The AMT provides an opportunity to observe variance-scale interaction for the open ocean over a wide range of scales by using underway sampling methods, including the impact of turbulence on plankton distributions.

Turbulence

Turbulence may carry plankton, and is an important influence on their distribution over several scales. Turbulence acts across a range of scales from 100s of km to centimetres. At the largest scales, turbulence occurs between two watermasses or currents caused by friction causing mesoscale eddies and rings. This large scale turbulence approximates to

being two dimensional, and is known as geotropic, and can cause eddies 100 km across, and hundreds of metres deep. Islands, tidal, wave and wind action may also cause turbulence. The turbulence cascades to smaller scales down to cm scales. Over scales of 1 km to 1 cm, turbulent diffusion is approximately isotropic, i.e. statistically equivalent in all three dimensions. Turbulence affects all passive tracers in the same way, e.g. heat, salinity and nutrients.

Small scale turbulence

At scales of less than 10 km, turbulence may be caused by friction between water layers, waves breaking or flows behind islands, and from the cascade of larger turbulent features. Phytoplankton are distributed by the turbulent field in a similar way to a passive tracer. Spectral analysis of chlorophyll concentration showed that it followed a similar pattern of variation to temperature and salinity over scales greater than 100m (Denman 1976, Fasham and Pugh 1976), following the –5/3 power law (Mann and Lazier 1996). However, this pattern may be modified by phytoplankton growth (e.g. Denman and Platt 1976, Bennett and Denman 1985). Zooplankton will also be affected by turbulence, but growth and active movement (i.e. swimming) will modify their distribution, and they are more patchily distributed particularly at smaller scales (Mackas and Boyd 1979). Differences in maturation time between zooplankton and phytoplankton can produce increased patchiness in zooplankton over small scales (Abraham 1998). Small scale turbulence also affects fish larval survival by increasing encounter rates with zooplankton prey (e.g. Gallego *et al.* 1996, Lough and Mountain 1996)

Turbulent Eddies and rings

Where there are strong currents between water masses such as in the Gulf Stream, the currents often meander, and the friction between water masses produces turbulent eddies

(Lalli and Parsons 1997). The Gulf Stream has a north south oscillation. As the stream oscillates, eddies are produced between the ocean and the coast, often appearing as finger-like projections. These eddies may form total loops, pinching off rings of water from the opposing water masses, within the top 1000 m. The rings drift off, either to rejoin the stream at a later date or diffuse into the watermass (Mann and Lazier 1991), carrying with them the plankton community.

The rings have been studied from a reductionist stance, analysing the properties and impact of individual structures. A cold core ring contains nutrient rich water from the coastal current within the anticyclonic gyre, for instance in the Sargasso Sea. The nutrient rich water within the euphotic zone leads to high primary productivity, as the warm waters mix with the rich cold ring water. Ring Bob had 50% higher primary production than the surrounding Sargasso Sea (Ring Group 1981), supporting between 30 and 80 % more zooplankton biomass, with high diversity and dominated by small species. As the ring aged, the zooplankton maximum moved deeper, away from the warmed surface waters to around 800 m; the old ring fauna eventually died out through reduced reproduction and growth as the zooplankton were separated from their food. After 17 months, none of the original ring fauna remained, and the zooplankton community was dominated by warm water species (Mann and Lazier 1991). Beckman *et al.* (1987) studied a one month old cold core eddy. The centre of the ring had a higher concentration of zooplankton than the surrounding waters in the upper 100 m, dominated by smaller species. However, the biomass was reduced at depth, and from 100 m to 400 m was dominated by larger species (> 600 μm). At the ring periphery, smaller species dominated in the upper 100 m.

Warm core rings formed from oligotrophic anticyclonic water budding off ocean gyres, brings warm nutrient poor water into the cold nutrient rich waters. Although this may be

expected to have no effect on productivity, this is not always the case. Surrounding the warm centre there may be an area of high productivity. Various hypotheses have been suggested: Yeutsch and Phinney (1985) proposed that isopycnal mixing brings up deep nutrient rich water in the periphery of the ring, or that convectional mixing followed by stabilisation allows the plankton to bloom. Initially zooplankton biomass within the rings is low. But zooplankton are advected into the warm core rings from the slope water, and with the in situ growth facilitated by the bloom, within a few months the zooplankton biomass may be greater than in the surrounding waters (Mann and Lazier 1991). The warm rings may also interact with the continental shelf. Warm water is sometimes intruded on to the coast, displacing the cold water and their communities. At certain times of the year, the coastal waters contain an abundance of planktonic fish larvae. If this water is displaced it can have a dramatic impact on the recruitment of fish stocks in that year due to reduced larval survival (Mann and Lazier 1991).

Ring behaviour is less well studied at the Falklands-Brazil confluence, through which the AMT track passes, although the mechanisms and effects are likely to be similar.

Large scale spatial variability

The understanding of the distribution and patterns of organisms is referred to as biogeography. Biogeography has six main aims according to McGowan (1971, 1974):

1. to determine what species are present
2. to describe, quantitatively, their patterns of abundance
3. to understand what maintains the patterns
4. to determine how and why the patterns developed
5. to describe and delineate communities
6. to determine how these community-ecosystems are structured and how they function.

Regional/climatic factors impose latitudinal gradients on the distribution through, for example, variations in solar radiation, which may play a role in determining the surface wind field and thermohaline circulation of the oceans (Angel 1997a). The environment controls the distributional patterns through the local biotic and abiotic conditions and ecological processes that maintain the current biodiversity patterns at all scales and levels of organisation. The evolutionary and geological origins of the pelagic communities, influenced by the long-term changes in the morphology of the oceans' basins resulting from the sea floor spreading and plate tectonics, affect the species pool from which the present patterns are being generated (Angel 1997a). The Atlantic is the youngest of the oceans and the least diverse (Angel 1997b).

Divisions of the ocean

Provinces have been defined from zooplankton assemblages (e.g. Pierrot-Bults *et al.* 1986 and references therein). Most of the major oceanic provinces were defined by the middle of this century based on qualitative presence absence data (Boltovskoy 1997). The oceans were divided into nine major regions: polar, subpolar, transitional (temperate), subtropical for northern and southern hemispheres, and equatorial or tropical (Figure 1.4). Through the 1960s and 1970s quantitative data was used and lead to changes in the concepts and structure of several marine systems, but changes to the basic biogeographic schemes were small (Figure 1.5).

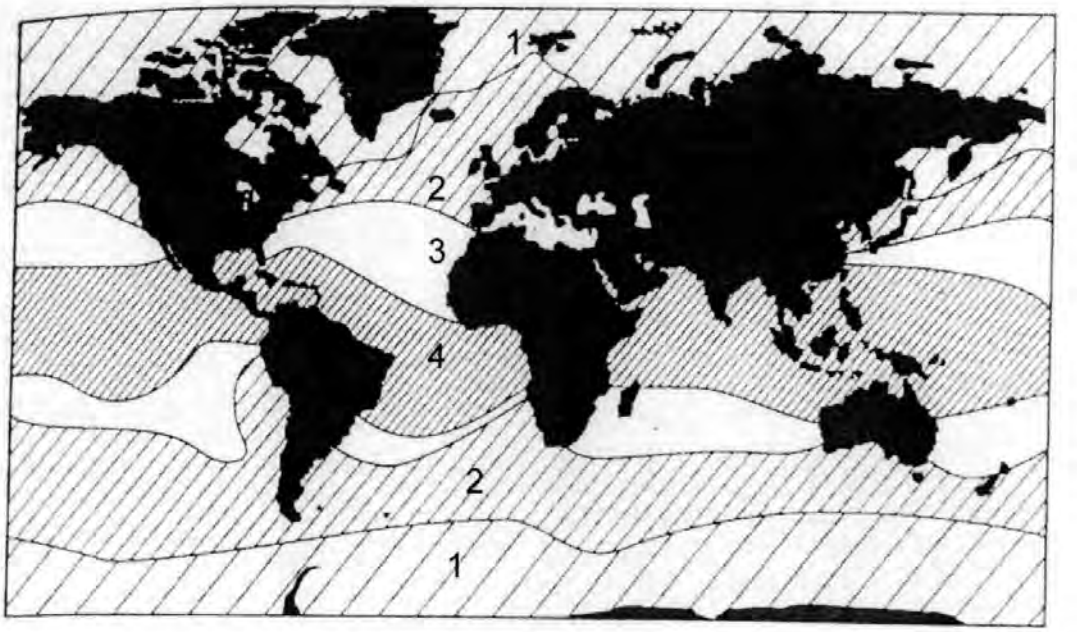

Figure 1.4: A biogeographic division of the world oceans in 1946 (adapted from Bobrinskii *et al.* 1946 in Boltovskoy 1998, 1-Polar, 2-Subpolar and Transitional (Temperate), 3-Subtropical and 4-Equatorial or Tropical).

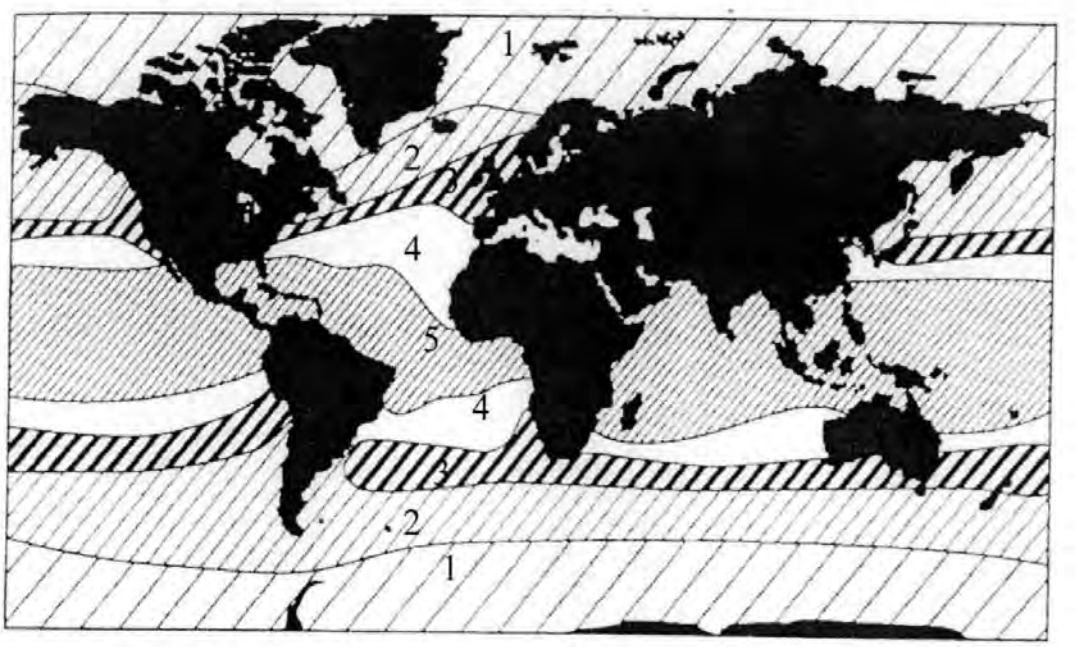

Figure 1.5: A current generalised biogeographic division of the world oceans (adapted from Boltovskoy 1998, 1-Polar, 2-Subpolar, 3-Transitional (Temperate), 4-Subtropical and 5-Equatorial or Tropical). Note the similarity of the schemes despite 40 years research.

These regions appear to contain a central core where all the characteristic fauna are present. The taxonomic structure in this core region appears to be consistent, independent of the abundance, so that the rank abundance shows significant agreement between localities (Fager and McGowan 1963). This suggests that the communities may have coevolved, and

therefore be considered to be ecosystems. The boundaries of individual species and groups do not always agree, tending to form a broad area of change (e.g. McGowan 1974), a transition zone or ecotone.

Divisions of the oceans have also been developed from the ocean physics and production regimes. Sverdrup *et al.* (1942) divided the oceans into constituent watermasses, which could be identified from their temperature-salinity profiles (McBarry 1964). More recently, Longhurst *et al.* (1995) have divided the oceans into biogeochemical provinces, each with its own physical, chemical and biological properties. These were divided by physical forcing factors, as these will determine the species assemblage, the magnitude of nutrient flux, the rate of vertical mixing and the stratification of the water column. The idea then was to be able to identify these zones from remotely sensed data (sea surface temperature, sea-elevation, wind stress and ocean colour; Platt *et al.* 1995; Longhurst 1998). The four major domains are Polar, Westerlies, Coastal and Trades.

The Polar Domain is typified by an ephemeral brackish period in spring and summer, due to fresh water inputs from ice melts. This layer induces stability early in the season, allowing algal blooms as soon as surface irradiance is sufficient. In the Atlantic, the Polar provinces are the Atlantic Arctic (ARCT) and the Atlantic subarctic (SARC) in the northern hemisphere, and the Antarctic (ANTA) and Austral Polar (APLR) in the southern hemisphere.

The West-Wind Domain includes the mid-latitudinal oceanic regions where westerly winds induce convective mixing, and spring blooms can be adequately described by Sverdrup's critical depth model (Sverdrup 1953). The Westerlies' defining characteristic is seasonality in wind stress imposed by the westerlies associated with atmospheric low pressure cells

(Aleutian, Iceland and Antarctic), with the seasonal radiation. These combine to give a deepening mixed layer (>500 m in parts of the northern hemisphere) and winter nitrate levels reaching 5-10 mmol. m^{-3}, and a vernal bloom. In the Atlantic, the provinces include North Atlantic Drift (NADR), the Gulf Stream (GFST; Florida to the bifurcation in the New Foundland Basin to 18 °C isotherm), the North Atlantic Subtropical Gyre (West and East defined by the mid-Atlantic ridge; NAST), the South Subtropical Convergence (SSTC), the Subantarctic (SANT).

The Trade Winds region has a characteristically stable pycnocline and a large eddy scale compared to higher latitudes, as a consequence of the diminishing Coriolis effect. Frictional wind stress is dominated by the trade winds causing momentum rather than mixing. Seasonal changes in the pycnocline are associated with seasonal shifts in the equatorial current system. Generally typical features are that the mixed layer algal blooms are not light limited. The depth of the mixed layer will change seasonally with wind field and curvature of the wind stress. The breakdown of the pycnocline and nutrient renewal will only occur at strong divergence (e.g. the equator). The provinces in the Atlantic include the North Atlantic Tropical Gyre (NATR), the Western Tropical Atlantic (WTRA), the Eastern Tropical Atlantic (ETRA), the Caribbean (CARB) and the South Atlantic Tropical Gyre (SATL).

The Coastal Boundary Zone is defined as the area under the influence and interaction with the coastal topography and the coastal wind regime modifies the circulation. The Coastal domain is often bounded by the shelf break, and includes coastal upwelling and associated eddies. Coastal features such as river plumes, tidal mixing, coastal upwelling and downwelling, and bottom roughness complicate the coastal regimes. This makes the coastal provinces more difficult to define, and Platt *et al.* (1995) are more sceptical about

the province definitions, as they are more variable. Atlantic coastal provinces include the Northeast Atlantic Continental shelf (NECS), Northwest Atlantic Continental Shelf (NWCS), the Canary Current (CNRY), the Guinea Coastal current (GUIN), the Guianas Coastal Current (GUIA), the Brazilian Coastal Current (BRAZ), the Southwest Atlantic Continental Shelf (FKLD) and the Benguela Coastal Current (BENG).

Sathyendranath *et al.* (1995) used deep chlorophyll maxima as a check for the boundaries because the depth of the chlorophyll maxima is consistently characteristic of domains.

Large scale divisions of the ocean based on the distribution of species, such as those in Figure 1.4 and 1.5, have mainly been derived from composite data sets taken at different times, seasons, with different sampling equipment, and analysed in different ways. Sampling coverage of the Atlantic Ocean is highly variable. The North Atlantic has been extensively sampled (e.g. Continuous Plankton Record sampling; Colebrook 1986). The southern Atlantic is relatively undersampled (e.g. Dadon 1997). These factors interact to impose limitations on the validity of different schemes and the robustness of these divisions. Gibbons (1997) tried to produce a scheme from the distribution of euphausiids using strict controls on the interpolation of data, and objective techniques such as cluster analysis to identify regions. However, because the data was from a variety of sources, it was reduced to presence/absence, which will not show community changes due to changes in dominance.

Environmentally based schemes are also expected to determine the distributions of organisms, directly through, for example, the temperature and salinity tolerances of the organism, but also indirectly via interactions with other organisms through feeding, predation and competition. This is born out by the similarity in distribution of many species

with the watermasses (e.g. McGowan 1974, Zeitzschel 1978). Production regimes are also likely to have a profound effect on the distributions of organisms.

The AMT traverses many of the proposed regions and their boundaries in the different schemes in the Atlantic over the 50°N to 50°S transect. With the regular sampling and consistent methodology, the AMT provides a platform for identifying large scale patterns in distributions. It will allow determination of whether zooplankton form identifiable communities or whether the gradients in the environment determine the distribution. Do the zooplankton really form communities which are directly determined by the environment as indicated by the watermasses or by the productivity regime, or are the changes modified significantly by the biological interactions, and are the schemes derived from species distributions really valid? Size structure has also been proposed as an important component of the community structure (above). If the size structure reflects changes in zooplankton community structure, it would also be expected to show divisions within the ocean, which might coincide with the changes in the taxonomic distribution.

Understanding zooplankton abundance

Estimation and understanding of zooplankton abundance is important for understanding carbon flux in the ocean (e.g. Banse 1995), and for estimating secondary production (Huntley and Lopez 1992). The environment will largely determine the zooplankton abundance through food supply and temperature-dependent processes. Biological processes (e.g. predation and behaviour) will also impact upon the zooplankton. Modelling zooplankton abundance has mainly been carried out within ecosystem models. The simplest of these models are NPZ (nutrients-phytoplankton-zooplankton; Evans and Parslow 1985, Steele and Henderson 1992), where nutrient input is determined by ocean physics, phytoplankton by nutrient input and grazing, and zooplankton by phytoplankton

and mortality. These models may be made more complex by sub-dividing compartments, e.g. having two nutrients (e.g. Aknes and Lie 1990, Franzs and Vehagen 1985), or by adding extra compartments e.g. fish (Walsh 1975) or detritus (Wroblewski 1977, Fasham *et al.* 1990). However, all these models must be calibrated and formulated for particular regions. The relationships between the compartments hold implicit assumptions (e.g. density dependence, linear or quadratic; Carlotti *et al.* 2000).

Simple empirical models have been developed, mainly for processes rather than zooplankton abundance (e.g. egg production; Calbet and Agustí 1999), using multiple regression. Multiple regression allows simple determination of the main factors influencing the process, and prediction is possible within the parameter range. The relationship between parameters is still implicit, and usually linear (multiple linear regression). Recently, neural networks have proved to be a useful approach in empirical ecosystem modelling, as they allow non-linear interactions between parameters without assuming the nature of the relationship. It is more complex to understand the impact of each parameter, but sensitivity analysis can be used, and may improve prediction over linear models particularly in non-linear systems (Lek and Guégan 1999). If zooplankton abundance is directly and indirectly determined by parameters of the physical environment, an empirical model of the zooplankton abundance should be possible, and may lead to increased understanding of how the environment impacts the zooplankton community.

Aims

Zooplankton heterogeneity has been analysed in several environments on various scales. However, there is a lack of integrated studies covering a wide range of spatial scales, particularly in the open ocean. This study aims to utilise the 50 ^{o}N and 50 ^{o}S Atlantic Meridional Transect cruises (AMT; Robins and Aiken 1996) to investigate spatial variation in mesozooplankton abundance, taxonomic composition and size structure over a range of scales. More specifically:

1. *To examine the scales of spatial zooplankton heterogeneity in the Atlantic*

- To utilise continuous data to identify the scales of variability in zooplankton abundance in the open ocean over a range from 10 to 1000 km.
- To compare heterogeneity in zooplankton abundance over a range of scales with chlorophyll and the physical environment.

2. *To identify large scale patterns in zooplankton community structure*

- To identify latitudinal trends in a variety of measures of zooplankton community structure including diversity, abundance and size.
- To identify large scale units of similarity in the zooplankton communities in terms of taxonomic and size structure, and compare with regions proposed by others.

3. *To understand and predict patterns of abundance of zooplankton*

- To model surface zooplankton abundance from empirical data

Chapter 2: Methods, inter-comparisons and validation

Introduction

Several methods for the measurement of different facets of community structure were utilised. These methods used are a combination of modern and traditional techniques. Some aspects of the methods are not fully validated, and the relationships between methods have not been fully investigated. The first zooplankton samples were analysed under the microscope qualitatively, by identification of species or higher taxonomic groups. Initially quantification, in terms of numerical abundance, was derived from microscope counts, and taxa counts still form the basis of much analysis of community structure. As theories about trophic structure and energetics have developed so too has the need for estimates of biomass and energy. Zooplankton biomass is now recognised as a fundamental yet difficult parameter to measure; it is the critical quantity for estimating zooplankton productivity (Huntley and Lopez 1992). Numerical abundance does not take into account the size of the organism. Size is important because smaller organisms tend to be more abundant, and larger organisms contain more energy. Size maybe measured directly from individuals. Several length to mass equations have been developed for different species (e.g. Mauchline 1998 and references therein), although the energy content may vary significantly between individuals and seasons. However, measurements of this nature are very time consuming. Recent developments such as digitising pads have gone some way to improving the speed of analysis. An alternative quick and simple way to size organisms is by separating through sieves.

Sieving has been employed as a sizing mechanism in several fields e.g. sediment, phytoplankton, particulate carbon, benthic, and freshwater and marine zooplankton studies. The size of mesh through which a particle will pass depends not only on the size of the

particle, but on its shape and orientation. It has been found with sediments that it is the second largest dimension that determines whether a particle can pass through a particular mesh (Dyer 1986). Seda and Dostolkova (1996) investigated the efficiency of sieving with the cladoceran *Daphnia galeata*. They found that the chance of an animal passing through a given mesh size was probabilistic, and related to the carapace length. However, they suggested that the carapace width might be more closely related to the mesh size. They concluded "our results demonstrated not only the usefulness of the technique, but also its reliability and accuracy". Other work has been done on capture characteristics of plankton nets (Smith *et al.* 1968; Tranter and Fraser, 1968; Evans and Sell, 1985). Joint Global Ocean Flux Study (JGOFS) protocols suggest the use of 200 μm mesh nets for mesozooplankton, and standardisation of sieving mesh sizes to 50, 200, 1000 and 2000 μm (Longhurst *et al.* 1990b), although reported using 200, 500, 1000 and 2000 μm meshes (Harris 1990). Despite these protocols, the exact procedure for sieving is not clearly defined. The care taken in sieving may significantly alter the proportion in each size category, and this will vary between people. Several people have undertaken the size fractionated carbon sieving on the AMT programme. To test whether differences in sieving were likely to be significant, thorough and normal sieving were compared.

Abundance can also be measured in terms of biomass or energy. There are several measures of biomass: biovolume, wet weight, dry weight, carbon, calorific value. Energy models require calorific values. However, carbon can be measured more quickly and easily than calorific value, and be converted to energy giving the same kind of precision as calorific measurements, and is precise even for small amounts (ca 1 μg; Båmstedt 1986; Salonen 1979; Salonen *et al.* 1976). Nitrogen is required for nutrient models and can be measured at the same time as carbon using a CHN elemental analyser. However, carbon and nitrogen analyses have their drawbacks. Samples must be dried, and this can lead to losses. Too slow drying allows deterioration of the samples, but too hot temperatures may

vaporise some carbon compounds. Lovegrove (1966) studied this problem extensively and recommended oven drying at 60°C, as does the JGOFS protocols (Longhurst *et al.* 1990b). Analysis requires a sophisticated instrument, unsuitable for use at sea. In addition, to be carried out economically, samples are processed in batches of around 100. This means that samples must be stored. In the past several techniques have been employed. Preservation in formalin can result in substantial losses (e.g. Williams and Robins 1982; Fudge 1968). This is thought to be due to either leeching caused by the osmotic pressure of the preservative (Williams and Robins 1982), or hydrolysis of lipids and degradation of polyunsaturated fatty acids (Morris 1972) and protein (Fudge 1968). Freezing is the other alternative for preservation. Varying results have been found depending on the exact method of freezing. Williams and Robins (1982) found substantial losses in *Calanus helgolandicus* of frozen individuals. However, frozen individuals were picked from the filter papers they were frozen on, so losses due to ruptured membranes caused by the freezing may have resulted in carbon leaking out of the animal on to the filter paper. Omori (1970) froze *Calanus cristanus* in individual cups, and the whole cup was analysed for carbon. He found the smallest losses by this method, as compared to drying or formalin preservation. Others have found little loss with freezing (e.g. Fudge 1968). Losses from two preservation methods convenient for use on board ship were estimated.

The introduction of automated systems can allow more sampling by reducing the cost and time required for analysis, as well as continuous sampling. One instrument developed for zooplankton analysis is the optical plankton counter (OPC). Extensive calibration and testing of the OPC in diverse environments has led to a greater understanding of the operational limitations (Herman 1988, Herman 1992, Herman *et al.* 1993, Sprules *et al.* 1998, Halliday and Coombs (in press)). The accuracy of abundance measurements has generally been estimated using the towed version (OPC-1T). However, in this study a laboratory version (OPC-1L) is used in the open ocean environment for processing net

samples and pumped through (underway) sampling. Accuracy and reliability of the OPC system for measuring numerical abundance for processing net samples and for underway sampling was tested by comparing with traditional microscope counts. The relationship between OPC measured biovolume and biomass in terms of carbon was investigated. This will allow the use of OPC data in the development of carbon based models.

Sizing by the OPC, and how it relates to other methods, is one of the contentious issues in the use of the OPC. The transparency of the organism has been found to play an important part, with fresh fish eggs before and after preservation been measured as different sizes (Sprules *et al.* 1992). The orientation of the animal as it passes the beam will also affect how it is measured. The initial calibration of the OPC is based on a spherical model, where the measured area is converted to a volume or equivalent spherical diameter (ESD). The simplification of zooplankton to spheres can introduce errors. Sprules *et al.* (1998) modified the model to improve the accuracy for cladocerans. Understanding sizing of organisms by different methods is also important for inter-comparison of methods. Here, the relationship between sieving, OPC and microscope measurement for sizing zooplankton is developed.

Another potential limitation in the use of the OPC is that at high concentrations two particles may pass through the beam at the same time and be counted as one. For the OPC-1T at concentrations of 7500 particles m^{-3}, only 37 % was estimated to have been counted (Herman 1988). Estimates of the relationship between coincidence and concentration have been proposed by Herman (1988) who derived a semi-empirical formula, and by Sprules *et al.* (1992, 1998) who used a theoretical approach based on the Poisson distribution. Sprules *et al.* (1998) predicted a change in the particle size measured by the OPC due to coincidence: a shift to fewer, larger particles, and an anomalously high biomass estimate. This high biomass is due to the OPC measuring in effect the area of the organism, which is

converted into ESD. The ESD is then used to calculate the biovolume of the sphere. Because of the non-linear conversion from area to biovolume, if two particles are in the beam, the biovolume of the particles will be overestimated (Sprules *et al.* 1998). In this study, coincidence is investigated using a range of concentrations of the diatom *Coscinodiscus wailesii*, to test the predictions of a theoretical model based on the Poisson distribution for the OPC-1L.

Methods

The L4 station

L4 is a traditional sampling site five miles off Plymouth (50 ° 15'N, 04° 15'W; Figure 2.1), in about 50m of water. Regular zooplankton vertical net samples were taken with WP2 200 μm mesh, integrated from approximately 50 m to the surface. Extra samples were taken for method validation and intercomparisons.

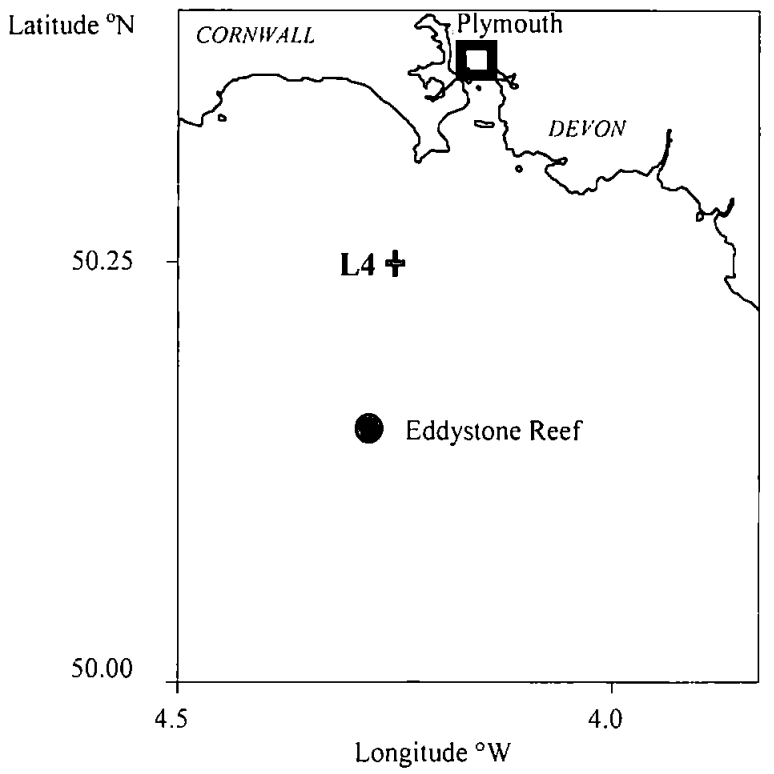

Figure 2.1: Station L4: 50 ° 15'N, 04° 15'W

Cruises

The Atlantic Meridional Transects (AMTs) were set up as part of a NERC (Natural Environment Research Council) programme investigating decadal change on the basin scale. They use the British Antarctic Survey vessel RRS James Clark Ross as a ship of opportunity, on its way to and from Antarctica for the Austral summer (Robins and Aiken 1996). Generally, this is between UK and Falklands, but AMT 6 was between South Africa (Cape Town) and UK. This is a multidisciplinary programme where several aspects of oceanography are investigated. Data and zooplankton samples were made available from AMT 1-3, and I undertook AMT 4-6 (Table 2.1, Figures 2.2 and 2.3). Details of station are in Appendix 1.

Sampling on the AMT cruises was based around a mid morning station, when a variety of optical measurements were taken. A CTD and bottle rosette was deployed to 200 m. Water collected was used for a variety of measurements including nutrients, primary productivity, phytoplankton samples and particulate carbon. Other measurements were made on some cruises. Details can be found in the cruise reports (Robins 1996, Robins *et al.* 1996, Bale 1996 and 1997, Aiken 1998, Aiken *et al.* 1998) and on the AMT website (http://www1.npm.ac.uk/amt/). Zooplankton sampling consisted of WP2 (Tranter and Fraser 1968) 200 μm net samples. In addition to these daily stations, some night and other extra stations were made with reduced data collected.

Between stations, fluorescence derived chlorophyll, temperature and salinity were measured using automated sensors from the uncontaminated seawater supply, and logged on the ocean logger. Samples for calibration were also taken regularly for chlorophyll derived fluorescence. The OPC also sampled the uncontaminated seawater supply. The uncontaminated seawater was pumped from beneath the ship's keel from an extensible

intake protruding approximately 30 cm, and at about 7m depth. The intake had a 6 mm steel mesh filter allowing mesozooplankton to pass through whilst removing larger objects that might damage the pumps.

Cruise	Dates	Track
AMT1	21st Sept. - 24th Oct. 1995	UK- Falklands
AMT2	22nd April - 22nd May 1996	Falklands-UK
AMT3	16th Sept. - 25th Oct. 1996	UK-Falklands
AMT4	21st April - 27th May 1997	Falklands-UK
AMT5	15th Sept. - 17th Oct. 1997	UK-Falklands
AMT6	14th May - 16th June 1998	South Africa-UK

Table 2.1: Summary of Cruises

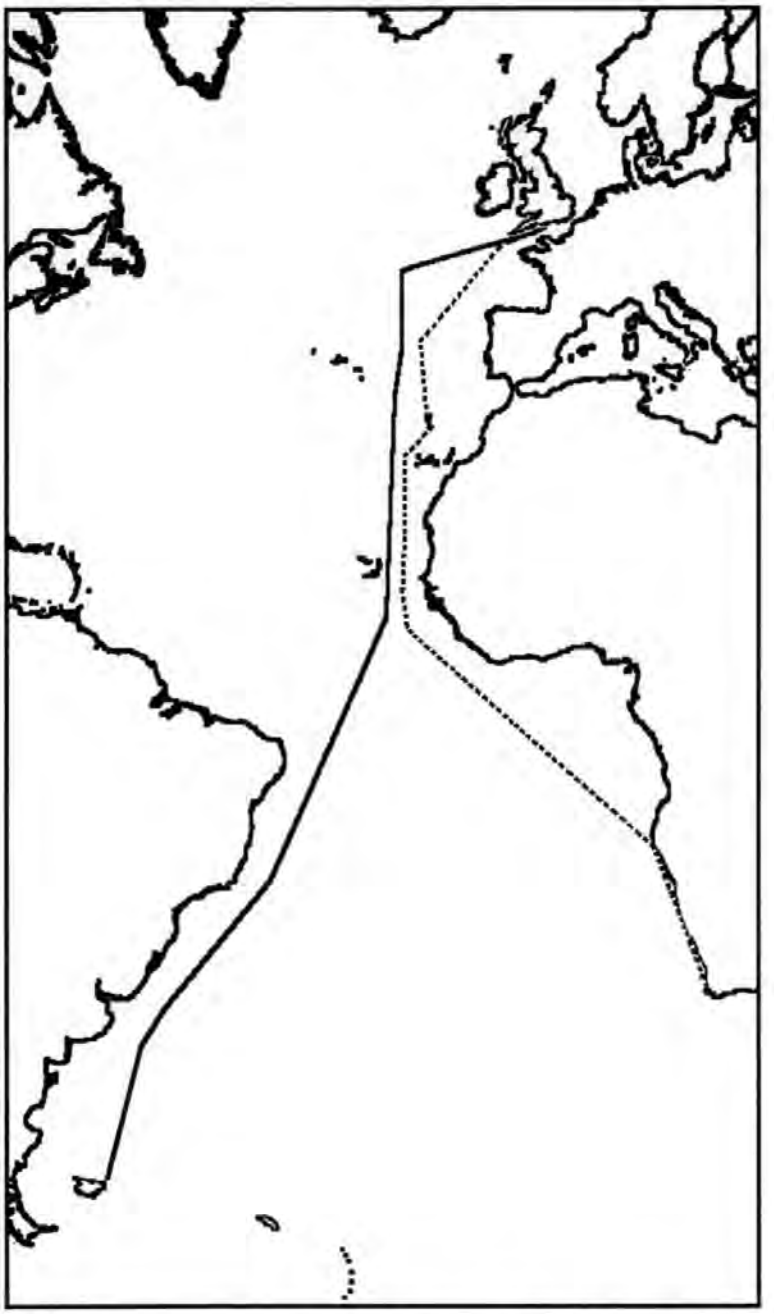

Figure 2.2 General AMT cruise track (—— AMT track for AMT 1-5 ····· AMT 6)

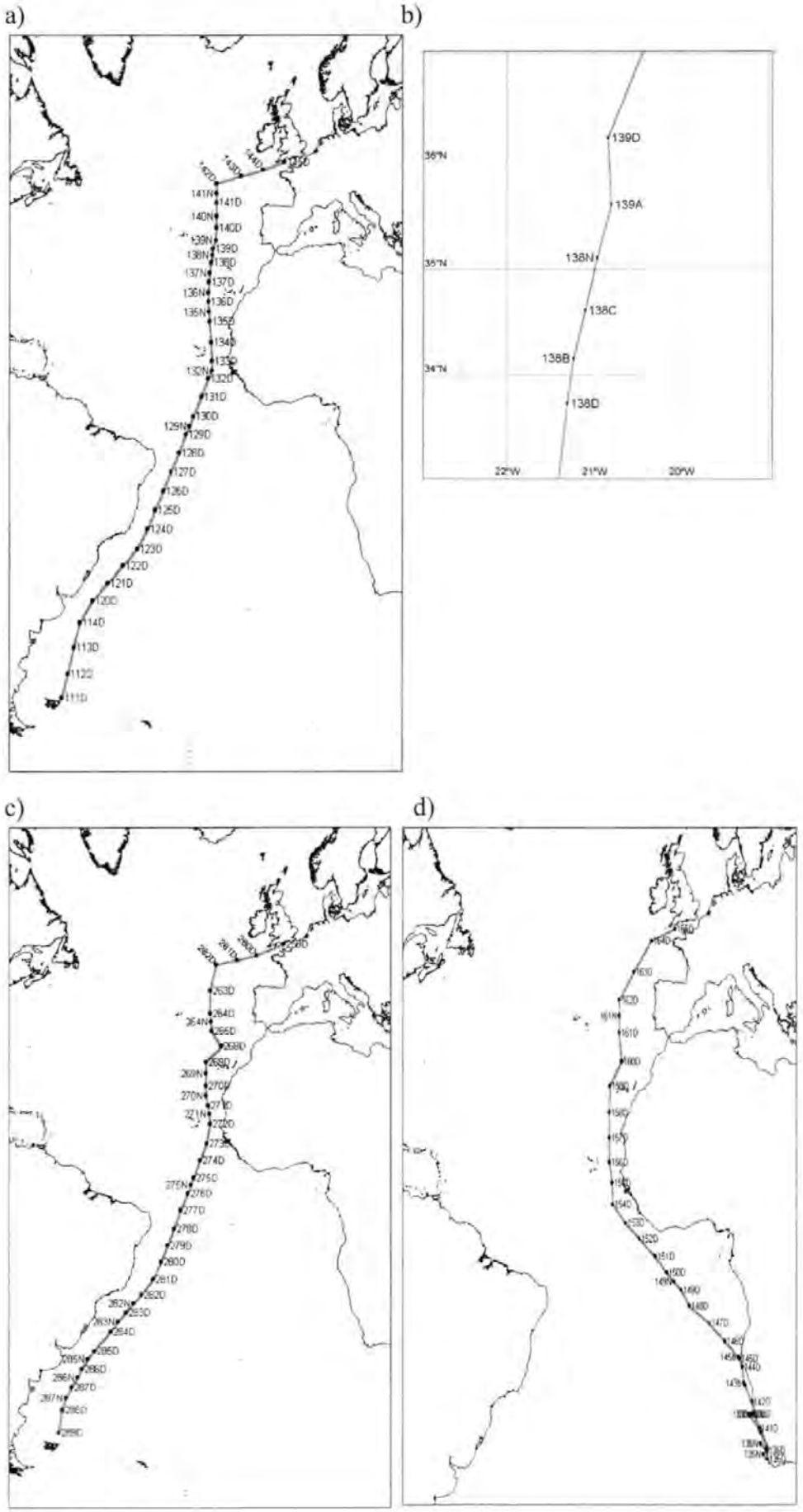

Figure 2.3 a) AMT 4 cruise track, b) AMT4 stations between 35 and 37 °N, c) AMT 5 cruise track, and d) AMT 6 cruise track with stations

Net sampling

At each daily station, two WP2 (200 μm mesh) net casts were made: one integrated 200 m to surface haul, and one integrated 20 m to surface. On night stations, a WP-2 (200 μm mesh) 0-200 m haul was taken only. The 20 m nets were processed through the OPC and preserved in 4% buffered formalin. The 200 m net was split in half using a Folsom plankton splitter. The first half of the sample was passed through the OPC, and collected and preserved (4% formalin), and the second half was sub-sampled for carbon analysis, with the remainder preserved. Conversions to concentrations assumed 100% filtering efficiency. Trials on earlier cruises with flowmeters suggested that the filtering efficiency was generally greater than 85%.

Carbon

The zooplankton net sample was size fractionated by screening the sample through 2000, 1000, 500 and 200 μm sieves, and rinsing through with filtered seawater, so that every particle came into direct contact with the mesh. This created fractions of 200-500, 500-1000, 1000-2000 and >2000 μm, the standard JGOFS size fractions (Longhurst *et al.* 1990b). Each size fraction was made up to 500 or 1000 ml with filtered seawater, depending on the density of zooplankton. Aliquots of 50 ml were filtered onto pre-ashed Whatman glass fibre GF/C filters (in triplicate), from each size fraction. Blanks were made by filtering 50 ml of the filtered seawater on to a pre-ashed Whatman GF/C filter. The sample and blank filters were dried for 48 hours at 60 °C, before being wrapped in aluminium foil and compacted, and stored at -20 °C or below. The samples were subsequently analysed for carbon and nitrogen using a Carlo Erba 1500 CHN analyser. Five standards of acetanilide between 0.2 and 2 mg were used to derive a calibration curve. Further standards and blanks were interspersed with the sample pellets. The carbon and nitrogen biomasses were corrected from the blanks and converted to mg m^{-3}, assuming 100% filtering efficiency.

The remainder of the sample was preserved with borax buffered formalin (4%) for later taxonomic identification. For AMTs 1-4 the sample fractions were preserved together, for AMT 5 the >2000 fraction was preserved separately as none was removed for carbon estimation, and for AMT 6 all the size fractions were preserved separately.

Effects of thoroughness of sieving

Four integrated 50m to surface WP2-200 μm zooplankton net samples were taken from L4 off Plymouth (Figure 2.1) at different times. The zooplankton samples were brought back to the laboratory and stored in a cold room until processed. The samples were split in half using a Folsom splitter. One half sample was sieved as normal for carbon. The second half was sieved 'thoroughly'. This involved spending extra time washing through the samples so as to ensure that every particle possible passed through the mesh. From each size fraction, 50 ml aliquots were taken using a ladle and filtered on Whatman GF/C filters for carbon analysis. Five aliquots were taken from each size fraction. The filters were frozen and subsequently dried and pelletted before processing through the Carlo Erba CHN elemental analyser.

Effects of preservation on carbon samples

An L4 sample was taken and stored as above. The sample was made up to 1000 ml. Aliquots were taken with a 50 ml ladle, and filtered on to Whatman GF/C filters. One from each triplicate was assigned at random to the three experiments, until five filters were in each of the three groups. The first group was dried and run through the Carlo Erba 1500 elemental analyser (CHN) immediately. The second was dried and pelletted immediately then frozen until the next carbon run (ca 2 months) before being run through the Carlo Erba and the third group were frozen (for ca 2 months) before being dried, pelletted and

run through the Carlo Erba. This was repeated for five more samples taken at different times.

Two-way ANOVA was used to analyse the results, to determine if the different treatments were significantly different from each other for both carbon and nitrogen. This was followed by a paired student T test, to determine which treatments were different. The mean percentage difference from the samples immediately analysed from those that were dried and frozen or frozen and dried was calculated.

Taxonomic analysis

The 200 m half net samples, preserved after part was removed for carbon analysis, were analysed for major zooplankton groups, and copepod genera within the four size classes (200-500, 500-1000, 1000-2000 and >2000 μm). The samples were washed to remove formalin before being size fractionated if required (i.e. for AMT 4 and 5). A sub-sample was taken from a known volume using a Stempel pipette, so that a minimum of 200 copepods was counted. All major zooplankton groups were identified; copepods were further analyzed to genus level where possible. Small calanoid copepods such as *Paracalanus, Pseudocalanus* and *Clausocalanus* were not distinguished. These were classified as *Para/Pseudocalanus*.

The 20m net preserved samples and the underway samples, which had been through the OPC, were analysed for major groups only, and were not size fractionated. The samples were washed to remove the formalin and made up to a known volume. A sub-sample was taken using a Stempel pipette, so that a minimum of 200 of the most abundant group, usually copepods, was counted. For some of the underway samples, it was necessary to analyse the whole sample.

The OPC

On the ship, the laboratory version of the optical plankton counter (OPC-1L, Focal Technologies; Herman 1988) was used. Herman (1988, 1992) describes its design and operation. Essentially the system consists of a 20 mm square flow cell through which the sample passes (Figure 2.4). A parallel light beam with a 4 mm width is detected by a sensor on the opposite side of the tube. As a particle passes the sensor, the light attenuation due to the passage of the particle is detected by the sensor and converted to an electrical pulse. The electrical pulse is sent to the deck unit where it is converted to digital size and a time stamp is added before being logged by the computer. The OPC software converts the digital size to equivalent spherical diameter (ESD), using a semi-empirical formula (Herman 1992). The ESD is the diameter of a theoretical sphere with the same digital size (or area) as the particle.

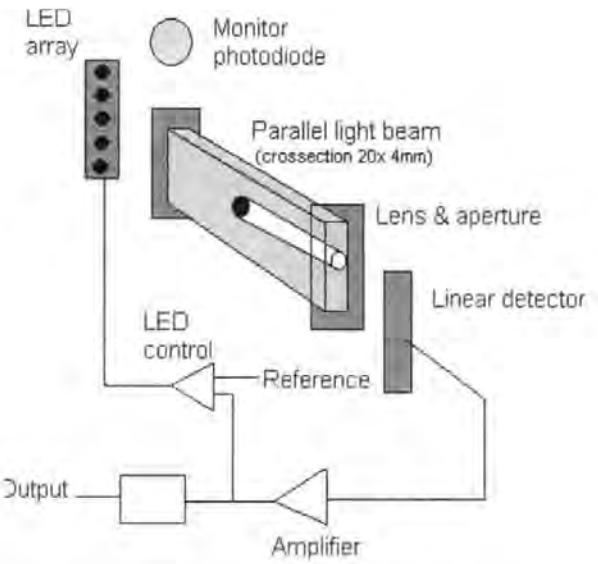

Figure 2.4: A schematic of the OPC. Redrawn from Focal Technologies Inc. (1995).

OPC processing of net samples

The OPC was set up as a recirculating system (Figure 2.5), using seawater from the uncontaminated seawater supply. On the OPC outflow, a collection vessel with a 130 μm mesh was used to collect any material and stop it from being recycled. The OPC was connected to a computer (PC) via a deck unit to record the data using the OPC software.

The recirculating system was run to remove particles from the seawater, until the counts were less than one in 10 sec. The collection vessel was rinsed out and replaced, and the system allowed to resettle before the net sample was added. The OPC software was set to save to a new file, and the sample was added slowly to the tank, to reduce bubbles and to control the rate of particles through the OPC. Once all of the sample had been added the count rate was allowed to return to zero (less than one count in 10 seconds), and a visual check was made to ensure all the organisms had been removed from the tank before the file was ended. The sample was recovered from the collection vessel and preserved in 4% borax buffered formalin.

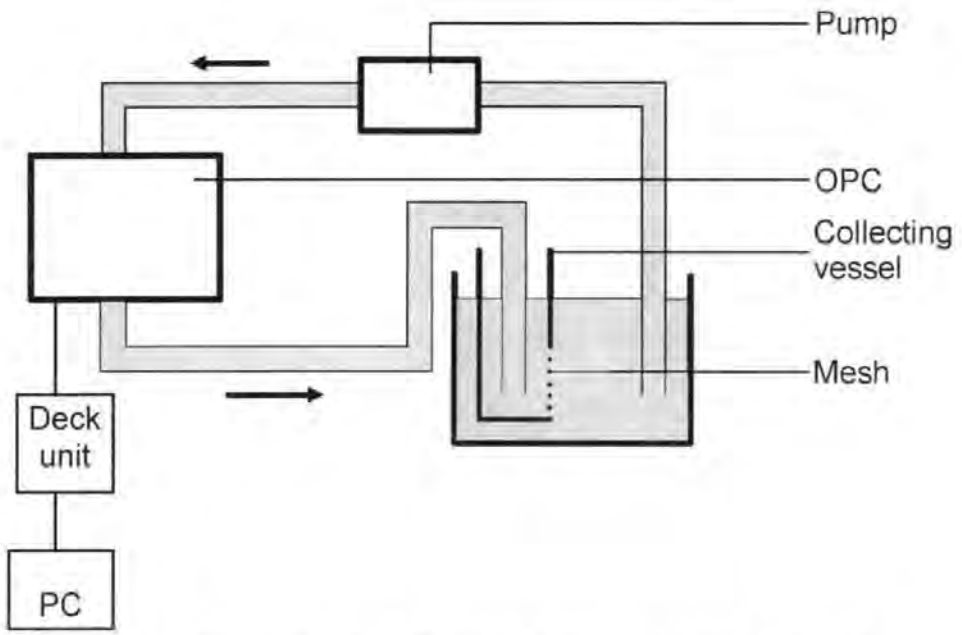

Figure 2.5: The OPC set up for processing net samples

OPC underway

The OPC was used in continuous flow-through mode during each cruise, using the uncontaminated seawater supply. This was interrupted only briefly at local dusk and dawn to change data files, and for about two hours each day on station to process the net samples, and carry out maintenance such as cleaning. The uncontaminated seawater supply passed through a debubbling device (Gallienne *et al.* 1996) before passing through the OPC and a flowmeter at a rate of approximately 20 L $min.^{-1}$ (Figure 2.6). In line samples, from the OPC outflow, were collected at least once a day, through a 200 μm mesh

collection vessel. These were preserved in 4% borax buffered formalin for subsequent taxonomic analysis to validate the OPC data.

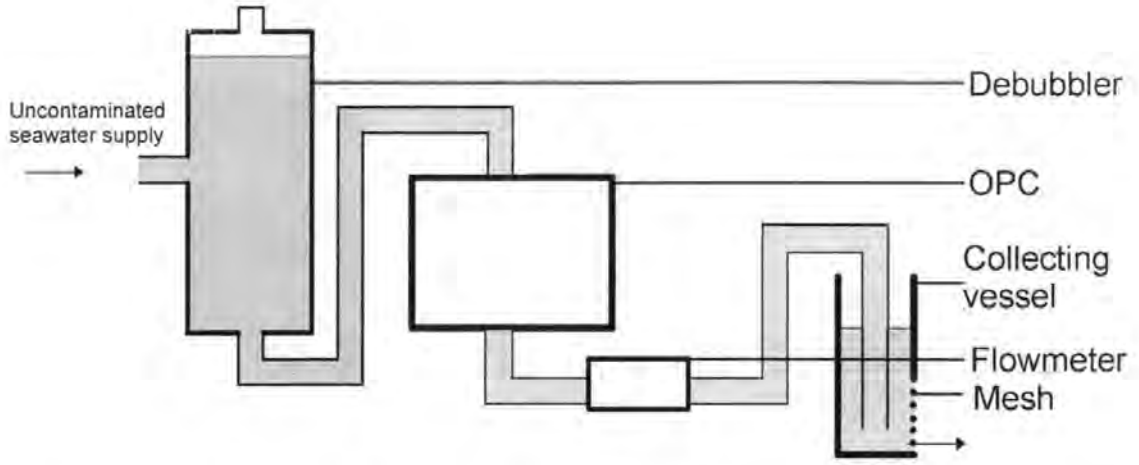

Figure 2.6: The OPC set up for sampling the uncontaminated seawater supply on ship

Comparison of OPC counts with microscope counts for net samples

The data from the AMT 200 m WP2 net samples were used to compare the OPC counts and the net counts. For the OPC, counts over 250 μm ESD were used, as the OPC is unreliable at smaller sizes. This is due to the signal to noise ratio in the OPC detector being too low to be consistently distinguished (Herman 1992). The counts were Log_e transformed to normalise the variance of the data. Functional (type 2; Kendall and Stuart 1961) regressions were calculated to give the symmetric relationship between OPC and microscope counts for AMT 1-6 totals and AMT 5 size fractions. The functional regression does not assume that one variable is dependent on the other, but gives the relationship between the two. This is the most suitable regression when there are errors in both variables (Krebs, 1999).

Comparison of OPC counts with microscope counts for underway samples

Underway samples were collected from the outflow of the OPC and analysed. The raw OPC counts were converted to counts per m^3, using a lower cut off of 250 μm. For AMT 1, samples were collected whilst the OPC was not running, so the microscope counts were

compared with OPC counts either side of the sample. In addition, for AMT 1, the volume of water passing through the OPC during sample collection was not recorded, thus counts were converted to counts per hour. OPC and microscope counts were Log_e transformed to normalise the variance, and then compared using symmetrical functional regressions for AMT 1-6.

Comparison of OPC biovolume with carbon biomass

Carbon biomass and OPC biovolume from AMT's 1-6 200 m WP2 net samples were compared, both as totals and for each size fraction. The carbon and biovolumes were Log_e transformed to normalise the variance. Symmetric functional regressions were used to determine the relationship between carbon and OPC biovolume.

Comparison of OPC size fractions and sieved size fractions

An L4 net sample was taken and stored as described above. It was size fractionated as for carbon (above). Each size fraction was run separately through the OPC. The distribution of sieved sizes in the OPC size classes (ESD) were compared. The mean ESD was also calculated from the OPC distribution.

Comparison of OPC and sieve sizing with microscope measurements

An L4 net sample was taken and stored as described above. It was size fractionated as for carbon (above). Individuals of a variety of major groups were taken and measured under the microscope using a calibrated graticule, from each size fraction. Each group from each size fraction was put slowly through the OPC separately. The mean and range of ESD was calculated from OPC and microscope measurements. Copepods, cladocereans and ostracods were assumed to be elipsoid and biovolume was calculated from:

$$V=4/3\ \pi\ r^2\ (L/2)$$

where V is the volume, r is the radius (half the diameter), and L is the total length.

Siphonophores were assumed to be conical, and biovolume calculated from:

$$V=1/3\ \pi\ r^2L$$

where V is the volume, r is the radius and L is the length. Fish eggs were assumed to be spherical and ESD was assumed to be the diameter, and the volume:

$$V=4/3\ \pi\ r^3$$

where V is the volume, and r is the radius. The organisms from the sieved size fractions were compared with various microscope measurements to try to determine which parameter predicted which fraction it was found in. OPC and microscope mean ESDs were compared.

Estimating coincidence for the OPC

A 200 μm net sample from AMT 6 (Figure 2.3, sample 140D) from the Benguela upwelling at 12° 00'E, 19° 00'S was predominantly composed of the centric diatom *Coscinodiscus wailesii* (Grant). Large additional organisms were removed by passing the sample through a 500 μm mesh before it was preserved in 4% borax buffered formalin. The 200-500 μm fraction of this sample was used as a test for coincidence, as the *Coscinodiscus* has a narrow size distribution (Figure 2.7 ESD SD. = 72 μm) and a similar size range to many small copepods (mean ESD 399 μm).

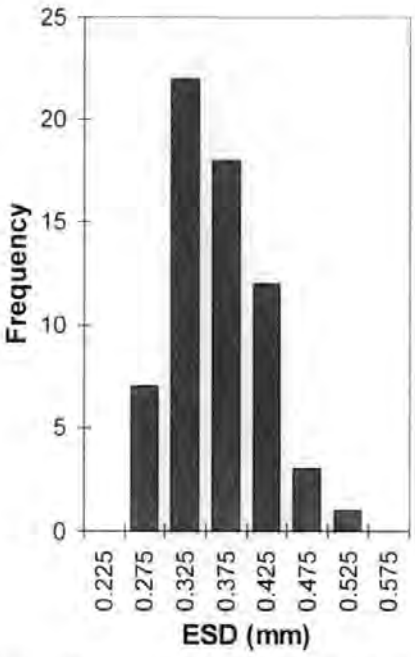

Figure 2.7: Estimate of ESD of *Coscinodiscus wailesii* (Mean ESD = 399 mm, SD = 72.)

The OPC-1L was set up in pump through mode (Figure 2.4). The sample of *Coscinodiscus wailesii* was added slowly at first to get low counts per sec (1-2 cts per sec) for estimating the mean ESD (Figure 2.7), and then at increasing concentrations, to give a range of count rates. The raw data was processed to give the counts and biovolume in 1 sec intervals using the OPC software. The mean biovolume of a particle was calculated by dividing the total biovolume by the number of counts.

Theory predicting coincidence and its effect on mean ESD

Sprules *et al.* (1992) derived a formula based on theory from the Poisson distribution, thus assuming random distribution. The average number (μ) in the beam is:

$$\mu = C \times V$$

where C is the concentration of animals, and V is the volume in the beam (i.e. 20 x 20 x 4 mm). From the average number in the beam, the average number counted can be calculated from the Poisson distribution ($P(Y) = e^{-\mu}. \mu^{Y}/Y!$, where P(Y) is the probability of Y particles in the beam, and μ is the mean number of particles in the beam). If more

than one organism is in the beam at one time, they will be counted as one (and with an area of both). The average number of organisms recorded by the OPC will therefore be:

$$\text{OPC av. no.} = P(0).0+P(1).1+P(2).1+...$$

$$= P(1)+P(2)+...$$

$$=1-P(0)$$

$$=1-e^{-\mu}$$

The coincidence factor =(av. no.)/(OPC av. no.)

The Poisson distribution was used to calculate the apparent OPC counts from the actual counts in a similar way to Sprules *et al.* (1992, 1998), but time was used instead of volume. Given a flow rate of 15 L min^{-1}, an area of 400 mm^2 (20*20 mm cross-section of the flow tube), the velocity of particles along the tube will be 625 mm s^{-1}. Two particles will be counted as one if any part of them is in the beam at the same time, so that a particle will have to travel the beam width plus its length without encountering another particle i.e. 4 mm + mean ESD. This will take (4 + mean ESD) / 625 mm s^{-1}. The average number of particles in the beam is given by the actual count rate / [(4 + mean ESD) / 625]. The probability of one or more particles in the beam is given by 1-P(0), or $1-e^{-(\text{av. no.})}$ (above).

For larger particles, it will take longer for a particle to completely clear the beam. Thus, the probability of coincidence would be expected to be higher at the same concentration (Figure 2.8a). Varying the flow rate will not alter the rate of coincidence if the concentration remains the same. However, the OPC does not measure concentration directly, but the count rate. The same concentration will have a lower count rate at lower flow rates. Thus at lower flow rates the coincidence will be greater for the same count rate (Figure 2.8b). For *Coscinodiscus wailesii* (mean ESD = 0.399 mm), the time to cross the beam will be $7.07 * 10^{-3}$ s. The theoretical response of OPC measured counts compared to the actual number of particles passing through the OPC is given in Figure 2.8c.

The Poisson distribution can also be used to estimate the probability of any number of particles being in the beam from the mean density of particles, given by $P(Y) = e^{-\mu}. \mu^{Y}/Y!$ (see above). This was calculated for up to 6 particles in the beam at one time. Greater than six particles would be expected to be very rare, even when densities are quite high. The apparent mean ESD is given by actual mean ESD x (P(1) x 1+P(2) x 2 +P(3) x 3....). The apparent mean ESD was calculated for a range of densities of *Coscinodiscus wailesii* Figure 2.8d shows how the measured mean ESD would be expected to increase with concentration.

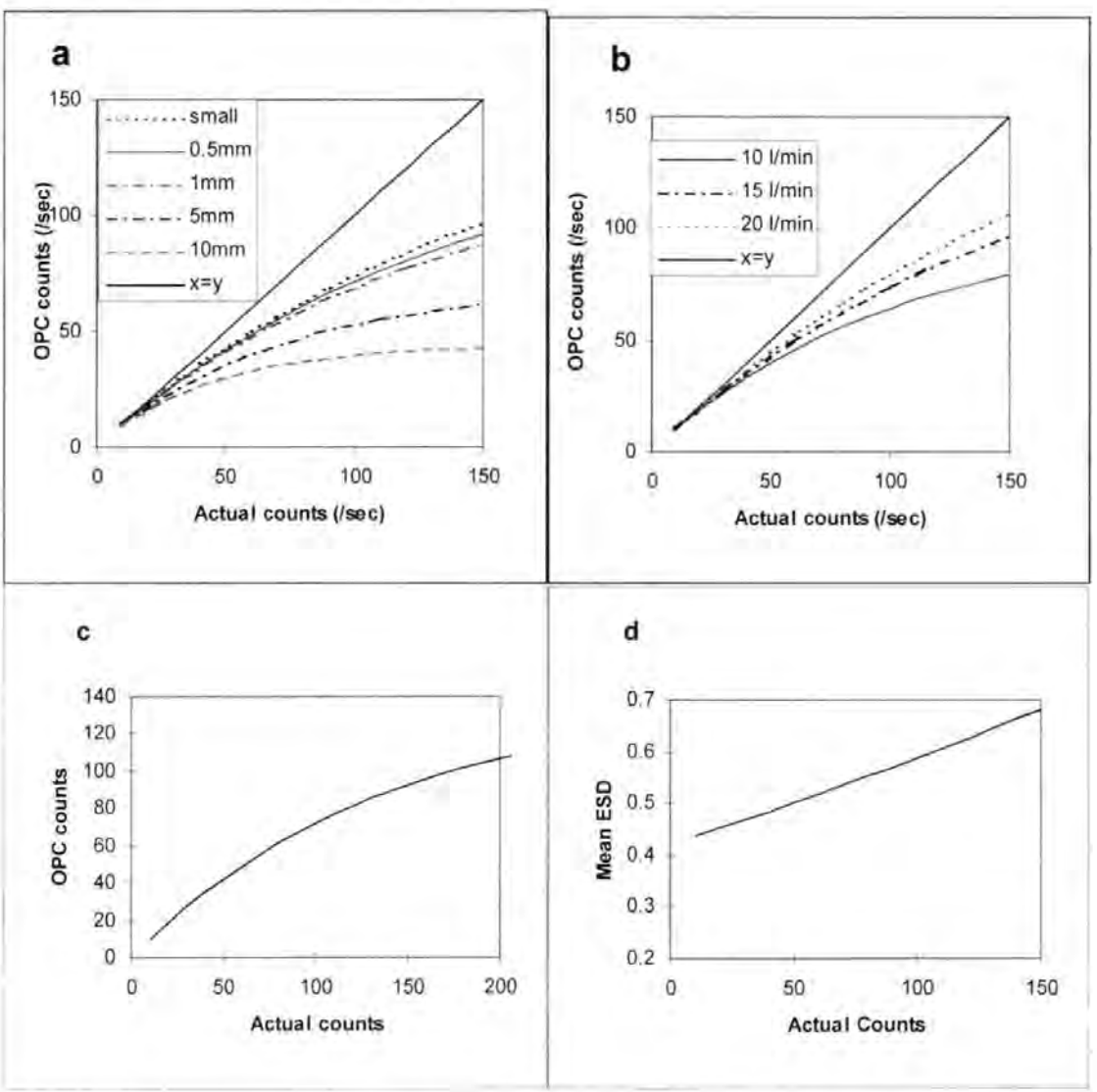

Figure 2.8: Predictions from the Poisson distribution for coincidence using the OPC-1L a) the effect of particle size on the expected coincidence at a flow rate of 15 L min-1, b) the effect of flow rate on coincidence for a small particle, c) predicted coincidence for *Coscinodiscus wailesii* at a flow rate of 15 L min-1, d) the predicted effect of coincidence on particle size for *Coscinodiscus wailesii*.

Maximum Count Rate

If it takes (4 mm + mean ESD)/625 seconds to cross the beam, and a further 4 ms for the system to reset itself (Sprules *et al.* 1998), the maximum count rate for different size particles can be calculated: 1 / ([(4 + ESD) / 625] + 0.004). This assumes that as soon as the system has reset, another particle enters the beam. The maximum count rate is predicted to decrease as the ESD increases (Figure 2.9a). The maximum count rate for *Coscinodiscus wailesii*, with a mean ESD of 399 μm will be 90.6 s^{-1}. The manufacturer's maximum counts rate of 200 s^{-1} is based on the maximum flow rate of the OPC, 4 m s^{-1}, and for a small particle. For the minimum flow rate and a particle of 250 μm, the maximum count rate is 68 s^{-1}.

The mean biovolume for the OPC measured count rate can now be predicted (Figure 2.9b) for *Coscinodiscus wailesii*. The maximum count rate is also shown.

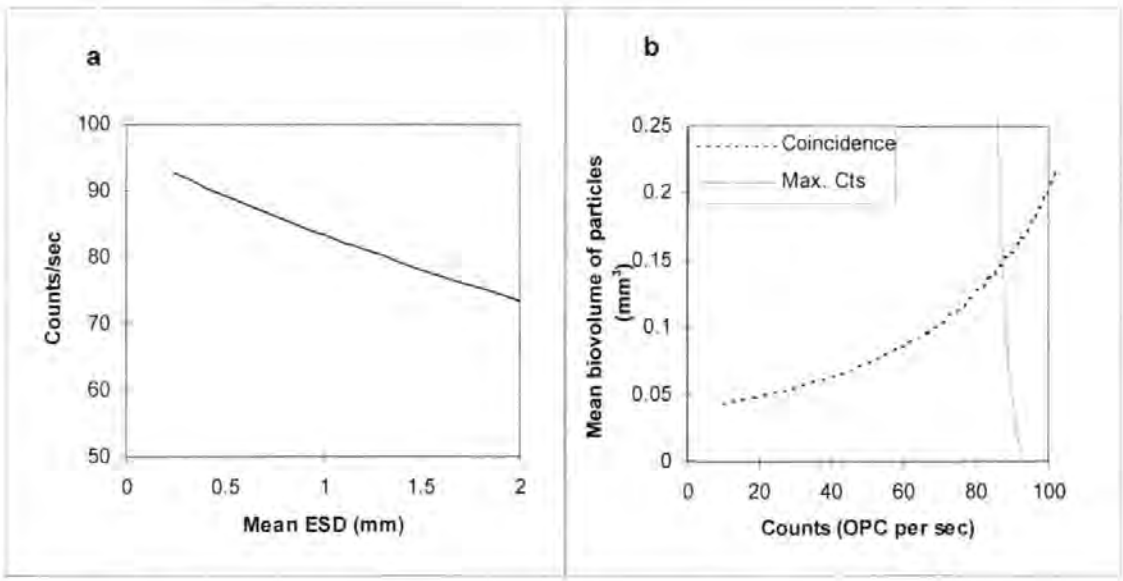

Figure 2.9: a) The maximum theoretical number of counts per second calculated for different sized particles, at a flow rate of 15 L min^{-1} b) The theoretical response of the OPC measured biovolume to the OPC measured count rate for *Coscinodiscus* spp., calculated from the Poisson distribution and from the maximum count rate at a flow rate of 15 L min^{-1}.

Results

Effects of thoroughness of sieving

The different sieving regimes appear to give similar results (Figure 2.10), although three-way ANOVA shows that for both carbon and nitrogen, thorough and normal sieving are significantly different from each other and there is a significant interaction between sieving thoroughness and size fraction (Table 2.2). The two-way ANOVA shows that the smallest size fraction (200-500 μm) is most significantly effected by sieving thoroughness for nitrogen and carbon with an average of 13% less in the normal sieved than the thorough sieved. For the 500-1000 μm fraction, sieving thoroughness is only just significantly different at the 5% level, with normal sieving being again 13 % less. The largest size fraction is not significantly effected for carbon or nitrogen (Table 2.3), although an average of 16 % more in the normal sieved sample was found. The total carbon and nitrogen in each sample was on average approximately 10 % less for normal compared to thorough sieving (Table 2.4).

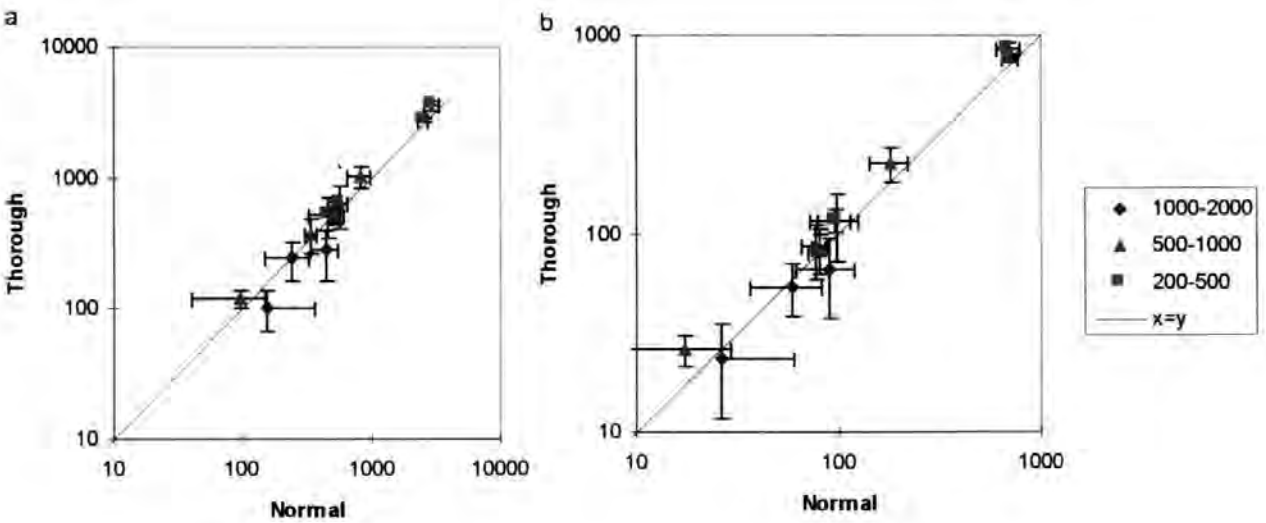

Figure 2.10: Comparison of thorough and normal sieving with standard error bars marked for a) carbon (mg) and b) nitrogen (mg).

a)

Source	Sum of squares	df	Mean square	F-ratio	Probability
Thoroughness of sieving	2.64E5	1	2.64E5	10.8	0.001
Sample	3.41E7	3	1.14E7	464.7	<0.001
size fraction	5.86E7	2	2.90E7	1197.9	<0.001
sieving thoroughness and size fraction	5.13E5	2	2.56E5	10.4	<0.001

b)

Source	Sum of squares	df	Mean square	F-ratio	Probability
Thoroughness of sieving	2.06E4	1	2.06E4	16.9	<0.001
Sample	2.35E6	3	7.85E5	643.6	<0.001
size fraction	3.97E6	2	1.98E6	1630.4	<0.001
sieving thoroughness and size fraction	3.18E4	2	1.59E4	13.0	<0.001

Table 2.2: Results of three-way ANOVA a) carbon, b) nitrogen (df – degrees of freedom)

a)

Source	Sum of squares	df	Mean square	F-ratio	Probability
Carbon sieving	6.99E5	1	6.99E5	14.1	<0.001
Carbon Sample	7.07E7	3	2.35E6	475.8	<0.001
Nitrogen sieving	4.85E4	1	4.85E4	19.2	<0.001
Nitrogen sample	5.00E6	3	1.66E5	659.2	<0.001

b)

Source	Sum of squares	df	Mean square	F-ratio	Probability
Carbon sieving	4.98E4	1	4.98E4	4.1	0.048
Carbon Sample	4.25E6	3	1.41E6	128.6	<0.001
Nitrogen sieving	3100	1	3100	4.9	0.031
Nitrogen sample	2.15E5	3	7.18E4	124.4	<0.001

c)

Source	Sum of squares	df	Mean square	F-ratio	Probability
Carbon sieving	2.8E4	1	2.8E4	2.4	0.21
Carbon Sample	9.95E5	3	3.31E5	27.9	<0.001
Nitrogen sieving	752	1	752	1.5	0.22
Nitrogen sample	2.39E4	3	7988	16.0	<0.001

Table 2.3: Results of two-way ANOVA for each size fraction a) 200-500, b)500-1000 c)1000-2000 (df – degrees of freedom)

Sample	Carbon			Nitrogen		
	Normal	Thorough	Difference	Normal	Thorough	Difference
1	706	742	36	141	166	25
2	1599	1700	101	259	281	22
3	3087	3331	247	840	901	60
4	4194	4863	668	962	1145	183
Mean	2396	2658	262 (9.9%)	551	623	72 (11.6%)

Table 2.4: Total Carbon and nitrogen for samples

Effects of preservation of carbon samples

The methods of preservation showed different effects for carbon and nitrogen. For carbon and nitrogen, the difference between samples was much more significant than the difference between preservation technique, although this was significant (Table 2.5, Figure 2.11). For carbon, both drying then freezing and freezing then drying resulted in a significantly lower carbon estimate than immediate processing, on average 11 and 12 % respectively (Table 2.6). Preservation did not significantly effect nitrogen (Table 2.5), with difference between immediate processing and freezing before or after drying being less than 6 %. In fact, freezing then drying, resulted on average with a higher nitrogen content, although this difference was just not significant at the 5% level.

a)

Source of Variation	SS	df	MS	F	Probability
Sample	1.22E+08	4	30497078	911.0	5.87E-53
Columns	964964.2	2	482482	14.4	7.73E-06
Interaction	954520.5	8	119315	3.6	0.001931
Within	2008534	60	33475		
Total	1.26E+08	74			

b)

Source of Variation	SS	df	MS	F	Probability
Sample	7293761	4	1823440	853.4	4.03E-52
Columns	21360	2	10680	5.0	0.00982
Interaction	99593	8	12449	5.8	1.68E-05
Within	128200	60	2136		
Total	7542915	74			

Table 2.5: Two-way ANOVA of preservation techniques a) Carbon b) Nitrogen (SS – sum of squares, df – degrees of freedom, MS – mean square, F – f ratio)

a)

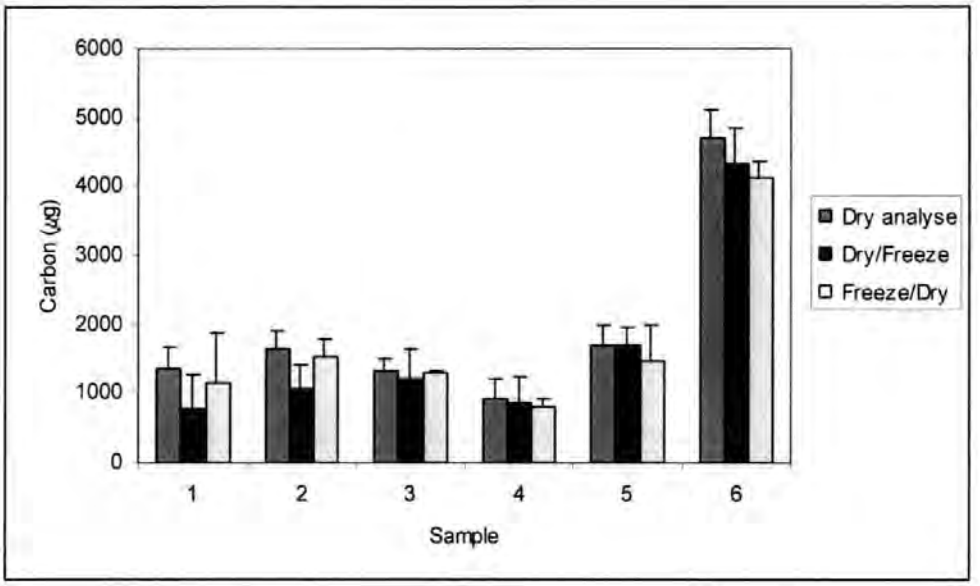

b)

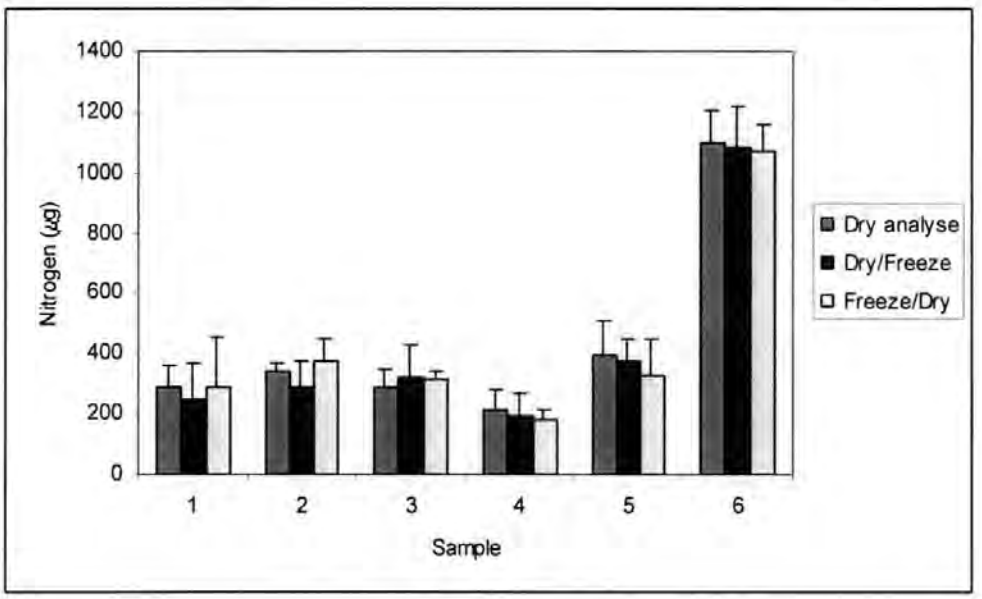

Figure 2.11: Comparison of preservation techniques for biomass a) carbon, b) nitrogen (error bars show 95% confidence limits)

	Carbon		Nitrogen	
	P	%	P	%
Dry/Analyze v Dry/freeze	<0.001	12.4	0.12	3.6
Dry/Analyze v Freeze/Dry	0.001	10.8	0.21	-5.2
Dry/freeze v Freeze/Dry	0.62		0.052	

Table 2.6: Paired T-test of the different preservation methods, with the mean percentage difference, compared to drying and immediate analysis.

Comparison of OPC counts with microscope counts for net samples

The net OPC and microscope counts showed similar patterns along the transects (Appendix 3), and the direct comparison, by regression, showed that counts were scattered around the 1:1 line, and were generally within a factor of two (Figure 2.12). AMT 4 net samples showed that OPC counts are lower than expected. The functional regression of Log_e transformed data showed a consistently significant correlation, although this was lower for AMT 4 (Table 2.7). The overall correlation for AMT 1-6 was reduced by including AMT 4 data, as demonstrated when this was removed.

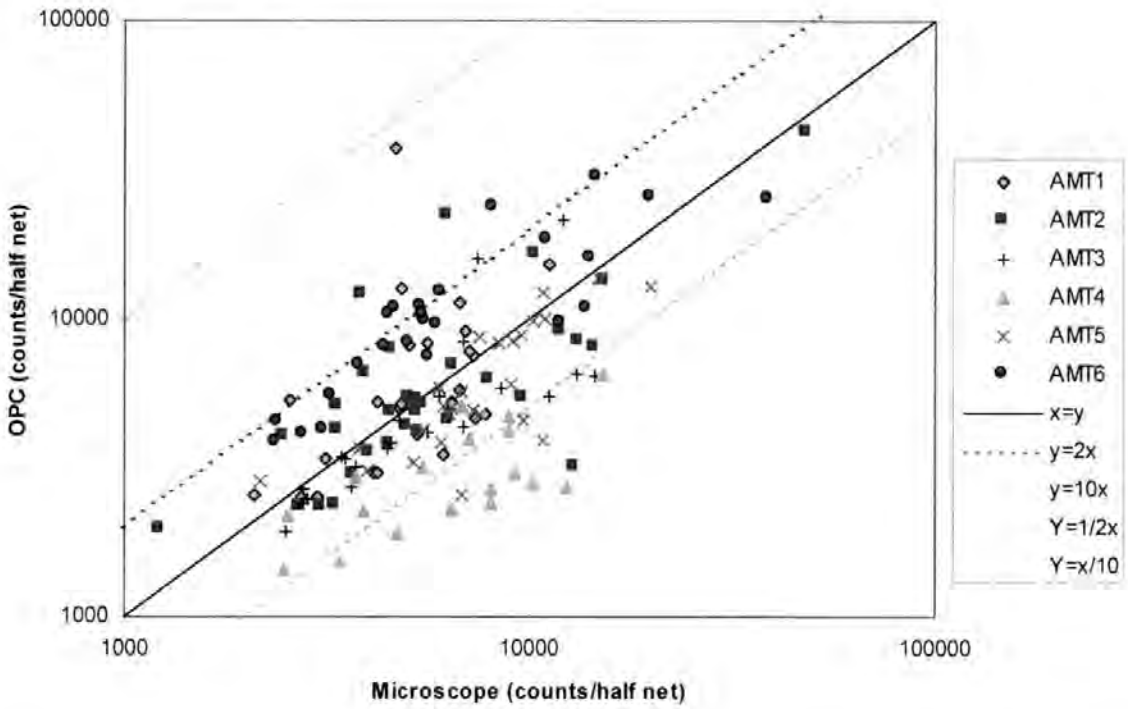

Figure 2.12: Comparison of half net counts by the OPC and by microscope counts for AMT 1-6

Cruise	R^2	F	P	Gradient	Intercept	95% confidence limits	
						+	-
AMT 1	0.44	18	<0.001	1.20	-1.67	1.24	1.13
AMT 2	0.51	32	<0.001	0.97	0.22	1.08	0.81
AMT 3	0.63	33	<0.001	1.15	-1.37	1.20	1.09
AMT 4	0.46	14	0.0018	0.76	1.58	0.92	0.53
AMT 5	0.66	44	<0.001	1.02	-0.25	1.09	0.92
AMT 6	0.74	65	<0.001	0.83	1.74	0.92	0.71
AMT 1-6	0.42	104	<0.001	1.13	-1.14	1.19	1.02
AMT 1-3,5-6	0.51	134	<0.001	1.06	-0.45	1.13	0.95

Table 2.7: Result of functional regression of Log_e transformed total OPC counts verses microscope counts. (F=f ratio, P=probability, 95% confidence limits are for the gradient.)

The size fractionated counts showed good agreement between OPC and microscope for all size fractions (Figure 2.13). The middle two size fractions, however, showed the strongest correlation with the regressions closest to the 1:1 line (Table 2.8). Overall a correlation of the $\log_e$ counts gives an R^2 value of 0.92 for the AMT 5 size fractions.

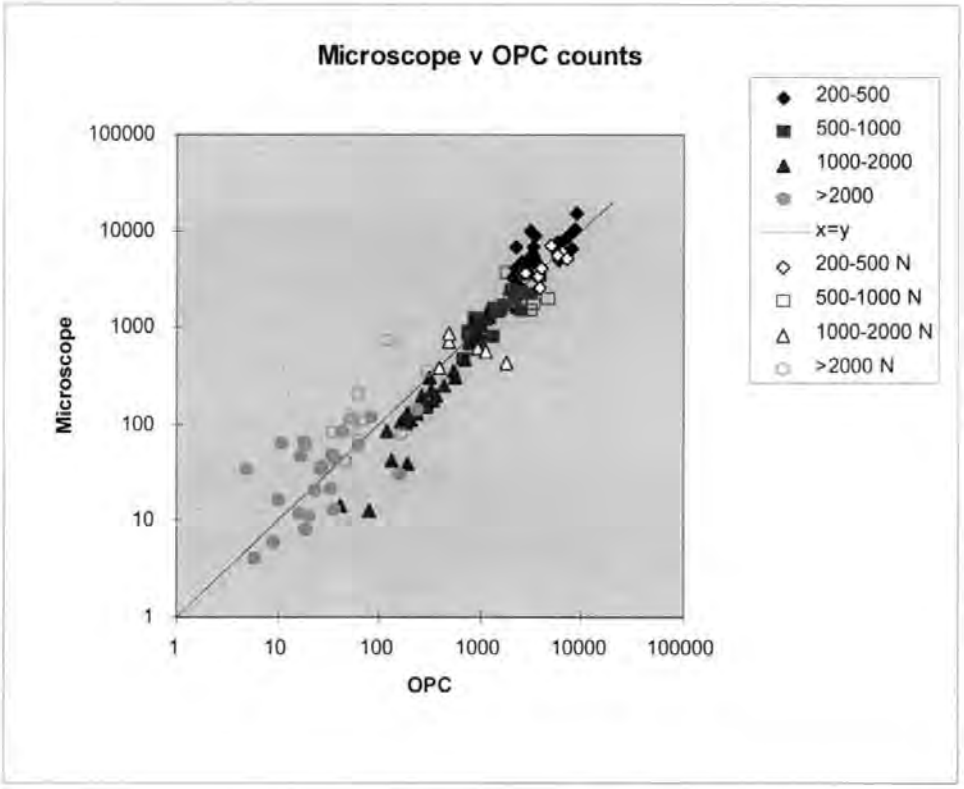

Figure 2.13: Comparison of size counts in each size fraction between OPC and microscope for AMT 5. Open symbols are from night nets.

Size fraction	R^2	F	P	Gradient	Intercept	95% confidence limits +	-
200-500	0.40	22	<0.001	0.75	138	1.02	0.21
500-1000	0.83	155	<0.001	0.98	50	1.08	0.83
1000-2000	0.89	265	<0.001	0.82	112	0.94	0.67
>2000	0.28	12	0.0012	0.51	13	0.77	0.14

Table 2.8: Results of functional regression of size fractionated counts for AMT 5. (Number of cases N = 35, F=f ratio, P=probability of occurring by chance, 95% confidence limits are for the gradient.)

Comparison of OPC counts with microscope counts underway samples

The microscope counts generally appeared on the line of the underway count concentrations (Appendix 4). The high variability of underway counts made it hard to

compare results. The regressions between underway OPC and microscope counts are all significant, except for AMT 3 where only five in line samples were taken (Figure 2.14; Table 2.9). Generally the OPC counts were higher than the corresponding microscope counts, and AMT 1 samples showed greater scatter than the other AMT samples. All the gradients of the Log_e transformed regressions were close to one, and overall the intercept was found to be 0.32. Thus the untransformed relationship between OPC and microscope is approximately linear with a ratio of 1:1.4 (microscope : OPC).

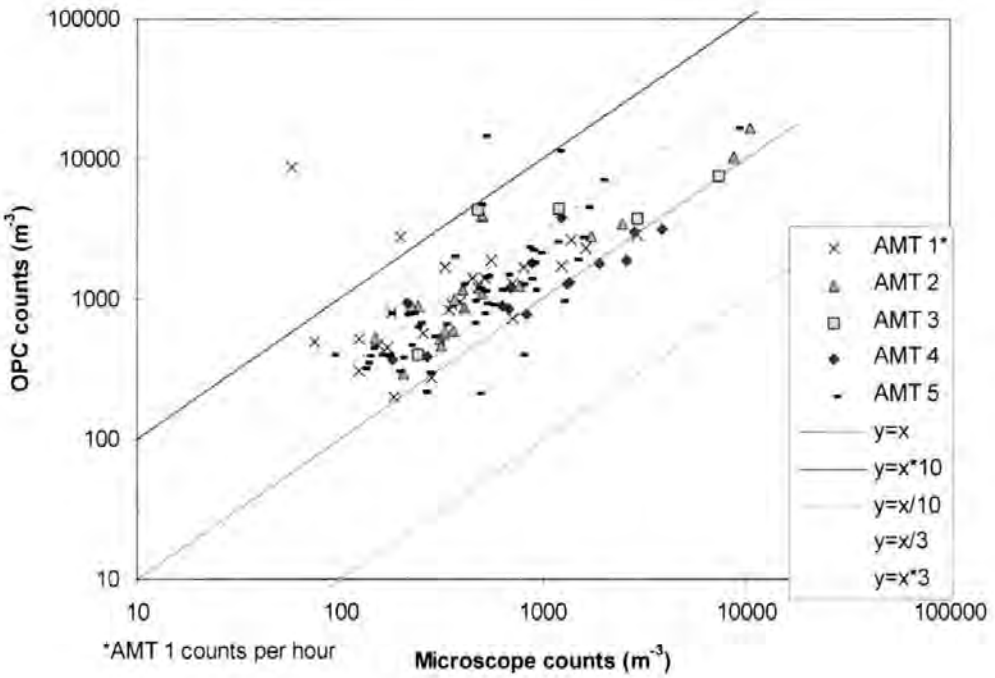

Figure 2.14: Comparison of underway counts by microscope and OPC (counts m^{-3})

Cruise	R^2	F	P	Gradient	Intercept	95% confidence limits +	-
AMT 1	0.531	26	<0.001	0.82	1.94	1.22	0.54
AMT 2	0.819	86	<0.001	0.87	1.57	1.11	0.67
AMT 3	0.572	4	0.138	0.84	2.00	2.31	0.24
AMT 4	0.497	13	0.003	0.84	1.46	1.54	0.43
AMT 5	0.587	73	<0.001	1.17	-0.19	1.54	0.90
AMT 6	0.506	63	<0.001	1.14	-1.31	1.51	0.87
AMT 1-6	0.408	124	<0.001	1.01	0.32	1.21	0.84

Table 2.9: Result of functional regression of Log_e transformed AMT total OPC counts verses microscope counts. (F=f ratio, P=probability of occurring by chance, 95% confidence limits are for the gradient.)

Comparison of OPC biovolume with carbon biomass

In general, the OPC biovolume followed the same pattern as the carbon estimates (Appendix 2). The largest discrepancies tended to be at high biomass. The regression analysis showed strong relationships between carbon and biovolume, although this was less good for AMT 1 (Figure 2.15; Table 2.10). For AMT 4, the ratio was noticeably lower than for the other AMTs. Overall, the transformed gradient was slightly less than 1 at 0.92, although not significantly (P > 5%). The conversion from carbon to biovolume is given by:

$$\text{Log}_e(\text{Biovolume})=0.919*\text{Log}_e(\text{Carbon})+3.25$$

Over the range of carbon values measured, the ratio of carbon : biovolume varies from 29.4 at 0.2 mg m^{-3} to 20.2 at 20 mg m^{-3}, and is 25.8 at 1 mg m^{-3}.

Cruise	R^2	F	P	Gradient	Intercept
AMT1	0.383	13	0.002	1.266	3.89
AMT2	0.685	48	<0.001	0.979	3.13
AMT3	0.852	139	<0.001	1.187	3.03
AMT4	0.579	38	<0.001	0.994	2.14
AMT5	0.703	82	<0.001	0.880	3.79
AMT6	0.765	104	<0.001	0.941	3.35
Overall	0.491	162	<0.001	0.919	3.25

Table 2.10: Results of functional regression of Log_e transformed size total carbon and biovolume for AMT 1-6, except >2000 which is 1-4 and 6 as AMT5 where no carbons were taken in this size fraction. (F=f ratio, P=probability of occurring by chance.)

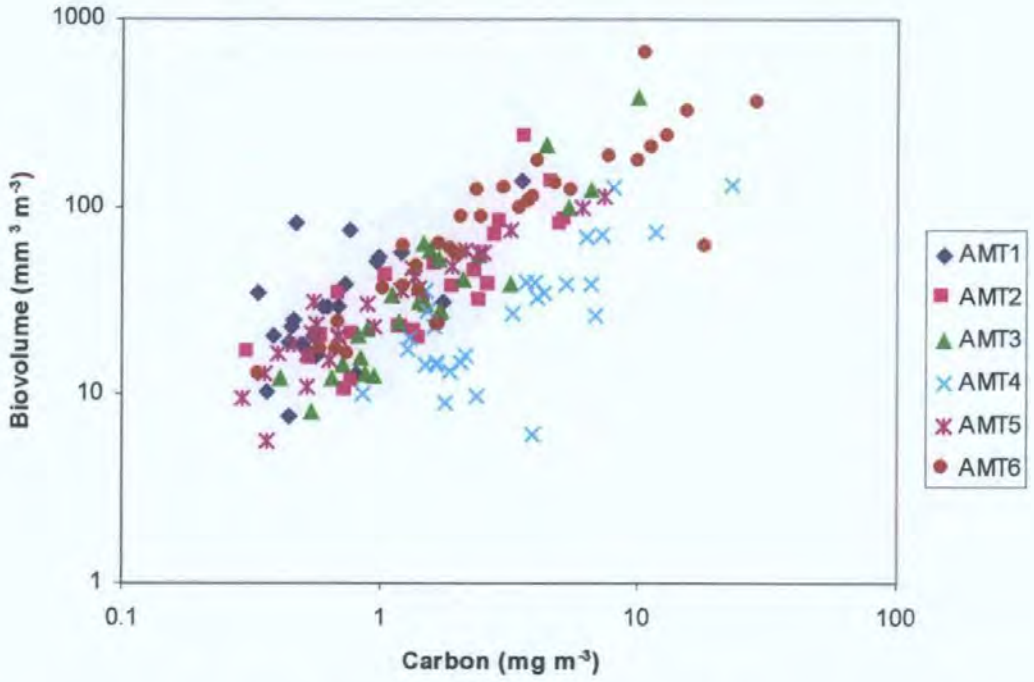

Figure 2.15: Comparison of AMT 1-6 total OPC biovolume and carbon biomass from 200 m net samples.

The comparison of size fractionated carbon to biovolume (Figure 2.16), showed a similar relationship. For the 200-500 μm size fraction the relationship was weakest (R^2=0.223), mainly due to the AMT 4 samples. AMT 4 biovolumes appeared lower than for other AMT samples in the other size fractions as well. The transformed gradients were all close to one, varying from 0.77 to 1.05, and the overall gradient was 1.03 (Table 2.11). The intercept varied from 2.09 for 200-500 μm size fraction to 3.52 for the 1000-2000 μm size fraction, and overall was 3.03. For all size fractions, biovolume is given by:

$$\text{Log}_e(\text{Biovolume}) = 1.026 * \text{Log}_e(\text{Carbon}) + 3.03$$

Over the range of carbon values measured, the ratio of carbon : biovolume varies from 19.8 at 0.2 mg m^{-3} to 22.4 at 20 mg m^{-3}, and is 20.7 at 1 mg m^{-3}.

Comparison of OPC size fractions and sieved size fractions

The biovolume distribution shifted to larger sizes with larger size fractions, but the size fractions showed considerable overlap in the OPC distribution (Table 2.12; Figure 2.17). In addition, the mean ESD increased with increasing size fractions for all but the largest size fraction from 573 to 843 μm (Figure 2.18). The biovolume was very low in the >2000 μm size fraction.

	size fraction	N	< 250	< 384	< 500	< 707	< 1000	< 1414	< 2000	< 2828	< 4000	>4000
mean	200-500	14	1.1	8.2	11.5	27.8	38.3	12.6	0.6	0.1	0.2	0.0
	500-1000	16	0.1	0.9	1.9	8.1	24.7	23.4	7.1	0.7	0.0	0.0
	1000-2000	16	0.1	0.4	0.7	1.9	4.6	9.1	8.8	1.8	0.2	0.0
	>2000	2	0.1	0.9	1.7	4.1	5.7	6.8	3.8	0.0	0.0	0.0
	Total	17	1.1	8.0	11.6	31.6	58.2	41.8	16.2	2.5	0.5	0.0
SD	200-500	14	2.8	14.1	8.9	20.3	30.0	11.5	0.7	0.3	0.7	0.0
	500-1000	16	0.0	0.4	0.6	3.0	17.7	18.3	5.8	1.7	0.0	0.0
	1000-2000	16	0.0	0.2	0.5	1.3	2.6	5.5	7.9	1.9	0.8	0.0
	>2000	2	0.0	0.1	0.5	0.9	2.0	3.8	2.7	0.0	0.0	0.0
	Total	17	2.9	14.6	11.6	29.8	47.0	25.5	11.1	2.1	1.1	0.0

Table 2.12: OPC size distribution of sieved size fractions (μm) OPC size classes are between one size class and the next. N = number of samples.

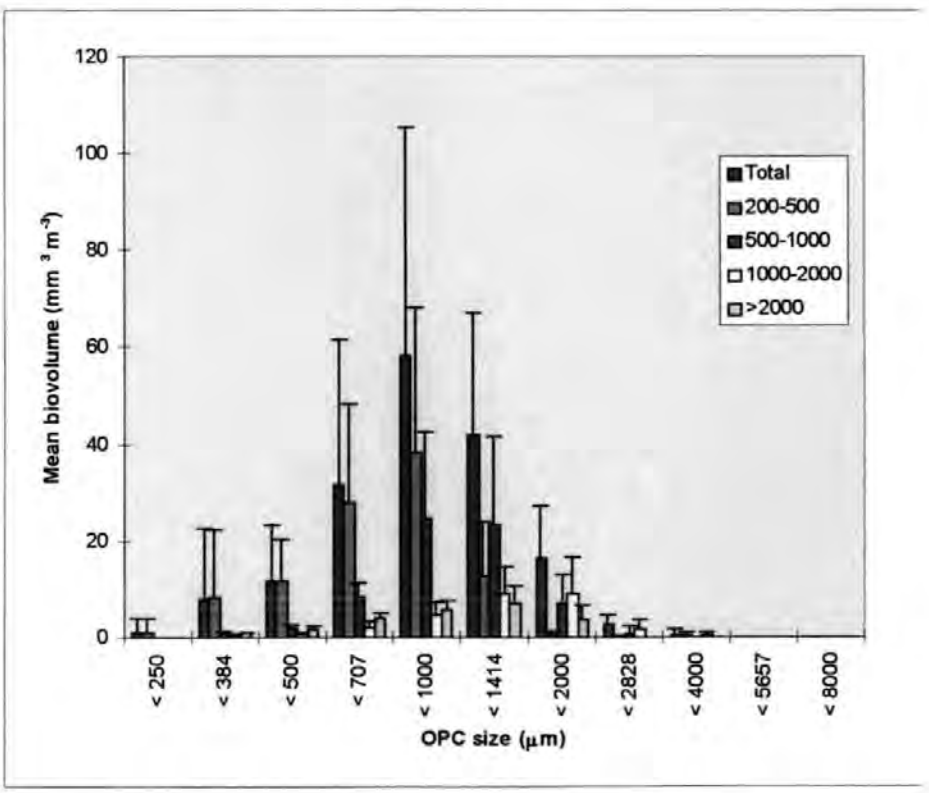

Figure 2.17: A comparison of sieve sizing and OPC sizing

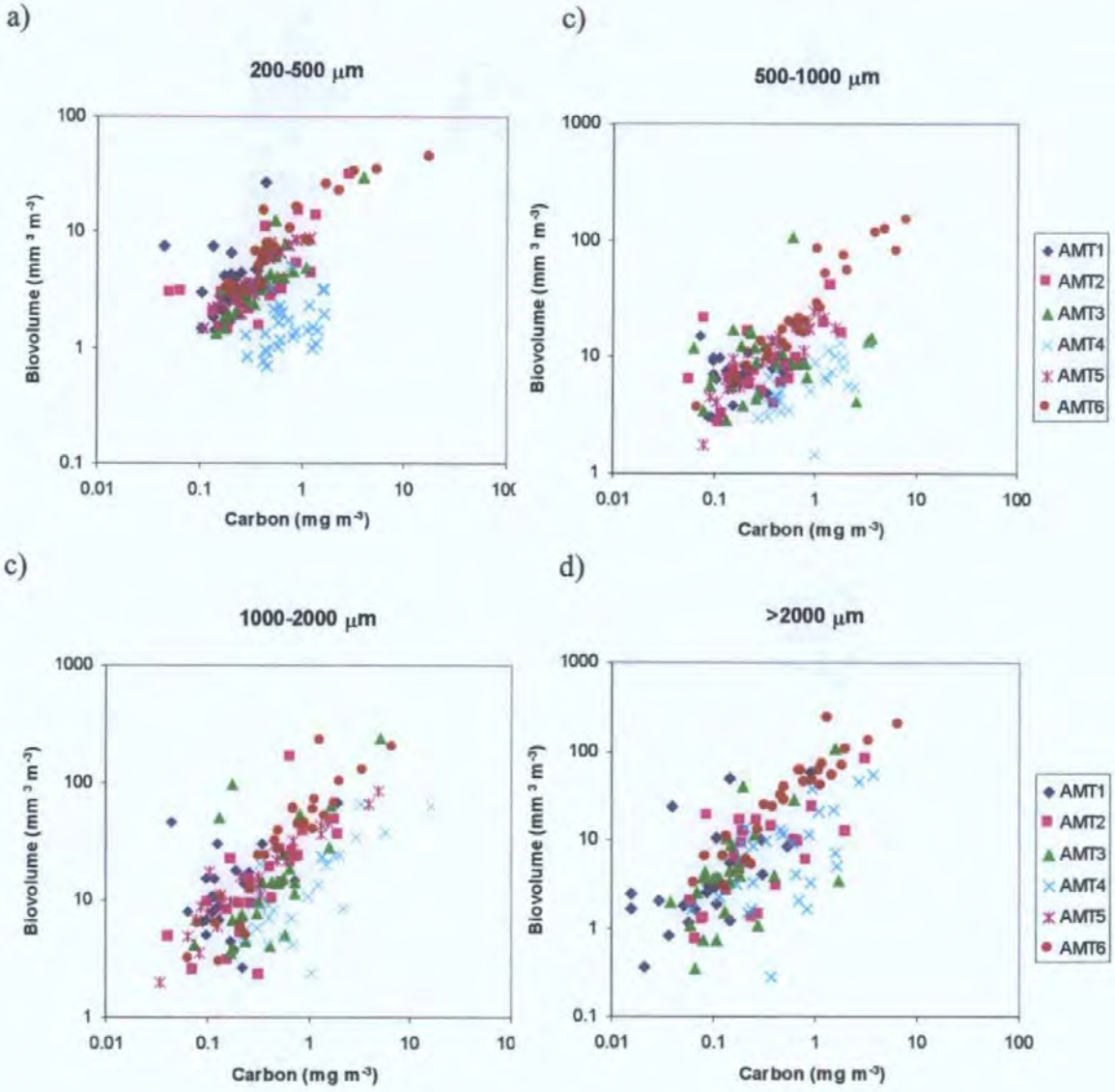

Figure 2.16: Comparison of AMT 1-6 OPC biovolume and carbon biomass from 200 m net samples for the four JGOFs size fractions. a) 200-500 µm, b) 500-1000 µm, c) 1000-2000 µm, d) >2000 µm.

Size fraction	R^2	F	P	Gradient	Intercept	95% confidence limits +	-
200-500	0.223	43	<0.001	0.931	2.09	1.23	0.70
500-1000	0.302	66	<0.001	0.767	2.92	0.94	0.62
1000-2000	0.451	125	<0.001	0.889	3.52	1.06	0.75
>2000	0.440	93	<0.001	1.045	3.21	1.30	0.84
All fractions	0.285	231	<0.001	1.026	3.03	1.39	0.76

Table 2.11: Results of functional regression of Log_e transformed size fractionated carbon and biovolume for AMT 1-6, except >2000 which is 1-4 and 6 as AMT5 where no carbons were taken in this size fraction. F=f ratio, P=probability of occurring by chance, 95% confidence limits are for the gradient.

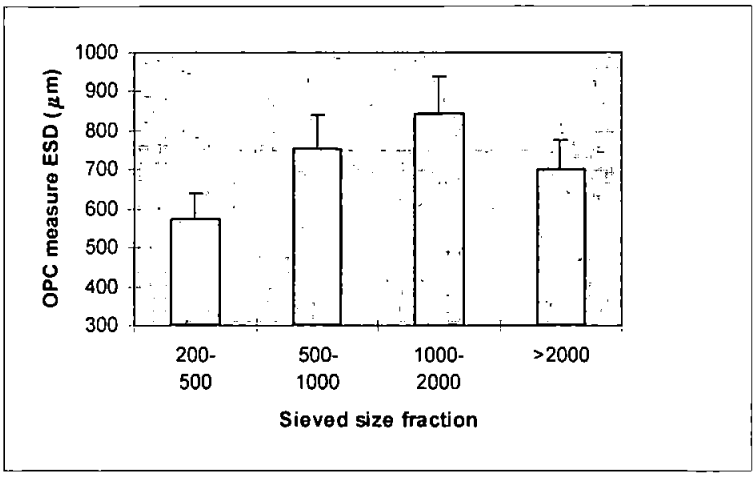

Figure 2.18: The OPC calculated mean ESD of sieved size fractions (error bars show standard deviations).

Comparison of OPC and sieve sizing compared to microscope sizing

Copepods minimum size to pass through a mesh appeared to be determined by their width (Figure 2.19 c), although they may not pass through a larger mesh. The size fraction which most of the copepods occurred in did not correspond to the equivalent spherical diameter (ESD), total length or cephalosome length (Figure 2.19).

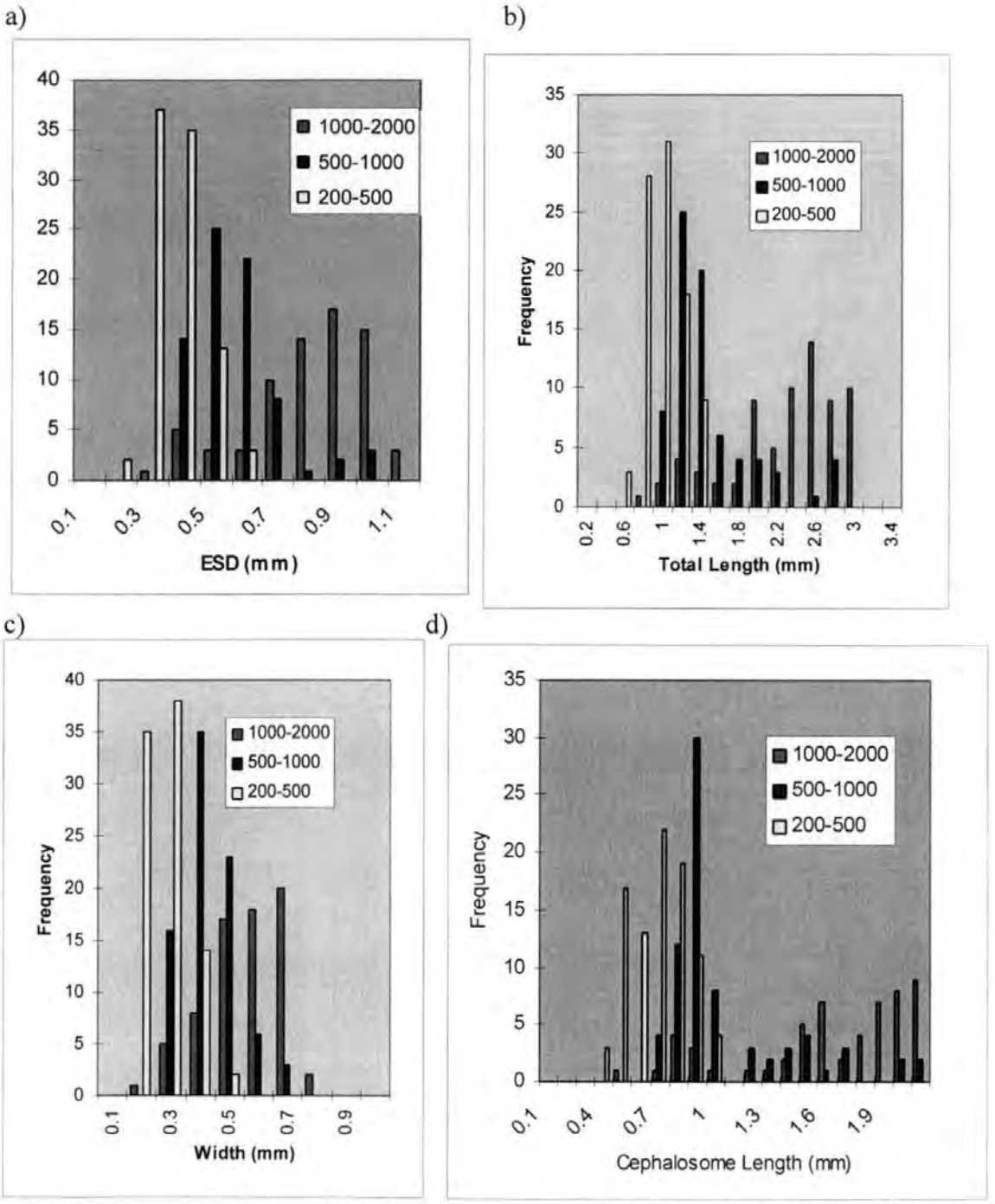

Figure 2.19 Comparison of the size distribution of copepods from three sieve size classes a) mean equivalent spherical diameter (ESD), b) total length, c) width d) cephalosome length

Comparing the size of zooplankters as measured under the microscope to those measured by the OPC, shows that there is generally a strong agreement between the two (Figure 2.20), with most falling within a factor of two. The Euphausiids were measured by the OPC to be much smaller than under the microscope, and the smallest cirripedi larvae much larger.

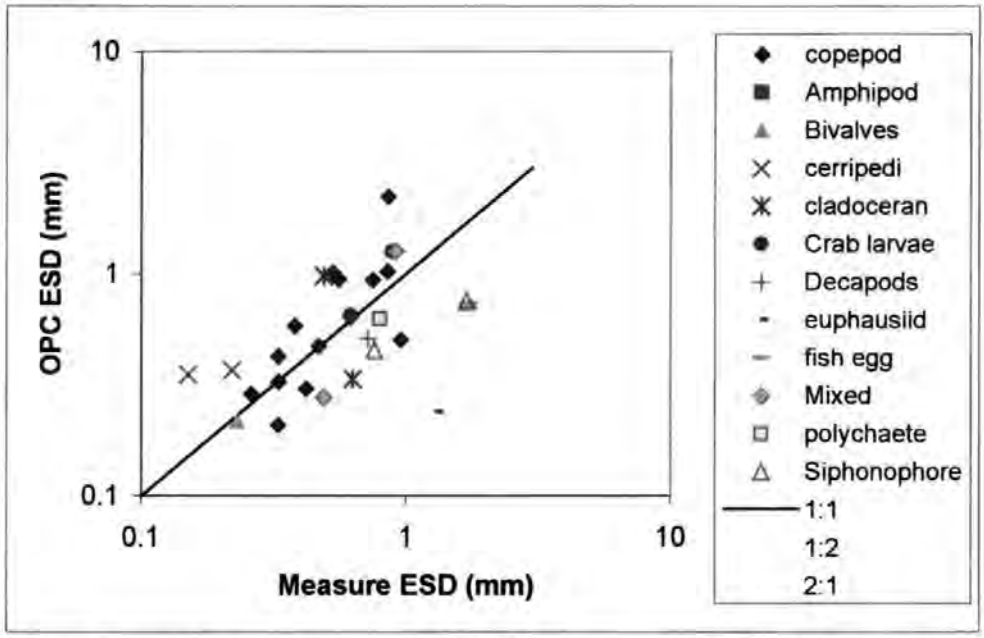

Figure 2.20: Comparison of measured and OPC mean ESD for different zooplankton groups.

Coincidence for the OPC

The mean biovolume increased with OPC counts, following the theoretical line predicted from the Poisson distribution up to about 60 OPC s^{-1} (Figure 2.21). No OPC counts were obtained greater than the theoretical maximum rate, with 80 s^{-1} being the most recorded, even though very high concentrations of *Coscinodiscus* were added. This is reflected by the high biovolumes of particles between 60 - 80 s^{-1}.

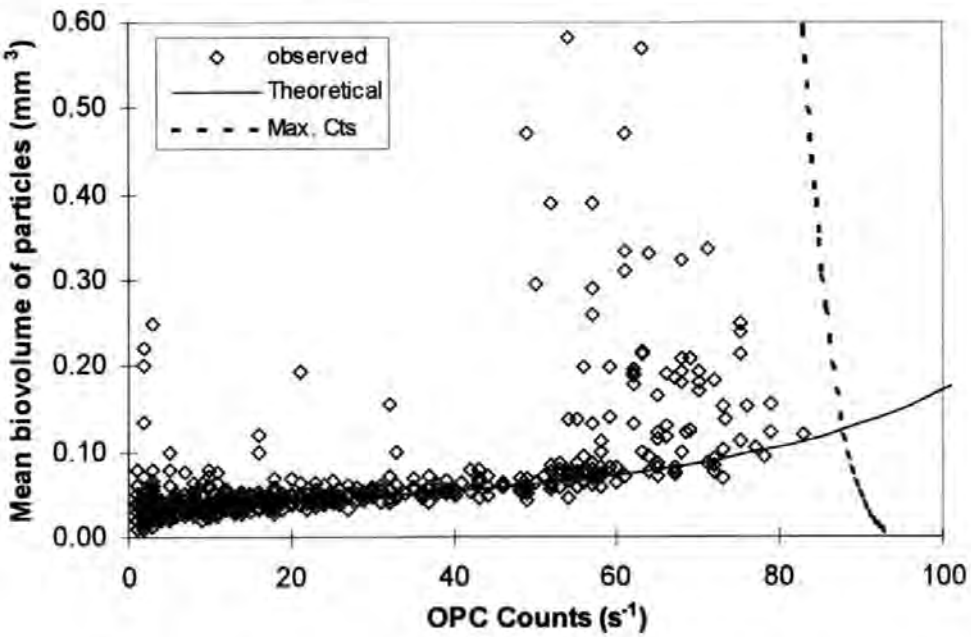

Figure 2.21: The effect of count rate on particle volume for *Coscinodiscus wailesii* at a flow rate of 15 L min^{-1}, observed compared to predicted.

Discussion

Effects of thoroughness of sieving

The thoroughness of sieving makes a significant difference to the apparent distribution of carbon and nitrogen in each size fraction. Although it is significant and appears substantial at 13% for 200-500 and 500-1000 size fractions, this difference is small when the standard deviation is frequently around 20 %, and changes in carbon and nitrogen of magnitude order are observed. The reduction in total carbon and nitrogen of around 10 % was unexpected. It might be that more remains in the greater than 2000 μm size fraction, although this is generally small, especially during the day, in the top 200 m of the open ocean. Differences due to different peoples sieving techniques would be expected to be less than 15 %.

Effects of preservation of carbon samples

Estimates of carbon were significantly affected by preservation by either freezing wet or dry, typically being around 10 % less than unpreserved samples. There was no difference between drying the samples first and then storing frozen, or by freezing the wet samples, and drying immediately before analysis. Although the effect of preservation is significant it is not substantial; it is within the expected error of the estimates. The estimates will, however, be biased, and this should be taken into consideration. Nitrogen was not significantly affected by preservation. Degradation of the samples appears to be due to decompositional losses, as the nutrient content (i.e. nitrogen) is maintained. These losses are likely to occur during the transition, i.e. during the drying, initial freezing and thawing periods. Thus these stages should be minimised and carried out as efficiently as possible. Fudge (1968) found negligible changes in chemical composition with either deep freezing or drying. Storing dry samples may make them more resistant to problems of short periods of thawing during transit for instance.

Comparison of OPC counts with microscope counts

Comparison of counts by two methods can be problematic where there is an arbitrary size cut-off at the lower part of the size range. Sizing by mesh (in effect with the microscope counts, as they were collected using a 200 μm mesh) and sizing by area (as in the OPC) will not necessarily size the same, or even consistently for different organisms. The shape and orientation of the organism will determine how large it appears to the OPC (Herman 1988) and whether it will pass through a particular mesh. This problem is exacerbated by small organisms tending to be the most numerically abundant (Sheldon *et al.* 1972). In spite of these problems, using an OPC cut off at 250 μm and a 200 μm mesh, OPC and microscope counts generally agreed well for net samples. However, low OPC counts were found for AMT 4 samples, probably due to the sample being processed too quickly, causing coincidence. The size fractionated counts from AMT 5 demonstrated good agreement between the two methods. The large scatter of the >2000 mm size fraction, is probably due to the low numbers, with different numbers being in each half of the sample. The 1000-2000 size fraction tended to fall below the 1:1 line, with OPC counts on average being higher than microscope counts. Small changes in the cut-off of size fractions, due to differences in sizing by the two methods, could also influence the agreement.

The transformed underway counts showed an overall 1:1 gradient, indicating a linear relationship between counts, and an untransformed relationship of 1.4, suggesting that OPC counts are marginally higher than actual. In coastal regions, filamentous algae and other large phytoplankton cell could be counted by the OPC. Flocculated detritus and other debris may also occur at high concentration, and may significantly increase OPC count rates. In the open ocean phytoplankton tend to be small and detritus is rare, so this is unlikely. It is more likely that different cut-offs or incomplete recovery of the sample for microscope analysis effects counts. The higher variability in AMT 1 underway samples

demonstrates that comparisons with samples displaced by quite a short time are less accurate. This suggests that the surface underway zooplankton abundance is highly variable over short scales, as observed in the OPC underway data (Appendix 4).

Comparison of OPC biovolume with carbon biomass

Using biovolume instead of counts reduces the problem of cut off at the lower end off the size spectrum. This is because, although numerically dominant, the small size classes usually make a less significant contribution to the total biovolume. However, estimates of biovolume to carbon in the literature vary considerably for zooplankton samples. Frequently several conversions are required, e.g. assuming biovolume to wet weight ratio of 1 (Chojnack 1983; 1.025:1), wet weight (or displacement volume):dry weight estimates vary from 6.95:1 (Sreepada *et al.* 1992) to 26.5:1 (Bé and Forns 1971) with an average around 1:0.13 (Lovegrove 1966). Krishnakumari and Nair (1988) found dry weight to carbon varying from 1:0.183 to 1:0.3249, with an average of 1:0.278. A more accepted value is 1:0.4 (Williams and Robins 1982; Omori and Ikeda 1986; Båmstedt 1986). Overall the expected conversion of wet weight to carbon would be around 1:0.05 A few measurements of wet weight to carbon exist in the literature; Dalal and Parulekar (1986) estimated 1:0.027, whilst Vinogradov and Shushkina (1987) estimated ratios of 1:0.04-0.05. In the present study, the Log_e regression, which as well as normalising the distribution of the results, down weights large values. The resultant ratio (biovolume : carbon) for total carbon ranged between 29.4:1 (1:0.034) for low biomass (0.2 mg C m^{-3}) to 20.2 (1:0.049) for high biomass (20 mg C m^{-3}) with a ratio of 23.6:1 (1:0.042) about the mean, and for all size fractions varies between 19.8:1 (0.05) and 22.4:1 (0.045) over the same range, with a mean of 20.7:1 (1:0.048). These are comparable to the literature values above, and similar to Wiebe *et al.* (1975) and Wiebe (1988) also using functional regression equations. It was also found that the gradient was less than 1 for both conversions of carbon to wet weight and to displacement volume, as with this study. For

wet weight to carbon, ratios varied from 27:1 (1:0.037) to 53.6:1 (1:0.019), and for displacement volumes to carbon, ratios varied from 20.3:1 (1:0.049) to 46.7:1 (1:0.021), between 0.2 and 20 mg C m^{-3}. Thus, it seems that for larger zooplankton samples, the concentration of carbon is lower. With the OPC measurements, coincidence causing an underestimation of biovolume is more likely to be a greater problem for larger samples, although the concentration was controlled. It does not explain why displacement volumes and wet weights should follow a similar pattern.

The individual size fractions show greater variation in the slope and the intercept. The 200-500 μm size fraction shows the weakest relationship ($R^2 = 0.223$). This size fraction, being the most numerically dominant will be most likely to suffer from coincidence. Coincidence will reduce the number of particles counted, and increase the estimated size of the particles (Sprules *et al.* 1998), and thus may be counted in a larger size fraction. The larger size fractions did not show a reduced gradient as might be expected if larger organisms on average had a lower concentration of carbon.

Sizing by different methods

The sieved sizes do show an increase in the abundance of the larger OPC size classes with increase in sieved size fraction. The mean ESD also increases. However, these changes are not as large as might be expected. The mean ESD of the 1000-2000 μm size fraction is only 840 μm, and the >2000 is actually lower. The >2000 size fraction had a very low biovolume, so it could be that the mean ESD is reduced by a small percentage of the more numerically dominant smaller organisms contaminating the size fraction. Alternatively, the >2000 size fraction may have gelatinous organisms such as siphonophores which are at least partially transparent to the OPC, and tend to have their size underestimated.

Sizing by sieves showed that the lower limit of mesh that the copepods could pass through appeared to be defined by their width, although the majority fell into larger size fractions. Vannucci (1968) found that often organisms passed through mesh of less than their diameter. What determines where the majority occurred was unclear. It did not appear to be total length, cephlasome length or mean ESD. Seda and Dostolkova (1996) suggested that it was 3/4 the length for cladocerans. Nichols and Thompson (1991), similarly, suggested that, for towed nets, mesh size of 75% of the copepod carapace width would catch 95% of the individuals of that size present in seawater. It is likely that the complex irregular shapes make the determination of whether a particular zooplankter could pass through the mesh difficult to predict. Chaetognaths tended to become caught in the mesh with half passing through one hole and half through another. Copepods with long antennules may catch in the mesh or may deform allowing the copepod to pass through it depending on the initial orientation of the individual.

Comparison of the measured and OPC sized copepods generally agreed (R^2=0.76), although the ESD had a larger variance for OPC measured copepods and frequently a peak in the distribution at around 200 μm. The peak is probably due to bubbles and small organisms. Several other investigators have found similar patterns (e.g. Herman 1992; Sprules *et al.* 1998). Grant *et al.* (2000) found that the OPC estimated the size of Antarctic copepods accurately. Estimates for other organisms were generally good, also falling within a factor of 2. The euphuasiid estimate was much lower, however, and this could be due to inaccurate estimation of the measured biovolume or the euphausiid being broken up by the pump. Large organisms such as euphausiids were commonly seen in pieces after processing through the OPC. Siphonophore size tended to be underestimated by the OPC. This could have been be caused by their transparency.

Test of Coincidence for the OPC

The results from the test of the Poisson distribution using *Coscinodiscus* spp. show that coincidence, and thus actual count rates can be predicted up to 50-60 s^{-1}. However, between 60 and 80 OPC s^{-1} (estimated from the Poisson distribution to be actual counts of 80 to 120), another factor comes into play. The high biovolumes of particles found between 60 and 80 s^{-1} suggest that actual counts can be very high in this range. The maximum count rate was calculated to be 90 s^{-1} for *Coscinodiscus* at these flow rates, although this will be reduced for larger sized particles. Thus the reset time and time to pass through the beam appear to become limiting. Sprules *et al.* (1992) suggested a maximum of 200 s^{-1} can be counted by the OPC. This may be the theoretical limit, but in practice the limit appears to be much lower at about 80 s^{-1} for this setup.

Given that the rate of coincidence can be approximated to the Poisson distribution, coincidence will be significant even at relatively low count rates. At 30 particles per sec, the OPC will count on average 27.3 particles per sec (9 % reduction), and at 10 particles per sec, 9.7 particles per sec (3 % reduction) will be counted. However, as the mean ESD of particles increases, coincidence increases, so that for a theoretical sample of 5 mm particle at 30 particles per sec only 25 (16.7% reduction) will be counted. To process net samples efficiently without loss of accuracy, samples with small ESD (<500 μm) should be processed to keep the count rate below 25 s^{-1}, by controlling the concentration of the sample. However, if using the OPC for processing net samples taken with 500 μm mesh or where the zooplankton community is dominated by larger organisms, lower count rates must be maintained. For the towed OPC-1T, which has a larger beam volume, coincidence would be expected to be greater at lower concentrations. For underway sampling, count rate is largely determined by the concentration of zooplankton. Altering the flow rate will not reduce the coincidence substantially (Figure 2.8b). Coincidence can be reduced by reducing beam volume e.g. by reducing the aperture (Sprules *et al.* 1998).

Conclusions

The methods selected and evaluated have different strengths and weakness (summarised in Table 2.12). At present, microscope analysis is the only method available to get detailed taxonomic information for analysis of community structure. In the near future, automated video systems may be able to at least give basic taxonomic groups (e.g. Gallienne 1997). For measures of zooplankton biomass or rough sizing of taxonomic groups, sieving is a useful tool, giving insight into the size structure. It is quick and simple, although differences in sieving techniques could lead to small differences in estimates, and the sizing of the zooplankton is complex. The OPC gives a more accurate and detailed measure of size structure, although the sizing of gelatinous organisms will tend to be underestimated.

The OPC, although probably not as accurate as carbon estimates, can give a good, rapid (real time) assessment of biomass. It is particularly suited to open ocean situations where concentrations of zooplankton are relatively low, phytoplankton are small, and debris is rare. In coastal waters contamination by non-zooplankton particles may be counted leading to high counts or high zooplankton concentrations may be encountered causing coincidence. The OPC-1L may be used for processing net samples and for underway measurements from pumped systems, with assessment of performance. Pumped systems do have inherent problems such as avoidance by large zooplankters (Omori and Ikeda 1984), but net sampling has similar problems associated with it. The pumped system may also allow mixing before reaching the sensor so that the resolution at the smallest scales may be lost. The towed version (OPC-1T) can be mounted on towed vehicles such as 'batfish' and undulating oceanographic recorder (UOR), allowing surveys of the water column, but it is harder to assess the reliability and precision of the data. Underway systems allow analysis

of zooplankton over all scales. The OPC software may be modified to give time stamps to the data, as opposed to time bins, for very small-scale analysis (e.g. Currie *et al.* 1998). Carbon analysis may be more accurate per se, but cannot be used to give the same resolution required to reliably estimate a highly spatially heterogeneous medium as the ocean. Using carbon analysis to calibrate the OPC optimises accuracy and spatial resolution to enable rapid assessment of zooplankton biomass for extensive surveys, over a wide a range of scales, such as with the AMT programme.

Method	Advantages	Disadvantages
Microscope analysis	Gain detailed taxonomic information useful for ecology Sample not damaged so can be used in future analyses	Time consuming Samples collected by nets (low spatial resolution) Assumptions about conversion equations to biomass
Carbon analysis	Accurate Automated system is less time consuming than microscope analysis	Rely on samples Expensive to analyse samples Samples need to be stored before analysis, which can reduce accuracy, and cannot be carried out at sea Cannot distinguish plant from animal material Destructive sampling Accuracy lost if carried out on formalin preserved samples
OPC	Accurate for open ocean Quick – real time on towed vehicles Can be used for net or underway sampling and vertical profiling, so can give information on any scale Can be used for estimating biomass for preserved samples Can give size structure which may have important ecological implications	Requires conversion to carbon Cannot distinguish plant or inorganic particles from animal material May loose accuracy at high concentrations, although the system can be adapted to cope with this

Table 2.13: Summary of the advantages and disadvantages of different methods.

Chapter 3: Spectral Analysis

Introduction

Spectral analysis can be used to understand spatial and temporal variability of zooplankton in two ways: to identify frequencies/spatial scales characteristic of zooplankton patches (i.e. by looking at 'spikes' in the spectrum), and for more general analysis of variability across scales by examining the gradient or 'role off' of the power spectrum. In addition, comparisons may be made with other variables such as temperature and chlorophyll, and with theoretical models, e.g. comparisons with random distribution or models of turbulence. These comparisons may be made between the spectra, or for real data taken at the same time, coherence maybe considered.

Spectral analysis is based on the Fourier transform, which describes a continuous data stream in terms of its component sine and cosine waves. The concept was first conceived by Bernoulli in the eighteenth century, but later developed by Fourier in 1822. With the advent of computers, Fast Fourier Transform (FFT) became established in the 1960s (e.g. Cooley and Tukey 1965). In the 1970s, spectral analysis started to be used to analyse spatial variability of physical and biological variables in marine ecosystems. Initially, chlorophyll and temperature spectra were produced (e.g. Denman 1976), and then zooplankton spectra as well (e.g. Mackas and Boyd 1979). Different scales have been studied from metres (e.g. Currie *et al* .1998) to thousands of kilometres (e.g. Piontkovski and Williams 1995). Generally, zooplankton have been found to be more patchy than phytoplankton, and phytoplankton more patchy than temperature, and a variety of gradients of the role off have been found. Temperature is considered to be a passive trace with the patchiness determined by turbulence. Chlorophyll is similar but modelled by including a growth term (e.g. Denman and Platt 1976, Denman *et al.* 1977).

In this study, transects of over 1000 km are used to analyse plankton patchiness over a range of scales from a few kilometres to 1000 km, to look at patterns in the patchiness and the relationship between the variation in different parameters over these scales.

Data Analysis

Spectral Analysis

Underway OPC data, chlorophyll, temperature and salinity were converted into ten minute bins (approx. spatial scale 3 km). OPC data were also converted to 2 minute bins (0.6 km). Part bins from ends of files were removed if they were less than half the standard bin length, to avoid erroneous estimations.

The power spectrum was estimated using the power spectral density (PSD) function in MATLAB, which is based upon FFT (below).

$$X_k = \sum_{m=-N/2+1}^{N/2} x_m e^{-i2\pi km/N}$$

where: N= length of series, X_k=Fourier coefficient, i=imaginary component, x_j=series

The frequency resolution is 1/T, where T is the total length of the series, and the highest frequency is the Nyquist frequency (Ny)

$$Ny = \frac{1}{2\Delta t}$$

where Δt is the sampling frequency

The power spectrum shows how much variation occurs at a particular frequency, i.e. spatial/temporal scale, so that one might expect a peak in zooplankton heterogeneity with a period of approximately 24 hours caused by diel migration in to the surface layer. In addition to identifying peaks of specific frequencies or patch sizes, the slope of the power

spectrum will indicate the general heterogeneity over a range of scales. PSD uses the Welch method to estimate the power spectrum; this involves dividing the series into lengths and calculating the FFT for each section. The sections may be overlapped. If overlapping is used, a window such as Hanning (suitable for 50% overlap) is required to down weight the overlapped section and prevent 'ringing'. The spectrum is averaged from these different spectra resulting in a smoother spectrum with smaller confidence intervals. The confidence intervals have an approximate chi squared distribution, and the number of degrees of freedom is given by twice the number of estimates averaged, assuming that the estimates are independent. Thus for overlapping sections, the estimates are unreliable.

The PSD was calculated for the corrected ten minute bin series for zooplankton and other data, using AMT 1-5 transects from 38°S-50°N. The southern end of the transect was excluded to avoid possible violations of the assumptions of stationarity (large shifts in the mean and standard deviation). Each series was standardised to zero mean and unit standard deviation, and the PSD calculated for an FFT of length 1024 (approx. 3400 km, 170 hours) with no overlap and boxcar window (equivalent to no window). The transect spectra from the five AMTs were averaged to reduce the variability (and the confidence limits). Log_{10} variance (PSD) was compared to log_{10} frequency. Peaks in the mean spectra were identified, and the equivalent wavelengths calculated assuming a ship speed of 20 km hr^{-1}. Linear regressions were calculated for the series mean spectra.

For AMT 5 38°S-50°N, the 2 min bins were calculated for OPC data for each day (after mid-morning station to the start of the following morning station). The PSD was calculated for each day and the mean of the resultant spectra taken.

The region south of Montevideo was analysed separately is a similar way to the 38°S-50°N region for 10 minute bins, but an FFT length of 256 was chosen due to the shorter series lengths.

Cross-spectral analysis

Cross-spectral analysis is the frequency domain equivalent to cross-correlation, so that it will show how two spectra vary in relation to one another. It has two components: the strength of the 'correlation' or the coherence, and the 'lag' or phase. Coherence estimates the agreement between spectra showing whether the same frequencies are important to each spectra. Coherence behaves in a similar way to the correlation coefficient, tending toward 1 when the power spectra are identical and zero when they are unrelated. The coherence of series x and y is:

$$\rho_{yx}^2(f_i) = \frac{|p_{yx}(f_i)|^2}{p_x(f_i)p_y(f_i)}$$

where p_x is the power (variance) at frequency f_i for series x.

The phase is calculated from the angle between the real and imaginary parts of the cross-spectral density, and is between $-\pi$ and $+\pi$ radians, (i.e. +-half a cycle). At these values the waves are out of phase, and at zero they are in phase. The confidence limits of the phase are largely determined by the coherence (Jenkins and Watts 1968). The smoothed phase estimate is given by:

$$\mathrm{var}(\phi_{yx}) \approx \frac{1}{2T}\left(\frac{1}{r_{yx}^2} - 1\right)$$

where r_{yx}^2 is the smoothed estimate of coherence and 1/T is the smoothing factor.

The coherence and phase between the physical and biological variables was calculated using MATLAB (Cohere and CSD angle) for the corrected 10 minute bin series, using AMT 1-5 transects from 38°S-50°N. FFT sections of 1024 samples were used, with no

overlap and boxcar window of 1024. The resultant coherence and phase were averaged across the 5 transects. The modulus of the phase was taken so that large values would be out of phase and small values in phase. Ten point moving average was calculated for both the coherence and phase modulus to further smooth the spectra. This was repeated for the Montevideo to Falklands section (38°S-50°S) using FFT lengths of 256. The shorter FFT length was used to increase the smoothing.

Results

Spectral analysis

Spectral analysis using FFT on underway data between UK and Montevideo (50°N-38°S) for zooplankton showed that the log variance for zooplankton was linearly related to the log frequency over large changes in scale (Figure 3.1), indicating that log patch size was inversely related to its frequency. Biovolume showed an approximately linear relationship with a gradient of –0.95, from 20 mins/7 km up to 22 hours/450 km. Counts had a similar gradient of –0.83, and ESD (equivalent spherical diameter) had a less steep gradient of –0.58, from 20 min/7 km up to 170hrs/3400km suggesting greater patchiness at small scale. Biovolume and ESD relationship showed distinct peaks at -1.33 (22hrs), and at 11 hours in ESD only and 16 hours in biovolume only. The peaks represent characteristic frequencies in the parameter variability. The 22 hour peak is likely to be associated with diel events, and the 11 hour represents a twice daily event.

a) Biovolume

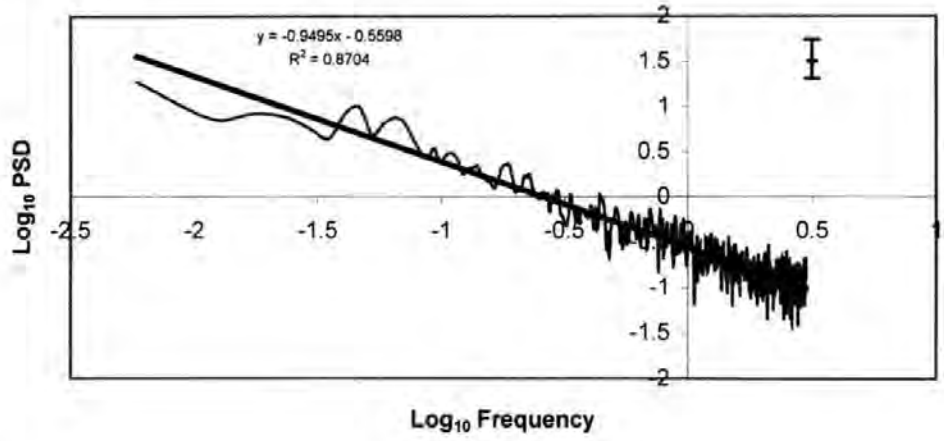

b) Counts

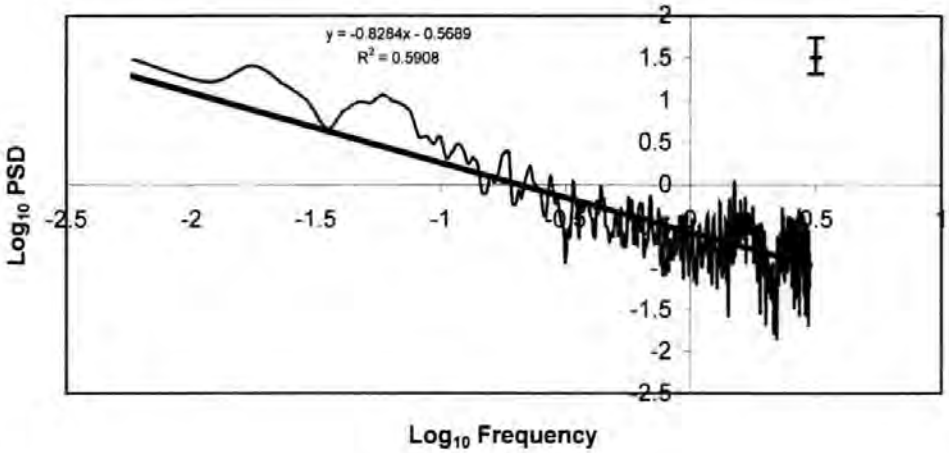

c) ESD

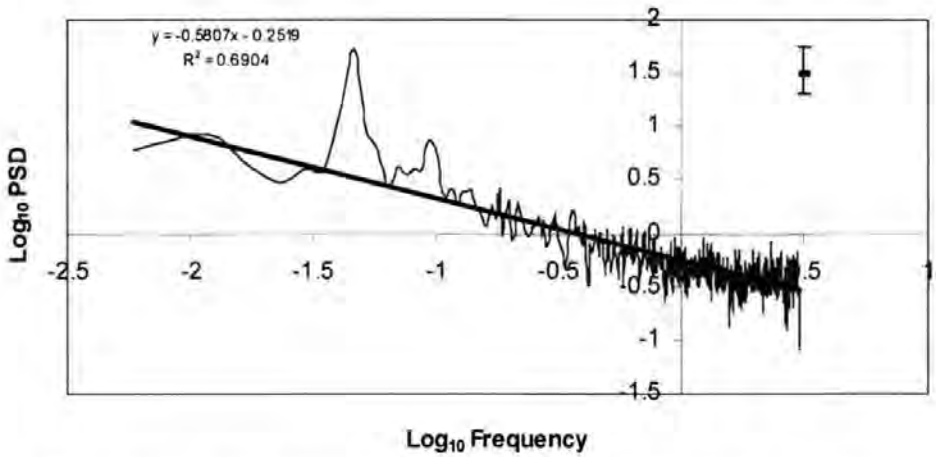

Figure 3.1: The mean spectral density (PSD) for AMT 1-5 38°S-50°N calculated from 10 min averages, for a) biovolume, b) counts c) ESD (equivalent spherical diameter), shown as $\log_{10}$ variance against $\log_{10}$ frequency (hr^{-1}), with the linear regression, and error bars showing 95 % confidence limits.

For the different size fractions, different behaviour is seen in the power spectra of the zooplankton biomass (Figure 3.2). The two smaller size fractions show very similar effects of scale on the heterogeneity, with the same gradient (-1.05). The slope is very similar to that of the total biovolume (-0.95, Figure 3.1a), but no peaks corresponding to diel migration are evident. The 1000-2000 μm size fraction has a similar gradient (-1) but displays the peaks at around 22 hours as seen in the total biovolume, associated with diel events. The >2000 μm size fraction has a reduced slope (-0.26), and a peak at 22 hours.

At smaller scales the slope becomes less steep (Figure 3.3). Biovolume and ESD, at scales 20 to 5 mins (7-1km), have an approximately zero slope at around –0.5. Flat spectra are associated with a random distribution. Totally random heterogeneity would be flat at around –0.66. For counts, at scales less than 45 mins (15 km), the slope is approximately 0.66, suggesting that the zooplankton are still patchy, and patch size and frequency are still related.

Chlorophyll, temperature and salinity over scales from 7 km to 3400 km showed linear relationships between log frequency and log variance (Figure 3.4). None of these spectra showed strong or significant peaks over the frequency range. The slopes were all around -1.4.

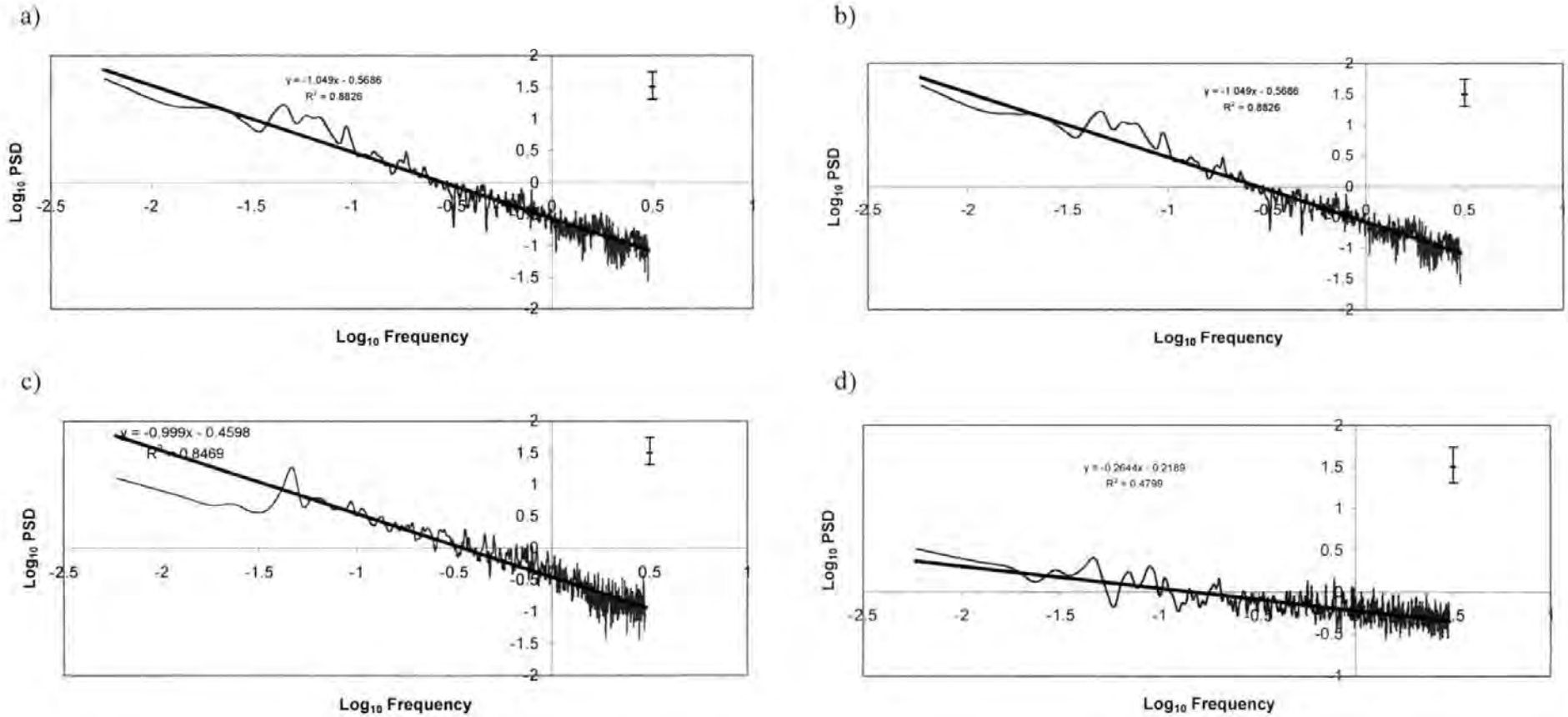

Figure 3.2: The mean spectral density (PSD) for AMT 1-5 38°S-50°N calculated from 10 min averages, for a) 200-500, b) 500-1000, c) 1000-2000 and d) >2000 μm, shown as $\log_{10}$ variance against $\log_{10}$ frequency (hr^{-1}), with the linear regression, and error bars showing 95 % confidence limits.

a)

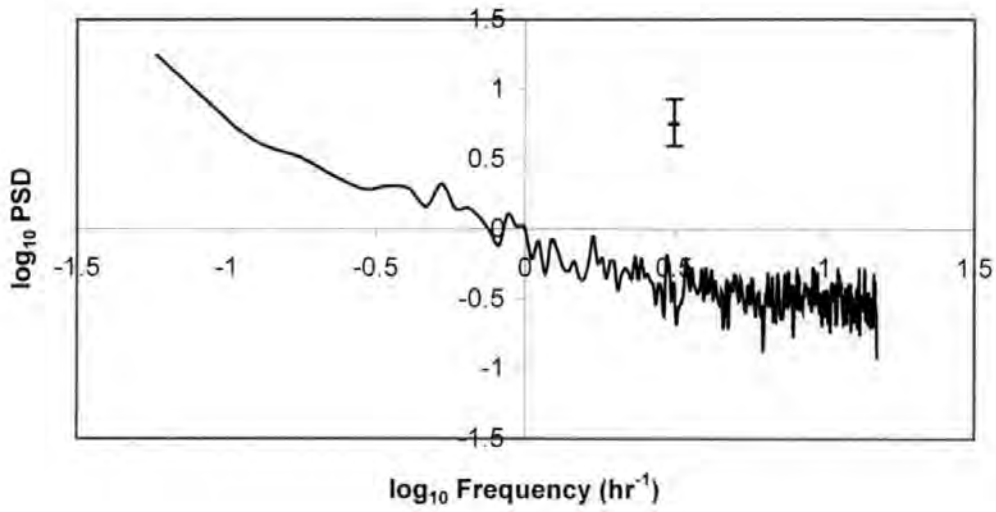

b)

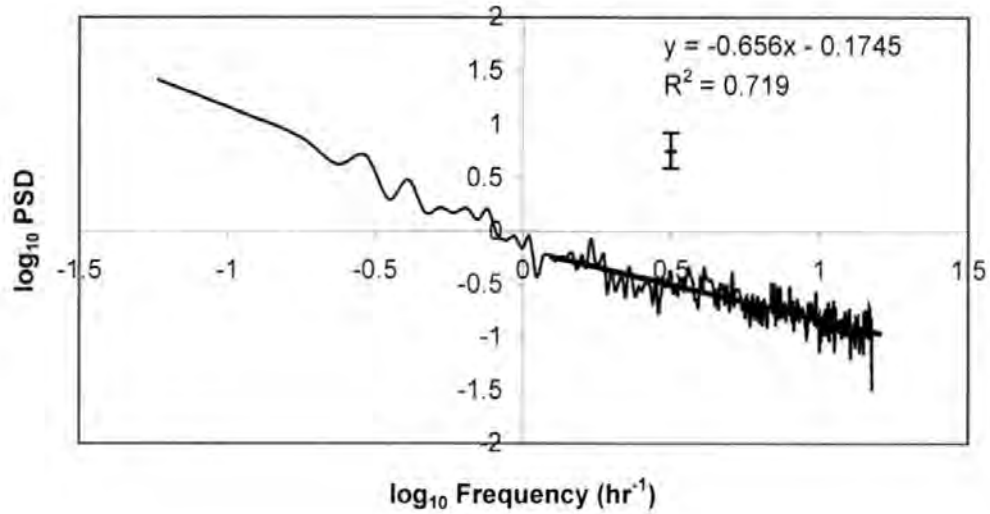

c)

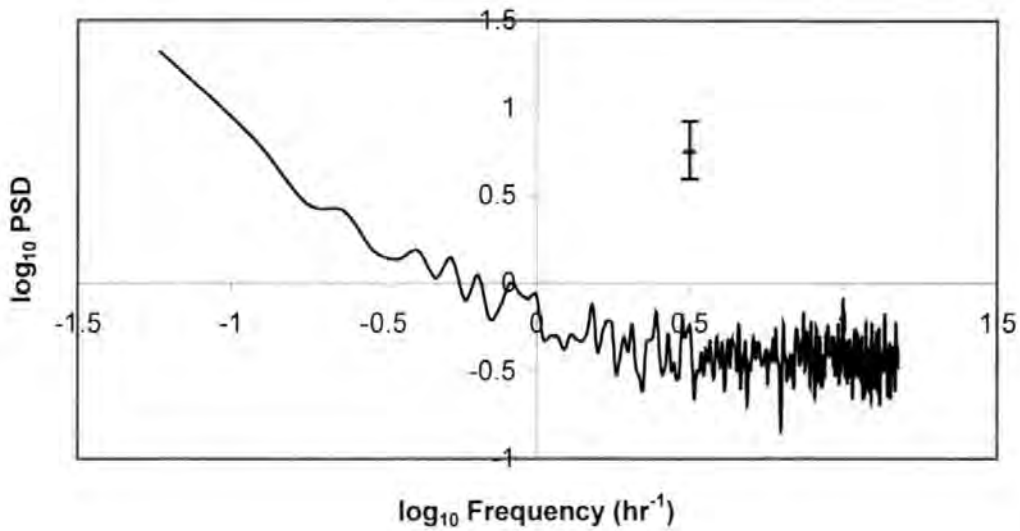

Figure 3.3 The mean spectral density (PSD) for AMT 5 38°S-50°N calculated from 2 min averages, for a) biovolume, b) counts (with the linear regression over 0.1-1.2 hr^{-1}) c) ESD, shown as log_{10} variance against log_{10} frequency (hr^{-1}), and error bars showing 95 % confidence limits.

a) Chlorophyll

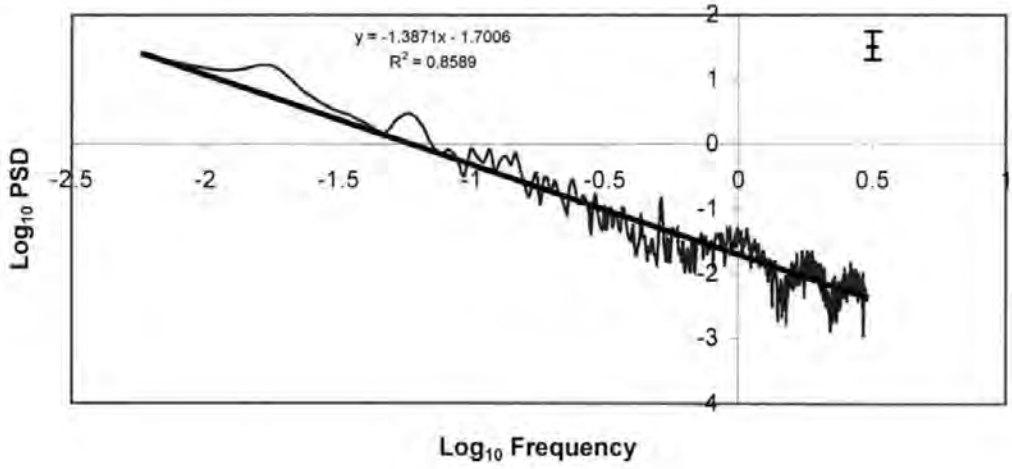

b) Temperature

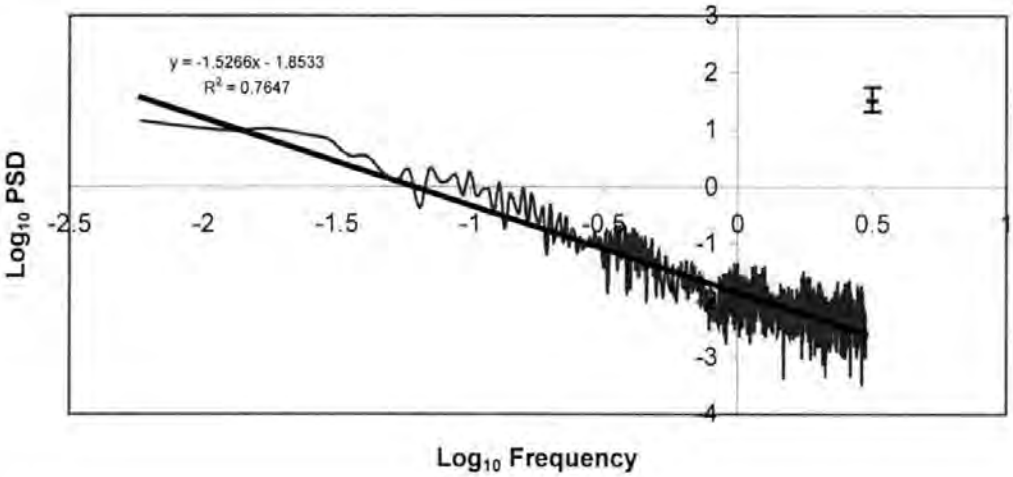

c) Salinity

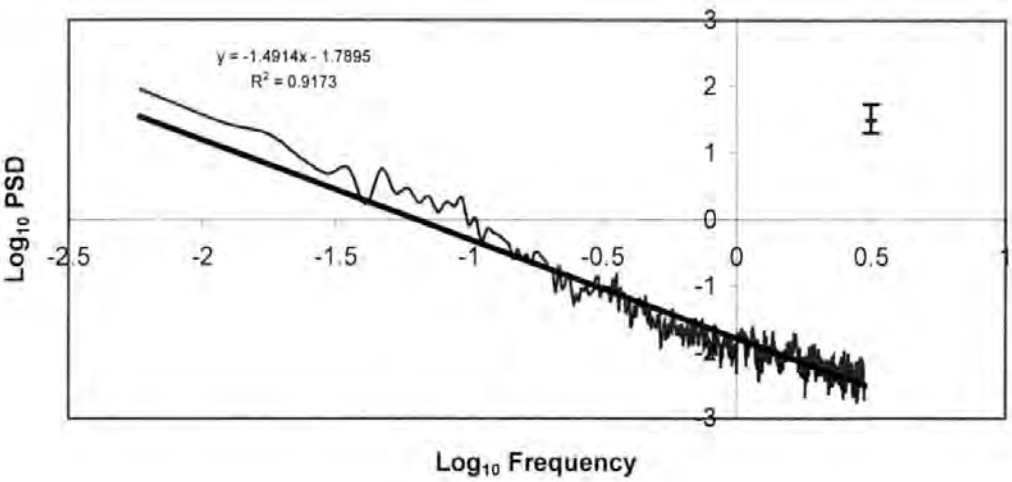

Figure 3.4: The mean spectral density (PSD) for AMT 1-5 38°S-50°N calculated from 10 min averages, for a) chlorophyll, b) temperature c) salinity, shown as $\log_{10}$ variance against $\log_{10}$ frequency (hr^{-1}), with the linear regression, and error bars showing 95 % confidence limits.

Comparing the regression lines between variables (Figure 3.1 and 3.4), showed that the zooplankton related variables (biovolume, ESD, counts) were similar to each other, and were distinctly less steep than chlorophyll, temperature and salinity which were hardly distinguishable. This shows that zooplankton have higher variability at smaller scales, ie. Are more patchily distributed, than either chlorophyll or the physical variables. Closer examination of the 'mesoscale' environment from 30 to 1000 km showed that chlorophyll, temperature and salinity gradients ranged between –1.8 and –2, whereas the zooplankton estimates ranged from –0.8 to –1.3, counts having the steepest gradient (Figure 3.5). Although the gradients are steeper, the relative positions are similar.

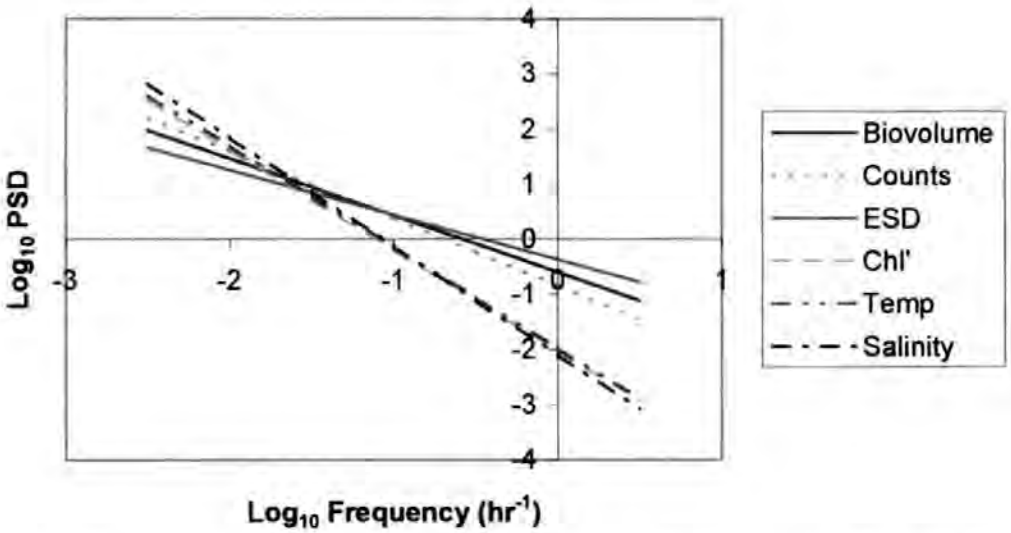

Figure 3.5: The regression of the mean spectral density (PSD) for AMT 1-5 38°S-50°N calculated from 10 min averages over spectral range 30 km to 1000 km, for Zooplankton measure (biovolume, counts and ESD), and other variables (chlorophyll, temperature, salinity) shown as $\log_{10}$ variance against $\log_{10}$ frequency (hr^{-1}).

Fourier analysis of Falklands to Montevideo (38°S-50°S) section of the transect gave similar results with the gradient of log variance against log frequency for zooplankton measures at around –1 (Figure 3.6) and slightly higher for chlorophyll, salinity and temperature at around –1.7 (Figure 3.7). However, neither the size (ESD) or the biovolume showed distinct peaks around 24 hours, although a series of peaks were present in all the zooplankton spectra.

a) Biovolume

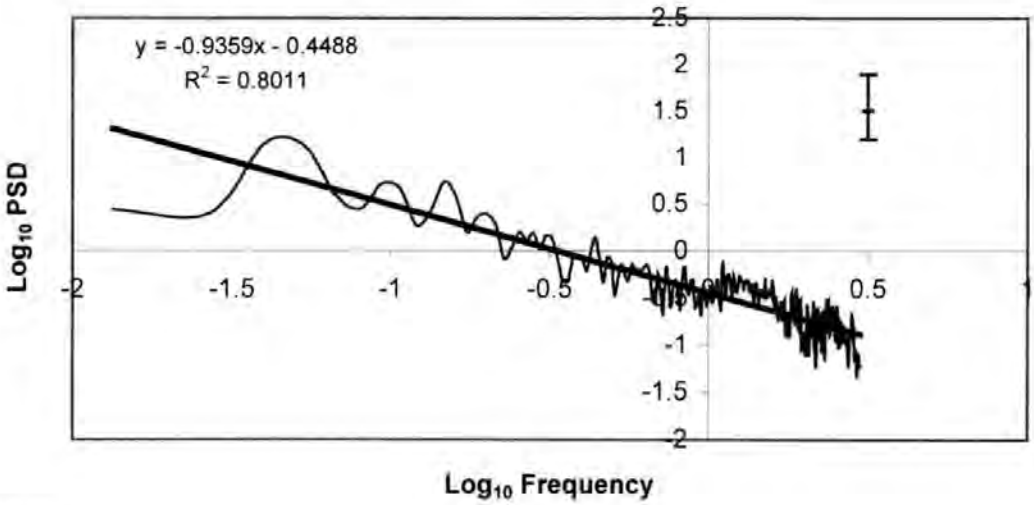

b) ESD

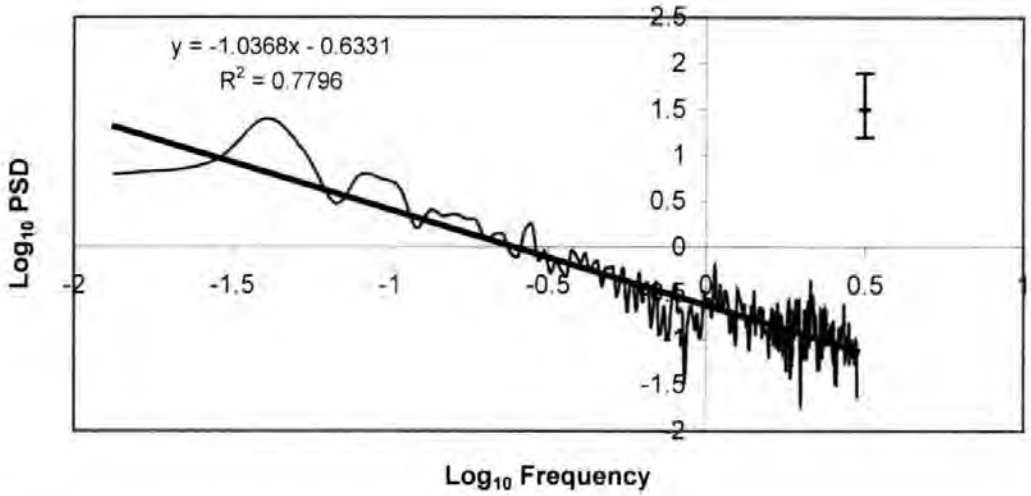

c) Counts

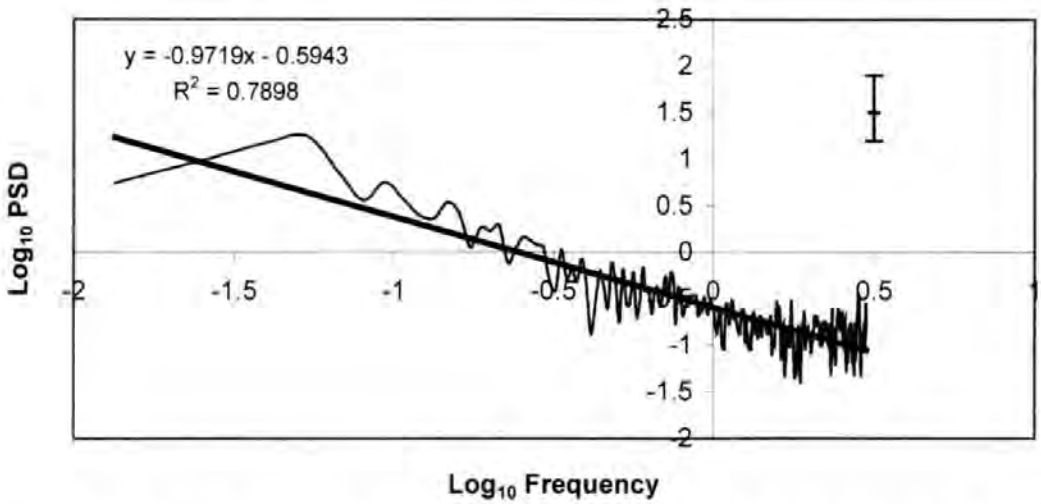

Figure 3.6: The mean spectral density (PSD) for AMT 1-5 38°S-50°S (Port Stanley – Monteovideo) calculated from 10 min averages, nfft (length of section for FFT)=256, for a) biovolume, b) mean equivalent spherical diameter (ESD) c) counts, shown as $\log_{10}$ variance against $\log_{10}$ frequency (hr^{-1}), with the linear regression, and error bars showing 95 % confidence limits.

a) Chlorophyll

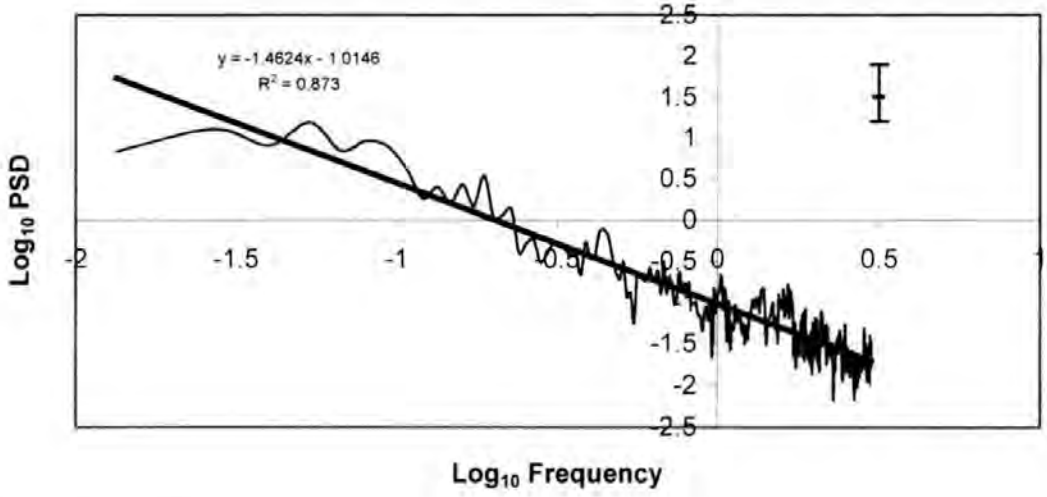

b) Temperature

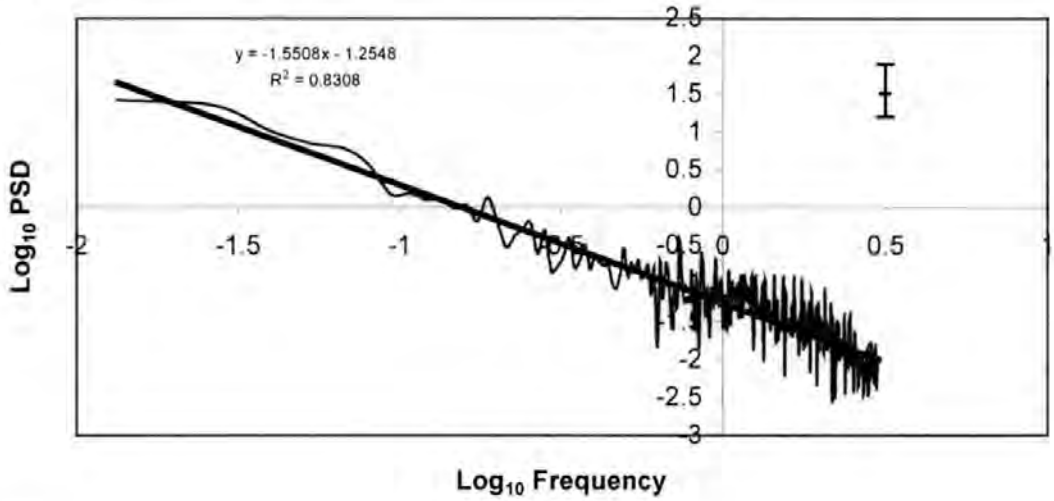

c) Salinity

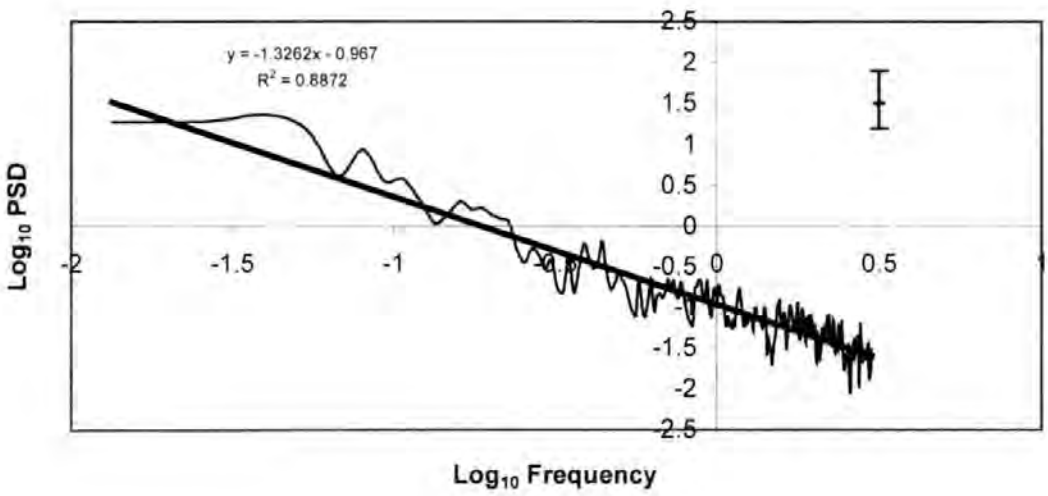

Figure 3.7: The mean spectral density (PSD) for AMT 1-5 38°S-50°S (Port Stanley – Monteovideo) calculated from 10 min averages, nfft (length of section for FFT) = 256 for a) chlorophyll, b) temperature c) salinity, shown as $\log_{10}$ variance against $\log_{10}$ frequency (hr^{-1}), with the linear regression, and error bars showing 95 % confidence limits.

Cross-spectral analysis

Coherence, the agreement between the power spectra, for zooplankton is highest for counts, particularly at low frequency, i.e. large spatial scales (>150 km), where it rises from around 0.7 to 0.9 (Figure 3.8). However, ESD compared to counts and biovolume showed only a coherence of around 0.5 and 0.6 respectively for the whole spectrum. The modulus of the phase is quite constant and low at around 0.4 for biovolume compared to counts and ESD, and 0.6 for counts compared to ESD, suggesting that the spectra are in phase. The coherence between the zooplankton biovolume with chlorophyll was quite high (mean around 0.6), and slightly lower for biovolume and salinity (around 0.5), although it was quite flat for both these variables (Figure 3.9). Biovolume and temperature showed quite low coherence over small scales (up to 5 hours/100km) at around 0.3. However, at larger scales coherence rose to around 0.6. The modulus of the phase is again low (mean 0.7), suggesting that the biovolume is close to being in phase with physical variables. The slightly higher modulus of the phase is probably due to the reduced coherence and thus accuracy of the phase estimation. The coherence between chlorophyll and the physical variables is quite high around 0.5, for all frequencies, and is in phase (Figure 3.10).

The coherence for the region south of Montevideo was in general much lower (Figure 3.11). Biovolume cohered to counts around 0.5-0.7 down to scales of 34minutes/11km, with a peak at 48 minutes/16km, then dropping to around 0.35 at smaller scales. Coherence between ESD and biovolume at large scales (>5hrs/100km) falls with smaller scales to around 0.2. Where coherence was large, the fluctuations were close to being in phase with each other. Coherence with chlorophyll and physical variables was low (0.1-0.3; Figure 3.12), except for temperature and salinity which showed strong coherence (0.65) at large scales dropping gradually to 0.55 at around 1 hr/20km. At smaller scales coherence fluctuated between 0.4 and 0.5. The temperature and salinity fluctuations were in phase (modulus of phase <0.05) with each other over all scales.

a)

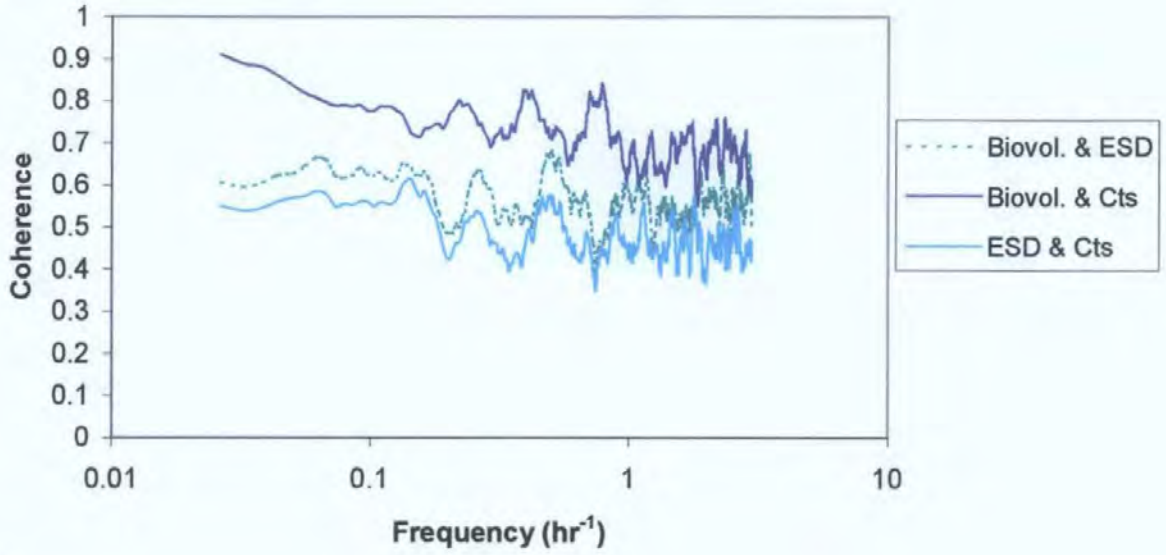

b)

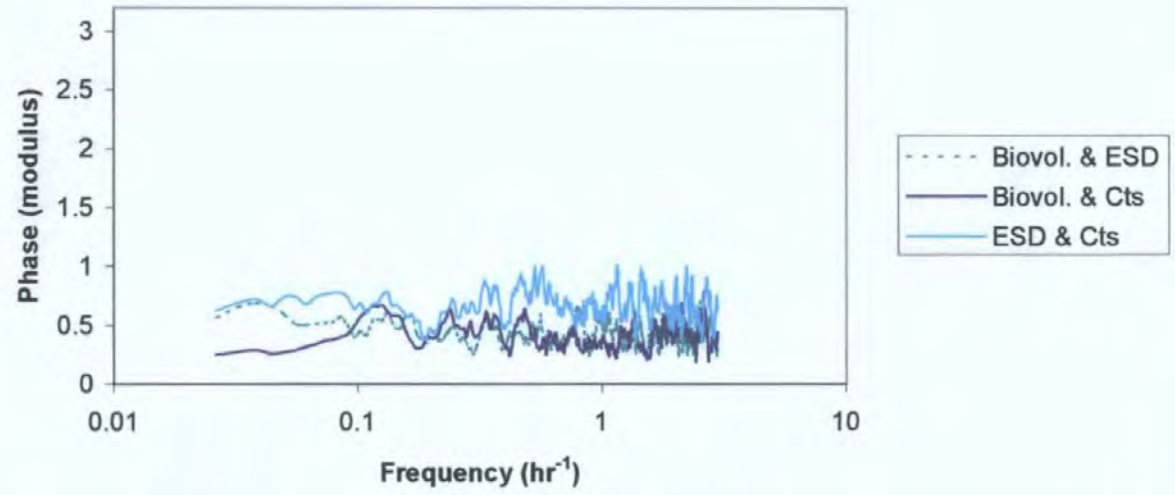

Figure 3.8: AMT 1-5 38°S-50°N calculated from 10 min averages a) Coherence and b) Phase (modulus) between different measures for zooplankton, biovolume (Biovol.), Counts (Cts), mean equivalent spherical diameter (ESD) (calculated as 10 point moving averages).

a)

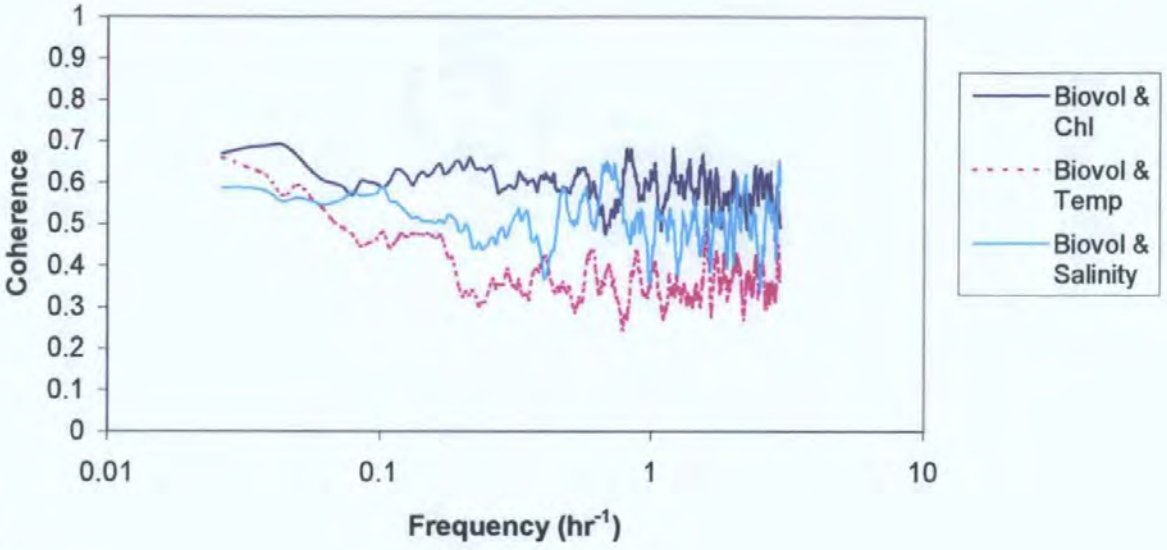

b)

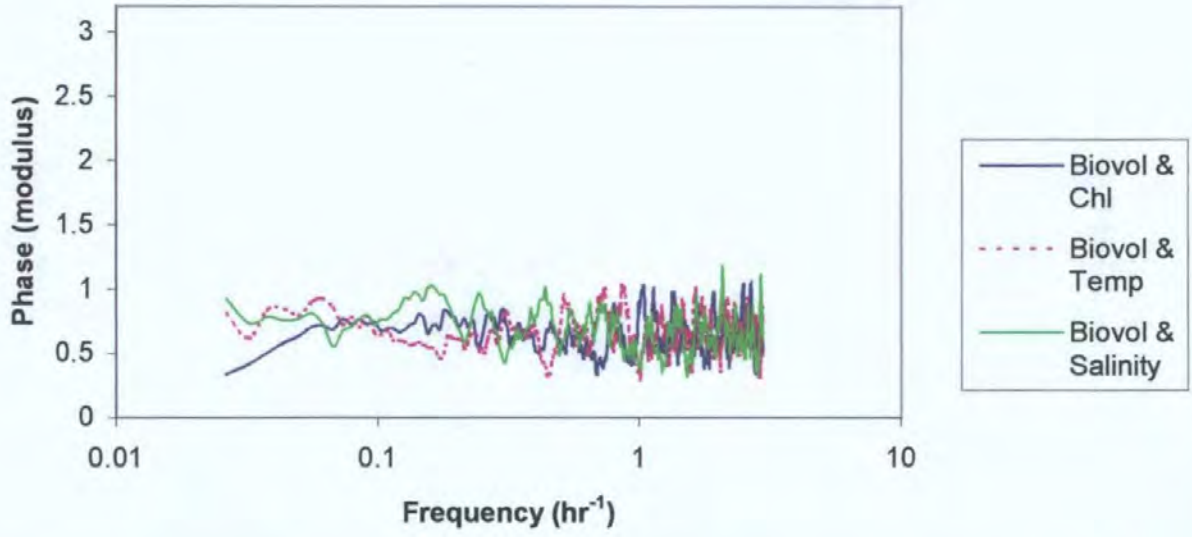

Figure 3.9: AMT 1-5 38°S-50°N calculated from 10 min averages a) Coherence and b) Phase (modulus) between zooplankton biovolume (Biovol.) and chlorophyll (Chl), temperature (Temp) and salinity (calculated as 10 point moving averages).

a)

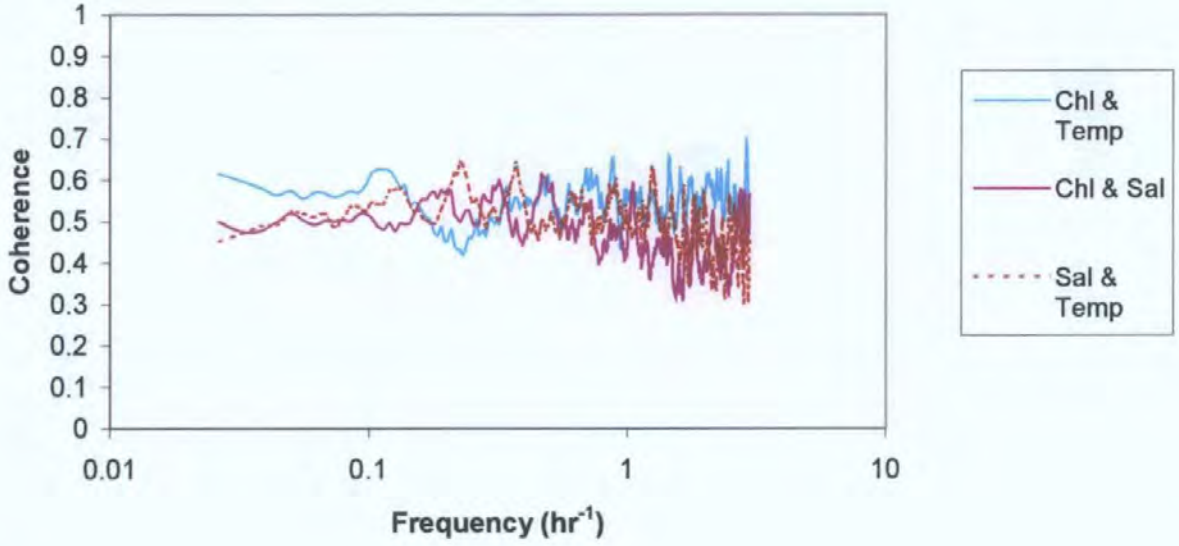

b)

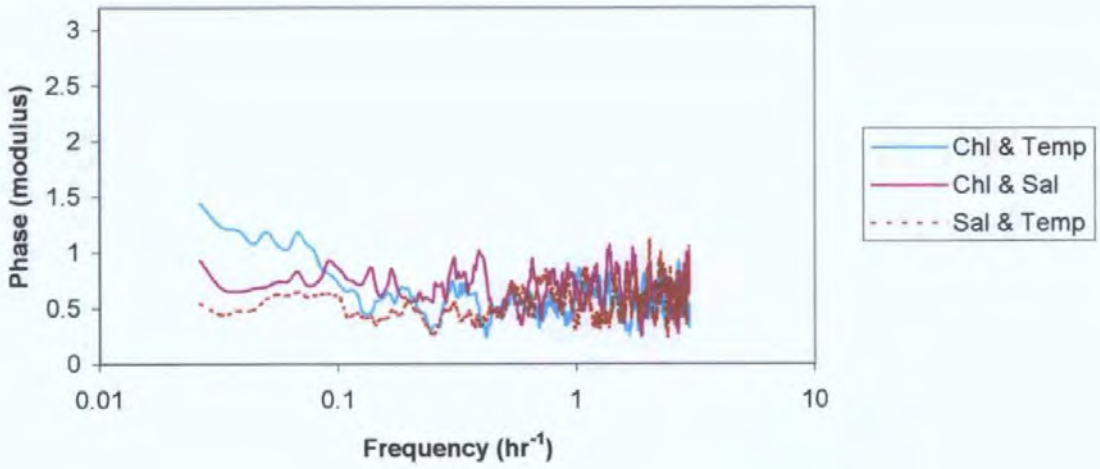

Figure 3.10: AMT 1-5 38°S-50°N calculated from 10 min averages a) Coherence and b) Phase (modulus) between chlorophyll (Chl), temperature (Temp) and salinity (calculated as 10 point moving averages).

a)

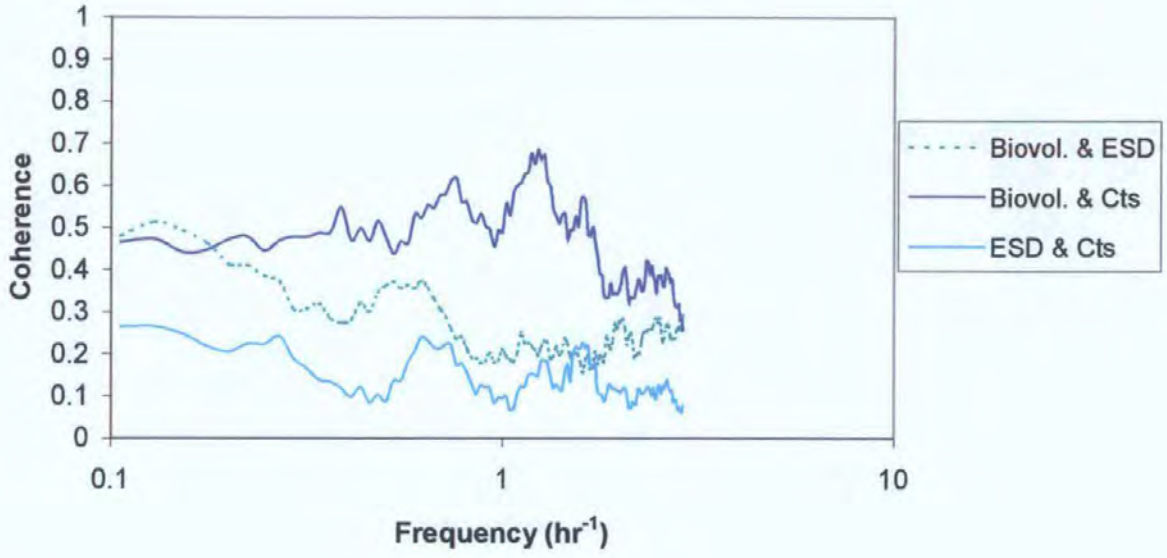

b)

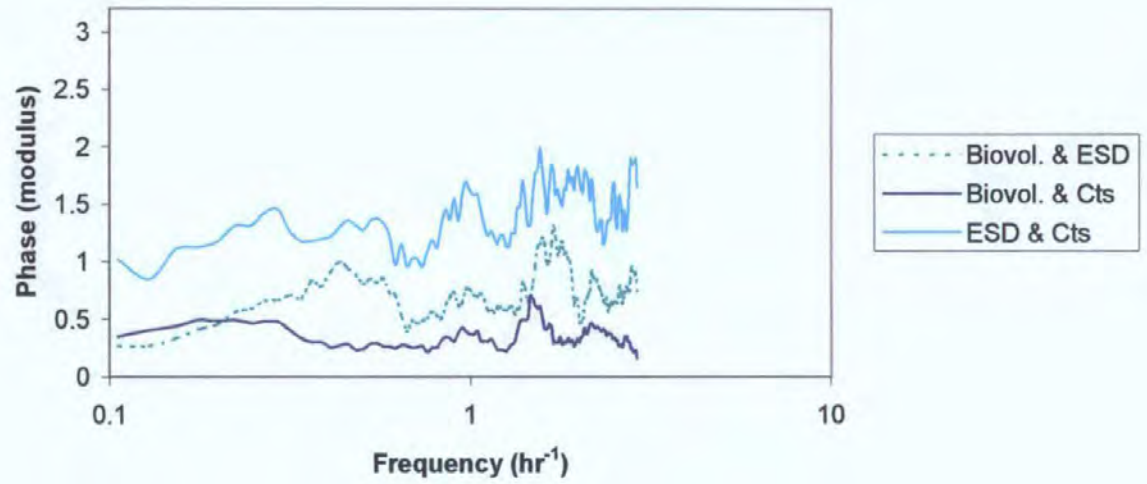

Figure 3.11: a) Coherence and b) Phase (modulus) between different measures for zooplankton, biovolume (Biovol.), Counts (Cts), mean equivalent spherical diameter (ESD) (calculated as 10 point moving averages) for Montevideo to Port Stanley (nfft=256).

a)

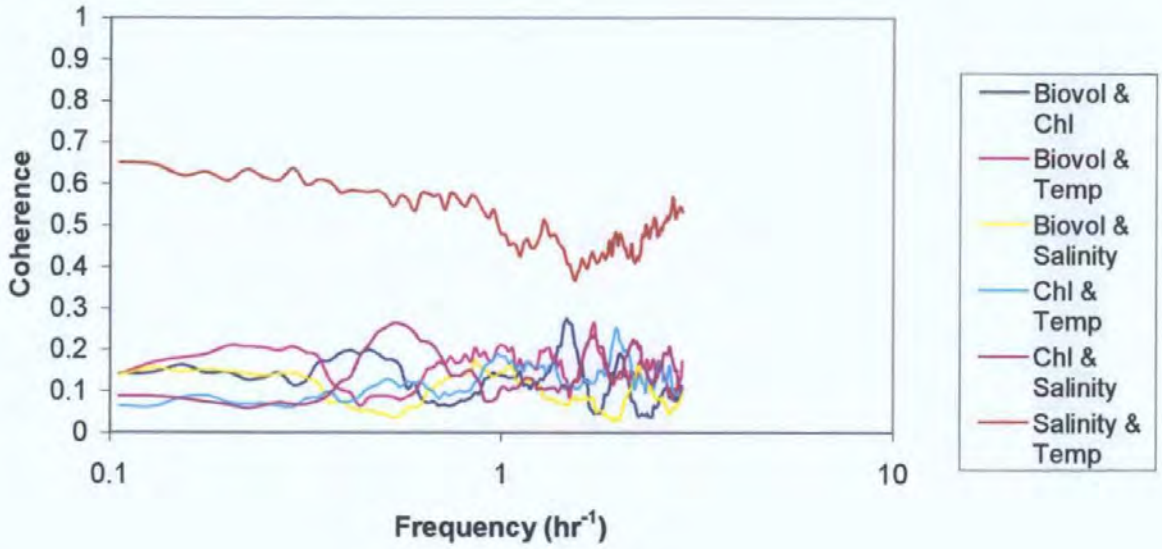

b)

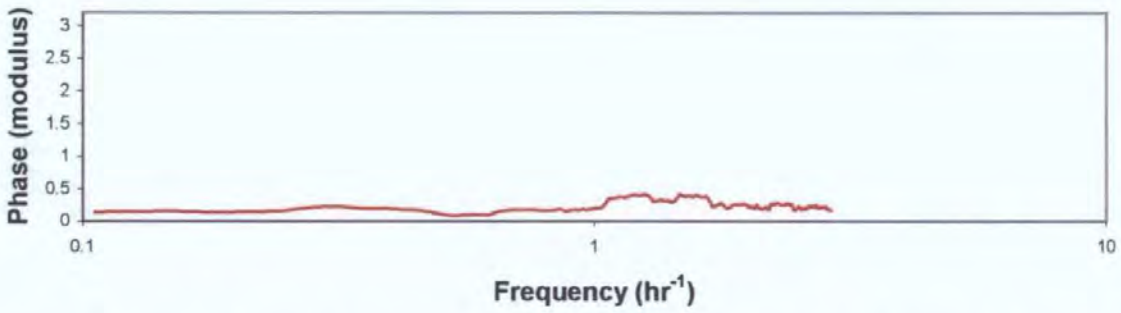

Figure 3.12: a) Coherence between zooplankton biovolume (Biovol.) and chlorophyll (Chl), temperature (Temp) and salinity, and b) Phase (modulus) for temperature with salinity (calculated as 10 point moving averages) for AMT1-5 Montevideo to Port Stanley (nfft=256).

Discussion

The interpretation of zooplankton patchiness over these transects is confused by crossing both spatial and temporal scales. The peaks in zooplankton biovolume and mean size at 22 hours / 440 km are likely to be temporal changes related to diel migration. The passive scalers (temperature and salinity; Figure 3.3) do not show peaks at this frequency. Cycles of 22 hours rather than 24 hours are evident due to the daily station of approximately two hours. The largest peak is in the mean size (ESD). Large zooplankton are known to undergo the strongest vertical migrations (Dam *et al.* 1993, Hays *et al.* 1994). The strongest peak in the size fractionated spectra occurs in the 1000-2000 μm size fraction at 22 hours, also suggesting that it is the larger zooplankton. The largest size fraction (>2000 mm) does have a peak at this frequency too, but the spectra is not as clear. This is likely to be due to under sampling. The spectrum is almost flat as would be expected from white noise, i.e. a random distribution. The diel cycles are also evident in the time domain (appendix 4 and 5). The secondary peak at 11 hours in the mean ESD is likely to be linked to the diel migration. It could be associated with peak near surface abundances at dawn and dusk, which for most of the transect will be approximately 12 hours apart (as the cruises were Spring and Autumn, so close to the equinox). An observed phenomenon in the time domain (appendix 4 and 5) and by others (Raymont 1983, Mauchline 1998) is 'midnight sinking' where the near surface abundance decreases after total darkness, around midnight. One possible explanation is that zooplankton in general and copepods in particular are thought to control their vertical migration by moving towards an optimum light level or following the change in the luminance. In the region south of Montevideo, 22 hour peaks are evident in all the zooplankton measures (Figure 3.6), although this is only just significant at the 95 % level in the biovolume and the peak is not very sharp in the numerical abundance (counts). Several other peaks can be distinguished. These may be associated with spatial features such as rings and fronts, which are abundant in this

dynamic region of the confluence of the Falkland and Brazil currents, as peaks are also visible in the chlorophyll and salinity spectra.

The zooplankton spectra showed a linear slope over the mesoscale, but at spatial scales greater than 250-1000 km, the linear relationship broke down, with the underlying spectrum becoming flatter with more distinct peaks. A similar relationship was observed in temperature and chlorophyll, although the linear relationship appeared to be maintained with the salinity for much larger scales. At large scales, frequency analysis of zooplankton becomes less useful. Understanding zooplankton distributions on large scales is better approached by different techniques based in the time domain. At the smaller end of the spectrum (Figure 3.3), the slopes of zooplankton spectra flatten. This is particularly evident in the mean equivalent size (ESD), and also in the biovolume, at scales less than 30 minutes /10 km, where the variance oscillates around -0.5. In theory, white noise has a flat spectrum at $1/\sqrt{\sigma^2}$, where σ^2 is the variance (Jenkins and Watts 1968). As the series were standardised to zero mean and unit standard deviation, white noise would be expected to be at –0.67 (on log scale). If measures are discrete, rather than continuous, the variance of the series increases. Thus at small spatial scales the zooplankton biovolume and mean ESD distributions behave like white noise i.e. have an apparently random distribution. Two explanations exist as to why the zooplankton appear randomly distributed at these small scales; either the zooplankton are randomly distributed or that there is a sampling error. The sampling error could be caused by the sampling volume being too small at these scales to distinguish patches, or the pumped system allowing mixing over small scales, randomising the zooplankton distribution. Considering that several other studies have shown patchiness at these scales and smaller (e.g. Mackas and Boyd 1979, Currie *et al.* 1998), it is likely that the sampling is contributing to the apparent randomness, although these other studies were generally based in coastal regions which may behave differently.

Over 'mesoscales', 30-1000 km, the gradient of zooplankton measure spectra were around -1 (Figure 3.7), less steep than chlorophyll, temperature and salinity at around –1.8 to -2, suggesting that zooplankton have greater spatial variability in their distribution at smaller scales, i.e. patchiness, than the physical parameters. Mackas and Boyd (1979) also found that the zooplankton gradient was less steep than chlorophyll and temperature over scales 100 m to 2 km, and Piontkovski and Williams (1995) found zooplankton were more heterogeneous than phytoplankton, over scales of 10s to 100s of kilometres in the tropical ocean. Levin *et al.* (1989) found Antarctic krill exhibited finer structure than the phytoplankton. There are also theoretical predictions from modelling that variability should be greater for zooplankton than for chlorophyll due to differences in lifecycles (e.g. Steele and Henderson 1992, Smith *et al.* 1996, Abraham 1998). For model of turbulent stirring of coupled phytoplankton and zooplankton populations, Abraham (1998) found that the spectral slope for chlorophyll had a gradient of 2.1 ± 0.20, and for zooplankton a gradient of 1.0 ± 0.16, over scales of 5 to 500 km. This model considers zooplankton to be truly planktonic, and the difference in zooplankton and phytoplankton to be a consequence of different growth rates and life spans. The model also predicts no coherence between zooplankton and phytoplankton at larger length scales. In addition, increasing maturation time would lead to flatter spectra. Generally, maturation time is longer for the same conditions for larger zooplankton (Hirst and Sheader 1997). Therefore the flatter slopes of the larger zooplankton size classes (Figure 3.2) could, at least in part, be a consequence of their longer maturation time. Other explanations of zooplankton patchiness include behavioural swarming (Levin *et al.* 1989) and vertical migration (Mackas, 1984).

It can also be seen that chlorophyll is behaving over these scales in the same way as temperature and salinity, which can be considered passive scalars of turbulence (Platt and Denman 1975). Other estimates for chlorophyll and temperature vary between –2 and –3 (e.g. Sanders, 1972; Holladay and O'Brian, 1975; Fasham and Pugh, 1976; Gower *et al*,

1980; Deschamps *et al.* 1981). Theoretical predictions of turbulence vary with scale and model. However, at large scales predictions vary between –2 and –3 depending on the assumptions (e.g. -2 for turbulence at fronts and eddies and –3 for two dimensional models; Denman and Platt, 1976).

There is strong coherence between the different zooplankton measures, particularly between numerical abundance (counts) and biovolume over the 38 °S to 50 °N part of the transect, as would be expected. The coherence between biovolume and counts increases at larger scales (>280 km, 14 hours). The mean size of zooplankton is less strongly related to the zooplankton abundance, but there is still coherence of around 0.5 and in phase. This suggests that at higher zooplankton abundances, the zooplankters are larger, or conversely that at low zooplankton abundances the zooplankters are smaller. It has been found that in the subtropical gyres, where zooplankton biomasses are low, the system tends to be dominated by small copepods (e.g. Chapter 4, Piontkovski and Van der Spoel 1997).

The relationship between zooplankton measures over the 38 °S to 50 °S, Falklands to Montevideo section, shows a different relationship. The coherence between biovolume and counts is lower (0.35-0.7), and at low frequencies (large scales, >5hours/100km), the coherence between biovolume with counts or ESD is the same. The relationship between abundance and zooplankter size is also not evident. This change in pattern suggests that the system is different, and the variability is influenced by different factors. It could be that this very dynamic ecotone is not close to being in equilibrium, and so the physical and biological systems have become uncoupled. Similar affects have been found in dynamic upwelling systems (Mitchell-Innes and Walker 1991, Pitcher *et al.* 1991, Bailey and Chapman 1991).

The coherence between zooplankton biovolume and temperature, salinity and chlorophyll is quite strong, and in phase over 38 °S to 50 °N. The strongest relationship is with chlorophyll; temperature is similar. Chlorophyll is expected to cohere with zooplankton biovolume at large scales, as large phytoplankton populations would support large zooplankton populations, although Abraham's model (1998) predicted no coherence at scales of 100s of km. However, at small scales, Piontkovski *et al.* (1995) found a negative relationship between zooplankton and chlorophyll, due grazing of the zooplankton on the chlorophyll. Between chlorophyll and the physical variables, coherence was approximately 0.5 over all scales, although at larger scales the relationship between chlorophyll and temperature was slightly higher. The phase was also higher suggesting that at large scales the temperature and chlorophyll may not be in phase, and that there is some lag. At the largest scales (>500km), the chlorophyll lags the temperature, reaching an approximate anti-phase, suggesting high temperatures are associated with low chlorophyll. Across the ocean, the highest temperatures are found in the subtropical gyres, which are characterised by a deep stable pycnocline with an oligotrophic mixed layer and low chlorophyll. Cooler waters occur at upwelling sites where deep nutrient rich waters come to the surface. Over the Falklands-Montevideo transect, the zooplankton biovolume shows no real relationships with other variables with coherence less than 0.2. In fact, the only variables showing coherence are salinity and temperature, which is strong especially at scales greater than 1 hour/20km, and these are in phase.

Conclusions

The spectral and cross-spectral analyses demonstrate the importance of scale in understanding zooplankton variability. The patterns and influences on zooplankton at large basin scales (500-1000 km) are different to that at smaller scales. At the smallest scales (<10 km), the data become unreliable for some applications and again the behaviour changes. The different behaviour and relationships observed in the section 38 °S to 50 °S to the rest of the transect, also suggests that the influence of factors on the zooplankton community structure may change over different regions of the ocean.

The spectral analysis demonstrates that zooplankton measures of biomass at the mesoscale have quite high variability at small scales, forming a log-log linear relationship with a gradient of approximately –1. In contrast, chlorophyll and the physical parameters have steeper gradients of around –2 over the same scales, suggesting that there is less variability at smaller scales in the chlorophyll and temperature. These gradients are consistent with others findings, and with Abraham's (1998) seeded turbulent advection model.

Chapter 4: Large scale patterns in zooplankton

Introduction

Large scale patterns are predicted because of the latitudinal changes in the physical environment, particularly light and temperature regimes. Several latitudinal changes in the zooplankton have been noted (e.g. Reid *et al.* 1978, Angel 1993). Angel (1997b) suggested that these included an increase in mean size and longevity of organisms at higher latitudes, and a decrease in diversity whilst variability in diversity increased at higher latitudes. In addition to these latitudinal changes, the characteristics of the watermasses and climate give rise to areas or regions of similar physical and derived biological properties. Understanding of pelagic marine biogeography forms a crucial part of understanding the biology of the oceans. It allows generalisations to be made over large areas. Several attempts have been made to divide the oceans into areas of similarity. These regions have been based on a variety of organisms (Euphausiids; Brinton 1962, Myctophidae; Backus *et al.* 1977, Thecosomata; Dadon and Boltovskoy 1982, Foraminifera; Bé 1977). Many of these schemes rely on a composite of data from several sources, and due to sampling differences are reduced to presence/absence data (e.g. Gibbons 1997), losing changes in community structure due to changes in abundance and dominance. They may also involve interpolation from physical boundaries and watermasses. Strong links are generally thought to be associated between the watermasses and the changes in community (e.g. Van der Spoel and Heyman 1983, Boltovskoy 1986, McGowan 1986). Platt *et al.* (1995) divided the oceans into 'provinces' based on 'ocean currents, fronts, topography and recurrent features in the sea surface chlorophyll'. Several world composites have been derived and reviewed (e.g. McGowan 1974, Van der Spoel and Heyman 1983, Backus 1986, Boltovskoy 1997). Traversing the length of the Atlantic, it may be possible to observe some of these changes, from samples that have been collected and processed consistently.

Two perspectives have been taken: latitude as a gradient (section 4.1), investigating continuous trends along the transect; and looking for areas of similarity (section 4.2).

With respect to the taxonomic community structure, two levels have been taken to analyse the structure in terms of the major groups to give a broad overview of the general zooplankton behaviour, and to carry out a more detailed study on the copepod genera. Copepods dominate the mesozooplankton over most of the oceans, frequently constituting more than 80% of the abundance (appendix 6), and form a diverse group. As a highly diverse group, the detailed species taxonomy has not been fully resolved. By utilising the genus rather than species level, many of these problems are circumvented. In addition, the problems associated with detailed species mapping such as expatriation will also be minimised by this approach, and this simplification may provide a clearer insight into the controls on community structure.

4.1 Latitudinal Changes

Introduction

There are several hypotheses and theories about how zooplankton communities change over latitudinal gradients. Angel (1997b) proposed four trends in pelagic ecosystem pattern:

1) There are latitudinal trends in species richness and dominance: high latitude communities are poor in species and dominated by very few species whereas most low latitude communities are rich in species and low in dominance.

2) The mean size of pelagic organisms tends to increase both Polewards and with increasing depth, at least to 1000 m.

3) Species richness also increases with depth to reach a maximum at 500-1000 m, but mostly as a result of an increase in the number of rare or infrequent species in the communities.

4) In high productivity areas such as coastal and oceanic upwelling zones, there is a high degree of dominance. Sample species richness also tends to be lower.

The AMT transect covers an extent approximately 50 ^{o}N to 50 ^{o}S, so presents an opportunity to investigate latitudinal changes. Using both the underway and net data from the cruises, I investigated changes in diversity and size with latitude and the pattern of carbon and biovolume in the surface 200 m mesozooplankton along the transects.

Diversity

Diversity is a key issue in ecology, and understanding patterns of diversity has been a major issue. Although diversity is not a new concept and generally widely understood, its definition and how it should be calculated is more complex. Traditionally, two aspects of species diversity have been considered: the species richness i.e. the number of species, and the evenness which is the distribution of individuals within each species. Thus a perfectly even sample would have the same number of individuals representing each species. Dominance is the opposite of evenness, so a low evenness sample has high dominance, i.e. will contain mainly one or two species.

The simplest measure of species richness is the number of species in a sample. However, the number of species will depend on the sample size (e.g. Soetaert and Heip 1990). Margalef's index (D_{mg}; equation 4.1) takes into account the number counted, but will still be sample size dependent.

$$D_{mg} = (S-1)/\ln N \qquad \text{(eq. 4.1)}$$

where S is the number of species, and N is the number of individuals counted. Menhinick's index (D_{mn}; equation 4.2) is similar.

$$D_{mn} = S / \sqrt{N} \qquad \text{(eq. 4.2)}$$

where S is the number of taxa, and N is the number of individuals. Both of these indices assume the relationship between species richness and sample size. However, this has been shown to vary depending on the system (e.g. Soetaert and Heip 1990), and thus these measures still show sample size dependency. If similar sized samples are used, they may be useful.

Diversity indices try to incorporate the richness and the evenness within the diversity. Shannon and Wiener (Pielou 1975) developed an index based on information theory, where diversity is a measure of 'bits' of information:

$$H^1 = -\Sigma\, p_i \ln p_i \qquad \text{(eq. 4.3)}$$

where H^1 is the Shannon Wiener diversity index, and p_i is the proportion of the ith taxa. This is one of the most widely used diversity indices. Yet it assumes that the community has been exhaustively sampled, and shows a strong sample size bias.

Species evenness is the quantification of the unequal representation against a theoretical community where all members are equal in abundance. One common index is Pielou's (1969) evenness:

$$J^1 = H^1(\text{obs})/H^1(\text{max}) \qquad \text{(eq. 4.4)}$$

where H^1 is the Shannon Wiener diversity index for the observed, and for the theoretical maximum, when all species are represented by the same number of individuals.

Dominance curves are not simple indices, but are ranked species abundance curves based on ranking species (or taxa) in decreasing order of their importance in terms of abundance.

The rank abundances are expressed as a percentage of the total, and are plotted against the relevant species. Log transforming of the axis can be used to emphasise or down-weight different sections of the curve. Logging the x axis enables better visualisation of the more common species. K-dominance curves are cumulative ranked abundances, plotted against species (or log species) abundance. To compare dominance separately from number of species the x axis may be rescaled to give relative species rank, producing Lorenz curves. These curves give a more in depth view of the community diversity. However, where diversity is being considered for lots of samples, the curves may be less clear and easy to compare than single indices.

Recently, the emphasis has shifted to 'biodiversity', rather than simply species diversity, with the taxonomic relatedness being important, and total genetic variability included (e.g. Van der Spoel 1994). The simplest way to include relatedness is to calculate diversity indices at different taxonomic levels (e.g. species, genus, family). But a more integrated approach has been to develop new indices including the taxonomic relatedness of the species. Vane-Wright *et al.* (1991) and May (1990) used detailed cladograms to determine weightings of related species and Faith (1992, 1994) defined phylogenetic diversity (PD) which includes the total length of all branches of the phylogenetic tree. Warwick and Clarke (1995) developed a more general hierarchical system based on the Linnean classifications. They defined two indices: taxonomic diversity, which is similar to Shannon-Wiener index (eq 4.5), but includes taxonomic relatedness, and taxonomic distinctness, which does not include the diversity. Taxonomic diversity (Δ) is the average path length between any two individual, and is given by:

$$\Delta = \frac{\sum\sum_{i<j} w_{ij} x_i x_j + \sum_i 0.x_i(x_i - 1)/2}{\sum\sum_{i<j} x_i x_j + \sum_i x_i(x_i - 1)/2} \qquad \text{(eq. 4.5)}$$

Taxonomic distinctness (Δ^*) is the average taxonomic distance between species, and is given by:

$$\Delta^* = \frac{\sum\sum_{i<j} w_{ij} x_i x_j}{\sum\sum_{i<j} x_i x_j} \qquad \text{(eq. 4.6)}$$

where x_i is the abundance of the *i*th species and w_{ij} is the distinctness weight linking species i and j . The weighting can be altered to emphasise different levels, or to adjust to the number of branches at each level (Clarke and Warwick 1999).

Patterns in diversity have been studied in a wide variety of environments. However, different sampling strategies, techniques and intensities have confounded the problem. For example, the diversity of marine harpacticoid copepods was most closely related to sampling effort, rather than latitude or environment type (Bodin 1999). Recently, there has been a drive to standardise sampling techniques and intensity to allow greater inter-comparison across a wide range of fields (e.g. benthic epifauna; Gee and Warwick (1996), termites, Jones and Eggleton 2000). In addition, there has been a development of measures of diversity such as taxonomic diversity which are not as sensitive to sample size as traditional measures.

Data Analysis

Latitudinal changes in diversity

The data on genera from AMT 4-6 0-200 m nets were used to calculate Margalef's species richness from the number of genera and from the number of major groups in the sample and the number of individuals counted (eq 4.1). Margalef's richness was employed because it is simple and easy to use, and even though it does not totally negate the effect of sample size, it gives an adequate normalisation if sample sizes are not too small (>100 individuals) and a similar number have been counted in all samples (Clarke and Warwick 1994). A

second order polynomial was fitted to the latitudinal transect of the data less the Benguela stations from AMT6. The samples were averaged into 5^{o} bands along the transect, so that for example 40^{o} was between 37.5^{o} and 42.5^{o}. The number of groups and genera in each band was calculated for each 5^{o} interval. Pielou's evenness, one of the most common measures of evenness, J^{1} (eq 4.4) was also calculated for both major groups and genera.

To incorporate the relatedness of the different taxa, taxonomic distinctness was calculated for the 200 m net samples using equal weights for each taxonomic level shown in Table 4.1. The phylogeny was taken for Calanoid copepods from Mauchline (1998) and for other sub-orders from Boltovskoy (1999). Para/pseuds were omitted as they could not be assigned to any group. However as they were present in all samples this should make little difference to the results. Taxonomic diversity represents an integrated measure of diversity including facets of richness, evenness and taxonomic distinctness and was also calculated.

Genus	Family	Super-family	Sub-order
Arietellus	Arietelidae	Arieteloidea	Calanoida
Augaptilus	Auguptilidae	Arieteloidea	Calanoida
Euagaptilus	Auguptilidae	Arieteloidea	Calanoida
Haloptilus	Auguptilidae	Arieteloidea	Calanoida
Heterorhabdus	Heterohabidae	Arieteloidea	Calanoida
Heteorstylites	Heterohabidae	Arieteloidea	Calanoida
Lucicutia	Lucicutidae	Arieteloidea	Calanoida
Metridia	Metridinidae	Arieteloidea	Calanoida
Pleuromamma	Metridinidae	Arieteloidea	Calanoida
Phyllopus	Metridinidae	Arieteloidea	Calanoida
Acartia	Acartiidae	Centropagoidea	Calanoida
Candacia	Candaciidae	Centropagoidea	Calanoida
Centropages	Centropages	Centropagoidea	Calanoida
Labidocera	Pontellidae	Centropagoidea	Calanoida
Pontellina	Pontellidae	Centropagoidea	Calanoida
Temora	Temoridae	Centropagoidea	Calanoida
Aetideus	Aetideidae	Clausocalanoidae	Calanoida
Euaetideus	Aetideidae	Clausocalanoidae	Calanoida
Euchirella	Aetideidae	Clausocalanoidae	Calanoida
Gaetanus	Aetideidae	Clausocalanoidae	Calanoida
Undeuchaeta	Aetideidae	Clausocalanoidae	Calanoida
Aetideopsis	Aetideidae	Clausocalanoidae	Calanoida
Pseudoeuchaeta	Aetideidae	Clausocalanoidae	Calanoida
Euchaeta	Euchaetidae	Clausocalanoidae	Calanoida
Phaenna	Phaennidae	Clausocalanoidae	Calanoida
Scolecithrix	Scolecithricidae	Clausocalanoidae	Calanoida
Scolethricella	Scolecithricidae	Clausocalanoidae	Calanoida
Scottocalanus	Scolecithricidae	Clausocalanoidae	Calanoida
Scaphocalanus	Scolecithricidae	Clausocalanoidae	Calanoida
Racovitzanus	Scolecithricidae	Clausocalanoidae	Calanoida
Eucalanus	Eucalanoidae	Eucalanoidae	Calanoida
Rhincalanus	Eucalanoidae	Eucalanoidae	Calanoida
Calanoides	Calanidae	Megacalanoidae	Calanoida
Calanus	Calanidae	Megacalanoidae	Calanoida
Undinula	Calanidae	Megacalanoidae	Calanoida
Neocalanus	Calanidae	Megacalanoidae	Calanoida
Mecynocera	Mecynoceridae	Megacalanoidae	Calanoida
Calocalanus	Paracalanidae	Megacalanoidae	Calanoida
Oithona	Oithonidae	Oithonidae	Cyclopoida
Corycaeus	Corycaeidae	Corycaeidae	Poecilostomatidae
Lubbockia	Oncaeidae	Oncaeidae	Poecilostomatidae
Pachos	Oncaeidae	Oncaeidae	Poecilostomatidae
Oncaea	Oncaeidae	Oncaeidae	Poecilostomatidae
Copilia	Sapphirinidae	Sapphirinidae	Poecilostomatidae
Sapphirina	Sapphirinidae	Sapphirinidae	Poecilostomatidae
Aegisthus	Aegusthidae	Cervinioidea	Harpacticoida
Clytemnestra	Clytemnesidae	Clytemnesidae	Harpacticoida
Macrosetella	Miraciidae	Miraciidae	Harpacticoida
Miracia	Miraciidae	Thalestroidea	Harpacticoida

Table 4.1: Summary of taxonomic groups used for calculating taxonomic relatedness.

Latitudinal changes in size

Changes in size along the AMT transects were investigated in several ways. The size fractionated counts for the 200 m net samples from AMT 4-6 were used to calculate the proportion represented by each size fraction. The absolute number in each size fraction was also used. For both the proportions and absolute numbers, the means for 5^{o} latitudinal blocks were calculated, excluding the Benguela stations. The mean carbon per individual was calculated by dividing the total carbon by the number of individuals. The mean equivalent spherical diameter (ESD) was calculated in 30 minute bins for the underway data from all six AMT transects. This was plotted with a moving 24 hour average to reduce the diel variation. Latitudinal comparisons were made for the AMTs for these variables.

Latitudinal changes in biomass

The carbon biomass and biovolumes from the 200m zooplankton nets from the transects were converted into mgC m^{-3}, and the latitudinal variation compared for AMT 1-6.

Results

Diversity

Margalef's richness (D_{mg}) for the major groups showed a slight but significant increase towards the equator (Figure 4.1; R^2=0.249, N=162, F=26.46, P<0.001; D_{mg} approximately 6 at the equator, and 4 at the highest latitudes). The scatter was considerable (approx. 3 units). Margalef's richness for the genera showed a much more pronounced dome (R^2=0.652, N=101 F=92.75, P<0.001), with much less scatter. Genera diversity was greatest just north of the equator to the equator with Dmg between 9 and 11), falling off to less than 4 in the south and around 5 in the north (Figure 4.2). The Benguela station

richness was significantly lower than the western Atlantic over the corresponding latitudinal range (Mann-Witney U-test $P<0.0001$), by an average of 4 units, although some were considerably lower than this.

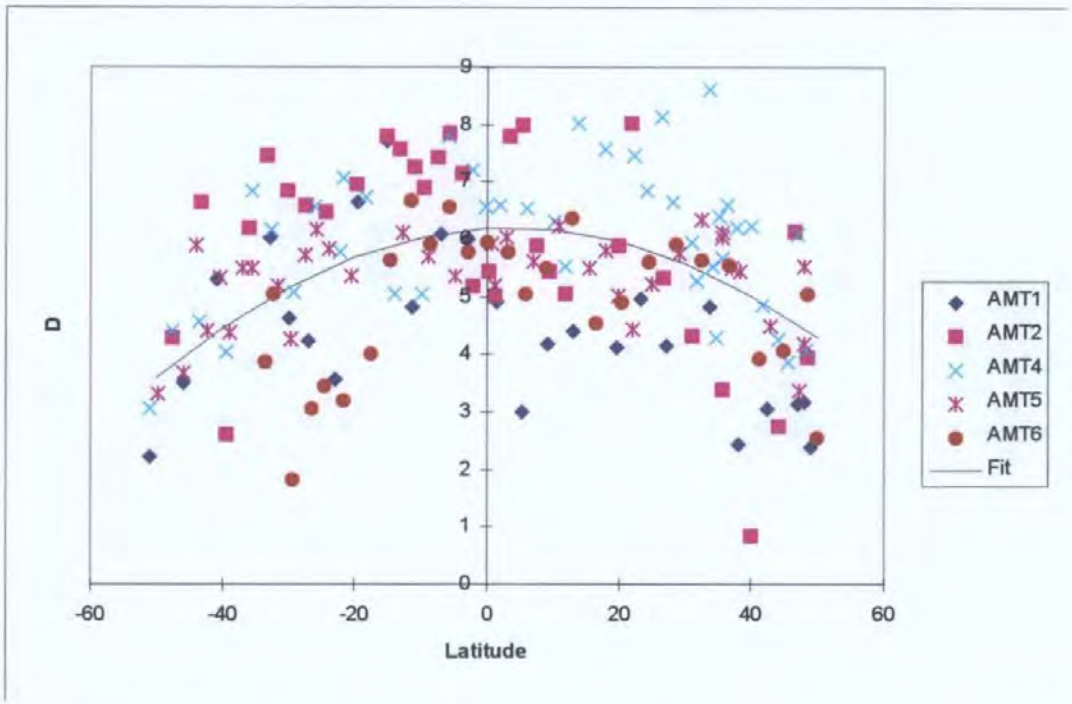

Figure 4.1 The relationship between Margalef's major group richness (D) and latitude for AMT 1,2, 4-6. A order 2 polynomial is fitted. $R^2 = 0.249$, $y = -0.00093 x^2 + 0.0067 x + 6.183$, $F=26.46$, $P<0.001$.

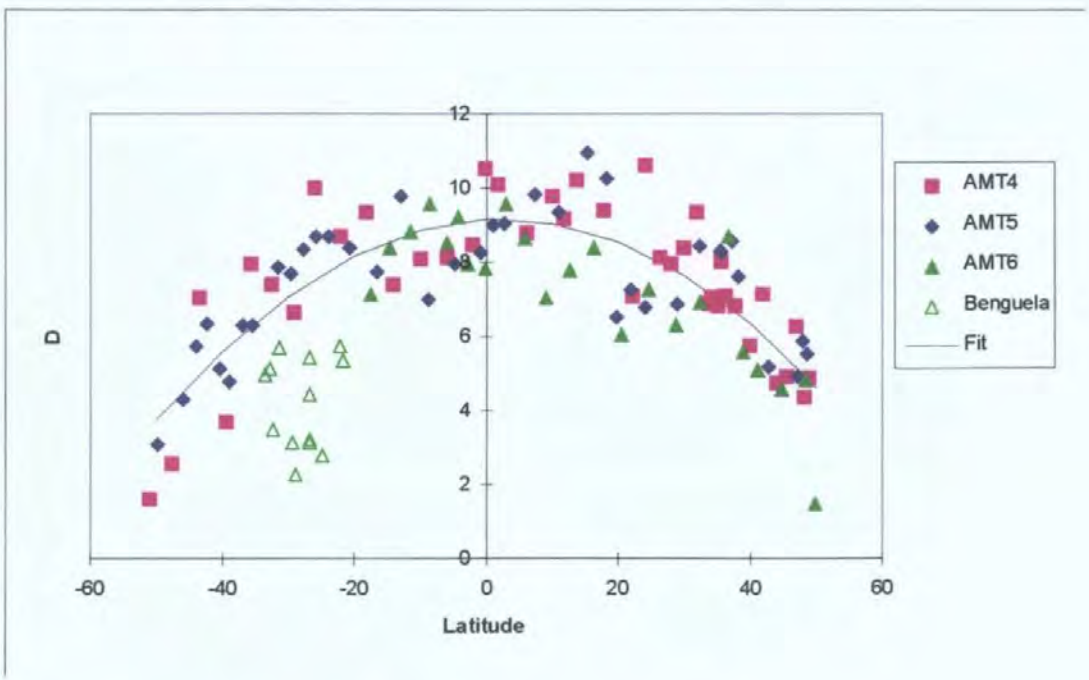

Figure 4.2: The relationship between Margalef's genera richness (D) and latitude for Amt 4-6. A order 2 polynomial is fitted, excluding the Benguela station. $R^2 = 0.652$, $y = -0.0020 x^2 + 0.0085 x + 9.159$,$F=92.75$, $P<0.001$.

The copepod subfamily and family richness in terms of number per sample showed a similar pattern to the copepod genera, although reduction in diversity with latitude was not as pronounced (Figure 4.3). The second order polynomial for family and subfamily was still significant, although the curve was quite flat over the tropical region for the families. But for both the number of families and subfamilies from the Benguela upwelling was considerably lower than for the corresponding latitudes of the open ocean.

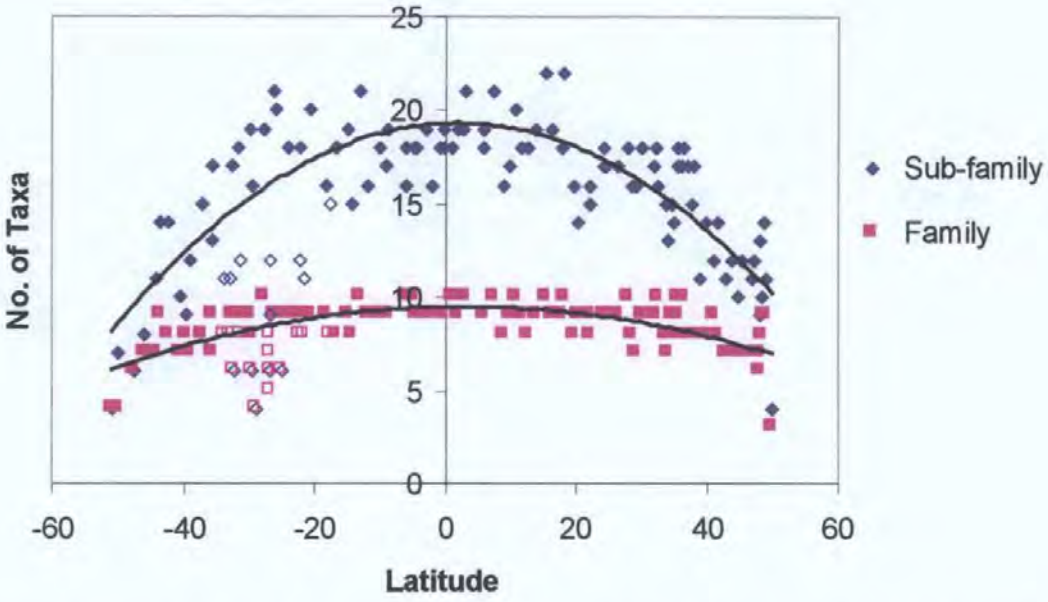

Figure 4.3: Number of subfamily and families along the AMT transect. Unfilled symbols are from the Benguela upwelling and are not included in the 2nd order polynomical fit. For sub-family R^2=0.674, N=100, $y=-0.004x^2+0.007x+19.33$, for family R^2=0.480, N=100, $y=-0.0012x^2+0.007x+9.49$.

For samples grouped in 5° bands, the number of major groups was found to be significantly affected by latitude (R^2=0.629, F=17.17, P=0.0001; Figure 4.4), being maximal in the northern hemisphere at around 25, and dropping south of the equator to approximately 15 at the southern end. The northern end of the transect does not show as pronounced a decline with over 20 groups still being present. The genera showed a reduction in richness at high latitudes, particularly in the Southern Hemisphere (R^2=0.673, F=17.48, P=0.0001; Figure 4.4), from over 35 genera around the equator to less than 20 in the south, and 25 in the north.

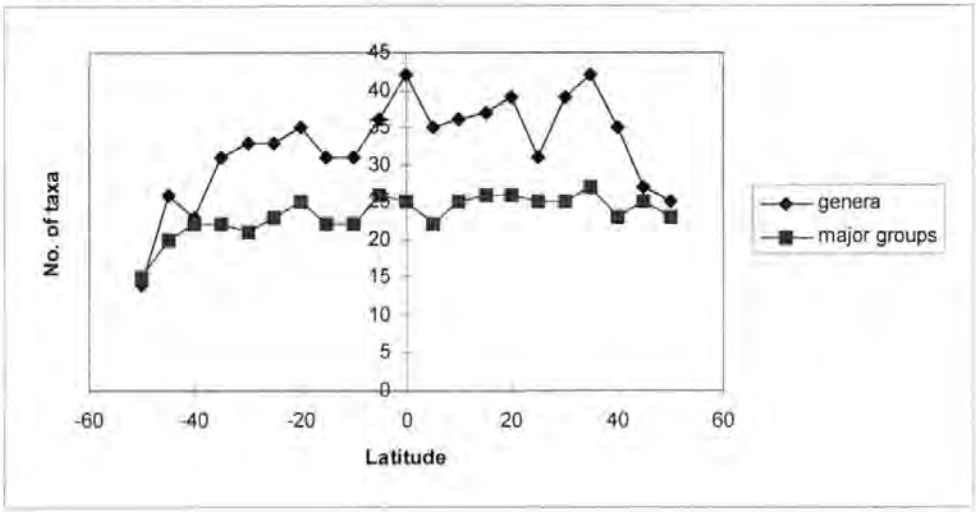

Figure 4.4: Number of genera and major groups along the AMT transect, when the samples are grouped by 5° latitude. For major groups, a second order polynomial regression R^2=0.629, N=19, F=17.17, P=0.0001, $y=-0.00159x^2+0.0571x+24.78$. For genera, a second order polynomial regression R^2=0.673, N=17, F=17.48, P=0.0001, $y=-0.00531x^2+0.0937x+37.06$.

Pielou's evenness for major groups was consistently low across the AMT transects varying between 0.019 and 0.56 (Figure 4.5), as samples tended to be dominated by copepods (Appendix 6). The polynomial regression was significant, but did not explain much of the variance (R^2=0.034, F=3.24, P=0.041). The evenness of the genera was higher and fairly stable at around 0.4 to 0.7 (Figure 4.6). However, at 40 °N there was a reduction in evenness to around 0.3 on all three transects. The second order polynomial was significant but the R^2 was low (R^2=0.127, F=7.23, P=0.0012), suggesting that the trend was not substantial.

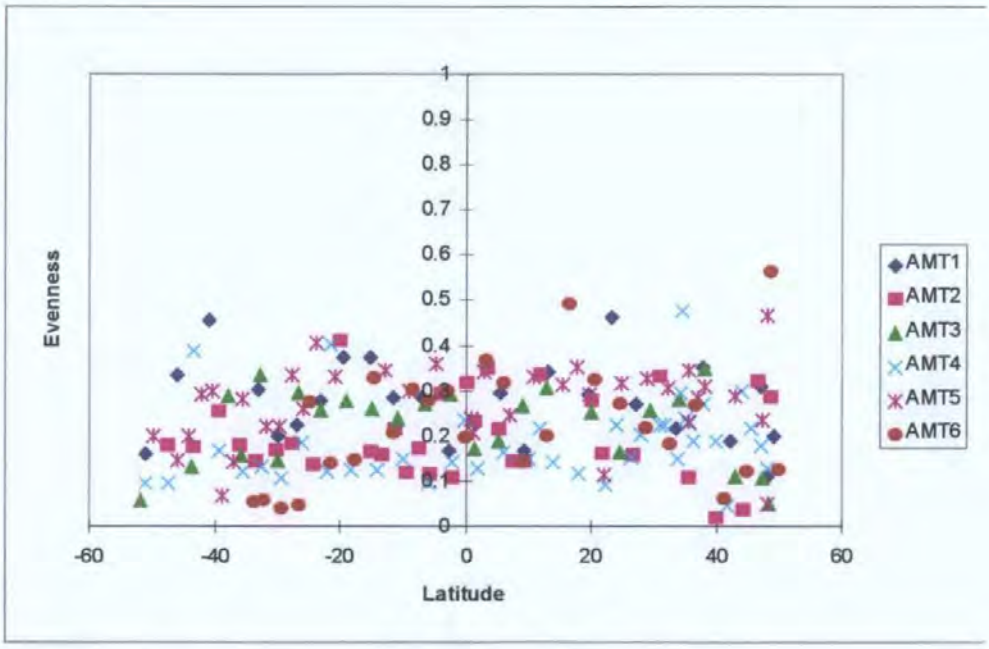

Figure 4.5: Pielou's evenness along the AMT transects for the major groups.

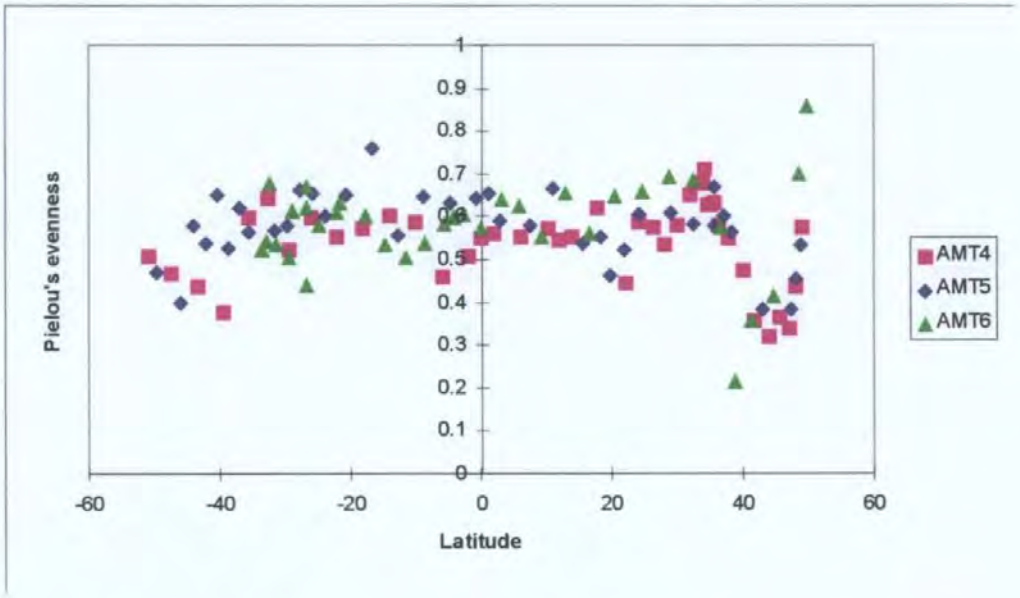

Figure 4.6: Pielou's evenness along the AMT transects for the copepod genera.

Taxonomic distinctness did not show any trend in its mean value across the transect, being consistently high with a mean of 3.2, over a scale of 1 (all the same genus) to 4 (all different suborders; Figure 4.7). However, the Benguela stations tended to show lower taxonomic distinctness, and at higher latitude (>40°) the variability also increased, with some estimates of diversity being similar to those in the Benguela region. The taxonomic diversity was quite consistent up to 35° latitude (Figure 4.8). However, at higher latitudes the diversity dropped

the diversity dropped rapidly, and became more variable. The net samples from the Benguela region showed a similar reduction in diversity and increase in variability to the high latitude samples.

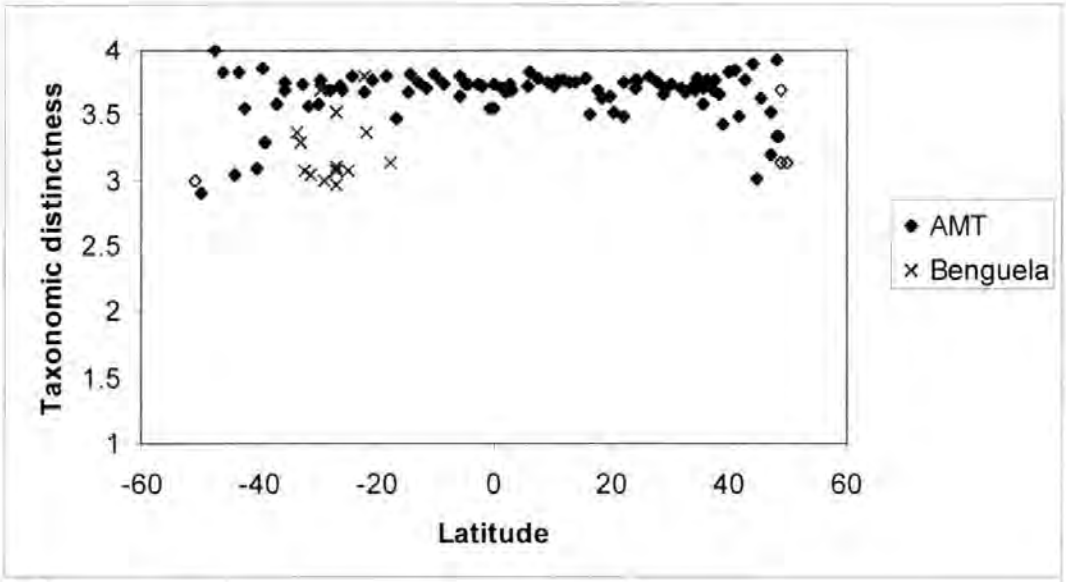

Figure 4.7: Taxonomic distinctness for copepod genera in 200m net samples (open symbols are samples taken on the shelf).

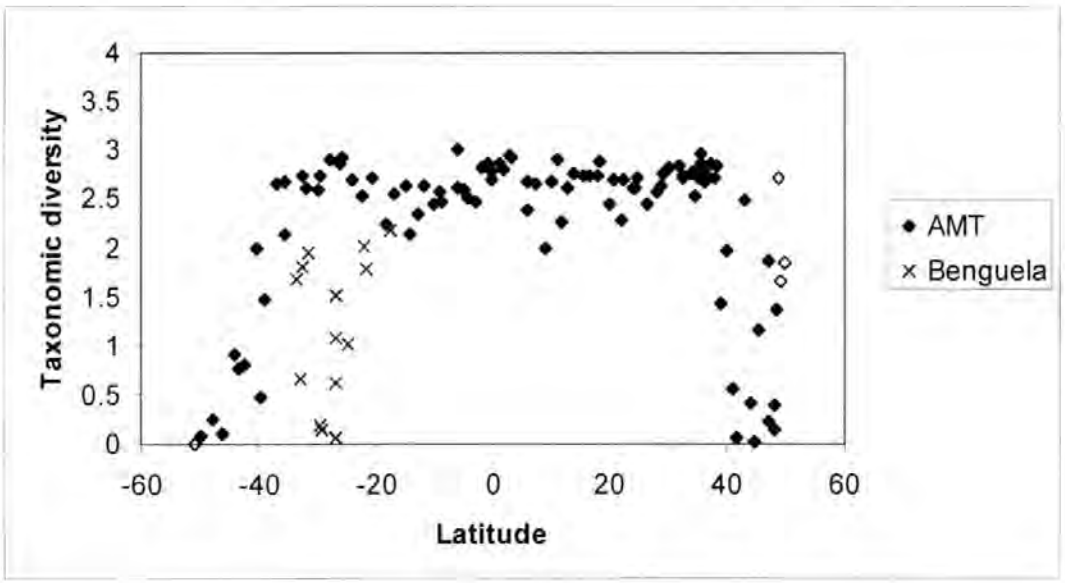

Figure 4.8: Taxonomic diversity for copepod genera in 200m net samples (open symbols are samples taken on the shelf).

Size

For the 200 m size fractionated net samples, neither the percentage in each size class nor the absolute number in each size class suggested any increase in size with latitudinal trend (Figure 4.9 and 4.10). If anything, size showed a decrease in size in the higher northern latitudes. In general, the number in each size class was quite uniform with a few stations with considerably more in. In addition, the proportion in each size was quite consistent, with the smallest size fraction dominating having on average 74 %, and only 1 % in the largest size fraction (Table 4.2). The Benguela stations did, however, have appreciably higher counts in the 500-1000 and 200-500 μm size categories.

Size fraction	Mean counts	Counts S.D.	Mean %	% S.D.
200-500	294	350	74	10.5
500-1000	75	83	20	7.6
1000-2000	17	19	5	4.0
>2000	2.6	4	1	1.3
Total	389	426	100	

Table 4.2: The number in each size fraction with standard deviation (S.D.), and percentage.

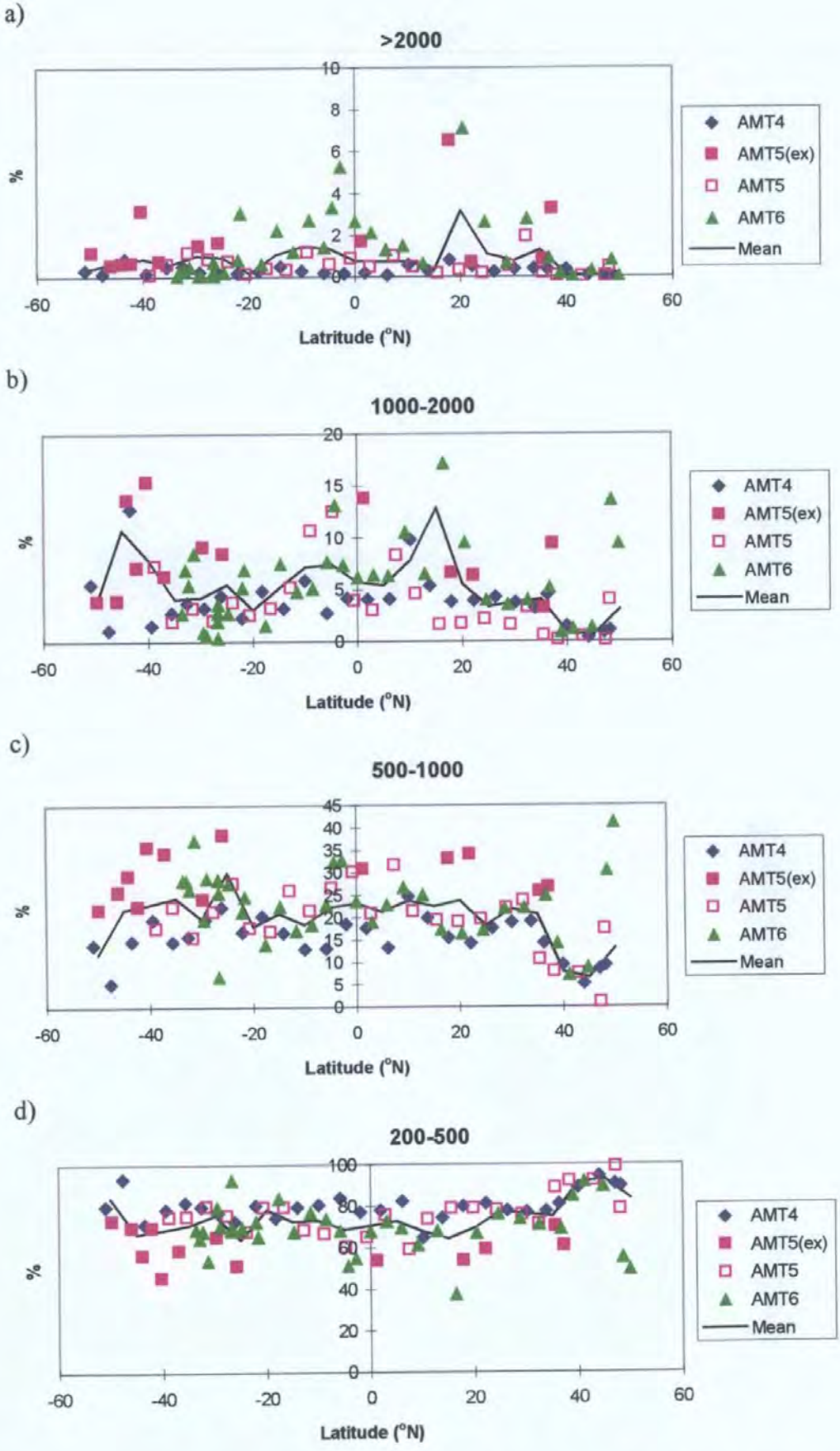

Figure 4.9: Percentage of the total number of copepods in each size fraction for AMT 4-6. a) >2000, b) 1000-2000, c) 500-1000 and d) 200-500 μm. The Mean is an average for 5 ° intervals, not including Benguela Stations. Note the change in scale.

a)

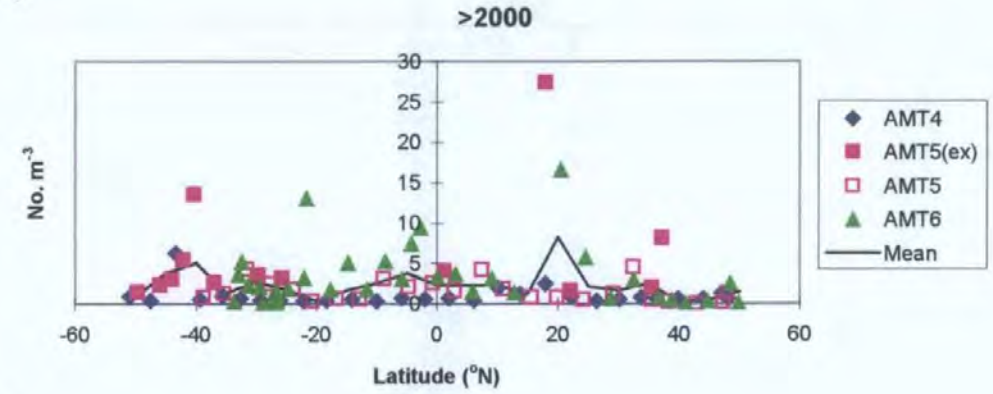

b)

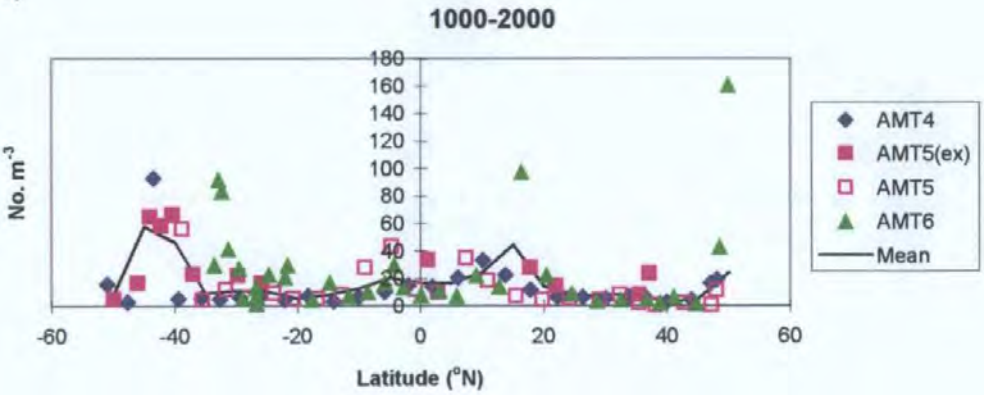

c)

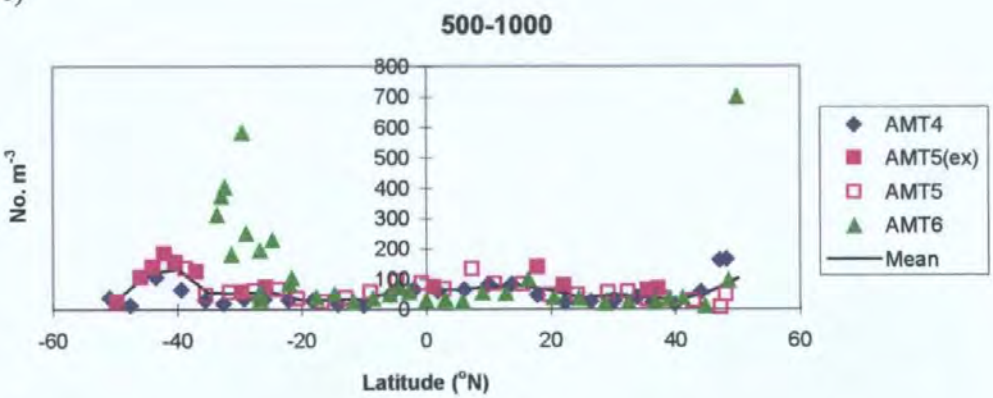

d)

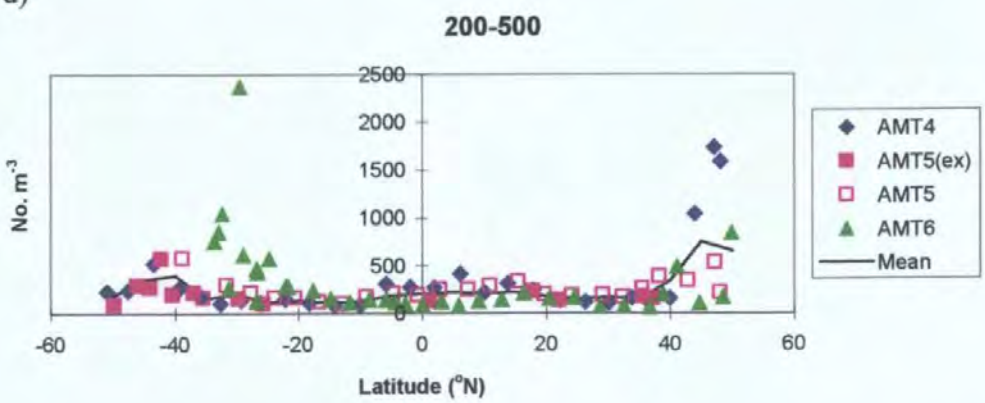

Figure 4.10: The total number of organisms in each size fraction for AMT 4-6. a) >2000, b) 1000-2000, c)500-1000 and d) 200-500 μm. The Mean is an average for 5 ° intervals, not including Benguela Stations.

The mean carbon per zooplankter varied (Figure 4.11), with the inter-quartile range of 0.003-0.01 mg C, and a maximum of 0.047 mg C. Carbon per zooplankter was generally lower on AMT 5 where the > 2000 μm size fraction was not included. AMT 6 showed two peaks in the Southern Hemisphere which were likely to be artefacts, one at 25°S and the other at 17°S. These samples contained large quantities of the large diatom *Coscinodiscus wailesii*, which was not counted. There was a peak at the southern end of the transect, most pronounced on AMT4 (0.03 mg C). The mean carbon per zooplankter was consistently low across the southern oligotrophic gyre, at around 0.01mg C on AMT4 and 0.0025 mg C on AMT5. One of the most pronounced features was a peak in mean zooplankter size between approximately 10 and 25 °N. Further north the mean carbon fell to similar levels to the southern oligotrophic gyre.

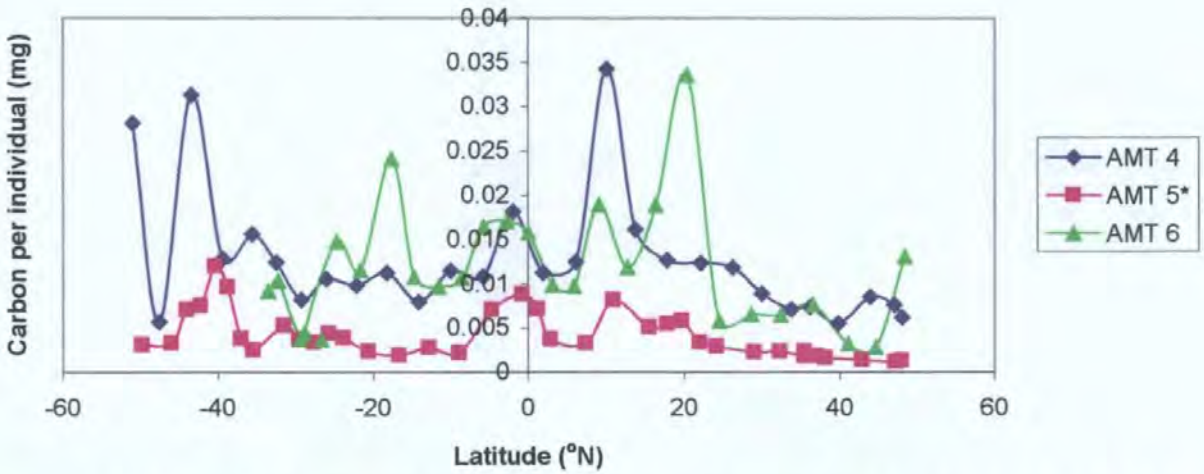

Figure 4.11: Variation in mean carbon per individual along the transect for AMT 4-6. *AMT 5 does not include >2000 size fraction, as no carbon was measured.

The mean size measured in terms of equivalent spherical diameter (ESD) using the OPC calculated in 30 min time bins for the surface underway data showed a substantial diel variation (Appendix 5). The 24 hr moving average ESD was quite consistent across the transects, generally between 400 and 600 μm. The daily minimum ESD is even more consistent along the transects, being around 350 on AMT 1-3 and 400 μm on AMT 4-6. However the 24 hr moving average showed a slight increase towards the southern end of

the transects. The increase in mean ESD was more pronounced in the odd numbered AMTs i.e. the austral spring.

Latitudinal changes in biomass

The zooplankton total biomass in the top 200m as measured by carbon and biovolume showed a consistent pattern along the AMT transects, which was similar for the two methods (Figure 4.12 and 4.13). High and highly variable biomass estimates (0.1-22 mg C m^{-3}, 10-350 mm^3 m^{-3}) were found at either end of the transects (>40°N/S). Between 38°S and 8 °S, and 40°N-20°N, the biomass is consistently low (0.2-3 mg C m^{-3}, 6-50 mm^3 m^{-3}). In the equatorial region (8°S-24°N) some quite high biomass estimates were found (0.6-13 mg C m^{-3}, 20-120 mm^3 m^{-3}, with one very high biovolume 650 mm^3 m^{-3}), and in the Benguela region (AMT 6, 40-15°S) the biomass estimates were high and variable (1-20 mg C m-3, 20-230 mm^3 m^{-3}).

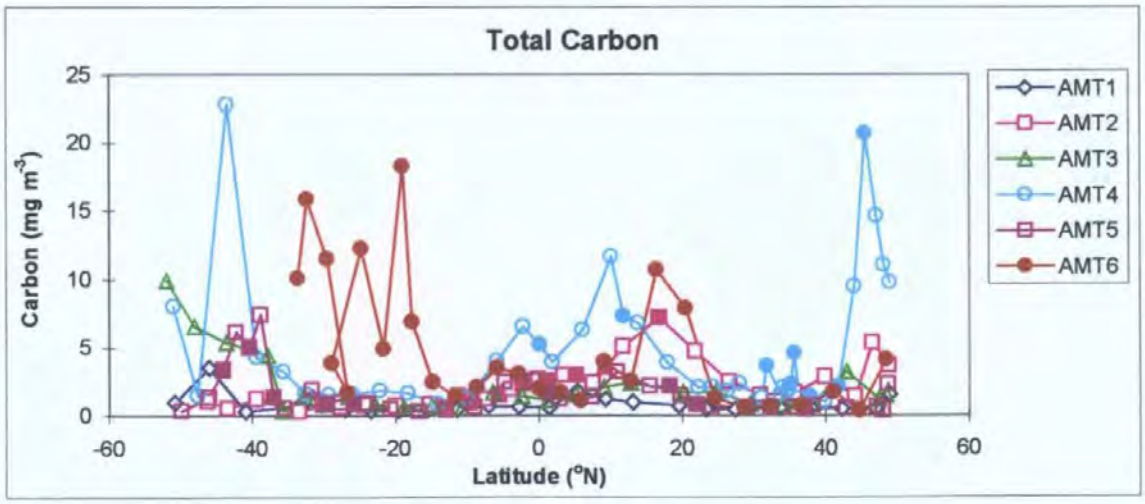

Figure 4.12: The pattern of zooplankton carbon from 200m nets along the AMT. AMT 5 does not include >2000 size fraction, as no carbon was measured.

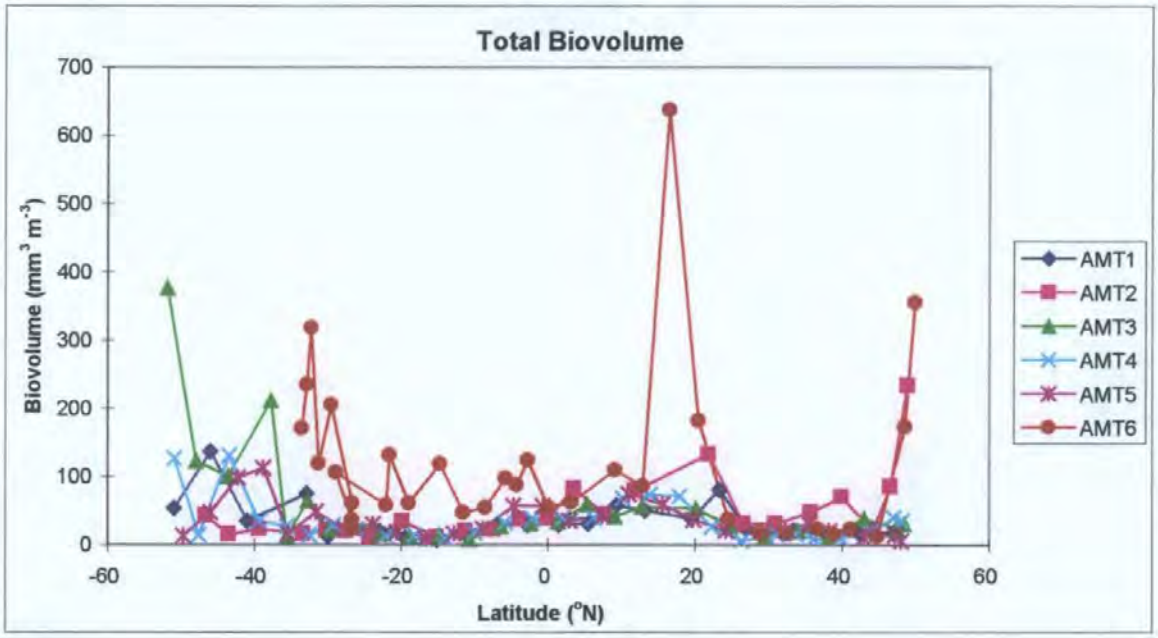

Figure 4.13: The pattern of zooplankton biovolume from 200m nets along the AMT.

Discussion

Diversity

An obvious trend can be seen in the diversity with latitude due to the taxon richness of the zooplankton, even observable in the major groups. Bé and Forns (1971) found a similar trend in zooplankton groups for the North Atlantic. They found that although all groups were found across the Atlantic, in any sample the most groups were found in the central Atlantic gyre where over 16 out of 27 groups occurred, whereas in temperate waters 12 or less groups were found. The copepod genera showed a more pronounced trend in richness, with Margalef's richness falling from around 9 at the equator to less than 5 at 40°. The copepod family and subfamily richness showed a similar latitudinal trend, although, not as pronounced as the genera. This demonstrates a generally observed trend found by others (e.g. Reid *et al.* 1978, Angel 1997a), that the diversity is more greatly effected with more detailed taxonomic resolution, so that species would be expected to show an even clearer trend with latitude. As the pattern of richness is maintained after grouping into 5° bands, it can be considered that it is not just the density of groups and genera which is effected by

latitude, but that the richness of the community is reduced at high latitudes. Data from the literature and from unpublished works (Table 4.3), suggested that the richness in the copepod community continues to decline at high latitudes (Figure 4.14). In addition, the latitudinal trend appears quite strong, becoming more pronounced at greater than 40° N/S, and is similar in northern and southern hemispheres.

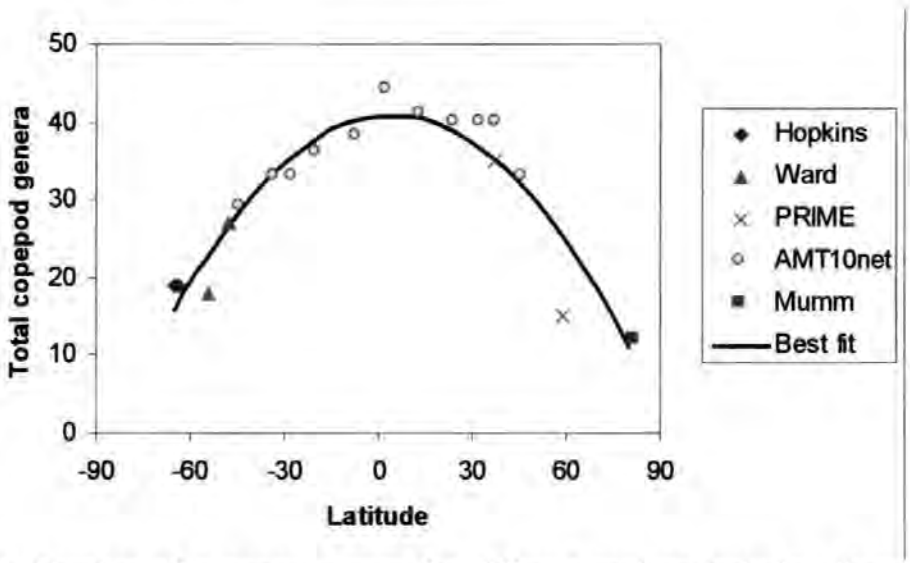

Figure 4.14: Number of copepod genera for different regions including literature data, showing the pattern for the Atlantic, details in table 4.3. AMT as 10 net totals. Best fit 2nd order polynomial $y=-0.0052x^2+0.045x+40.76$, $R^2=0.872$.

Author	Latitude	Location	Net
Hopkins (1985)	64°S	Croker Passage, Antarctic Peninsula	162 μm mesh present in top 200m
Hopkins and Torr (1988)	64°S	Weddell Sea (48°W)	162 μm mesh present in top 200m
Ward (unpublished)	48-51°S 52-53°S	Falklands –Polar Front Polar Front-South (38-43°W)	WP2 200μm mesh 0-200m
PRIME (unpublished)	59°N and 35°N	N. Atlantic (20°W)	WP2 200μm mesh 0-200m
Mumm (?)	82-85°N	Nansen Basin, Barents Sea	300 μm mesh multinet 0-200m

Table 4.3: Details of source data used for extended transect.

The samples from the Benguela upwelling region (AMT 6) showed lower diversity in terms of richness than those samples from the open ocean, most obviously observed in the copepod genera (Figure 4.2), as proposed by Angel (1997b). Piontkovski *et al.* (1997) found that the diversity of copepods increased further offshore from the Benguela upwelled

waters. The reduction in diversity could be caused by the system being considered to be 'immature', with frequent newly upwelled water being considered as a 'new' ecosystem, starting succession. Immature, newly formed ecosystems tend to be low diversity (Whitaker 1975). As the water moves off shore, the system matures and species richness increases. However, the system is more complex with specialist species able to exploit the high productivity of the system, and maintain themselves within the coastal zone. *Calanoides carinatus* is typical of upwelling systems, and its lifecycle appears to be adapted to allow maintenance within the Benguela upwelling (Verheye *et al.* 1992). Angel (1997b) also suggested that the dominance would increase in upwelling areas. Dominance is the inverse of evenness, so that we would expect to see a reduction in the evenness for Benguela samples. This is not at all obvious from the copepod genera, although the major groups' evenness from the Benguela did tend to be particularly low, mainly in the Southern Benguela (AMT6, south of 28° 40'S) where Pielou's evenness was less than 0.1 (Figure 4.5).

The evenness along the oceanic transect did not show a latitudinal gradient for either genera or major groups. The evenness of the major groups was consistently low along the transect. The samples were heavily dominated by copepods, generally making up around 80% by number (appendix 6). The evenness of the genera became less consistent at the southern end of the transect, showing a slight decline. However, the most noticeable feature was the sharp fall in the evenness at around 40-45 °N on all three transects. This appears to be due to an increase in abundance of the small copepods *Para/Pseudocalanus*, *Oithona* and *Oncaea* (appendix 7). This is in the region of the Azores front. Perhaps the enhanced primary production is being exploited by the small fast growing copepods.

Taxonomic distinctness was generally high throughout the transect, close to its maximum of 4. This suggests that the different levels were consistently represented. Some samples

lower taxonomic distinctness at higher latitudes, but not all. Taxonomic diversity which incorporates all three facets of diversity (richness, abundance and distinctness) was quite stable for much of the transect (35 °S-35 °N). However, in the temperate regions, the diversity dropped dramatically. This reduction in taxonomic diversity is seen in the extensions of the AMT transect north and south (Figure 4.15). However, there are still samples with relatively high taxonomic diversity, even at these extremes. In fact, there may be a slight increase in the mean diversity south of 55 °S in the circumpolar current. This current links the oceans and therefore may enhance diversity through incorporating genera from other ocean basins.

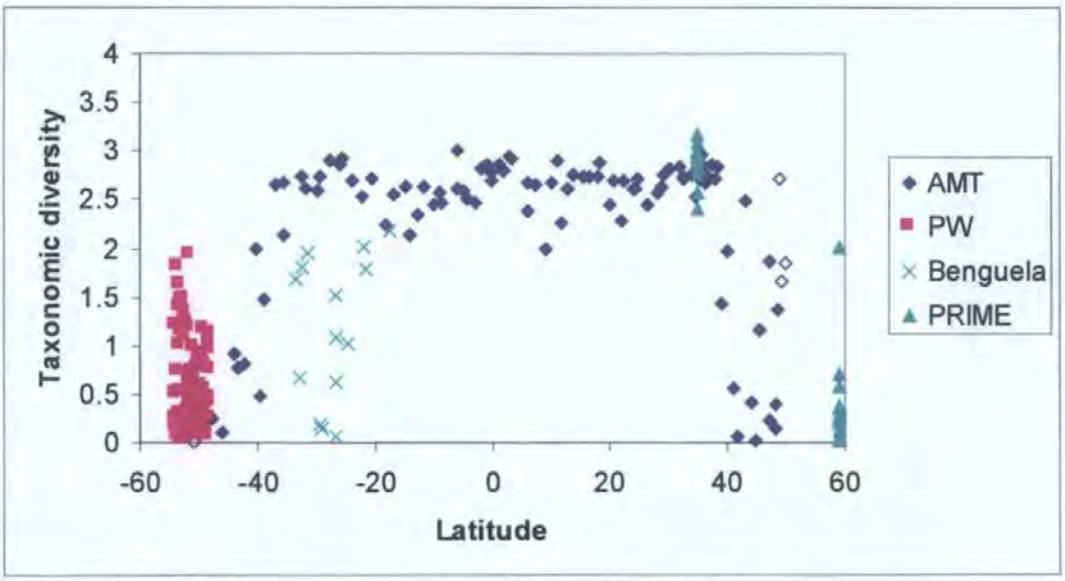

Figure 4.15: Taxonomic diversity along the transect, extended with unpublished data from Dr Peter Ward, and the PRIME cruise (analysed by Dr Alistair Lindley).

The variability of the sample diversity in richness for copepod genera or major groups showed no clear latitudinal trend. The evenness showed an increase in range in the high latitudes of the southern hemisphere for the copepod genera and to a lesser extent at either end of the transect of major groups. However, for the taxonomic distinctness, at greater than 35 °, the variability in the distinctness increased, with some samples having substantially lower distinctness (<3). These three factors combined to give much higher variability in the taxonomic diversity at high latitudes. This, with the drop in diversity,

emphasises the change in the communities in the temperate regions as compared to the warm-water regions.

Several theories have been proposed to explain latitudinal gradients. Rutherford *et al.* (1999) suggested that sea surface temperature was more closely related to diversity than latitude, at least for oceanic foraminifera. Comparing the number of genera per samples to the temperature at the surface (Figure 4.16), it can be seen that sea surface temperature is closely related to diversity with an R^2 of 0.66 for AMT data. Rutherford suggested a non-linear relationship between temperature and diversity, although there is no evidence for that from the AMT copepod species richness, or any theoretical basis to predict the shape of the curve. Rutherford's relationship would approximate to linear between 7 and 22 °C, but higher than this the diversity is reduced. Northern and southern samples follow the same relationship. Extension of the transect south of the Falklands to lower temperatures, does suggest a reduction in the slope at these low temperatures. The Benguela data does lie closer to the regression line, but still tend to fall below it, suggesting that although temperature may predict some of the reduction in diversity, other factors are likely to be important.

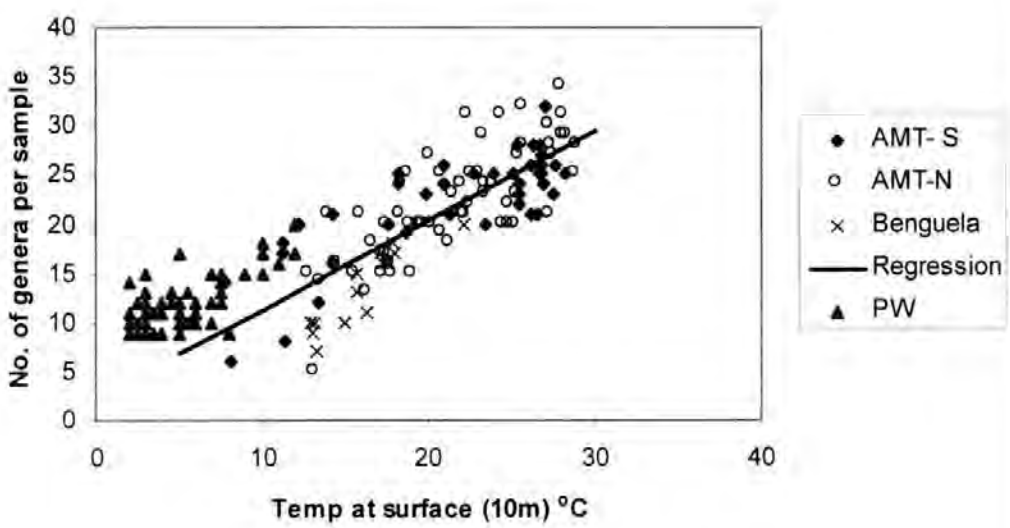

Figure 4.16: The relationship between sea surface temperature and species richness for AMT data. Linear regression y=0.907x+2.224, R^2 = 0.66. In addition data from Falklands to Antarctica (48-53 °S) made available by Dr Peter Ward (BAS) taken with 200 m WP2 nets is shown (PW).

The relationship of temperature with taxonomic diversity is more complex (Figure 4.17). The Benguela stations are not distinguishable from the other AMT stations and an increase in diversity is associated with an increase in temperature. However, the change does not appear to be linear, and the drop in diversity starts at around 18-19 °C. This corresponds to a latitude of approximately 38 °N/S. Northern and southern samples appear to show the same pattern, although some of the southern stations are at lower sea temperatures. Thus it appears that copepod diversity is not primarily determined by temperature, although some aspects may co-vary. Data from south of the Falkland Islands demonstrates an apparent increase in diversity at less than 5 °C, suggesting at the lowest temperatures, species richness is not related to sea surface temperature. These lowest temperatures are found south of the Polar Front in the circumpolar current. As the name suggests, the current is continuous around Antarctica, joining all the ocean basins. The Atlantic is the youngest of the ocean basins and also tends to have lower diversity (particularly compared to the Pacific, e.g. Ekman 1953). It is therefore possible that the circumpolar current is richer due the increase in the richness of the species pool available from the other ocean basins. Rutherford *et al.* (1999) proposed that sea surface temperature was an indicator of the water column structure, and this was related to niche availability. However, this hypothesis makes several assumptions, for which there is little evidence.

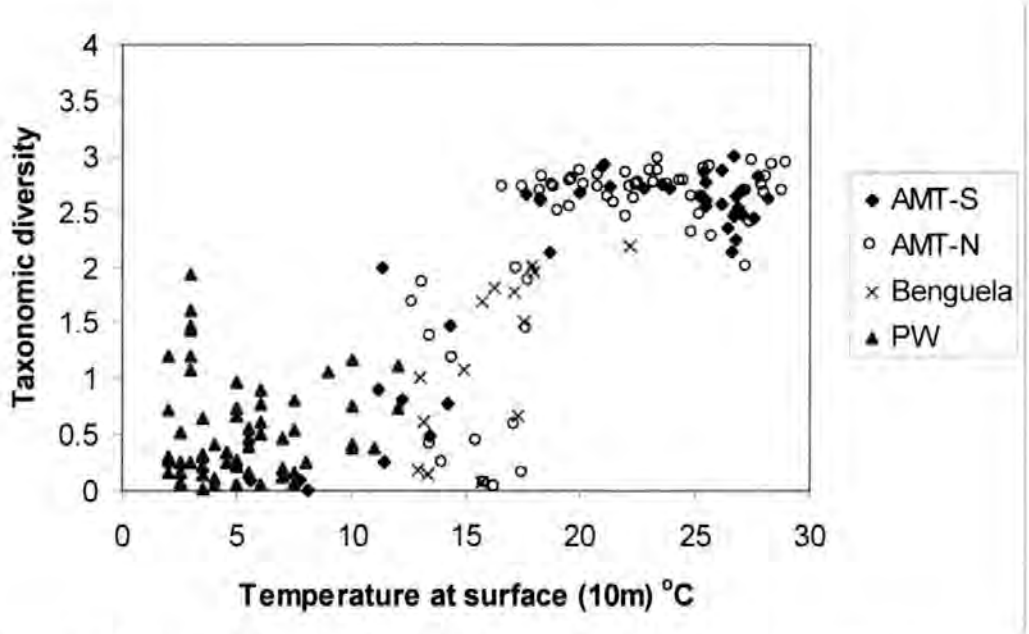

Figure 4.17: The relationship between sea surface temperature and taxonomic diversity. In addition to AMT data, data from Falklands to Antarctica (48-53 °S) made available by Dr Peter Ward (BAS) taken with 200 m WP2 nets during the austral summer is shown (PW).

Although temperature may be related to the gradient in diversity, it does not explain the underlying cause. Others have invoked past events such as ice-ages as mechanisms determining the gradient (Angel 1997a). However, zooplankton are not bound by physical barriers within ocean basins. Between ocean basins there is evidence of restriction with the Pacific tending to be the most diverse and the Atlantic the least (Ekman 1953). Temperature and salinity regimes may restrict high latitudinal species from mixing with species at the opposite pole, but this does not explain the cline in diversity. Seasonality is a co-variant with latitude, and will have a profound effect on the water structure and primary productivity cycles. In tropical regions productivity is low over the whole year. In temperate regions, productivity is pulsed being highest in spring, dropping with a second lower maxima in autumn before falling to close the zero over winter. At higher latitudes, the winter period of close to zero productivity is extended until only one maxima in productivity is observed. Particular life strategies are employed to allow survival and exploitation of the seasonal cycles. The more extreme the seasonality, the more adaptations are required. Close to Antarctica, large fat storing copepods such as *Calanus*, *Calanoides* and *Rhincalanus*, which may have diapause stages, are prevalent (Raymont 1983). Life

history strategies such as these will not prevent survival at lower latitudes. Thus new taxa utilising these strategies will not be prevented from invading the warmer waters. The Benguela upwelling shows lower diversity, and at least in the south it is seasonal (Verheye *et al.* 1992). In addition, copepods may require specific adaptations to enable maintenance and survival in this dynamic region.

Size

The size of zooplankton, indicated by the number and particularly the proportion in each size class taken from 200 m net samples is remarkably stable along the AMT transect, with around 74% in 200-500, 20 % in 500-1000, 5 % in 1000-2000 and 1% >2000 μm, and does not show an obvious trend with latitude. An increase in size has previously been most marked at the very high latitudes, in the polar and subpolar seas (e.g. Reid *et al.* 1978). These areas were not sampled on the transects. In addition, the northern and southern extremes of the transects have been in shelf seas and coastal waters, which have very different communities as demonstrated by those stations from the Benguela region. Another possible explanation is that the larger copepods frequently undergo diel migration, rising towards the surface at dusk, and sinking at dawn. As most of the net samples were taken during the day, many of the larger zooplankton would be expected to be below 200m. Future inclusion of more night stations and deeper net samples, possibly with open-ocean, high latitude stations is required to distinguish these hypotheses.

The mean carbon per individual did show a pattern, with high carbon, suggesting large individual size, at the southern end of the transect. Low individual size across the southern oligotrophic gyre, rising around the equator and a large peak around 20 °N, possibly associated with the West African upwelling, and small size in the northern oligotrophic gyre. This is consistent with the view that small copepods are thought to dominate the zooplankton of the oligotrophic gyres (e.g. Piontkovski and Van der Spoel 1997). It has

been proposed that more productive areas have large zooplankton (Thiel 1975). The latitudinal pattern does show that in the areas of high zooplankton biomass, the mean zooplankter size is larger. Comparing directly biomass and mean zooplankter size (Figure 4.18), it can be seen that there is a significant relationship (R^2=0.57), although there is substantial scatter, particularly for AMT 6. High carbon estimates on AMT 6 may be due to substantial phytoplankton contamination (e.g. *Coscinodiscus* and *Phaeocystis*).

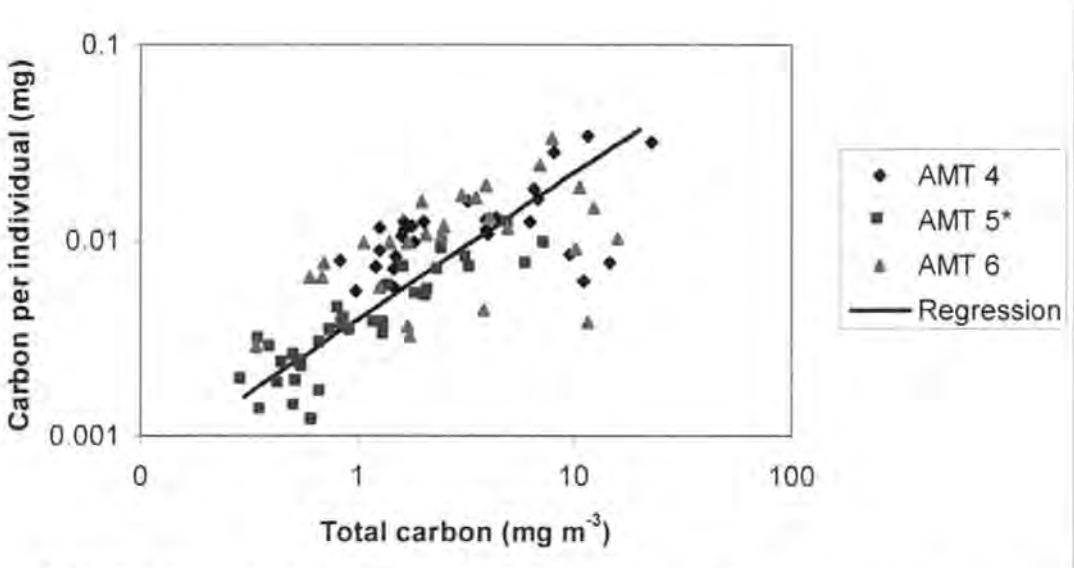

Figure 4.18: Total zooplankton carbon from 200m net samples compared to mean carbon content per individual, on a log scale. The regression is a functional regression y*=0.747x*-5.545, where y* is Ln (total carbon), and x* is Ln(carbon per individual), and R^2 =0.567.

The underway mean ESD showed considerable small scale variability, mostly associated with diel variation. The daily mean ESD was quite consistent across the transects, generally between 400 and 600 μm. The minimum ESD is even more consistent along the transects, being around 350 on AMT 1-3 and 400 μm on AMT 4-6. This suggests that the population of small zooplankters remains in the surface waters throughout the transects, and at night the larger zooplankters migrate to the surface. However, on the austral spring cruises (AMT 1, 3 and 5) an increase in the daily mean ESD at the southern end of the transects was observed. This is likely to be due to an increase in large copepods migrating to the surface at night, and feeding on spring phytoplankton blooms. It is unclear why a similar trend is not seen in the north. It could be linked to patterns of seasonal vertical migration of

large copepods. Several species of large copepods have been shown to overwinter at depth (e.g. Richter 1995, Schnack-Schiel and Hagen 1995).

Zooplankton carbon and biovolume follow a consistent pattern across the transect. The highest biomasses occur at either end of the transects (>40°), and also in the Benguela region. They vary considerably, typically being between 5 and 25 mgC m^{-3}, 500-5000 p.p.b. Estimates for the temperate North Atlantic vary over a similar range (e.g. Longhurst and Williams 1992, Dam *et al.* 1993, Lenz *et al.* 1993). The Benguela region zooplankton carbon are comparable with values reviewed by Verheye *et al.* (1992), although higher biomasses would be expected in the southern Benguela during the austral summer when upwelling is maximal. The equatorial region also tended to have quite high biomasses (3-13 mgC m^{-3}). In between, in the oligotrophic gyres, the biomass was low and stable between 0.2 and 3 mgC m^{-3}. Bé and Forns (1971) found dry weight to be less than 5 mg m^{-3} for the top 100 m of the northern tropical gyre. Given carbon is equivalent to approximately 40 % of dry weight (Lovegrove 1966), these are very similar.

4.2 Global Provinces

Introduction

There have been several attempts to divide the world's oceans according to its characteristics dating back to the earliest oceanographers. Ekman (1953) produced a world scheme that included most of the worlds regions. Others have produced different schemes for parts of the oceans or for particular organisms, generally based on a composite of data from a wide variety of sources. The relationship between the pelagic organisms and the physical environment has also been attempted particularly with respect to the water masses (e.g. Van der Spoel and Heyman 1983, McGowan 1974). More recently, Longhurst (1998) has developed a system of biogeochemical biomes and provinces based on the production regimes throughout the world oceans.

The AMT transects cross several oceanographic regions, providing an extensive survey of the Atlantic sampled consistently. This provides a very strong database to investigate zooplankton community structure. Copepods dominate the zooplankton so form a meaningful test group for taxonomic regions as well as the less detailed major groups. The size structure may give a quick way of recognising zooplankton communities, as well as allowing inferences about the community properties. Specific aims include:

- Do zooplankton form large scale regions of similar community structure in terms of major groups, copepod genera and size structure?
- How do these areas compare with each other and with published schemes?
- How are these regions defined?

Data Analysis

Taxonomic regions

The AMT 4-6 200 m net samples analysed for genera and major groups, formed the basis of taxonomic regions analysis (Appendix 6 and 7). Major groups from AMT 4-6 200 m net samples were transformed (root and double root), and used to produce a Bray-Curtis similarity matrix between samples. The mild root transformation still maintains much of the abundance information and emphasises the common taxa, whereas the double root transformation reduces the effect of the abundance, and emphasises the rarer species. The Bray-Curtis similarity index is recommended for taxonomic data, although choice of similarity index tends to have less effect on the matrix than the transformation (Clarke and Warwick 1994). Multidimensional scaling (MDS) was carried out on the similarity matrix, using PRIMER (Plymouth routines in multivariate ecological research), a package based on non-parametric statistics suitable for taxonomic analysis. Groupings were identified from the ordination by identifying clusters of similar latitudes, so that latitudinal regions were defined. This was repeated using the copepod genera data from AMT 4-6. MDS was repeated on temperate with Benguela, and tropical stations for copepod genera separately, allowing greater detail to be observed within each of these areas. Cluster analysis was not used as the similarities were too variable, and formed more of a gradient than totally separate regions.

Analysis of similarity (ANOSIM) was carried out on the derived regions to see if these apparent groupings were all different from each other. Similarity of percentages (SIMPER) was used to examine which genera were significant in determining the groups of stations.

Comparisons of groups with published areas

The regions from different schemes in the literature were compared. Their ability to describe the pattern of genera similarities was calculated by taking the boundaries where the AMT transect crossed, and using ANOSIM to test the significance of the regions for double root transformed Bray-Curtis similarities of the copepod genera.

OPC groups

The OPC 200m net data were converted into $\log_2$ biovolume size classes for AMTs 4-6. The data was standardised to give equal weighting to each size class, (but untransformed), and principal components analysis (PCA) was carried out on it, to investigate latitudinal changes. PCA is easier to interpret than MDS, as the factors are derived directly from the size classes. However, violations of normality weaken its strength. MDS was also carried out after double root transformation and standardisation to provide an alternative scheme.

The underway data from AMTs 1-6 was converted onto the $\log_2$ biovolume size classes in 30 minute bins. Part files, less than half the bin length, were deleted. Daily averages were calculated (midnight to midnight). The daily averages were double root transformed to normalise the data, and standardised to give equal weighting to each size class. PCA was carried out on this. The first three principal components were plotted against latitude. Multidimensional scaling (MDS) was carried out using Euclidean distance on the double root transformed standardised data for AMT 3-6, as the package had a maximum of 125 samples, and this included two autumn and two spring cruises. ANOSIM was used to discover if the size structure was related to the latitudinal regions defined using the station genera. The regions developed by Backus (1986) were also tested using ANOSIM. Finally, this was modified by comparing with the MDS plot, and the improvement tested with ANOSIM.

Results

Taxonomic regions

The major groups did not show very distinctive groupings either root or double root transformed (Figure 4.19). However, the higher latitude stations with those from the Benguela region were scattered around a core of tropical and subtropical stations. The Benguela stations were more similar to the southern temperate stations than the northern temperate stations for the root transformed similarities.

In contrast to the major groups, the copepod genera showed a clear distinction between the temperate with the Benguela stations and subtropical-tropical stations both for the root and double root transformed similarities (Figure 4.20). The tropical-subtropical group (38°N-38°S) were much tighter, more similar, than the temperate and Benguela group. The separate MDS plot for temperate and Benguela stations showed that the Benguela stations are different, even though they do not form a totally separate group, but there was no obvious difference between the northern and southern temperate (Figure 4.21). The tropical and subtropical MDS ordination is harder to interpret (Figure 4.22). However, there do appear to be some latitudinal groupings. The subtropical stations (19°-39 °N, 29 °-39 °S) appeared to partially separate from the tropical stations (18 °N-28 °S). The tropical stations showed some separation into equatorial (8°S-18°N) and southern tropical (8°-28°S).

a)

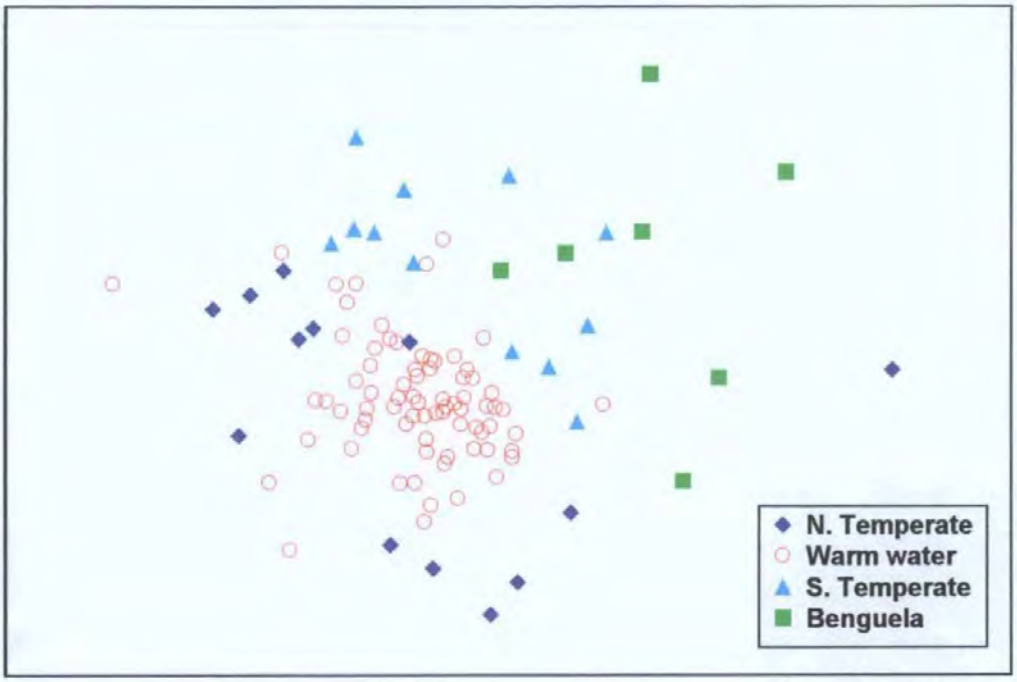

b)

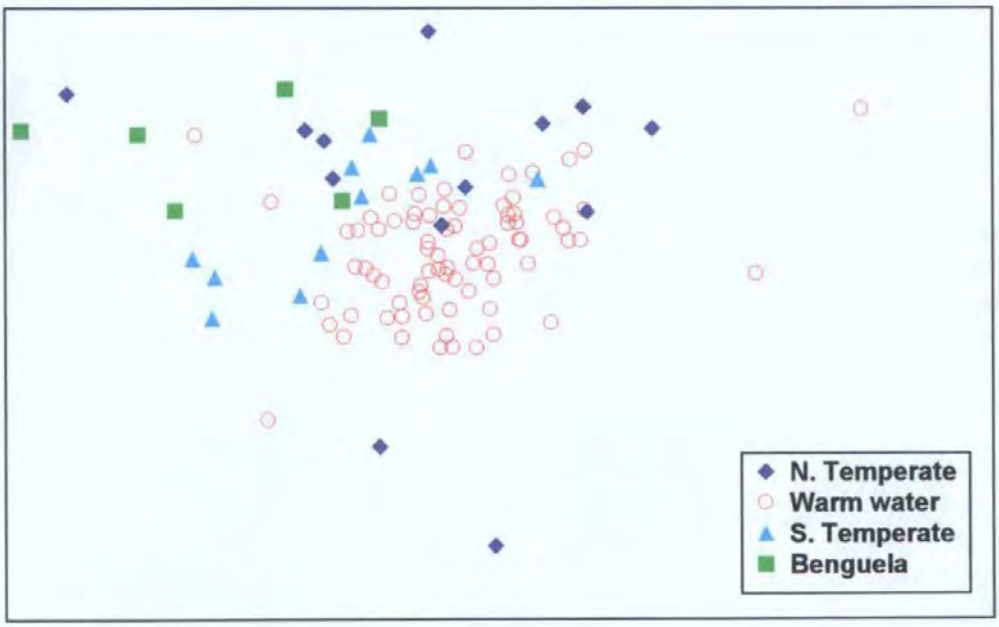

Figure 4.19: MDS ordination for major groups (AMT1-6), Bray-Curtis similarity a) Root transformed, stress = 0.13 b) double root transformed, stress = 0.21. Temperate is taken as $> 40^{o}$.

a)

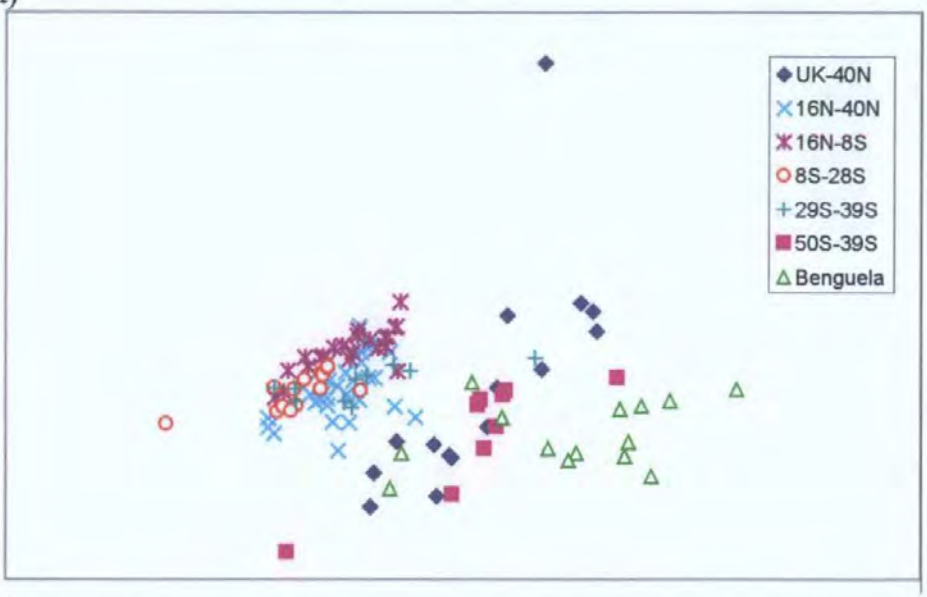

b)

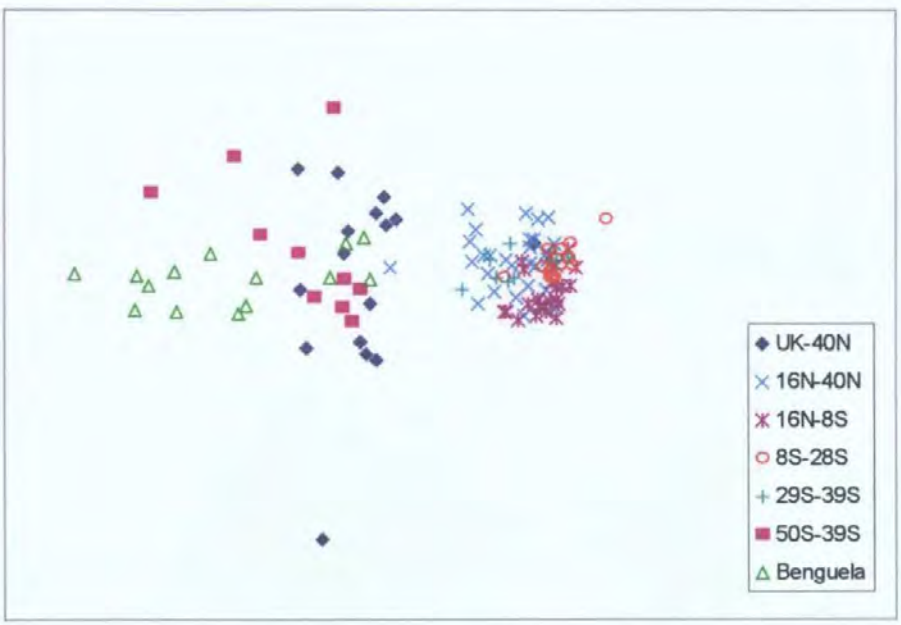

Figure 4.20: MDS ordination for copepod genera (AMT4-6), Bray-Curtis similarity a) Root transformed, stress = 0.12 b) double root transformed, stress = 0.14.

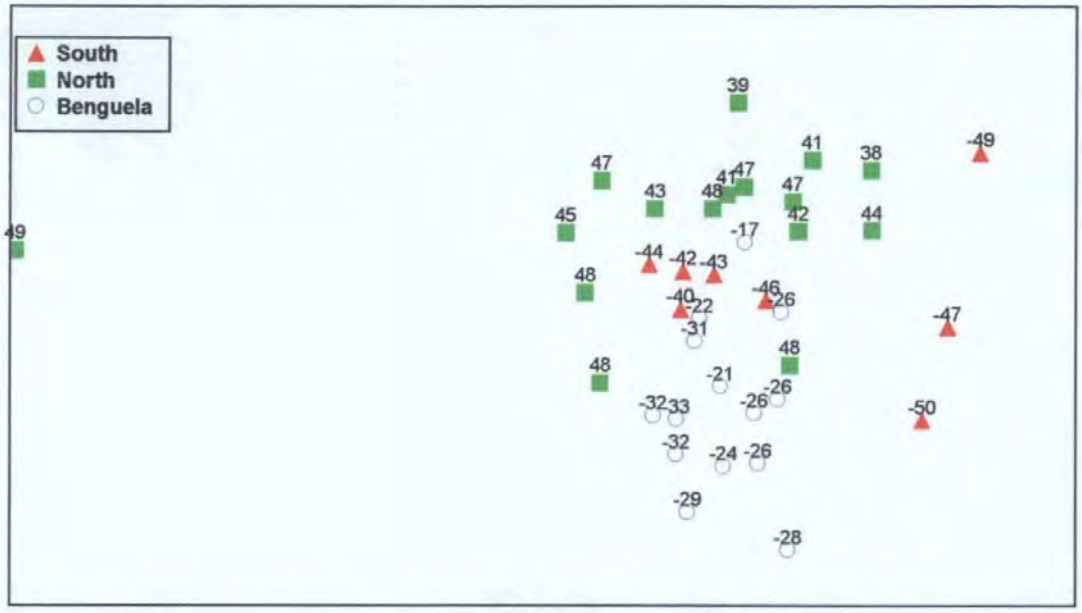

Figure 4.21: MDS ordination for copepod genera (AMT4-6) for temperate and the Benguela stations, Bray-Curtis similarity double root transformed, stress = 0.14. Latitude is shown above the symbol.

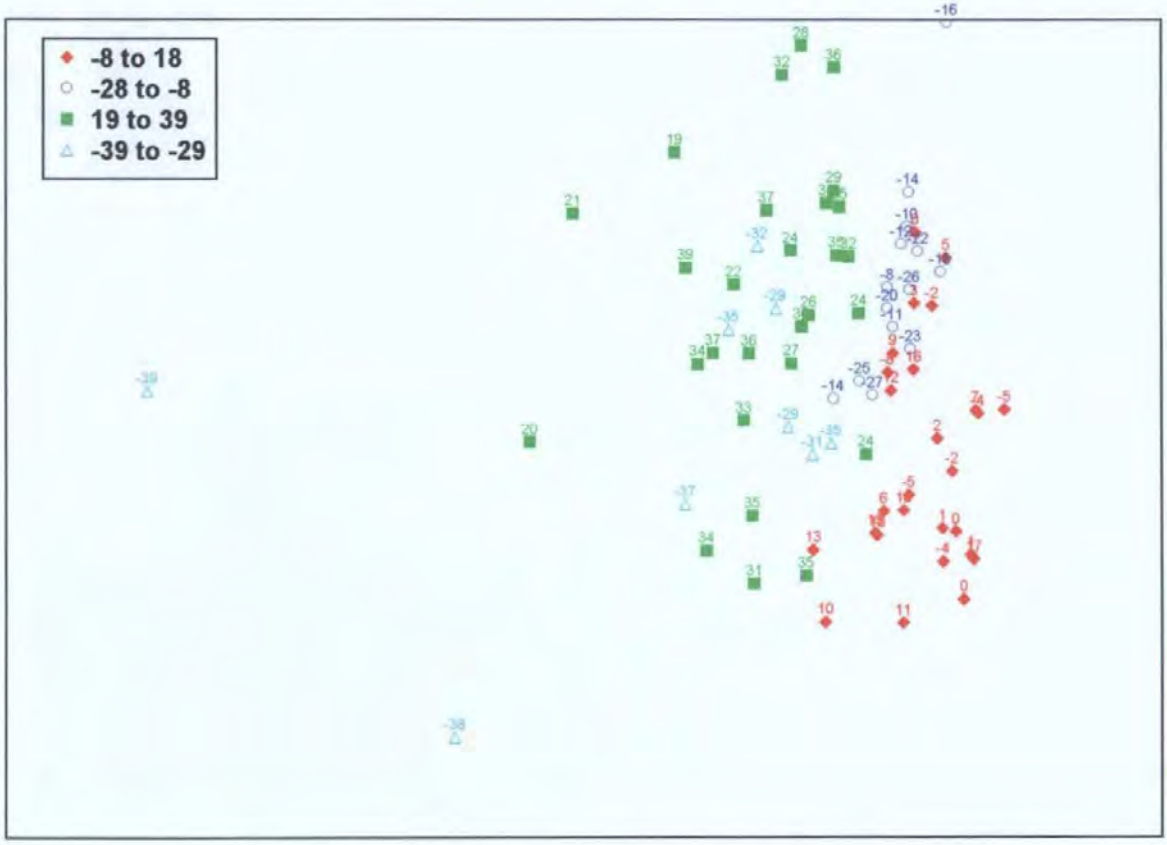

Figure 4.22: MDS ordination for copepod genera (AMT4-6) for the tropical and subtropical stations, Bray-Curtis similarity double root transformed, stress = 0.14. Latitude is shown above the symbol.

The analysis of the significance of the latitudinally derived groups using ANOSIM for double root transformed similarity of genera showed that all groups were significantly different from each other, apart from the northern and southern temperate, the northern and southern subtropical, and the northern temperate and southern subtropical (Table 4.4). The root transformed ANOSIM gave similar results.

	Double root transformed (R=0.569)			Root transformed (R=0.565)		
Groups Used	R	Significant Statistics	Significance Level	R	Significant Statistics	Significance Level
(1, 2)	0.686	0	0.0%	0.778	0	0.0%
(1, 3)	0.815	0	0.0%	0.727	0	0.0%
(1, 4)	0.633	0	0.0%	0.583	0	0.0%
(1, 5)	**0.129**	**588**	**11.8%**	**0.089**	**805**	**16.1%**
(1, 6)	**0.035**	**1415**	**28.3%**	**-0.066**	**3950**	**79.0%**
(1, 7)	0.460	0	0.0%	0.296	0	0.0%
(2, 3)	0.443	0	0.0%	0.392	0	0.0%
(2, 4)	0.177	20	0.4%	0.164	63	1.3%
(2, 5)	**-0.035**	**2978**	**59.6%**	**0.064**	**1354**	**27.1%**
(2, 6)	0.916	0	0.0%	0.934	0	0.0%
(2, 7)	0.949	0	0.0%	0.907	0	0.0%
(3, 4)	0.294	0	0.0%	0.394	0	0.0%
(3, 5)	0.482	0	0.0%	0.437	0	0.0%
(3, 6)	0.944	0	0.0%	0.920	0	0.0%
(3, 7)	0.989	0	0.0%	0.944	0	0.0%
(4, 5)	0.507	0	0.0%	0.372	6	0.1%
(4, 6)	0.893	0	0.0%	0.904	0	0.0%
(4, 7)	0.971	0	0.0%	0.907	0	0.0%
(5, 6)	0.568	1	0.0%	0.540	1	0.0%
(5, 7)	0.876	0	0.0%	0.695	0	0.0%
(6, 7)	0.511	0	0.0%	0.396	0	0.0%

Table 4.4: Analysis of similarity of the genera derived groups (double root transformed. Global R=0.569, P<0.1%, N=115, root transformed Global R=0.565, P<0.1%, N=115), with 5000 permutations used. Bold highlights the non-significant comparisons. Group1: northern temperate (>38 °N), group 2: northern subtropical (18-38 °N), group 3: equatorial (8 °S-18 °N), group 4: southern tropical (8-28 °S), group 5: southern subtropical (28-38 °S), group 6: southern temperate (>38 °S), group7: Benguela.

The analysis of the genera determining the groups (SIMPER) revealed that for the root transformed abundance, very few genera were important in determining the groupings. Generally these were *Para/Pseudocalanus, Oithona, Oncaea, Corycaeus* and *Calanus*, the abundant and common genera (Table 4.5). *Euchaeta* was important in differentiating

between tropical and subtropical groups (2-5), and *Pleuromamma* was important in differentiating group 6, the southern temperate region where it was abundant (Table 4.7).

For the double route transformed SIMPER, more genera were important in determining the differences between the groupings (Table 4.6), although the pattern of similarity was similar. In addition, the groups were more similar to each other, with less dissimilarity between groups. One genus never explained more than 10 % of the difference, and the same genera were not always important. The high abundance of *Para/Pseudocalanus* and low abundance of *Lucicutia* and *Corycaeus* were important in defining group 1, the northern temperate stations. Group 2 and group 5 (northern and southern subtropical) had high *Acartia*, groups 3 and 4 (equatorial and southern tropical) had no genera which consistently discriminated from other groups, and group 6 had high *Oithona*, low *Oncaea* and *Corycaeus*. Generally, the temperate stations have fewer genera than the tropical and subtropical stations, and are more dominated by *Para/Pseudocalanus* and *Oithona* (Table 4.7).

Groups	1v2	1v3	4v1	5v1	6v1	3v2	4v2	5v2	6v2	4v3	5v3	6v3	5v4	6v4	6v5
Mean dissimilarity (%)	38.9	46.4	48.3	42.1 (NS)	39.9 (NS)	31.7	28.1	26.0 (NS)	47.0	31.5	29.6	47.1	28.2	50.5	42.8
Genera															
Para/Pseudocalanus	1(20)	1(16)	1(23)	1(19)	1(19)	2 (9)	1(11)	1(10)	2(11)	1(13)	2 (9)	3 (9)	1(14)	2(14)	2(10)
Oithona	2(13)	2(11)	2(13)	2 13)	2(17)	4 (6)	5 (5)	6 (6)	1(15)	3 (6)	4 (6)	1(13)	6 (5)	1(15)	1(16)
Oncaea	3 (7)	3(10)	4 (7)	3 (8)	4 (6)	1(10)	3 (8)	5 (7)	4 (7)	2(12)	1 (9)	2(11)	2 (8)	5 (6)	3 (9)
Corycaeus	4 (6)	4 (7)	3 (7)	5 (6)			4 (6)	3 (8)	5 (7)			4 (8)		3 (8)	4 (7)
Calanus	6 (5)	5 (5)	5 (5)	4 (7)	3 (9)			3 (7)	6 (7)	6 (5)	6 (5)	5 (5)	5 (7)	4 (7)	5 (7)
Acartia	5 (6)			6 (5)		3 (7)		2 (8)	3 (7)	3 (7)	3 (7)		3 (8)		6 (7)
Euchaeta						5 (6)	2 (9)			5 (5)	5 (6)				
Eucalanus						6 (5)				4 (5)					
Pleuromamma					6 (5)			4 (7)			7 (5)				7 (6)
Metridia													4 (8)		
Copepodites					5 (6)										
Calocalanus								7 (5)							

Table 4.5: The rank importance of genera (root transformed) for determining the differences between groups for genera explaining 5% or more of the total difference, with the % in brackets. The mean dissimilarity between groups and if it was not significant (NS) in the ANOSIM is also shown. Group 1: northern temperate, group 2: northern subtropical, group 3: equatorial, group 4: southern tropical, group 5: southern subtropical, group 6: southern temperate.

Groups	1v2	1v3	4v1	5v1	6v1	3v2	4v2	5v2	6v2	4v3	5v3	6v3	5v4	6v4	6v5
Mean dissimilarity (%)	39.2	41.9	41.9	36.7 (NS)	37.1 (NS)	28.9	26.3	25.2 (NS)	44.8	24.9	27.0	46.3	24.5	48.0	41.5
Genera															
Para/Pseudocalanus	1 (6)	4 (5)	1 (7)	3 (6)	2 (6)					3 (4)			3 (5)	4 (4)	
Oithona	4 (5)		3 (5)	5 (5)	1 (6)				3 (5)			3 (4)		2 (5)	5 (5)
Oncaea		2 (5)			3 (6)				4 (5)	1 (5)		2 (6)		5 (4)	3 (6)
Corycaeus	3 (6)	1 (5)	2 (6)	2 (6)					1 (7)			1 (7)		1 (8)	1 (8)
Calanus					7 (5)										
Copepodites															
Acartia	5 (5)			4 (5)	6 (5)	3 (5)	4 (5)	3 (5)	2 (7)		1 (5)		2 (6)		2 (7)
Euchaeta															
Eucalanus						1 (5)	5 (4)			2 (5)					
Pleuromamma					5 (6)		1 (5)	2 (5)		4 (4)	4 (4)		1 (8)		
Metridia					4 (6)			5 (4)				4 (4)	5 (4)	3 (5)	
Lucicutia	2 (6)	3 (5)	4 (5)	1 (6)					5 (5)			5 (4)			4 (5)
Solecithrix		5 (4)	5 (4)												
Undinula						2 (5)	2 (5)								
Macrosetella						4 (4)					2 (5)				
Calocalanus						5 (4)	3 (5)	1 (6)			3 (5)		4 (4)		6 (5)
Temora								4 (4)							
Rhincalanus										5 (4)	5 (4)				

Table 4.6: The rank importance of genera (double root transformed) for determining the differences between groups for genera explaining either 5% or more of the total difference or the top 5 ranked, with the % in brackets. The mean dissimilarity between groups and if it was not significant (NS) in the ANOSIM is also shown. Group 1: northern temperate, group 2: northern subtropical, group 3: equatorial, group 4: southern tropical, group 5: southern subtropical, group 6: southern temperate.

Group Genera	1	2	3	4	5	6	Overall
Para/Pseudocalanus	373	69	96	44	90	157	125
Oithona	172	25	34	24	31	137	59
Oncaea	18	21	56	18	25	6.5	28
Corycaeus	8.2	0.1	14	12	8.1	0.1	9.4
Calanus	24	5.9	13	5.1	14	29	13
Acartia	4.9	11	3.7	2.0	8.9	0.1	5.6
Euchaeta	2.1	2.9	10	3.5	2.4	0.03	4.6
Eucalanus	1.8	1.3	5.6	0.5	0.7	0.8	2.3
Pleuromamma	2.1	2.6	1.1	0.6	6.7	9.8	2.9
Metridia	4.4	0.5	0.1	0.1	0.4	4.6	1.3
Copepodites	24	7.5	9.2	4.9	7.7	17	11
Lucicutia	0.04	2.8	2.6	1.6	3.4	0.4	2.0
Solecithrix	0.01	0.2	1.3	0.7	0.3	0.01	0.5
Undinula	0.01	0.05	1.7	0.5	0.3	0.00	0.6
Macrosetella	0.3	0.1	1.8	0.2	0.04	0.00	0.6
Calocalanus	1.3	1.6	0.5	1.6	2.7	0.03	1.2
Temora	0.02	0.1	1.3	0.5	0.7	0.28	0.5
Rhincalanus	0.86	0.06	0.9	0.1	0.03	1.9	0.6
Total no. of genera	35	46	44	39	32	29	48
Average similarity (root transformed)	58.14	74.04	73.65	76.43	75.85	64.62	
Double root transformed	63.96	74.13	76.89	80.08	77.93	65.8	

Table 4.7: Mean abundance of the genera important in determining the dissimilarities, for each group and overall (per sample), with the number of genera and the average similarity of the group groups (root transformed and double root transformed). Group 1: northern temperate, group 2: northern subtropical, group 3: equatorial, group 4: southern tropical, group 5: southern subtropical, group 6: southern temperate.

Comparisons between groups

The results of ANOSIM carried out on different schemes for oceanographic regions showed how well the AMT sample similarity fitted the different schemes. The different schemes of regions showed great variation in how well the AMT data fitted, as demonstrated by the global R (Table 4.8). The derived grouping fits the pattern of genera similarity substantially better than the others, having the highest R value. Bé's regions for Foraminifera and Backus's regions for pelagic organisms are both quite strong. Both divide the ocean into five groups. It is the lack of difference between the northern and southern pairs for temperate (transition) and subtropical regions which brings down the global R (Table 4.9).

Scheme	Author	Global R
Genera	This paper	0.569
Pelagic organisms	Backus (1986)	0.446
Zooplankton	Boltovskoy (1997)	0.378
Pelagic organisms	Van der Spoel and Heyman (1983)	0.137
General oceanographic	Van der Spoel and Heyman (1983)	0.031
Foraminifera	Bé (1977)	0.470
Watermasses	Van der Spoel and Heyman (1983)	0.416
Biogeochemical	Platt *et al.* (1995)	0.425

Table 4.8: Strength of groupings by different schemes for copepod genera double root transformed

	Bé		Backus	
Groups	Stat Value	Significance (%)	Stat Value	Significance (%)
1, 2	0.646	0	0.728	0
1, 3	0.879	0	0.811	0
1, 4	0.697	0	0.577	0
1, 5	0.019	30.4	0.041	29.8
2, 3	0.315	0	0.261	0
2, 4	0.068	12.2	0.075	5.5
2, 5	0.705	0	0.858	0
3, 4	0.148	0.9	0.313	0
3, 5	0.891	0	0.936	0
4, 5	0.794	0	0.764	0

Table 4.9: Pairwise comparison of groups for Backus (1986) and Bé (1977) schemes from ANOSIM (significances are not adjusted for multiple comparisons, 1 – northern temperate/ transitional, 2-northern subtropical, 3 – tropical, 4 – southern subtropical, 5 – southern temperate)

OPC groups

The PCA of the 200m net in log_2 biovolume size classes (standardised) showed that the first principal component was chiefly a measure of biomass, being negative for all but the largest size fraction (Table 4.10). The second principal component was negative for small particles (ESD <1.2 mm), but positive for large. The third component differentiated between medium (negative, ESD 1.2-3.6 mm) and large. The principal components showed some latitudinal patterns (Figure 4.23). The Benguela stations (AMT6 south of 15 °S) were variable, but generally highly negative for PC1, negative for PC2 and positive for PC3. For Montevideo to Falklands (south of 38 °S), PC1 was highly negative, PC2 positive, and PC3 highly negative. From about 30 °S to 5 °N, the first three principal components were quite stable (except the Benguela stations), although there was some fluctuation in PC1. Between about 10°N and 30°N, PC1 drops, PC2 is high, and PC3 is very variable. On AMT 5 at about 35°N, there is a large peak in PC2 and PC3. The three northern most extra stations on AMT4 were night stations, these were high for PC2, compared to the day stations. PC 2 and PC 3 (Figure 4.24) show some separation of the above areas, in spite of much overlap.

Log_2 Biovolume	PC1	PC2	PC3	PC4	PC5
Eigen value	7.11	3.2	1.77	0.86	0.71
% of variation	47.4	21.4	11.8	5.7	4.8
-6	-0.316	-0.128	0.059	-0.18	0.366
-5	-0.329	-0.19	0.114	-0.124	0.265
-4	-0.329	-0.204	0.154	-0.13	0.152
-3	-0.332	-0.189	0.145	-0.121	0.06
-2	-0.331	-0.184	0.133	-0.028	-0.14
-1	-0.337	-0.12	0.061	0.129	-0.33
0	-0.327	0.001	-0.044	0.272	-0.44
1	-0.291	0.166	-0.169	0.335	-0.29
2	-0.234	0.299	-0.305	0.22	0.217
3	-0.214	0.352	-0.305	0.084	0.3
4	-0.203	0.379	-0.19	-0.114	0.165
5	-0.122	0.386	0.059	-0.568	-0.19
6	-0.043	0.392	0.303	-0.353	-0.32
7	-0.011	0.275	0.531	0.293	0.202
8	0.014	0.245	0.536	0.341	0.141

Table 4.10: The principal components from PCA on the 200 m net log_2 OPC biovolume size classes (standardised), with the eigenvalues, variation explained the by the principal component and the eigenvectors for each of the size classes.

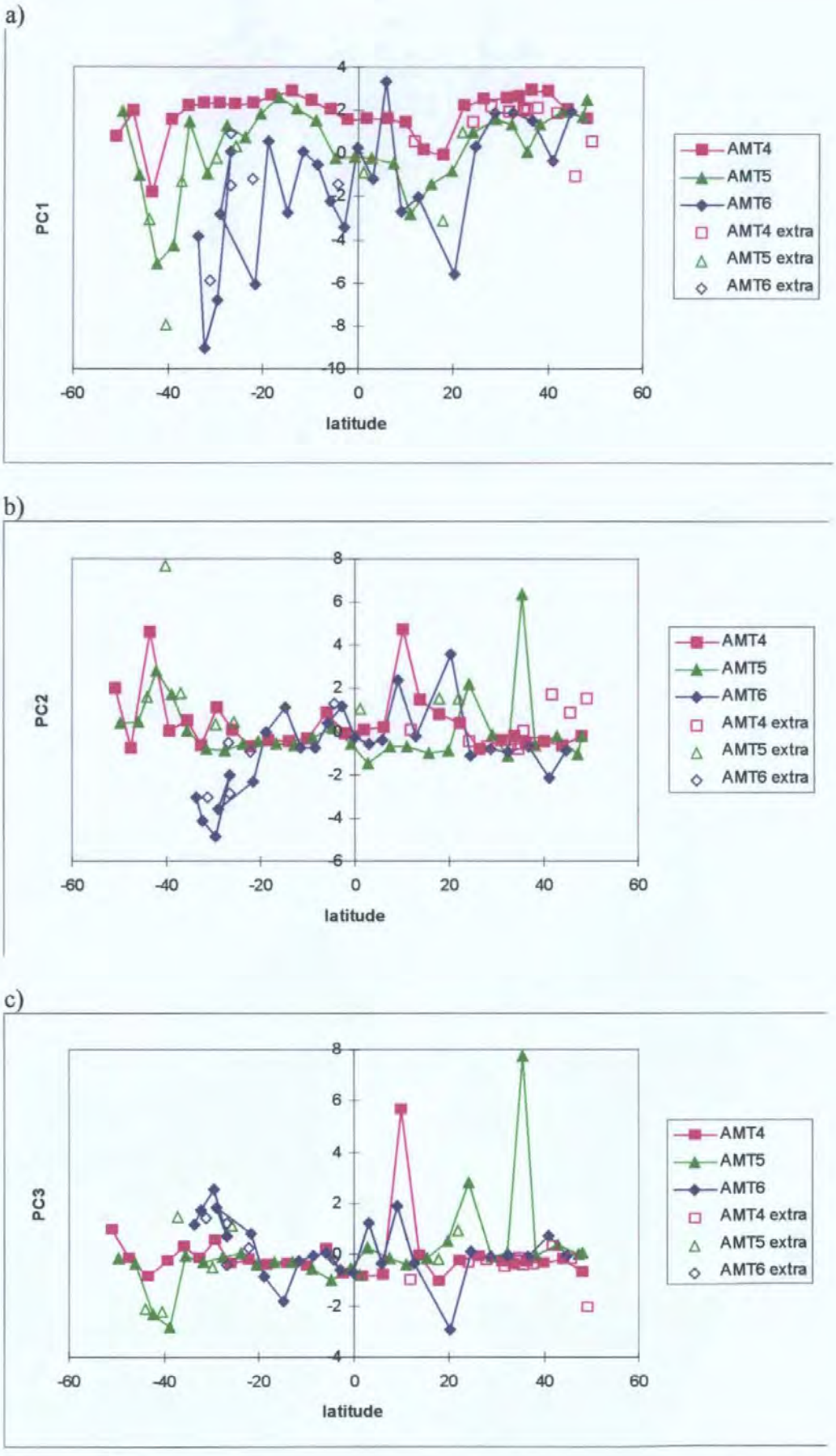

Figure 4.23: Principal components analysis on 200 m net samples OPC size fractions, standardised for AMT 4-6, a) principal component (PC) 1 (Eigen value 7.11, 47.4 % of the variation), b) PC 2 (Eigen value 3.2, 21.4 % of the variation), c) PC 3 (Eigen value 1.77, 11.8 % of the variation), latitudinal transects. Extra nets are mainly night stations.

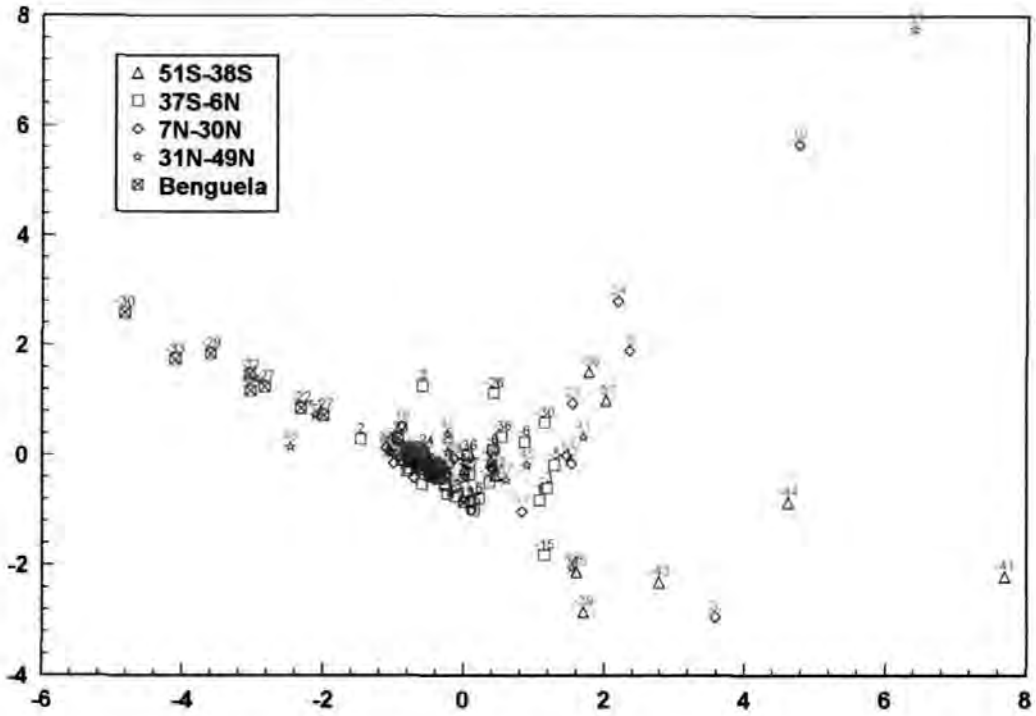

Figure 4.24: PC (Principal component) 2 (Eigen value 3.2, 21.4 % of the variation) and PC3 (Eigenvalue 1.77, 11.8 % of the variation), for 200 m net samples OPC size fractions, standardised for AMT4-6. Latitude is shown above the symbol.

MDS of the double root transformed and standardised $\log_2$ 200 m net samples showed no obvious latitudinal groupings or trends (Figure 4.25). ANOSIM was used to investigate if the similarities fitted with the genera derived groups (above). The ANOSIM showed that size based similarities did not fit the genera based regions, with most northern hemisphere groups not being different from each other or from the southern groups (Table 4.11). The southern groups showed greater differentiation, with southern tropical being different from southern subtropical, temperate, the Benguela and the northern temperate, and the Benguela also different from equatorial, southern subtropical and temperate regions. Comparison with Backus' regions was less significant; only Benguela was different from southern temperate and equatorial stations, and northern temperate and equatorial stations were different (Table 4.12).

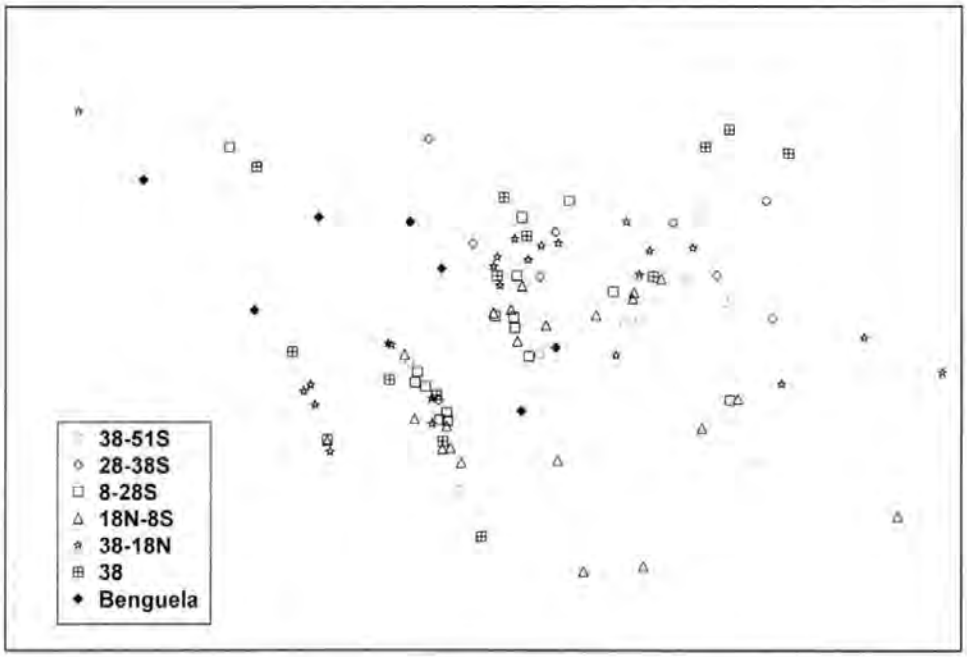

Figure 4.25: MDS of $\log_2$ OPC biovolumes for AMT 4-6 for 200 m net samples, double square root transformed and standardised, based on Euclidean distance (stress=0.11).

Groups Used	Stat Value	Significant Statistics	Significance Level
(1, 2)	**0.001**	**4409**	**44.1%**
(1, 3)	0.112	417	4.2%
(1, 4)	0.139	233	2.3%
(1, 5)	**-0.009**	**4756**	**47.6%**
(1, 6)	**0.053**	**1699**	**17.0%**
(1, 7)	**0.064**	**1336**	**13.4%**
(2, 3)	**-0.001**	**4181**	**41.8%**
(2, 4)	**0.021**	**2342**	**23.4%**
(2, 5)	**0.035**	**3385**	**33.9%**
(2, 6)	**0.010**	**3957**	**39.6%**
(2, 7)	**0.030**	**3161**	**31.6%**
(3, 4)	**0.042**	**985**	**9.9%**
(3, 5)	**0.173**	**611**	**6.1%**
(3, 6)	**0.042**	**2559**	**25.6%**
(3, 7)	0.236	63	0.6%
(4, 5)	0.407	32	0.3%
(4, 6)	0.274	38	0.4%
(4, 7)	0.257	36	0.4%
(5, 6)	**0.060**	**2069**	**20.7%**
(5, 7)	0.341	53	0.5%
(6, 7)	0.453	2	0.0%

Table 4.11: Analysis of similarity of the genera derived groups (double root transformed), carried out on OPC 200 m nets for AMT 4-6, with 10,000 permutations used (Euclidean distance for double root transformed and standardised $\log_2$ size classes). Global R=0.088, P=0.3%, N=105. Group1: northern temperate (>38 ^{o}N), group 2: northern subtropical (18-38 ^{o}N), group 3: equatorial (8 ^{o}S-18 ^{o}N), group 4: southern tropical (8-28 ^{o}S), group 5: southern subtropical (28-38 ^{o}S), group 6: southern temperate (>38 ^{o}S), group7: Benguela.

Groups Used	Stat Value	Significant Statistics	Significance Level
(1, 2)	**0.088**	**1428**	**14.2%**
(1, 3)	0.191	197	2.0%
(1, 4)	**0.060**	**1505**	**15.1%**
(1, 5)	**0.036**	**2494**	**24.9%**
(1, 6)	0.100	850	8.5%
(2, 3)	**-0.005**	**4825**	**48.3%**
(2, 4)	**-0.014**	**5969**	**59.7%**
(2, 5)	**0.034**	**3359**	**33.6%**
(2, 6)	**0.076**	**2013**	**20.1%**
(3, 4)	**0.004**	**3485**	**34.9%**
(3, 5)	**0.095**	**1667**	**16.7%**
(3, 6)	0.270	92	0.9%
(4, 5)	**0.055**	**2239**	**22.4%**
(4, 6)	**0.142**	**556**	**5.6%**
(5, 6)	0.509	3	0.0%

Table 4.12: Analysis of similarity of the Backus' (1986) regions carried out on OPC 200 m net samples, with 10000 permutations used (Euclidean distance for double root transformed and standardised $\log_2$ size classes). Global R=0.065, P=2.3%, N=115. Group1: northern temperate (>40 °N), group 2: northern subtropical (14-40 °N), group 3: equatorial (8 °S-14 °N, AMT 6 21 °S-14 °N), group 4: southern subtropical (8-40 °S), group 5: southern temperate (>40 °S), group 6: Benguela (21-40 °S).

OPC underway groups

PCA carried out on averaged daily underway $\log_2$ OPC biovolumes, double root transformed and standardised showed similar results to the 200 m net samples (Table 4.13). The first principal component was positive for all size classes, the second was negative for small size classes (ESD <1.2 mm), and the third was negative for medium size classes (0.62-2.5 mm), and positive for large and small. The latitudinal transects of the principal components (Figure 4.26) showed some patterns. The Benguela stations tended to have high PC1, variable PC2 and highly negative PC3. The southern high latitudes had high PC1, PC2 and variable PC3. Between 30 °S and the equator, PC 1 was negative, reaching a minimum around 15 °S, PC2 and 3 were stable and close to zero. North of the equator PC1 rose, peaking around 18 °N, with PC 2 and 3 remaining stable, becoming more variable North of 20°N. PC1 fell to a minimum around 30 °N rising again steadily to 50 °N. PC2 fell north of 40°N. PC3 became positive between 30-48°N, before becoming variable.

Log_2 Biovolume	PC1	PC2	PC3
Eigen value	9.29	1.79	1.25
% of variation	61.97	11.97	8.34
-6	0.231	-0.395	0.331
-5	0.287	-0.373	0.231
-4	0.286	-0.320	0.084
-3	0.309	-0.217	0.009
-2	0.311	-0.143	-0.117
-1	0.305	-0.090	-0.289
0	0.295	-0.031	-0.395
1	0.288	0.105	-0.359
2	0.276	0.319	-0.192
3	0.275	0.379	-0.004
4	0.264	0.332	0.132
5	0.251	0.274	0.350
6	0.205	0.289	0.521

Table 4.13: Principal components analysis of 24 hour underway log_2 biovolume size classes, double root transformed and standardised, for AMT 1-6 with the eigenvalues, variation explained the by the principal component and the component weights for each of the size classes.

a)

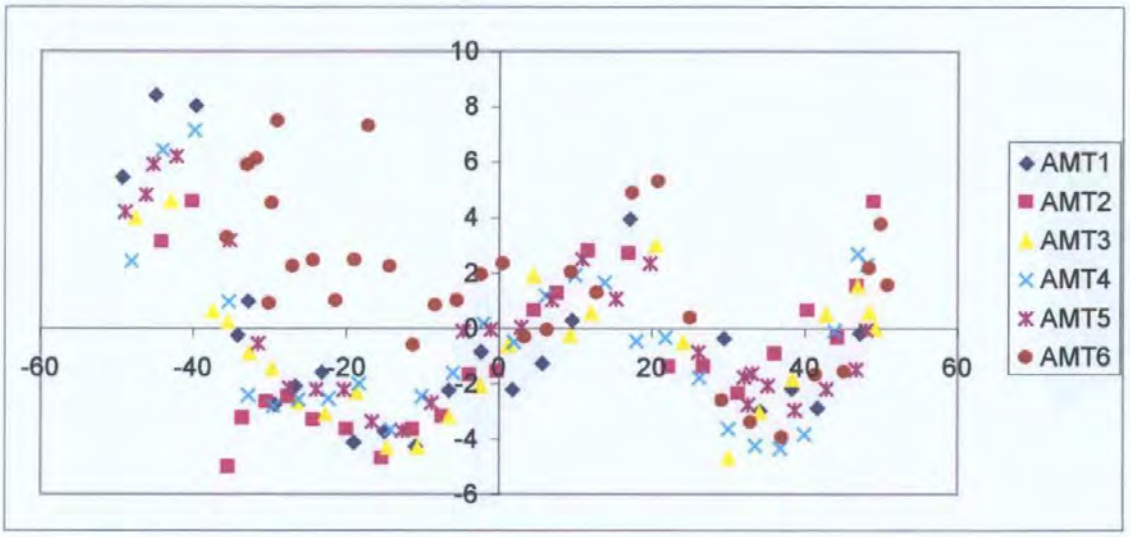

b)

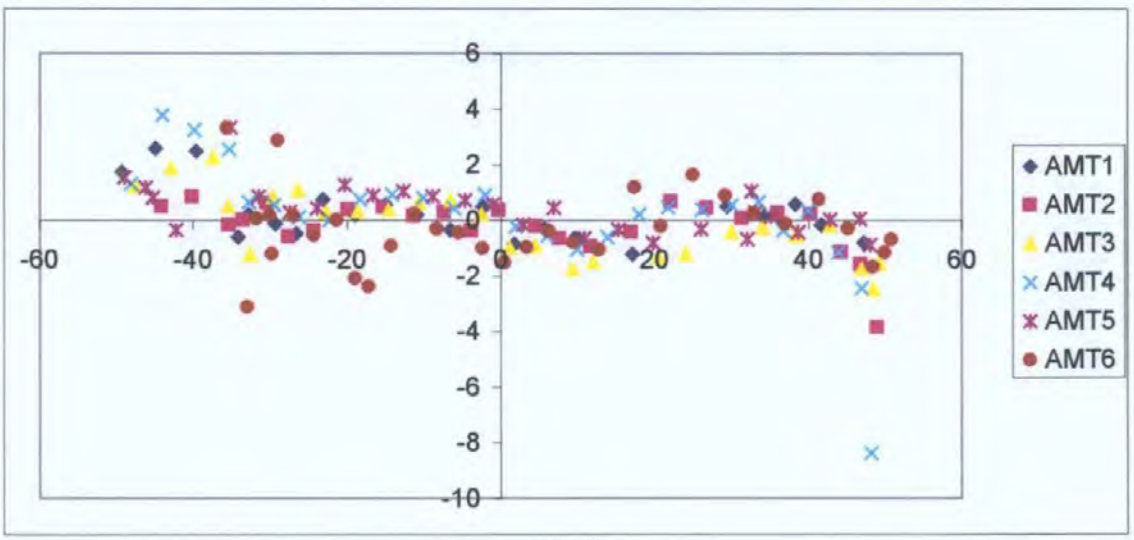

c)

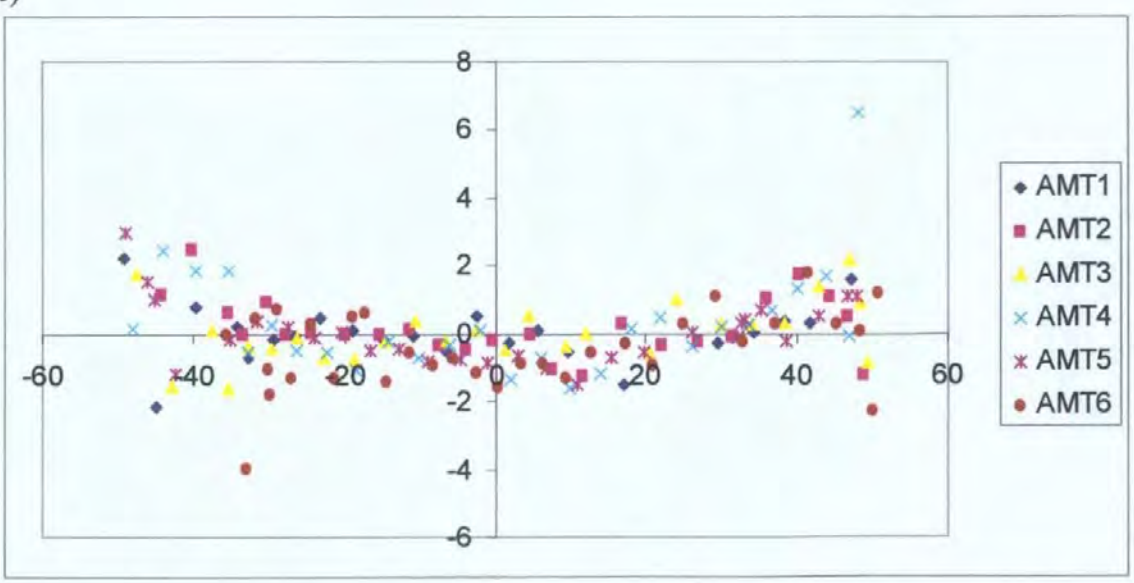

Figure 4.26: Principal components analysis of 24 hour underway log_2 biovolumes, double root transformed and standardised along the latitudinal transect, for AMT 1-6. a) PC1 (Eigenvalue 9.29, 62.0 % of the variation), b) PC 2 (Eigenvalue 1.80, 11.9 % of the variation), c) PC 3 (Eigenvalue 1.25, 8.4 % of the variation), latitudinal transects.

Multidimensional scaling of the log_2 size classes for double root transformed Euclidean distances between 24 hours averaged underway biovolumes slight grouping into latitudinal regions (Figure 4.27). ANOSIM used to see if the genera derived latitudinal groups were significant, found that most of the groups were significantly different from each other (Table 4.14). The northern subtropical was not significantly different from the northern temperate, southern subtropical or Benguela regions. The Benguela region was also not significantly different from the southern subtropical region. When compared to Backus' regions using ANOSIM (Table 4.15), again the northern subtropical was not significantly different from the northern temperate, southern subtropical regions and the Benguela was only just significantly different from the southern subtropical region. Modification of the boundary between the northern temperate and northern subtropical region to 35 ^{o}N, improved the differentiation of these regions (P=0.7%), although the northern and southern subtropical regions were not significantly different from each other (Table 4.16), and the overall fit was still quite low (global R = 0.248).

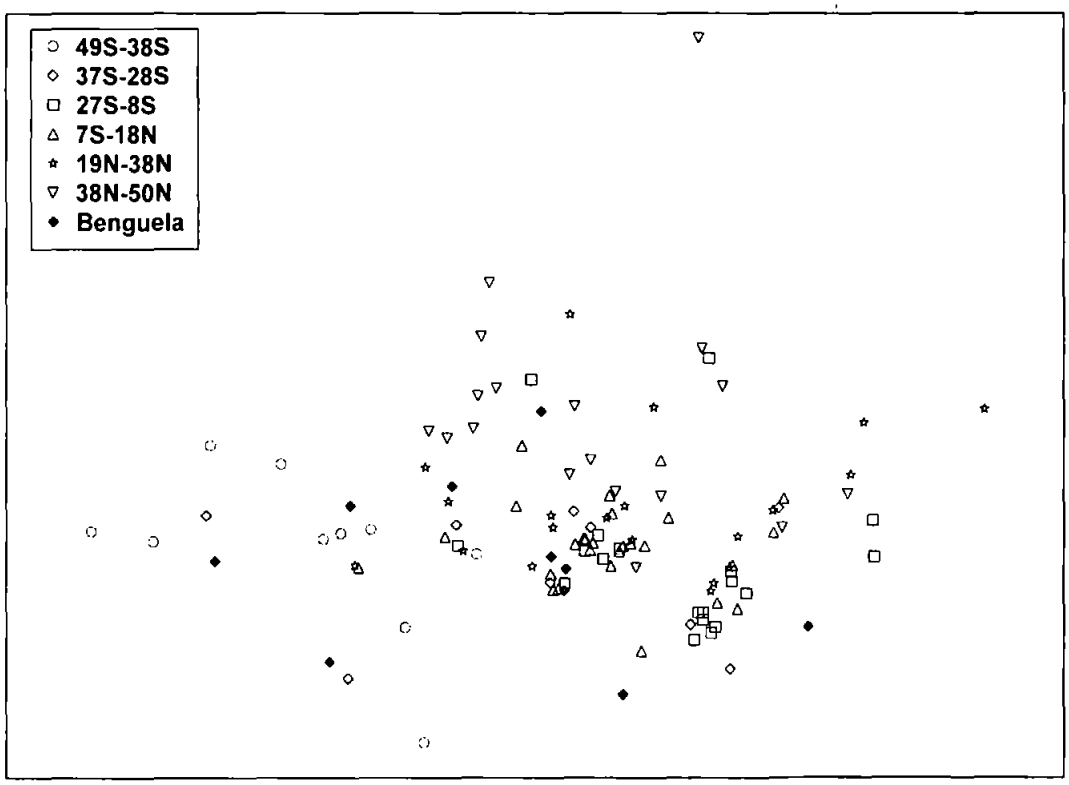

Figure 4.27: MDS of underway OPC biovolumes in log_2 size classes averaged over 24 hours, for AMT 3-6. Symbols represent latitudinal group.

Groups Used	Stat Value	Significant Statistics	Significance Level
(1, 2)	**0.054**	**352**	**7.1%**
(1, 3)	0.332	0	0.0%
(1, 4)	0.277	0	0.0%
(1, 5)	0.229	31	0.6%
(1, 6)	0.534	0	0.0%
(1, 7)	0.189	91	1.8%
(2, 3)	0.144	9	0.2%
(2, 4)	0.075	127	2.6%
(2, 5)	**0.085**	**707**	**14.2%**
(2, 6)	0.504	0	0.0%
(2, 7)	**0.117**	**393**	**7.9%**
(3, 4)	0.089	144	2.9%
(3, 5)	0.336	13	0.3%
(3, 6)	0.773	0	0.0%
(3, 7)	0.387	6	0.1%
(4, 5)	0.165	234	4.7%
(4, 6)	0.777	0	0.0%
(4, 7)	0.314	11	0.2%
(5, 6)	0.333	29	0.6%
(5, 7)	**0.030**	**1381**	**27.6%**
(6, 7)	0.230	77	1.6%

Table 4.14: Analysis of similarity of the genera derived groups (double root transformed) using 5000 permutations, carried out on OPC 24 hour underway averages for AMT 3-6 (Euclidean distance for double root transformed and standardised $\log_2$ size classes). Global R=0.261, P<0.1%, N=115. Group1: N. temperate (>38 °N), group 2: N. subtropical (18-38 °N), group 3: equatorial (8 °S-18 °N), group 4: S. tropical (8-28 °S), group 5: S. subtropical (28-38 °S), group 6: S. temperate (>38 °S), group7: Benguela.

Groups Used	Stat Value	Significant Statistics	Significance Level
(1, 2)	**0.057**	**1559**	**15.6%**
(1, 3)	0.381	0	0.0%
(1, 4)	0.286	3	0.0%
(1, 5)	0.531	0	0.0%
(1, 6)	0.240	69	0.7%
(2, 3)	0.118	8	0.1%
(2, 4)	0.080	109	1.1%
(2, 5)	0.462	0	0.0%
(2, 6)	**0.124**	**964**	**9.6%**
(3, 4)	0.125	7	0.1%
(3, 5)	0.827	0	0.0%
(3, 6)	0.440	8	0.1%
(4, 5)	0.548	1	0.0%
(4, 6)	0.196	315	3.2%
(5, 6)	0.216	187	1.9%

Table 4.15: Analysis of similarity of the Backus' (1986) regions carried out on OPC underway 24 hour averages (Euclidean distance, double root transformed, standardised $\log_2$ size classes), with 10,000 permutations. Global R=0.248, P<0.1%, N=115. Group1: N. temperate (>40 °N), group 2: N. subtropical (14-40 °N), group 3: equatorial (8 °S-14 °N, AMT 6 21°S-14°N), group 4: S. subtropical (8-40 °S), group 5: S. temperate (>40 °S), group 6: Benguela (21-40 °S).

Groups Used	Stat Value	Significant Statistics	Significance Level
(1, 2)	0.108	67	0.7%
(1, 3)	0.333	0	0.0%
(1, 4)	0.251	0	0.0%
(1, 5)	0.526	0	0.0%
(1, 6)	0.254	88	0.9%
(2, 3)	0.143	45	0.5%
(2, 4)	0.088	220	2.2%
(2, 5)	0.491	0	0.0%
(2, 6)	**0.135**	**794**	**7.9%**
(3, 4)	0.125	11	0.1%
(3, 5)	0.827	0	0.0%
(3, 6)	0.440	5	0.1%
(4, 5)	0.548	0	0.0%
(4, 6)	0.196	326	3.3%
(5, 6)	0.216	220	2.2%

Table 4.16: Analysis of similarity of the adjusted Backus' (1986) regions carried out on OPC underway 24 hour averages (Euclidean distance for double root transformed and standardised $\log_2$ size classes), using 10,000 permutations. Global R=0.263, P<0.1%, N=115. Group1: northern temperate (>35 °N), group 2: northern subtropical (14-35 °N), group 3: equatorial (8 °S-14 °N, AMT 6 21°S-14°N), group 4: southern subtropical (8-40 °S), group 5: southern temperate (>40 °S), group 6: Benguela (21-40 °S).

Discussion

Taxonomic groups

The zooplankton major groups region analysis did not show any clear latitudinal groupings. However, as the high latitude and Benguela stations were scattered around a central core of warm water stations, the composition of the cooler station can be seen to be more variable with the warm water stations appearing to be more similar to each other. This could be due to the same major groups being present at high latitudes, but the individual samples being more variable, as suggested by Bé and Forns (1971) and the latitudinal gradient analysis (above).

The copepod genera from the AMT cruises fall into two major groups of similarity: the warm water stations, and the temperate and Benguela stations. This difference is also

suggested from the taxonomic diversity based on copepod genera (above), which shows a rapid reduction in diversity and increase in variance, starting between 35 and 40 °N/S. This boundary at approximately 38° in the south is associated with the boundary of the sub-arctic water, and South Atlantic Central Water (Sverdrup *et al.* 1942). No such obvious physical boundary exists in the north. Further analysis of the similarity differentiates the temperate from the Benguela stations. The warm water stations can be further broken down into equatorial, tropical and subtropical regions, although these are not completely distinct and overlap in the similarity. Analysis of similarity showed that the north and south temperate stations were not significantly different from each other, neither were the north and south subtropical stations; more surprisingly, the north temperate and south subtropical were not significantly different. The similarity of the north and south pairs of temperate and subtropical regions may be due to genera being used rather than more detailed taxonomy, as sympatriots are frequently found in each hemisphere e.g. *Calanus helgolandicus* and *Calanus australis* (Van der Spoel and Heyman 1983). Others have found that the same species are present in both the northern and southern subtropical zone, e.g. Ekman (1953) notes the abundance of "warm water cosmopolites". If species data was available, it is likely that the patterns would be stronger and more separation between the regions would be evident.

Several other attempts have been made to divide the ocean into meaningful areas based on physical, chemical and biological properties. The boundaries of these regions, although they may be similar and even overlapping, are not the same. Figure 4.27 shows the boundaries of several proposed regions traversed by the AMT cruises between UK and Falklands. The schemes for the North Atlantic show close agreement for the biologically based regions, particularly as the regional boundaries are not necessarily sharp due to expatriation (e.g. Ekman 1953), and vary by a few degrees depending on season and currents (e.g. Boltovskoy 1997, Backus 1986). The southern ocean shows a more profound

variability in its regions. This is partly an artefact of the AMT track being closer to the coast in the Southern Hemisphere, but there are fundamental differences in the division of the southern ocean. The southern ocean has also suffered historically from under sampling (e.g. Boltovskoy 1997, Gibbons 1997). The watermasses and biogeochemical provinces are distinct from the biologically derived regions.

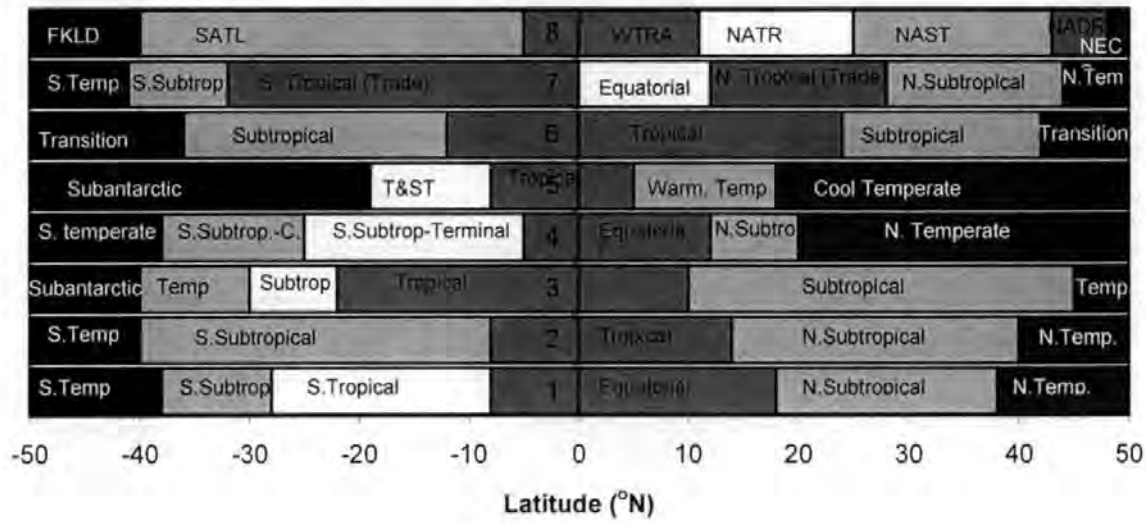

Figure 4.28: Inter-comparison of latitudinal groups along the AMT. 1 – genera derived groups, 2- pelagic organisms (Backus 1986), 3 - pelagic (Boltovskoy 1997), 4 – zooplankton (Van der Spoel and Heyman 1983), 5 – generalised oceanographic regions (Van der Spoel and Heyman 1983), 6 – Foraminifera (Bé 1977), 7 - Watermasses (Van der Spoel and Heyman 1983), 8 - biogeochemical (Longhurst and Platt 1995). (FKLD – SW Atlantic shelf, SALT – S. Atlantic gyre, WTRA – W. tropical Atlantic, NATR – N. Atlantic tropical gyre, NAST – N. Atlantic subtropical gyre, NADR – N. Atlantic drift, NECS – N.E. Atlantic shelf, Temp. – temperate, Subtrop. – subtropical, T&ST – temperate and subtropical.)

Overall, the copepod genera derived groups match closely with Bé (1977) and Backus (1986), except that this study identified an extra region between 28 and 38 °S. Backus (1986) admitted feeling uneasy with his divisions of the southern Atlantic Ocean. Van der Spoel and Heyman's (1983) scheme for the zooplankton of the southern ocean is very similar to this study's. Analysis of the groups showed that Bé (1977) and Backus (1986) schemes fitted the copepod genera, and that it was only the pairs northern and southern temperate and subtropical which were not significantly different from each other. Thus it can be seen that the copepod genera similarities fit with the traditional ideas of pelagic biogeography (e.g. Ekman 1953).

Size structure

The zooplankton size structure showed clear latitudinal patterns as the ocean provinces are crossed, consistent between cruises for both the net samples and the underway 24 hour daily averages. PCA of the $\log_2$ biovolume size classes identified the overall abundance (PC1), the difference in size contrasting large and small (PC2), and the medium compared to large (PC3) as being the most important components of the size structure. PC 1, 2 and 3 were all distinctive for stations in the Benguela upwelling, showing that the community structure was very different from the oceanic community, having high biovolume (negative PC 1), dominated by small size classes (negative PC 2) and with high numbers medium zooplankton (positive PC3). This is probably because the productivity regime was very different. Large zooplankton tend to be associated with productive systems with high zooplankton standing stock (above). Overall, PC 1 followed the inverse pattern of biovolume. PC 2 was steady and low from approximately 0^{o} to 38^{o}S, suggesting the size structure was stable and dominated by small zooplankton. Oligotrophic gyres are typified by dominance of small copepods (e.g. Pointkovski and Van der Spoel 1997), thus be dominated by the smaller size classes.

The MDS from the size structure did not show strong latitudinal groupings. Comparison of the size structure similarity with the groupings derived from the copepod genera, showed that although the groupings were similar, the size structure was not as strongly or consistently grouped. This suggests that size structure is not as sensitive a measure of community structure as taxonomy. Adjustment of the boundaries of Backus (1986) groups for the underway size fractions found that most groups were significantly different from each other, but not very strongly, having low R values.

Conclusion

There is a clear latitudinal trend in the richness of copepod genera along the Atlantic Ocean, evident in both the overall richness and the richness per sample. This decrease in richness towards the poles is associated with a decrease in sea surface temperature, which in turn may indicate the structure and niche availability of the water column. However, increased seasonality towards the poles is an alternative hypothesis. The Benguela upwelling region has lower richness than the open ocean, and may be considered immature. Evenness showed no trend over the transect, and taxonomic distinctness increased in variability at high latitudes. These facets combined in the taxonomic diversity showed stability across the open ocean between 35 ^{o}N and 35 ^{o}S. At greater latitudes, the taxonomic diversity fell rapidly and increased in variability, suggesting a change in the community. This change in community structure is likely to be associated with the change in the environment, and the uncoupling of primary and secondary productivity.

A clear distinction in copepod composition can be seen between the warm water stations (38 ^{o}N-38 ^{o}S) and the temperate and upwelling areas. The temperate and upwelling areas also show higher variability in composition as also indicated by the increase in variance of the taxonomic diversity. The southern boundary approximates to the physical front of the Subantarctic and South Atlantic Central Waters. The northern boundary did not appear to be physical, although it may be associated with less well defined changes in the ocean structure. The temperate regions had similar taxonomic compositions, but analysis to species may have exposed differences. The Benguela upwelling region had a significantly different composition to the temperate region. The warm water region could be separated into sub-regions, although these were not totally separated, and north and south subtropical regions were indistinguishable using the genera composition. Comparing with other schemes divisions showed that these were similar to other pelagic biological systems, but

did not fit well with the watermasses or Longhurst and Platt's biogeochemical provinces. It is surprising that neither the watermasses or the production regimes corresponded with the changes in community structure, as both are thought to be important in determining zooplankton distributions.

Size of individual zooplankters has in the past been found to increase at high latitudes. However, there is no evidence of this from the current data. Mean size does appear to be positively related to the zooplankton standing sock. Others may have found mean size increasing with latitude as biomass tends to be seasonally high at high latitudes. Size structure, although varying along the transect, is not as sensitive a measure of community structure as taxonomy, but may be related to the productivity of the ecosystem.

Chapter 5: Modelling surface zooplankton

Introduction

Modelling surface zooplankton abundance has two benefits: to enable prediction of zooplankton abundance, and to increase understanding of the system and the influence of different factors. Here two approaches are taken: multiple linear regression and neural networks. Multiple linear regression is an extension of univariate regression, which fits linear combinations of factors to the dependent variable using least squares. It is simple to interpret, but assumes a linear interaction between the independent and dependent variables. 'New variables' can be constructed from the product of the original variables, or by transforming them. A potential problem occurs when the independent variables are related. Correlations between the variables (multicolinearity) mean that the presence of one variable in the model will influence the impact of another. Thus a factor that may appear insignificant may just be related to a factor already in the model, which is accounting for the same variance within the data.

Zooplankton abundance has generally been modelled from a theoretical perspective within ecosystem models rather than to model zooplankton themselves, as in for example NPZ (nutrients-phytoplankton-zooplankton) models (e.g. Frost & Franzen 1992, Frost 1993), where several assumptions at each trophic level are made about their interactions. However, Aoki *et al.* (1999) modelled zooplankton biomass empirically in response to long-term changes in the hydrography, in the northeastern sea area of Japan. The model could predict smoothed mean annual abundance of zooplankton quite accurately within this region (root mean square error <10%). Other empirical zooplankton models tend to concentrate on production of part of the lifecycle or other specific aspects of zooplankton e.g. copepod egg production (Prestige *et al.* 1995), diel migration (Richards *et al.* 1996).

Other studies have looked at the relationship of zooplankton abundance with specific hydrographic events e.g. flows in the northeastern Atlantic (Stephens *et al.* 1998), shifts in the Gulf Stream (Taylor 1995). But, in general, models predicting biomass are restricted to particular regions.

Multiple regression has been used in a wide range of applications within marine biology due to its flexibility. Calbet and Agustí (1999) used multiple regression to test the influence of temperature and food availability on copepod egg production. White and Roman (1992) used it to differentiate the effects of different foods and physical variables on egg production of the copepod *Acartia tonsa.* Chow-Fraser and Maly (1991) looked at factors affecting clutch size in *Diatomus* copepods. Waife and Frid (1996) used multiple regression to assess the temporal variation in zooplankton community composition in light of turbulent mixing. Haury *et al.* (1992) used multiple linear regression to give insight into the relationships between physical factors and zooplankton community structure.

Neural networks do not assume any particular relationship between the variables, but allow non-linear mapping of the independent variables and their interactions on to the dependent variable. The immediate appeal of neural networks is the ease in which they may be applied, especially for prediction, and the removal of assumptions as to the nature of the interaction between the variables. Sarle (1994) has shown that many statistical analysis techniques have equivalent artificial neural network models. For example, the multi-layer feed forward neural networks, used here, can be considered equivalent to multivariate non-linear regression.

Feed forward neural networks are widely used (Lek and Guégan 1999). The structure consists of a layer of nodes that accept various inputs (the independent variables). These inputs are fed to various further layers of nodes and ultimately a layer of outputs. The

network is 'trained' so that the response to a given set of inputs corresponds to the desired output. Multi-layer feed-forward networks can approximate any continuous function provided that there are sufficient nodes. The system is 'trained' on a set of inputs and output pairs. Initially the connections between the nodes and thus the variables are given small random weights. The outputs are compared to the actual outputs and the weightings of the connections are modified to minimise the discrepancy between the input and output signals. The process of modification is repeated resulting in an optimised network. The network is subsequently tested on more input output pairs.

One drawback of neural networks is that it is harder to interpret the impact of individual components or independent variables, as the weightings and connections of the nodes are concealed. However, sensitivity analysis may be used to give insight into the systems behaviour, and the effects of the individual inputs.

Artificial neural networks of this type have been used in a wide variety of applications. Initially developed for insight into the working of actual neural networks within the nervous system and brain (e.g. Rosenblatt 1961), their use has extended into pattern recognition (e.g. Simpson *et al.* 1992), control systems and robotics (e.g. Reeve and Hallam 1995). Recently neural networks have become increasingly used in fields such as ecosystem dynamics, because the underlying relationship between variables is not assumed, and non-linear elements may be added. Scardi (1996) and Scardi and Harding (1999) developed an empirical model of primary production based on a feed-forward neural network using easily measured hydrographic factors. They found that predictions of primary production were much more reliable than those derived from linear multiple regression, even with very simple networks. Aoki *et al.* (1999) used neural networks for the prediction of zooplankton biomass in responses to long term changes in climate and oceanography. Guégan *et al.* (1998) used neural networks to predict riparian fish diversity,

and to test theoretical predictions. Frequently in ecological systems, empirical models from neural networks out performed multiple linear regression models, in terms of reliability and accuracy of the predictions (e.g. Brey *et al.* 1996; Guégan *et al.* 1998; Scardi 1996; Manel *et al.* 1999).

The main aim of this study is to use easily measured environmental parameters to estimate empirically surface zooplankton biomass. Two methods, multiple linear regression and artificial neural networks, are used and compared.

Analysis

Data manipulation

The underway data from the OPC and physical variables for AMT 2 to AMT 5 was binned into one hour means. Any part bins of less than 30 minutes were considered unreliable and removed. The variable 'diel time' was calculated as a sine wave with an amplitude of one and period twice the length of the time between sunrise and sunset for day bins, and between sunset and sunrise the following day for night samples.

For day,

$$T = \mathrm{Sin}\,(\pi[\,t-t_r]/[t_s-t_r])$$

At night,

$$T = -\mathrm{Sin}\,(\pi\,[t-t_s]/[t_r-t_s])$$

where T is modelled diel time, t is actual time, t_r is sunrise and t_s is sunset.

The Julian day was included with time to enable the correct sunset and sunrise, and to avoid negatives. Thus diel time was zero at sunrise and sunset, negative during the night and positive during the day. Season was coded as spring -1 and autumn 1.

The OPC biovolume for mean ESD 250 to 2000 μm was used to avoid unusual high biovolumes from occasional large individuals, and at smaller biovolumes the OPC becomes unreliable. This size range is also close to what is considered to be the 'mesozooplankton' (200-2000 μm; Lenz *et al.* 1993). The biovolume (250-2000 μm) was $\log_e$ transformed, to normalise the distribution, and thus reduce the influence of unusually high biovolume measures. It is also more appropriate to use a log scale as it is the changes in magnitude that are interesting.

AMT 4 and 5 data sets were used to develop the models, whereas AMT2 and 3 were kept separate to test the generalisation capabilities of the models.

Multiple regression

The one hour binned underway data was used for multiple regression analysis. Initially, the whole of the cruise track was used to calculate the regression with variables: latitude, temperature, change in temperature, salinity, change in salinity, density, change in density, sea surface height from TOPEX imagery, chlorophyll, total incident radiation (TIR), diel time and season for AMT 4 and 5 data sets. A backward elimination procedure was used in Statgraphics to remove insignificant variables. Care was taken with temperature, salinity and density to check which combination was most appropriate, as the multicolinearity (correlation between the variables) made automatic selection unreliable. The procedure was repeated on parts of the transect separately. Temperate (>38°) and tropical regions (38°N-38°S) were separated, as were the regions defined by copepod genera and the transect without the southern temperate region. Whole transects were reconstructed from the parts, and compared with the actual results, from AMT 4 and 5. The equations were used to predict biovolumes for AMT 2 and 3, and compared with the measured biovolumes.

Neural networks

The one hour binned underway data was used for the neural network analysis. A two-layered feed forward artificial neural network was used, otherwise known as a backpropagation network (Figure 5.1). The network was set up using MATLAB. Initially the hidden layer was set up with 15 nodes plus a constant. The hidden nodes have hyperbolic tangent sigmoid transfer functions allowing non-linearity, and the linear transfer functions are used in the output layer. The network was trained for 40 epochs (runs), using alternate samples from the AMT 4 and 5 data set. The other samples were used to test the network. The performance was tested by repeating the training and testing process 100 times, giving a better indication of the behaviour of the network.

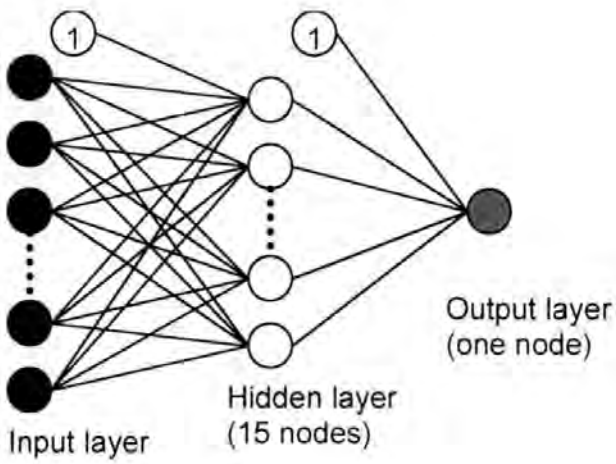

Figure 5.1: Diagram of the two layer feed forward artificial neural network used. The number of input nodes varied between models, but was initially 8 plus a constant. 15 nodes were used in the hidden layer plus a constant. Connections between inputs and hidden layer are hyperbolic tangent sigmoid transfer functions, and to the output linear transfer functions.

Initially variables that were found to be important in the multiple regression analysis were used over the whole of the AMT 4 and 5 transects, with two minimisation functions. The first, the Levenberg-Marquardt algorithm, minimises the least squares of the output. The second measures the performance of the Artificial Neural Network model as a combination of the mean sum of the squares of the network residuals and the mean sum of the squares of the network weights and biases as suggested by MacKay (1992). This smoothing of the

response is important if the model is to predict outside the initial area of the input parameters, and reduces the likelihood of over-fitting the data.

Optimisation of the variables was performed with an algorithm that included the smoothing element by sequentially removing one variable and seeing the effect on the model. The variable that made the least difference to the model performance was removed and the process repeated until the model's accuracy was significantly affected. The performance of the simplified model was tested for generality on totally new data sets, the AMT 2 and 3 transects.

To understand the influence of the factors on the model, sensitivity analysis was carried out on the model with the optimised variables. The model was first retrained with all four AMT data sets to improve the robustness of the model. The median values for each variable were calculated and used in the model whilst one variable was changed across the parameter's range, and the output recorded. This was carried out for each of the regions defined by the copepod genera.

Results

Multiple regression

The multiple regression of $\log_e$ biovolume (250-2000μm ESD) for the whole transect showed that the important components in predicting the biovolume were: latitude, temperature, density, chlorophyll, total incident radiation (TIR) and diel time (Table 5.1). These variables explained 55% of the variation. In general, the prediction was good across the transect (Figure 5.2), although the prediction of the extreme low and high values was less good than the intermediate estimates. The predicted biovolume followed the general trend and the diel cycle of the actual biovolume (Figure 5.2). However, the high

biovolumes in the southern temperate region in the austral autumn (AMT 4) were not predicted, although they were in the spring. The biovolumes north of the equator tended to be underestimated by the model in AMT 4. Figure 5.3 shows how each component affects the model. Temperature and salinity form the basic shape, modified by latitude and chlorophyll at either end of the transect. Diel time and total incident radiation combine to simulate the cyclic diel migration component to the model.

Variable	Whole transect	Warm water	Temperate	N. Temperate	N. Subtropical	Equatorial	S. Tropical	S. Subtropical	S. Temperate	Whole with no S. Temp
Constant	22.48	22.16	11.64	135.2	5.83	-73.9	19.76	6.40	16.62	20.87
Latitude	0.006	0.008	-	0.23	-0.07	0.044	-0.03	-	0.234	0.007
	(6.3)	(6.8)		(3.88)	(-10)	(9.5)	(-3.5)		(7.5)	(7.6)
Temperature	-0.13	0.067	-	-0.59	-	5.67	-0.19	-0.15	-	-
	(-16)	(7.7)		(-2.8)		(4.1)	(-3.2)	(-5.8)		
Change in temperature	-	-	-	-	-	-	-	-	-	-
Salinity	-	-0.55	-0.43	-	-	-13.8	-	-	-0.86	-0.27
		(-14)	(-8.5)			(-4.1)			(-6.3)	(-6.9)
Change in salinity	-	-	-	-	-	-	-	-	-	-
Density	-0.69	-	0.29	-5.03	-	17.9	-0.49	-	1.08	-0.30
	(-19)		(3.8)	(-5.5)		(4.1)	(-3.1)		(7.3)	(-12)
Change in density	-	-	-	-	-	-	-	-	-	-
Sea surface height	-	-	-	0.121	-	-	-	-	-	-
				(3.0)						
Chlorophyll	0.688	0.752	0.471	0.479	-	2.43	-	0.412	-	0.963
	(20)	(9.35)	(9.4)	(3.7)		(4.7)		(4.3)		(16)
TIR (x1000)	-1.17	-1.27	-1.60	-	-1.34	-0.98	-2.19	-	-1.41	-1.14
	(-8.7)	(-9.0)	(-4.9)		(-9.1)	(-5.5)	(-15)		(-2.9)	(-8.6)
Diel time	-0.39	-0.29	-0.44	-0.72	-	-0.34	-	-0.78	-0.78	-0.34
	(-8.0)	(-5.4)	(-4.5)	(-9.9)		(-5.8)		(-8.6)	(-5.1)	(-6.9)
Season	-	-0.12	4.69	-0.84	0.44	-	-	-	-	-
		(4.69)		(-3.7)	(10.3)					
Adjusted R^2	0.55	0.53	0.57	0.74	0.60	0.61	0.55	0.64	0.51	0.54

Table 5.1: Coefficients for variables from multiple regression of $\log_e$ transformed biovolume (<2000μm) for AMT 4 and 5 with R^2 of the regression, adjusted for degrees of freedom. The T statistic is shown in brackets below the coefficient. The larger the T statistic, the more significant the factor, the sign indicates whether the relationship is negative or positive. TIR – total incident radiation

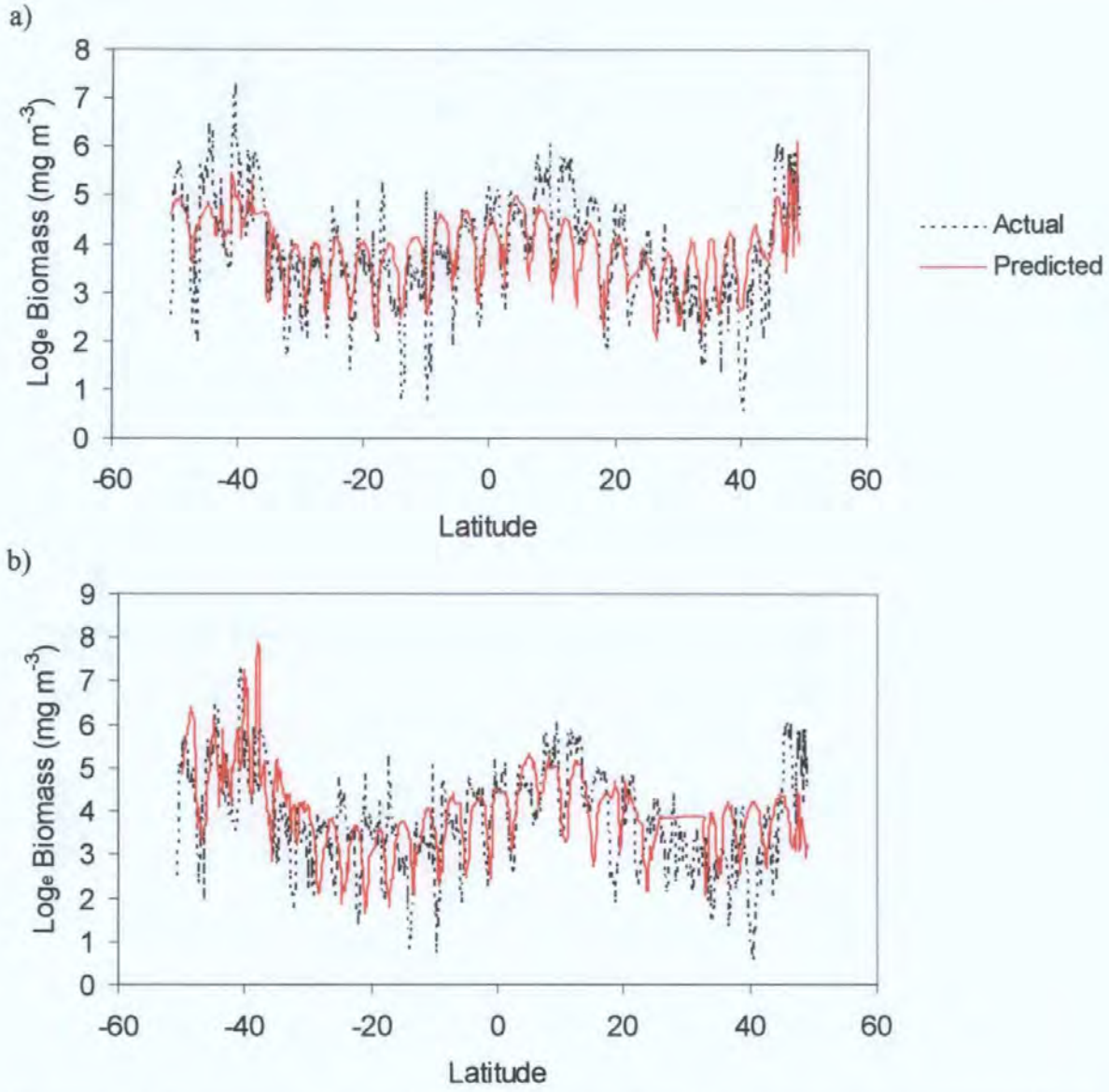

Figure 5.2: Linear regression models of biovolume from the whole transect compared with actual biovolumes for a) AMT 4, b)AMT 5.

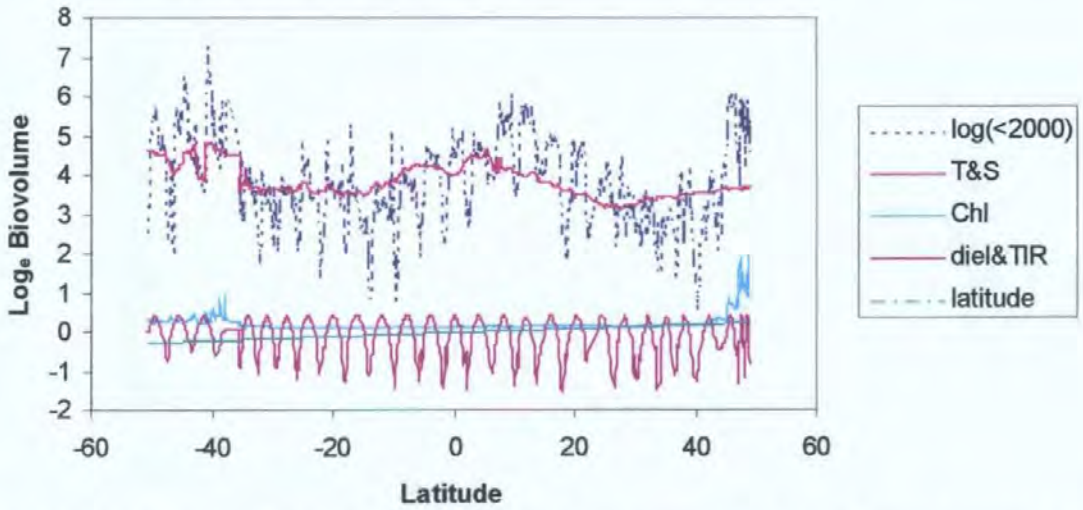

Figure 5.3: The contribution of the different components to the whole transect model derived from the linear regression equation compared to the actual $\log_e$ transformed biovolume (log(<2000)) for the AMT 4 transect. T&S – the contribution of the constant, temperature and salinity, Chl – the contribution of chlorophyll, diel&TIR – the contribution of diel time and total incident radiation.

Regression models of the different areas could explain more of the variability (up to 75%; Table 5.2). However, the factors tended to be similar. A combination of temperature, salinity and density were used in all, but the northern subtropical region, and generally two out of three factors were significant, demonstrating the importance of the oceanographic physics. Chlorophyll was in all models except the northern subtropical, southern tropical and southern temperate. Time of day as modelled by diel time and solar time was a consistently important factor, generally using both measures, and season, spring and autumn was important for temperate and northern regions.

The transects comparing the estimates of biovolume from the linear regression models with the actual biovolumes for AMTs 4 and 5 show good agreement, with R^2 between 0.54 and 0.70 for whole transects (Table 5.2; Figures 5.4 to 5.7). Where the transect has been divided into smaller sections the agreement is generally better. The separate model for the temperate region gave very similar results to the whole transect model (Figure 5.5). The separate regions analysis showed a much better fit, with the predictions being very close to the actual for the whole transect (Figure 5.6). The inclusion of the northern temperate with the warm water region did not affect the warm water region, but improved the fit of the northern temperate over its prediction from the temperate region (Figure 5.7). This suggests that the behaviour of the northern temperate is quite similar to the rest of the transect, and that the southern temperate region is quite different.

Model	R^2
Whole transect	0.55
Warm water/Temperate	0.56
Regions	0.70
Warm water & N/S temperate	0.62
All & south temperate	0.59

Table 5.2: Correlation coefficients of multiple regression models for the whole transects made from the component models of the transect sections for AMT 4 and 5.

a)

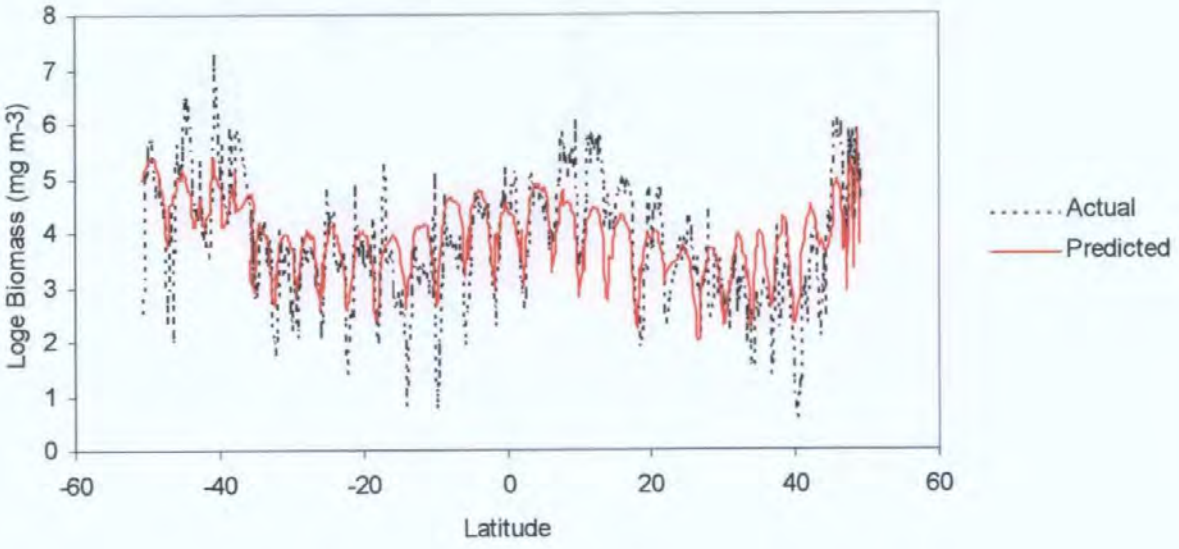

b)

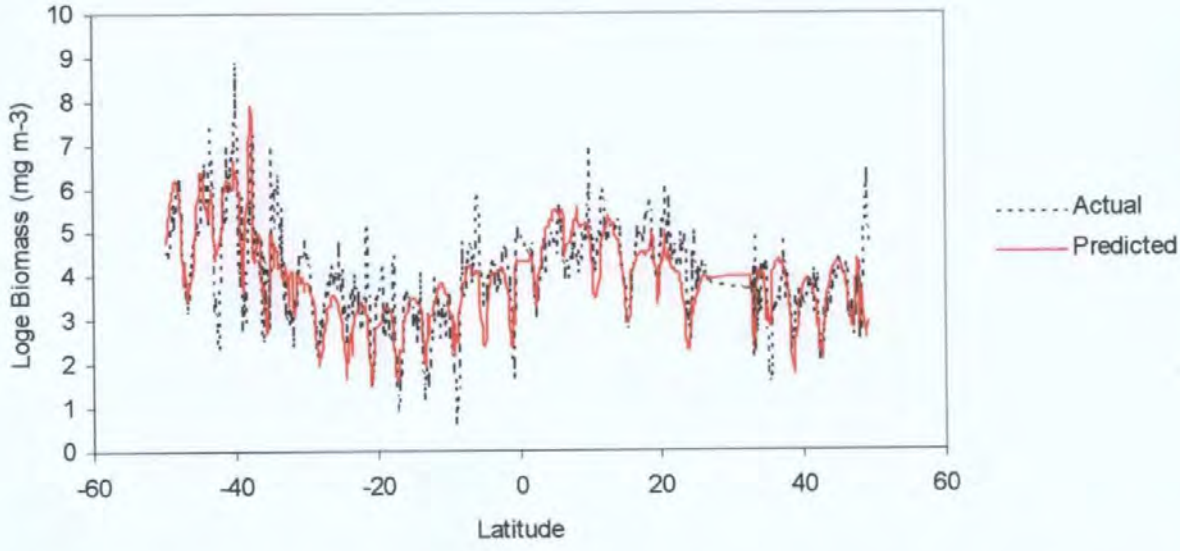

Figure 5.4: Linear regression models of biovolume from the separate temperate and warm water regions compared with actual biovolumes for a) AMT 4, b)AMT 5.

a)

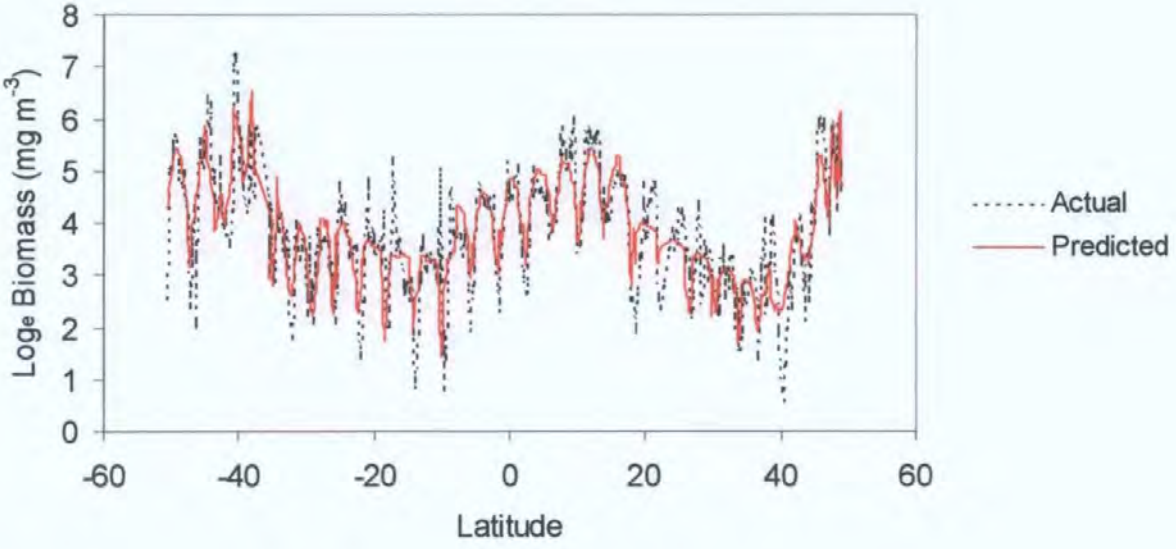

b)

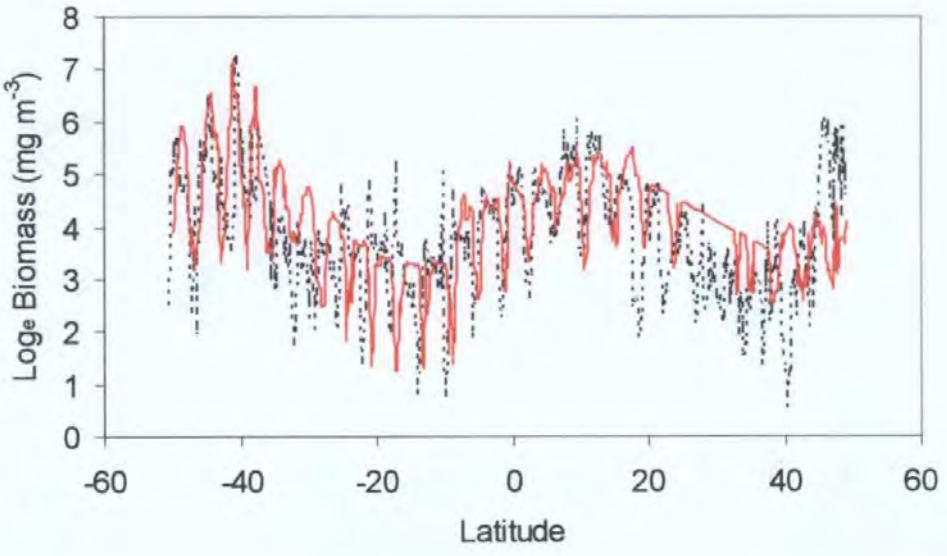

Figure 5.5: Linear regression models of biovolume from the separate regions compared with actual biovolumes for a) AMT 4, b)AMT 5.

a)

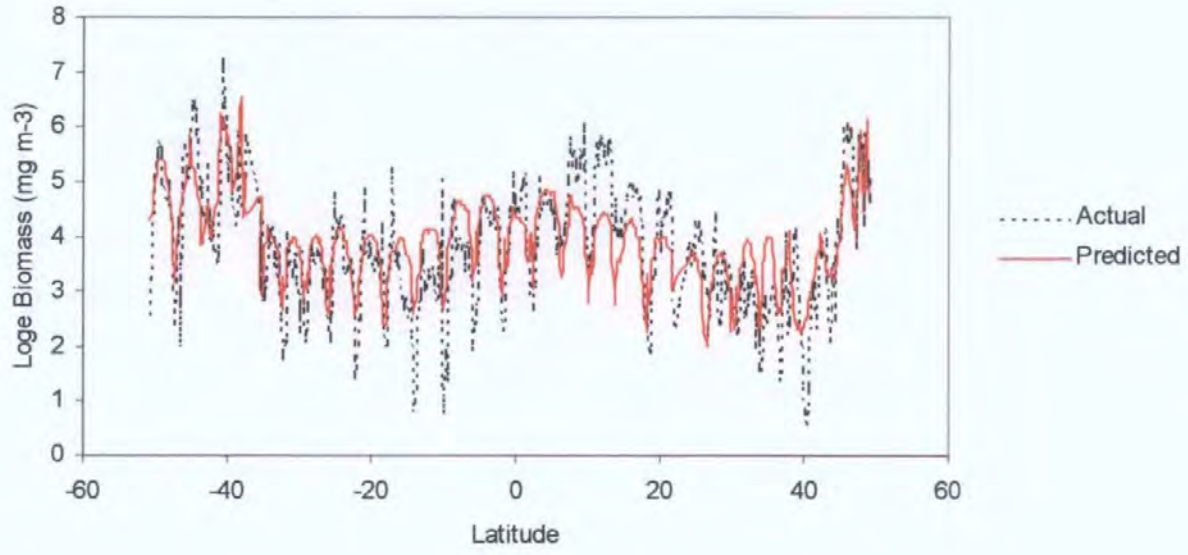

b)

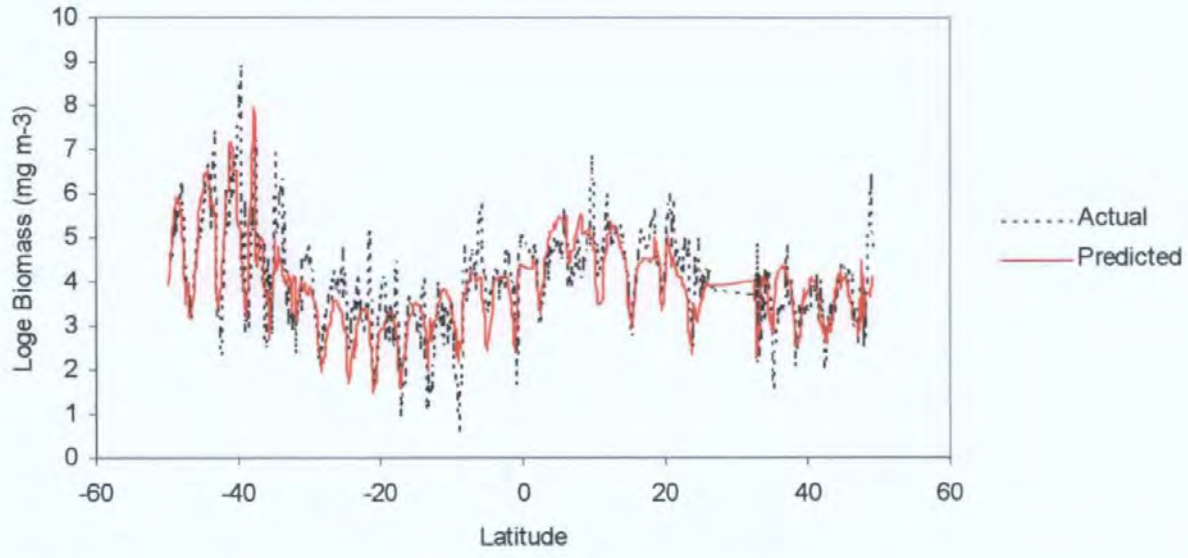

Figure 5.6: Linear regression models of biovolume from the separate warm water and north and south temperate regions compared with actual biovolumes for a) AMT 4, b)AMT 5.

a)

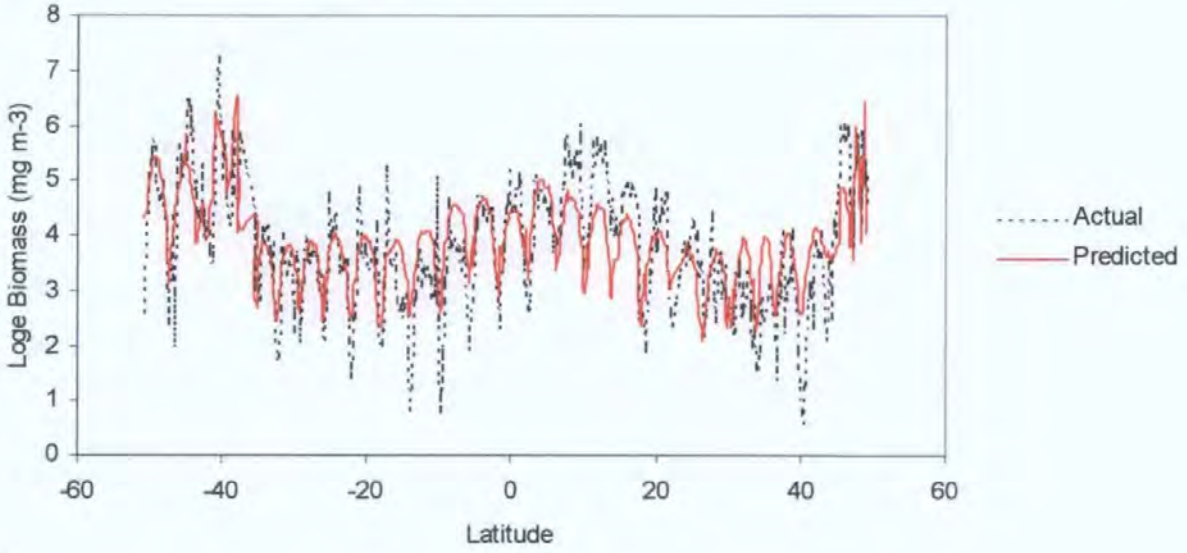

b)

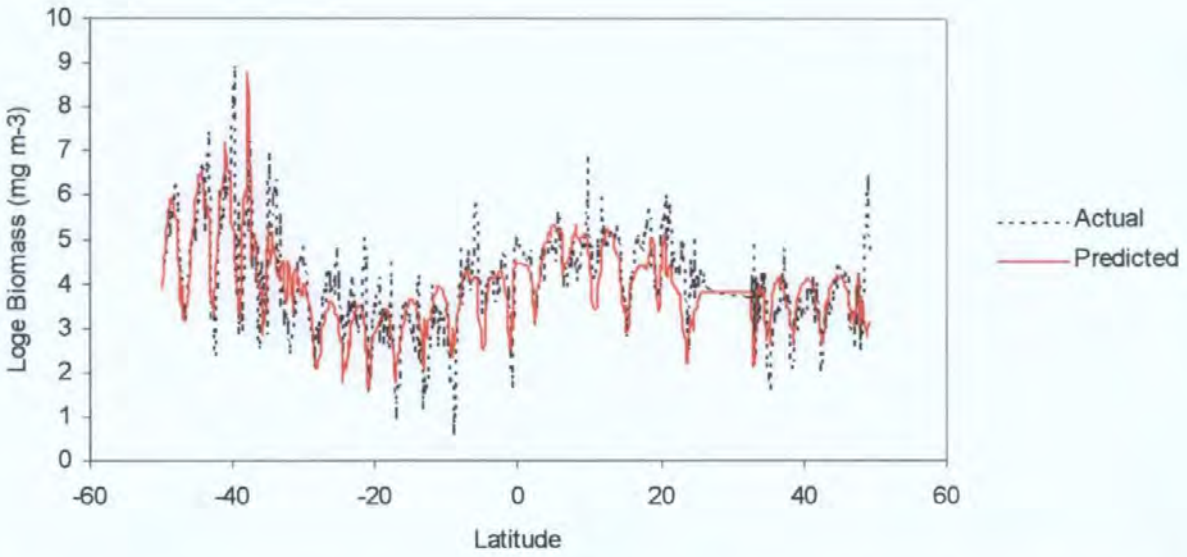

Figure 5.7: Linear regression models of biovolume from the separate warm water and north and south temperate regions compared with actual biovolumes for a) AMT 4, b)AMT 5.

Prediction of the biovolumes from the AMT 4 and 5 models, for AMT2 and 3 showed less good agreement with actual biovolumes, with R^2 varying between 0.33 and 0.42 (Table 5.3). The whole transect model prediction was reasonable, apart from the southern temperate region, which was particularly inaccurate on AMT 3 (Figure 5.8). The best models were the regions model (Figure 5.9) and the model which separated the southern temperate from the rest of the transect (Figure 5.10). The regions model predictions appeared to follow the actual biovolume more closely, although the R^2 was very similar.

Model	R^2
Whole transect	0.34
Warm-water/Temperate	0.39
Regions	0.42
Warm-water & N/S temperate	0.33
All & south temperate	0.42

Table 5.3: Correlation coefficients of multiple regression models for the whole transects made from different components compared with AMT2 and 3.

a)

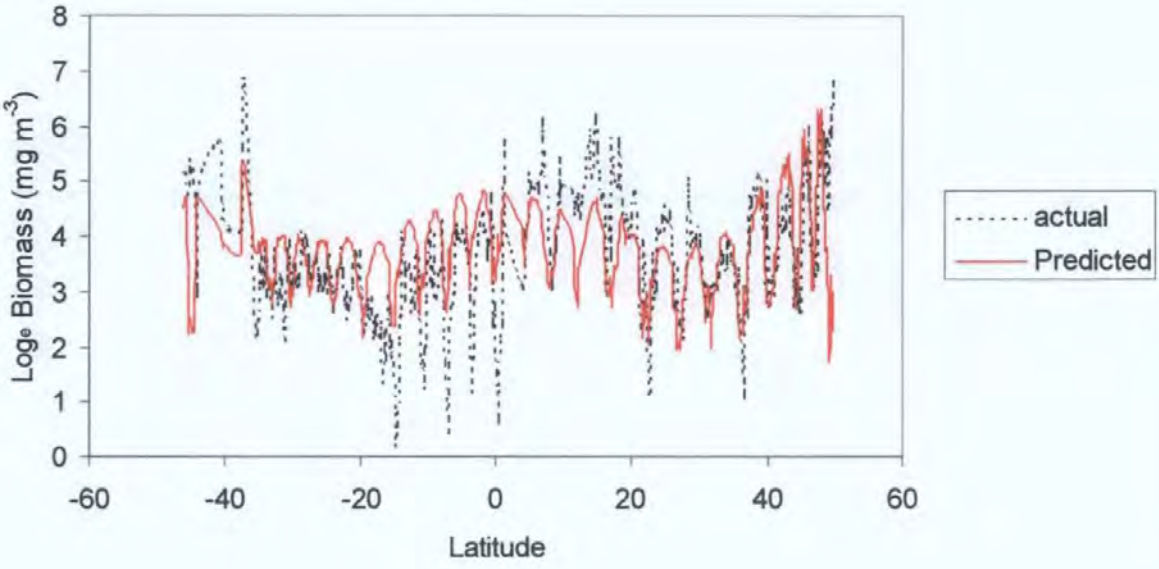

b)

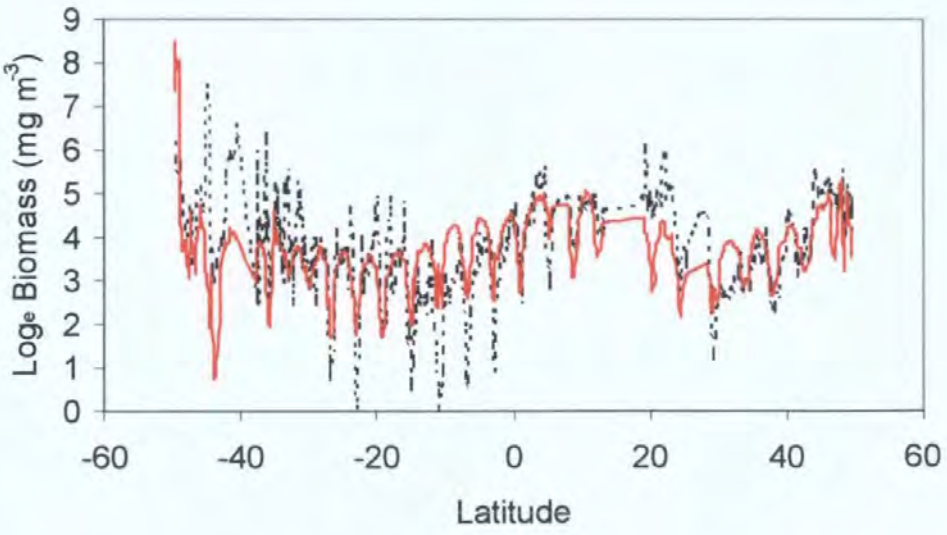

Figure 5.8: Comparison of predicted biovolume from regression model of the whole transect with actual biovolumes for a) AMT 2, b)AMT 3.

a)

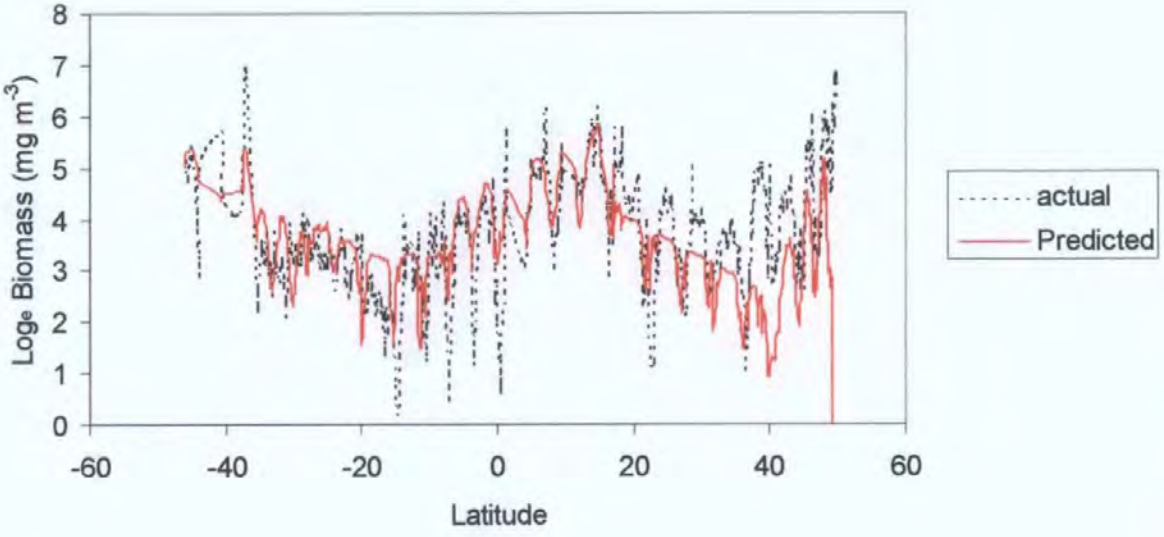

b)

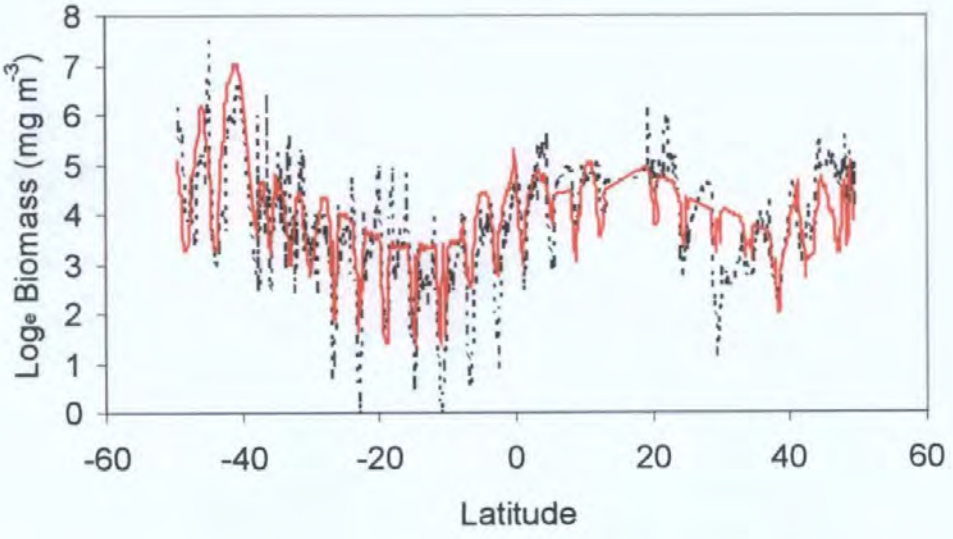

Figure 5.9: Comparison of predicted biovolume from regression model of the regions with actual biovolumes for a) AMT 2, b)AMT 3.

a)

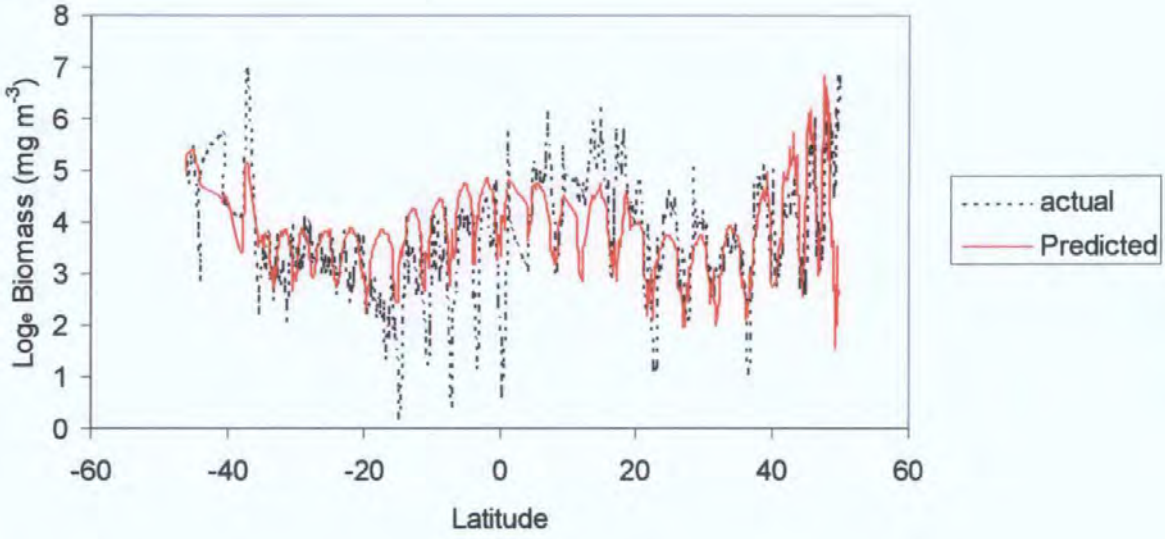

b)

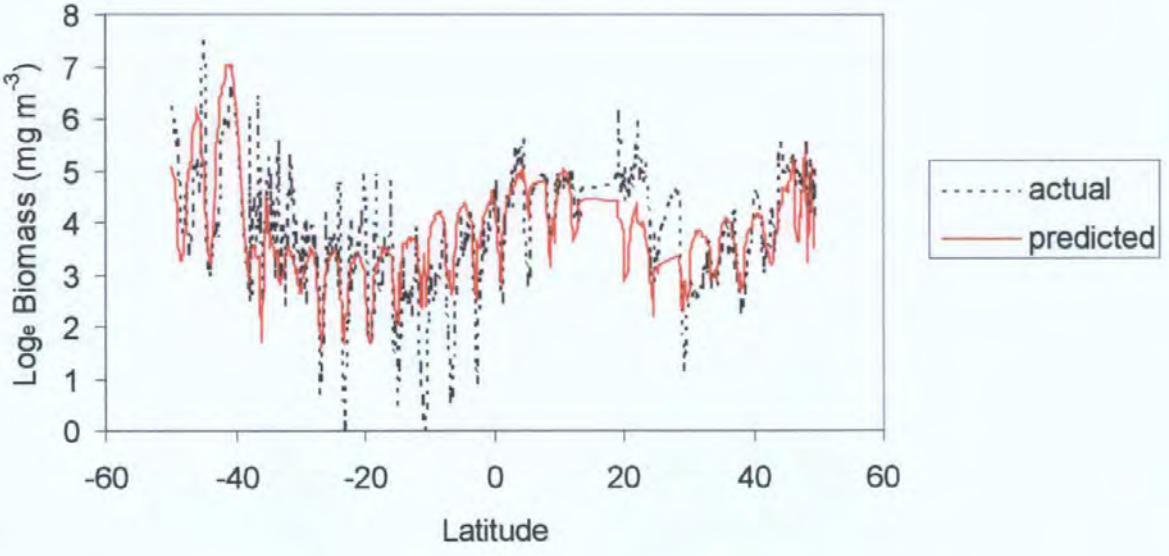

Figure 5.10: Comparison of predicted biovolume from regression model with the S.Temperate calculated separately with actual biovolumes for a) AMT 2, b)AMT 3.

Neural Networks

The model with all the initial variables (latitude, temperature, salinity, density, chlorophyll, TIR, diel time and season) showed good agreement over the transect with an R^2 of 0.77 for Levenberg-Marquardt, and 0.78 with the smoothing algorithm (Figure 5.11).

a)

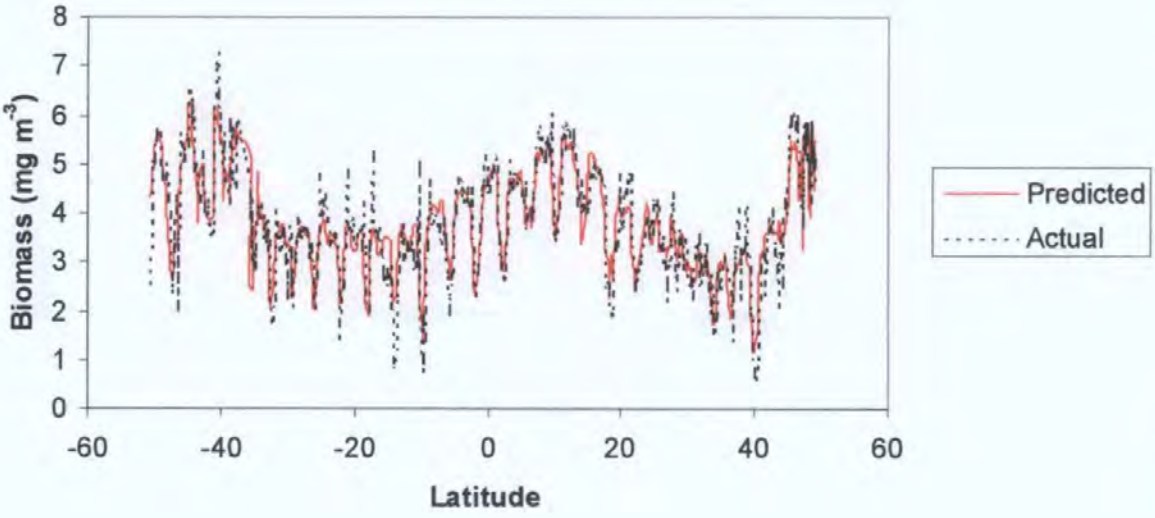

b)

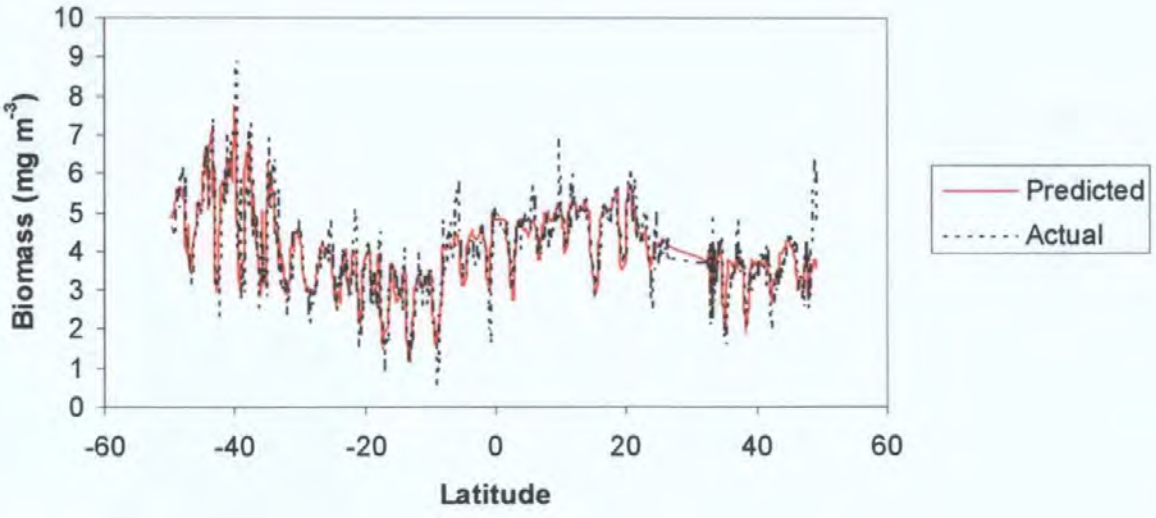

Figure 5.11: Artificial neural network model of biovolume of the original parameter set using the smoothed algorithm, compared with measured biomass (R^2= 0.78), for a) AMT 4, b) AMT 5. (Parameters: latitude, temperature, salinity, density, chlorophyll, TIR, diel time and season)

Optimisation of variables allowed three variables to be lost (density, TIR and season), without significantly affecting the model on either the training or the new data sets (Table 5.4). The predicted biovolumes still followed the measured biovolume very closely (Figure 5.12). Testing of the optimal model on AMT 2 and 3 gave a reduced R^2 of 0.47. This was higher than for the initial model (Table 5.4) or for multiple linear regression models (Table 5.2). The model picked up the major features of zooplankton abundance along the transect (Figure 5.13), but the lowest biovolumes tended to be overestimated on AMT2, and the highest biovolumes were overestimated just south of the equator. Although the peaks in the southern temperate region were predicted, on AMT 3 their magnitude was also overestimated.

Latitude	Temperature	Salinity	Density	Chlorophyll	TIR	Diel time	Season	AMT 4 & 5 R^2	AMT 2 & 3 R^2	
x	x	x	x	x	x	x	x	0.782	0.311	Initial model
x	x	x	x	x		x	x	0.782	0.391	
x	x	x		x		x	x	0.768	0.465	
x	**x**	**x**		**x**		**x**		**0.766**	**0.474**	**Optimal model**
x	x	x				x		0.758	0.428	

Table 5.4: Summary of neural networks optimising variables for the whole transect, showing the results at each stage of subtraction. The variables included in the model are marked with x, with R^2 for the training set (AMT 4 and 5) and independent test cruises (AMT2 and 3). Bold highlights the final accepted model.

a)

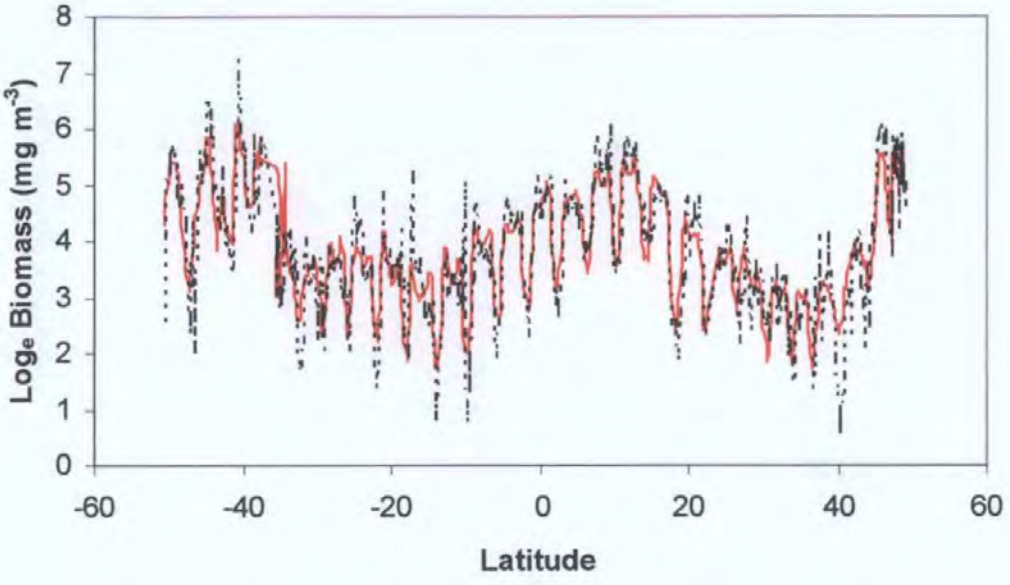

b)

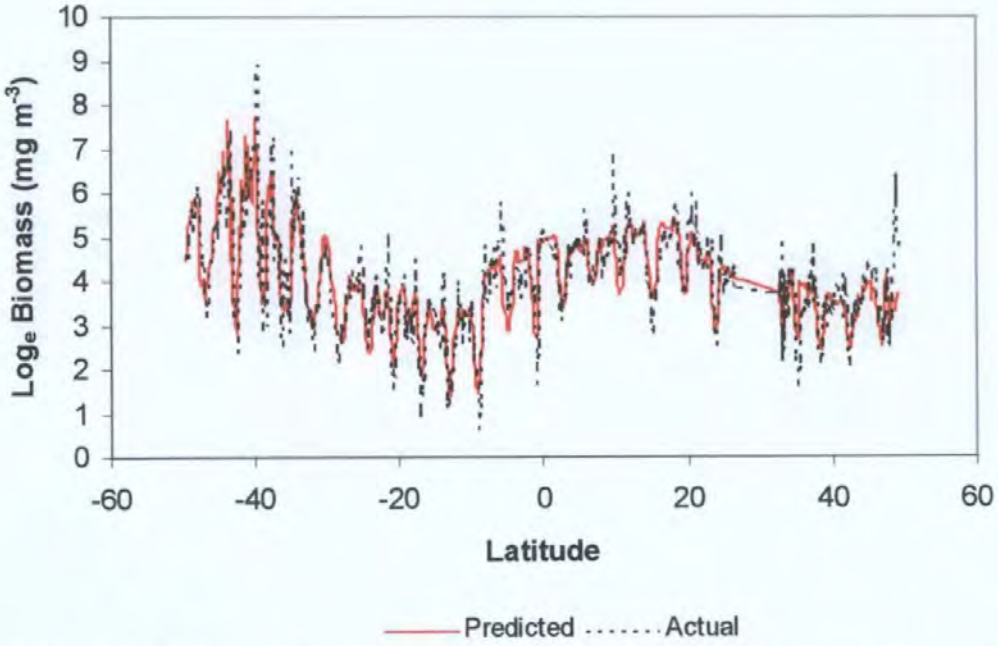

Figure 5.12: Artificial neural network model of biomass of the optimised parameter set compared with measured biomass (R^2= 0.77), for a) AMT 4, b)AMT 5. (Parameters: latitude, temperature, salinity, chlorophyll and diel time)

a)

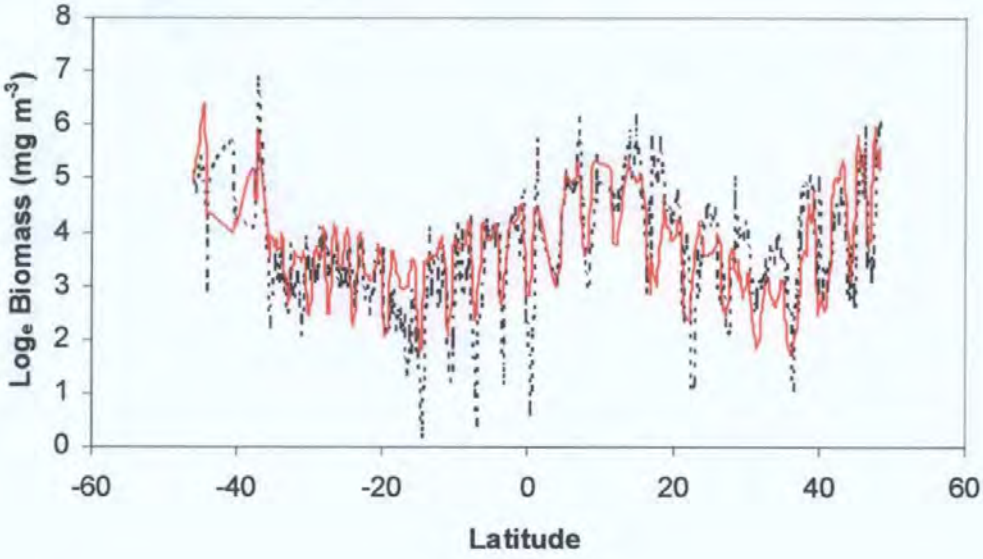

b)

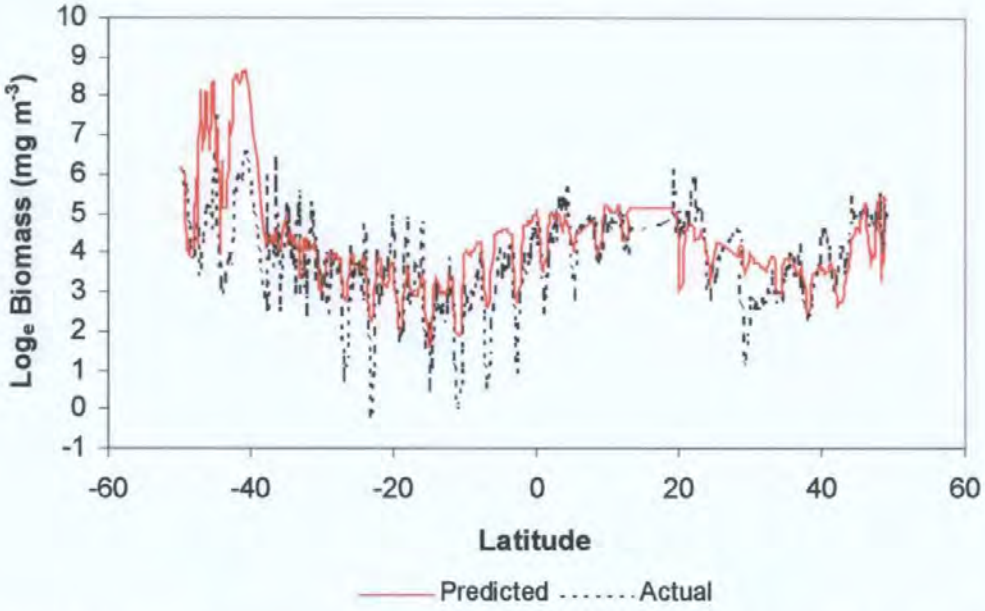

Figure 5.13: Artificial neural network model of biovolume of the optimised parameter set compared with measured biovolume (R^2= 0.47), for a) AMT 2, b)AMT 3. (Parameters: latitude, temperature, salinity, chlorophyll and diel time)

Optimisation with the same variables for the regions separately generally did not improve the model substantially with R^2 values varying between 0.55 and 0.88 (Table 5.5). However, the R^2 for the northern temperate region was greater. Using the variables significant in the multiple regression analysis for each region did not improve the model behaviour either, and in many cases the R^2 value was lower than with the optimised model variables.

Region	Latitude	Temperature	Salinity	Density	Chlorophyll	TIR	Diel time	Season	AMT 4 & 5 R^2
Warm water	x	x	x		x		x		0.786
Temperate	x	x	x		x		x		0.757
S.Temperate	x	x	x		x		x		0.551
S.Subtropical	x	x	x		x		x		0.756
S.Tropical	x	x	x		x		x		0.727
Equatorial	x	x	x		x		x		0.765
N.Subtropical	x	x	x		x		x		0.741
N.Temperate	x	x	x		x		x		0.878
Whole with no S.Temp.	x	x	x		x		x		0.750
Warm water	x	x	x		x	x	x		0.775
Temperate			x	x	x	x	x	x	0.709
S.Temperate	x		x			x	x		0.591
S.Subtropical		x			x		x		0.736
S.Tropical	x	x		x	x	x	x		0.647
Equatorial	x	x	x	x		x		x	0.756
N.Subtropical	x					x		x	0.596
N.Temperate	x	x		x	x		x	x	0.878
Whole with no S.Temp.	x		x	x	x	x	x		0.757

Table 5.5: Summary of neural network models optimised for each region with optimal model variables, and with variables significant in multiple regression by region. The variables included in the model are marked with x, with R^2 for the training set (AMT 4 and 5, N=1138, P<0.01 for all).

Comparison of neural network with multiple linear regression

The optimal neural network model showed improved performance over the linear multiple regression model, with higher R^2 values for both the training data sets (AMT 4 and 5), and for the novel set (AMT 2 and 3). An alternative approach to evaluating the model is to investigate the distribution of the residuals. Figure 5.14 compares the distribution of the residuals between the multiple linear regression and the neural network models. Both show bias tending to overestimate the amount of zooplankton, although this is more pronounced with the multiple linear regression model (mean residual of 0.0058) than the neural network model (mean residual of 0.00057). The multiple regression model also has a larger spread of residuals with greater maximum residuals (-3.4 and +3.0); even so 67% are with

an untransformed factor of 2. For the neural network model 85% are within these limits, with maximum residuals –2.9 to +2.3.

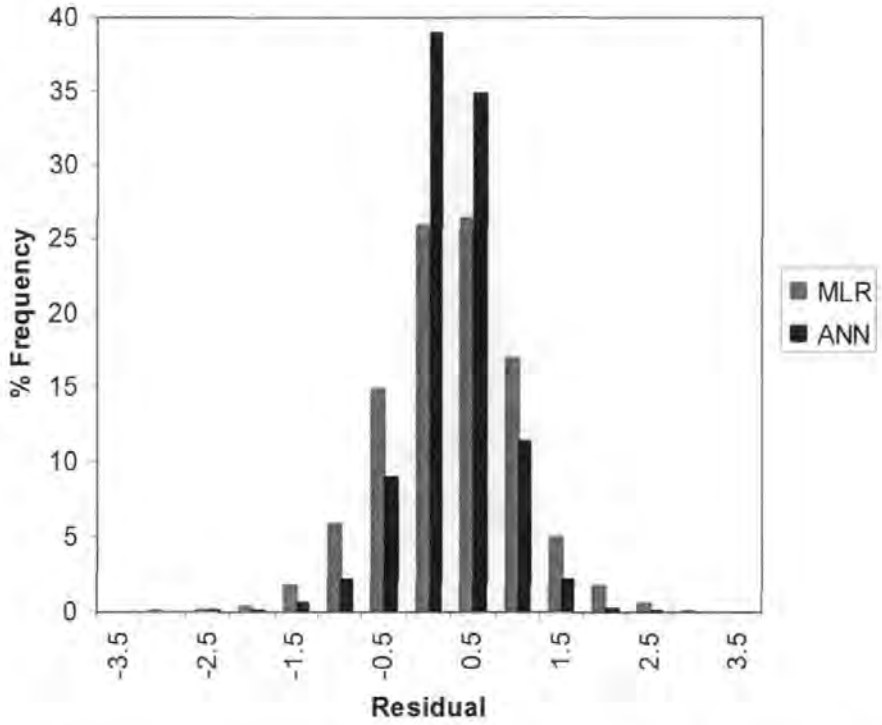

Figure 5.14 Comparison of residuals between multiple linear regression (MLR) and artificial neural network (ANN) models of zooplankton for AMT 4 &5 data sets.

Analysis of neural network model behaviour

Sensitivity analysis of the different factors in the different regions showed how the complex interactions were involved, with the relationships with the biovolume varying substantially between regions. Latitude had the greatest effect in the equatorial region, with more northerly areas having higher biovolumes, making c. 2 log units difference (7x) in zooplankton abundance over the regions (Figure 5.15). In the northern subtropical region, latitude had virtually no effect. In the northern temperate there was a slight increase in zooplankton with latitude. In the southern temperate, the reverse trend was apparent with the furthest south having lower biovolumes. The southern tropical and subtropical regions showed a slight increase in biovolume further south.

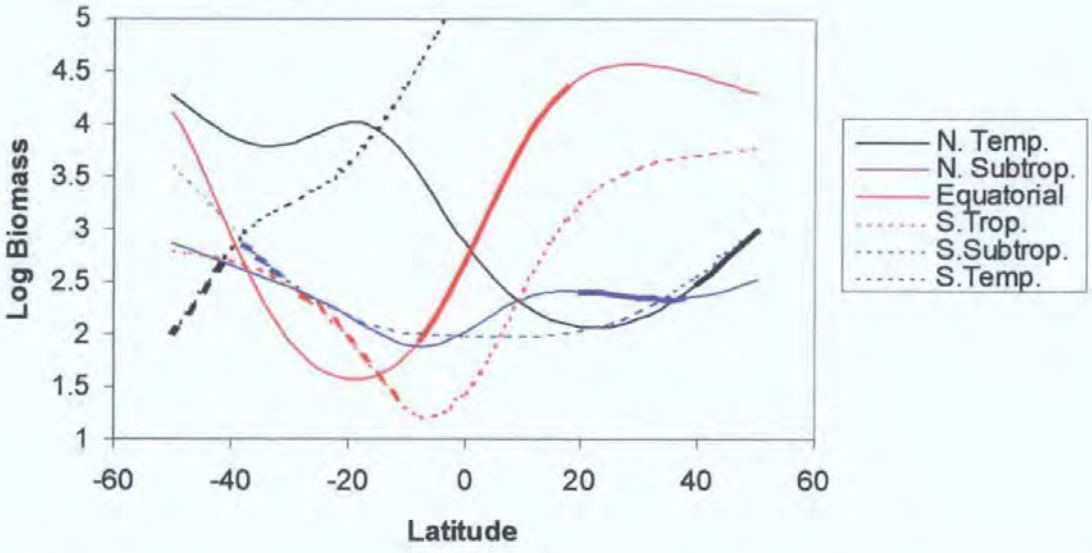

Figure 5.15: Sensitivity analysis of latitude, showing the effect on biovolume in the different regions. Bold lines show the latitudinal range of each region. (N. Temp 38-50°N, N. Subtrop. 18-38°N, Equatorial 8°S-18°N, S. Trop. 28-8°S, S.Temp. 28-38°S)

Temperature showed a complex pattern over the transect (Figure 5.16). For southern subtropical, southern tropical and equatorial regions, lower temperatures were generally associated with higher biomass, although the relationship varied. Cooler temperatures in these regions may be associated with upwelled water or increased mixing with cold, higher nutrient waters from below the thermocline, and therefore higher productivity. In the southern temperate region lower temperatures were associated with higher biomass, possibly due to the warm waters of the Brazil current supporting lower production than the cool seasonally mixed waters of the Falklands current. In the northern temperate and subtropical regions, biomass minima were associated with intermediate temperatures (16°C and 21°C respectively), with biomass increasing at higher and lower temperatures. This more complex pattern may be due to productive coastal regions having warmer waters and being more productive or due to a seasonal effect.

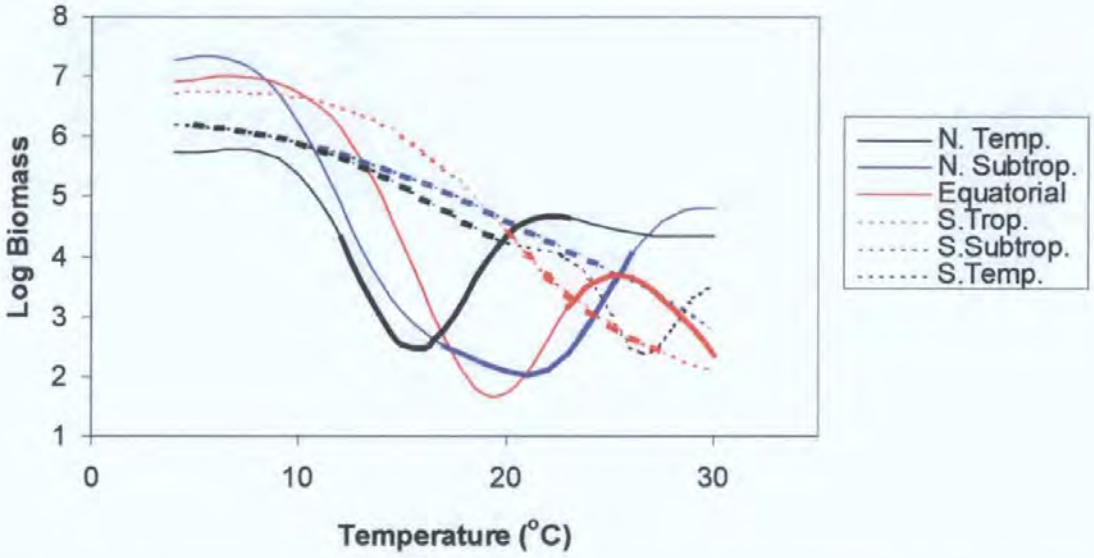

Figure 5.16: Sensitivity analysis of temperature (°C), showing the effect on biovolume in the different regions. Bold lines show the temperature range experienced within each region. (N. Temp 38-50°N, N. Subtrop. 18-38°N, Equatorial 8°S-18°N, S. Trop. 28-8°S, S.Subtrop. 28-38°S, S.Temp 38-50°S)

Salinity in general showed a trend of increasing biomass with decreasing salinity, although the relationship was not always straightforward (Figure 5.17). For instance, salinities around 34.5‰ were associated with lower biomass in the southern temperate region. The overall relationship followed the expected pattern with the lowest biomass associated with the highest salinities, which are found in the oligotrophic gyres. The effect of salinity was greatest in the northern temperate region where over less than one unit, the log biomass increased by 3 $\log_e$ units (20x). This may be due to an additional coastal effect where low salinity is associated with the highly productive inshore waters.

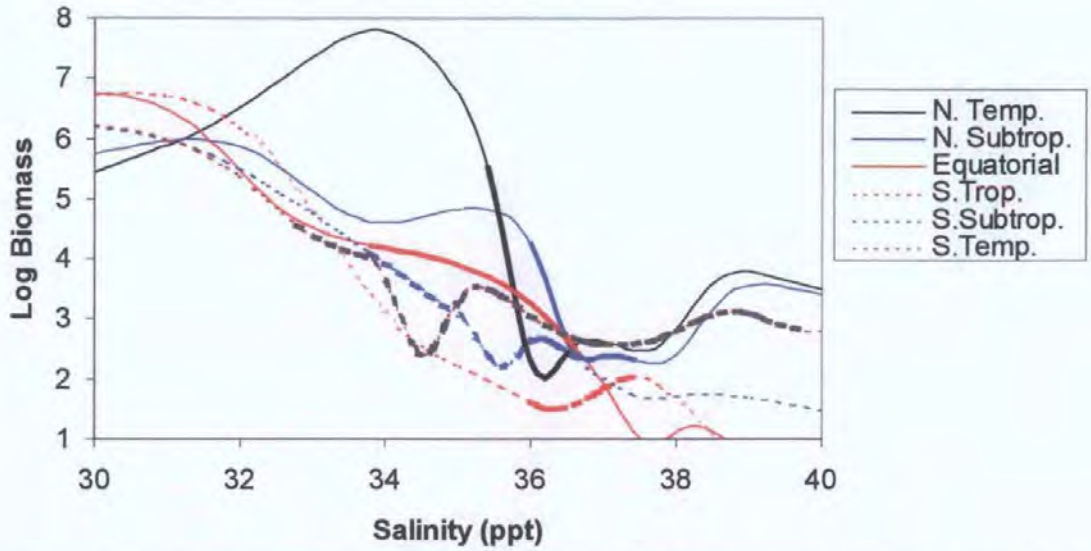

Figure 5.17: Sensitivity analysis of salinity (‰), showing the effect on biovolume in the different regions. Bold lines show the salinity range experienced within each region. (N. Temp 38-50°N, N. Subtrop. 18-38°N, Equatorial 8°S-18°N, S. Trop. 28-8°S, S.Subtrop. 28-38°S, S.Temp 38-50°S)

Chlorophyll was generally, but not always associated with higher biomass, at least over the range associated with that region making between 1 and 2 log units difference (Figure 5.18). Outside this range estimates showed different relationships. The northern and southern subtropical and equatorial regions showed a rapid drop in biomass at chlorophyll levels higher than the range. The northern temperate region reached an asymptote at 2mg chl m^{-3}. This suggests that the neural network may be unreliable outside the training range. In the southern temperate and subtropical regions, minimum biomasses were associated with intermediate chlorophyll concentrations.

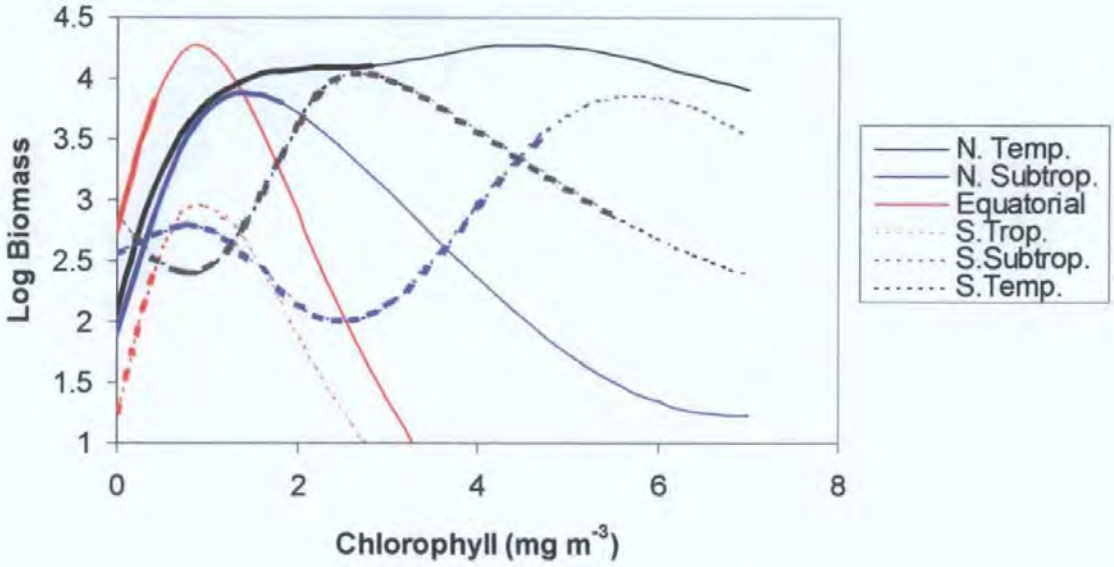

Figure 5.18: Sensitivity analysis of chlorophyll (mg m^{-3}), showing the effect on biovolume in the different regions. Bold lines show the chlorophyll range experienced within each region. (N. Temp 38-50°N, N. Subtrop. 18-38°N, Equatorial 8°S-18°N, S. Trop. 28-8°S, S.Subtrop. 28-38°S, S.Temp 38-50°S)

Diel time showed a consistent trend across the transect, with high zooplankton biovolumes at night (-1) and low biovolumes during the day (+1), making between 1 and 2.5 log units between maximum and minimum biovolumes (Figure 5.19). This is equivalent to a factor between 3 and 12 for day:night. The exact nature of the diel changes varied across the regions. Figure 5.20 shows the diel changes for a standard day, with 0 midnight , 6 dawn, 12 noon, 18 dusk and 24 midnight. During the day, the biovolume approximates to half a sine curve, over the whole transect. In the southern temperate region, the night follows the sine wave too. However, for the other regions there is a distinct flattening between dusk and dawn, with a peak evident at these times. The dawn/dusk peak is most pronounced in the southern tropical region.

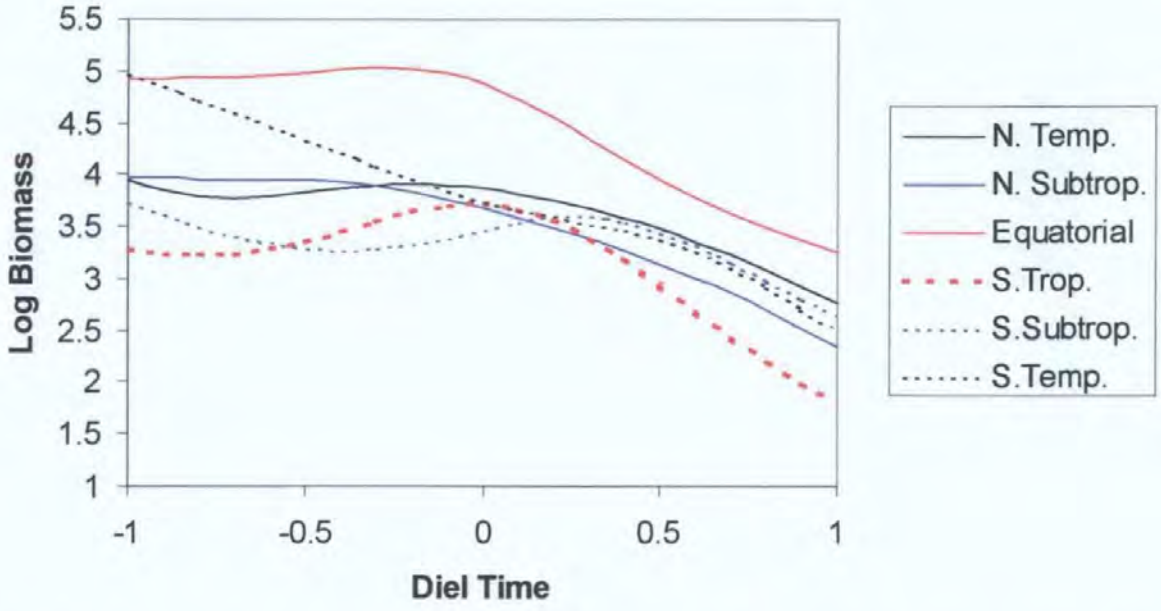

Figure 5.19: Sensitivity analysis of diel time, showing the effect on biovolume in the different regions. (N. Temp 38-50°N, N. Subtrop. 18-38°N, Equatorial 8°S-18°N, S. Trop. 28-8°S, S.Subtrop. 28-38°S, S.Temp 38-50°S)

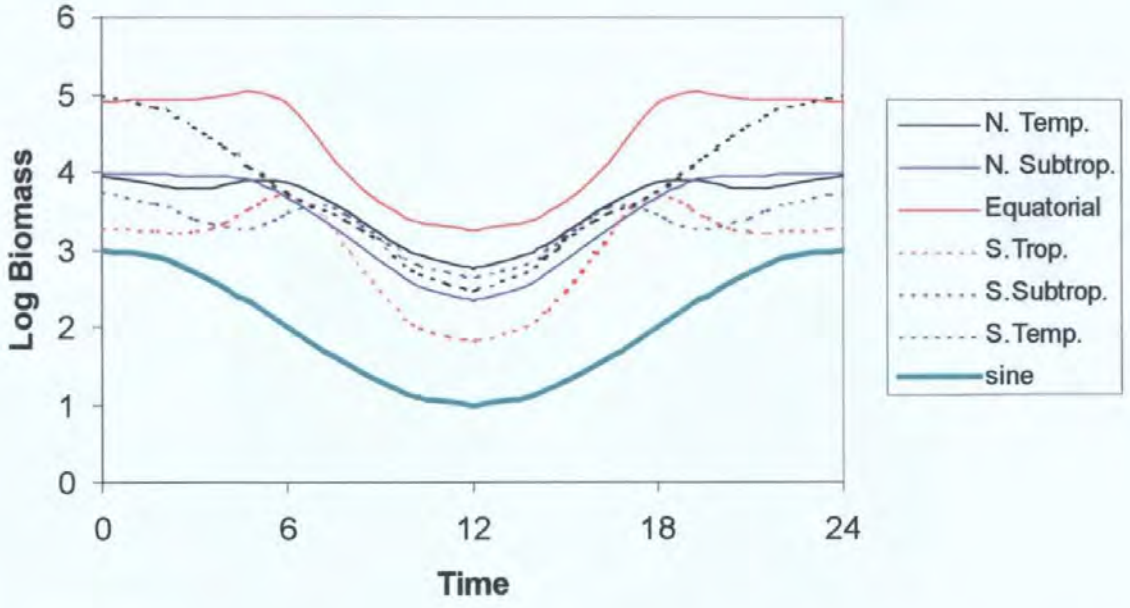

Figure 5.20: The neural network model of diel changes in surface zooplankton for the different regions on a standardised day (N. Temp 38-50°N, N. Subtrop. 18-38°N, Equatorial 8°S-18°N, S. Trop. 28-8°S, S.Subtrop. 28-38°S, S.Temp 38-50°S, 0 midnight, 6 sunrise, 12 noon, 18 sunset, 24 midnight). Sine is a sine wave of amplitude 1 (-diel time, the input).

Discussion

Multiple regression model

Linear multiple regression can explain approximately half the variability of the log transformed biovolume, and is most accurate for values close to the mean, tending to underestimate the very high values and overestimate very low ones. Others (e.g. Scardi 1996) have found similar effects using linear regression models. The consistently important factors for predicting the zooplankton biovolume are latitude, the ocean physics (temperature, salinity and density), the amount of phytoplankton (chlorophyll), time of day (total solar radiation and diel time) and time of year (season). Maravelias and Reid (1997) noted the changes in abundance of zooplankton associated with oceanographic features, and phytoplankton abundance is known to be an important factor in influencing zooplankton abundance (e.g. Koppelmann and Weikert 1992) and productivity (e.g. Calbet and Agustí 1999, Zhang *et al.* 1995). The physics and chlorophyll, modified for season and latitude add to give the overall abundance of the zooplankton. Season may help to give a historical aspect, an influence of the timing within the system. The influence of latitude is quite small for the overall model, adding an asymmetry to the effects of the other variables. The time of day affecting surface zooplankton abundance is unlikely to reflect changes in the actual abundance of zooplankton in the water column, but be due to diel migration of the zooplankters. Diel migration of zooplankton has long been recognised and is associated with changes in light level, as indicated here by the importance of total incident radiation. The sine wave is a very simple model of the diel migration. A more complex model including 'midnight sinking' might improve the predictability. The linear model does not allow for changes in the extent of migration with factors such as changes in the zooplankton community structure (Roman *et al.* 1995), presence of predators (Bollens *et al.* 1994), latitude and food supply (e.g. Fiksen and Giske 1995; Calbet and Agustí 1999) that are known to have an affect on diel migratory behaviour.

Tests on novel data sets (AMT2 and 3), showed reduced R^2 values of between 0.3 and 0.42. The R^2 of the novel data sets gives an indication of the generality of the model. Even though the R^2 is reduced the general pattern of zooplankton biomass is still being followed by the model. The high biomass of the southern temperate region is not being predicted accurately, and, on AMT 2, the equatorial region shows less good agreement. The model for the whole transect can be improved by dividing into regions, or at least by treating the southern temperate region (38°S-50°S) separately. The division into regions allows optimisation of factors without 'over fitting'. It also suggests that the magnitude of influences of factors on zooplankton abundance may not be constant across the ocean, particularly in the dynamic southern temperate region. The southern temperate region is very dynamic, coinciding with the confluence of the warm oligotrophic Brazil current and the cold relatively nutrient rich Falklands current. Thus the dynamic of this regime is closely coupled to the physical parameters, behaving differently from other regions. Alternatively, improved model performance may reflect the non-linearity of the systems which is being inadequately modelled.

The multiple regression model is simple to interpret. The t statistic shows the strength of each factor. However, it does have limitations. The model assumes a linear relationship between the independent and dependent variables, although 'new' variables can be made by multiplying factors together or transforming them. The combination of independent variables alters the effect of each variable, particularly when variables are closely related and co-vary (multicolinearity), as with temperature, salinity and density. The model may be improved by including interactions between variables and by allowing non-linear relationships. More complex models such as generalised additive models used by Maravelias and Reid (1997) may give further insight into the influences and controls on zooplankton.

Neural networks

The neural networks showed improved estimation of the zooplankton biomass over the multiple regression, with an R^2 of 0.78 for the initial model with eight inputs. This highlights the non-linear relationship between zooplankton abundance and the parameters. Reducing the inputs to 5 did not affect the R^2 greatly (0.77). The predictive power of the model with fewer inputs demonstrated the redundancy in much of the original data. Testing of the optimal model on AMT 2 and 3 data sets, showed a reduced R^2 (0.47), but this was greater than for the multiple regression analysis. The original model showed a lower R^2 suggesting that it tended to 'overfit' the data, reducing the robustness of the model for new data sets. In addition to the higher R^2 of the neural network model over the linear multiple regression model, the residuals also showed less bias and a narrower distribution.

The variables selected included latitude, temperature, salinity, chlorophyll and diel time. These are almost identical to the variables that were selected from the multiple regression for the whole transect (salinity has replaced density, and TIR is not included). Optimisation for the different regions with the same variables or for regions with the significant variables from multiple regression analysis did not significantly improve the models. This is likely to be due to two factors: the non-linear network being able to model zooplankton abundance adequately across the whole transect, and the smaller training sets being insufficient to optimise the parameters fully.

Future improved model performance may be obtained by using more data to train the network, so that the parameter space is more extensively covered. Further optimisation may be reached by changing the model architecture or input parameters. 'Top down' effects of predators on the system, which have been shown to be important in certain situations (e.g. Steele and Henderson 1995; Hutchings *et al.* 1995), are not included.

Sampling errors in the original data will also reduce the predictability. However, the model is unlikely to reach the 'perfect' prediction of an R^2 of 1, about the 1:1 line, due to the fundamental nature of zooplankton. Zooplankton are known to show greater variability at smaller scales than the ocean physics (Piontkovski and Williams 1995). Interactions within the zooplankton such as swarming behaviour (e.g. Ueda *et al.* 1983, Kimoto *et al.* 1988, Omori and Hamner 1982), and predator-prey interactions will tend to introduce errors/noise into the predictions. However, some degree of smoothing may be considered beneficial for overall predictability.

Sensitivity analysis demonstrated the impact of the different parameters in the different regions. In general, the relationships followed expected trends. High chlorophyll was associated with high biomass, high salinity and temperatures associated with the oligotrophic gyres coinciding with low biomass, and night with high biomass due to diel migration. However, within these trends, the parameters appear to have opposite effects in different regions, and sometimes they are counterintuitive. This could be due to the interactive effects of the variables, particularly where the variables are covariate. Thus for example, although chlorophyll is generally associated with high zooplankton abundance, in some regions (e.g. southern subtropical 1-2mg chl m^{-3}) the relationship is negative. Over this parameter space, it could be that temperature and salinity are overestimating zooplankton abundance, or it could be that the zooplankton are lower due to predation for example. It is interesting to note that none of these unexpected effects are apparent in the diel time, even though the impact of diel time does vary between regions. The modelling of the diel migration gives insight into the differences in diel migration in the different regions. In the southern temperate region, the difference between day and night biomass is greatest (12x), and reaches a maximum at midnight, closely following the sine curve. This region also has many large zooplankton which are known to undergo much greater diel migrations (e.g. Zhang *et al.*1995), and thus take longer to reach the surface waters after

dusk. Throughout the rest of the transect day-night change in zooplankton abundance varies between 3 and 5 times, and maximum abundance is frequently at dawn/dusk, either plateauing or dropping in darkness, in a similar manner as described by Mauchline (1998).

By modelling zooplankton using spatial (ocean physics, chlorophyll) and temporal parameters (diel time), the spatial and temporal components to the distribution can be at least to a certain extent separated. Figure 5.21 demonstrates how zooplankton biovolume would be expected to vary over the transect if sampling was at midnight only. In the future, such insights might allow more accurate comparison of samples taken during the day and night.

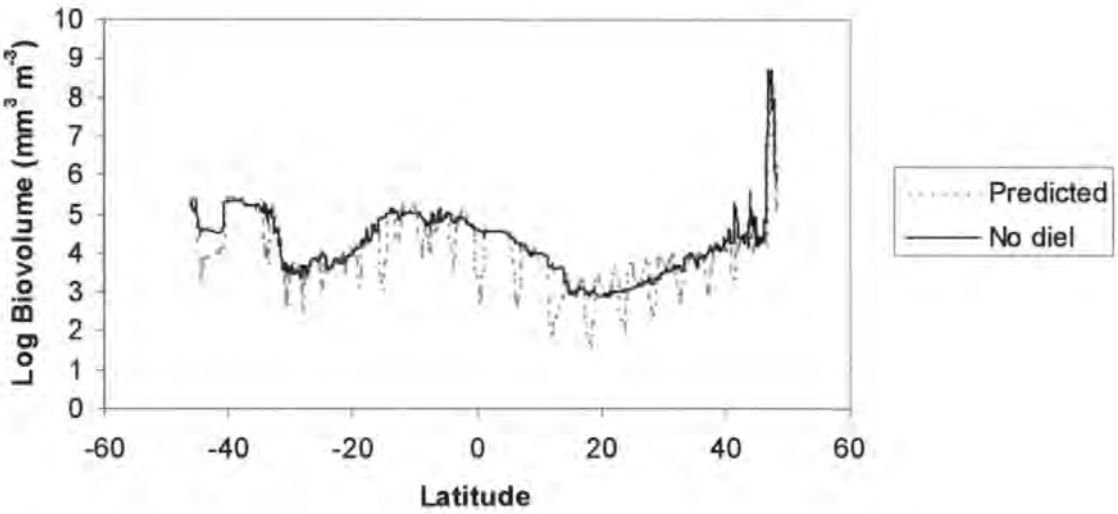

Figure 5.21: Optimised model comparing the predicted biovolume if sampling was at night, with the model including diel migration for AMT 4.

Possible extensions of this neural network approach could include extension to use over wider areas using satellite data, to give a global estimate of zooplankton biomass. As Huntley and Lopez's (1992) suggested that zooplankton productivity can be estimated from the biomass and temperature, it is conceivable that global secondary production may be estimated. Alternatively, neural networks could be used for prediction patterns of zooplankton diversity, and testing of different hypotheses in a similar way to Guégan *et al.*

(1998), or more complex neural networks with multiple outputs to model changes in taxonomic or size community structure.

Conclusions

The amount of surface zooplankton can be predicted using a few easily measured parameters. The ocean physics and chlorophyll influences the abundance in the water column, and time of day influences the proportion within the surface layer. Neural network models enhance the predictability over multiple linear regression, especially for large areas and do not require separate models for different areas, even though the influence of different parameters is easier to understand using multiple linear regression. The effect of different parameters is complex for neural networks, but can be revealed using sensitivity analysis. It is therefore apparent that multiple linear regression models can be enhanced by using neural networks for prediction in ecosystem modelling. In the future the neural network approach could allow prediction of several properties of zooplankton community structure.

Chapter 6: Discussion

The importance of scale in understanding variability in zooplankton communities has long been recognised. Haury *et al.* (1978) produced a Stommel diagram showing the heterogeneity at different scales in time and space. Pinel-Alloul (1995) recognised the usefulness of automated systems such as fluorometers, optical plankton counters and acoustic systems that allow collection of data at high resolution, yet covering large spatial scales, giving insight into heterogeneity over a large range of scales. With the extensive nature of the data, detail such as taxonomy is lost. Although the OPC gives some insight into the size structure of the community, taxonomic aspects of the system cannot be deduced, except in very simple ecosystems where one size range is dominated by a single taxa. To this end, the OPC has been successfully utilised for *Calanus finmarchicus* distributions (Heath *et al.* 1999). By using automated devices in conjunction with traditional techniques their use can be validated, and greater insight can be brought to bear on questions such as scale and variability. Further improvements may be made by using the OPC in conjunction with an acoustic Doppler current profiler (ADCP), which measures size range from large copepods upwards (Smith *et al.* 1992). Overlap in the size range with the OPC has allowed some inter-comparison, and has shown similar results (e.g. Gallienne *et al.* in press). Future developments of automated video systems (e.g. Davis *et al.* 1992, Gallienne 1997) may allow greater accuracy in predicting zooplankton biomass and allow some degree of taxonomic resolution.

The AMT has provided a valuable and cost-effective resource, making it possible to study basin-scale variation in zooplankton and other oceanic properties in an integrated way. Future collaborative projects with similar ships of opportunity will bring greater understanding of the workings of the oceans, particularly the undersampled oligotrophic

gyres that make up a large proportion of the world's oceans. With the satellite information now readily available, a truly global approach to oceanography is possible.

Scale is emerging as one of the critical problems that must be considered in community ecology (Allen and Hoekstra 1991). Previously 'holistic' approaches to spatial variation in zooplankton abundance have been dominated by coastal and shelf sea studies (e.g. Denman 1976, Horwood 1976, Mackas and Boyd 1979, Steele and Henderson 1979, Gallager *et al.* 1996). In the present study, spectral analysis has used in order to gain a holistic perspective of zooplankton heterogeneity of the oceans over a wide range of scales (10-1000 km). The spectral analysis of continuous data from the surface has emphasised the change in the nature of variability at different spatial scales. At the largest scales, greater than 500 km, there are regular frequencies of variation in zooplankton, phytoplankton and temperature. At these scales changes in zooplankton biomass can be considered in terms of changes in regimes of temperature, water column structure, seasonality and ocean circulation patterns. The patterns appear to be dominated by the physical forcing. These give rise to latitudinal trends and ocean provinces.

At intermediate scales, between scales of 100's and 10's of km, zooplankton patch frequency follows a power law close to –1 with patch size, although this changes between regions. The Falklands-Montevideo part of the transect showed a slightly steeper gradient compared to the rest of the transect. Piontkovski *et al.* (1997) found steeper slopes of zooplankton heterogeneity in the tropical Atlantic Ocean of –2 to-3, over similar scales (10-200 km). Over these scales of 100's and 10's of km, the salinity, temperature and chlorophyll patch frequency is related to scale by a power law of approximately –2. A –2 power law is similar to previous studies in coastal environments and oceanic environments where values between –2 and –3 are typical (e.g. Horwood 1976, Gower *et al.* 1980, Piontkovski *et al.* 1997). This suggests that zooplankton are more patchy, particularly at

smaller scales than phytoplankton or passive traces of turbulence in the open ocean as well as coastal systems. Abraham (1998) proposed that this could be as a result of differences in maturation time. Larger zooplankton tend to have longer maturation times (Hirst and Sheader 1997), and thus are predicted to have flatter power spectra. The size fractionated biomass demonstrated that indeed larger zooplankton were more patchy at smaller scales. Piontkovski and Williams (1995) suggested that in the tropics predators were patchily distributed as compared with their prey in tropical oceans, i.e. zooplankton were patchy compared to phytoplankton, and fish were patchy compared to zooplankton. This has also been seen in the present study. At these intermediate scales, heterogeneity in zooplankton biomass appears to cohere with phytoplankton biomass, with peaks in phytoplankton and zooplankton coinciding.

At small scales, >10 km, zooplankton abundance appears to become random. This could be due to the zooplankton distributing themselves randomly, or due to under sampling giving the appearance of randomness. Others have found that zooplankton are patchy on smaller scales. Currie *et al.* (1998) demonstrated that zooplankton were patchy on the metre scale. Mackas and Boyd (1979) found zooplankton more patchy on a scale of 100-1000 m in the North Sea. Thus it is probable that undersampling is at least contributing to the change in slope. In future, if analysis over these scales is to be studied, a greater volume needs to be sampled or numbers rather than biomass used.

The spectral analysis suggested that large scale zooplankton heterogeneity was associated with large scale changes in the environment. This is likely to apply to other aspects of zooplankton community structure and biomass. Large scale patterns have been proposed, and demonstrated with varying degrees of success for zooplankton and other organisms. Latitudinal clines in diversity have been demonstrated in a wide variety of environments: marine (e.g. Rex *et al.* 1993, Culver and Buzas 2000), freshwater (e.g. Barbour and Brown

1974) and terrestrial (e.g. Simpson 1964, Silvertown 1985). In the pelagic realm, the broad scale and use of different sampling gear and analytic protocols has brought doubt on the validity of general patterns such as latitudinal trends and biogeographic schemes, which frequently used published data from several sources. Others have used collative data qualitatively, not utilising abundance (e.g. Gibbons 1997). Here, although the taxonomic detail is more limited than some studies and only from the surface waters (top 200 m), it did concentrate on the most numerous component of the zooplankton, the copepods. The samples were taken and analysed in the same manner, so are internally consistent, and sampling effort was similar over much of the transect with good coverage. Extension of the AMT using data from samples taken and processed in a similar way, with overlap, has enabled greater spatial coverage.

The latitudinal gradient in zooplankton richness is apparent in even the types of zooplankton, and is profound in the copepod genera for the open ocean. The gradient of richness of the copepod genera appears not only in the density of genera, but also in the total surface community. Comparing with data from further north and south than the AMT transect, it can be seen that this trend extends into the Arctic and Antarctic waters. Boltovskoy *et al.* (1999) show a slightly different pattern for the South Atlantic, with copepod species richness being slightly lower at the equator than the central/subtropical region (10-35 ^{o}S), and then dropping rapidly at the transition zone (35 ^{o}S). Boltovskoy *et al.* (1999) noted the difficulty in getting reliable data, and only considered 101 copepod species. A similar trend was found in the class and subclass analysis of copepods, suggesting that the reduction in richness occurs at all taxonomic levels within the copepods.

The causes of the latitudinal gradients are not fully understood. Sea surface temperature has been shown to have a strong relationship with diversity (Rutherford 1999), but the

mechanism has not been demonstrated. Rutherford (1999) suggested that temperature reflects the water column structure and niche availability. A covariant with latitude is seasonality. Seasonality affects the physical structure of the ocean and the productivity regime directly through solar radiation. More pronounced seasonality in production will act as a stress, and reduce the range of successful life-histories. At low latitudes, primary production is more or less constant throughout the year, allowing close coupling between phytoplankton and zooplankton. Boltovskoy *et al.* (1999) suggest that this coupling may be an important factor in determining diversity. Biological interactions emphasise these differences through feedback mechanisms. There is evidence to suggest that more complex food webs can support a wider range of organisms, for example predators have been found to increase prey diversity (e.g. Dodson 1970, Hall *et al.* 1970, Crooks 1999). Stability of the system may enable tighter interactions, specialisation and thus narrow niches in a similar way to hypotheses for rainforest diversity. Stevens (1989) reported that high latitude species had wider latitudinal ranges (Rapopart's rule), and suggested that this might be related to niche breadth. Rhode (1992) suggested that greater diversity at low latitudes was due to faster evolution at higher temperatures due to shorter generation times, higher mutation rates and faster physiological processes.

Taxonomic diversity shows a rather different pattern, in that diversity is stable across the central part of the ocean (35 ^{o}N – 35 ^{o}S), but then rapidly falls with an increase in the variance as well. This suggests that there is a dramatic change in community structure, which is also seen in the sample similarity of copepod genera. At greater latitudes than 38 ^{o}N/S, the variability in the taxonomic structure increases and shifts. The size structure did not reflect this change. The model indicates important parameters predicting the zooplankton biomass, and showed that the role of factors changed in these temperate areas, particularly in the southern temperate region. The 38 ^{o}S boundary coincides with the boundary of the South Atlantic Central Water and the Sub Antarctic Water. The physics

and productivity regimes of the watermasses are quite different. The spectral analysis suggested that the scales of variability were different. This is a dynamic area in which eddies and ring structures are common, increasing the heterogeneity at scales of the order of 100 km. In the Northern Hemisphere, there is no corresponding change in watermass, and although the community structure change is as strong, the behaviour of the system is less so. Longhurst (1998) proposed that at around 40 ^{o}N was the boundary between the subtropical and the temperate gyre systems. It appears that temperature and seasonality may interact to cause the latitudinal gradient in species richness.

The Benguela upwelling region off southern Africa showed a distinct taxonomic community of copepods, and a suggestion of a different zooplankton size structure. The diversity was lower than expected from its latitude, similar to the temperate region. It has been suggested that this is associated with the water temperature. However, the diversity was lower than was expected from the sea surface temperature. All these factors support the hypothesis that coastal upwelling systems such as the Benguela are separate systems and parameters affecting the ecosystem dynamics will be different. The zooplankton community shows in several cases adaptation to the environment (e.g. Verheye *et al.* 1992).

The warm water region appears to be quite uniform, with the copepod community being quite similar throughout. However, on close inspection subtle changes in the community can be seen, and this area can be divided into a number of sub-regions. The northern and southern subtropical regions were not distinguishable from each other in the generic composition, and are intermediate in similarity between temperate and the equatorial/tropical. The equatorial and southern tropical regions are significantly different from each other and the subtropical regions. The division of the warm-water area is similar to other biological schemes, but does not appear to be so closely related to the watermasses

or Longhurst (1998)'s regions. The size structure of the zooplankton does not appear to reflect the changes in the taxonomic structure. Future analysis of copepods to species may make these sub-regions clearer and define the boundaries more precisely.

Size structure of a community is a fundamental property and may influence the productivity and energy flow within the ecosystem (Peters 1983). Generally the size structure of marine pelagic systems follows a relationship where the biomass in logarithmic size classes remains constant (e.g. Sheldon *et al.* 1972, 1977), although individual spectra may have peaks in abundance over specific size ranges (e.g. Wieland *et al.* 1997), or different slopes (e.g. Piontkovski *et al.* 1995). In the current study, it can be seen that the zooplankton community size structure varies considerably over the Atlantic in terms of the total abundance, mean size and proportion in each size fraction. However, these changes in size structure do not appear to be directly related to changes in the taxonomic structure or to latitudinal changes. Thiel (1975) hypothesised that reduced levels of resource supply (productivity) led to communities with smaller individual size. There is some evidence to support this hypothesis: Pavoni (1963) suggested that nannoplankton dominate oligotrophic lakes whereas larger phytoplankton are more common in eutrophic lakes, and Davis (1980) found an increase in mean adult size of freshwater lakes in more productive waters. In this study, it has been demonstrated that mean zooplankton size is correlated to zooplankton standing stock.

Others have found that zooplankton abundance and size structure is an important part of aquatic ecosystem functioning. Sprules and Holtby (1979) found that the size structure of lake zooplankton was more closely related to the lake type than the species composition. Zhou and Huntley (1997) estimated population growth based on the size structure of the zooplankton. Huntley and Lopez (1992) found that secondary production could be predicted from the biomass and temperature more reliably and easily than from individual

species. Models including size structure may provide more realistic predictions than those based on individual species (Armstrong 1999). Thus it appears that the abundance and size structure of zooplankton may give a more general insight into the ecosystem functioning and energy transfer than detailed taxonomic studies. However, functioning of specific ecosystems will still be improved by taxonomic, behavioural and life-history information (e.g. Davis 1987).

The modelling of zooplankton biomass showed that surface zooplankton abundance could be predicted from a few easily measured parameters (temperature, salinity, chlorophyll, time of day and latitude). The parameters were affecting the zooplankton to different extents in the different regions, as demonstrated by the multiple linear regression regions model and neural network sensitivity analysis. At large scales, it appears that patterns in zooplankton community structure are dominated by physical forcing, in agreement with much of the literature (e.g. Haury *et al.* 1978, Barry and Dayton 1991, Pinel-Alloul 1995). However, the physical processes appear to be reinforced by the biological attributes. Diel migration i.e. a behavioural response, appears critical in abundance of zooplankton in the surface waters. Haury *et al.* 1978 noted that diel vertical migration affects zooplankton abundance over a wide range of scales. The change in the pattern of diel vertical migration over the transect demonstrates the interaction between physical environment and the biological community in determining the structure. The model of zooplankton biomass also suggests that complex non-linear interactions between the parameters can account for the variability in zooplankton biomass. Future understanding may be gained from more complex sensitivity analysis co-varying more than one parameter. Better generalisation capabilities require a more diverse range of data sets over the same region and from other transects. It may be possible to develop neural network models to utilise satellite imagery and thus be able to predict zooplankton biomass on the ocean scale. The neural network

approach may also be applied to other problems in zooplankton ecology such as understanding patterns in diversity and community structure.

As well as the spatial variability explicitly analysed, temporal variability is also evident. Seasonal differences are apparent, particularly in the temperate regions. These are evident in the zooplankton biomass and sea surface temperature, although the taxonomic structure did not reflect these changes. Diel changes are very pronounced over the whole transect, affecting all the abundance (described above) and other measures of zooplankton community structure in the surface layer. The spectral analysis of zooplankton showed that diel variation was particularly evident in the mean ESD, thus suggesting a change in size structure. Larger zooplankters tend to migrate to the surface at night, whereas many of the smaller copepods remain in the surface waters throughout the diel cycle. There were two frequencies associated with diel migration (11 and 22 hours). Piontkovski *et al.* (1997) noted a similar finding. The zooplankton abundance for the surface layer shows that zooplankton abundance increases between 1 and 2.5 $\log_e$ units (biomass increases by a factor of c 2.5 to 12) from day to night. The greatest migration is seen in the southern temperate region. Although diel migration approximates to a sine wave during the day, the pattern of diel migration appears to differ between regions at night. In the southern subtropical region, zooplankton abundance peaks at dawn and dusk, sinking over the hours of darkness. Many other areas do not show such a pronounced sinking, but more of a plateau at night where zooplankton abundance is more constant. The southern temperate region is closest to the sine wave at night. This is also the region of highest migration, and where high abundances of large copepods such as *Calanus* and *Rhincalanus* are abundant. If these larger species are migrating further (Dam *et al.* 1993, Hays *et al.* 1994), it could be that they do not reach the surface layer until later in the night.

Conclusions

The methods selected have complimentary strengths. Microscope analysis allows detailed taxonomy. Carbon analysis gives accurate but not real time estimate of biomass. The OPC gives an accurate size distribution and rapid assessment of biomass, calibrated from carbon and microscope analyses.

Spectral analysis demonstrated the importance of scale in understanding zooplankton heterogeneity in the open ocean. At basin scales, heterogeneity is associated with ocean circulation, and is largely determined by the physics. Over mesoscales, zooplankton abundance follows a log-log linear relationship of –1, and is more patchy at smaller scales than temperature or chlorophyll. Zooplankton and phytoplankton show some covariance over these mesoscales, and it is over the mesoscale that the biological physical properties of the ocean show the greatest interaction.

Very few data sets are evident in the zooplankton literature traversing several ocean provinces and covering a large latitudinal range, where sampling and analysis are consistent. At the large scale, copepod richness shows a strong, symmetrical reduction in richness towards high latitudes. This is strongly correlated with temperature. However, the taxonomic diversity (including dominance and relatedness as well as richness) and copepod community structure (indicated by MDS) show a sudden change at around 35-40°N/S with a reduction in diversity and an increase variance of the community structure at higher latitudes. This boundary corresponds to the approximate location of the end of the permanent pycnocline (Longhurst 1998). It is proposed that the seasonality in production may account for the change in community structure. The warm waters of the Atlantic between 38°N and 38°S can be subdivided into areas of similar communities. The boundaries of these regions do not appear to coincide with changes in ocean physics, e.g.

with water masses or biogeochemical provinces, but are similar to other biologically derived divisions of the ocean. This suggests that although the environment must determine the communities, it is not a simple relationship. The Benguela region has low diversity and a community adapted to the upwelling environment.

The size structure did not follow a latitudinal gradient in the same way as the diversity or share the same regional divisions as the copepod community, but was related to the productivity. Larger mean size was associated with higher standing stock of zooplankton.

Modelling of zooplankton abundance has shown that it could be predicted from a few readily measured parameters. Neural networks show enhanced performance over multiple linear regression. This approach has potential for extension to a global prediction of zooplankton abundance.

References

Abraham, E.R. (1998) The generation of plankton by turbulent stirring. *Nature* **391**, 577-580.

Aiken, J. (1998) *AMT 6 cruise report.* Pp 1-75. Plymouth: Plymouth Marine Laboratory.

Aiken, J., Cummings, D.G., Gibb, S.W., Rees, N.W., Woodd-Walker, R.S., Woodward, E.M.S., Woolfenden, J., Hooker, S.B., Berthon, J.-F., Dempsey, C.D., Suggett, D.J., Wood, P., Donlon, C., Gonzalez-Benitez, N., Huskin, I., Quevedo, M., Barciela-Fernandez, R., deVargas, C. and McKee C. (1998) *Volume 2, AMT-5 Cruise Report.* Hooker, S.B. and Firestone, E.R. (Eds.) NASA/TM-1998-206892v, pp.1-113. Greenbelt, Maryland: Laboratory for Hydrospheric Processes.

Aksnes, D.L. and Lie, U. (1990) A coupled physical-biological model of a shallow sill fjord. *Estuarine, Coastal and Shelf Science* **31**, 459-486.

Alldredge, A.L., Robison, B.H., Fleminger, A. and Hamner, W.M. (1984) Direct sampling and in situ observation of a persistent copepod aggregation in the mesopelagic zone of the Santa Barbara Basin. *Marine Biology* **80**, 75-81.

Allen, T.F.H. and Hoekstra, T.W. (1991) Role of heterogeneity in scaling of ecological systems under analysis. In: Kolasa, J. and Picketts, S.T.A. (Eds.) *Ecological heterogeneity*, pp. 47-68. New York: Springer-Verlag.

Angel, M.V. (1993) Biodiversity of the pelagic ocean. *Conservation Biology* **7**, 760-772.

Angel, M.V. (1997a) Pelagic biodiversity. In: Ormond, R.F.G., Gage, J.D. and Angel, M.V. (Eds.) *Marine biodiversity: patterns and processes*, pp. 35-68. Cambridge: Cambridge University Press.

Angel, M.V. (1997b) Importance of biogeography in global change and biodiversity studies. *IOC workshop report* **142**, 27-35.

Aoki, I., Komatsu, T. and Hwang, K. (1999) Prediction of response of zooplankton biomass to climatic and oceanic changes. *Ecological Modelling* **120**, 261-270.

Armstrong, R.A. (1999) Stable model structures for representing biogeochemical diversity and size spectra in plankton communities. *Journal of Plankton Research* **21**, 445-464.

Backus, R.H. (1986) Biogeographic boudaries in the open ocean. In: Pierrot-Bults, A.C., van der Spoels, S., Zahuranec, B.J. and Johnson, R.K. (Eds.) *Pelagic biogeography*, pp. 9-13. Paris: UNESCO.

Backus, R.H., Craddock, J.E., Haedrich, R.L. and Robinson, B.H. (1977) Atlantic mesopelagic zoogeography. Fishes of the Western North Atlantic. *Mem. Sears Fdn Marine Research* **1**, 266-287.

Baily, G.W. and Chapman, P. (1991) Short term variability during an Anchor Station study in the southern Benguela upwelling system. Chemical and physical oceanography. *Progress in Oceanography* **28**, 9-37.

Bale, A.J. (1996) AMT-3 cruise report. Pp 1-102. Plymouth: Plymouth Marine Laboratory

Bale, A.J. (1997) AMT-4 cruise report. Pp 1-120. Plymouth: Plymouth Marine Laboratory

Båmsedt, U. (1986) Chemical composition and energy content. In: Corner, E.D.S. and O'Hara, S.C.M. (Eds.) *The biological chemistry of marine copepods*, pp. 1-58. Oxford: Clarendon Press.

Banse, K. (1995) Zooplankton: Pivotal role in the control of ocean production. *ICES Journal of Marine Science* **52**, 265-277.

Barbour, C.D. and Brown, J.H. (1974) Fish species diversity in lakes. *American Naturalist* **108**, 473-489.

Barry, J.P. and Dayton, P.K. (1991) Physical heterogeneity and the organisation of marine communities. In: Kolasa, J. and Picketts, S.T.A. (Eds.) *Ecological heterogeneity*, pp. 270-320. New York: Spriner-Verlag.

Bé, A.W.H. (1977) An ecological, zoogeographic and taxonomic review of recent planktonic foraminifera. In: Ramsey, A.T.S. (Ed.) *Oceanic Micropalaeontology*, pp. 1-100. London: Academic Press.

Bé, A.W.H. and Forns, J.M. (1971) Plankton abundance in the North Atlantic Ocean. In: Kostlow, J.D. (Ed.) *Fertility of the sea, volume 1*, pp. 17-50. London: Gordon & Breach Science Publishers.

Beckmann, W., Auras, A. and Hemleben, C. (1987) Cyclonic cold core eddy in the eastern North Atlantic III Zooplankton. *Marine Ecology Progress Series* **39**, 165-173.

Bennett, A.F. and Denman, K.L. (1985) Phytoplankton patchiness: inferences from particle statistics. *Journal of Marine Research* **43**, 307-335.

Bodin, P. (1999) Marine harpacticoid copepod species richness and diversity: comparison between temperate and tropical zones. *7th International Conference on Copepoda* P.62 (Abstract)

Bollens, S.M., Frost, B.W. and Cordell, J.R. (1994) Chemical, mechanical and visual cues for vertical migration behaviour of a marine copepod *Acartia hudsonica*. *Journal of Plankton Research* **16**, 555-564.

Boltovskoy, D. (1986) Biogeography of southwestern Atlantic: overview, current problems and perspectives. In: Pierrot-Bults, A.C., van der Spoels, S., Zahuranec, B.J. and Johnson, R.K. (Eds.) *Pelagic biogeography.* pp. 14-24. Paris: UNESCO.

Boltovskoy, D. (1997) Pelagic biogeography: background, gaps and trends. In: Pierrot-Bults, A.C. (Ed.) *Pelagic biogeography ICoPB II.* pp. 53-64. Paris: IOC/UNESCO.

Boltovskoy, D. (1999) *South Atlantic zooplankton*, pp 1-1709. Lieden: Backhuys.

Boltovskoy, D., Gibbons, M.J., Hutchings, L. and Binet, D. (1999) General biological features of the South Atlantic. In: Boltovskoy, D. (Ed.) *South Atlantic Zooplankton*, pp. 1-42. Lieden: Backhuys.

Boudreau, P.R. and Dickie, L.M. (1992) Biomass size spectra of aquatic ecosystems in relation to fisheries yield. *Canadian Journal of Fisheries and Aquatic Science* **49**, 1528-1536.

Boyd, C.M. (1973) Small scale spatial patterns of marine zooplankton examined by an electronic insitu zooplankton detecting device. *Netherlands Journal of Sea Research* **7**, 103-111.

Brey, T., Jarre-Teichmann, A. and Borlich, O. (1996) Artificial neural networks versus multiple linear regression: predicting P/B ratios from empirical data. *Marine Ecology Progress Series* **140**, 251-256.

Brinton, E. (1962) The distribution of Pacific Euphausiids. *Bulletin of the Scripps Institution of Oceanography of the University of california* **8**, 51-270.

Calbet, A. and Agusti, S. (1999) Latitudinal changes of copepod egg production rates in Atlantic waters: temperature and food availability as the main driving factors. *Marine Ecology Progress Series* **181**, 155-162.

Carlotti, F., Giske, J. and Werner, F. (2000) Modelling zooplankton dynamics. In: Harris, R.P., Wiebe, P.H., Lenz, J., Skjoldal, H.R. and Huntley, M. (Eds.) *Zooplankton methodology manual*, pp. 571-668. London: Academic Press.

Cassie, R.M. (1963) Microdistribution of plankton. In: Barnes, H. (Ed.) *Oceanography Marine Biology Annual review.* pp. 223-252. London: George Allen and Unwin Ltd.

Chojnacki, J. (1983) Standard weights of the Pomeranian Bay copepods. *Internationale Revue der gesamten Hydrobiologie* **68**, 435-441.

Chow-Fraser, P. and Maly, E.J. (1991) Factors governing clutch size in two species of *Diaptomus* (Copepoda: Calanoida). *Canadian Journal of Fisheries and Aquatic Science* **48**, 364-370.

Clarke, K.R. and Warwick, R.M. (1994) *Change in marine communities: An approach to statistical analysis and interpretation*, Plymouth: Plymouth Marine Laboratory.

Clarke, K.R. and Warwick, R.M. (1999) The taxonomic distinctness measure of biodiversity: weighting of step lengths between heirarchical levels. *Marine Ecology Progress Series* **184**, 21-29.

Colebrook, J.M. (1986) Environmental influences on long-term variability in marine plankton. *Hydrobiologia* **142**, 309-325.

Cooley, J.W. and Tukey, J.W. (1965) A algorithm for the machine calculation of complex Fourier series. *Mathmatical Computation* **19**, 297-301.

Crooks, K.R. and Soule, M.E. (1999) Mesopredator release and avifaunal extinctions in a fragmented system. *Nature* **400**, 563-566.

Culver, S.J. and Buzas, M.A. (2000) Global latitudinal species diversity gradient in deep-sea benthic foraminifera. *Deep Sea Research I* **47**, 259-275.

Currie, W.J.S., Claereboudt, M.R. and Roff, J.C. (1998) Gap and patches in the ocean: a one-dimensional analysis of planktonic distributions. *Marine Ecology Progress Series* **171**, 15-21.

Cushing, D.H. (1990) Plankton production and year class strength in fish populations: An update of the match/mismatch hypothesis. *Advances in Marine Biology* **26**, 249-294.

Dadon, J.R. (1997) Environmental structure, scale of analysis and biogeography of the Thecosomata (Gastropoda, Opisthobranchia) in the South Atlantic. In: Pierrot-Bults, A.C. (Ed.) *Pelagic Biogeography ICoPB II*, pp. 97-142. Paris: IOC/UNESCO.

Dadon, J.R. and Boltovskoy, D. (1982) Zooplanktonic recurrent groups (Pteropoda, Euphausia, Chaetognatha) in the southwestern Atlantic ocean. *Physis (Buenos Aires)* **41**, 63-83.

Dalal, S.G. and Parulekar, A.H. (1986) Validity of zooplankton biomass estimates and energy equivalent in the Indian Ocean. *Indian Journal of Marine Science* **15**, 264-266.

Dam, H.G., Miller, C.A. and Jonasdottir, S.H. (1993) The trophic role of mesozooplankton at 47°N, 20°W during the North Atlantic Bloom Experiment. *Deep Sea Research II* **40**, 197-212.

Davies, I.J. (1980) Relationships between dipteran emergence and phytoplankton production in the experimental lakes area, northwestern Ontario. *Canadian Journal of Fisheries and Aquatic Science* **37**, 523-533.

Davis, C.S. (1987) Components of the zooplankton production cycle in the temperate oceans. *Journal of Marine Research* **45**, 947-983.

Davis, C.S., Flierl, G.R., Wiebe, P.H. and Franks, P.J.S. (1991) Micropatchiness turbulence and recruitment in plankton. *Journal of Marine Research* **49**, 109-152.

Davis, C.S., Gallager, S.M., Berman, M.S., Haury, L.R. and Strickler, J.R. (1992) The Video Plankton Recorder (VPR): design and initial results. *Archiv fur Hydrobiologie. Ergebnisse der Limnologie* **36**, 67-81.

De Nie, H.W., Bromley, H.J. and Vijverberg, J. (1980) Distribution patterns of zooplankton in Tjeukemeer, The Netherlands. *Journal of Plankton Research* **2**, 317-334.

Denman, K.L. (1976) Covariability of chlorophyll and temperature in the sea. *Deep Sea Research* **23**, 539-550.

Denman, K.L. and Platt, T. (1976) The variance spectrum of phytoplankton in a turbulent ocean. *Journal of Marine Research* **34**, 593-601.

Denman, K.L., Okubo, A. and Platt, T. (1977) The chlorophyll fluctuation spectrum in the sea. *Limnology and Oceanography* **22**, 1033-1038.

Deschamp, P.Y., Frouin, R. and Wald, L. (1981) Satellite determination of the mesoscale variability of the sea surface temperature. *Journal of Physical Oceanography* **11**, 864-870.

Dickie, T. (1993) Sampling and observational systems. Report of the first meeting of an International GLOBEC Working Group. 3, pp.1-99. Paris: GLOBEC International.

Dodson, S.I. (1970) Complementary feeding niches sustained by size selection predation. *Limnology and Oceanography* **15**, 131-137.

Dussart, B.M. (1965) Les different categories de plancton. *Hydrobiologia* **26**, 72-74.

Dyer, K.R. (1986) *Coastal and estuarine sediment dynamics*, Pp 342. Chichester: Wiley.

Ekman, S. (1953) *Zoography of the sea*, London: Sidgewick &Jackson.

Evans, G.T. and Parslow, J.S. (1985) A model of annual plankton cycles. *Biological Oceanography* **3**, 327-347.

Evans, M.S. and Sell, D.W. (1985) Mesh size and collection characteristics of 50-cm diameter conical plankton nets. *Hydrobiologia* **122**, 97-104.

Fager, E.W. and McGowan, J.A. (1963) Zooplankton spesies groups in the North Pacific. *Science* **140**, 453-460.

Faith, D.P. (1992) Conservation evaluation and phylogenetic diversity. *Biological Conservation* **61**, 1-10.

Faith, D.P. (1994) Phylogenetic pattern and the quantification of organismal biodiversity. *Philosophical Transactions of the Royal Society of London Series B* **3456**, 45-58.

Fasham, M.J.R. (1978) The application of some stochastic processes to the study of plankton patchiness. In: Steele, J.H. (Ed.) *Spatial pattern in plankton communities.* pp. 131-156. New York: Pleneum Press.

Fasham, M.J.R. and Pugh, P.R. (1976) Observations on the horizontal coherence of chlorophyll a and temperature. *Deep Sea Research* **23**, 527-538.

Fiksen, O. and Giske, J. (1995) Vertical distribution and population dynamics of copepods by dynamic optimization. *ICES Journal of Marine Science* **52**, 483-503.

Focal technologies Inc. (1995) Optical plankton Counter user's guide. 216-0401-00, pp.1-30. Dartmouth, Canada: Focal Technologies inc.

Fransz, H.G. and Verhagen, J.H.G. (1985) Modelling research on the production cycle of phytoplankton in the southern Bight of the North Sea in relation to river-bourne nutrient loads. *Netherlands Journal of Sea Research* **19**, 241-250.

Frontier, S. (1973) Etude statistique de la dispersion du zooplancton. *Journal of Experimental Marine Biology and Ecology* **12**, 229-262.

Frost, B.W. (1993) A modelling study of process regulating plankton standing stock and production in the open subarctic Pacific Ocean. *Progress in Oceanography* **32**, 17-56.

Frost, B.W. and Franzen, N.C. (1992) Grazing and iron limitation in the control of phytoplankton stock and nutrient concentration: a chemostat analogue of the Pacific equatorial upwelling zone. *Marine Ecology Progress Series* **83**, 291-303.

Fudge, H. (1968) Biochemical analysis of preserved zooplankton. *Nature* **219**, 380-381.

Gallager, S.M., Davis, C.S., Espstein, A.W., Solow, A. and Beardsley, R.C. (1996) High-resolution observations of plankton spatial distributions correlated with hydrography in the Great South Channel, Georges Bank. *Deep Sea Research II* **43**, 1627-1663.

Gallego, A., Heath, M.R., McKenzie, E. and Cargill, L.H. (1996) Environmentally induced short-term variability in the growth rates of larval herring. *Marine Ecology Progress Series* **137**, 11-23.

Gallienne, C.P. (1997) *The development of novel techniques for characterisation of marine zooplankton*. University of Plymouth.

Gallienne, C.P., Robins, D.B. and Pilgrim, D.A. (1996) Measuring abundance and size distribution of zooplankton using an optical plankton counter in underway mode. *Underwater Technology* **21**, 15-21.

Gallienne, C.P., Robins, D.B. and Woodd-Walker, R.S. (In Press) Abundance and distribution of mesozooplankton along a 20° west meridional transect of the north Atlantic Ocean. *Deep Sea Research* (PRIME Special Issue).

Gee, J.M. and Warwick, R.M. (1996) A study of global biodiversity patterns in the marine motile fauna of hard substrata. *Journal of Marine Biological Association, UK* **76**, 177-184.

Gibbons, M.J. (1997) Pelagic biogeography of the South Atlantic Ocean. *Marine Biology* **129**, 757-768.

Gower, J.F.R., Denman, K.L. and Holyer, R.J. (1980) Phytoplankton patchiness indicates the fluctuation of mesoscale oceanic structure. *Nature* **288**, 157-159.

Grant, S., Ward, P., Murphy, E., Bone, D. and Abbott, S. (2000) Field comparison of an LHPR net sampling system and an Optical Plankton Counter (OPC) in the Southern Ocean. *Journal of Plankton Research* **22**, 618-638.

Guégan, J.-F., Lek, S. and Oberdorff, T. (1998) Energy availability and habitat heterogeneity predict global riverine fish diversity. *Nature* **391**, 382-384.

Haeckel, E. (1891) Plankton Studien. *Jena Zeitschrift fur Naturwissenschaft* **25**, 232-336.

Haedrich, R.L. (1986) Size spectra in mesopelagic fish assembleges. In: Pierrot-Bults, A.C., van der Spoels, S., Zahuranec, B.J. and Johnson, R.K. (Eds.) *Pelagic Biogeography.* pp. 107-112. Paris: Unesco.

Hall, D.J., Cooper, W.E. and Werner, E.E. (1970) An experimental approach to the production dynamics and structure of freshwater animal communities. *Limnology and Oceanography* **15**, 839-928.

Halliday, N.C. and Coombs, S.H. (In Press) Vertical distribution of zooplankton in a Norwegian fjord and a comparison of LHPR and OPC data. *Sarsia*

Harris, R. (1990) North Atlantic bloom experiment. Report of the first data workshop. 4, pp.61-65. Kiel: JGOFS Buro.

Haury, L.R., McGowan, J.A. and Wiebe, P.H. (1978) Patterns and processes in the time-space scales of plankton distributions. In: Steele, J.H. (Ed.) *Spatial patterns in plankton communities*, pp. 277-328. New York: Plenum Press.

Haury, L.R., Yamazaki, H. and Fey, C.L. (1992) Simultaneous measurements of small-scale physical dynamics and zooplankton distributions. *Journal of Plankton Research* **14**, 513-530.

Haury, L.R. and Pieper, R.E. (1988) Zooplankton: scales of biological and physical events. In: Soule, D.F. and Klepper, G.S. (Eds.) *Marine organisms as indicators.* pp. 35-72. London: Springer-Verlag.

Hays, G.C., Proctor, C.A., John, A.W.G. and Warner, A.J. (1994) Interspecific differences in the diel vertical migration of marine copepods - the implications of size, colour, and morphology. *Limnology and Oceanography* **39**, 1621-1629.

Heath, M.R., Dunn, J., Fraser, J.G., Hay, S.J. and Madden, H. (1999) The use of an optical plankton counter to survey the distribution of *Calanus finmarchicus*. *Fisheries Oceanography* **8**, 13-24.

Herman, A.W. (1988) Simultaneous measurement of zooplankton and light attenuance with a new optical plankton counter. *Continental Shelf Research* **8**, 205-221.

Herman, A.W. (1992) Design and calibration of a new optical plankton counter capable of sizing small zooplankton. *Deep Sea Research* **39**, 395-415.

Herman, A.W., Sameoto, D.D. and Longhurst, A.R. (1981) Vertical and horizontal distribution patterns of copepods near the shelf break south of Nova Scotia. *Canadian Journal of Fisheries and Aquatic Science* **38**, 1065-1076.

Herman, A.W., Cochrane, N.A. and Sameoto, D.D. (1993) Detection and abundance estimation of euphausiids using an optical plankton counter. *Marine Ecology Progress Series* **94**, 165-173.

Hirst, A.G. and Sheader, M. (1997) Are in situ weight-specific growth rates body-size independent in marine planktonic copepods? A re-analysis of the global synthesis and a new empirical model. *Marine Ecology Progress Series* **154**, 155-165.

Holladay, C.G. and O'Brian, J.J. (1975) Mesoscale variability of sea surface temperature. *Journal of Physical Oceanography* **5**, 761-772.

Hopkins, T.L. (1985) The zooplankton community of Croker Passage, Antarctic Peninsular. *Polar Biology* **4**, 161-170.

Hopkins, T.L. and Torres, J.J. (1988) The zooplankton community in the vicinity of the ice edge, western Weddell Sea, march 1986. *Polar Biology* **9**, 79-87.

Horne, E.P.W. and Platt, T. (1984) The dominant space and time scales of variability in the physical and biological fields on continetal shelves. *Rapport Proces. verb. Conseil International Exploration de Mer* **183**, 9-19.

Horwood, J. (1976) Variation of fluorescence, particle size groups, and environmental parameters in the North Sea. *Journal du Conseil CEIM* **39**, 593-601.

Huntley, M.E. and Lopez, M.D.G. (1992) Temperature dependent production of marine copepods: a global synthesis. *American Naturalist* **140**, 201-242.

Hutchings, L., Verheye, H.M., Mitchell-Innes, B.A., Peterson, W.T., Huggett, J.A. and Painting, S.J. (1995) Copepod production in the southern Benguela system. *ICES Journal of Marine Science* **52**, 439-455.

Ikeda, T. (1985) Metabolic rates of epipelagic marine zooplankton. *Marine Biology* **85**, 1-11.

Jenkins, G.M. and Watts, D.G. (1968) *Spectral analysis and its applications*, pp1-525. San Francisco: Holden-Day.

Jenkins, J.T. (1901) The methods and results of the German plankton investigation, with special reference to the Hensen nets. *Proceedings and Transactions of the Liverpool Biological Society* **15**, 279-341.

Jones, D.T. and Eggleton, P. (2000) Sampling termite assemblages in tropical forests: testing a rapid biodiversity assessment protocol. *Journal of Appied Ecology* **37**, 191-203.

Jumers, P.A., Penry, D.L., Baross, J.A., Perry, M.J. and Frost, B.W. (1989) Closing the microbial loop: dissolved carbon pathway to heterotrophic bacteria from incomplete ingestion, digestion and absorption in animals. *Deep Sea Research* **36**, 483-495.

Kendall, M.G. and Stuart, A. (1961) *The advanced theory of statistics*, London: Griffin.

Kerr, S.R. (1974) Theory of size distribution in ecological communities. *Journal of Fisheries Research Board Canada* **31**, 1859-1862.

Kimoto, K., Uye, S.-i. and Onbe, T. (1988) Direct observation of copepod swarm in a small inlet of Kyushu, Japan. *Bulletin of the Seikai Regional Fisheries Research Laboratory* **66**, 41-58.

Koppelman, R. and Weikert, H. (1992) Full-depth zooplankton profiles over the deep bathyal of the NE Atlantic. *Marine Ecology Progress Series* **86**, 263-272.

Krebs, C.J. (1999) *Ecological methodology*, Pp 1-654. New York: Harper Collins Publishers.

Krishnakumari, L. and Nair, V.R. (1988) Biomass, organic carbon and calorific content of zooplankton from the Arabian Sea off central west coast of India. *Indian Journal of Marine Science* **17**, 78-80.

Lalli, C.M. and Parsons, T.R. (1997) *Biological oceanography an introduction*, 2nd edn. Pp 1-314. Oxford: Butterworth-Heinemann.

Landry, M.R. (1978) Predatory feeding behaviour of a marine copepod, *Labidocea trispinosa*. *Limnology and Oceanography* **23**, 1103-1113.

Landry, M.R., Peterson, W.K. and Lorenzen, C.J. (1995) Zooplankton grazing, phytoplankton growth, and export flux: inferences from chlorophyll tracer methods. *ICES Journal of Marine Science* **52**, 337-346.

Lasker, R. (1975) Field criteria for survival of anchovie larvae: the relationship between inshore chlorophyll layers and success at first feeding. *US Fisheries Bullettin* **71**, 453-462.

Lasker, R. and Zweifel, J. (1978) Growth and survival of first feeding northern anchovy larvae (*Engraulis mordax*) in patches containing different proportions of large and small prey. In: Steele, J.H. (Ed.) *Spatial pattern in plankton communities*, pp. 329-355. London: Plenum Press.

LeBrasseur, R.J., Barraclough, W.E., Kennedy, O.D. and Parsons, T.R. (1969) Production studies in the straits of Georgia. Part III. Oberservations on the food of larval and juvenile fish in the Fraser River plume, February to May, 1967. *Journal of Experimental Marine Biology and Ecology* **3**, 39-50.

Lehman, J.T. and Scavia, D. (1982) Microscale nutirent patches produced by zooplankton. *Proceedings of the National Academy of Science* **79**, 5001-5005.

Lek, S. and Guégan, J.F. (1999) Artificial neural networks as a tool for ecological modelling, an introduction. *Ecological Modelling* **120**, 65-73.

Lenz, J., Morales, A. and Gunkel, J. (1993) Mesozooplankton standing stock during North Atlantic spring bloom study in 1989 and its potential grazing pressure on phytoplankton: a comparison between low, medium and high latitudes. *Deep Sea Research II* **40**, 559-572.

Levin, S.A., Morin, A. and Powell, T.M. (1989) Pattern and processes in the distribution and dynamics of Antarctic krill. VII/BG/20, pp.281-296. Scientific Report for the commission for the conservation of Antarctic marine living resources (CCAMLR).

Longhurst, A.R. (1981) Significance of spatial variability. In: Longhurst, A.R. (Ed.) *Analysis of Marine Ecosystems*, pp. 415-442. London: Academic Press.

Longhurst, A. (1998) *Ecological geography of the sea*, pp1-398 London: Academic Press.

Longhurst, A.R. and Harrison, W.G. (1988) Vertical nitrogen flux from the oceanic euphotic zone by diel migrant zooplankton and nekton. *Deep Sea Research* **35**, 881-889.

Longhurst, A. and Williams, R. (1992) Carbon flux by seasonal vertical migrant copepods is a small number. *Journal of Plankton Research* **14**, 1495-1509.

Longhurst, A.R., Bedo, A.W., Harrison, W.G., Head, E.J.H. and Sameoto, D.D. (1990a) Vertical flux of respiratory carbon by oceanic diel migrant biota. *Deep Sea Research* **37**, 685-694.

Longhurst, A., Fransz, G., Lenz, J., Harris, R. and Small, L. (1990b) Core measurements protocols. *Report of the core measurements working group. 6*, p.24 Kiel: JGOFS Buro.

Longhurst, A., Sathyendranah, S., Platt, T. and Carverhill, C. (1995) An estimate of global primary production in the ocean from satellite radiometer data. *Journal of Plankton Research* **17**, 1245-1271.

Lough, R.G. and Mountain, D.G. (1996) Effect of small scale turbulence on feeding rates of larval cod and haddock in stratified waters on Gearges Bank. *Deep Sea Research II* **43**, 1745-1772.

Lovegrove, T. (1966) The determination of the dry weight of plankton and the effect of various factors on the values obtained. In: Barnes, H. (Ed.) *Some contemporary studies in marine science*, pp. 429-467. London: George Allen and Unwin Ltd.

Lussenhop, J. (1974) Victor Hensen and the development of sampling methods in ecology. *Journal of Historical Biology* 7, 319-337.

Mackas, D.L. (1984) Spatial autocorrelation of plankton community composition in a continental shelf ecosystem. *Limnology and Oceanography* **29**, 451-471.

Mackas, D.L. and Boyd, C.M. (1979) Spectral analysis of zooplankton heterogeneity. *Science* **204**, 62-64.

Mackas, D.L., Denman, K.L. and Abbott, M.R. (1985) Plankton patchiness: biology in the physical vernacular. *Bulletin of Marine Science* **37**, 652-674.

MacKay, D.J.C. (1992) Bayesian interpolation. *Neural Computation* **4**, 415-447.

Manel, S., Dias, J.-M. and Ormerod, S.J. (1999) Comparing discriminant analysis, neural networks and logistic regression for predicting species distributions: a case study with a Himalayan river bird. *Ecological Modelling* **120**, 337-347.

Mann, K.H. and Lazier, J.R.N. (1991) *Dynamics of marine ecosystems. Biological and physical interactions in the oceans.* Pp 1-466. Oxford: Blackwell Scientific Publications.

Mann, K.H. and Lazier, J.R.N. (1996) *Dynamics of marine ecosystems. Biological and physical interactions in the oceans.* 2nd edn. Pp 1-394. Oxford: Blackwell Scientific Publications.

Maravelias, C.D. and Reid, D.G. (1997) Identifying the effects of oceanographic features and zooplankton on prespawning herring abundance using generalized additive models. *Marine Ecology Progress Series* **147**, 1-9.

Marrase, C., Costello, J.H., Granata, T. and Strickler, J.R. (1990) Grazing in a turbulent environment: Energy dissapation, encounter rates, and efficiency of feeding currents in *Centropages hamatus. Proceedings of the National Academy of Science* **87**, 1653-1657.

Mauchline, J. (1998) *The biology of calanoid copepods*, London: Academic Press.

May, R.M. (1990) Taxonomy as destiny. *Nature* **347**, 129-130.

McBarry, K. (1964) *Journal of Fisheries Research Board of Canada* **21**, 183-202.

McGowan, J.A. (1971) Ocean biogeography of the Pacific. In: Funnel, B.M. and Reidel, W.R. (Eds.) *The Micropalaentology of Oceans*, pp. 3-74. Cambridge: Cambridge University Press.

McGowan, J.A. (1974) The nature of oceanic ecosystems. In: Miller, C.B. (Ed.) *The biology of the oceanic Pacific*, pp. 9-28. Oregon State University Press.

Mitchell-Innes, B.A. and Walker, D.R. (1991) Short-term variability during an Anchor Station study in the southern Benguela upwelling system. Phytoplankton production and biomass in relation to species changes. *Progress in Oceanography* **28**, 65-89.

Morales, C.E. (1999) Carbon and nitrogen fluxes in the oceans: the contribution by zooplankton migrants to active transport in the North Atlantic during the Joint Global Ocean Flux Study. *Journal of Plankton Research* **21**, 1799-1808.

Morris (1972) The occurrence of wax esters in crustaceans from the north east Atlantic Ocean. *Marine Biology* **16**, 102-107.

Mumm, N. (1991) On the summerly distribution of mesozooplankton in the Nansen Basin, Arctic Ocean. *Berichte zur Polarforschung* **92**, 1-146.

Neill, W.E. and Peacock, A. (1980) Breaking through the bottleneck: Interactions of invertebrate predators and nutrients in oligotrophic lakes. In: Kerfoot, W.C. (Ed.) *Evolution and ecology of zooplankton communities*, pp. 715-724. University Press of New England, London.

Nichols, J.H. and Thompson, A.B. (1991) Mesh selection of copepodite and nauplius stages of four calanoid copepod species. *Journal of Plankton Research* **13**, 661-671.

Noda, M., Kawabata, K., Gushima, K. and Kakuda, S. (1992) Importance of zooplankton patches in the foraging ecology of the planktivorous fish *Chromis chrysurus* (Pomacentridae). *Marine Ecology Progress Series* **87**, 251-263.

Omori, M. (1970) Variations in length, weight, respiratory rate, and chemical composition of *Calanus cristanus* in relation to its food and feeding. In: Steele, J.H. (Ed.) *Marine food chains*, pp. 113-126. Edinburgh: Oliver and Boyd.

Omori, M. and Hamner, W.M. (1982) Patchy distribution of zooplankton: behaviour, population assessment and sampling problems. *Marine Biology* **72**, 193-200.

Omori, M. and Ikeda, T. (1984) *Methods in marine zooplankton ecology*, pp 1-332. New York: John Wiley & Sons.

Paffenhofer, G.A. and Knowles, S.C. (1979) Ecological implications of faecal pellet size, production and consumption by copepods. *Journal of Marine Research* **37**, 35-49.

Paffenhofer, G.A. and Knowles, S.C. (1980) Omnivorousness in marine planktonic copepods. *Journal of Plankton Research* **2**, 355-365.

Pavoni, M. (1963) Die Bedeutung des nannoplanktons im Vergleich zum netzplankton. *Schweizerische Zeitschrift fur Hydrobiologie* **25**, 220-231.

Pavshitilics (1975) Zvereva, Z.A. (Ed.) *Geographical and seasonal variability of marine plankton*, pp. 200-247. Jerusalem: Israel Program for Scientific Translations

Peters, R.H. (1983) *The ecological implications of body size.* Pp 1-379. Cambridge: Cambridge University Press.

Pielou,E.C. (1975) *Ecological diversity.* New York: Wiley.

Pierrot-Bults, A.C., van der Spoels, S., Zahuranec, B.J. and Johnson, R.K. (1986) Pelagic biogeography. 49. 1-295. Paris: UNESCO.

Pinel-Alloul, B. (1995) Spatial heterogeneity as a multiscale characteristic of zooplankton community. *Hydrobiologia* **300/301**, 17-42.

Piontkovski, S.A. and van der Spoel, S. (1997) Similarities in size, in taxonomic and in ecological mesoscale structure of tropical zooplankton communities, *IOC workshop report* **142**, 297-306.

Piontkovski, S.A. and Williams, R. (1995) Multiscale variability of tropical ocean zooplankton biomass. *ICES Journal of Marine Science* **52**, 643-656

Piontkovski, S.A., Williams, R. and Melnik, T.A. (1995) Spatial heterogeneity, biomass and size structure of the Indian Ocean: some general trends. *Marine Ecology Progress Series* **117**, 219-227.

Piontkovski, S.A., Williams, R., Peterson, W.T., Yunev, O.A., Minkina, N.I., Vladimirov, V.L. and Blinkov, A. (1997) Spatial heterogeneity of the plankton fields in the upper mixed layer of the open ocean. *Marine Ecology Progress Series* **148**, 145-154.

Pitcher, G.C., Walker, D.R., Mitchell-Innes, B.A. and Moloney, C.L. (1991) Short-term variability during an Anchor Station study in the southern Benguela upwelling system. Phytoplankton dynamics. *Progress in Oceanography* **28**, 39-64.

Platt, T. and Denman, K.L. (1975) Spectral analysis in ecology. *Annual Review of Ecology and Systematics* **6**, 189-210.

Platt, T., Sathyendranah, S. and Longhurst, A. (1995) Remote sensing of primary production in the ocean: promise and fulfilment. *Philosophical Transactions of the Royal Society of London Series B* **348**, 191-202.

Prestige, M.C., Harris, R.P. and Taylor, A.H. (1995) A modelling investigation of copepod egg production in the Irish Sea. *ICES Journal of Marine Science* **52**, 693-703.

Raymont, J.E.G. (1983) *Plankton and productivity in the oceans. Volume 2: Zooplankton.* 2nd edn. Pp 1-824. Oxford: Pergamon Press.

Reeve, R.E. and Hallam, J. (1995) Control of walking by Central Pattern Generators. In: Rumbold, U., Dillman, R., Hertzberger, L.O. and Kanade, T. (Eds.) *Intelligent autonomous systems IAS-4*, pp. 695-701.

Reid, J.L., Brinton, E., Fleminger, A., Venrick, E.L. and McGowan, J.A. (1978) Ocean circulation and marine life. In: Charnock, H. and Deacon, G. (Eds.) *Advances in oceanography*, pp. 65-130. London: Plenum Press.

Rex, M.A., Stuart, C.T., Hessler, R.R., Allen, J.A., Sanders, H.L. and Wilson, G.D.F. (1993) Global-scale latitudinal patterns of species diversity in the deep-sea benthos. *Nature* **365**, 636-639.

Rhode, K. (1992) Latitudinal gradients in species diversity: the search for the primary cause. *Oikos* **65**, 514-527.

Richards, S.A., Possingham, H.P. and Noye, J. (1996) Diel vertical migration: modelling light-mediated mechanisms. *Journal of Plankton Research* **18**, 2199-2222.

Richter, C. (1995) Seasonal changes in the vertical distribution of mesozooplankton in the Greenland Sea Gyre (75°N): distribution strategies of Calanoid copepods. *ICES Journal of Marine Science* **52**, 533-539.

Ricklefs, R.E. (1990) Scaling pattern and process in marine ecosystems. In: Sherman, K., Alexander, L.M. and Gold, B.D. (Eds.) *Large patterns, marine processes and ecosystem yields.* pp. 169-178. American Association for the Advancement of Science.

Riley, G.A. (1976) A model of zooplankton patchiness. *Limnology and Oceanography* **21**, 873-880.

Ring Group (1981) Gulf Stream cold-core rings: their physics, chemistry and biology. *Science* **212**, 1091-1100.

Robins, D.B. (1996) *AMT-2 cruise report.* Pp 1-54 (+appendices). Plymouth: Plymouth Marine Laboratory.

Robins, D.B. and Aiken, J. (1996) The Atlantic Meridional Transect: an oceanographic research programme to investigate physical, chemical, biological and optical variables of the Atlantic Ocean. *Underwater Technology* **21**, 8-14.

Robins, D.B., Bale, A.J., Moore, G.J., Rees, N.W., Hooker, S.B., Gallienne, C.P., Westbrook, A.G., Maranon, E., Spooner, W.H. and Laney, S.R. (1996) *AMT-1 Cruise report and preliminary results.* Robins, D.B. (Ed.) 35. Maryland, USA: NASA Goddard Space Flight Centre.

Roman, M.R., Dam, H.G., Gauzens, A.L., Urban-Rich, J., Foley, D.G. and Dickey, T.D. (1995) Zooplankton variability on the equator at 140°W during the JGOFS EqPac study. *Deep Sea Research II* **42**, 673-693.

Rosenblatt, F. (1961) *Principles of neurodynamics*, Washington DC: Spartan Press.

Rothchild, B.J. and Osborn, T.R. (1988) Small scale turbulence and plankton encounter rates. *Journal of Plankton Research* **10**, 465-474.

Rutherford, S., D'Hondt, S. and Prell, W. (1999) Environmental controls on the geographic distribution of zooplankton diversity. *Nature* **400**, 749-753.

Salonen, K. (1979) A versitile method for the rapid and accurate determination of carbon by high temperature combustion. *Limnology and Oceanography* **24**, 177-183.

Salonen, K., Sarvala, J., Hakala, I. and Viljanen, M.L. (1976) The relation of energy and organic carbon in aquatic invertebrates. *Limnology and Oceanography* **21**, 724-730.

Sanders, P.M. (1972) Space and time variability of temperature in the upper ocean. *Deep Sea Research* **19**, 467-480.

Sarle (1994) Neural networks and statistical models. *Proceeding of the nineteenth Annual SAS Users Group International Conference* Pp. 1-13

Sathyendranath, S., Longhurst, A., Carverhill, C. and Platt, T. (1995) Regionally and seasonally differentiated primary production in the North Atlantic. *Deep Sea Research* **42**, 1773-1802.

Scardi, M. (1996) Artificial neural networks as empirical models for estimating phytoplankton production. *Marine Ecology Progress Series* **139**, 289-299.

Scardi, M. and Harding, L.W. (1999) Developing an empirical model of phytoplankton primary production: a neural network case study. *Ecological Modelling* **120**, 213-223.

Seda, J. and Dostalkova, I. (1996) Live sieving of freshwater zooplankton: a technique for monitoring community size structure. *Journal of Plankton Research* **18**, 513-520.

Sheldon, R.W., Prakash, A. and Sutcliffe, W.H. (1972) The size distribution of particles in the ocean. *Limnology and Oceanography* **17**, 327-340.

Sheldon, R.W., Sutcliffe, W.H. and Paranjape, M.A. (1977) Structure of pelagic food chains and relationship between plankton and fish production. *Journal of Fisheries Research Board of Canada* **34**, 2344-2353.

Silvertown, J. (1985) History of latitudinal diversity gradient; woody plants in Europe 13,000-1000 years B.P. *Journal of Biogeography* **12**, 519-525.

Simpson, G.G. (1964) Species diversity of North American recent mammals. *Systematics in Zoology* **13**, 57-73.

Simpson, R., Williams, R., Ellis, R. and Culverhouse, P.F. (1992) Biological pattern recognition by neural networks. *Marine Ecology Progress Series* **79**, 303-308.

Smith, C.L., Richards, K.L. and Fasham, M.J.R. (1996) The impact of mesoscale eddies on plankton dynamics in the upper ocean. *Deep Sea Research I* **43**, 1807-1832.

Smith, P.E., Counts, R.C. and Clutter, R.I. (1968) Changes in filtration efficiency of plankton nets due to clogging under tow. *Journal du Conseil CEIM* **32**, 232-248.

Smith, S.L., Pieper, R.E., Moore, M.V., Rudstam, L.G., Greene, C.H., Zamon, C.N. and Williamson, C.E. (1992) Acoustic techniques for the in situ observations of zooplankton. *Archiv fur Hydrobiologie. Ergebnisse der Limnologie* **36**, 23-43.

Soetaert, K. and Heip, C. (1990) Sample-size dependence of diversity indices and determination of sufficient sample size in a high-diversity deep-sea environment. *Marine Ecology Progress Series* **59**, 305-307.

Sprules, W.G. and Holtby, L.B. (1979) Body size and feeding ecology as alternatives to taxonomy for studies of limnetic zooplankton community structure. *Journal of Fisheries Research Board of Canada* **36**, 1354-1363.

Sprules, W.G., Bergstrom, B., Cyr, H., Hargreaves, B.R., Kilham, S.S., MacIsaac, H.J., Matsushita, K., Stemberger, R.S. and Williams, R. (1992) Non-video optical instruments for studying zooplankton distribution and abundance. *Archiv fur Hydrobiologie. Ergebnisse der Limnologie* **36**, 45-58.

Sprules, W.G., Herman, A.W. and Stockwell, J.D. (1998) Calibration of an optical plankton counter for use in fresh water. *Limnology and Oceanography* **43**, 726-733.

Sreepada, R.A., Rivonker, C.U. and Parulekar, A.H. (1992) Biochemical composition and calorific potential of zooplankton from Bay of Benal. *Indian Journal of Marine Science* **21**, 70-73.

Steele, J.H. (1978) Some comments on plankton patches. In: Steele, J.H. (Ed.) *Spatial pattern in plankton communities*, pp. 1-20. London: Plenum Press.

Steele, J.H. and Henderson, E.W. (1979) Spatial patterns in North Sea plankton. *Deep Sea Research* **26A**, 955-963.

Steele, J.H. and Henderson, E.W. (1992) The role of predation in plankton models. *Journal of Plankton Research* **14**, 157-172.

Steele, J.H. and Henderson, E.W. (1995) Predation control of zooplankton demography. *ICES Journal of Marine Science* **52**, 565-574.

Stephens, J.A., Jordan, M.B., Taylor, A.H. and Proctor, R. (1998) The effects of fluctuations in the North Sea flows on zooplankton abundance. *Journal of Plankton Research* **20**, 943-956.

Stevens, G.C. (1989) The latitudinal gradient in geographical range: how so many species coexist in the tropics. *American Naturalist* **133**, 240-256.

Sverdrup, H.U. (1953) On conditions of the vernal blooming of phytoplankton. *Journal du Conseil Perm. International Exploration de la Mer* **18**, 287-295.

Sverdrup, H.U., Johnson, M.W. and Fleming, R.H. (1942) *The oceans: physics, chemistry and general biology*, New Jersey: Prentice-Hall.

Taylor, A.H. (1995) North-South shifts of the Gulf Stream and their climatic connections with the abundance of zooplankton in the UK and its surrounding seas. *ICES Journal of Marine Science* **52**, 711-721.

Tessier, A.J. (1983) Coherence and horizontal movement of patches of *Holopedium gibberum* (Cladoceran). *Oecologia* **60**, 71-75.

Thiel, H. (1975) The size structure of the deep-sea benthos. *Internationale Revue der gesamten Hydrobiologie* **60**, 575-606.

Thiriot, A. (1978) Zooplankton communities in the West African upwelling area. In: Boje, R. and Tomczak, M. (Eds.) *Analysis of Upwelling Systems*, pp. 32-60. Berlin: Springer.

Tranter, D.J. and Fraser, J.H. (1968) *Zooplankton sampling*, pp 56 Paris: Unesco Press.

Ueda, H., Kuwahara, A., Tanaka, M. and Azeta, M. (1983) Underwater observations on copepod swarms in temperate and subtropical waters. *Marine Ecology Progress Series* **11**, 165-171.

van der Spoel, S. and Heyman, R.P. (1983) *A comparative atlas of zooplankton, biological patterns in the oceans*, Utrecht: Wetenschappelijke uitgeverji Bunge.

Vane-Wright, R.I., Humphries, C.J. and Williams, P.H. (1991) What to protect?-Systematics and agony of choice. *Biological Conservation* **55**, 235-254.

Vannucci, M. (1968) Loss of organisms through the meshes. In: Tranter, D.J. (Ed.) *Zooplankton sampling*, pp. 77-86. Paris: The UNESCO Press.

Verheye, H.M., Hutchings, L., Huggett, J.A. and Painting, S.J. (1992) Mesozooplankton dynamics in the Benguela ecosystem, with emphasis on the herbivorous copepods. *South African Journal of Marine Science* **12**, 561-584.

Vinogradov, M.E. and Shushkina, E.A. (1984) Quantitative estimation of epipelagic population in the world ocean. *Dokl. An S. S. S. R.* **274**, 410-412.

Waife, G. and Frid, C.L.J. (1996) Short-term temporal variation in coastal zooplankton communities: the relative importance of physical and biological mechanisms. *Journal of Plankton Research* **18**, 1485-1501.

Walsh, J.J. (1975) A spatial simulation of the Peru upwelling ecosystem. *Deep Sea Research* **22**, 201-236.

Warwick, R.M. and Clarke, K.R. (1995) New 'biodiversity' measures reveal a decrease in taxonomic distinctness with increasing stress. *Marine Ecology Progress Series* **129**, 301-305.

Whitaker (1975) *Communities and ecosystems*, 2nd edn. New York: MacMillan.

White, J.R. and Roman, M.R. (1992) Egg production by the calanoid copepod Acartia tonsa in the mesohaline Chesapeake Bay: the importance of food resources and temperature. *Marine Ecology Progress Series* **86**, 239-249.

Wiebe, P.H. (1988) Functional regression equations for zooplankton displacement volume, wet weight, dry weight, and carbon: a correction. *Fishery Bulletin* **86**, 833-835.

Wiebe, P.H., Boyd, S. and Cox, J.L. (1975) Relationships between zooplankton displacement volume, wet weight, dry weight, and carbon. *Fishery Bulletin* **73**, 777-786.

Wieland, K.W., Peterson, D. and Schnack, D. (1997) Estimates of zooplankton abundance and size distribution with the Optical Plankton Counter (OPC). *Arch. Fish. Mar. Res.* **45**, 271-280.

Williams, R. and Robins, D.B. (1982) Effects of preservation on wet weight, dry weight, nitrogen and carbon contents of *Calanus helgolandicus* (Crustacea: Copepoda). *Marine Biology* **71**, 271-281.

Williamson, C.E. (1993) Linking predation risk models with behavioral mechanisms: identifying population bottlenecks. *Ecology* **74**, 320-331.

Williamson, C.E. and Butler, N.M. (1986) Predation on rotifers by suspension feeding calanoid copepod *Diaptomus pallidus*. *Limnology and Oceanography* **31**, 393-402.

Yentsch, C.S. and Phinney, D.A. (1985) Rotary motions and convection as a means of regulating primary production. *Journal of Geophysical research* **90**, 3237-3248.

Zeitzschel, B. (1978) Oceanographic factors influencing the distribution of plankton in space and time. *Micropaleontology* **24**, 139-159.

Zhang, X., Dam, H.G., White, J.R. and Roman, M.R. (1995) Latitudinal variations in mesozooplankton grazing and metabolism in the central tropical Pacific during the U.S. JGOFS EqPac study. *Deep Sea Research II* **42**, 695-714.

Zhou, M. and Huntley, M.E. (1997) Population dynamics of plankton based theory on biomass spectra. *Marine Ecology Progress Series* **159**, 61-73.

Appendices

Appendix 1: Station details

AMT1

Day	Time	Date	Lat (°)	Lon (°)	Depth (m)	Deep Net OPC	Deep Net carbon
268	12:42	25/9	48 55.8N	09 08.9W	100	X	X
269	12:36	26/9	47 55.9	14 50.7	200	X	X
270	10:00	27/9	47 00.4	19 56.6	200	X	X
271	12;38	28/9	42 15.1	20 00.9	200	X	X
272	12:35	29/9	37 54.3	19 59.7	200	X	X
273	12:36	30/9	33 35.9	20 53.0	200	X	X
			Arrived Madeira				
275	14:00	2/10	27 22.8	21 50.0	200	X	X
276	12:38	3/10	23 17.3	20 09.8	200	X	X
277	10:42	4/10	19 29.9	20 23.3	200	X	X
278	16:00	5/10	13 03.3	20 26.0	200	X	X
279	14:01	6/10	09 14.5	22 12.7	200	X	X
280	14:00	7/10	05 21.1	23 58.3	200	X	X
281	14:00	8/10	01 23.8	25 42.1	200	X	X
282	14:00	9/10	02 45.5S	27 31.4	200	X	X
283	14:00	10/10	07 00.7	29 30.5	200	X	X
284	14:58	11/10	11 28.1	31 33.1	200	X	X
285	15:03	12/10	15 34.5	33 26.8	200	X	X
286	14:59	13/10	19 38.9	35 21.8	200	X	X
287	15:00	14/10	23 47.2	37 23.2	200	X	X
288	14:55	15/10	27 02.3	40 08.5	200	X	X
289	14:58	16/10	30 17.2	43 23.3	200	X	X
290	14:59	17/10	33 11.1	46 25.8	200	X	X
			Montevideo port-call				
295	17:19	22/10	40 57.0	55 14.0	200	X	X
296	16:00	23/10	46 00.2	56 17.1	200	X	X
297	14:02	24/10	50 48.3	57 25.0	100	X	X

AMT 2

Day	Start	Date	Lat (°)	Lon (°)	Depth (m)	Deep net OPC	Deep net Carbon	20m OPC
114	13:15	23/4	47 38.0 S	55 56.4 E	200	X	X	
115	13:30	24/4	43 25.6	54 44.2	200	X	X	
116	13:58	25/4	39 24.3	53 19.5	200	X	X	
	Montevideo port-call							
120	17:00	29/4	36 03.1	49 48.7	200	X	X	
121	13:13	30/4	33 23.0	46 37.5	200	X	X	
122	13:07	1/5	30 18.0	43 25.2	200	X	X	
123	13:00	2/5	27 27.1	40 42.6	200	X	X	
124	12:18	3/5	24 21.2	37 51.9	200	X	X	
125	11:59	4/5	19 54.3	35 31.3	200	X	X	
126	12:08	5/5	15 10.3	33 18.4	200	X	X	
126	23:00	5/5			200	X	X	
127	12:00	6/5	11 14.7	31 27.7	200	X	X	
127N	22:49	6/5	09 38.6	30 44.6	200	X	X	
128	12:02	7/5	07 28.8	29 45.3	200	X	X	
128N	22:59	7/5	05 49.8	29 03.5	200	X	X	X
129	11:00	8/5	03 55.0	28 12.6	200	X	X	X
129N	22:04	8/5	02 16.1	27 25.4	200	X	X	X
130	11:05	9/5	00 11.7	26 24.1	200	X	X	X
130N	22:00	9/5	01 17.5N	20 44.7	200	X	X	X
131	11:05	10/5	03 24.1	24 47.7	200	X	X	X
131N	22:06	10/5	05 21.1	24 03.1	200	X	X	X
132	11:01	11/5	07 34.6	22 56.6	200	X	X	X
132N	21:58	11/5	09 21.6	22 04.9	200	X	X	X
133	10:57	12/5	11 44.4	21 03.1	200	X	X	
135N	01:36	14/5	19 54.3	21 19.2	200	X	X	
135	10:57	14/5	21 45.8	21 28.1	200	X	X	
136	09:56	15/5	26 32.3	21 47.8	200	X	X	X
137	09:58	16/5	30 55.0	21 16.3	200	X	X	X
138	09:57	17/5	35 39.9	20 25.1	200	X	X	X
139	09:57	18/5	39 53.9	19 59.8	200	X	X	
140	09:53	19/5	44 07.7	20 00.9	200	X	X	X
141	08:56	20/5	46 29.7	14 03.7	200	X	X	X
142	08:58	21/5	48 45.1	08 06.0	100	X	X	X

AMT 3

						Deep Net		20m
Day	GMT	Date	Lat (°)	Lon (°)	Depth (m)	OPC	Carbon	OPC
266	08:00	22/9	49 40.5N	05 41.4W	100	X	X	
267	09:30	23/9	48 24.7	12 30.0	200	X	X	X
268	10:30	24/9	47 22.0	18 12.7	200	X	X	X
269	10:30	25/9	42 54.0	19 59.5	200	X	X	X
270	11:25	26/9	38 10.1	20 00.8	200	X	X	X
271	11:25	27/9	34 02.0	21 15.5	200	X	X	X
272	11:25	28/9	29 29.6	21 48.5	200	X	X	X
273	11:25	29/9	24 40.6	21 24.1	200	X	X	X
274	10:55	30/9	20 05.1	20 37.7	200	X	X	X
No hydrographic station due to EEZ restrictions								
276	10:55	2/10	12 45.6	20 32.7	200	X	X	X
277	10:55	3/10	09 03.1	22 16.6	200	X	X	X
278	10:55	4/10	05 10.2	24 01.0	200	X	X	X
279	10:55	5/10	01 17.4	25 46.9	200	X	X	X
280	10:55	6/10	02 23.4S	27 27.3	200	X	X	X
281	10:55	7/10	06 29.0	29 16.2	200	X	X	X
282	11:55	8/10	10 46.8	31 14.5	200	X	X	X
283	12:15	9/10	14 53.4	33 07.3	200	X	X	X
284	11:55	10/10	18 51.9	35 02.8	200	X	X	X
285	11:55	11/10	22 55.9	36 57.3	200	X	X	X
286	11:55	12/10	26 36.9	39 36.0	200	X	X	X
287	12:00	13/10	29 51.0	42 54.7	200	X	X	X
288	12:00	14/10	32 48.0	46 07.0	200	X	X	X
289	12:30	15/10	35 42.7	49 34.0	200	X	X	X
290	11:50	16/10	37 48.4	52 11.6	200	X	X	X
Montevideo port-call								
297	12:55	23/10	43 34.7	55 01.4	200	X	X	X
298	12:55	24/10	48 00.1	55 52.8	200	X	X	X
299	11:00	25/10	51 55.9	57 53.6	70	X	X	X

AMT 4

Day	Start	Date	Lat (°)	Lon (°)	Depth (m)	Deep net OPC	Deep net Carbon	20m OPC
111	17:00	21/4	50 58.4S	57 17.7W	100	X	X	X
112	14:00	22/4	47 37.2	55 56.5	200	X	X	X
113	13:55	23/4	43 28.9	54 24.0	200	X	X	X
114	14:04	24/4	39 26.2	52 58.2	200	X	X	X
	Montevideo port-call							
120	13:43	30/4	35 39.0	49 49.0	200	X	X	X
121	13:15	1/5	32 36.6	46 12.0	200	X	X	X
122	13:00	2/5	29 19.7	42 38.5	200	X	X	X
123	13:00	3/5	26 06.2	39 11.0	200	X	X	X
124	13:00	4/5	22 09.5	36 37.2	200	X	X	X
125	11:55	5/5	18 16.1	34 46.3	200	X	X	X
126	11:55	6/5	14 06.9	32 50.3	200	X	X	X
127	11:50	7/5	10 02.1	30 56.8	200	X	X	X
128	11:55	8/5	05 54.0	29 05.0	200	X	X	X
129	11:50	9/5	02 01.5	27 19.7	200	X	X	X
129N	00:00	10/5	00 07.9	26 28.4	200	X	X	X
130	11:55	10/5	01 53.9N	25 37.1	200	X	X	X
131	11:55	11/5	06 04.9	23 38.3	200	X	X	X
132	12:00	12/5	10 03.4	21 55.4	200	X	X	X
132N	00:00	13/5	11 44.4	21 05.3	200	X	X	X
133	11:50	13/5	13 44.6	20 59.9	200	X	X	X
134	10:50	14/5	17 47.0	21 13.0	200	X	X	X
135	10:45	15/5	22 10.1	21 33.3	200	X	X	X
135N	22:55	15/5	24 10.0	21 42.4	200	X	X	X
136	10:55	16/5	26 16.6	21 52.7	200	X	X	X
136N	22:55	16/5	27 57.6	21 57.8	200	X	X	X
137	10:50	17/5	30 02.6	21 45.6	200	X	X	X
137N	22:30	17/5	31 48.4	21 33.6	200	X	X	X
138a	10:50	18/5	33 43.8	21 18.1	200	X	X	X
138b	17:00	18/5	34 09.3	21 13.7	200	X	X	X
138c	20:45	18/5	34 36.7	21 05.9	200	X	X	X
138e	00:50	19/5	35 06.3	20 57.7	200	X	X	X
139f	04:33	19/5	35 36.1	20 47.9	200	X	X	X
139	10:45	19/5	36 13.0N	20 50.0W	200	X	X	X
139N	22:30	19/5	37 45.5	20 04.0	200	X	X	X
140	10:55	20/5	39 51.9	20 00.1	200	X	X	X
140N	23:00	20/5	41 43.4	20 01.5	200	X	X	X
141	11:00	21/5	43 58.0	19 58.9	200	X	X	X
49	16:00	21/5	44 30.8	19 57.9	200	X	X	X
141N	23:00	21/5	45 29.2	19 59.4	200	X	X	X
142	10:00	22/5	47 00.2	19 59.9	200	X	X	X
142N	11:00	23/5	48 03.5	13 59.1	200	X	X	X
143	10:00	24/5	48 57.3	08 46.0	200	X	X	X
144	10:00	25/5	50 04.1	03 28.1	100	X	X	X
145	08:50	26/5	51 43.0	01 47.2E				X

AMT5

Day	Time	Date	Lat (°)	Long (°)	Depth (m)	Deep net OPC	Deep net Carbon	20m OPC
259	14.22	16-Sep	50 27.6'N	01 39.1'W				
260	16.05	17-Sep	48 40.2'	08 27.4'	200	X	X	X
261	10.08	18-Sep	47 59.0'	13 12.3'	200	X	X	X
262	10.13	19-Sep	47 10.4'	18 28.9'	200	X	X	X
263	10.10	20-Sep	42 50.5'	19 57.8'	200	X	X	X
264	10.10	21-Sep	38 43.0'	20 00.7'	200	X	X	X
264N	21:05	21-Sep	37 07.3'	19 51.9'	200	X	X	
265	09.07	22-Sep	35 26.7'	19 31.4'	200	X	X	X
			Madeira					
268	13.47	25-Sep	32 18.6' N	17 13.6' W	200	X	X	X
269	11.03	26-Sep	29 02.8' ,	20 58.1'	200	X	X	X
270	11.06	27-Sep	24 08.1'	20 59.9'	200	X	X	X
270N	23.00	27-Sep	21 59.4'	20 59.3'	200	X	X	
271	11.03	28-Sep	19 43.2'	20 31.7'	200	X	X	X
271N	23.00	28-Sep	19 03.0'	20 25.1'	200	X	X	
272	11.06	29-Sep	15 29.5'	20 00.6'	200	X	X	X
273	11.04	30-Sep	10 55.3'	20 52.2'	200	X	X	X
274	11.02	01-Oct	07 01.6'	22 28.3'	200	X	X	X
275	11.06	02-Oct	02 49.0'	24 09.8'	200	X	X	X
275	23.00	02-Oct	01 11.2'	24 51.2'	200	X	X	
276	10.39	03-Oct	00 46.7' S	25 39.8'	200	X	X	X
277	11.40	04-Oct	04 47.2'	27 22.1'	200	X	X	X
278	11.37	05-Oct	08 58.0'	29 06.9'	200	X	X	X
279	11.35	06-Oct	12 52.6'	30 42.3'	200	X	X	X
280	11.35	07-Oct	16 41.1'	32 21.8'	200	X	X	X
281	11.45	08-Oct	20 39.7'	34 13.5'	200	X	X	X
282	11.45	09-Oct	23 54.2'	37 17.1'	200	X	X	X
282N	24.00	09-Oct	25 48.8'	39 06.5'	200	X	X	
283	11.35	10-Oct	27 41.4'	40 58.6'	200	X	X	X
283N	24.00	10-Oct	29 40.3'	42 55.9'	200	X	X	
284	12.00	11-Oct	31 37.2'	44 52.0'	200	X	X	X
285	12.43	12-Oct	35 28.6'	48 51.6'	200	X	X	X
285N	01.00	12-Oct	36 42.3'	50 05.7'	200	X	X	
286	12.00	13-Oct	38 50.1'	51 55.4'	200	X	X	X
286N	01.00	13-Oct	40 23.6'	52 58.4'	200	X	X	
287	12.40	14-Oct	42 14.3'	54 27.3'	200	X	X	X
287N	01.00	14-Oct	44 04.6'	55 49.6'	200	X	X	
288	12.14	15-Oct	46 02.7'	56 42.0'	200	X	X	X
289	12.43	16-Oct	49 47.7'	57 39.6'	200	X	X	X

AMT 6

Station					Deep Net		20m net
J Day	Date	Lat (°) Long (°)	Time	Depth (m)	OPC	Carbon	OPC
135	15/05/98	33 37.1'S, 18 00.2'E	11:15	100	x	x	x
135	15/05/98	32 55.4'S, 17 05.4'E	20:00	200	x	x	
136	16/05/98	32 20.2'S, 17 52.6'E	08:00	100	x	x	x
136	16/05/98	31 17.3'S, 16 20.8'E	20:00	200	x	x	
137	17/05/98	29 31.2'S, 16 27.2'E	08:00	100	x	x	x
138	18/05/98	26 42.6'S, 14 47.9'E	04:00	200		x	
138	18/05/98	26 41.8'S, 14 14.8'E	08:30	200	x	x	x
138	18/05/98	26 42.4'S, 13 57.5'E	11:20	200		x	
138	18/05/98	26 41.8'S, 13 30.1'E	15:00	200		x	
141	21/05/98	28 55.8'S, 16 11.3'E	08:00	100	x	x	x
142	22/05/98	24 45.0'S, 14 19.5'E	08:00	100	x	x	x
143	23/05/98	22 05.5'S, 12 36.7'E	04:00	200		x	
143	23/05/98	21 39.3'S, 12 24.4'E	08:00	200	x	x	x
144	24/05/98	19 00.0'S, 12 00.0'E	08:00	200	x	x	x
145	25/05/98	17 40.0'S, 11 20.0'E	06:00	200	x	x	
145	25/05/98	17 26.5'S, 11 04.5'E	11:30	200		x	
146	26/05/98	14 44.6'S, 07 51.6'E	08:30	200	x	x	x
147	27/05/98	11 37.2'S, 04 08.3'E	08:30	200	x	x	x
148	28/05/98	08 37.6'S, 00 36.5'E	08:30	200	x	x	x
149	29/05/98	05 51.9'S, 02 37.1'W	08:30	200	x	x	x
149	29/05/98	04 22.2'S, 04 20.7'W	21:00	200	x	x	
150	30/05/98	02 48.7'S, 06 09.8'W	08:30	200	x	x	x
151	31/05/98	00 01.7'S, 08 51.0'W	08:15	200	x	x	x
152	01/06/98	03 04.3'N, 12 46.2'W	09:00	200	x	x	x
153	02/06/98	05 51.7'N, 16 04.9'W	09:00	200	x	x	x
154	03/06/98	09 03.7'N, 19 07.2'W	09:00	200	x	x	x
155	04/06/98	12 47.1'N, 19 14.7'W	09:00	200	x	x	x
156	05/06/98	16 22.5'N, 20 00.0'W	09:00	200	x	x	x
157	06/06/98	20 24.3'N, 20 00.1'W	09:00	200	x	x	x
158	07/06/98	24 30.3'N, 20 00.0'W	09:00	200	x	x	x
159	08/06/98	28 41.0'N, 19 52.2'W	09:00	200	x	x	x
160	09/06/98	32 39.4'N, 17 09.7W	09:00	200	x	x	x
161	10/06/98	36 36.8'N, 17 30.2'W	09:00	200	x	x	x
161	10/06/98	38 52.8'N, 17 30.0'W	22:00	200	x	x	x
162	11/06/98	41 05.2'N, 17 02.9'W	09:00	200	x	x	x
163	12/06/98	44 40.8'N, 14 00.6'W	08:30	200	x	x	x
164	13/06/98	48 27.0'N, 09 41.8'W	09:45	200	x	x	x
165	14/06/98	49 50.2'N, 04 09.5'W	09:00	20	x	x	x

Appendix 2: AMT 200m net carbon and biovolume estimates

AMT 1

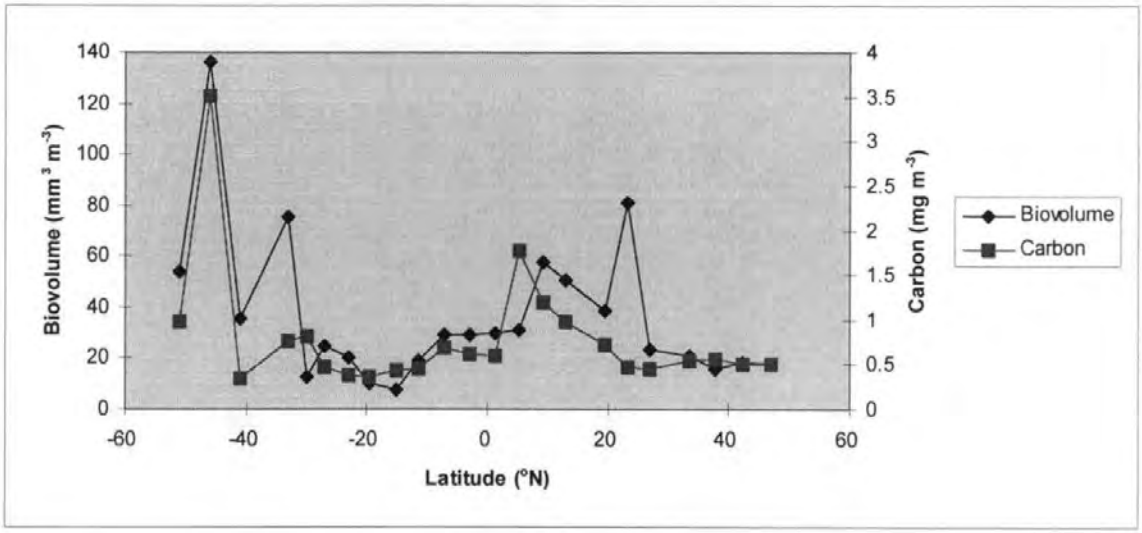

AMT 2

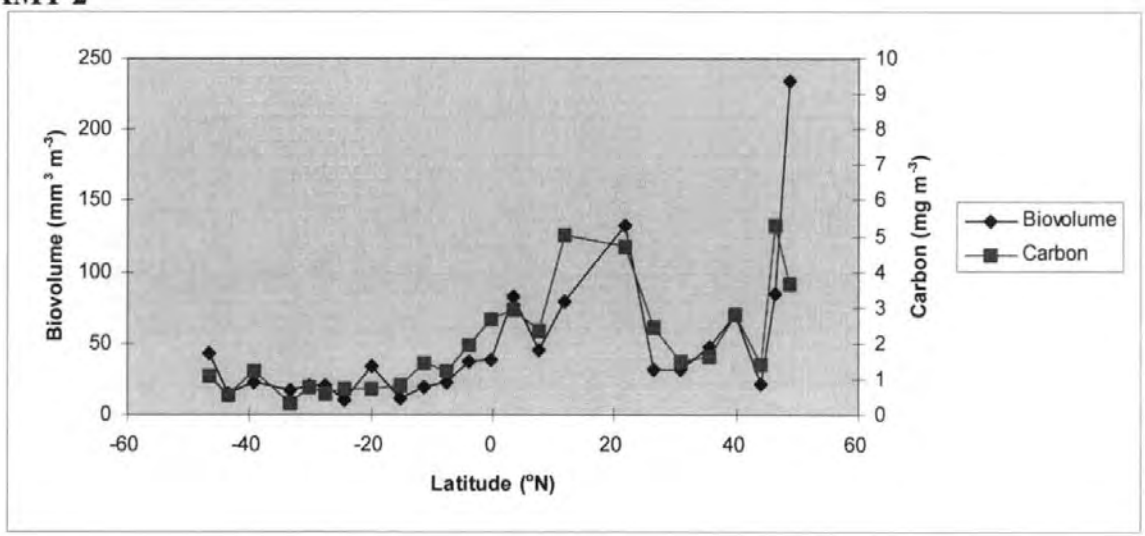

AMT 3

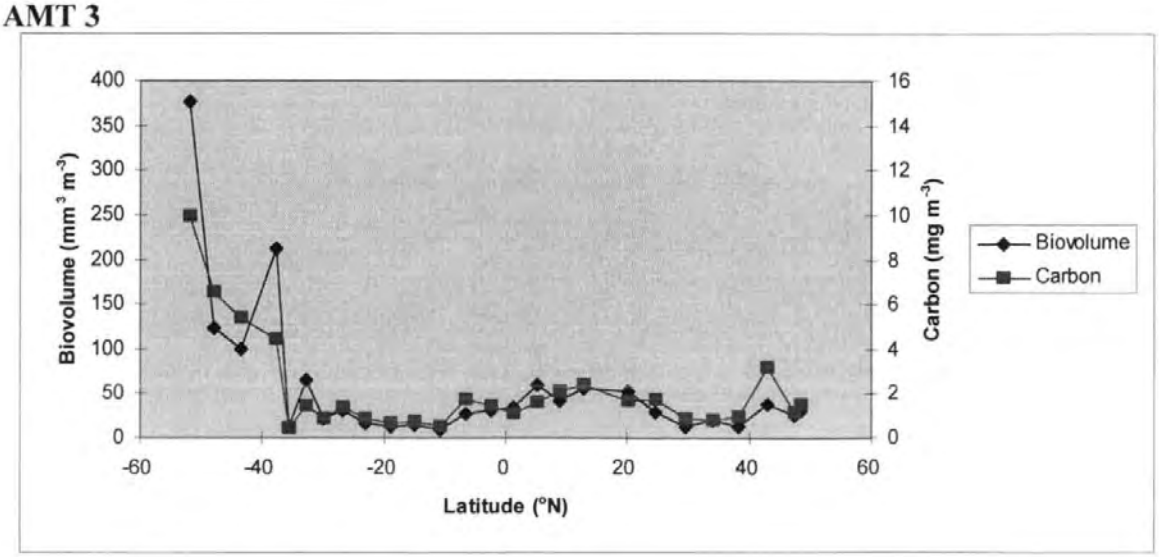

AMT 4

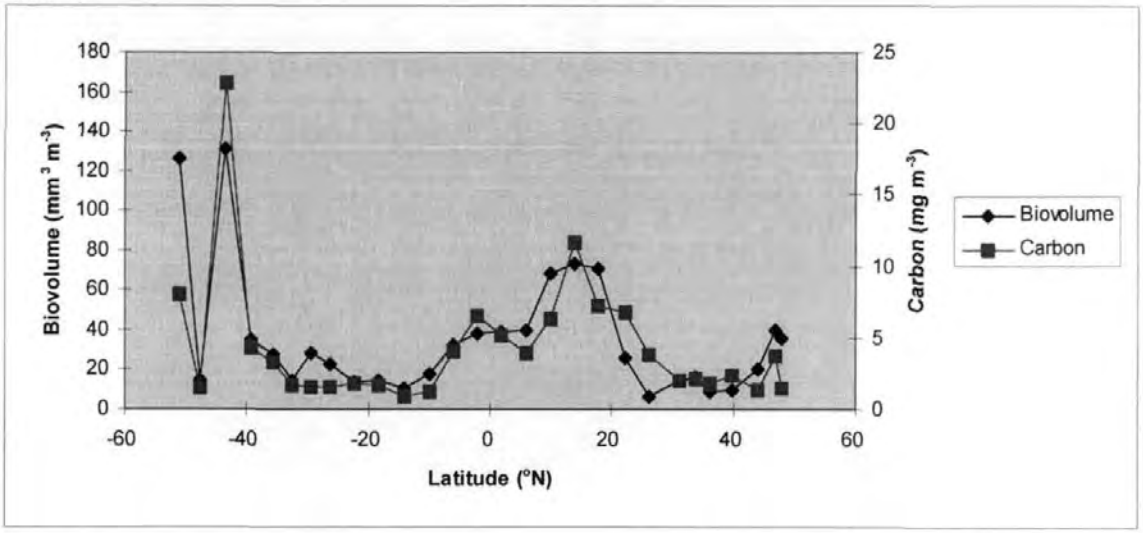

AMT 5

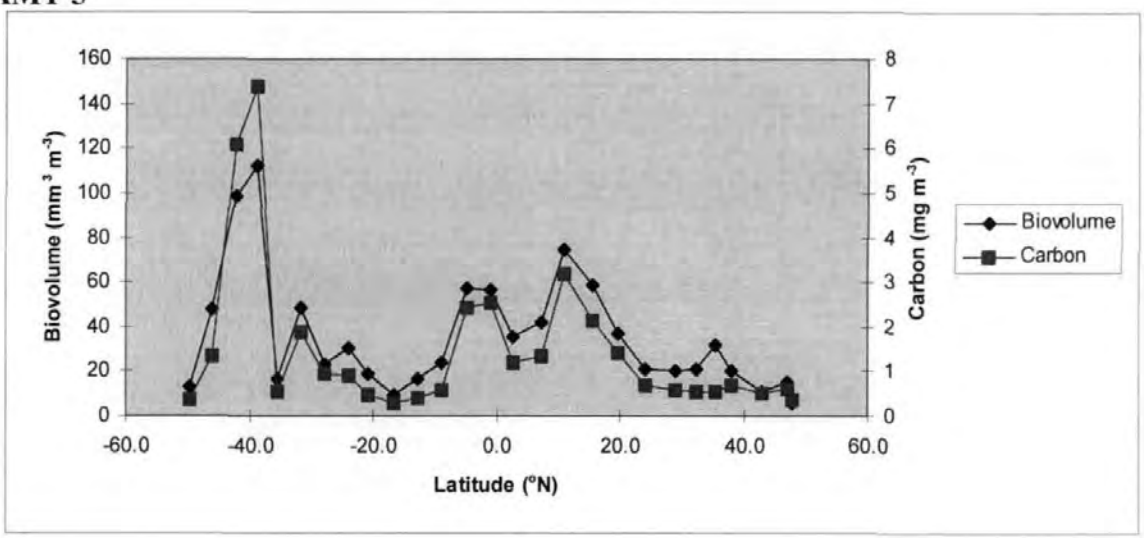

AMT 6

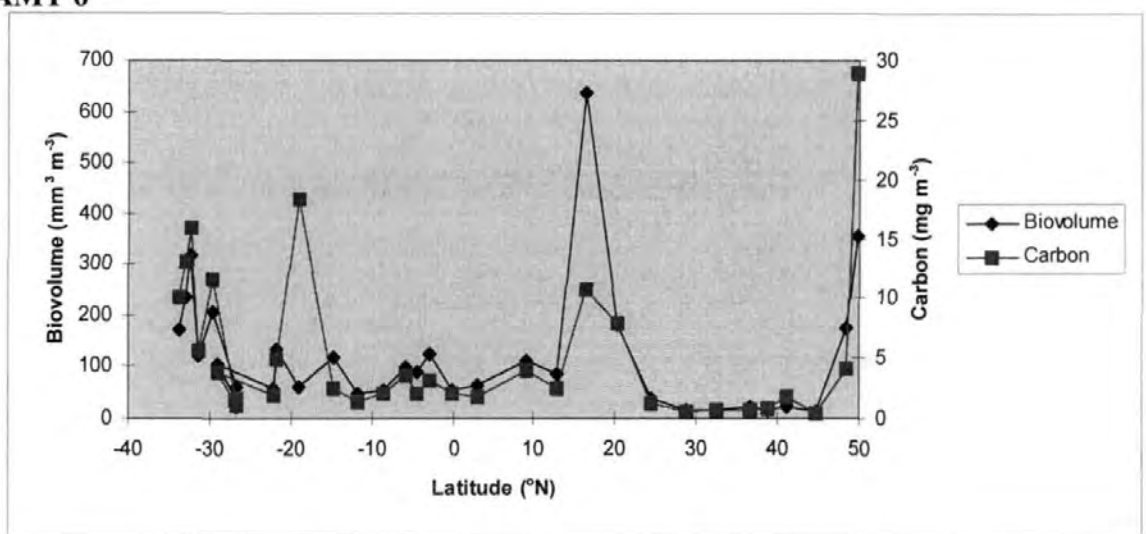

Appendix 3: AMT 200m net samples, numerical abundance estimated from OPC and microscope for transects 1-6

AMT 1

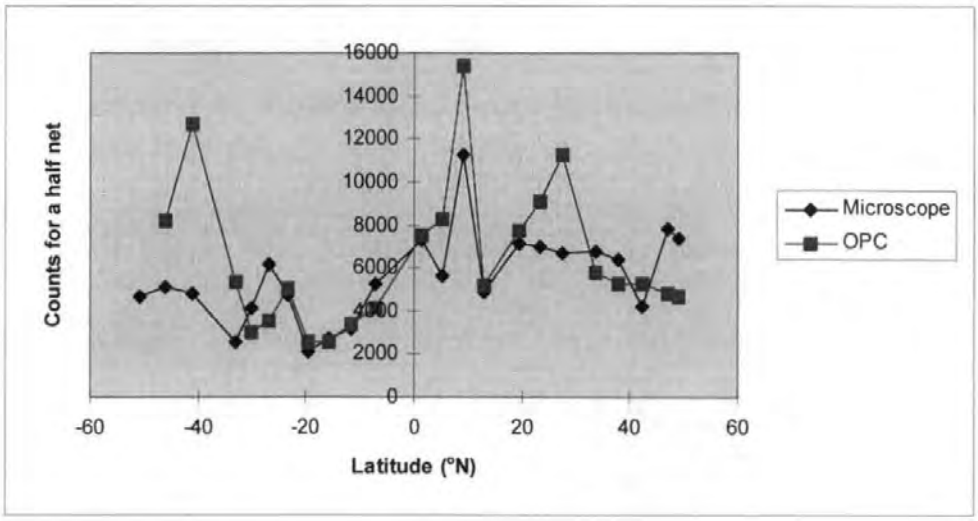

AMT 2

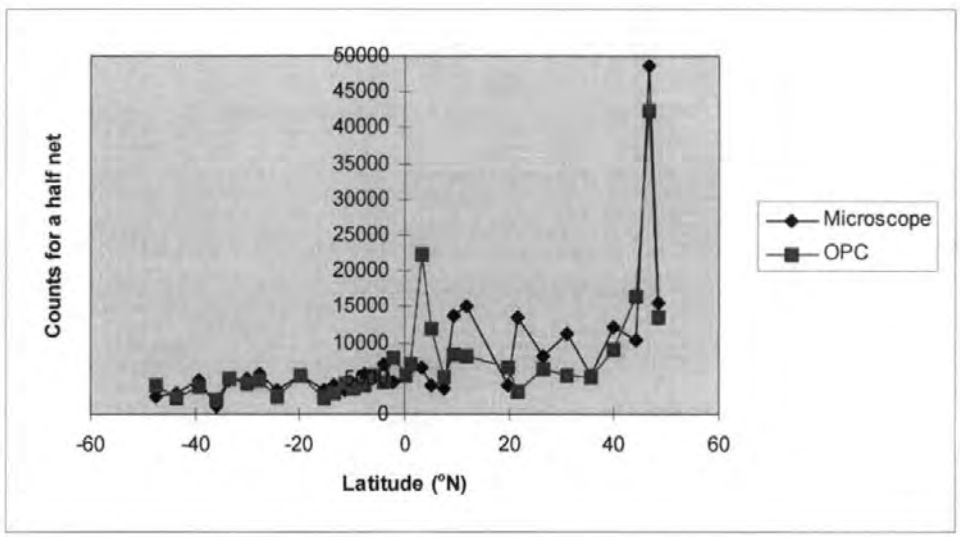

AMT 3

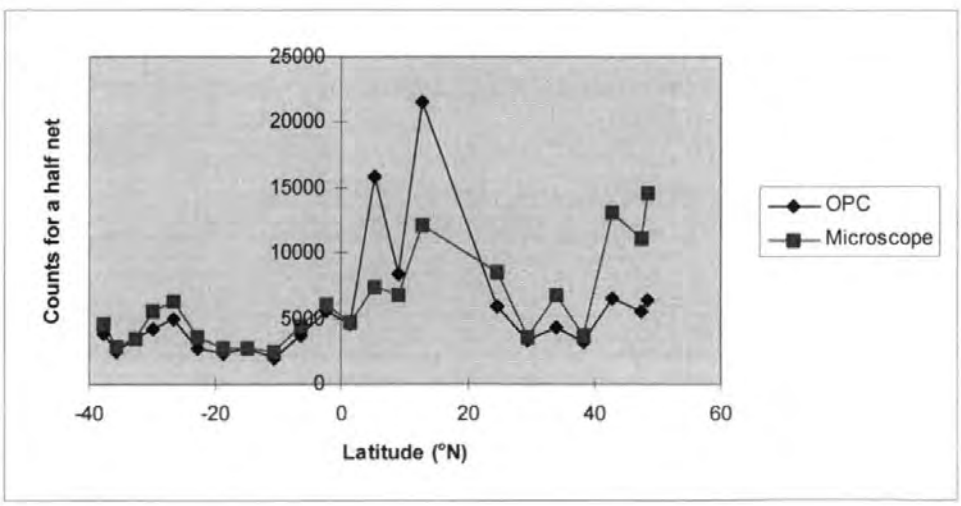

AMT 4

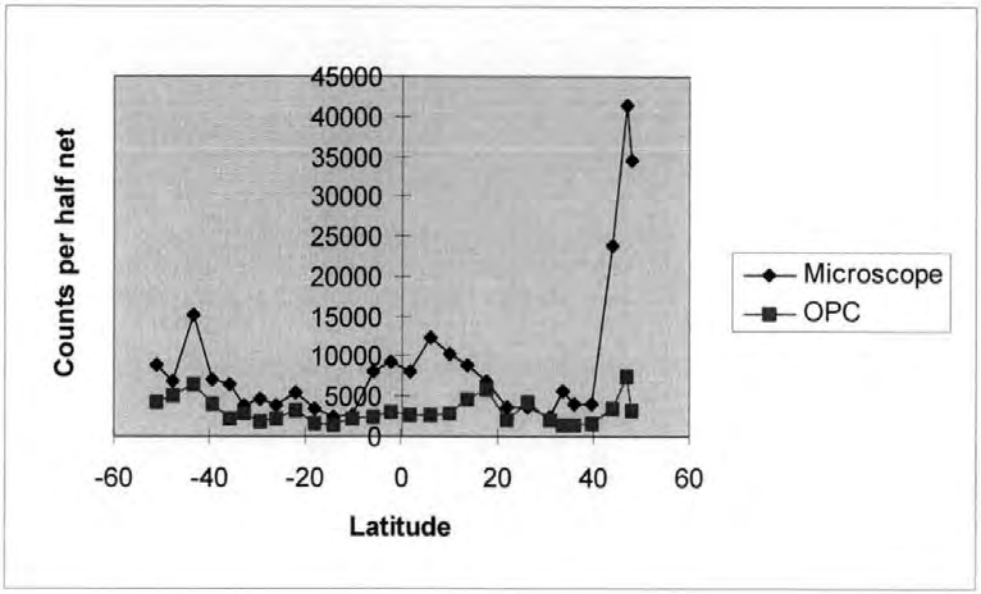

AMT 5

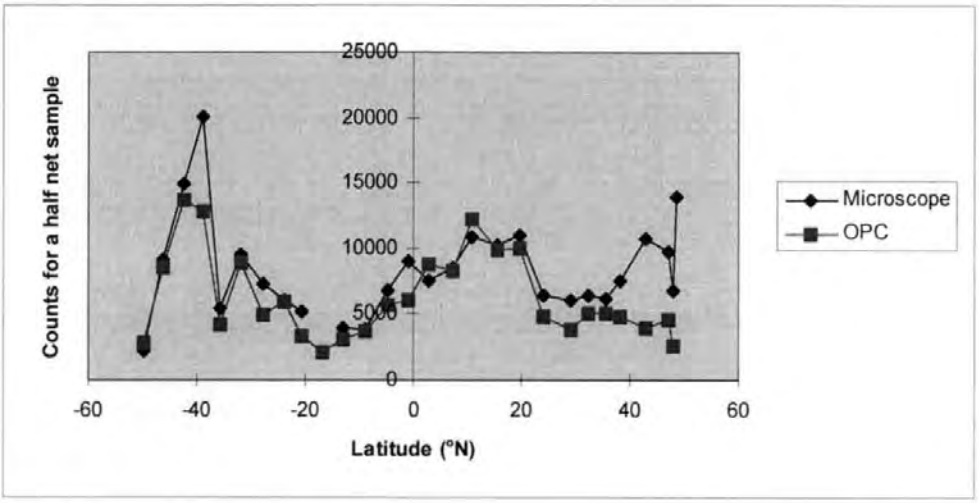

AMT 6

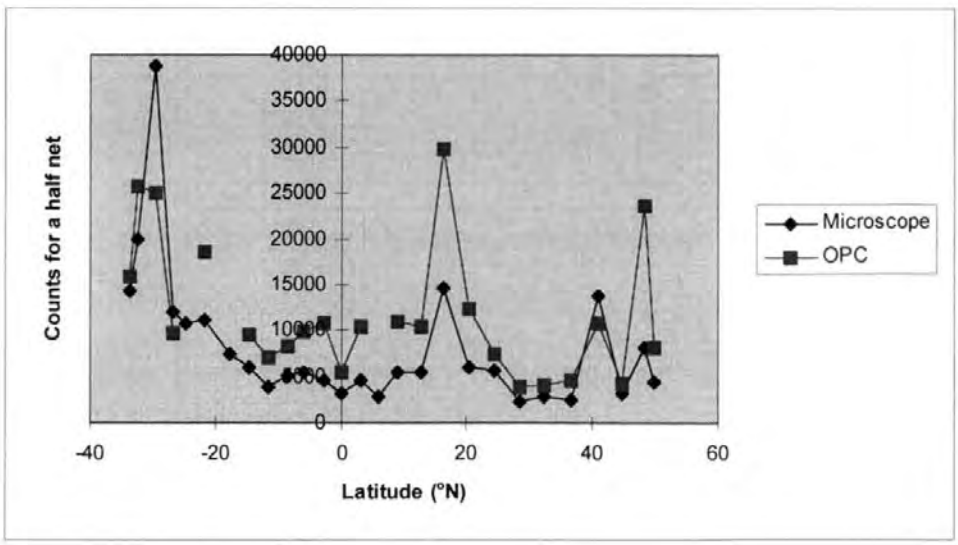

Appendix 4: AMT underway OPC counts compared with microscope counts for the six transects

AMT 1

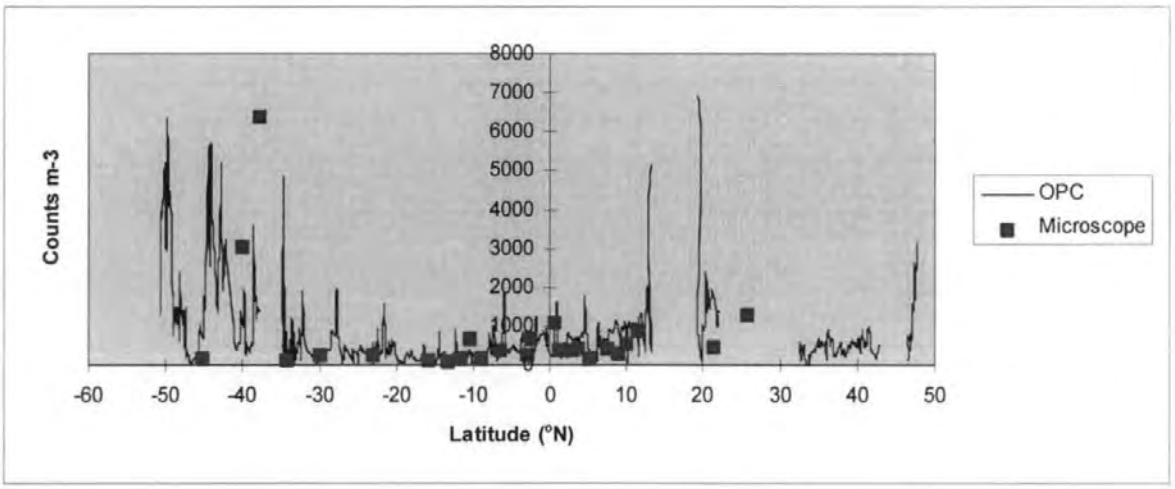

AMT 2

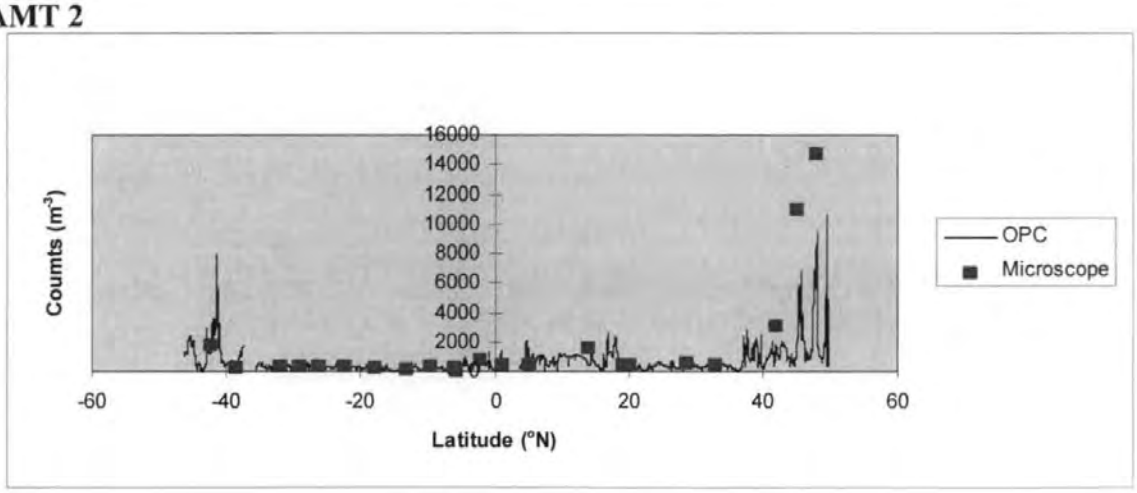

AMT 3

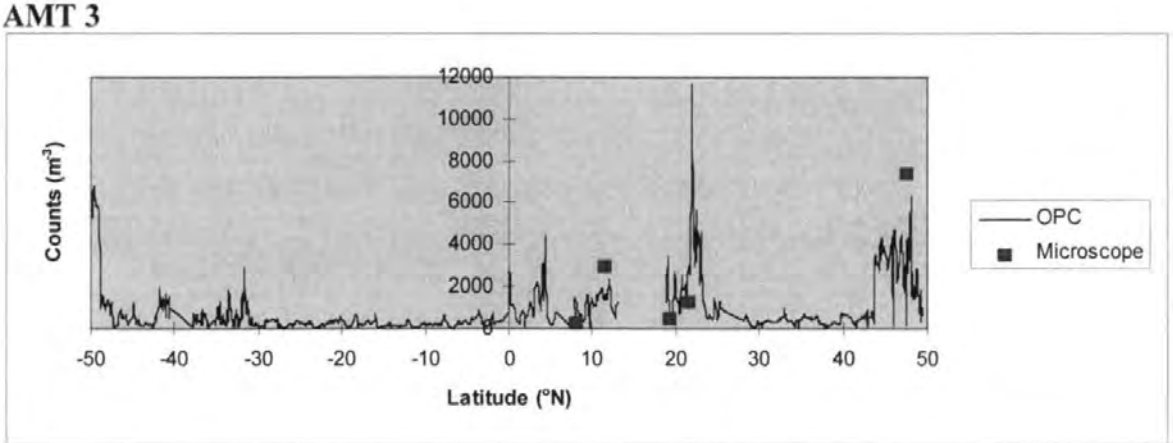

AMT 4

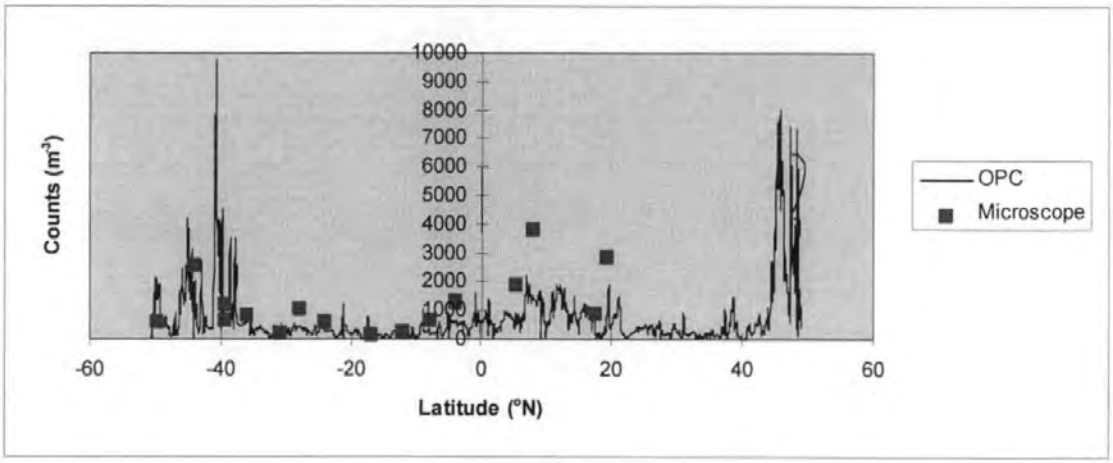

AMT 5

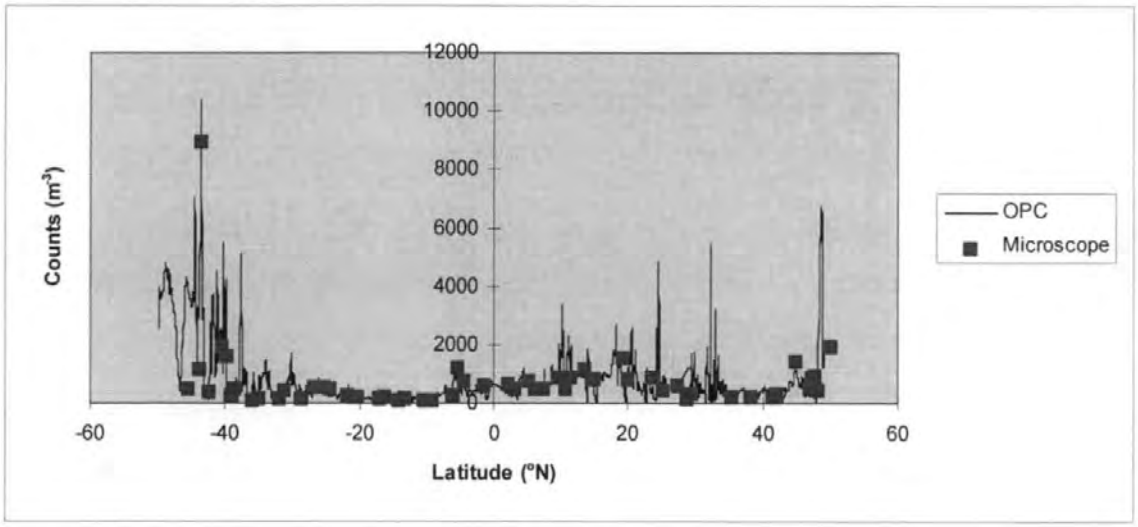

AMT 6

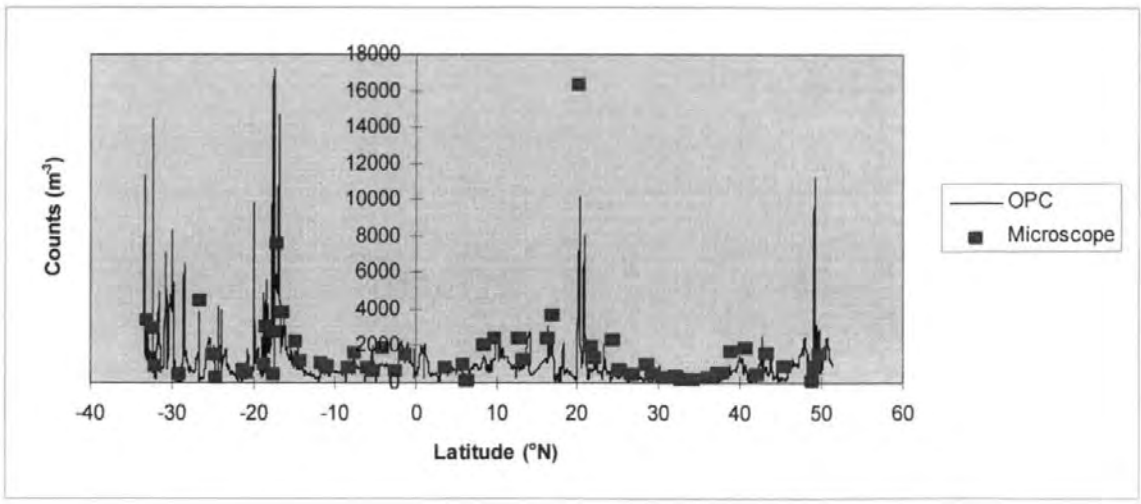

Appendix 5: AMT 1-6 OPC underway mean ESD derived from 30 min bins, with 24 hour moving averages

AMT 1

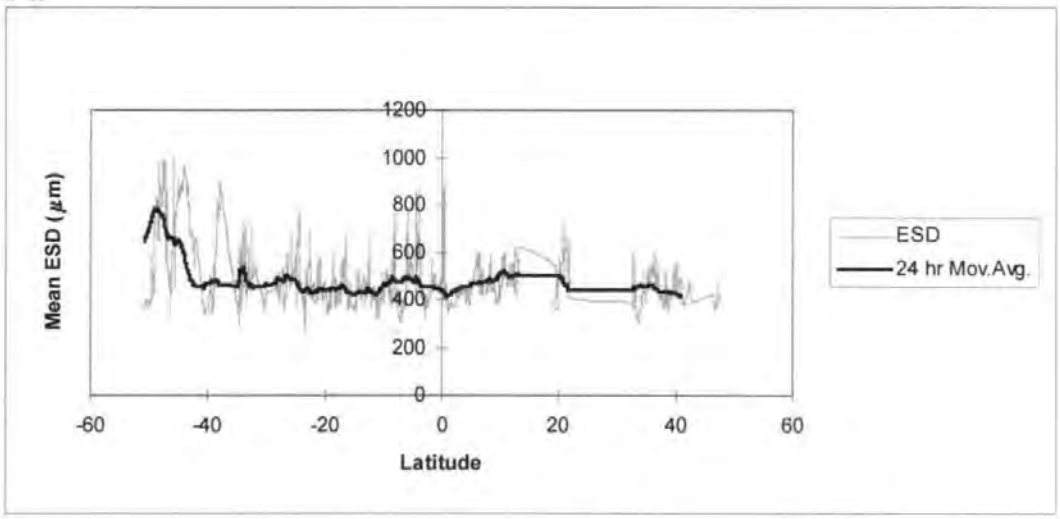

AMT 2

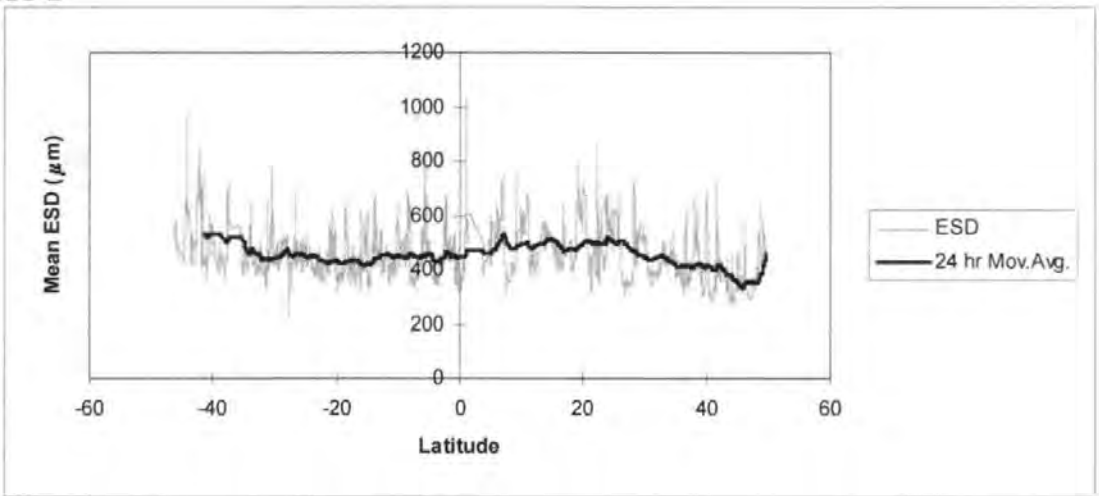

AMT 3

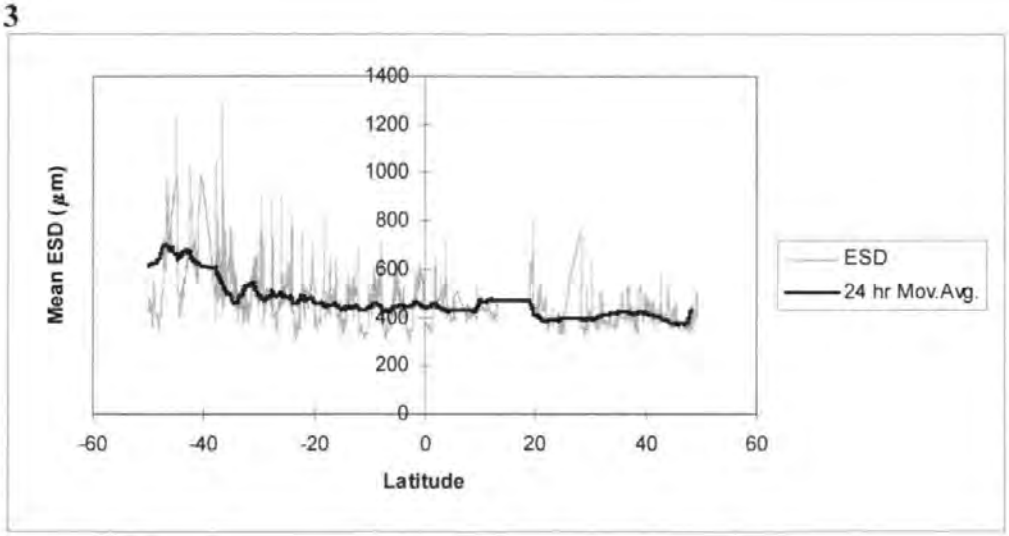

AMT 4

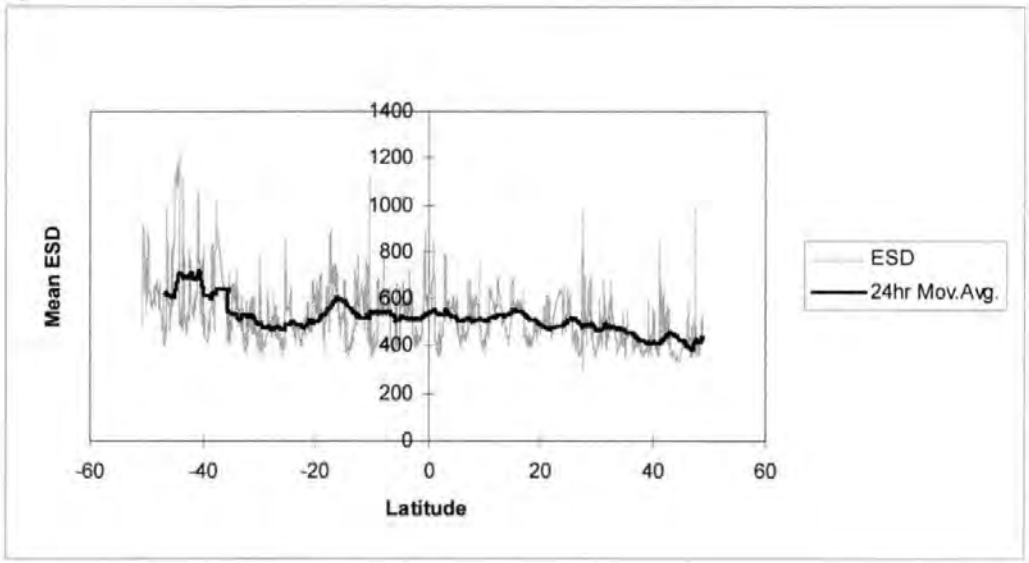

AMT 5

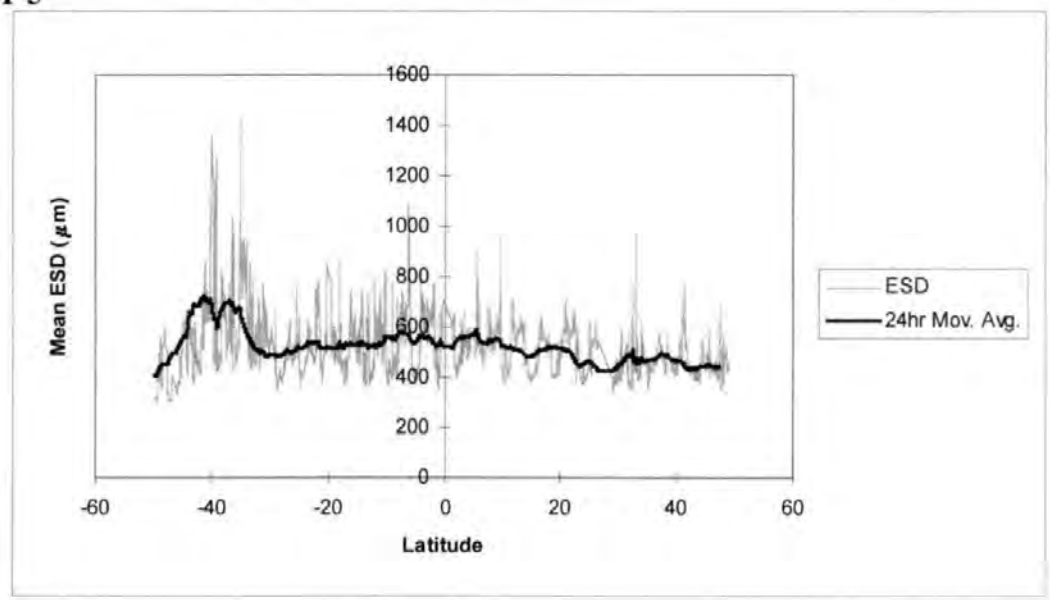

AMT 6

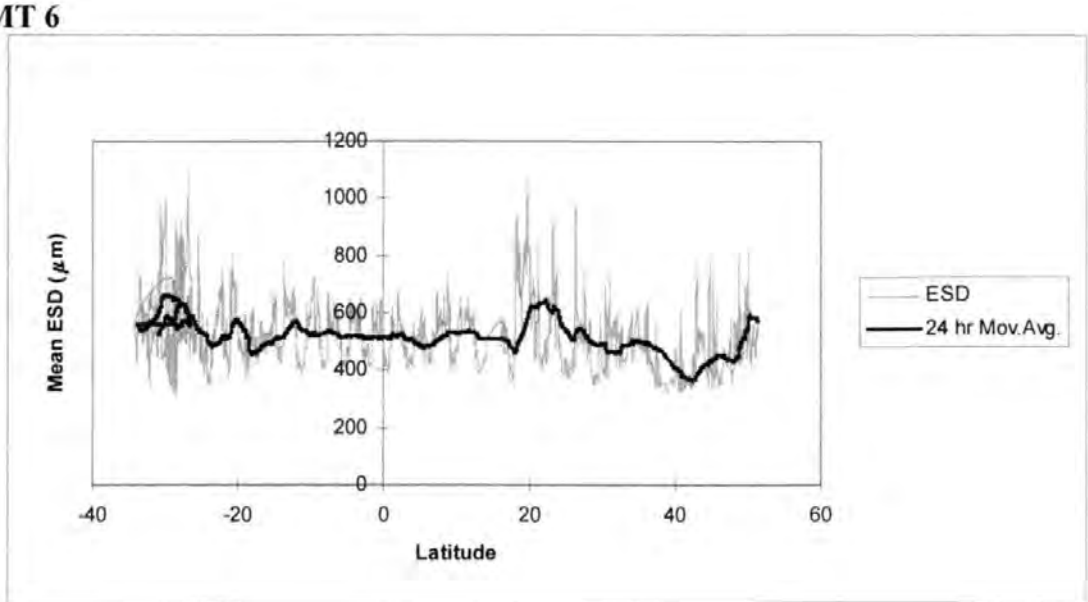

Appendix 6: AMT 1-6 Major groups analysis from deep nets (m^{-3})

AMT 1

Date	24/10	23/10	22/10	17/10	16/10	15/10	14/10	13/10	12/10	11/10	10/10	09/10	08/10
Julian Day	297	296	295	290	289	288	287	286	285	284	283	282	281
Latitude	-51	-46	-41	-33	-30	-27	-23	-19	-15	-11	-7	-3	1
Copepoda	117.3	104.2	93.5	58.6	55.8	146.0	112.0	28.1	33.4	75.2	149.0	198.4	241.4
Naupli	7.8	2.1	7.1	0.7	-	2.1	-	0.1	0.3	1.4	3.0	1.0	6.1
Clad/Ost	0.7	9.3	5.7	2.8	0.7	7.1	7.8	3.0	2.8	1.4	22.4	10.2	11.2
Euph/Mysids	0.0	1.3	0.2	0.2	0.0	0.7	-	0.4	0.2	0.4	1.6	0.2	0.6
Amphipods	0.1	0.2	0.0	0.2	0.1	0.2	0.1	0.3	0.0	0.0	0.3	0.1	0.1
Decapod l.	-	-	-	-	-	-	-	-	-	-	0.1	0.0	-
Cirrepedi	-	0.7	1.4	-	-	-	-	-	-	-	-	-	-
Chaetognatha	0.2	5.1	9.1	3.0	5.4	3.0	3.0	0.5	5.3	3.0	0.7	1.3	0.9
Polychaeta	-	-	3.6	0.1	0.3	0.2	1.4	0.1	0.1	0.0	0.5	0.2	0.5
Ptero/gastro	-	3.6	2.8	2.1	0.0	2.8	5.7	1.4	1.4	-	3.0	1.0	3.0
Bivalve	-	-	-	-	-	-	-	-	-	-	0.0	-	-
Salpa	-	-	-	2.4	0.1	-	-	0.0	0.0	-	-	-	-
Doliolid	-	-	0.0	0.0	-	-	-	-	0.1	0.1	0.0	0.1	0.1
Appendicularia	-	-	5.7	0.3	0.3	1.4	0.3	0.1	0.2	2.8	1.0	6.1	9.1
Siphonophores	-	0.1	2.1	0.2	0.2	0.3	0.2	2.3	1.4	2.8	3.0	0.5	3.0
Medusa	-	-	0.0	0.1	-	-	-	-	0.0	-	-	0.0	0.0
Ctenophores	-	-	-	-	-	-	-	-	-	-	-	-	-
Echinoderm	-	-	-	-	-	-	0.0	0.1	0.0	-	-	-	0.0
Fish larvae	-	-	-	-	-	0.0	-	-	-	-	-	0.0	-
Amphioxus	-	-	-	-	-	-	-	-	-	-	0.0	-	-
Total	126.1	126.4	131.5	70.7	62.9	164.0	130.7	36.5	45.6	88.1	185.0	219.4	276.1

AMT 1 continued

Date	07/10	06/10	05/10	04/10	03/10	02/10	30/09	29/09	28/09	27/09	26/09	25/09
Julian Day	280	279	278	277	276	275	273	272	271	270	269	268
Latitude	5.3	9.2	13.0	19.4	23.2	27.0	33.5	37.9	42.2	47.0	47.9	48.9
Copepoda	186.0	371.6	154.5	234.8	146.8	221.6	221.2	202.6	145.7	253.6	267.5	253.6
Naupli	1.0	2.0	3.0	2.0	3.0	1.0	-	-	-	0.8	0.8	1.7
Clad/Ost	10.2	7.1	2.0	8.1	11.2	19.3	12.6	22.6	11.7	4.2	5.9	1.7
Euph/Mysids	-	0.3	2.0	4.1	0.2	2.0	0.2	-	0.3	2.5	0.1	2.5
Amphipods	1.0	0.1	-	1.0	0.2	-	0.1	-	0.0	-	0.2	-
Decapod l.	-	-	-	1.0	-	-	-	-	-	-	-	-
Cirrepedi	-	-	-	-	-	-	-	-	-	-	-	-
Chaetognatha	3.0	6.1	4.1	5.1	1.7	3.0	2.1	1.7	0.4	13.4	4.1	4.2
Polychaeta	-	0.1	2.0	4.1	0.4	1.0	0.5	1.7	-	0.8	-	-
Ptero/gastro	1.0	2.0	-	8.1	3.0	1.0	5.9	3.3	1.7	-	0.8	-
Bivalve	-	-	-	-	-	-	-	-	-	-	-	-
Salpa	-	-	1.0	-	83.4	-	-	-	-	-	-	-
Doliolid	-	0.2	2.0	-	-	2.0	0.3	-	-	2.5	-	2.5
Appendicularia	12.2	7.1	8.1	1.0	6.1	2.0	0.6	-	0.2	2.5	0.2	-
Siphonophores	2.0	6.1	7.1	4.1	2.0	4.1	8.4	13.4	0.9	20.9	0.3	8.4
Medusa	-	-	1.0	-	-	1.0	0.1	0.8	-	-	-	-
Ctenophores	-	-	-	-	5.1	-	-	-	-	-	-	-
Echinoderm	-	-	-	-	0.0	-	0.0	-	-	-	-	-
Fish larvae	-	-	-	-	-	-	-	-	-	-	-	-
Amphioxus	-	-	-	-	-	-	-	-	-	-	-	-
Total	216.5	402.8	187.0	273.4	263.1	258.2	252.0	246.1	161.0	301.4	280.0	274.6

AMT 2

Julian Day	115	116	120	121	122	123	124	125	126	126	127
Date	24/04	25/04	29/04	30/04	01/05	02/05	03/05	04/05	05/05	05/05	06/05
Depth	200	200	200	200	200	200	200	200	200	200	200
Time	13:34	13:35	14:03	17:02	13:14	13:10	13:06	12:22	12:00	12:10	22:51
Latitude	-47.6	-43.4	-39.4	-36.1	-33.4	-30.3	-27.6	-24.4	-19.9	-15.2	-13.3
Copepoda	62.5	109.8	16.5	98.7	116.5	111.3	70.9	124.2	28.5	82.8	75.4
Naupli	0.2	0.1	-	-	0.1	0.1	-	-	1.8	0.1	1.4
Cladocerans	-	-	-	0.2	-	-	-	-	-	-	-
Ostracods	4.9	5.6	0.7	1.1	1.8	5.2	3.7	2.6	1.5	2.1	1.7
Euphausiid	0.2	0.2	-	0.4	0.1	0.0	0.1	0.0	0.1	0.5	0.2
Mysid	-	-	-	-	0.2	0.1	0.1	-	-	-	0.1
J. euph/mysid	0.1	0.4	-	0.3	0.2	0.3	0.1	0.3	0.1	0.2	-
Amphipoda	0.0	0.1	0.0	-	0.1	0.1	-	0.1	0.1	0.3	-
Decapod l.	-	0.1	-	-	0.1	0.1	0.0	0.2	0.1	0.1	0.1
Cerripedi	-	-	-	-	-	-	-	0.2	11.4	-	0.1
Chaetognath	0.4	1.5	0.2	2.0	0.8	1.7	1.0	1.7	0.4	1.3	0.3
Polychaete	-	0.3	0.2	0.8	0.3	0.6	0.4	0.2	0.1	0.4	0.3
Pteropoda	0.1	0.5	0.3	0.6	-	0.5	0.1	0.1	0.1	0.3	0.5
Gastropoda	0.2	1.3	0.2	1.6	0.1	0.9	0.7	0.6	0.5	1.2	0.5
Bivalva	-	0.2	-	0.0	-	-	-	-	-	0.0	0.0
Salpa	-	-	-	-	-	-	-	-	-	-	-
Doliolid	-	0.1	-	0.0	1.6	0.2	0.1	0.5	0.0	0.0	0.0
Larvacea	0.3	0.1	0.2	1.4	1.2	0.0	0.1	0.4	0.2	0.0	0.1
Siphonophore	0.2	1.1	0.4	1.1	1.5	1.4	0.8	1.1	0.5	0.9	0.7
Medusa	-	0.0	-	0.1	0.1	-	-	0.3	-	0.2	-
Ctenophora	-	-	-	0.0	0.0	-	-	-	-	-	-
Echinoderm	-	0.0	-	0.0	0.5	0.2	0.5	0.2	0.2	0.1	0.3
Ophuroides	-	-	-	-	-	-	-	-	-	-	-
Bryozoan	-	-	-	-	-	0.0	0.0	0.0	0.0	-	-
Amphioxus	-	-	-	-	-	-	-	-	-	-	0.0
Fish egg	-	-	-	-	-	-	-	-	-	-	0.0
Fish larvae	0.1	-	-	-	-	-	-	-	-	0.0	-
Total	69.1	121.5	18.5	108.2	125.2	122.7	78.6	132.7	45.5	90.4	81.9

AMT 2 continued

Julian Day	127	128	128	129	129	130	130	131	131	132	132
Date	06/05	07/05	07/05	08/05	08/05	09/05	09/05	10/05	10/05	11/05	11/05
Depth	200	200	200	200	200	200	200	200	200	200	200
Time	12:05	22:51	12:03	23:01	11:03	22:05	11:06	22:21	11:07	22:07	11:02
Latitude	-11.2	-9.6	-7.5	-5.8	-3.9	-2.3	0.2	1.3	3.4	5.2	7.6
Copepoda	80.5	129.3	114.5	156.7	96.8	134.1	138.4	146.3	67.1	75.3	311.8
Naupli	1.4	1.4	2.8	0.3	2.8	2.1	1.4	4.3	2.1	-	7.8
Cladocerans	-	-	0.0	-	-	-	-	-	0.0	-	0.1
Ostracods	2.0	2.6	2.3	4.3	1.5	1.8	9.3	2.0	1.4	1.9	7.1
Euphausiid	0.7	0.1	0.5	0.3	0.5	0.2	1.0	0.2	0.5	-	0.7
Mysid	-	-	-	0.0	0.0	-	-	-	-	0.2	-
J. euph/mysid	0.2	0.3	0.2	0.3	0.1	0.4	-	0.1	0.0	0.4	0.2
Amphipoda	0.2	0.1	0.3	0.1	0.4	-	0.5	0.2	1.0	0.3	1.2
Decapod l.	0.3	0.1	0.3	0.5	-	-	0.5	-	0.2	0.2	0.3
Cerripedi	-	-	-	0.2	-	-	-	-	-	-	-
Chaetognath	1.2	0.8	0.7	1.0	1.0	0.4	1.2	1.8	0.8	2.7	3.0
Polychaete	0.5	0.3	0.5	0.7	0.5	0.1	0.5	1.0	1.0	0.7	0.8
Pteropoda	0.5	0.2	0.3	0.4	0.0	-	0.4	0.1	-	0.0	0.1
Gastropoda	1.7	0.5	0.8	0.3	0.5	0.3	0.6	0.1	0.2	0.2	0.7
Bivalva	0.0	0.0	-	-	-	-	-	-	0.0	-	-
Salpa	-	-	0.4	0.0	17.1	-	18.5	-	26.3	0.2	0.6
Doliolid	-	0.1	0.3	0.1	0.2	-	0.1	10.7	-	0.7	0.5
Larvacea	0.3	0.0	-	0.3	-	0.2	-	0.3	-	0.7	-
Siphonophore	1.0	0.7	1.4	0.6	1.9	0.8	0.5	1.0	0.2	1.3	0.4
Medusa	0.0	-	0.1	0.1	0.0	0.0	1.7	-	0.8	0.1	-
Ctenophora	-	-	-	0.1	-	-	-	-	-	-	-
Echinoderm	0.2	0.2	0.1	-	-	-	-	-	-	-	-
Ophuroides	-	-	-	-	-	-	-	-	-	-	-
Bryozoan	-	-	-	-	-	-	-	-	-	0.0	-
Amphioxus	-	-	-	0.0	0.0	-	-	-	-	0.0	-
Fish egg	-	0.2	-	-	-	0.0	-	-	0.0	0.1	0.2
Fish larvae	0.2	-	0.1	-	0.1	0.0	0.1	-	0.0	0.1	0.3
Total	90.7	137.1	125.6	166.4	123.5	140.6	174.7	168.1	101.8	85.3	336.0

AMT 2 continued

Julian Day	133	134N	135	136	137	138	139	140	141	142	144
Date	12/05	14/05	14/05	15/05	16/05	17/05	18/05	19/05	20/05	21/05	23/05
Depth	200	200	200	200	200	200	200	200	200	200	200
Time	21:59	10:59	1:36	11:02	9:59	10:01	9:59	9:59	10:00	9:03	9:04
Latitude	9.4	11.7	19.9	21.8	26.5	30.9	35.7	39.9	44.1	46.5	48.5
Copepoda	344.4	70.7	287.9	178.6	234.3	102.1	302.7	158.2	1283	301.0	54.7
Naupli	7.8	0.1	2.1	0.7	0.0	0.2	-	-	-	5.7	-
Cladocerans	-	-	-	0.6	0.0	-	-	-	-	62.6	-
Ostracods	9.3	1.6	8.5	12.1	17.1	11.4	0.7	-	0.6	0.7	2.9
Euphausiid	0.1	0.5	0.3	0.1	-	-	-	-	0.1	0.1	0.3
Mysid	-	-	-	0.0	-	-	-	-	-	-	-
J. euph/mysid	0.1	-	1.2	0.1	0.1	0.0	-	-	0.2	-	-
Amphipoda	0.2	0.7	0.0	0.2	1.0	15.7	0.7	0.0	12.8	0.2	0.2
Decapod l.	0.2	0.2	4.0	0.6	0.3	0.2	0.1	-	0.1	0.5	0.0
Cerripedi	0.1	-	-	-	-	-	-	-	-	-	-
Chaetognath	2.7	0.1	3.9	1.2	0.7	0.2	3.0	0.4	2.8	3.3	1.8
Polychaete	0.8	0.1	0.2	0.2	0.6	0.2	0.2	-	0.2	0.4	0.0
Pteropoda	0.9	0.0	0.0	-	-	0.1	0.1	-	0.2	0.9	1.0
Gastropoda	2.5	1.1	0.4	1.5	3.7	0.4	0.2	-	-	0.4	2.6
Bivalva	0.1	-	0.1	-	0.2	-	-	-	-	0.2	-
Salpa	-	28.5	15.7	0.1	-	-	9.3	-	-	-	-
Doliolid	-	-	17.8	0.1	0.1	-	-	-	-	-	-
Larvacea	0.2	-	-	0.8	-	0.0	-	-	-	-	0.8
Siphonophore	2.2	0.0	0.6	1.1	1.1	2.3	0.3	-	0.7	29.9	0.1
Medusa	0.0	0.0	5.0	0.2	-	-	-	-	-	0.0	-
Ctenophora	-	-	-	-	-	-	-	-	-	0.1	-
Echinoderm	-	-	-	0.1	0.0	-	-	-	-	5.7	-
Ophuroides	-	-	-	-	-	-	-	-	-	0.1	-
Bryozoan	-	-	0.0	-	-	-	-	-	-	-	-
Amphioxus	-	-	-	-	-	-	-	-	-	-	-
Fish egg	-	-	0.0	0.1	0.0	-	0.1	-	-	0.1	-
Fish larvae	-	-	-	0.1	-	-	-	-	-	0.1	-
Total	372.0	103.8	348.0	198.4	259.2	132.7	317.3	158.7	1301	412.2	64.4

AMT 3

Date	22/09	23/09	24/09	25/09	26/09	27/09	28/09	29/09	02/10	03/10	04/10	05/10	06/10
Latitude	48	47	43	38	34	30	25	20	13	9	5	1	-2
Copepoda	1321	530.5	408.7	361.9	121.6	219.3	124.2	272.6	367.4	220.1	259.5	167.9	192.9
Nauplii	13.0	0.5	0.8	2.4	0.1	1.1	0.2	2.1	2.6	1.5	3.1	2.1	2.3
Cladocera	-	0.1	0.1	8.3	0.6	1.5	0.2	0.9	-	7.2	-	1.6	-
Ostrocoda	-	10.1	7.0	7.9	2.6	6.3	5.1	12.0	13.9	0.1	9.4	0.6	6.1
Euphausiid	0.3	0.1	0.2	0.7	0.1	0.5	0.2	1.7	0.2	13.2	0.4	0.6	1.1
J. Euph.	0.3	0.2	-	0.7	-	0.3	0.4	0.4	0.5	0.8	0.7	0.7	4.0
Mysid	0.2	-	-	-	-	0.1	0.1	0.5	0.1	0.1	0.0	-	-
Amphipoda	-	-	0.8	0.2	-	0.1	0.1	0.4	0.4	0.7	0.6	0.3	0.2
Decapod L.	2.1	0.0	0.2	0.2	0.2	-	-	0.1	-	1.4	0.1	0.2	0.1
Chaetognatha	0.3	3.6	2.7	4.6	1.5	1.3	0.6	0.9	2.7	1.7	3.6	2.3	5.1
Polychaeta	0.3	1.3	-	0.6	0.5	1.0	0.7	0.2	1.0	0.3	0.2	0.6	1.5
Gastropoda	-	0.5	1.5	1.0	0.5	0.3	2.1	1.7	2.8	0.8	-	-	-
Pteropoda	-	0.7	-	0.8	0.1	0.5	0.3	1.1	1.3	-	0.6	-	1.5
Salpa	0.3	-	-	1.1	-	0.0	-	-	0.3	3.2	-	-	-
Doliolid	4.8	-	-	89.7	0.7	1.6	0.0	-	0.9	0.1	0.5	0.1	-
Medusa	2.8	0.2	-	1.5	0.5	0.3	0.0	-	-	0.0	-	-	0.1
Siphonophore	1.0	0.1	0.1	0.6	1.3	1.5	0.8	1.2	0.9	1.0	1.9	1.3	4.2
Cnideria	-	-	-	-	1.0	1.5	-	0.2	2.0	0.7	1.1	0.7	1.9
Larvacea	0.6	7.4	4.0	16.7	3.2	0.9	0.3	3.8	3.9	5.9	3.6	2.3	5.5
Echinoderm L.	-	-	-	-	-	-	-	-	-	0.1	-	-	-
Amphioxus	-	-	-	-	-	-	-	0.1	-	-	-	-	0.2
Fish eggs	0.5	0.9	-	1.3	3.1	21.8	0.2	27.4	48.3	0.6	0.2	0.9	-
Fish larvae	-	0.1	-	-	-	-	-	0.2	0.2	0.1	-	0.1	0.1
Foraminifera	-	2.9	2.8	2.6	6.4	1.6	0.4	0.6	19.6	4.5	2.2	1.0	4.9
Radiolaria	-	0.3	0.2	-	-	1.5	-	-	-	-	-	-	-
Total	1348	559	429	502	144	263	136	328	468	264	287	183	231

AMT 3 continued

Date	07/10	08/10	09/10	10/10	11/10	12/10	13/10	14/10	15/10	16/10	23/10	25/10
Latitude	-6	-11	-15	-19	-23	-27	-30	-33	-36	-38	-44	-52
Copepoda	144	83	91	88	118	201	201	91	101	126	279	4626
Nauplii	1.8	0.1	-	0.5	2.6	4.0	0.5	0.2	0.1	-	2.3	71.3
Cladocera	-	0.2	0.5	0.5	-	-	-	-	-	-	-	-
Ostrocoda	5.8	7.3	2.8	2.7	7.0	4.9	3.7	1.1	1.8	1.8	7.4	0.2
Euphausiid	0.8	0.2	0.2	0.3	1.0	0.6	0.1	0.2	0.0	0.3	2.1	0.7
J. Euph.	0.3	0.3	0.2	0.4	0.6	0.8	0.6	0.3	0.3	0.1	0.5	0.9
Mysid	-	-	-	-	0.1	-	-	-	-	-	-	-
Amphipoda	0.2	0.1	0.2	0.3	0.4	0.5	-	0.1	0.1	0.2	0.3	-
Decapod L.	-	0.2	0.1	-	0.1	0.1	-	0.2	0.1	-	-	-
Chaetognatha	3.8	0.8	1.1	0.8	1.8	5.5	2.2	3.1	1.4	2.1	3.8	1.5
Polychaeta	0.8	0.6	1.3	0.8	0.3	0.6	0.3	-	0.2	0.2	0.2	2.8
Gastropoda	-	0.0	-	-	-	-	-	-	-	-	-	-
Pteropoda	2.1	0.9	1.3	0.5	1.1	1.1	-	0.3	0.7	0.3	0.2	0.9
Salpa	0.3	-	0.2	-	0.0	-	0.9	30.0	0.6	41.7	0.2	-
Doliolid	0.1	-	0.2	-	0.2	1.1	0.2	0.1	-	-	-	-
Medusa	0.1	-	0.3	0.2	0.0	0.2	-	0.0	0.0	0.1	-	-
Siphonophore	1.3	0.4	2.3	0.5	2.5	3.2	1.0	0.5	0.8	0.8	0.4	-
Cnideria	3.1	0.6	0.8	0.3	0.8	1.0	0.2	0.9	0.5	0.2	0.5	-
Larvacea	4.0	1.2	1.4	0.7	0.6	9.5	3.2	1.2	0.5	0.7	-	24.5
Echinoderm L.	-	-	0.8	0.6	0.3	0.5	-	-	-	-	-	-
Amphioxus	0.2	-	-	-	-	-	-	-	-	-	-	-
Fish eggs	0.1	0.3	0.2	-	0.2	2.0	0.2	1.3	0.1	-	-	-
Fish larvae	0.1	-	-	-	0.0	-	-	0.1	-	0.2	-	-
Foraminifera	1.5	0.6	0.8	0.1	0.8	1.7	1.3	0.9	0.4	0.1	-	-
Radiolaria	0.2	-	0.7	9.6	1.4	1.8	0.3	0.5	0.4	0.4	0.5	-
Total	171	96	107	107	140	240	216	132	109	175	297	4729

AMT 4

Julian Day	111	112	113	114	120	121	122	123	124	125	126	127
Date	21/04	22/04	23/04	24/04	30/04	01/05	02/05	03/05	04/05	05/05	06/05	07/05
Latitude	-51	-48	-43	-39	-36	-33	-29	-26	-22	-18	-14	-10
Depth	100	200	200	200	200	200	200	200	200	200	200	200
Copepoda	339.3	249.8	460.9	253.7	220.5	133.0	177.6	127.8	193.0	112.6	86.9	84.6
Naupli	-	-	0.8	-	-	-	2.5	0.1	1.7	0.2	0.3	1.3
Cladocera	-	-	-	-	-	-	-	-	-	-	-	-
Ostracods	1.9	6.2	33.5	18.6	2.7	3.6	0.8	4.7	2.5	2.5	2.1	1.4
Euphausid	0.5	0.0	1.0	-	0.2	0.1	0.1	0.1	-	0.3	0.5	0.2
J. euph/mysid	-	0.1	2.3	0.2	0.2	0.6	0.3	0.1	0.3	0.3	0.1	0.0
Mysid	-	-	-	-	0.0	0.1	-	-	-	-	-	-
Amphipoda	0.2	0.1	1.9	0.2	0.3	0.3	-	-	0.1	0.3	0.1	0.1
Decapod l.	-	0.2	0.4	-	0.2	0.0	-	1.1	0.2	0.2	-	-
Cerripedi	-	0.0	0.1	-	-	-	-	-	-	-	-	-
Chaetognatha	0.7	2.9	11.2	2.9	4.0	3.5	1.2	1.5	1.4	1.0	1.0	1.5
Polychaeta	0.0	0.0	0.5	0.3	0.5	0.1	0.0	0.2	0.7	-	0.5	0.4
Pteropod	0.0	-	0.2	0.2	0.2	-	0.0	-	-	-	0.0	-
Gastropoda	4.7	1.0	70.3	1.0	1.7	0.3	0.4	1.9	1.0	0.6	0.2	0.5
Bivalva	0.1	-	0.7	-	-	-	0.0	-	-	-	-	-
Squid	-	-	-	-	-	-	-	-	-	-	-	-
Salps	-	-	-	-	-	0.1	-	-	-	-	-	-
Doliolid	-	-	-	-	0.1	-	-	0.2	0.2	-	0.0	-
Larvacea	-	-	-	-	0.0	0.0	2.7	0.3	0.7	0.0	-	0.0
Siphonophore	-	0.1	0.1	0.4	1.4	0.5	0.0	0.9	1.0	0.7	-	0.2
Medusa	-	-	-	0.1	0.3	-	-	0.1	-	0.1	-	-
Ctenophores	-	-	-	-	-	-	-	-	-	-	-	-
Echinoderm l.	-	-	-	-	-	-	-	0.4	-	0.0	0.0	-
Anthozoan	-	-	-	-	-	-	-	-	-	-	-	-
Ophuroides	-	-	-	-	-	-	-	-	-	-	-	-
Bryozoan	-	-	-	-	-	-	-	-	-	-	-	-
Amphioxus	-	-	-	-	-	-	-	-	-	-	-	-
Fish larvae	-	-	-	-	0.0	-	-	0.0	0.1	-	0.0	-
Fish egg	-	-	-	0.5	0.1	0.0	-	-	0.0	0.1	-	-
Fish	-	-	-	-	-	-	-	-	-	-	-	-
Total	347	260	584	278	233	142	186	139	203	119	92	90

AMT 4 continued

Julian Day	128	129	129	130	131	132	132	133	134	135	135	136
Date	08/05	09/05	09/05	10/05	11/05	12/05	12/05	13/05	14/05	15/05	15/05	16/05
Latitude	-6	-2	1	2	6	10	12	14	18	22	25	26
Depth	200	200	200	200	200	200	200	200	200	200	200	200
Copepoda	288.4	312.7	164.4	271.0	272.4	432.2	143.4	336.7	451.6	342.2	193.5	228.4
Naupli	0.8	0.0	-	0.6	0.2	1.7	-	0.0	1.8	0.0	0.0	0.3
Cladocera	0.1	-	3.5	-	-	-	0.1	0.0	-	0.1	-	0.0
Ostracods	4.1	5.0	6.5	5.0	18.4	19.3	1.6	3.9	3.9	3.9	0.7	3.8
Euphausid	0.3	1.1	0.3	1.6	0.8	0.2	0.0	0.2	0.7	-	0.2	0.5
J. euph/mysid	0.3	0.3	2.3	2.4	0.6	-	0.1	0.0	0.5	0.1	0.0	0.8
Mysid	0.3	-	-	-	0.0	-	-	-	-	-	0.3	-
Amphipoda	0.3	1.2	0.3	0.2	0.5	0.5	0.1	0.7	0.5	0.2	0.5	0.4
Decapod l.	-	0.5	-	0.2	0.5	1.0	-	0.5	0.8	0.6	-	0.3
Cerripedi	0.1	-	3.3	-	-	0.0	-	0.0	-	-	0.0	0.0
Chaetognatha	1.2	3.2	1.9	1.7	1.4	2.8	0.5	5.0	4.7	3.0	0.1	7.8
Polychaeta	1.4	0.9	1.3	0.8	0.6	0.6	0.2	0.5	0.5	0.5	0.1	0.7
Pteropod	0.8	0.8	1.0	0.3	0.2	0.3	0.0	0.7	0.4	0.9	-	0.2
Gastropoda	1.1	0.5	1.0	0.6	1.1	3.9	0.4	2.2	1.5	0.5	-	0.4
Bivalva	-	-	-	-	-	-	0.0	0.0	0.1	0.0	-	0.2
Squid	-	-	-	0.0	-	-	-	-	-	0.0	-	-
Salps	-	6.8	-	1.7	0.2	0.4	-	0.0	1.3	-	-	1.4
Doliolid	0.0	0.1	0.2	0.4	0.6	0.2	-	1.9	0.1	0.9	-	0.2
Larvacea	0.4	0.8	2.4	0.1	0.2	3.0	0.3	4.5	6.8	1.2	0.2	0.1
Siphonophore	0.6	2.5	3.7	1.2	2.4	0.7	1.8	4.1	1.4	1.5	0.5	4.2
Medusa	0.1	0.1	0.0	-	0.1	-	-	0.0	0.0	-	0.0	0.1
Ctenophores	-	-	-	-	-	-	-	-	-	-	-	-
Echinoderm l.	-	-	-	-	-	-	-	-	-	-	-	-
Anthozoan	-	-	-	-	-	-	-	-	-	0.0	-	-
Ophuroides	-	-	-	-	-	-	-	-	-	-	-	-
Bryozoan	-	0.0	-	-	-	-	-	-	-	-	-	-
Amphioxus	0.3	-	-	-	-	-	-	-	-	-	0.0	-
Fish larvae	0.0	0.1	0.7	0.2	0.1	0.1	0.0	0.1	0.3	0.1	0.0	0.0
Fish egg	-	0.1	-	-	-	0.1	-	0.4	0.1	0.9	-	0.1
Fish	0.0	-	-	-	-	-	-	-	-	-	-	-
Total	301	337	193	288	301	467	149	362	477	357	196	250

AMT 4 continued

Julian Day	136	137	137	138	139	139	140	141	142	143
Date	16/05	17/05	17/05	18/05	19/05	19/05	20/05	21/05	22/05	23/05
Latitude	28	31	32	34	36	38	40	44	47	48
Depth	200	200	200	200	200	200	200	200	200	200
Copepoda	900	120	1561	211	114	1268	134	71	206	191
Naupli	0.0	0.1	5.0	0.3	2.5	35.2	0.0	-	0.0	-
Cladocera	-	-	-	0.3	0.3	-	2.6	0.2	-	0.2
Ostracods	2.4	2.4	4.5	7.0	3.0	1.3	5.1	12.1	7.1	2.4
Euphausid	0.3	0.0	1.8	0.9	-	0.6	0.4	0.4	0.5	-
J. euph/mysid	0.3	0.5	0.4	0.2	0.4	2.2	0.3	0.2	0.4	0.2
Mysid	-	-	-	-	-	-	-	-	-	-
Amphipoda	4.2	0.1	3.7	0.6	0.2	0.9	0.2	0.4	0.3	0.3
Decapod l.	0.0	0.4	-	0.0	0.1	0.2	0.1	0.2	0.1	-
Cerripedi	-	-	-	0.1	-	0.0	-	-	0.4	-
Chaetognatha	2.8	5.0	4.0	1.4	1.6	1.7	0.7	0.8	4.3	3.7
Polychaeta	-	0.3	0.1	0.1	0.6	0.5	0.5	0.3	0.8	0.3
Pteropod	0.1	0.2	0.1	0.3	0.1	0.2	0.0	0.4	0.2	0.1
Gastropoda	-	2.0	0.1	1.8	0.8	1.1	1.2	1.1	2.5	0.7
Bivalva	-	-	-	0.0	-	0.0	-	-	0.2	-
Squid	-	-	-	-	-	-	-	-	-	-
Salps	-	0.0	-	0.2	0.1	-	-	-	-	-
Doliolid	-	-	-	0.3	0.0	-	0.0	0.0	0.2	0.2
Larvacea	-	0.5	0.0	1.0	0.4	0.2	0.3	-	0.2	0.0
Siphonophore	0.4	3.0	0.3	2.2	1.3	1.4	2.1	1.2	3.7	3.0
Medusa	-	0.2	-	0.0	0.1	-	-	-	0.0	-
Ctenophores	-	-	-	-	-	-	-	-	-	-
Echinoderm l.	-	-	-	-	-	-	-	-	-	0.1
Anthozoan	-	-	-	-	-	-	-	-	-	-
Ophuroides	-	-	-	-	-	-	-	-	-	-
Bryozoan	-	-	-	-	-	-	-	-	0.0	-
Amphioxus	-	-	-	-	-	-	-	-	-	-
Fish larvae	0.0	-	-	0.3	0.0	0.0	0.2	0.0	0.1	-
Fish egg	0.1	-	-	0.1	-	1.1	-	-	0.0	0.2
Fish	-	-	-	-	-	-	-	-	-	-
Total	911	135	1581	228	126	1315	148	89	228	203

AMT 5

Date	17-9	18-9	19-9	20-9	21-9	22-9	25-9	26-9	27-9	28-9	29-9	30-9	1 10
latitude	48.0	48.0	47.2	42.8	38.2	35.4	32.3	29.0	25.0	19.7	15.5	10.9	7.0
Day	260	261	262	263	264	265	268	269	270	271	272	273	274
Copepods	66.8	524.8	313.2	198.5	224.0	181.7	199.0	161.9	184.1	327.0	319.2	322.3	279.4
nauplii	6.0	3.2	1.5	1.0	0.4	0.2	1.3	0.7	0.2	6.7	6.2	7.4	4.6
Ostrocod	0.5	1.5	1.5	0.8	12.5	10.8	15.6	8.3	7.1	1.2	13.1	14.5	15.4
Cladocera	4.8	0.5	0.1	0.4	0.9	0.9	1.1	0.7	0.7	-	-	0.2	-
Euphausiid	1.0	0.3	0.1	0.1	0.3	0.1	0.8	0.1	0.1	0.3	0.7	0.8	0.1
Juv.Euph	0.0	-	-	0.2	0.4	-	0.5	0.3	-	0.7	1.4	0.4	0.5
Decapod l.	0.7	0.1	-	-	0.2	0.4	0.4	0.1	-	-	0.3	0.2	0.1
Amphipods	0.1	0.2	0.4	0.1	-	0.1	0.2	-	0.0	0.0	-	0.7	0.8
Mollusc l.	1.5	0.5	-	-	0.2	-	-	-	-	-	0.2	-	-
Pteropods	5.1	-	1.0	1.0	0.3	1.5	3.3	0.6	0.9	1.1	1.4	1.1	1.3
Polychaetes	-	-	-	0.1	1.3	0.9	1.6	0.8	-	0.1	0.7	3.0	1.7
Chaetognath	2.2	0.9	1.9	0.4	1.3	2.5	2.8	1.2	1.1	4.2	6.5	5.5	2.7
Cnidarians	0.2	0.1	-	0.3	0.7	0.9	0.5	0.1	0.1	0.2	1.1	2.6	0.4
Medusae	-	-	-	-	-	0.2	0.1	-	-	-	0.1	0.6	-
Siphonophore	7.0	-	-	0.3	0.7	2.3	0.6	2.5	2.2	1.6	2.1	2.3	2.3
Salpa	0.4	0.1	-	-	0.4	19.0	0.2	0.1	0.0	0.4	0.4	2.1	1.9
Doliolid	158.9	1.1	0.4	0.1	0.4	0.2	0.3	0.2	-	0.2	0.2	0.9	-
Larvacea	10.8	0.1	2.5	1.5	6.2	1.8	7.1	1.1	3.6	1.6	10.5	3.8	4.3
Fish larvae	0.8	-	-	-	-	0.4	0.2	0.1	0.1	-	-	0.2	0.2
Fish eggs	0.7	-	-	-	-	-	-	-	0.2	0.9	0.4	1.1	0.3
Radiolaria	1.0	-	46.6	207.6	33.0	5.3	3.1	2.2	2.4	59.5	5.3	3.8	2.2
Foraminifera	6.5	0.9	3.1	0.8	3.2	3.7	1.3	0.7	38.9	10.3	7.4	5.6	4.4
Total	278	535	373	414	288	237	247	233	245	421	395	416	325

AMT 5 continued

Date	2/10	3/10	4/10	5 /10	6/10	8/10	9/10	10/10	11/10	12/10	13/10	14/10	15/10	16/10
latitude	2.8	0.8	-4.8	-9.0	-12.9	-20.7	-23.9	-27.7	-31.6	-35.5	-38.8	-42.2	-46.0	-49.8
Day	275	276	277	278	279	281	282	283	284	285	286	287	288	289
Copepods	227.7	299.0	200.0	120.7	101.9	147.9	160.8	218.8	321.7	177.4	748.0	661.6	382.9	107.6
nauplii	5.3	2.6	2.9	2.2	1.5	1.1	2.2	3.5	0.4	4.0	1.4	85.2	-	-
Ostrocod	9.7	10.2	6.0	5.8	2.6	4.8	13.4	7.5	3.0	1.5	1.6	33.4	9.7	3.4
Cladocera	-	0.2	-	-	0.1	-	0.4	-	-	-	-	-	-	-
Euphausiid	0.4	0.8	2.6	0.1	0.1	0.5	0.4	0.2	2.0	1.0	0.8	0.2	0.1	0.4
Juv.Euph	1.0	2.7	7.1	0.2	0.1	0.4	0.5	0.7	2.9	2.5	3.4	16.4	0.2	0.1
Decapod l.	0.1	0.2	-	-	0.1	0.1	-	0.1	-	-	0.0	0.2	0.0	-
Amphipods	0.3	0.1	0.4	0.3	0.1	0.1	0.1	0.1	0.1	0.0	-	-	1.1	-
Mollusc l.	-	-	-	-	-	0.9	-	-	-	-	-	-	-	-
Pteropods	0.9	1.6	3.3	2.6	0.9	1.1	1.6	1.8	1.3	1.6	-	-	-	1.1
Polychaetes	0.7	3.1	1.1	-	0.1	0.4	0.9	0.9	1.0	0.8	1.1	1.8	0.0	0.9
Chaetognath	3.6	4.1	3.9	2.2	1.2	1.4	3.2	3.8	5.8	2.5	4.0	7.6	3.3	1.6
Cnidarians	0.8	1.3	0.0	0.0	0.3	-	-	0.5	0.1	0.4	-	-	-	-
Medusae	-	0.0	0.0	0.1	-	0.1	0.2	-	0.0	-	-	-	-	0.1
Siphonophore	3.7	4.7	2.7	0.6	1.5	0.5	2.0	2.1	4.1	1.6	0.2	2.2	1.0	0.5
Salpa	3.7	-	2.4	0.4	0.3	0.1	0.3	0.2	1.1	0.1	0.2	-	-	-
Doliolid	0.4	0.2	-	0.1	0.1	-	0.2	0.2	0.3	-	-	-	-	-
Larvacea	12.9	7.9	1.7	2.1	1.9	1.3	12.1	8.7	14.6	4.0	4.5	-	-	-
Fish larvae	0.5	-	-	0.2	-	-	-	-	-	0.2	0.2	-	-	-
Fish eggs	1.1	0.9	0.4	-	-	-	0.2	0.2	5.5	5.9	1.1	1.1	-	0.1
Radiolaria	6.6	2.4	2.4	0.7	1.1	4.0	2.9	7.9	2.2	5.2	0.4	-	-	-
Foraminifera	5.4	2.9	23.2	6.3	0.9	3.1	1.8	2.9	0.4	1.0	1.1	7.7	11.9	2.8
Total	289	345	260	147	153	199	232	281	366	210	770	810	398	116

AMT6

Date	15/05	16/05	17/05	18/05	22/05	23/05	25/05	26/05	27/05	28/05	29/05	30/05	31/05	01/06
J Day	135	136	137	138	142	143	145	146	147	148	149	150	151	152
Latitude	-33.6	-32.3	-29.5	-26.7	-24.8	-21.7	-17.7	-14.7	-11.6	-8.6	-5.9	-2.8	0.0	3.1
Time	11:15	8:00	8:00	8:30	8:00	8:00	0:00	8:30	8:30	8:30	8:30	8:30	8:15	9:00
Depth	100	100	100	200	100	200	200	200	200	200	200	200	200	200
Copepoda	1077	1500	2948	456	685	400	261	181	128	159	178	147	112	129
Naupli	2.0	8.0	10.0	3.5	63.5	2.5	16.6	2.7	1.1	0.7	2.9	3.3	3.1	1.1
Cladocera	-	2.6	-	-	-	-	-	-	-	-	-	-	-	-
Ostracoda	-	0.5	-	0.1	2.6	2.7	-	3.9	6.0	6.5	7.6	5.5	1.8	5.4
Euphausiid	2.9	5.1	0.3	0.0	57.6	-	0.2	2.4	0.1	0.7	1.3	0.6	0.5	0.2
Mysids	-	-	-	-	-	-	-	-	0.0	0.0	0.1	0.0	0.0	-
J. euph/mys	-	0.2	2.1	-	1.8	2.3	2.8	2.0	0.7	1.1	1.5	0.4	0.4	1.1
Amphipoda	0.1	2.6	0.7	-	1.4	-	-	0.3	0.1	0.7	1.4	0.8	0.1	0.5
Decapod l.	-	-	-	-	-	-	0.1	0.4	-	-	0.4	-	-	0.1
Cerripedi	-	-	-	-	-	-	-	-	-	-	-	-	-	-
Chaetognath	3.3	3.0	20.8	0.9	8.3	12.6	2.1	7.2	2.0	5.2	3.8	5.1	1.3	4.8
Polychaete	-	-	-	-	0.4	0.6	0.1	0.3	0.3	0.5	0.2	0.5	0.1	0.4
Pteropoda	-	0.3	-	-	-	0.5	0.1	3.8	0.1	3.0	1.5	0.2	0.4	0.9
Gastropoda	-	-	-	-	-	1.0	0.2	3.8	0.1	0.4	0.4	0.4	0.6	0.4
Bivalva	3.0	0.1	-	0.5	0.9	-	-	-	-	-	-	-	-	-
Salpa	-	-	-	-	-	-	0.1	5.3	0.1	0.2	0.3	0.4	-	0.4
Doliolid	0.7	3.1	-	-	-	-	0.1	0.1	0.1	0.6	0.5	3.3	0.6	1.5
Larvacea	1.0	0.1	-	-	0.9	-	1.1	1.0	1.0	3.4	2.8	2.0	1.9	11.0
Siphonophore	2.2	0.3	-	-	6.3	1.1	0.2	2.3	1.3	2.2	1.6	0.8	0.5	2.0
Medusa	-	-	-	-	0.1	-	-	-	0.0	-	-	-	-	-
Ctenophora	-	-	-	-	-	-	-	-	-	-	-	-	0.0	-
Echinoderm l.	-	-	-	-	-	-	-	-	0.1	-	-	-	-	-
Ophuroidea	1.0	-	-	-	-	-	-	-	-	-	-	-	-	-
Bryozoa	-	2.5	-	-	-	-	-	-	-	-	-	-	-	-
Anthozoa	-	-	-	-	-	-	-	-	-	-	0.0	-	-	-
Amphioxus	-	-	-	-	-	-	-	-	-	-	-	0.2	-	-
Fish	-	-	-	-	-	-	-	-	-	-	-	-	-	-
Fish larvae	0.7	2.1	-	0.2	-	-	0.0	0.1	0.0	0.1	0.1	-	0.0	0.0
Fish egg	0.8	2.5	-	1.9	-	0.8	-	0.1	0.1	0.1	0.4	0.2	0.4	0.1
Squid	-	-	-	-	-	-	-	-	-	-	-	-	-	-
Foramnifera	3.0	-	-	0.1	-	0.5	-	9.4	3.5	7.8	5.7	4.2	0.6	12.4
Radiolaria	-	2.0	1.3	0.1	-	1.2	-	0.9	1.3	2.1	2.3	3.3	0.4	1.1
Total	1098	1535	2983	463	829	425	284	227	147	194	212	179	125	173

AMT 6 continued

Date	02/06	03/06	04/06	05/06	06/06	07/06	08/06	09/06	10/06	11/06	12/06	13/06	14/06
J Day	153	154	155	156	157	158	159	160	161	162	163	164	165
Latitude	5.9	9.1	12.8	16.4	20.4	24.5	28.6	32.4	36.6	41.1	44.7	48.5	49.8
Time	9:00	9:00	9:00	9:00	9:00	9:00	9:00	9:00	9:00	9:00	8:30	9:45	9:00
Depth	200	200	200	200	200	200	200	200	200	200	200	200	20
Copepoda	90	193	188	278	186	183	80	95	79	519	113	167	1610
Naupli	1.1	0.4	2.7	21.0	1.0	1.1	0.3	-	0.3	-	0.8	39.2	11.2
Cladocera	-	-	-	-	-	0.0	2.5	0.0	0.3	0.0	0.0	0.3	5.8
Ostracoda	7.6	4.6	5.7	1.3	1.9	5.3	4.5	4.6	3.6	2.2	1.1	3.9	-
Euphausiid	0.1	0.5	0.1	0.5	4.4	0.2	0.2	0.1	0.1	-	0.0	3.5	3.6
Mysids	-	0.1	0.1	-	-	0.1	0.1	-	0.0	-	-	-	-
J. euph/mys	0.4	0.5	0.4	2.4	0.9	0.3	0.1	0.2	0.1	-	0.4	6.1	-
Amphipoda	0.3	0.1	-	1.3	0.3	0.2	0.3	0.1	0.4	0.2	0.5	-	-
Decapod l.	0.0	-	-	-	0.0	2.8	-	-	-	-	-	2.7	1.2
Cerripedi	-	-	-	-	-	-	-	0.5	1.6	1.0	-	-	-
Chaetognath	4.1	2.4	2.3	6.8	6.4	4.1	0.5	1.3	1.1	0.2	0.4	3.6	1.2
Polychaete	0.3	0.3	0.2	0.8	0.4	0.4	0.1	0.1	-	0.0	-	-	-
Pteropoda	0.1	1.1	0.7	2.5	0.7	0.4	0.4	0.3	0.8	-	-	1.5	-
Gastropoda	1.0	0.5	-	32.8	6.2	7.2	0.6	0.0	0.5	2.1	-	2.4	-
Bivalva	-	0.1	1.1	0.3	-	-	-	-	-	-	-	-	-
Salpa	-	-	-	185.7	0.3	1.1	0.1	0.4	-	-	-	-	-
Doliolid	1.0	-	0.5	-	-	0.1	-	0.1	0.5	-	0.0	3.9	-
Larvacea	2.0	1.0	3.6	2.3	0.7	4.2	0.3	0.6	0.8	4.1	0.0	50.6	-
Siphonophore	1.5	1.0	0.3	2.1	2.5	2.7	1.1	1.4	2.2	0.4	0.0	18.5	52.0
Medusa	-	-	0.0	-	-	-	-	-	-	-	-	0.2	-
Ctenophora	-	-	-	-	-	-	-	-	-	-	-	-	-
Echinoderm l.	-	-	-	-	-	-	-	-	-	-	-	-	-
Ophuroidea	-	-	-	-	-	-	-	-	-	-	-	-	-
Bryozoa	-	-	-	-	-	-	-	-	-	-	-	-	-
Anthozoa	-	-	-	-	-	-	-	-	-	-	-	-	-
Amphioxus	-	-	-	-	-	-	-	-	-	-	-	-	-
Fish	-	-	-	-	-	-	-	-	-	-	-	-	-
Fish larvae	-	0.0	0.0	-	0.1	-	0.1	0.1	0.1	0.0	-	0.5	-
Fish egg	0.3	0.3	0.7	1.3	0.1	0.3	0.0	0.1	-	-	-	-	8.5
Squid	-	-	0.0	-	-	-	-	-	-	-	-	-	-
oramnifera	-	0.8	1.7	5.3	15.1	3.1	0.2	0.3	0.3	1.0	3.5	7.5	-
Radiolaria	0.9	1.2	2.7	22.1	6.7	0.6	0.4	0.6	1.0	1.2	0.1	0.2	-
Total	111	208	211	566	233	217	91	106	92	532	120	313	1702

Appendix 7: AMT 4-6 Copepod genera from deep nets (m^{-3})

AMT 4

SYD	111	112	113	114	120	121	122	123	124	125	126	127	128	129
Latitude	-51.0	-47.6	-43.5	-39.4	-35.7	-32.6	-29.3	-26.1	-22.2	-18.3	-14.1	-10.0	-5.9	-2.0
Acartia	-	-	0.5	-	-	3.4	1.2	0.5	0.6	0.8	0.5	0.4	-	2.5
Aegisthus	-	-	-	-	-	-	-	-	-	-	-	-	-	-
Aetideopsis	-	-	-	-	-	-	-	-	-	-	-	-	-	-
Aetideus	-	-	0.9	0.4	-	-	-	-	-	0.1	-	-	-	0.0
Arietellus	-	-	-	-	-	-	-	-	-	-	-	0.0	-	-
Auguptilus	-	-	-	-	-	-	-	-	-	-	-	-	-	-
Calanoides	-	-	0.2	0.1	0.0	0.1	0.0	0.1	0.0	0.2	0.0	-	0.3	0.1
Calanus	68.5	4.6	14.8	4.0	11.9	2.5	4.9	3.0	1.5	4.6	4.4	4.0	8.9	23.0
Calocalanus	-	-	-	-	0.8	0.2	-	0.8	0.6	-	0.5	-	-	-
Candacia	-	-	-	-	0.2	0.1	0.8	1.1	0.7	0.5	0.4	0.7	0.5	0.9
Centropages	-	-	2.2	1.9	0.2	-	0.3	0.6	0.0	-	-	0.0	0.1	0.5
Clytemnestra	-	2.5	0.8	0.6	-	-	-	-	-	-	-	-	0.2	-
Copepodites	2.9	5.2	14.2	6.7	7.2	5.0	7.5	6.7	5.8	4.9	3.5	3.3	5.3	1.6
Copilia	-	-	-	-	-	0.0	-	0.7	0.5	0.1	0.1	0.1	-	0.0
Corycaeus	-	-	0.9	-	10.8	8.0	16.1	17.1	34.4	6.0	6.3	11.6	33.0	22.5
Euaetideus	-	0.0	-	-	-	-	0.1	0.0	0.3	0.1	0.2	0.1	-	0.8
Euagaptilus	-	-	0.2	-	-	-	-	0.0	-	-	-	-	-	0.1
Eucalanus	-	-	2.6	0.3	2.1	0.2	0.4	0.2	0.0	0.4	-	0.3	0.2	0.6
Euchaeta	-	-	1.0	0.5	3.3	0.7	2.9	5.9	0.2	0.8	1.3	3.3	10.9	11.7
Euchirella	-	-	0.0	-	-	-	-	-	-	-	-	-	0.1	-
Gaetanus	-	-	-	-	-	-	-	-	-	0.1	-	-	0.0	-
Haloptilus	-	-	-	-	0.1	0.3	0.2	0.3	0.6	0.6	0.6	0.7	0.2	0.2
Heteorstylites	-	-	0.6	0.1	0.3	0.3	0.3	0.6	0.2	0.5	0.0	0.2	0.8	0.6
Heterorhabdus	-	-	-	-	0.2	0.9	0.2	0.3	0.2	0.0	0.1	0.1	0.2	0.1
Labidocera	-	-	-	-	-	-	-	-	-	-	-	-	-	-
Lubbockia	-	-	-	-	-	-	-	-	-	0.6	-	-	-	-
Lucicutia	-	-	-	-	2.4	3.9	0.2	0.4	1.8	1.3	0.9	0.4	1.7	2.8
Macrosetella	-	-	-	-	0.2	-	-	0.2	0.1	0.1	0.1	-	-	2.7
Metridia	0.1	0.1	4.1	4.8	0.6	0.2	-	-	-	-	-	-	-	-
Miracia	-	-	-	-	-	-	-	-	-	-	-	-	-	-
Oithona	416.2	82.7	136.7	70.3	32.4	14.2	20.8	17.9	19.2	33.1	28.4	25.3	50.1	44.3
Oncaea	-	0.1	11.3	3.3	29.9	23.3	10.9	14.6	17.3	10.9	6.5	5.0	15.6	29.6
Pachos	-	-	-	-	-	-	-	-	-	0.1	-	-	0.0	-
Para/pseuds	184.6	90.9	181.3	202.6	72.0	33.0	83.1	39.1	38.0	29.9	24.4	32.3	165.3	165.6
Phaenna	-	-	-	-	-	0.1	-	0.1	-	-	-	0.1	0.0	-
Phyllopus	-	-	-	-	-	-	-	-	-	-	-	-	-	-
Pleuromamma	-	-	1.7	-	2.3	2.0	0.4	0.2	-	0.1	-	0.1	-	-
Pontellina	-	-	-	-	-	-	-	0.2	-	-	-	-	-	-
Pseudoeuchaeta	-	-	0.0	-	-	-	-	-	-	-	-	-	-	-
Rhincalanus	0.2	-	0.1	-	-	-	-	-	0.1	-	-	-	0.2	0.1
Sapphirina	-	-	-	-	0.1	-	-	0.0	0.1	0.1	0.1	0.0	0.1	0.7
Scaphocalanus	-	-	-	-	-	-	-	-	-	-	-	-	-	-
Scolecithrix	-	-	0.1	-	0.7	0.1	0.8	0.3	0.2	0.7	0.5	1.2	0.8	2.2
Scolethella	-	-	-	-	0.2	-	0.8	0.2	0.8	0.9	1.0	0.6	0.2	1.3
Scottocalanus	-	-	-	-	-	-	-	-	-	-	-	-	-	-
Temora	-	-	2.8	-	3.1	0.5	0.3	0.6	0.2	-	-	-	-	-
Undeuchaeta	-	-	-	-	-	-	-	-	-	0.0	-	-	0.1	0.0
Undinula	-	-	-	-	0.3	-	-	0.3	0.0	0.8	0.3	0.3	3.5	1.7
Total	672	186	377	296	181	99	152	112	123	98	80	90	298	316

AMT 4 continued

SYD	129	130	131	132	132	133	134	135	135	136	136	137	137
Latitude	-0.1	1.9	6.1	10.1	11.7	13.7	17.8	22.2	24.2	26.3	28.0	30.0	31.8
Time	22:00	10:00	10:00	10:00	22:00	10:00	10:00	10:00	22:00	10:00	22:00	10:00	22:00
Acartia	-	0.6	2.5	2.5	14.3	11.6	22.4	8.3	6.4	5.0	3.6	2.2	21.5
Aegisthus	-	-	-	-	-	-	-	-	-	-	-	-	-
Aetideopsis	-	-	-	-	-	-	-	-	-	-	-	-	-
Aetideus	-	-	0.4	-	0.2	0.0	-	-	-	-	-	-	-
Arietellus	-	-	-	-	-	-	-	-	-	-	-	-	-
Auguptilus	-	-	-	-	-	-	-	-	-	-	-	-	0.0
Calanoides	0.1	-	0.8	2.3	0.3	0.4	0.7	0.0	0.1	0.2	0.3	0.1	0.3
Calanus	10.6	17.1	20.4	30.8	23.7	9.7	17.6	2.4	5.9	2.8	4.6	3.1	10.4
Calocalanus	-	0.0	0.0	-	-	0.0	-	-	-	-	-	0.0	0.0
Candacia	0.1	0.4	0.5	0.2	0.2	0.2	0.7	0.0	0.8	0.2	0.1	0.4	-
Centropages	0.1	1.5	-	0.1	-	1.4	0.2	0.0	-	-	-	-	-
Clytemnestra	-	-	-	-	-	-	-	-	-	-	0.2	-	-
Copepodites	11.7	6.9	13.1	7.5	17.9	5.5	9.3	4.8	8.2	4.1	6.6	4.5	11.8
Copilia	0.0	0.6	0.1	0.2	0.0	0.1	0.0	-	0.0	-	-	-	-
Corycaeus	23.1	20.8	8.0	21.1	20.4	11.1	6.4	0.9	15.2	4.8	8.2	7.4	13.3
Euaetideus	0.1	0.9	0.3	2.5	1.1	0.8	0.8	0.1	0.4	0.3	1.0	0.7	0.5
Euagaptilus	0.2	-	-	1.2	1.4	1.5	0.4	-	0.0	-	-	-	0.1
Eucalanus	1.3	0.5	1.8	4.3	21.2	15.0	6.5	0.1	1.3	0.5	0.8	1.0	7.4
Euchaeta	6.7	18.5	18.8	22.6	19.6	11.8	8.0	1.8	4.9	2.6	4.5	3.4	4.2
Euchirella	0.0	0.5	0.1	0.9	-	0.1	0.1	-	0.1	-	-	0.1	-
Gaetanus	0.3	0.1	-	-	-	0.0	0.2	-	0.2	0.0	0.1	0.1	0.2
Haloptilus	0.2	0.7	0.6	0.3	0.4	0.6	0.9	0.7	1.1	1.9	0.9	1.7	2.5
Heteorstylites	2.1	0.8	3.6	3.0	2.8	2.5	2.3	0.1	1.0	0.5	0.7	0.5	0.8
Heterorhabdus	0.6	0.3	0.8	0.4	0.4	0.6	-	0.4	0.9	0.3	0.0	0.1	0.5
Labidocera	1.1	-	-	-	-	-	-	-	-	-	-	-	-
Lubbockia	-	-	-	-	-	0.4	1.0	-	-	0.6	-	0.2	0.4
Lucicutia	2.8	5.0	3.5	3.0	3.8	4.8	1.9	0.9	3.9	3.1	2.5	3.5	7.8
Macrosetella	0.8	0.2	1.3	2.2	2.1	1.3	1.6	0.1	0.2	1.1	-	-	-
Metridia	-	-	-	0.2	-	-	-	-	-	-	-	-	-
Miracia	-	0.1	1.0	0.6	-	-	-	-	-	-	-	0.3	-
Oithona	41.6	33.3	69.7	49.3	46.1	48.3	49.5	9.0	48.1	32.7	28.3	19.8	43.1
Oncaea	62.0	57.6	134.9	89.3	229.3	77.7	46.9	12.2	19.7	13.1	9.9	13.2	42.8
Pachos	-	0.1	-	0.1	-	-	-	-	0.0	-	-	-	-
Para/pseuds	102.3	122.3	120.4	133.6	180.5	143.2	88.6	78.7	59.9	48.8	80.9	51.5	66.0
Phaenna	0.3	-	-	-	0.2	-	0.1	-	0.1	-	0.1	0.0	0.1
Phyllopus	-	-	-	-	-	-	-	-	-	-	-	-	-
Pleuromamma	6.3	2.1	0.1	0.7	0.9	0.5	0.8	0.4	1.5	0.1	1.1	0.1	3.1
Pontellina	-	0.3	0.7	-	-	-	-	-	-	0.1	-	-	-
Pseudoeuchaeta	0.1	0.0	-	-	-	-	-	-	-	-	-	-	0.0
Rhincalanus	1.0	0.4	0.2	0.0	0.0	0.2	0.0	0.3	0.0	0.0	-	0.0	0.1
Sapphirina	0.8	0.7	1.0	0.0	1.9	0.8	0.4	-	0.1	0.1	0.1	0.6	1.3
Scaphocalanus	-	-	-	-	-	-	-	-	-	-	-	-	-
Scolecithrix	1.8	3.0	3.2	1.8	0.2	0.2	2.9	0.1	0.8	0.2	0.0	0.1	-
Scolethella	0.0	0.3	-	0.1	0.2	0.1	1.6	0.1	1.1	0.0	0.2	-	-
Scottocalanus	0.0	-	-	-	0.2	-	-	-	0.0	-	-	-	0.0
Temora	0.2	-	-	-	14.1	6.0	1.6	-	0.3	-	0.2	-	0.1
Undeuchaeta	0.0	0.1	0.8	0.0	-	-	-	-	0.5	-	-	-	0.3
Undinula	0.7	4.5	6.8	2.4	0.4	0.5	0.4	-	0.2	-	-	-	-
Total	279	300	415	383	604	357	274	122	183	123	155	115	239

AMT 4 continued

SYD	138	138	138	138	139	139	139	140	140	141	141	142	143	144
Latitude	33.7	34.2	34.6	35.1	35.6	36.2	37.8	39.9	41.7	44.0	45.5	47.0	48.1	49.0
Time	10:00	16:00	19:45	23:30	04:30	10:00	22:00	10:00	22:00	10:00	22:00	10:00	10:00	10:00
Acartia	13.8	21.1	17.6	17.7	17.4	10.3	3.7	6.8	0.2	5.2	23.2	18.9	9.4	-
Aegisthus	-	-	-	-	-	-	-	-	-	-	-	-	-	-
Aetideopsis	-	-	-	-	-	-	-	-	-	-	-	-	-	-
Aetideus	-	-	-	-	-	-	-	-	0.4	-	-	0.2	1.0	-
Arietellus	-	0.0	-	-	-	-	-	-	-	-	-	-	-	-
Auguptilus	-	-	0.0	-	0.0	-	-	-	-	-	-	-	-	-
Calanoides	-	0.1	-	-	-	-	-	-	-	-	-	0.1	-	1.3
Calanus	7.1	6.7	5.7	6.9	11.7	3.1	4.4	1.1	1.6	7.4	104.2	61.7	74.6	61.6
Calocalanus	-	-	-	-	-	-	-	-	-	-	-	-	-	-
Candacia	0.0	-	0.2	-	0.7	0.0	1.4	0.0	-	0.0	0.1	-	-	-
Centropages	-	-	-	-	-	-	0.5	-	0.1	2.0	0.2	-	-	0.5
Clytemnestra	-	-	0.2	-	0.6	0.2	-	-	0.2	-	-	-	-	0.5
Copepodites	10.5	11.4	13.4	12.1	11.3	4.4	8.7	5.3	16.0	36.2	112.8	42.7	58.4	3.9
Copilia	-	-	-	-	0.7	-	0.1	-	-	-	-	-	-	-
Corycaeus	7.7	8.3	5.0	7.0	10.1	6.3	5.5	1.5	0.1	-	-	0.1	-	2.1
Euaetideus	0.4	0.4	0.0	-	0.5	0.1	0.3	0.2	0.1	1.9	-	2.0	-	-
Euagaptilus	-	0.1	-	-	-	-	-	-	-	-	-	9.4	-	-
Eucalanus	5.2	7.4	0.4	2.1	1.3	4.5	-	0.5	-	3.2	1.8	9.6	1.2	7.4
Euchaeta	3.9	8.3	1.3	7.5	8.2	1.1	2.2	2.3	0.9	1.8	1.7	4.1	1.2	2.4
Euchirella	-	-	0.0	-	0.5	0.0	0.3	-	-	0.1	0.1	0.7	0.4	-
Gaetanus	-	-	-	0.4	0.9	-	0.3	-	0.1	-	-	-	-	-
Haloptilus	0.7	1.4	0.3	0.4	1.0	1.1	0.3	0.5	0.1	0.1	-	0.0	-	-
Heteorstylites	0.1	0.6	-	-	-	-	-	-	-	-	-	0.1	-	-
Heterorhabdus	0.7	0.5	0.2	0.0	0.1	0.1	0.3	0.2	0.3	1.3	1.9	2.5	1.2	-
Labidocera	-	-	-	-	-	-	-	-	-	-	-	-	-	-
Lubbockia	0.5	0.4	-	0.6	-	-	-	-	-	-	-	-	-	-
Lucicutia	4.7	7.7	1.1	3.0	6.0	0.8	1.4	0.5	0.1	-	-	-	-	-
Macrosetella	-	-	-	0.2	0.6	-	-	-	-	-	-	-	-	0.5
Metridia	0.2	-	0.2	-	-	-	-	0.1	0.1	-	-	0.1	16.5	38.7
Miracia	-	-	-	-	-	-	-	-	-	-	-	-	-	-
Oithona	33.6	42.6	35.0	36.3	27.4	23.8	20.0	25.6	80.9	196.3	213.7	492.5	942.9	49.2
Oncaea	25.9	32.4	21.0	25.2	62.4	13.6	17.6	7.6	0.1	9.9	34.4	8.2	47.1	2.7
Pachos	-	-	-	-	-	-	-	-	-	-	-	-	-	-
Para/pseuds	58.7	57.1	54.7	85.4	100.7	57.1	80.7	81.6	116.0	704.3	1323	1114	331.3	138.6
Phaenna	-	-	-	-	-	-	-	-	-	-	-	-	-	-
Phyllopus	-	-	-	-	-	-	-	-	0.0	-	-	-	-	-
Pleuromamma	1.4	3.7	4.4	3.6	10.6	0.3	1.4	0.5	2.4	1.5	13.3	2.3	-	-
Pontellina	-	-	-	-	-	-	-	-	-	-	-	-	-	-
Pseudoeuchaeta	-	0.2	-	-	-	-	-	-	-	-	-	-	-	-
Rhincalanus	0.1	0.5	-	0.1	-	0.0	-	-	-	-	0.1	0.1	11.3	0.1
Sapphirina	-	-	-	0.2	-	0.1	-	-	-	-	-	-	-	-
Scaphocalanus	-	-	-	-	-	-	-	-	-	-	-	-	-	-
Scolecithrix	-	-	0.0	-	-	-	-	-	0.1	-	-	-	-	-
Scolethella	0.0	-	-	-	1.6	0.0	0.5	-	-	-	0.1	-	-	0.5
Scottocalanus	-	-	-	-	-	-	-	-	-	-	-	-	-	-
Temora	0.2	-	-	-	-	0.2	-	0.1	-	-	-	-	-	-
Undeuchaeta	-	-	-	0.0	0.7	-	0.1	-	1.1	-	0.5	0.1	0.0	-
Undinula	-	-	-	0.0	0.3	-	-	-	-	-	-	-	-	-
Total	175	211	161	209	275	127	150	135	221	971	1831	1770	1497	310

AMT 5

J Day	260	261	262	263	264	264	265	265	268	269	270	270	271
Latitude	48.7	48.0	47.2	42.8	38.2	37.1	35.4	35.4	32.3	29.0	24.1	22.0	19.7
Time	16:00	10:00	10:00	10:00	10:00	22:00	10:00	07:00	13:30	11:00	11:00	23:00	11:00
Acartia	-	0.4	4.1	0.8	7.8	11.6	9.6	7.6	1.3	4.4	17.7	24.5	49.2
Aegisthus	-	-	-	-	-	-	-	-	-	-	-	0.4	-
Aetideopsis	-	-	-	-	-	-	-	-	-	-	-	0.4	-
Aetideus	-	0.1	0.2	0.7	0.9	0.1	-	0.2	-	0.2	-	-	-
Amallothrix	-	-	-	-	-	-	-	-	-	-	-	-	-
Arietellus	-	-	-	-	-	-	-	-	-	-	-	-	-
Augaptilus	-	-	-	-	-	-	0.1	-	-	-	-	-	-
Calanoides	3.8	0.3	-	-	-	-	-	-	0.0	-	-	0.1	0.0
Calanus	8.9	3.0	3.6	3.3	6.5	9.7	13.4	3.7	7.7	7.2	4.7	2.0	10.1
Calocalanus	-	15.8	0.1	0.4	1.0	8.4	5.4	7.4	1.4	2.3	1.4	0.2	2.0
Candacia	11.9	-	0.1	-	0.2	0.3	0.7	0.3	0.3	-	0.1	0.5	0.0
Centropages	16.9	0.5	20.7	8.4	-	-	-	-	-	-	-	-	1.4
Clytemnestra	4.5	-	-	-	-	-	-	-	0.5	-	-	-	-
Copepodites	10.0	20.0	12.3	4.4	8.6	17.6	8.9	3.0	8.7	2.4	3.2	2.3	4.0
Copilia	-	-	-	-	0.3	-	0.1	-	0.1	0.1	0.1	-	-
Corycaeus	103	0.1	1.2	3.5	14.7	14.9	15.5	13.4	15.9	11.3	7.8	0.4	10.6
Euaetideus	-	0.0	0.1	-	-	0.1	-	0.1	0.5	0.1	0.2	-	0.2
Euagaptilus	-	-	-	-	-	-	-	-	-	-	0.2	-	-
Eucalanus	1.1	-	-	-	-	-	0.7	-	-	-	0.3	0.0	0.1
Euchaeta	2.7	1.2	2.5	0.5	1.1	1.6	0.4	0.2	1.6	7.4	3.4	0.9	0.0
Euchirella	-	-	-	-	-	-	-	-	-	-	-	0.2	-
Gaetanus	-	-	-	-	-	0.2	-	-	-	-	-	-	-
Haloptilus	-	-	-	0.3	3.5	4.6	1.9	1.8	2.9	3.5	2.6	-	0.1
Heterorhabdus	0.0	0.5	-	-	-	0.4	0.5	0.9	0.2	0.1	0.2	0.3	0.2
Labidocera	-	-	-	-	-	-	-	-	-	-	-	-	-
Lubbockia	-	-	-	-	-	-	-	-	-	-	-	-	-
Lucicutia	-	-	-	-	1.5	1.2	2.5	1.2	3.7	2.8	1.9	0.4	-
Macrosetella	3.8	-	0.1	-	0.1	-	-	0.2	-	1.0	-	-	-
Metridia	5.3	-	-	0.4	0.1	0.1	4.6	-	0.1	0.1	-	0.5	0.0
Neocalanus	-	-	-	-	-	-	0.5	-	-	-	-	-	-
Oithona	73.0	106	16.8	18.4	10.9	35.8	18.7	25.2	18.4	28.0	29.1	19.2	16.6
Oncaea	116	1.1	2.6	9.2	26.9	28.6	16.7	15.8	34.2	10.8	12.5	9.5	19.1
Pachos	-	-	-	-	-	-	-	-	-	-	-	-	-
Para/pseuds	399	93.1	195	150	93.2	105	60.1	71.6	71.8	69.0	65.5	72.3	170
Phaenna	-	-	-	-	0.1	0.5	0.1	0.1	0.0	0.1	-	-	2.0
Phyllopus	-	-	-	-	-	0.2	-	-	-	-	-	-	-
Pleuromamma	0.0	0.5	2.4	0.3	1.4	2.9	0.3	0.3	0.0	0.1	0.3	13.3	-
Pontellina	-	-	-	-	-	0.1	0.3	-	0.0	-	0.1	-	-
Pseudoeuchaeta	-	-	-	-	-	-	-	-	-	-	-	-	-
Rhincalanus	-	-	-	-	-	-	-	-	-	-	-	-	-
Sapphirina	-	-	-	-	0.2	1.3	1.2	0.3	0.5	-	-	-	-
Scaphocalanus	-	-	-	-	-	0.2	-	-	-	-	-	-	-
Scolecithrix	-	-	-	-	0.7	0.1	0.5	0.1	0.9	0.6	0.5	0.3	0.4
Scolethella	0.9	0.1	-	-	-	1.3	0.2	1.8	1.4	-	-	0.2	0.1
Scottocalanus	-	-	-	-	-	-	-	-	-	-	-	0.0	-
Temora	-	0.1	-	-	0.7	-	-	0.6	-	-	-	-	-
Undeuchaeta	0.0	-	-	-	-	-	-	0.1	-	-	-	-	-
Undinula	-	-	-	0.1	-	-	0.7	-	-	-	-	-	-
Total	762	244	262	201	180	246	164	156	172	151	152	148	287

AMT 5 continued

J Day	271	271	272	273	274	275	275	276	277	278	279	280	281
Latitude	19.7	18.2	15.5	10.9	7.4	2.8	1.2	-0.8	-4.8	-9.0	-12.9	-16.7	-20.7
Time	11:00	23:00	11:00	11:00	11:00	11:00	23:00	10:30	11:30	11:30	11:30	11:30	11:30
Acartia	49.2	11.8	6.3	8.0	5.6	0.9	0.9	0.1	-	0.9	0.5	0.8	1.6
Aegisthus	-	0.2	0.1	-	-	-	-	-	-	-	-	-	-
Aetideopsis	-	-	-	-	-	-	-	-	-	-	-	-	-
Aetideus	-	0.2	0.1	-	0.3	-	-	-	-	-	0.1	0.1	0.1
Amallothrix	-	-	-	-	-	-	-	-	-	-	-	-	-
Arietellus	-	-	0.0	-	-	-	0.0	-	-	-	-	-	-
Augaptilus	-	-	-	-	-	-	-	-	-	-	-	-	-
Calanoides	0.0	-	0.5	-	0.1	0.1	-	-	0.1	-	-	-	-
Calanus	10.1	12.8	10.7	15.2	5.0	11.6	11.5	14.5	11.0	6.5	4.6	3.0	5.4
Calocalanus	2.0	2.2	2.0	1.0	3.7	0.1	-	0.2	-	0.7	1.2	0.5	2.7
Candacia	0.0	2.3	0.4	0.5	0.2	1.6	1.0	1.0	0.1	0.3	0.5	0.5	0.5
Centropages	1.4	4.9	-	-	-	-	-	-	0.1	-	0.2	-	-
Clytemnestra	-	-	-	0.1	0.4	1.4	0.6	0.5	0.4	-	0.1	-	-
Copepodites	4.0	10.6	5.8	12.4	17.7	17.4	9.0	8.9	6.0	3.6	3.4	0.8	5.7
Copilia	-	-	0.5	0.1	0.4	0.3	-	-	-	0.2	0.1	-	-
Corycaeus	10.6	19.6	21.7	9.6	16.0	19.7	21.5	21.0	4.8	8.9	6.5	2.3	17.2
Euaetideus	0.2	0.0	0.2	1.6	0.5	0.2	0.8	0.2	-	0.1	0.1	-	0.2
Euagaptilus	-	-	-	-	-	-	-	-	-	-	-	-	-
Eucalanus	0.1	4.3	7.4	8.0	0.6	0.3	12.1	24.0	7.0	0.3	0.1	0.1	0.3
Euchaeta	0.0	0.6	10.2	14.5	7.0	10.3	19.9	11.5	12.0	6.3	4.5	2.1	3.6
Euchirella	-	0.7	0.2	0.4	-	0.1	0.6	0.1	0.1	-	0.1	-	-
Gaetanus	-	-	0.0	-	-	-	0.1	-	-	-	-	-	-
Haloptilus	0.1	0.5	0.4	0.3	0.2	0.4	0.2	0.4	0.2	0.6	0.5	1.2	1.0
Heterorhabdus	0.2	0.5	0.1	0.4	0.2	0.4	-	-	-	0.2	0.3	0.2	0.8
Labidocera	-	0.1	0.1	-	0.1	-	-	-	-	-	-	-	0.1
Lubbockia	-	-	-	-	-	-	-	-	-	-	-	-	-
Lucicutia	-	1.9	4.0	6.7	4.0	2.7	1.2	2.3	1.3	2.1	0.8	1.0	6.2
Macrosetella	-	0.3	4.8	11.3	2.7	5.8	1.0	0.8	0.5	0.2	0.2	0.1	0.5
Metridia	0.0	1.0	0.8	0.7	-	-	0.2	0.3	0.1	-	-	-	0.4
Neocalanus	-	-	0.0	-	-	-	0.0	-	-	-	-	-	-
Oithona	16.6	17.3	59.7	50.8	36.3	24.9	41.2	38.5	41.4	27.6	22.7	8.1	38.0
Oncaea	19.1	49.9	90.2	67.0	66.6	38.2	22.5	21.8	30.8	10.1	4.2	1.3	18.1
Pachos	-	-	0.1	-	-	-	-	-	-	-	-	-	-
Para/pseuds	170.7	140.5	149.3	75.7	83.7	103.7	55.4	96.3	46.9	32.0	35.0	4.7	30.8
Phaenna	2.0	0.2	0.3	0.1	0.3	0.1	-	0.3	0.2	-	0.1	0.1	0.1
Phyllopus	-	-	-	-	-	-	0.1	-	-	-	-	-	-
Pleuromamma	-	9.8	1.1	0.5	0.7	0.9	1.5	0.2	0.1	-	0.1	0.1	-
Pontellina	-	-	-	-	-	-	0.1	-	-	-	0.1	0.2	-
Pseudoeuchaeta	-	-	-	-	-	-	-	-	-	-	-	-	-
Rhincalanus	-	0.1	0.5	0.2	-	-	0.3	10.9	0.7	-	-	-	-
Sapphirina	-	0.4	0.2	1.6	0.1	0.7	0.1	-	0.5	0.1	0.1	-	0.1
Scaphocalanus	-	-	-	-	-	-	-	-	-	-	-	-	-
Scolecithrix	0.4	0.9	0.9	3.1	1.5	1.3	0.9	1.4	2.3	0.9	0.6	1.1	0.9
Scolethella	0.1	1.1	0.5	0.4	0.4	0.3	0.1	0.2	-	-	0.1	0.3	0.1
Scottocalanus	-	0.1	-	-	-	-	-	-	-	-	-	-	-
Temora	-	0.6	5.6	3.1	0.2	-	-	1.1	0.2	0.3	-	-	0.1
Undeuchaeta	-	0.1	-	0.1	0.1	0.2	-	0.1	-	-	-	-	-
Undinula	-	0.8	1.2	3.6	0.8	2.6	1.7	4.2	3.2	0.5	0.1	0.1	0.4
Total	287	296	386	297	255	246	205	261	170	102	87	29	135

AMT 5 continued

J Day	282	282	283	283	284	285	285	286	286	287	287	288	289
Latitude	-23.9	-25.8	-27.7	-29.7	-31.6	-35.5	-37.0	-38.8	-40.4	-42.2	-44.1	-46.0	-49.8
Time	11:30	00:00	11:30	00:00	11:30	12:30	01:00	12:00	01:00	12:30	01:00	12:00	12:30
Acartia	3.6	4.1	3.0	16.0	19.5	8.6	13.8	0.5	-	0.0	-	-	-
Aegisthus	-	-	-	-	-	-	-	-	-	-	-	-	-
Aetideopsis	-	-	-	-	-	-	-	-	-	-	-	-	-
Aetideus	0.1	-	-	-	0.1	0.1	-	-	0.9	0.9	1.7	0.1	0.3
Amallothrix	-	-	-	-	-	-	-	-	-	-	-	-	-
Arietellus	-	-	-	0.0	-	-	-	-	-	-	-	-	-
Augaptilus	-	-	-	-	-	-	-	-	-	-	-	-	-
Calanoides	-	-	-	-	-	-	-	6.7	1.5	0.4	0.3	0.1	-
Calanus	2.8	7.2	9.5	28.5	33.2	3.8	16.4	78.8	43.4	17.4	44.4	21.1	2.2
Calocalanus	3.5	6.0	5.0	1.9	7.6	5.0	3.6	0.3	-	-	-	-	-
Candacia	1.0	0.8	0.7	0.0	0.3	-	-	-	0.2	0.1	0.2	-	-
Centropages	0.1	0.4	-	-	-	-	-	0.5	3.8	0.6	-	0.3	-
Clytemnestra	-	-	0.5	-	-	-	-	-	-	0.3	-	-	-
Copepodites	5.3	5.3	5.3	7.0	11.0	5.9	10.0	58.5	23.3	30.2	15.1	12.6	1.2
Copilia	0.1	0.0	0.1	-	0.1	-	-	-	-	-	-	-	-
Corycaeus	9.2	22.5	15.5	5.2	8.8	3.1	4.3	-	-	-	-	-	-
Euaetideus	0.2	0.8	-	0.2	0.1	0.1	-	-	0.7	-	-	0.2	-
Euagaptilus	-	-	-	-	-	-	-	-	-	-	-	-	-
Eucalanus	1.0	2.0	0.8	0.9	0.4	0.6	0.6	1.1	0.5	1.9	1.1	0.1	-
Euchaeta	7.5	3.8	3.9	1.7	4.0	1.8	2.9	0.9	3.5	1.7	5.1	1.6	0.1
Euchirella	0.1	-	-	0.5	0.6	0.1	0.3	1.1	1.1	0.7	4.0	-	-
Gaetanus	0.2	0.0	-	-	-	-	-	0.3	-	-	-	-	-
Haloptilus	0.7	0.5	0.1	0.1	0.0	0.3	-	-	0.1	0.2	-	-	0.1
Heterorhabdus	-	0.2	0.7	0.4	0.2	0.5	0.3	0.7	-	1.2	0.5	-	0.1
Labidocera	-	4.4	-	-	-	-	-	-	-	-	-	-	-
Lubbockia	-	-	-	-	-	-	-	-	-	-	-	-	-
Lucicutia	2.1	1.5	2.3	2.6	3.2	2.6	8.5	1.8	-	0.6	1.5	-	-
Macrosetella	0.4	-	0.6	0.0	-	-	0.0	-	-	-	-	-	-
Metridia	0.5	-	-	-	0.9	-	1.2	-	17.5	4.6	13.2	0.8	0.8
Neocalanus	-	-	-	0.0	-	-	-	-	-	-	-	-	-
Oithona	31.3	29.4	23.0	24.3	42.6	34.7	45.5	112.6	53.7	125.9	134.2	224.4	15.9
Oncaea	38.3	32.1	34.9	30.2	35.7	9.2	37.2	22.3	11.5	9.4	5.0	2.4	-
Pachos	-	-	-	-	-	-	-	-	-	-	-	-	-
Para/pseuds	53.0	57.6	59.7	94.7	147.5	75.3	130.1	376.5	141.1	116.0	131.4	120.4	26.0
Phaenna	0.0	0.0	0.2	-	0.1	-	-	-	-	-	-	-	-
Phyllopus	-	-	-	-	-	-	-	-	-	-	-	-	-
Pleuromamma	-	3.3	4.6	6.0	2.6	0.9	32.5	39.7	18.9	13.5	22.7	1.1	0.2
Pontellina	-	-	-	-	-	-	-	-	-	-	-	-	-
Pseudoeuchaeta	-	-	-	-	-	-	-	-	-	-	-	-	-
Rhincalanus	-	-	0.2	-	-	0.2	-	-	10.2	4.7	3.1	0.2	-
Sapphirina	0.3	0.3	0.3	0.1	0.3	-	0.0	-	-	-	-	-	-
Scaphocalanus	-	-	-	-	-	-	-	-	-	-	-	-	-
Scolecithrix	0.3	0.7	0.3	0.1	0.5	-	-	-	-	-	0.0	-	-
Scolethella	-	0.5	-	-	-	-	0.0	-	-	-	-	-	-
Scottocalanus	-	-	-	-	-	-	-	-	-	-	0.0	-	-
Temora	-	0.7	5.5	0.0	0.7	-	-	-	-	-	-	-	-
Undeuchaeta	-	-	-	0.0	-	-	0.1	-	-	-	-	-	-
Undinula	0.6	0.3	0.4	0.1	1.4	0.4	0.0	-	-	-	-	-	-
Total	162	184	177	221	321	153	307	702	332	330	384	386	47

AMT 6

J Day	135	136	137	138	142	143	145	146	147	148	149	150	151	152
Latitude	-33.6	-32.3	-29.5	-26.7	-24.8	-21.7	-17.7	-14.7	-11.6	-8.6	-5.9	-2.8	0.0	3.1
Time	11:15	08:00	08:00	08:30	08:00	08:00	00:00	08:30	08:30	08:30	08:30	08:30	08:15	09:00
Acartia	-	-	-	-	-	-	0.2	10.1	1.2	1.0	1.2	0.4	0.1	0.3
Aegisthus	-	-	-	-	-	-	-	-	-	-	-	-	-	0.5
Aetideus	0.2	-	-	-	-	1.5	0.5	-	0.3	0.2	-	0.4	0.2	2.2
Amallothrix	-	-	-	-	-	-	-	-	0.1	-	-	-	-	0.1
Calanoides	163.6	184.6	5.8	5.8	115.8	47.5	17.4	0.5	0.0	-	-	-	-	-
Calanus	1.6	11.7	0.2	0.5	1.4	1.6	3.8	8.1	5.5	6.1	9.1	16.2	10.8	3.9
Calocalanus	-	-	-	2.0	-	-	-	0.0	1.1	0.7	0.7	0.3	0.4	0.2
Candacia	1.5	-	-	-	-	2.1	0.5	0.0	0.2	0.9	0.7	0.3	0.4	0.8
Centropages	83.6	130.4	14.4	12.5	21.4	5.3	23.2	1.0	-	-	-	-	-	-
Clytemnestra	-	-	-	-	-	-	-	-	-	-	0.2	-	-	-
Copepodites	14.7	62.1	38.4	9.7	58.3	45.6	8.2	9.1	4.1	6.5	6.0	5.1	2.9	7.9
Copilia	-	-	-	-	-	-	-	-	0.0	0.1	0.1	0.1	-	0.0
Corycaeus	1.3	-	-	0.1	-	0.0	0.7	5.5	4.8	7.3	9.3	5.0	4.7	10.0
Euaetideus	-	-	-	-	-	0.0	-	0.5	0.2	0.2	0.2	-	-	0.3
Euagaptilus	-	-	-	-	-	-	-	-	-	-	-	-	-	-
Eucalanus	0.5	0.3	-	-	-	0.0	0.8	1.1	0.2	0.7	4.9	2.1	2.4	1.1
Euchaeta	0.2	-	-	0.2	-	0.6	0.2	2.2	2.5	4.6	7.6	3.6	3.7	10.1
Euchirella	-	-	-	-	-	-	-	-	0.0	0.1	0.1	-	0.0	-
Gaetanus	-	0.4	-	-	-	-	-	-	-	-	-	-	-	-
Haloptilus	-	-	-	-	-	-	-	0.9	0.6	0.4	0.2	0.1	0.4	0.9
Heterorhabdus	-	-	-	-	-	-	0.8	0.4	0.8	-	0.2	0.1	0.3	0.2
Labidocera	-	-	-	-	-	-	-	-	-	-	-	-	0.1	-
Lubbockia	-	-	-	-	-	-	-	-	-	-	-	-	-	1.2
Lucicutia	-	-	-	-	-	-	0.1	0.7	1.0	1.1	3.5	0.4	0.9	1.8
Macrosetella	1.3	-	-	-	-	0.0	-	0.0	0.0	0.2	2.8	0.7	0.6	2.4
Mecynocera	-	-	-	-	-	-	-	-	-	-	-	-	-	-
Metridia	25.5	123.1	804.0	16.4	3.8	90.7	1.8	-	-	-	-	-	-	-
Neocalanus	-	-	-	-	-	-	-	-	-	-	-	-	-	-
Oithona	181	212.3	1352	219.3	83.6	82.2	11.8	25.4	14.3	15.8	10.2	18.4	9.2	14.0
Oncaea	25.4	16.0	20.0	0.1	3.1	16.4	4.8	14.1	24.4	40.8	22.2	35.2	5.7	22.7
Para/pseuds	546	593.7	458.0	178.6	432.6	104.2	56.8	89.5	73.3	64.1	82.7	45.1	47.5	39.3
Phaenna	-	-	-	-	-	-	0.0	0.2	-	0.1	0.1	0.6	0.0	0.0
Pleuromamma	-	0.5	0.1	0.2	-	0.0	0.2	-	-	0.1	-	0.3	-	0.1
Pontellina	-	-	-	-	-	-	-	-	-	-	-	0.5	-	0.1
Pseudoeuchaeta	-	-	-	-	-	-	-	-	-	-	-	-	-	-
Rhincalanus	0.1	2.4	3.4	0.3	8.3	0.3	-	0.6	0.1	0.7	1.1	1.9	2.0	0.3
Sapphirina	-	-	-	-	-	-	-	0.1	0.7	0.7	0.1	0.5	0.0	0.2
Scolecithrix	-	-	-	-	-	-	-	0.8	0.5	1.1	0.4	0.8	0.5	0.2
Scolethella	-	-	-	-	-	-	-	0.0	0.2	0.1	-	0.4	0.2	0.1
Temora	-	-	-	-	-	-	0.8	0.2	-	0.3	-	-	-	0.0
Undeuchaeta	-	-	-	-	-	-	0.0	-	0.1	0.0	0.3	-	-	-
Undinula	-	-	-	-	-	-	-	0.5	2.2	0.5	2.5	-	-	-
Total	1047	1337	2696	446	728	398	133	172	138	154	166	138	93	121

AMT 6 continued

J Day	153	154	155	156	157	158	159	160	161	162	163	164	165
Latitude	5.9	9.1	12.8	16.4	20.4	24.5	28.6	32.4	36.6	41.1	44.7	48.5	49.8
Time	09:00	09:00	09:00	09:00	09:00	09:00	09:00	09:00	09:00	09:00	08:30	09:45	09:00
Acartia	0.4	0.6	2.2	1.4	2.8	6.7	2.6	1.9	1.4	0.2	-	-	510.2
Aegisthus	-	-	-	-	0.1	-	-	-	-	2.0	-	-	-
Aetideus	0.5	0.8	2.1	0.9	-	0.2	0.6	0.1	0.5	2.6	0.2	1.6	-
Amallothrix	-	-	-	-	-	-	-	-	-	-	-	-	-
Calanoides	-	-	-	0.1	0.7	-	-	-	-	-	-	-	-
Calanus	3.8	6.4	10.8	19.3	3.3	6.0	4.3	4.7	1.5	4.1	1.2	39.9	431.9
Calocalanus	1.2	0.3	0.4	0.1	-	2.9	3.0	6.0	1.9	-	1.2	-	-
Candacia	0.4	0.0	-	0.9	-	0.4	0.3	0.3	0.1	-	-	0.4	-
Centropages	-	-	-	-	7.6	-	0.1	-	0.1	1.6	0.3	0.9	42.9
Clytemnestra	-	-	-	-	-	-	-	0.2	0.1	-	-	-	-
Copepodites	7.5	4.3	13.8	16.2	17.4	6.9	2.0	1.0	3.5	10.2	4.1	22.8	286.1
Copilia	0.0	-	-	-	-	0.0	0.2	-	0.2	-	-	-	-
Corycaeus	7.4	10.2	4.4	2.3	0.3	10.2	2.5	8.0	2.7	2.2	-	2.0	-
Euaetideus	0.2	0.8	0.6	0.8	-	0.3	-	-	0.2	-	-	-	-
Euagaptilus	-	-	-	-	-	-	-	-	0.0	-	-	-	-
Eucalanus	1.3	3.9	4.2	8.6	-	1.2	-	0.0	0.0	0.0	0.1	2.3	-
Euchaeta	1.7	6.4	9.9	3.5	2.1	2.1	1.4	1.0	0.5	5.3	1.0	4.2	-
Euchirella	-	-	-	-	-	-	-	-	-	-	-	-	-
Gaetanus	-	-	-	-	-	-	-	-	-	0.1	-	-	-
Haloptilus	0.5	-	1.2	1.0	-	1.1	0.8	0.7	0.7	-	-	-	-
Heterorhabdus	0.2	0.4	0.3	1.2	1.5	0.3	0.7	0.6	1.9	0.9	0.3	-	-
Labidocera	-	-	0.1	23.3	-	-	-	-	-	-	-	-	-
Lubbockia	-	-	-	-	-	-	-	0.3	-	-	-	-	-
Lucicutia	0.9	1.5	1.5	2.0	2.0	5.0	2.6	3.3	1.0	-	-	-	-
Macrosetella	0.1	-	-	-	-	0.4	-	-	-	-	-	-	-
Mecynocera	-	-	-	-	-	-	-	-	0.2	-	-	-	-
Metridia	-	-	-	-	6.4	-	-	-	-	-	-	0.2	-
Neocalanus	-	-	-	-	2.0	0.8	-	-	-	-	-	-	-
Oithona	12.3	17.6	23.3	7.8	17.5	28.8	15.8	21.1	12.9	116.3	59.9	32.7	123.5
Oncaea	21.2	88.0	43.3	31.0	27.4	41.1	9.1	8.3	9.6	5.3	0.0	3.3	-
Para/pseuds	26.8	48.1	45.0	121.3	80.3	44.9	25.3	27.0	33.1	336.5	41.1	21.4	-
Phaenna	0.1	0.0	0.4	0.5	-	-	0.2	-	0.1	-	-	-	-
Pleuromamma	0.1	1.0	0.9	0.5	19.2	-	0.0	1.2	0.5	4.4	0.5	3.4	-
Pontellina	0.1	-	-	-	-	-	-	-	-	-	-	-	-
Pseudoeuchaeta	-	-	-	-	-	-	-	0.1	-	-	-	-	-
Rhincalanus	0.1	0.1	0.1	0.2	0.4	-	-	-	-	-	0.4	0.3	-
Sapphirina	0.3	-	-	1.4	-	0.0	-	0.6	0.2	-	-	-	-
Scolecithrix	0.5	0.8	1.1	0.3	0.3	0.4	-	-	-	-	-	-	-
Scolethella	0.2	1.4	0.2	0.1	0.6	2.0	-	-	-	-	-	-	-
Temora	-	0.4	0.2	0.1	0.0	0.5	-	-	-	-	-	-	-
Undeuchaeta	-	-	-	-	-	-	-	-	0.1	0.0	-	-	-
Undinula	-	-	-	-	-	-	-	-	-	-	-	-	-
Total	88	193	166	245	192	162	71	86	73	492	110	135	1395

Journal of Plankton Research Vol.22 no.3 pp.473–483, 2000

A test model for optical plankton counter (OPC) coincidence and a comparison of OPC-derived and conventional measures of plankton abundance

Rachel S.Woodd-Walker, Christopher P.Gallienne[1] and David B.Robins[1]

Institute of Marine Studies, University of Plymouth, Drake Circus, Plymouth PL4 8AA and [1]Centre for Coastal & Marine Science, Plymouth Marine Laboratory, Prospect Place, West Hoe, Plymouth PL1 3DH, UK

Abstract. The use of the optical plankton counter (OPC) for processing zooplankton net samples is explored. A comparison of OPC counts and microscope counts from net samples was reasonable. Similarly, OPC biovolume and carbon had a ratio of 23:1 (biovolume:carbon). Coincidence was modelled using the Poisson distribution, and tested with a large diatom *Coscinodiscus wailesii*. Agreement appeared to be good up to 60 s^{-1}; above this, the maximum response rate of the system became limiting.

Introduction

The optical plankton counter (OPC; Herman, 1988, 1992) was developed for automated counting and sizing of zooplankton, and has been used extensively in submersible towed mode (OPC-1T) and with the shorter beam length laboratory version (OPC-1L) in continuous pump-through mode, or with discrete net samples.

Extensive calibration and testing of the OPC in diverse environments has led to a greater understanding of the operational limitations (Herman, 1988, 1992; Herman *et al.*, 1993; Sprules *et al.*, 1998). Coincidence, i.e. two particles in the beam at the same time, can be a major problem at high particle concentrations. Estimates of the relationship between coincidence and concentration have been proposed by Herman (Herman, 1988) who derived a semi-empirical formula, and by Sprules *et al.* (Sprules *et al.*, 1992, 1998) who used a theoretical approach based on the Poisson distribution. Sprules *et al.* predicted a change in the particle size measured by the OPC due to coincidence: a shift to fewer, larger particles, and an anomalously high biomass estimate (Sprules *et al.*, 1998).

In this study, to validate use of the OPC-1L for net samples, a comparison of OPC with conventional measures is presented, using the OPC and microscope counts, and carbon and OPC biovolume from field net samples. In addition, coincidence is investigated using a range of concentrations using an organism of small size and narrow size distribution, *Coscinodiscus wailesii*, to test the predictions of a theoretical model based on the Poisson distribution for the OPC-1L.

Method and results

The optical plankton counter

The OPC-1L [Focal Technologies Ltd (Herman, 1988)] design and operation is described by Herman (Herman, 1992). Essentially, the system consists of a 20 mm

© Oxford University Press 2000

square flow cell through which the sample passes. A parallel light beam of 4 mm width is detected by a sensor on the opposite side of the tube. As a particle passes the sensor, the light blocked due to the passage of the particle is measured. The digital size is recorded and converted by a semi-empirical formula to equivalent spherical diameter [ESD (Herman, 1992)].

Field samples

Sampling was carried out on six Atlantic Meridional Transects (AMT) cruises on RRS 'James Clark Ross' (Robins and Aiken, 1996) and the Plankton Reactivity in the Marine Environment [PRIME; (Gallienne *et al.*, 2000)] cruise on RRS 'Discovery' between 1995 and 1998 (Table I; Figure 1). Vertical net samples were taken along the transects from 200 m to the surface with a WP2 (200 μm mesh) net, on daily mid-morning stations with occasional night stations. The net sample was divided in half with a Folsom splitter and half the sample was used for carbon and taxonomic analysis. This half-sample was made up to a known volume (500 or 1000 ml), and three 50 ml aliquots taken and filtered individually onto Whatman glass fibre (GF/C) filters. The filters were dried for 48 h at 60°C, before being wrapped in aluminium foil, pelleted, and analysed for carbon content with a Carlo Erba NA 1500 elemental analyser. The biomass of carbon (m^{-3}) was then calculated. The remainder of the half-sample was preserved in 4% buffered formalin. A subsample of this was subsequently taken using a Stempel pipette for microscopic taxonomic identification and counting, so that a minimum of 200 individuals were counted.

The second half of the 0–200 m net sample was circulated through the OPC. Water was recirculated from a tank through the OPC at a rate of 15 l min^{-1}. The sample was added slowly to the tank, with minimum disturbance, to avoid producing bubbles. On the outflow, a collecting container with 170 μm mesh was used to filter the water (Figure 2).

Microscope and OPC counts were compared for the net samples (Figure 3). The functional regression (Kendall and Stuart, 1961) was significant with an R^2 of 0.42, and the slope was not significantly different to the 1:1 line ($N = 147$, $t = 1.21$, $P = 0.2$), with an untransformed slope about the mean of 0.98.

Comparison of counts by two methods can be problematic where there is an arbitrary size cut-off at the lower part of the size range. Sizing by mesh (in effect with the microscope counts, as they were collected using a 200 μm mesh) and

Table I. Summary of cruises

Cruise	Dates	Track
AMT1	September–October 1995	UK–Falklands
AMT2	April 1996	Falklands–UK
PRIME	July 1996	Iceland–UK
AMT3	September–October 1996	UK–Falklands
AMT4	April–May 1997	Falklands–UK
AMT5	September–October 1997	UK–Falklands
AMT6	May–June 1998	South Africa–UK

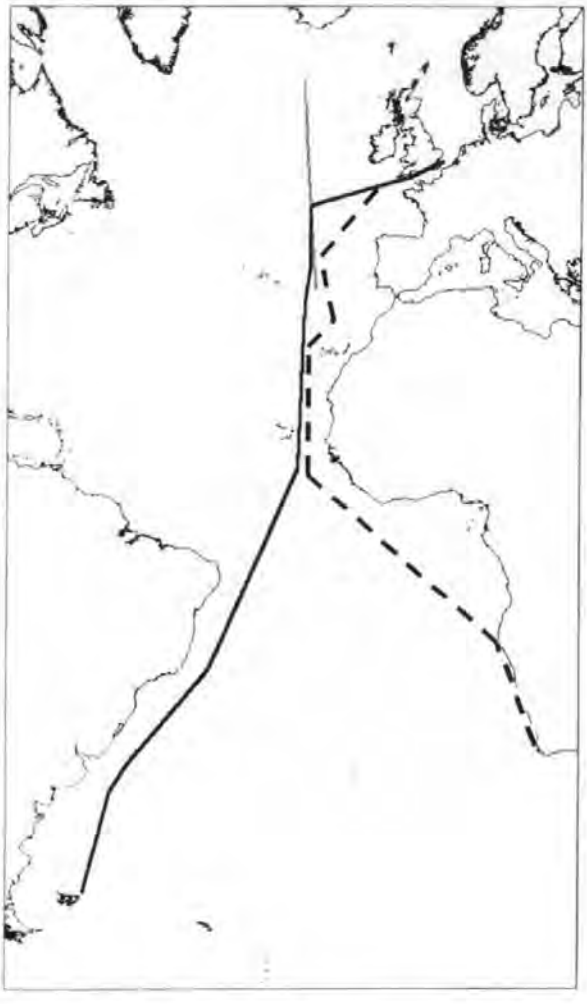

Fig. 1. The Atlantic Ocean showing cruises from which data were collected. ——— AMT, the AMT track for AMT1-5; — — — AMT6, South Africa–UK, May–June 1998; ——— PRIME, July 1996.

sizing by area (as in the OPC) will not necessarily size the same, or even consistently, for different organisms. The shape and orientation of the organism will determine how large it appears to the OPC (Herman, 1988) and whether it will pass through a particular mesh. This problem is exacerbated by small organisms tending to be the most numerically abundant. In spite of these problems, using an OPC cut-off at 250 and 200 μm mesh, OPC and microscope counts agreed well, but coincidence can cause a reduction in OPC counts, causing a low estimate of numerical abundance. Debris and large phytoplankton may also be counted. In the surface waters of open ocean, phytoplankton tend to be small and detritus is

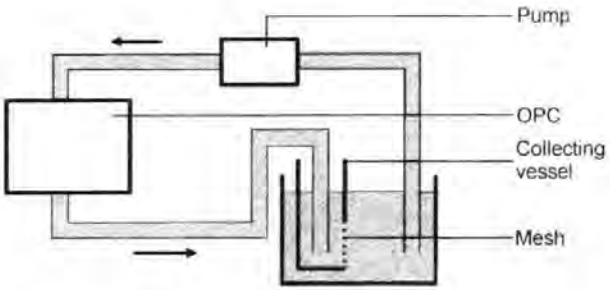

Fig. 2. The OPC-1L set-up for processing samples.

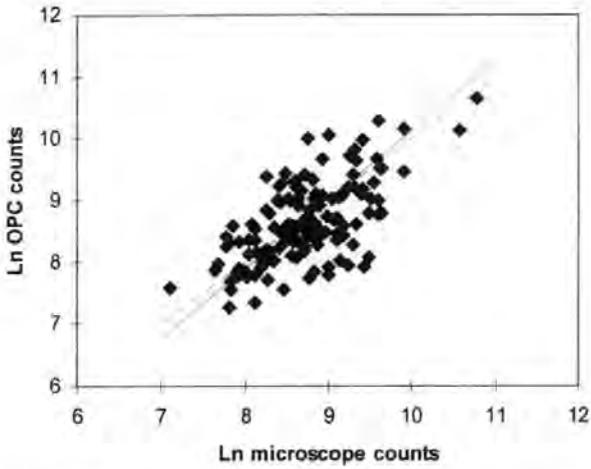

Fig. 3. A comparison of the total counts by the OPC with manual microscope counting for half net samples for AMT 1–6. The dashed line is $y = x$. Regression (solid line) $y^* = 1.125x^* - 1.1$, where y^* = ln OPC counts and x^* = ln microscope counts, $R^2 = 0.418$. Gradient 95% confidence limits are 1.375–0.923.

rare. In coastal regions, filamentous algae and other large phytoplankton could be counted. Flocculated detritus and other debris may also occur at high concentration, and may significantly increase count rates.

OPC biovolume was calculated using a spherical model and compared with total carbon. A $\log_e$ transformation of both sets of data was used to normalize the distribution of the variance of these data, a symmetrical functional regression (Kendall and Stuart, 1961) was carried out, and the confidence limits calculated (Figure 4). Regression of $\log_e$ values resulted in a linear ratio at the lowest carbon biomass of 26.8:1 (1:0.037) and at the highest carbon biomass of 21.3:1 (1:0.047), with a ratio about the mean of 22.9:1 (1:0.044). The gradient of the $\log_e$ regression is significantly less than 1 ($P < 0.05$), suggesting that at higher biovolumes the biovolume to carbon ratio is lower. Using biovolume instead of counts reduces the problem of cut-off at the lower end of the size spectrum. This is

because, although numerically dominant, the small size classes usually make a less significant contribution to the total biovolume. Establishing biovolume to carbon relationships is important to allow OPC data to be used in carbon-based models. However, estimates of biovolume to carbon in the literature vary considerably for zooplankton samples. Dalal and Parulekar (Dalal and Parulekar, 1986) estimated a ratio of 1:0.027, whilst Vinogradov and Shushkina (Vinogradov and Shushkina, 1987) estimated ratios of 1:0.04–0.05. A generally accepted conversion of wet weight to carbon is around 1:0.05, very similar to here (1:0.037–0.047).

Test of coincidence

A 200 μm net sample from AMT 6 (Table I) from the Benguela upwelling at 12°00′E, 19°00′S was predominantly composed of the centric diatom *C.wailesii* (Gran & Angst). Large additional organisms were removed by filtering the sample through a 500 μm mesh prior to preservation in 4% borax-buffered formalin. The 200–500 μm fraction of this sample was used as a test for coincidence, as *Coscinodiscus* has a similar size range to many small copepods (mean ESD 399 μm), at the lower end of the OPC's size range, and a narrow size distribution (Figure 5; ESD SD = 72 μm).

The OPC-1L was set up in pump-through mode (Figure 2). The sample of *Coscinodiscus* was added slowly at first to get a low count rate (1–2 s^{-1}) for estimating the mean ESD (Figure 5), and then at increasing concentrations, to give a range of count rates. The raw data were processed to give the counts and biovolume (which is calculated using a spherical model), in 1 s intervals, using the OPC

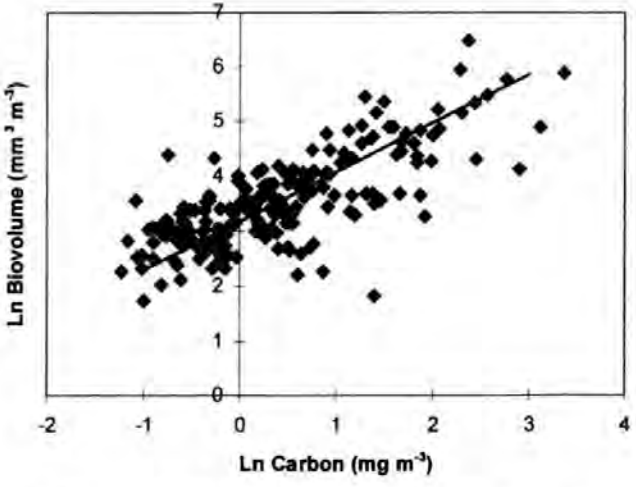

Fig. 4. OPC biovolume compared with carbon for AMT 1–6 and PRIME cruises. Ln regression $y^* = 0.89x^* + 3.181$, where y^* = Ln biovolume and x^* = Ln carbon, $R^2 = 0.561$. Gradient 95% confidence limits are 0.911–0.860.

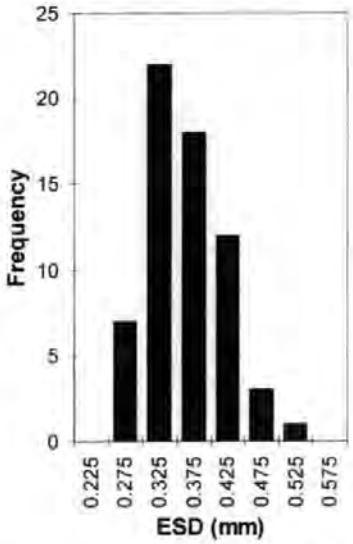

Fig. 5. Estimate of mean ESD of *Coscinodiscus* spp. Mean ESD = 399 mm, SD = 72.

software. The mean biovolume of a particle was calculated by dividing the total biovolume by the number of counts.

Theory predicting coincidence and its effect on mean ESD

Sprules *et al.* derived a formula based on theory from the Poisson distribution, thus assuming random distribution (Sprules *et al.*, 1992). The average number (μ) in the beam is:

$$\mu = C/V$$

where C is the concentration of animals and V is the volume of the beam (i.e. $20 \times 20 \times 4$ mm). From the average number in the beam, the distribution of the number in the beam can be calculated from the Poisson distribution [$P(Y) = e^{-\mu} \cdot \mu^{Y}/Y!$, where $P(Y)$ is the probability of Y particles in the beam and μ is the mean number of particles in the beam]. If more than one organism is in the beam at one time, they will be counted as one (but with an area equal to the sum of areas). The average number (av. no.) of organisms recorded by the OPC will therefore be:

$$\begin{aligned} \text{OPC av. no.} &= P(0).0 + P(1).1 + P(2).1 + \ldots \\ &= P(1) + P(2) + \ldots \\ &= 1 - P(0) \\ &= 1 - e^{-\mu} \end{aligned}$$

The coincidence factor = (av. no.)/(OPC av. no.).

The Poisson distribution was used to calculate the apparent OPC counts (number of particles counted by the OPC) from the actual counts (number of particles actually passing the sensor) in a similar way to Sprules *et al.* (Sprules *et al.*, 1992, 1998), but time was used instead of volume. Given a flow rate of 15 l min^{-1} and an area of 400 mm^2 (20 × 20 mm cross-section of the flow cell), the velocity of particles along the tube will be 625 mm s^{-1}. Two particles will be counted as one if any part of them is in the beam at the same time, so that a particle will have to travel the beam width plus its length without encountering another particle, i.e. 4 mm + mean ESD. This will take (4 + mean ESD)/625 s. The average number of particles in the beam is given by the actual count rate × [(4 + mean ESD)/625]. The probability of one or more particles being in the beam is given by $1 - P(0)$, or $1 - e^{-(\text{av. no.})}$ (see above).

For larger particles, it will take longer for a particle to clear the beam completely. Thus, the probability of coincidence would be expected to be higher at the same concentration. Varying the flow rate will not alter the rate of coincidence if the concentration remains the same. However, the OPC does not measure concentration directly, but the count rate. The same concentration will have a lower count rate at lower flow rates. Thus, at lower flow rates, the coincidence will be greater for the same count rate. For *Coscinodiscus* (mean ESD = 0.399 mm), the time to cross the beam will be 7.04×10^{-3} s. The theoretical response of OPC measured counts for actual counts is given in Figure 6a.

The Poisson distribution can also be used to estimate the probability of any number of particles being in the beam from the mean density of particles, given by $P(Y) = e^{-\mu} \cdot \mu^{Y}/Y!$ (see above). This was calculated for up to six particles in the beam at one time. Greater than six particles should be very rare, even when densities are quite high. The apparent mean ESD is given by actual mean ESD × $(P(1) \times 1 + P(2) \times 2 + P(3) \times 3 \ldots)/(1 - P(0))$, assuming that no particles overlap.

The apparent mean ESD was calculated for a range of densities of *Coscinodiscus*. Figure 6b shows how the measured mean ESD would be expected to increase with concentration. ESD was converted into biovolume using the spherical model, and this compared with the apparent OPC counts to give the predicted model for *Coscinodiscus* (Figure 8).

Maximum count rate

A particle takes (4 mm + mean ESD)/625 s to cross the beam, and a further 4 ms for the system to reset itself (Sprules *et al.*, 1998); the maximum count rate for different size particles can be calculated from 1/([4 + ESD)/625] + 0.004). This assumes that as soon as the system has reset, another particle enters the beam. The maximum count rate is predicted to decrease as the ESD increases (Figure 7). The maximum count rate for *Coscinodiscus*, with a mean ESD of 399 μm, will be 90.6 s^{-1}. The maximum count rate as it changes with ESD is shown in Figure 8. The manufacturer's maximum counts rate of 200 s^{-1} is based on the maximum flow rate of the OPC, 4 m s^{-1}, and for small particles. For the minimum flow rate, 0.4 m s^{-1}, and a particle of 250 μm, the maximum count rate is 68 s^{-1}.

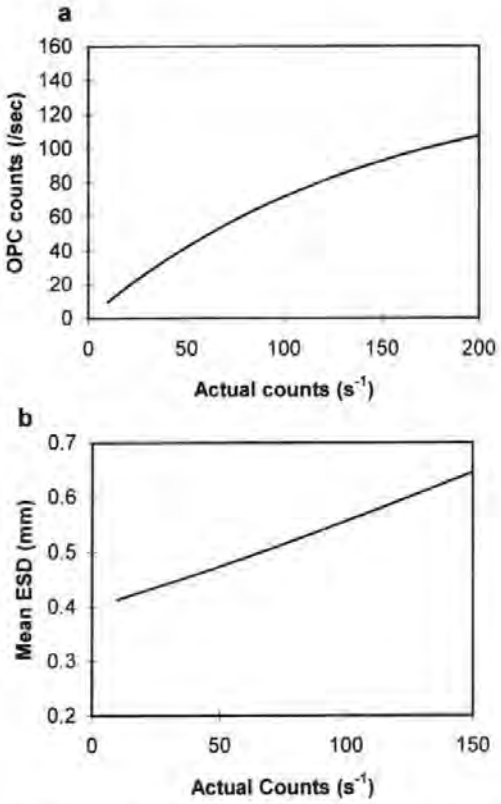

Fig. 6. Predictions from the Poisson distribution for coincidence using the OPC-1L. (**a**) Predicted coincidence for *Coscinodiscus* spp. at a flow rate of 15 l min^{-1}. (**b**) The predicted effect of coincidence on particle size for *Coscinodiscus* spp.

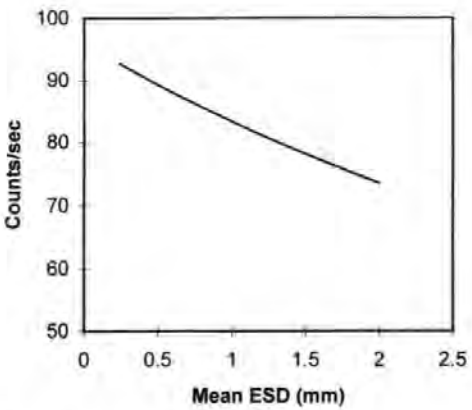

Fig. 7. The maximum theoretical number of counts per second calculated for different sized particles.

The test of the Poisson distribution using *Coscinodiscus* shows that coincidence, and thus actual count rates, can be predicted up to 50–60 s^{-1} (Figure 8a), with the residuals being evenly scattered around the line (Figure 8b). However, between 60 and 80 OPC counts s^{-1} (estimated from the Poisson distribution to be actual counts of 80–120), another factor comes into play. The high biovolumes of particles found between 60 and 80 OPC counts s^{-1} suggest that actual counts can be very high in this range, much higher than predicted. The maximum count rate was calculated to be 90 s^{-1} for *Coscinodiscus* at a flow rate of 15 l s^{-1}. Thus, the reset time and time to pass through the beam appear to become limiting.

The Poisson model suggests that coincidence is appreciable even at relatively low count rates. For a small particle, at 30 s^{-1}, the OPC will count on average 27.3 s^{-1} (9% reduction), and at 10 particles s^{-1}, 9.7 s^{-1} (3% reduction) will be counted.

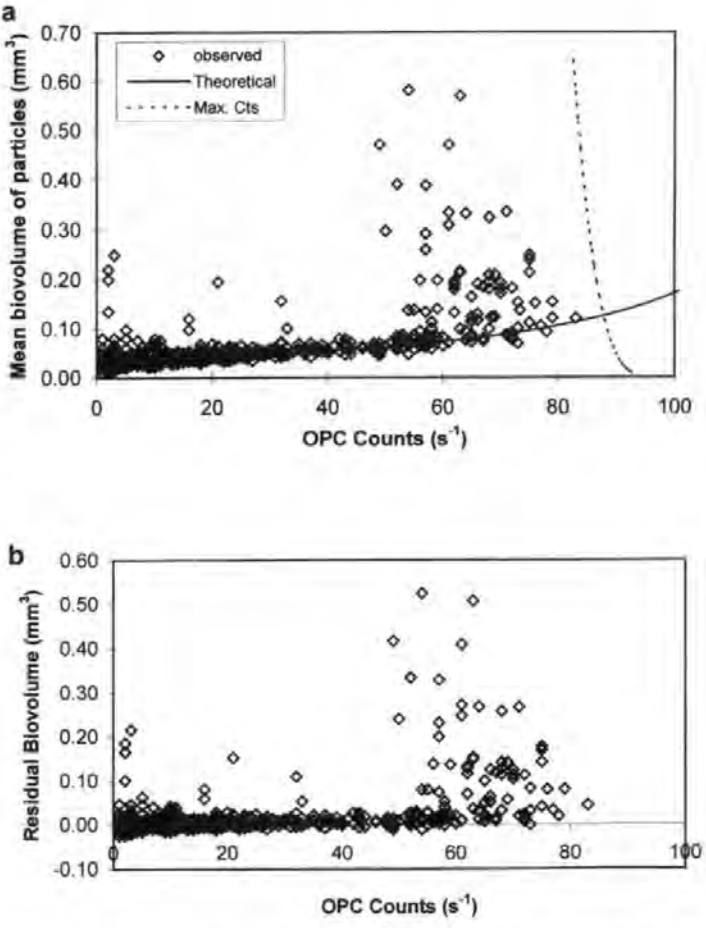

Fig. 8. The effect of count rate on particle volume for *Coscinodiscus wailesii* at a flow rate of 15 l min^{-1}. (**a**) Observed compared with predicted. (**b**) Residuals.

However, as the mean ESD of particles increases, coincidence increases, so that for a theoretical sample of 5 mm mean ESD, at 30 s^{-1} only 25 (16.7% reduction) will be counted. For the towed OPC-1T, which has a larger beam volume, coincidence would be expected to be greater at lower concentrations. Coincidence can be reduced by reducing beam volume, e.g. by reducing the aperture (Sprules *et al.*, 1998), or by reducing the concentration of the sample.

Conclusions

The OPC can be reliably used to process mixed zooplankton net samples, giving reasonable estimates of counts and a good estimate of biovolume and carbon (using a ratio of 23:1), even using a simple spherical model. However, coincidence can be a problem even at low concentrations. Samples should be diluted so that the OPC count rate is maintained below 10 s^{-1} for small zooplankton (mean ESD around 400 μm). With larger zooplankton, lower count rates should be used. The maximum count rate is largely determined by the flow rate and may be considerably less than the frequently quoted 200 s^{-1}.

Acknowledgements

We wish to thank the officers and crew of the British Antarctic Survey research ship RRS 'James Clarke Ross', and the officers and crew of RRS 'Discovery', for their help during the AMT and PRIME cruises. We are most grateful to Bob Head (CCMS-PML) for his help with the carbon analysis, and to Dave Conway (CCMS-PML) for his comments on the manuscript. This work was supported by the Natural Environmental Research Council PRIME special topic grant (GST/02/1068). R.W.-W. is supported by a University of Plymouth studentship. This is publication no. 41 of the AMT programme.

References

Dalal,S.G. and Parulekar,A.H. (1986) Validity of zooplankton biomass estimates and energy equivalent in the Indian Ocean. *Indian J. Mar. Sci.*, **15**, 264–266.

Gallienne,C.P., Robins,D.B. and Woodd-Walker,R.S. (2000) Abundance and distribution of mesozooplankton along a 20° west meridional transect of the north Atlantic Ocean. *Deep-Sea Res.*, in press.

Herman,A.W. (1988) Simultaneous measurement of zooplankton and light attenuance with a new optical plankton counter. *Cont. Shelf Res.*, **8**, 205–221.

Herman,A.W. (1992) Design and calibration of a new optical plankton counter capable of sizing small zooplankton. *Deep-Sea Res.*, **39**, 395–415.

Herman,A.W., Cochrane,N.A. and Sameoto,D.D. (1993) Detection and abundance estimation of euphausiids using an optical plankton counter. *Mar. Ecol. Prog. Ser.*, **94**, 165–173.

Kendall,M.G. and Stuart,A. (1961) *The Advanced Theory of Statistics*, Vol 2. Griffin, London.

Robins,D.B. and Aiken,J. (1996) The Atlantic Meridional Transect: an oceanographic research programme to investigate physical, chemical, biological and optical variables of the Atlantic Ocean. *Underwater Technol.*, **21**, 8–14.

Sprules,W.G., Bergstrom,B., Cyr,H., Hargreaves,B.R., Kilham,S.S., MacIsaac,H.J., Matsushita,K., Stemberger,R.S. and Williams,R. (1992) Non-video optical instruments for studying zooplankton distribution and abundance. *Arch. Hydrobiol. Ergebn. Limnol.*, **36**, 45–58.

Sprules,W.G., Herman,A.W. and Stockwell,J.D. (1998) Calibration of an optical plankton counter for use in fresh water. *Limnol. Oceanogr.*, **43**, 726–733.
Vinogradov,M.E. and Shushkina,E.A. (1984) Quantitative estimation of epipelagic population in the world ocean. *Dokl. Akad. Nauk. SSSR*, **274**, 410–412.

Received on March 29, 1999; accepted on October 6, 1999

SPATIAL DISTRIBUTIONS OF COPEPOD GENERA ALONG THE ATLANTIC MERIDIONAL TRANSECT

Rachel S. Woodd-Walker

[1]Institute of Marine Studies, University of Plymouth, Drake Circus, Plymouth PL4 8AA, United Kingdom, email: rwoodd-walker@plymouth.ac.uk

CCMS Plymouth, Prospect Place, West Hoe, Plymouth PL1 3DH, United Kingdom.

[1]correspondance address

Abstract

The distribution of copepod taxa at a basin scale was analysed using three Atlantic transects (UK - Malvinas 1997, Malvinas - UK 1997, and South Africa - UK 1998). Integrated 200 m to surface zooplankton samples were taken daily, using WP2-200 μm nets. The zooplankton were size-fractionated and sub-samples taken for carbon analysis. The remainder of the samples were preserved for taxonomic analysis of copepod genera. Multidimensional scaling (MDS) was used to identify zoogeographic regions from the copepod data. Seven regions were identified: northern temperate, northern subtropical, equatorial, southern tropical, southern sub-tropical, southern temperate, and Benguela upwelling. Analysis of similarity showed that all regions were significantly different from each other except: northern temperate and southern temperate, northern temperate and southern subtropical, and northern subtropical and southern subtropical. The genera significant in determining the regions were identified. These regions were compared to other schemes of biological and hydrographic areas. The MDS also showed that the copepod composition in the tropical and subtropical regions was less variable than the temperate and Benguela stations. Latitudinal trends were also investigated. Copepod genera showed a reduction in richness at higher latitudes. Copepod size did not show any substantial or consistent change with latitude along these transects, as demonstrated by both the numerical abundances in each size category, and the carbon biomass per individual. The proportion in each size fraction was quite uniform over the transect.

Key words: copepod, biogeography, biomass, zooplankton

Introduction

Pelagic marine biogeography forms a crucial part of understanding the biology of the oceans, by allowing generalisations to be made over large spatial scales. Several attempts have been made to divide up the oceans into areas of zoogeographic similarity. These regions have been based on a variety of organisms (Euphausiids, Brinton, 1962; Myctophidae, Backus et al., 1977; Thecosomata, Dadon & Boltovskoy, 1982; Foraminifera, Bé, 1977). Many of these schemes relied on a composite of data from several sources, and because of sampling differences were reduced to presence/absence data (e.g. Gibbons, 1997), losing changes in community structure due to changes in abundance and dominance. The development of these schemes may also involve interpolation from physical boundaries and watermasses. Strong links are generally assumed between the watermasses and the changes in community (e.g., van der Spoel & Heyman ,1983; Boltovskoy, 1986; McGowan, 1986). Longhurst et al. (1995) divided the oceans into 'provinces' based on 'ocean currents, fronts, topography and recurrent features in the sea surface chlorophyll'. Several world composites have been derived and reviewed (e.g., Boltovskoy, 1997; Backus, 1986; van der Spoel & Heyman, 1983; McGowan, 1974).

Another approach to understanding large scale patterns has been from gradients. Several latitudinal changes have been noted (e.g. Angel, 1993; Reid et al., 1978). Angel (1997) suggested that these included an increase in mean size and longevity of organisms at higher latitudes, and diversity decreasing whilst variability in diversity increased at higher latitudes.

Copepods form the dominant component of the mesozooplankton, frequently making up over 80% (e.g. Gallienne et al., in press; Bainbridge, 1972). They are important herbivores (e.g. Colebrook, 1982), as well as food for higher trophic levels (e.g. Williams et al., 1994). By

using genus level analysis, may give a clearer indication of the major trends in zooplankton community structure whilst avoiding problems associated with misidentification, synonyms in such a diverse group.

In this study of copepod genera, I investigated the regional groups based on similarities in assemblages along transects from 50°N to 50°S taken over three cruises, collected and analysed in a similar way, and compared these to some of the other regions in the Atlantic. Possible latitudinal trends in richness and size were analysed.

Method

Sampling was carried out on three Atlantic Meridional Transects (AMT) cruises on RRS James Clark Ross (Robins & Aiken, 1996) between 1997 and 1998 (Table 1, Fig. 1). Net samples were taken daily at approximately 400 km intervals.

Vertical net samples were taken from 200 m to the surface with a WP2 (200 μm mesh, mouth 0.25 m^2) net, on daily mid-morning stations, with occasional night stations. A 100% filtering efficiency was assumed. The zooplankton net samples were size-fractionated by screening the sample through 2000, 1000, 500 and 200 μm sieves to create fractions of 200-500, 500-1000, 1000-2000 and >2000 μm. Each size fraction was made up to 500 or 1000 ml with filtered seawater, depending on the density of zooplankton. Aliquots of 50 ml were filtered onto pre-ashed Whatman glass fibre GF/C filters (in triplicate), from each size fraction. Blanks were made by filtering 50 ml of the filtered seawater on to identical filters. The sample and blank filters were dried for 48 hours in a 60 °C oven before being wrapped in aluminium foil and compacted and stored at -20 °C. The samples were subsequently analysed for carbon and

nitrogen using a Carlo Erba 1500 CHN analyser. Five standards of acetanilide between 0.2 and 2 mg were used to derive a calibration curve. Further standards and blanks were interspersed with the sample pellets. The carbon and nitrogen biomass was corrected from the blanks and converted to mg m^{-3}.

The remainder of the sample was preserved with borax-buffered formalin (4%) for subsequent taxonomic identification. Copepod genera were identified within the four size classes (200-500, 500-1000, 1000-2000 and >2000 μm). A sub-sample was taken from a known volume using a Stempel pipette, so that a minimum of 200 copepods were identified. Where the number of copepods was less than 200 in the size fraction, the entire size fraction was counted. Copepods were analysed to genus level where possible. Small calanoid copepods such as *Paracalanus, Pseudocalanus* and *Clausocalanus* were not easily distinguished, and were grouped as "small calanoids".

Data analysis

The copepod genera abundances per cubic metre from the 200 m net samples were calculated. These abundances were transformed (double root), and used to produce a Bray-Curtis similarity matrix between samples. The double root transformation reduces the effect of the abundance, and emphasises the rarer genera. Multidimensional scaling (MDS) was carried out on the similarity matrix, using PRIMER (Plymouth routines in multivariate ecological research; Clarke & Warwick, 1994). MDS was used as it does not make parametric assumptions and condenses the information into an interpretable form, where the relative distances between samples is a measure of the sample similarity. Groupings of samples taken at similar latitudes were identified from the ordination. To allow greater detail of analysis of groups, the stations were separated into two groups: the temperate and Benguela stations, and

the warm water stations. MDS was carried out separately on each group. Regions identified visually were tested using analysis of similarity (ANOSIM) from PRIMER. SIMPER was used to identify the genera that were critical in differentiating regions.

The copepod genera from 0-200 m nets were used to calculate Margalef's richness using the number of genera and the number of individuals counted. Margalef's richness aims to compensate for differences in sample sizes. Although it does not entirely compensate, it is sufficient if the number counted is similar.

$D_{mg} = (S-1)/\ln N$

where D_{mg} is Margalef's richness, S is the number of genera counted, and N is the number of individuals counted. A second order polynomial was fitted to the genera richness related to latitude, after excluding the station from the Benguela region.

Changes in size along the AMT transects were investigated in several ways. The size fractionated counts for the 200 m net samples were used to calculate the proportion represented by each size fraction. The absolute number in each size fraction was also used. For each both the percentage and number 5 ^{o} means were calculated. The mean carbon content of an individual was calculated by dividing the total carbon by the number of individuals.

Results

Regions analysis

The MDS by genera similarity showed a clear distinction between the temperate plus the Benguela stations, and subtropical-tropical stations, for the double root transformed similarities (Fig. 2). The tropical-subtropical group showed greater similarity than the temperate and Benguela group. The separate MDS plot for temperate and Benguela stations

showed that the Benguela stations were different, but there was no obvious difference between the northern and southern temperate (Fig. 3). The tropical and subtropical MDS ordination is harder to interpret (Fig. 4). However, there do appear to be some latitudinal groupings. The subtropical stations (19°-39 °N, 29 °-39 °S) appear to separate from the tropical stations (18 °N-28 °S). The tropical stations showed partial separation into equatorial (8°S-18°N) and southern tropical (8°-28°S).

Analysis of the significance of the derived groups using ANOSIM showed that all groups were significantly different from each other, apart from the northern and southern temperate groups, the northern and southern subtropical groups, and the northern temperate and southern subtropical groups (Table 2). The R values, which indicate the strength of the grouping, were generally quite high. However, the R values were low for the northern subtropical and southern tropical comparison, and the northern and southern temperate groups' comparisons with the Benguela stations, in addition to those that were not significant, suggesting that these groups overlap.

Analysis of the genera determining the groups (SIMPER) revealed several genera were important in determining the differences between the groupings (Table 3). No genus explained more than 10 % of the difference, and the same genera were not always important. The high abundance of small calanoids, and the low abundance of *Lucicutia* and *Corycaeus* were important in defining Group 1, the northern temperate stations. Group 2 and Group 5 (northern and southern subtropical) had high *Acartia*, groups 3 and 4 (equatorial and southern tropical) had no genera which consistently discriminated them from other groups, and Group 6 had high *Oithona*, and low *Oncaea* and *Corycaeus*. Generally, the temperate stations had

fewer genera than the tropical and subtropical stations, and were more dominated by small calanoids and *Oithona* (Table 4).

Latitudinal changes

Margalef's richness for the copepod genera along the transect showed a significant dome (R^2=0.652, N=101 F=92.75, P<0.001), with genera diversity being greater closer to the equator, although the Benguela stations from AMT6 fell into a cluster below the main curve (Fig. 5). For samples grouped in 5° bands, the number of copepod genera was significantly affected by latitude (R^2=0.673, F=17.48, P=0.0001), being maximal north of the equator and decreasing south of the equator.

For the 200 m size fractionated net samples, neither the percentage nor the absolute number in each size class suggested any increase in size with latitudinal trend (Fig. 6 & 7). If anything, size decreased in the higher northern latitudes. In general, the number in each size class was quite uniform, with a few stations with considerably higher abundances. In addition, the proportion in each size class was quite consistent, with the smallest size fraction dominating having on average 74 %, and only 1 % in the largest size fraction (Table 5). The Benguela stations did, however, have appreciably higher counts in the 500-1000 and 200-500 μm size categories.

Mean carbon content per zooplankter varied (Fig. 8), with the interquartile range of 0.003-0.01 mg C, and a maximum of 0.047 mg C. Carbon per zooplankter was generally lower on AMT 5 as expected as no >2000 μm fraction was included in the analysis. AMT 6 showed two peaks in the southern hemisphere which were likely to be artefacts, one at 25°S and the other at 17°S. These samples contained large quantities of the large diatom *Coscinodiscus*

wailesii, which was not counted. In all other samples the amount of phytoplankton was negligible. There was a peak at the southern end of the transect, most pronounced on AMT4 (0.03 mg C). The mean carbon per zooplankter was consistently low across the southern oligotrophic gyre, at around 0.01mg C on AMT4 and 0.0025 mg C on AMT5. One of the most pronounced features was a peak in mean zooplankter size between approximately 10 and 25 ^{o}N. Further north the mean carbon fell to similar levels as in the southern oligotrophic gyre.

Discussion

Regions

The copepod genera from the AMT cruises fell into two major groups of similarity: the warm water stations, and the temperate and Benguela stations. Further analysis differentiated the temperate from the Benguela stations. The warm water stations could be further subdivided into equatorial, tropical and subtropical regions. Analysis of similarity showed that the north and south temperate stations were not significantly different from each other, neither were the north and south subtropical stations; more surprisingly, the north temperate and south subtropical stations were not significantly different. The similarity of the north and south pairs of temperate and subtropical regions may be a result of generic level classification; more detailed taxonomy may have distinguished these regions, as sympatriots are frequently found in each hemisphere, e.g. *Calanus helgolandicus* and *Calanus australis* (van der Spoel & Heyman, 1983). Others have found that the same species are present in both the northern and southern subtropical zone, e.g. Ekman (1953) noted the abundance of "warm water cosmopolites".

Several other attempts have been made to divide the ocean into meaningful areas based on physical, chemical and biological properties. However, the present study is one of the few

extensive surveys using data from one study rather than composite. The boundaries of the divisions of the different schemes, although they may be similar and even overlapping, are not the same. Fig. 9 illustrates a number of biogeographic schemes commonly used to characterise the Atlantic Ocean. The schemes do not agree closely, even considering the regional boundaries are not necessarily sharp due to expatriation (e.g. Ekman, 1953), and vary by a few degrees depending on season and currents (e.g. Boltovskoy, 1997; Backus, 1986). Overall, the groups derived from copepod genera derived groups most closely match those of Backus (1986), except that this study identified an extra region between 28 and 38 °S. Backus (1986) admitted feeling uneasy with his divisions of the southern Atlantic Ocean.

Latitudinal changes

The latitudinal analysis of copepod genera richness showed a pronounced trend, with Margalef's richness falling from around 9 at the equator to less than 5 at 40°. This demonstrated a trend found for other organisms (e.g. Angel, 1993; Reid et al., 1978; Rutherford et al., 1999). The samples from the Benguela upwelling region (AMT 6) showed lower diversity in terms of copepod genera richness than those samples from the open ocean. Upwelling areas frequently show lower diversity than the adjacent open ocean (Angel, 1993).

The mean size of copepods, indicated by the number and the proportion in size fraction, is remarkably stable along the AMT transect, with around 74% in 200-500, 20 % in 500-1000, 5 % 1000-2000 and 1% >2000 μm, and does not show an obvious trend with latitude. Many of the larger copepods undergo considerable diel vertical migration, so may not be present in the surface 200m during the day. Either more night net samples or deeper nets are required to test whether diel migration is affecting observed trends. The mean carbon per individual did show a pattern, with low individual size was found across the northern and southern oligotrophic

gyre. Large size was also found in the Benguela upwelling where *Calanoides carinatus* is frequently the dominant copepod (Verheye et al., 1992). The small size in the tropical gyres is consistent with the view that small copepods dominate the zooplankton of the oligotrophic gyres (e.g. Piontkovski & van der Spoel, 1997).

Conclusions

The copepod genera can be used to divide the ocean into regions of similarity. The temperate and Benguela regions showed very different taxonomic structure than the warm water stations. Northern and Southern temperate and subtropical areas are more similar to each other than to adjacent areas. Temperate stations also varied more in their taxonomic structure than warm water stations. Further subdivision of the regions derived latitudinal regions similar to those developed by Backus (1986) from pelagic systems.

Copepod genera richness decreased towards higher latitudes. In addition, copepod genera richness is lower in the Benguela upwelling than in the open ocean at similar latitude. The size distribution of copepods did not show strong trends over these 50 ^{o}N to 50 ^{o}S transects. But the numbers and proportions in each size fraction were quite consistent. The mean size indicated by the mean carbon per individual suggests that the mean size of zooplankton was lower in the oligotrophic gyres.

Acknowledgements

I wish to thank the officers and crew of the British Antarctic Survey research ship RRS James Clarke Ross during the AMT cruises. I am most grateful to Bob Head (CCMS-PML) for his help with the carbon analysis, to Dave Conway for his help identifying copepods, and to my supervisors Roger Harris, Derek Pilgrim and Dave Robins for their support and advice. This

work was supported by the Natural Environmental Research Council PRIME special topic grant (GST/02/1068) and by a University of Plymouth studentship. This is publication no. 42 of the AMT programme.

References

Angel, M. V., 1993. Biodiversity of the pelagic ocean. Cons. Biol. 7: 760-772.

Angel, M. V., 1997. Pelagic biodiversity. In R. F. G. Ormond, J. D. Gage, & M. V. Angel (eds.), Marine Biodiversity: Patterns and Processes. Cambridge University Press. Cambridge: 35-68.

Backus, R. H., 1986. Biogeographic boundaries in the open ocean. In: A. C. Pierrot-Bults, S. van der Spoel, B. J. Zahuranec, & R. K. Johnson (Eds.), Pelagic Biogeography. UNESCO, Paris: 9-13.

Backus, R. H., J. E. Craddock, R. L. Haedrich & B. H. Robinson, 1977. Atlantic mesopelagic zoogeography. Fishes of the western North Atlantic. Mem. Sears Fdn Mar. Res.1: 266-287.

Bainbridge, V., 1972. The zooplankton of the Gulf of Guinea. Bull. Mar. Ecol. 8: 61-97.

Bé, A. W. H., 1977. An ecological, zoogeographic and taxonomic review of recent planktonic Foraminifera. In A. T. S. Ramsey (ed.), Oceanic Micropalaeontology. Academic Press, London: 1-100.

Boltovskoy, D., 1997. Pelagic biogeography: background, gaps and trends. In: A. C. Pierrot-Bults, S. van der Spoel, B. J. Zahuranec, & R. K. Johnson (Eds.), Pelagic Biogeography. UNESCO, Paris: 53-64.

Boltovskoy, D., 1986. Biogeography of southwestern Atlantic: overview, current problems and perspectives. In: A. C. Pierrot-Bults, S. van der Spoel, B. J. Zahuranec, & R. K. Johnson (Eds.), Pelagic Biogeography. UNESCO, Paris: 14-24.

Brinton, E., 1962. The distribution of Pacific Euphausiids. Bull. Scripps Inst. Oceanogr. Uni. California 8: 51-270.

Clarke, K. R. & R. M. Warwick, 1994. Change in marine communities: An approach to statistical analysis and interpretation. Plymouth Marine Laboratory. Plymouth, 144 pp.

Colebrook, J. M., 1982. Continuous Plankton Records: seasonal variation in the distribution and abundance of plankton in the North Sea. J. Plankton Res. 4:435-462.

Dadon, J. R. & D. Boltovskoy, 1982. Zooplanktonic recurrent groups (Pteropoda, Euphausia, Chaetognatha) in the southwestern Atlantic ocean. Physis (Buenos Aires) 41: 63-83.

Ekman, S., 1953. Zoogeography of the Sea. Sidgewick & Jackson, London 417pp.

Gallienne, C. P., D. B. Robins & R. S. Woodd-Walker, In Press. Abundance and distribution of mesozooplankton along a 20° west meridional transect of the north Atlantic Ocean. Deep Sea Res.

Gibbons, M. J., 1997. Pelagic biogeography of the South Atlantic Ocean. Mar. Biol. 129: 757-768.

Longhurst, A., S. Sathyendranah, T. Platt, & C. Carverhill, 1995. An estimate of global primary production in the ocean from satellite radiometer data. J. Plankton Res. 17: 1245-1271.

McGowan, J. A., 1974. The nature of oceanic ecosystems. In: C. B. Miller (Ed.), The Biology of the Oceanic Pacific. Oregon State University Press, Oregon: 9-28.

McGowan, J.A., 1986. The biogeography of pelagic ecosystems. In: A. C. Pierrot-Bults, S. van der Spoel, B. J. Zahuranec, & R. K. Johnson (Eds.), Pelagic Biogeography. UNESCO, Paris: 191-200.

Piontkovski, S. A. & S. van der Spoel, 1997. Similarities in size, in taxonomic and in ecological mesoscale structure of tropical zooplankton communities. Intergovernmental Oceanographic Commission Workshop Report 142: 297-306.

Reid, J. L., E. Brinton, A. Fleminger, E. L. Venrick, & J. A. McGowan, 1978. Ocean circulation and marine life. In: H. Charnock & G. Deacon (Eds.), Advances in Oceanography. Plenum Press, London: 65-130.

Robins, D. B., & J. Aiken, 1996. The Atlantic Meridional Transect: an oceanographic research programme to investigate physical, chemical, biological and optical variables of the Atlantic Ocean. Underwater Technol. 21:8-14.

Rutherford, S., D'Hondt, S. & Prell, W. (1999) Environmental controls on the geographic distribution of zooplankton diversity. Nature 400: 749-753.

van der Spoel, S., & R. P. Heyman, 1983. A Comparative Atlas of zooplankton, Biological Patterns in the Oceans. Wetenschappelijke Uitgeverji Bunge, Utrecht, 186 pp.

Verheye, H.M., Hutchings, L., Huggett, J.A. and Painting, S.J. (1992) Mesozooplankton dynamics in the Benguela ecosystem, with emphasis on the herbivorous copepods. South African Journal of Marine Science 12: 561-584.

Williams, R., D. V. P. Conway, & H. G. Hunt, 1994. The role of copepods in the planktonic ecosystems of mixed and stratified waters of the European shelf seas. Hydrobiologia 292: 521-530.

Tables

Table 1: Summary of Cruises

Cruise	Dates	Track
AMT4	April-May 1997	Falklands-UK
AMT5	Sept-Oct 1997	UK-Falklands
AMT6	May-June 1998	South Africa-UK

Table 2: Analysis of similarity of the genera derived groups (double root transformed. Global R=0.569, P<0.1%,N=115), with 5000 permutations used. Group1: northern temperate (>38 °N), Group 2: northern subtropical (18-38 °N), Group 3: equatorial (8 °S-18 °N), Group 4: southern tropical (8-28 °S), Group 5: southern subtropical (28-38 °S), Group 6: southern temperate (>38 °S), group7: Benguela. * groups that were not significantly different from each other.

Groups Used	R	Significant Statistics	Significance Level
(1, 2)	0.686	0	0.0%
(1, 3)	0.815	0	0.0%
(1, 4)	0.633	0	0.0%
(1, 5)	0.129	588	11.8%*
(1, 6)	0.035	1415	28.3%*
(1, 7)	0.460	0	0.0%
(2, 3)	0.443	0	0.0%
(2, 4)	0.177	20	0.4%
(2, 5)	-0.035	2978	59.6%*
(2, 6)	0.916	0	0.0%
(2, 7)	0.949	0	0.0%
(3, 4)	0.294	0	0.0%
(3, 5)	0.482	0	0.0%
(3, 6)	0.944	0	0.0%
(3, 7)	0.989	0	0.0%
(4, 5)	0.507	0	0.0%
(4, 6)	0.893	0	0.0%
(4, 7)	0.971	0	0.0%
(5, 6)	0.568	1	0.0%
(5, 7)	0.876	0	0.0%
(6, 7)	0.511	0	0.0%

Table 3: The rank importance of genera for determining the differences between groups for genera explaining either 5% or more of the total difference or the top 5 ranked, with the % in brackets. The mean dissimilarity between groups and if it was not significant (NS) in the ANOSIM is also shown. Group 1: northern temperate, Group 2: northern subtropical, Group 3: equatorial, Group 4: southern tropical, Group 5: southern subtropical, Group 6: southern temperate.

Groups	1v2	1v3	4v1	5v1	6v1	3v2	4v2	5v2	6v2	4v3	5v3	6v3	5v4	6v4	6v5
Mean dissimilarity (%)	39.2	41.9	41.9	36.7 (NS)	37.1 (NS)	28.9	26.3	25.2 (NS)	44.8	24.9	27.0	46.3	24.5	48.0	41.5
Genera															
small calanoids	1 (6)	4 (5)	1 (7)	3 (6)	2 (6)					3 (4)			3 (5)	4 (4)	
Oithona	4 (5)		3 (5)	5 (5)	1 (6)				3 (5)			3 (4)		2 (5)	5 (5)
Oncaea		2 (5)			3 (6)				4 (5)	1 (5)		2 (6)		5 (4)	3 (6)
Corycaeus	3 (6)	1 (5)	2 (6)	2 (6)					1 (7)			1 (7)		1 (8)	1 (8)
Calanus					7 (5)										
Copepodites															
Acartia	5 (5)			4 (5)	6 (5)	3 (5)	4 (5)	3 (5)	2 (7)		1 (5)		2 (6)		2 (7)
Euchaeta															
Eucalanus						1 (5)	5 (4)			2 (5)					
Pleuromamma					5 (6)		1 (5)	2 (5)		4 (4)	4 (4)		1 (8)		
Metridia					4 (6)			5 (4)				4 (4)	5 (4)	3 (5)	
Lucicutia	2 (6)	3 (5)	4 (5)	1 (6)					5 (5)			5 (4)			4 (5)
Solecithrix		5 (4)	5 (4)												
Undinula						2 (5)	2 (5)								
Macrosetella						4 (4)					2 (5)				
Calocalanus						5 (4)	3 (5)	1 (6)			3 (5)		4 (4)		6 (5)
Temora								4 (4)							
Rhincalanus										5 (4)	5 (4)				

Table 4: Mean abundance of the genera (m^{-3}), for each Group. (Group 1: northern temperate, Group 2: northern subtropical, Group 3: equatorial, Group 4: southern tropical, Group 5: southern subtropical, Group 6: southern temperate, Group 7: Benguela. – indicates absence, 0.0 indicates mean abundance <0.1 m^{-3})

Genera	1	2	3	4	5	6	7
Acartia	34.5	11.2	2.8	1.9	7.7	0.1	0.4
Aegisthus	0.2	0.0	-	-	-	0.3	-
Aetideopsis	-	0.0	-	-	-	-	-
Aetideus	0.6	0.1	0.2	0.1	0.0	0.3	0.2
Arientellus	-	0.0	0.0	0.0	0.0	0.5	-
Augaptilus	-	0.0	-	-	-	-	-
Calanoides	0.3	0.1	4.8	1.1	16.1	15.4	50.9
Calanus	48.1	6.1	13.8	5.0	12.2	15.0	3.2
Calocalanus	1.1	1.7	1.3	1.4	2.4	0.0	0.3
Candacia	0.8	0.4	0.4	0.6	0.4	0.5	0.3
Centropages	5.6	0.5	6.2	1.6	21.1	0.7	34.4
Clytemnestra	0.3	0.1	0.1	0.0	-	8.7	-
Copepodites	38.7	7.5	9.7	5.1	10.4	8.5	38.3
Copilia	0.0	0.1	0.1	0.1	0.0	0.0	-
Corycaeus	7.7	8.6	7.4	11.0	6.4	0.1	0.5
Euaetideus	0.3	0.2	0.1	0.2	0.0	0.1	0.1
Euagaptilus	0.6	0.0	0.0	0.0	-	0.4	-
Eucalanus	1.6	1.4	0.6	0.5	0.6	1.1	0.1
Euchaeta	2.0	2.9	2.7	3.3	2.3	1.1	0.1
Euchirella	0.1	0.1	0.2	0.0	0.2	0.4	-
Gaetanus	0.0	0.1	0.0	0.0	0.0	0.0	-
Haloptilus	0.3	1.3	0.3	0.6	0.1	0.1	-
Heteorstylites	0.0	-	-	-	-	-	-
Heterorhabdus	0.5	0.5	0.3	0.3	0.3	0.1	-
Labidocera	0.0	0.0	0.1	0.3	-	-	-
Lubbockia	-	0.1	0.0	0.0	-	0.2	-
Lucicutia	0.1	2.8	1.5	1.5	2.6	0.2	0.0
Macrosetella	0.3	0.2	0.1	0.2	0.0	-	0.1
Metridia	3.6	0.5	2.6	0.2	4.9	70.9	139.0
Miracia	-	0.0	-	-	-	-	-
Oithona	144.0	26.1	72.6	23.2	91.1	71.9	240.8
Oncaea	23.5	22.3	15.4	17.3	22.0	81.8	12.3
Pachos	-	0.0	0.0	0.0	-	2.3	-
Phaenna	0.0	0.1	0.0	0.1	0.0	4.9	-
Phyllopus	0.0	0.0	-	-	-	-	-
Pleuromamma	2.0	2.9	4.9	0.6	7.8	4.9	1.3
Pontellina	-	0.0	0.0	0.0	-	0.0	-
Pseudoeuchaeta	-	0.0	0.0	-	-	0.9	-
Rhincalanus	0.7	0.1	0.6	0.1	0.1	0.9	1.6
Sapphirina	0.0	0.3	0.1	0.2	0.1	0.0	-
Scaphocalanus	-	0.0	-	-	-	-	-
Scolecithrix	0.0	0.2	0.4	0.6	0.2	0.0	0.0
Scolethricella	0.1	0.5	0.2	0.3	0.1	0.1	-
Scottocalanus	-	0.0	0.0	-	-	0.0	-
Small calanoids	313.8	71.0	99.9	45.0	126.7	78.5	284.3
Temora	0.1	0.1	0.4	0.5	0.5	0.1	-
Undeuchaeta	0.1	0.1	0.0	0.0	0.1	-	-
Undinula	0.0	0.1	0.4	0.5	0.3	0.0	0.0
No. Samples	17	27	36	16	9	10	11
No. Genera	38	47	41	39	33	39	22

Table 5: The number in each size fraction with standard deviation (S.D.), and percentage

Size fraction	Mean counts	Counts S.D.	Mean %	% S.D.
200-500	294	350	74	10.5
500-1000	75	83	20	7.6
1000-2000	17	19	5	4.0
>2000	2.6	4	1	1.3
Total	389	426	100	

Figure captions

Fig. 1: AMT cruise track

—— AMT track for AMT 4&5

····· AMT 6

Fig. 2: Multidimensional scaling (MDS) ordination for copepod genera (AMT 4-6), Bray-Curtis similarity double root transformed, stress = 0.14. Distance between points shows the similarity in copepod composition and is relative. Legend refers to stations within that latitudinal band, except Benguela Stations 17-35 °S on AMT 6.

Fig. 3: Multidimensional scaling (MDS) ordination for copepod genera (AMT4-6) for north and south temperate and the Benguela stations, Bray-Curtis similarity double root transformed, stress = 0.14. Distance between points shows the similarity in copepod composition, and is relative. Latitude is shown above the symbol.

Fig. 4: Multidimensional scaling (MDS) ordination for copepod genera (AMT4-6) for the tropical and subtropical stations, Bray-Curtis similarity double root transformed, stress = 0.14. Distance between points shows the similarity in copepod composition and is relative. Legend refers to stations within that latitudinal band (- is south)

Fig. 5: The relationship between Margalef's genera richness (D) and latitude. A 2nd order polynomial is fitted, excluding the stations from the Benguela upwelling, as these appear to be less diverse. $R^2 = 0.652$, $y = -0.0020 x^2 + 0.0085 x + 9.159$, $F=92.75$, $P<0.001$. (- south, + north)

Fig. 6: Percentage of the total number of copepods in each size fraction for AMT 4-6. a) >2000, b) 1000-2000, c)500-1000 and d) 200-500 μm. The mean is the average for 5 ° intervals, not including Benguela Stations.

Fig. 7: The total number of organisms in each size fraction for AMT 4-6. a) >2000, b) 1000-2000, c)500-1000 and d) 200-500 μm. The mean is the average for 5 ° intervals, not including Benguela Stations.

Fig. 8: Variation in mean carbon per individual along the transect for AMT 4-6. AMT 5 does not include >2000 size fraction, as no carbon was measured.

Fig. 9: Inter-comparison of latitudinal groups along the AMT. 1 – genera derived groups, 2-pelagic organisms (Backus 1986), 3 - pelagic (Boltovskoy 1997), 4 – zooplankton (van der Spoel & Heyman 1983), 5 – generalised oceanographic regions (van der Spoel & Heyman 1983), 6 – Foraminifera (Bé 1977), 7 - Watermasses (van der Spoel & Heyman 1983), 8 - biogeochemical (Longhurst & Platt 1995). (FKLD – SW Atlantic shelf, SALT – S. Atlantic gyre, WTRA – W. tropical Atlantic, NATR – N. Atlantic tropical gyre, NAST – N. Atlantic subtropical gyre, NADR – N. Atlantic drift, NECS – N.E. Atlantic shelf, Temp. – temperate, Subtrop. – subtropical, T&ST – temperate and subtropical.)

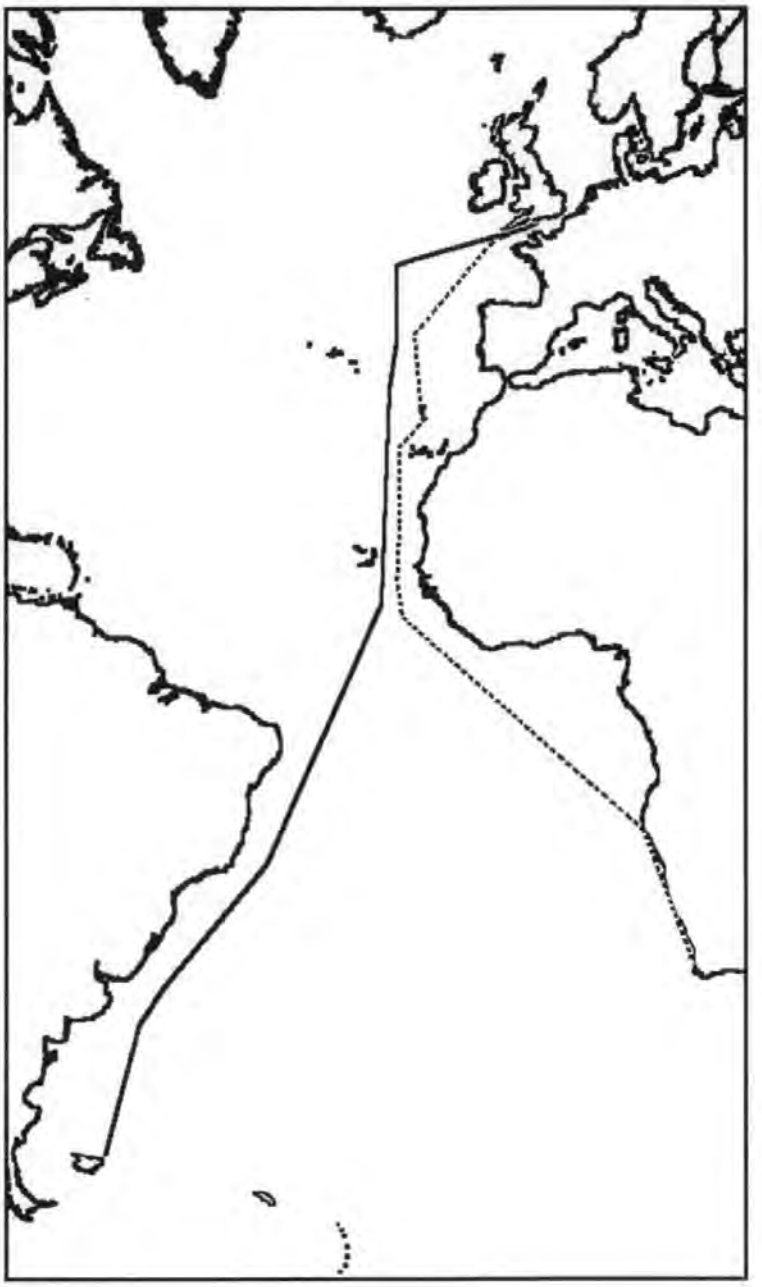

Fig. 1

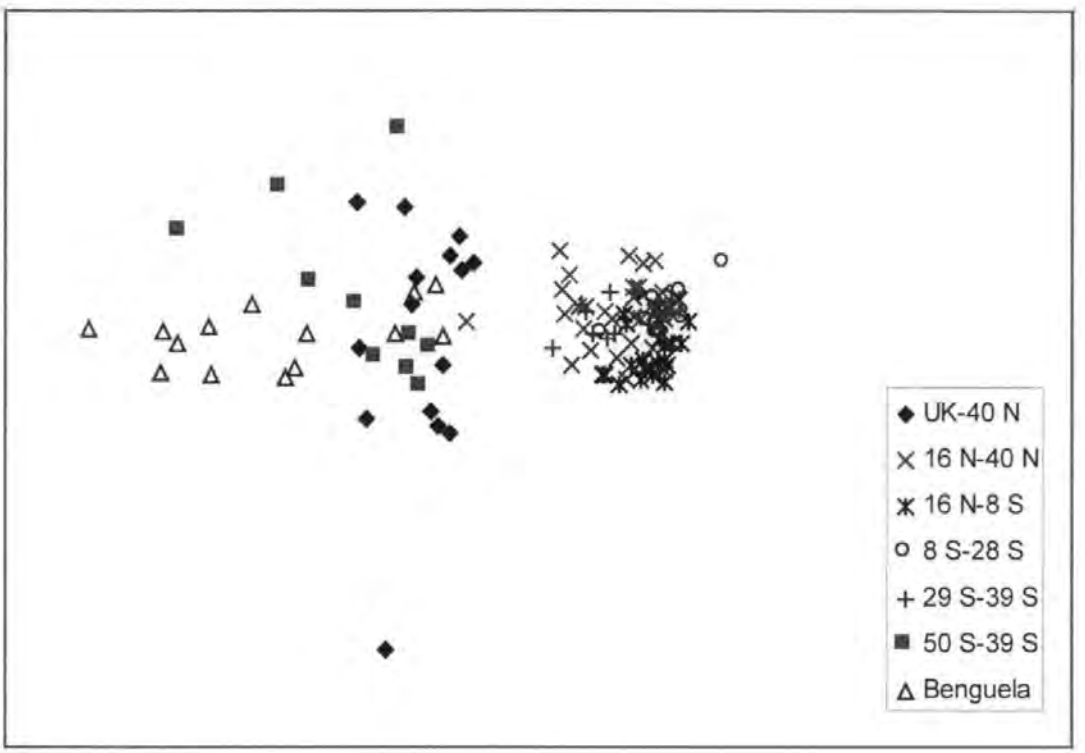

Fig. 2

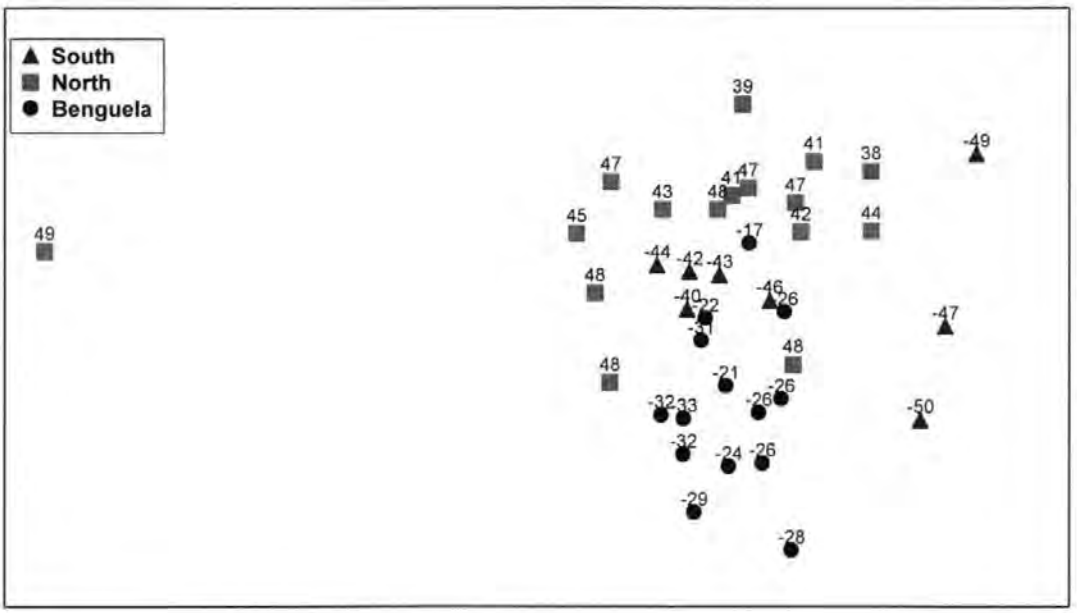
South
North
Benguela
39
41
38
-49
47
47
41
47
43
48
42
44
45
-17
49
-44
-42
-43
48
-40
-46
-26
-47
48
48
-21
-26
-32
33
-26
-50
-32
-24
-26
-29
-28

Fig. 3

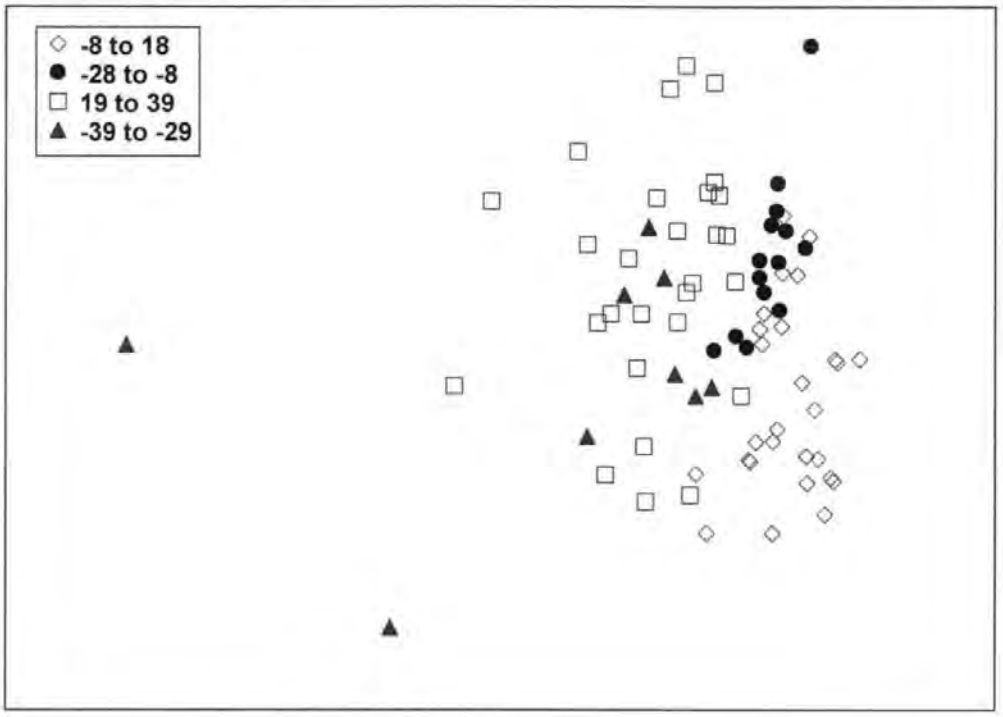

Fig. 4

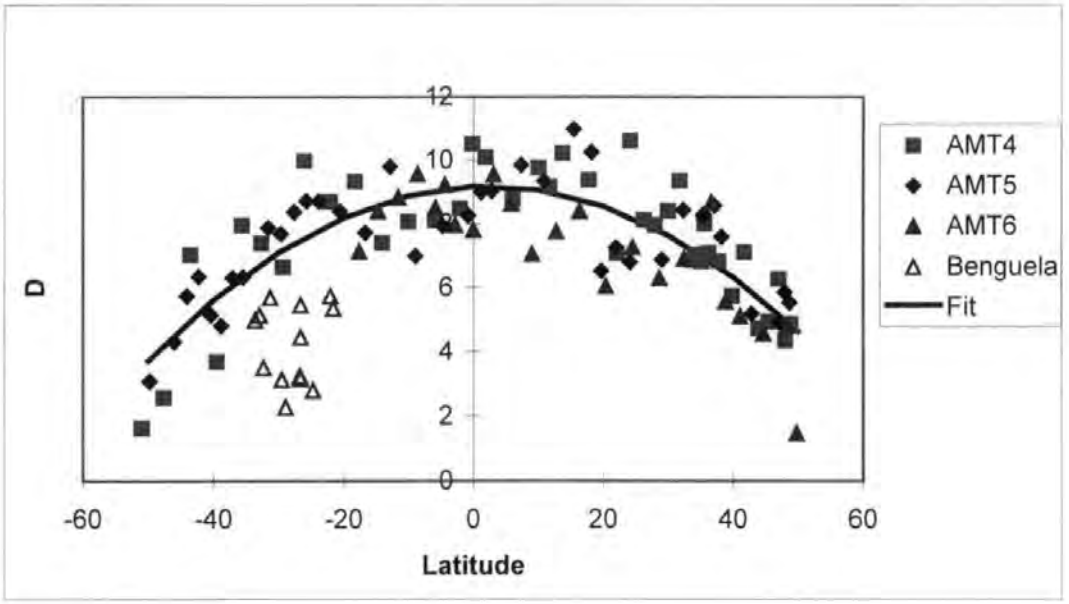
12
10
8
6
4
2
0
D
-60
-40
-20
0
20
40
60
Latitude
AMT4
AMT5
AMT6
Benguela
Fit

Fig. 5

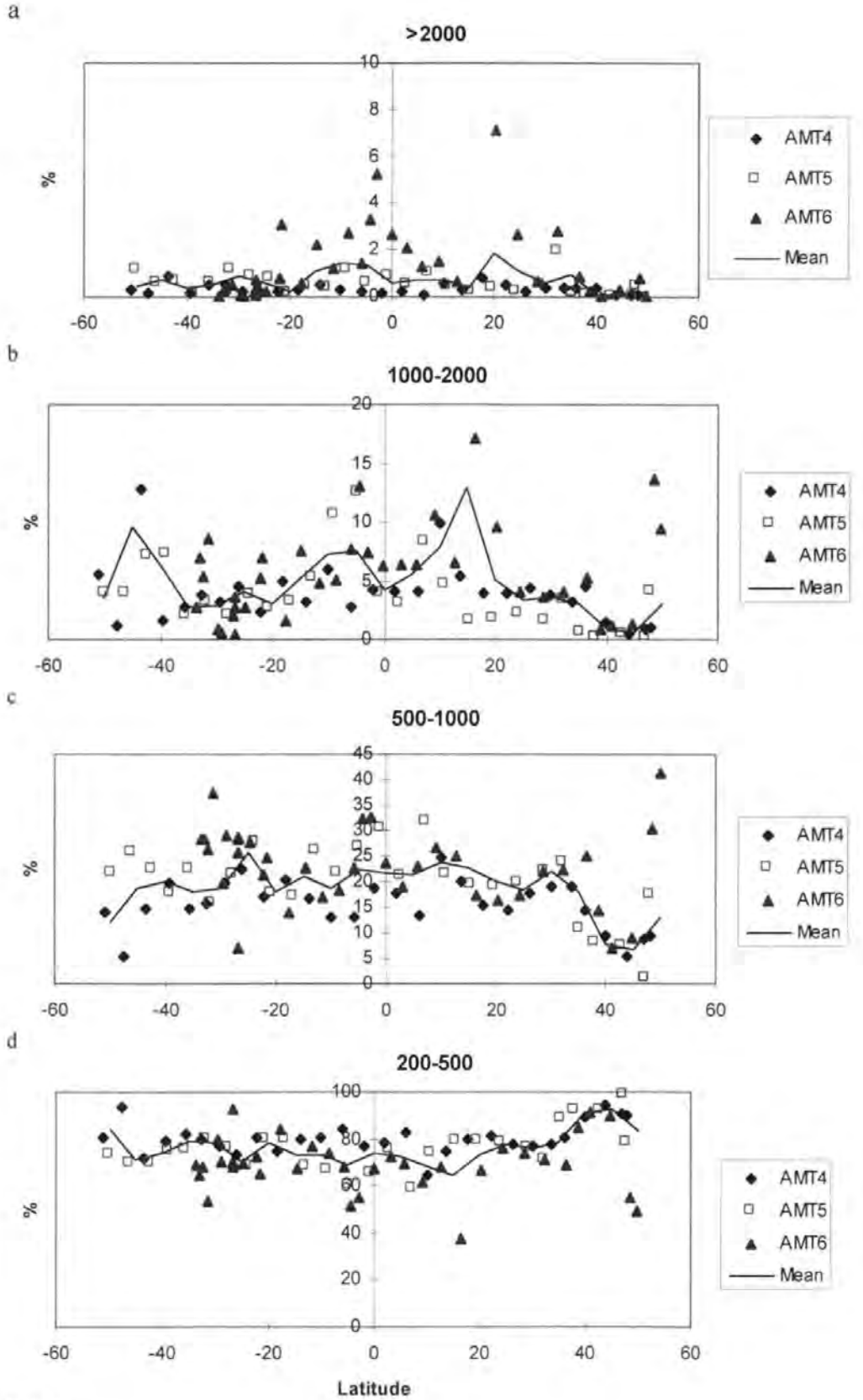
a
>2000
%
AMT4
AMT5
AMT6
Mean
b
1000-2000
%
AMT4
AMT5
AMT6
Mean
c
500-1000
%
AMT4
AMT5
AMT6
Mean
d
200-500
%
AMT4
AMT5
AMT6
Mean
Latitude

Fig. 6

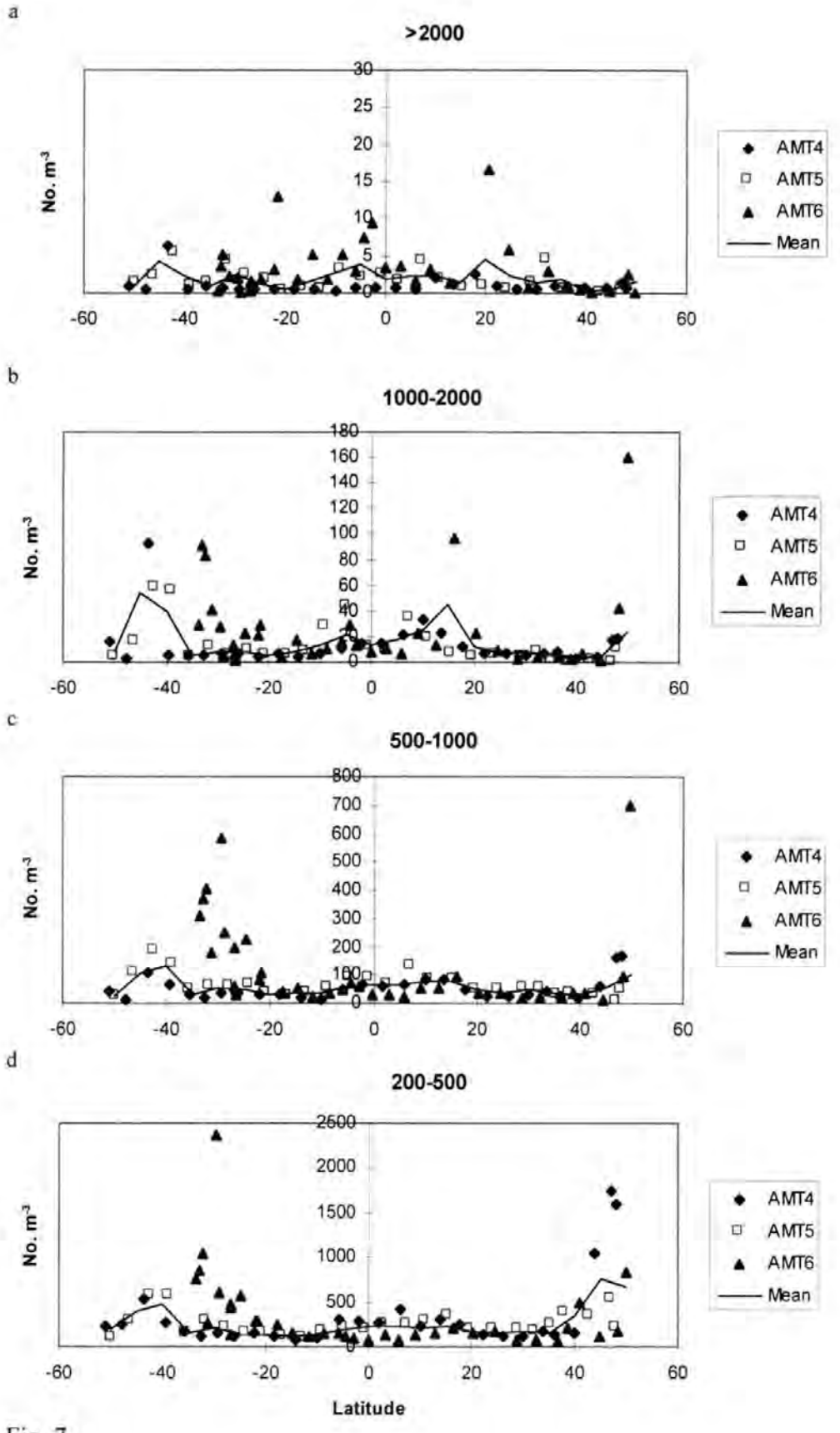
a
>2000
No. m-3
AMT4
AMT5
AMT6
Mean
b
1000-2000
No. m-3
AMT4
AMT5
AMT6
Mean
c
500-1000
No. m-3
AMT4
AMT5
AMT6
Mean
d
200-500
No. m-3
AMT4
AMT5
AMT6
Mean
Latitude

Fig. 7

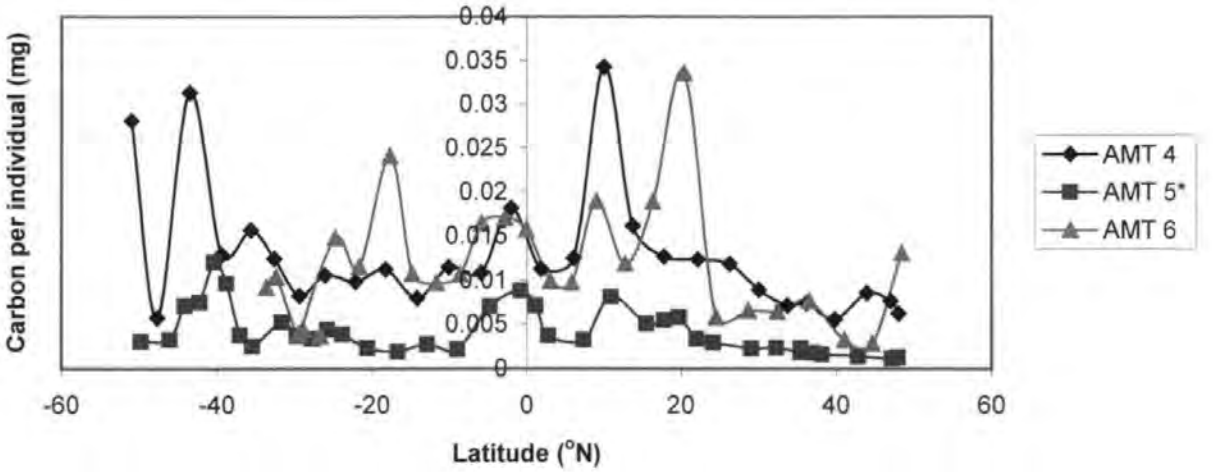
Carbon per individual (mg)
0.04
0.035
0.03
0.025
0.02
0.015
0.01
0.005
0
-60
-40
-20
0
20
40
60
Latitude (°N)
AMT 4
AMT 5*
AMT 6

Fig. 8

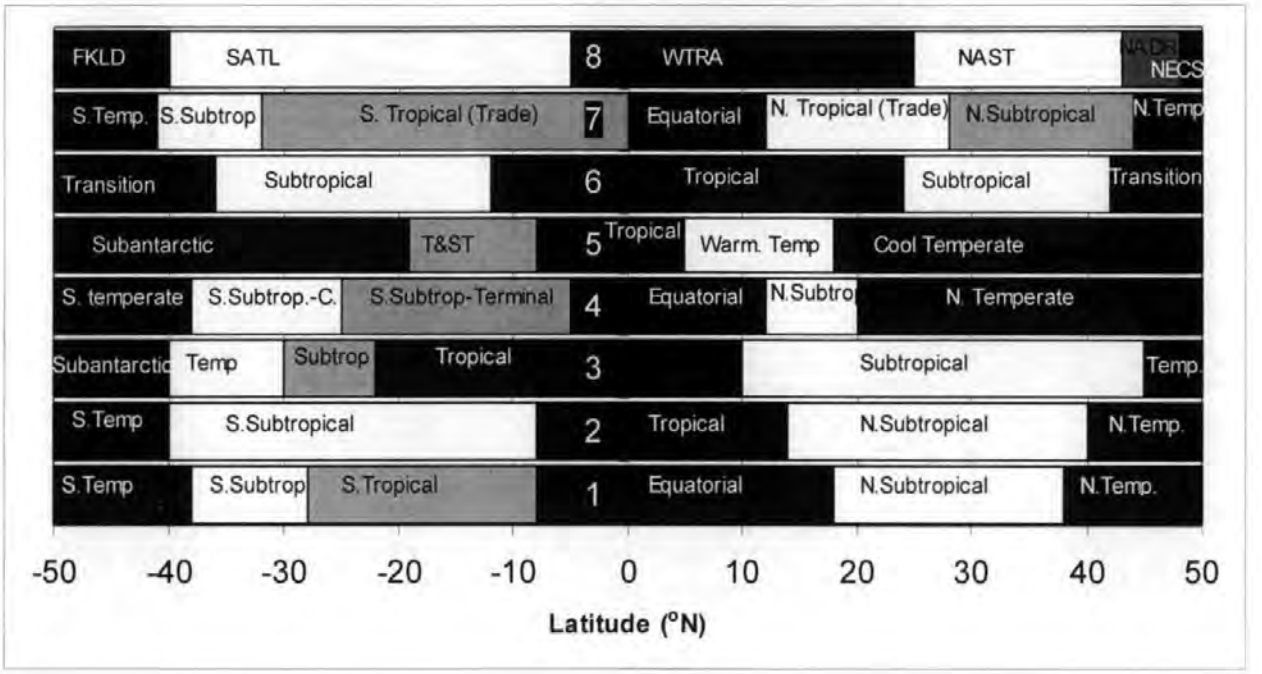
FKLD
SATL
8
WTRA
NAST
NECS
S.Temp.
S.Subtrop
S. Tropical (Trade)
7
Equatorial
N. Tropical (Trade)
N.Subtropical
N.Temp
Transition
Subtropical
6
Tropical
Subtropical
Transition
Subantarctic
T&ST
5
Tropical
Warm. Temp
Cool Temperate
S. temperate
S.Subtrop.-C.
S.Subtrop-Terminal
4
Equatorial
N.Subtro
N. Temperate
Subantarctic
Temp
Subtrop
Tropical
3
Subtropical
Temp.
S.Temp
S.Subtropical
2
Tropical
N.Subtropical
N.Temp.
S.Temp
S.Subtrop
S.Tropical
1
Equatorial
N.Subtropical
N.Temp.
-50
-40
-30
-20
-10
0
10
20
30
40
50
Latitude (°N)

Fig. 9

Using neural networks to predict surface zooplankton biomass along a 50°N to 50°S transect of the Atlantic

Woodd-Walker, R.S.[1], K.S. Kingston[1], C.P. Gallienne[2]

[1]Institute of Marine Studies, University of Plymouth, Drake Circus, Plymouth PL4 8AA, United Kingdom, email: r.woodd-walker@plymouth.ac.uk

[2]CCMS-Plymouth, Prospect Place, West Hoe, Plymouth PL1 3DH, United Kingdom

Abstract

Four Atlantic transects between UK and Falkland Islands were carried out during spring and autumn as part of the Atlantic Meridional Transect (AMT) programme. These 50°N to 50°S transects cross several ocean regions. An optical plankton counter (OPC-1L) sampled continuously along the transects from the ship's uncontaminated seawater supply, giving a surface distribution of zooplankton abundance and size. Measurements of underway fluorescence derived chlorophyll, sea surface temperature and salinity were also taken from the uncontaminated seawater supply. The relationship between zooplankton biomass and these variables was investigated using multiple linear regression and neural network techniques. In the analysis, $\log_e$ transformed biomass was used to reduce the impact of extreme values. Two transects were used to develop the models, and two to test the generalisation capabilities of the models. Multiple linear regression could explain up to 55% of the observed variation in the transformed biovolume, and demonstrated the impact of hydrographic variables and diel migration on the surface zooplankton community. Neural networks, starting with the same set of variables, were able to explain up to 78% of the variability, showing an increased performance over the multivariate analysis. An optimised model

accounted for 77% of the variance in the original data. However, it showed greater generalisation capabilities (R^2=0.47) when applied to new data sets than either the original neural network model (R^2=0.37) or the multiple linear regression model (R^2=0.34). This study highlights the non-linear nature of the parameters' impact on the zooplankton biomass and their variability between oceanographic regions.

Key words: neural networks, zooplankton, biomass, multiple linear regression

Introduction

Zooplankton play a vital role in marine ecosystems. Zooplankton impact systems through grazing and nutrient recycling, affecting the productivity of the system (e.g. Banse 1995). In addition, zooplankton impact higher trophic levels, with higher abundance of zooplankton frequently associated with higher concentrations of fish (e.g. Maravelias and Reid 1997, Aoki and Komatsu 1997). Transport of biomass from the surface waters to depth is increased by the zooplankton via their vertical migration and through sinking faecal pellets (Longhurst and Harrison 1988, Longhurst *et al.* 1990, Morales 1999). Huntley and Lopez (1992) suggest that zooplankton biomass is the most important factor in determining zooplankton productivity. Thus understanding what controls zooplankton abundance is necessary for understanding carbon uptake by the oceans and for fisheries studies.

Zooplankton abundance has generally been modelled from a theoretical perspective within ecosystem models rather than to model zooplankton themselves, as in for example NPZ (nutrients-phytoplankton-zooplankton) models (e.g. Frost 1993, Frost &

Franzen 1992). Ecosystem models make several assumptions at each trophic level about their interactions. However, Aoki et al. (1999) modelled zooplankton biomass empirically in response to long-term changes in the hydrography, in the northeastern sea area of Japan. The model could predict smoothed mean annual abundance of zooplankton quite accurately within this region (root mean square error <10%). Other empirical zooplankton models tend to concentrate on production of part of the lifecycle or other specific aspects of zooplankton e.g. copepod egg production (Calbet & Agustí 1999, Prestige et al. 1995), diel migration (Richards et al. 1996). Other studies have looked at the relationship between zooplankton abundance and specific hydrographic events e.g. flows in the northeastern Atlantic (Stephens et al. 1998), shifts in the Gulf Stream (Taylor 1995). But, in general, models predicting biomass are restricted to particular regions.

Here, we take an empirical approach to modelling surface zooplankton abundance across a wide range of oceanic regimes from easily measured parameters to allow future prediction and to give insight into the physical forcing on zooplankton abundance. Initially we use simple multiple linear regression, which is straightforward to interpret, but limited by the underlying assumption of linearity. The model is extended by using the more advanced technique of artificial neural networks (Rummelhart et al. 1986) which has recently been employed as a tool for modelling complex ecological systems (Lek and Guégan 1999), allowing non-linear interactions to be incorporated.

Method

Field sampling

Sampling was carried out on four Atlantic Meridional Transects (AMT) cruises on the RRS James Clark Ross between UK and Falklands (Robins & Aiken 1996; Table 1, Fig. 1). This 50°N to 50°S transect passes through a wide range of oceanographic regimes from temperate seasonal stratified, through subtropical oligotrophic gyres to equatorial current systems.

Fluorescence derived chlorophyll, temperature, salinity and zooplankton biovolume were measured using automated sensors from the uncontaminated seawater supply. The uncontaminated seawater was pumped from beneath the ship's keel from an extensible intake protruding approximately 30cm, and at about 7m depth. The intake had a 6mm steel mesh filter allowing mesozooplankton to pass through whilst removing larger objects which might damage the pumps. Fluorescence was measured using a Turner Model 10 fluorometer. The temperature and salinity were measured using a thermosalinograph (Sea-Bird Electronics). The data from the fluorometer and thermosalinograph, and total incident solar radiation (TIR) were logged into the ship's Ocean Logger system. An optical plankton counter (OPC-1L; Focal Technologies) also sampled the uncontaminated seawater supply for zooplankton biovolume continuously, except for about two hours per day when the ship was stationary. During this time, data storage and maintenance of the system was carried out (Gallienne et al. 1996). The OPC was set up at a flow rate of approximately 20 L min^{-1}, with a debubbler to remove contaminant air, and a flow meter enabling conversion of biovolume to concentration (ml m^{-3}). Checks on the accuracy of the OPC was carried out by periodic sampling and microscope analysis of the outflow from the OPC (Woodd-Walker 2000b), and by comparison with 20 net samples (Gallienne and Robins 1998).

Data manipulation

Modelling zooplankton requires zooplankton abundance data, and corresponding data for the parameters that may influence it. The underway data from the OPC and ocean logger were aggregated into one hour intervals. The OPC biovolume for equivalent spherical diameter (ESD) values greater than 250μm was used as below this threshold the OPC becomes unreliable (Herman 1992). The upper size limit was 2000μm, to avoid unusually high biovolumes from occasional large individuals. The 200-2000μm size range is also close to the range considered to be the 'mesozooplankton' (Lenz et al. 1993). The biovolume (mm^3 m^{-3}) was converted to biomass (wet weight, mg m^{-3}) using a specific gravity of 1. Literature values for zooplankton vary, but are generally close to 1 (e.g. 1.025; Chojnacki 1983). The OPC biovolume can also be reliably converted into carbon (e.g. Woodd-Walker et al. 2000). The biomass (250-2000μm) was $\log_e$ transformed, to normalise the distribution, and to improve the performance of the linear regression. It is also more appropriate to use a log scale as it is the changes in magnitude that are of most interest.

Other parameters that might influence the zooplankton biomass were calculated. Derived variables were calculated (first derivative of temperature, density and salinity). Diel time was calculated as a sine curve passing through zero at dawn and dusk, being positive in the day and negative at night. Season was coded as –1 for spring and 1 for autumn.

Multiple regression

The data from one autumn and one spring cruise (AMT 4 and 5) were used to calculate the regression for the zooplankton biomass over the whole transect. The independent variables used were latitude, temperature, first derivative of temperature, salinity, first derivative of salinity, density, first derivative of density, chlorophyll, total incident radiation (TIR), diel time and season. The first derivative of temperature, salinity and density was included as changes in these variables are associated with fronts and associated with enhanced biological activity (ref?). A backward stepwise selection procedure was used to eliminate insignificant variables. Care was taken with temperature, salinity and density to check which combination was most appropriate, as the multicolinearity (correlation between the variables) made automatic selection unreliable. The procedure was repeated on parts of the transect separately. Temperate (>38°N/S) and warm-water regions (38°N-38°S) were separated, as were regions derived from the zooplankton taxonomic structure from the same transects (Woodd-Walker in press).

Whole transects were reconstructed from the parts, and compared with the actual biomass, from AMT 4 and 5. The generalisation capabilities of the models were tested by using the equations from the regression analysis to predict biomass for AMT 2 and 3, and comparing with the measured biomass.

Neural networks

The multiple regression model presented in the previous section suffers from the limitation of being essentially a linear modelling approach. There is no reason why the relationship between biomass and the independent variables should be linear; hence

the problem of the most appropriate non-linear model to adopt arises. To overcome this difficulty it was decided to use an Artificial Neural Network to model the system. This non-linear input-output modelling technique essentially adopts the most appropriate model which it then optimises. They have been used extensively in areas such as non-linear forecasting and real-time systems analysis. For a more extensive description of the technique numerous descriptive texts are available, for example see Rosenblatt (1961), Bishop (1995).

This study adopts a two-layered feed forward artificial neural network. Alternate samples from the AMT 4 and 5 data set were used to train and test the Artificial Neural Network models. The network weights were trained using a Levenberg-Marquardt algorithm. Training was conducted for 40 epochs with 15 nodes in the hidden layer. The performance of the Artificial Neural Network model was measured as a combination of the mean sum of the squares of the network residuals and the mean sum of the squares of the network weights and biases as suggested by MacKay (1992). This measure known as regularisation helps to ensure that the developed Artificial Neural Network model generalises well. As the performance of the resulting network is to some extent a function of the original randomly chosen weights, the training procedure for each model was repeated 100 times, giving a better statistical indication of the behaviour of the network.

Initially, variables that were found to be important in the multiple regression analysis were used as inputs to the Artificial Neural Network. Optimisation of the set of input variables was performed by sequentially removing one variable and observing the effect on the model. The variable that made the least difference was removed and the

process repeated until the accuracy was significantly affected. To assess the quality (generalisation capabilities) of the developed Artificial Neural Network models, the models were tested on new data, the AMT 2 and 3 transects.

To understand the influence of the factors on the model, a sensitivity analysis was carried out on the optimal model. This model was created from the optimal set of input variables, and trained on alternate values from all four cruises to improve the robustness and generality of the model. To perform the sensitivity analysis, the median values for each variable were calculated over the range of each region, and used in the model whilst one variable was changed across the parameter's range, and the output recorded.

The model was optimised for the same regions as were considered in the multiple regression. Initially, the same variables were used, but calibration was carried out using the data for that latitudinal range, and subsequently, variables suggested to be important from the multiple regression were added.

Results

Multiple regression

The multiple regression of $\log_e$ biomass (250-2000μm ESD) for the whole transect showed that the important parameters in predicting the biomass were: latitude, temperature, density, chlorophyll, total incident radiation (TIR) and diel time (Table 2). These variables accounted for 55% of the variation. In general, the prediction was good across the transect (Fig. 2a&b), although the prediction of the extreme low and high values was less good than the intermediate estimates. Fig. 3 shows how each

component affects the model. Temperature and salinity form the basic shape, modified by chlorophyll at either end of the transect and latitude. Diel time and total incident radiation combine to simulate the cyclic diel migration component of the model.

Regression models developed for specific areas could explain more of the variability (up to 75%; table 2). However, the factors tended to be similar. A combination of temperature, salinity and density were used in all but the northern subtropical region, and generally two out of three of these factors were significant, demonstrating the importance of the ocean physics. Chlorophyll was significant in all models except the northern subtropical, southern tropical and southern temperate. Time of day as modelled by diel time and total incident radiation was a consistently important factor, generally using both measures. The effect of time of year, i.e. spring and autumn, was important for temperate, warm-water, northern temperate and northern subtropical regions.

The transects constructed from the different area models of biomass compared well with the measured biomass for AMT 4 and 5, with R^2 values of between 0.54 and 0.70 for the entire transect (table 3). Where the transect has been divided into smaller sections the agreement is generally better. Thus the best model appears to be where each region has been analysed separately (Fig. 2c and d). However, for the models where the northern temperate region was analysed with the warm water stations the R^2 was higher than when this region was analysed with the southern temperate.

Prediction of the biomass from the AMT 4 and 5 models, for AMT 2 and 3 showed a poorer agreement with actual biomass, with R^2 varying between 0.33 and 0.42 (table

3). The whole transect model prediction was reasonable apart from the southern temperate region, which was particularly inaccurate on AMT 3 (Fig. 4b). The best models were the regions model (Fig. 4c&d) and the model which separated the southern temperate from the rest of the transect. The regions model predictions appeared to follow the actual biomass more closely, although the R^2 was very similar.

Neural networks

The neural network modelled from all eight of the parameters which had been important in multiple regression analysis showed good agreement over the transect with an R^2 of 0.78. Optimisation of variables showed that the number of input parameters could be reduced without substantial loss in the accuracy of the model, and with an increase in the accuracy of prediction of the novel data set (table 4). The optimal variables for the neural network were latitude, temperature, salinity, chlorophyll and diel time. These variables accounted for 77% of the variability in zooplankton biomass of the AMT 4 and 5 data sets, and followed the actual pattern of zooplankton biomass closely (Fig. 5a&b). Training the model on separate regions did not improve the model, nor did changing the variables to those significant for multiple linear regression (Table 6). Comparison of the residuals (predicted-measured) from multiple regression and neural networks showed that both were normally distributed, but the bias for the multiple linear regression was 0.0058 compared to 0.00057 for the neural network. The range of the residuals was lower for the neural networks than for the multiple linear regression (Fig. 6), with 87% and 67% respectively of the biomass estimates being within a factor of two of the measured biomass.

Testing of the optimal model on AMT 2 and 3 gave a reduced R^2 of 0.47. This was higher than for the initial model (table 4). The model picked up the major features in zooplankton abundance along the transect (Fig. 5c&d), but the lowest biomasses tended to be overestimated. Although the peaks in the southern temperate region were predicted, their magnitude was also over estimated.

Sensitivity analysis of the developed model in the different regions demonstrated the complex interaction of parameters, with their relationships with the biomass varying substantially in the different regions (Fig. 7). Latitude had the greatest effect in the equatorial region, with more northerly areas having higher biomass, making approx. 2 log units difference (7x) in zooplankton abundance over the regions (Fig. 7a&b). In the northern subtropical region, latitude had virtually no effect. In the northern temperate region there was a slight increase in zooplankton with latitude. In the southern temperate region, the reverse trend was apparent with the more southerly latitudes being associated with lower biomass. The southern tropical and subtropical regions showed a slight increase in biomass further south.

Temperature showed a complex pattern over the transect (Fig. 7c&d). For southern subtropical, southern tropical and equatorial regions, lower temperatures were generally associated with higher biomass, although the relationship varied. Cooler temperatures in these regions may be associated with upwelled water or increased mixing with cold, higher nutrient waters from below the thermocline, and therefore higher productivity. In the southern temperate region lower temperatures were associated with higher biomass, possibly due to the warm waters of the Brazil current supporting lower production than the cool seasonally mixed waters of the Falklands

current. In the northern temperate and subtropical regions, biomass minima were associated with intermediate temperatures (16°C and 21°C respectively), with biomass increasing at higher and lower temperatures. This more complex pattern may be due to coastal regions having warmer waters and being more productive or due to a seasonal effect.

Salinity in general showed a trend of increasing biomass with decreasing salinity, although the relationship was not always straightforward (Fig. 7e&f). For instance, salinities around 34.5‰ were associated with lower biomass in the southern temperate region. The overall relationship followed the expected pattern with the lowest biomass associated with the highest salinities, which are found in the oligotrophic gyres. The effect of salinity was greatest in the northern temperate region where over less than one unit, the log biomass increased by 3 $\log_e$ units (20x). This may be due to an additional coastal effect where low salinity is associated with the highly productive inshore waters.

Chlorophyll was generally, but not always associated with higher biomass, at least over the range associated with that region making between 1 and 2 log units difference (Fig. 7g&h). Outside this range estimates showed different relationships. The northern and southern subtropical and equatorial regions showed a rapid drop in biomass at chlorophyll levels higher than the range. The northern temperate region reached an asymptote at 2mg m^{-3} chl. This suggests that the neural network may be unreliable outside the training range. In the southern temperate and subtropical regions, minimum biomass were associated with intermediate chlorophyll concentrations.

Diel time showed a consistent trend across the transect, with high zooplankton biomass at night and low biomass during the day, making between 1 and 2.5 log units between maximum and minimum biomass (Fig. 8a). This is equivalent to a factor between 3 and 12 for night : day. The exact nature of the diel changes varied across the regions. Fig. 8b shows the diel changes for a standard day, with 0 midnight, 6 dawn, 12 noon, 18 dusk and 24 midnight in each of the regions. During the day, the biomass approximates to half a sine curve, over the whole transect. In the southern temperate region, the night follows the sine wave too. However, for the other regions there is a distinct flattening between dusk and dawn, with a peak evident at these times. The dawn/dusk peak is most pronounced in the southern tropical region, suggesting midnight sinking is occurring (Raymont 1983).

Discussion

Multiple regression model

Linear multiple regression can explain approximately half the variability of the log transformed biomass, and is most accurate for values close to the mean, tending to underestimate the very high values and overestimate very low ones. Others (e.g. Scardi 1996) have found similar effects using linear regression models. The consistently important factors for predicting the zooplankton biomass are latitude, the ocean physics (temperature, salinity and density), the amount of phytoplankton (chlorophyll), time of day (total solar radiation and diel time) and time of year (season). Maravelias and Reid (1997) noted the changes in abundance of zooplankton associated with oceanographic features, and phytoplankton abundance is known to be an important factor in influencing zooplankton abundance (e.g. Koppelmann and Weikert 1992) and productivity (e.g. Calbet and Agustí 1999, Zhang et al. 1995). The

physics and chlorophyll, modified for season and latitude add to give the overall abundance of the zooplankton. Season may help to give a chronological aspect, i.e. an influence of the timing within the system. The influence of latitude is quite small for the overall model, adding an asymmetry to the effects of the other variables. Other latitudinal influences may be expressed by other factors such as temperature, or may be non-linear reducing the impact in the multiple linear regression model. The time of day affecting surface zooplankton abundance is unlikely to reflect changes in the actual abundance of zooplankton in the water column. Rather this may be due to diel migration of the zooplankters. Diel migration of zooplankton has long been recognised and is associated with changes in light level, as indicated here by the importance of total incident radiation. The sine wave is a very simple model of the diel migration. A more complex model including 'midnight sinking' might improve the predictability. The linear model does not allow for changes in the extent of migration with factors such as changes in the zooplankton community structure (Roman *et al.* 1995), presence of predators (Bollens *et al.* 1994), or latitude and food supply (e.g. Fiksen and Giske 1995; Calbet and Agustí 1999) that are known to have an effect on diel migratory behaviour.

Tests on novel data sets (AMT2 and 3), showed reduced R^2 values of between 0.3 and 0.42. The R^2 of the novel data sets gives an indication of the generality of the model. Even though the R^2 is reduced the general pattern of zooplankton biomass is still being followed by the model. The high biomass of the southern temperate region is not being predicted accurately, and, on AMT 2, the equatorial region shows less good agreement. The model for the whole transect can be improved by dividing into regions, or at least by treating the southern temperate region (38°S-50°S) separately.

The division into regions allow optimisation of factors without 'over fitting'. It also suggests that the magnitude of influences of factors on zooplankton abundance may not be constant across the ocean, particularly in the dynamic southern temperate region. The southern temperate region is very dynamic, coinciding with the confluence of the warm oligotrophic Brazil current and the cold relatively nutrient rich Falklands current. Thus the dynamic of this regime is closely coupled to the physical parameters, behaving differently from other regions. Alternatively, improved model performance may reflect the non-linearity of the systems which is being inadequately modelled.

The multiple regression model is simple to interpret. The t statistic shows the strength of each factor. However, it does have limitations. The model assumes a linear relationship between the independent and dependent variables, although 'new' variables can be made by multiplying factors together or transforming them. The combination of independent variables alters the effect of each variable, particularly when variables are closely related and co-vary (multicolinearity), as with temperature salinity and density. The model may be improved by including interactions between variables and by allowing non-linear relationships. More complex models such as generalised additive models such as used by Maravelias and Reid (1997) may give further insight into the influences and controls on zooplankton.

Neural networks

The neural networks showed improved estimation of the zooplankton biomass over the multiple regression, with an R^2 of 0.78 for the initial model with eight inputs. This highlights the non-linear relationship between zooplankton abundance and the

parameters. Reducing the inputs to 5, did not affect the R^2 greatly (0.77). The predictive power of the model with fewer inputs demonstrated the redundancy in much of the original data. Testing of the optimal model on AMT 2 and 3 data sets, showed a reduced R^2 (0.47), but this was still higher than for the multiple regression analysis. The original data showed a lower R^2 suggesting that it tended to 'overfit' the data, reducing the robustness of the model for new data sets.

The selected variables included latitude, temperature, salinity, chlorophyll and diel time. These are almost identical to the variables that were selected from the multiple regression for the whole transect (salinity has replaced density, and TIR is not included). Optimisation for the different regions with the same variables or for regions with the significant variables from multiple regression analysis did not significantly improve the models. This is likely to be due to two factors: the non-linear network being able to model zooplankton abundance adequately across the whole transect, and the smaller training sets being insufficient to optimise the parameters fully.

Future improved model performance may be obtained by using more data to train the network, so that the parameter space is more extensively covered. Further optimisation may be possible by changing the model architecture or input parameters. 'Top down' effects of predators on the system, which have been shown to be important in certain situations (e.g. Steele and Henderson 1995; Hutchings *et al.* 1995), are not included. However, if the abundance of predators co-varied with the other variables, e.g. latitude or temperature, their effect may already be included in the model as Huse & Gjøsæster (1999) suggest for capelin. Sampling errors in the original data will also reduce the predictability. However, the model is unlikely to reach the

'perfect' prediction of an R^2 of 1, about the 1:1 line, due to the fundamental nature of zooplankton. Zooplankton are known to show greater variability at smaller scales than the physics (Piontkovski and Williams 1995). Interactions within the zooplankton such as swarming behaviour (e.g. Omori & Hamner 1982, Ueda *et al.* 1983, Kimoto *et al.* 1988), and predator-prey interactions will tend to increase errors/noise into the predictions. The smoothing by the model may be considered desirable as it may allow greater reliability of prediction and understanding of the system.

Sensitivity analysis demonstrated the impact of the different parameters in the different regions. In general, the relationships followed expected trends. High chlorophyll was associated with high biomass, high salinity and temperatures associated with the oligotrophic gyres coinciding with low biomass, and night with high biomass due to diel migration. However, within these trends, the parameters appear to have opposite effects in different regions, and sometimes they are counterintuitive. This could be due to the interactive effects of the parameters, particularly where the parameters are covariate. Thus for example, although chlorophyll is generally associated with high zooplankton abundance, in some regions (e.g. southern subtropical 1-2mg chl m^{-3}) the relationship is negative. Over this parameter space, it could be that temperature and salinity are overestimating zooplankton abundance, or it could be that the zooplankton are lower due to predation for example. It could also be that in this region, chlorophyll is not a good measure of primary productivity (Marañón & Holligan 1999), and much of the phytoplankton is too small to be available to most zooplankton (ref?). None of these unexpected effects are apparent in the diel time, even though the impact of diel time does vary between regions. The modelling of the diel migration gives insight into the differences in diel

migration in the different regions. In the southern temperate region, the difference between day and night biomass is greatest (12x), and reaches a maximum at midnight, closely following the sine curve. This region also has many large zooplankton which are known to undergo much greater diel migrations (e.g. Zhang et al.1995), and thus take longer to reach the surface waters after dusk. Throughout the rest of the transect day-night change in zooplankton abundance varies between 3 and 5 times, and maximum abundance is frequently at dawn/dusk, either plateauing or dropping in darkness, in a similar manner as described by Mauchline (1998).

Conclusions

The amount of surface zooplankton can be predicted with a RMS error of < 2.5, using a few easily measured parameters, giving whole transect estimates within 50%. The ocean physics and phytoplankton abundance influences the zooplankton abundance in the water column, and time of day influences the proportion within the surface layer. Neural network models enhance the predictability over multiple linear regression, especially for large areas, by allowing non linear interactions of the parameters. However, the influence of different parameters is easier to understand using multiple linear regression, whereas more complex sensitivity analysis is required for neural networks. Thus we feel that by using neural networks to build on multiple linear regression, increased understanding and prediction in ecosystem modelling may be accomplished.

Acknowledgements

We wish to thank the officers and crew of the British Antarctic Survey research ship RRS James Clarke Ross during the AMT cruises. We are most grateful to Roger

Harris, Derek Pilgrim, Mark Davidson and Dave Robins for their support and advice. This work was supported by the Natural Environmental Research Council PRIME special topic grant (GST/02/1068) and Rachel Woodd-Walker and Ken Kingston are supported by University of Plymouth studentships. This is publication no. XX of the AMT programme.

References

Aoki, I. and Komatsu, T. (1997) Analysis and prediction of the fluctuation of sardine abundance using a neural network. Oceanologia Acta 20:81-88.

Aoki, I., Komatsu, T. and Hwang, K. (1999) Prediction of response of zooplankton biomass to climatic and oceanic changes. Ecol Mod 120:261-270.

Banse, K. (1995) Zooplankton: Pivotal role in the control of ocean production. ICES J Mar Sci 52:265-277.

Bishop, C.M. (1995) Neural networks for pattern recognition Oxford University Press, Oxford.

Bollens, S.M., Frost, B.W. and Cordell, J.R. (1994) Chemical, mechanical and visual cues for vertical migration behaviour of a marine copepod *Acartia hudsonica*. J Plankton Res 16, 555-564.

Calbet, A. and Agustí, S. (1999) Latitudinal changes of copepod egg production rates in Atlantic waters: temperature and food availability as the main driving factors. Mar Ecol Prog Ser 181:155-162.

Chojnacki, J. (1983) Standard weights of the Pomeranian Bay copepods. Int Rev ges Hydrobiol 68:435-441.

Fiksen, O. and Giske, J. (1995) Vertical distribution and population dynamics of copepods by dynamic optimization. ICES J Mar Sci 52:483-503.

Frost, B.W. (1993) A modelling study of process regulating plankton standing stock and production in the open subarctic Pacific Ocean. Prog Oceanog 32:17-56.

Frost, B.W. and Franzen, N.C. (1992) Grazing and iron limitation in the control of phytoplankton stock and nutrient concentration: a chemostat analogue of the Pacific equatorial upwelling zone. . Mar Ecol Prog Ser 83:291-303

Gallienne, C.P., Robins, D.B. and Pilgrim, D.A. (1996) Measuring abundance and size distribution of zooplankton using an optical plankton counter in underway mode. Underwater Technol 21, 15-21.

Herman, A.W. (1992) Design and calibration of a new optical plankton counter capable of sizing small zooplankton. Deep Sea Res 39:395-415.

Hutchings, L., Verheye, H.M., Mitchell-Innes, B.A., Peterson, W.T., Huggett, J.A. and Painting, S.J. (1995) Copepod production in the southern Benguela system. ICES J Mar Sci 52, 439-455.

Kimoto, K., Uye, S.-i. and Onbe, T. (1988) Direct observation of copepod swarm in a small inlet of Kyushu, Japan. Bull Seikai Regional Fish Res Lab 66: 41-58.

Koppelman, R. and Weikert, H. (1992) Full-depth zooplankton profiles over the deep bathyal of the NE Atlantic. Mar Ecol Prog Ser 86:263-272.

Lek, S. and Guegan, J.F. (1999) Artificial neural networks as a tool for ecological modelling,an introduction. Ecol Mod 120:65-73.

Lenz, J., Morales, A. and Gunkel, J. (1993) Mesozooplankton standing stock during North Atlantic spring bloom study in 1989 and its potential grazing pressure on phytoplankton: a comparison between low, medium and high latitudes. Deep Sea Res II 40:559-572.

Longhurst, A.R., Bedo, A.W., Harrison, W.G., Head, E.J.H. and Sameoto, D.D. (1990) Vertical flux of respiratory carbon by oceanic diel migrant biota. Deep Sea Res 37, 685-694.

Longhurst, A.R. and Harrison, W.G. (1988) Vertical nitrogen flux from the oceanic euphotic zone by diel migrant zooplankton and nekton. Deep Sea Res 35, 881-889.

MacKay, D.J.C. (1992) Bayesian interpolation. Neural Comp 4:415-447.

Maravelias, C.D. and Reid, D.G. (1997) Identifying the effects of oceanographic features and zooplankton on prespawning herring abundance using generalized additive models. . Mar Ecol Prog Ser 147:1-9.

Mauchline, J. (1998) The biology of calanoid copepods. Academic Press, London.

Morales, C.E. (1999) Carbon and nitrogen fluxes in the oceans: the contribution by zooplankton migrants to active transport in the North Atlantic during the Joint Global Ocean Flux Study. J Plankton Res 21, 1799-1808.

Omori, M. and Hamner, W.M. (1982) Patchy distribution of zooplankton: behaviour, population assessment and sampling problems. Mar Biol 72:193-200.

Piontkovski, S.A. and Williams, R. (1995) Multiscale variability of tropical ocean zooplankton biomass. ICES J Mar Sci 52:643-656.

Prestige, M.C., Harris, R.P. and Taylor, A.H. (1995) A modelling investigation of copepod egg production in the Irish Sea. ICES J Mar Sci 52:693-703.

Raymont, J.E.G. (1983) Plankton and productivity in the oceans. Volume 2: Zooplankton. 2nd edn. Pergamon Press, Oxford.

Richards, S.A., Possingham, H.P. and Noye, J. (1996) Diel vertical migration: modelling light-mediated mechanisms. J Plankton Res18:2199-2222.

Robins, D.B. and Aiken, J. (1996) The Atlantic Meridional Transect: an oceanographic research programme to investigate physical, chemical, biological and optical variables of the Atlantic Ocean. Underwater Techol 21:8-14.

Roman, M.R., Dam, H.G., Gauzens, A.L., Urban-Rich, J., Foley, D.G. and Dickey, T.D. (1995) Zooplankton variability on the equator at 140°W during the JGOFS EqPac study. Deep Sea Res II 42:673-693.

Rosenblatt, F. (1961) Principles of neurodynamics. Spartan Press, Washington DC.

Scardi, M. (1996) Artificial neural networks as empirical models for estimating phytoplankton production. . Mar Ecol Prog Ser 139:289-299.

Steele, J.H. and Henderson, E.W. (1995) Predation control of zooplankton demography. ICES J Mar Sci 52, 565-574.

Stephens, J.A., Jordan, M.B., Taylor, A.H. and Proctor, R. (1998) The effects of fluctuations in the North Sea flows on zooplankton abundance. J Plankton Res 20:943-956.

Taylor, A.H. (1995) North-South shifts of the Gulf Stream and their climatic connections with the abundance of zooplankton in the UK and its surrounding seas. ICES J Mar Sci 52:711-721.

Ueda, H., Kuwahara, A., Tanaka, M. and Azeta, M. (1983) Underwater observations on copepod swarms in temperate and subtropical waters. Mar Ecol Prog Ser 11:165-171.

Woodd-Walker, R.S. (in press) Spatial distribution of copepod genera along the Atlantic Meridional Transect. Hydrobiologia

Woodd-Walker, R.S., Gallienne, C.P. and Robins, D.B. (2000) A test model for optical plankton counter (OPC) coincidence and a comparison of OPC derived and conventional measures of zooplankton abundance. J Plankton Res (In Press)

Zhang, X., Dam, H.G., White, J.R. and Roman, M.R. (1995) Latitudinal variations in mesozooplankton grazing and metabolism in the central tropical Pacific during the U.S. JGOFS EqPac study. Deep Sea Research II 42:695-714.

Tables

Table 1: Summary of Cruises

Cruise	Dates	Track
AMT2	22nd April - 22nd May 1996	Falklands-UK
AMT3	16th Sept. - 25th Oct. 1996	UK-Falklands
AMT4	21st April - 27th May 1997	Falklands-UK
AMT5	15th Sept. - 17th Oct. 1997	UK-Falklands

Table 2 Coefficients for variables from multiple regression of $\log_e$ transformed biovolume (<2000μm) for AMT 4 and 5 with R^2 of the regression, adjusted for degrees of freedom. The T statistic is shown in brackets below the coefficient. The larger the T statistic, the more significant the factor, the sign indicates whether the relationship is negative or positive ($P<0.05$ for all variables). TIR – total incident radiation.

Variable	Whole transect	Warm water	Temperate	N. Temperate	N. Subtropical	Equatorial	S. Tropical	S. Subtropical	S. Temperate	Whole with no S. Temp
Constant	22.48	22.16	11.64	135.2	5.83	-73.9	19.76	6.40	16.62	20.87
Latitude	0.006	0.008	-	0.23	-0.07	0.044	-0.03	-	0.234	0.007
	(6.3)	(6.8)		(3.88)	(-10)	(9.5)	(-3.5)		(7.5)	(7.6)
Temperature	-0.13	0.067	-	-0.59	-	5.67	-0.19	-0.15	-	-
	(-16)	(7.7)		(-2.8)		(4.1)	(-3.2)	(-5.8)		
Change in temperature	-	-	-	-	-	-	-	-	-	-
Salinity	-	-0.55	-0.43	-	-	-13.8	-	-	-0.86	-0.27
		(-14)	(-8.5)			(-4.1)			(-6.3)	(-6.9)
Change in salinity	-	-	-	-	-	-	-	-	-	-
Density	-0.69	-	0.29	-5.03	-	17.9	-0.49	-	1.08	-0.30
	(-19)		(3.8)	(-5.5)		(4.1)	(-3.1)		(7.3)	(-12)
Change in density	-	-	-	-	-	-	-	-	-	-
Chlorophyll	0.688	0.752	0.471	0.479	-	2.43	-	0.412	-	0.963
	(20)	(9.35)	(9.4)	(3.7)		(4.7)		(4.3)		(16)
TIR (x1000)	-1.17	-1.27	-1.60	-	-1.34	-0.98	-2.19	-	-1.41	-1.14
	(-8.7)	(-9.0)	(-4.9)		(-9.1)	(-5.5)	(-15)		(-2.9)	(-8.6)
Diel time	-0.39	-0.29	-0.44	-0.72	-	-0.34	-	-0.78	-0.78	-0.34
	(-8.0)	(-5.4)	(-4.5)	(-9.9)		(-5.8)		(-8.6)	(-5.1)	(-6.9)
Season	-	-0.12	4.69	-0.84	0.44	-	-	-	-	-
		(4.69)		(-3.7)	(10.3)					
Adjusted R^2	0.55	0.53	0.57	0.74	0.60	0.61	0.55	0.64	0.51	0.54
N	1128	821	307	171	137	281	230	118	134	996

Table 3: Correlation coefficients of multiple regression models for the whole transects made from the component models of the transect sections for AMT 4 and 5 (Training, N=1138, P<0.01 for all) and AMT 2 and 3 (Testing, N=994, P<0.01 for all) data sets.

Model	Training R^2	Testing R^2
Whole transect	0.55	0.34
Warm water/Temperate	0.56	0.39
Regions	0.70	0.42
Warm water & N/S temperate	0.62	0.33
All & south temperate	0.59	0.42

Table 4: Summary of neural networks optimising variables for the whole transect, showing the results at each stage of subtraction. The variables included in the model are marked with x, with R^2 for the training set (AMT 4 and 5, N=1138, P<0.01 for all) and independent test cruises (AMT 2 and 3, N=994, P<0.01 for all). Bold highlights the final accepted model.

Latitude	Temperature	Salinity	Density	Chlorophyll	TIR	Diel time	Season	Training R^2	Testing R^2
x	x	x	x	x	x	x	x	0.782	0.311
x	x	x	x	x		x	x	0.782	0.391
x	x	x		x		x	x	0.768	0.465
x	**x**	**x**		**x**		**x**		**0.766**	**0.474**
x	x	x				x		0.758	0.428

Table 5: Summary of neural network models optimised for each region with optimal model variables, and with variables significant in multiple regression by region. The variables included in the model are marked with x, with R^2 for the training set (AMT 4 and 5, N=1138, P<0.01 for all).

Region	Latitude	Temperature	Salinity	Density	Chlorophyll	TIR	Diel time	Season	Training set R^2
Warm water	x	x	x		x		x		0.786
Temperate	x	x	x		x		x		0.757
S.Temperate	x	x	x		x		x		0.551
S.Subtropical	x	x	x		x		x		0.756
S.Tropical	x	x	x		x		x		0.727
Equatorial	x	x	x		x		x		0.765
N.Subtropical	x	x	x		x		x		0.741
N.Temperate	x	x	x		x		x		0.878
Whole with no S.Temp.	x	x	x		x		x		0.750
Warm water	x	x	x		x	x	x		0.775
Temperate			x	x	x	x	x	x	0.709
S.Temperate	x		x			x	x		0.591
S.Subtropical		x			x		x		0.736
S.Tropical	x	x		x	x	x	x		0.647
Equatorial	x	x	x	x		x		x	0.756
N.Subtropical	x					x		x	0.596
N.Temperate	x	x		x	x		x	x	0.878
Whole with no S.Temp.	x		x	x	x	x	x		0.757

Figure legends

Fig. 1: The AMT cruise track with regions shown (N. Temp 38-50°N, N. Subtrop. 18-38°N, Equat. 8°S-18°N, S. Trop. 28-8°S, S.Subtrop. 28-38°S, S.Temp 38-50°S)

Fig. 2: Linear regression models of biomass from the whole transect compared with actual biovolumes (R^2= 0.55), for training data sets, a) AMT 4, b)AMT 5, and for the model derived from separate regions (R^2= 0.70) for c) AMT 4, d) AMT 5.

Fig. 3: The contribution of the different components to the whole transect model compared to the actual $\log_e$ transformed biomass (log(<2000)) for the AMT 4 transect. T&S – constant, temperature and salinity, Chl – chlorophyll, diel&TIR – diel time and total incident radiation.

Fig. 4: Linear regression models of biomass from the whole transect compared with actual biovolumes (R^2= 0.34), for testing data sets a) AMT 2, b)AMT 3, and for the model derived from separate regions (R^2= 0.42) for c) AMT 2, d) AMT 3.

Fig. 5: Artificial neural network model of biomass of the optimised parameter set compared with measured biomass (Parameters: latitude, temperature, salinity, chlorophyll and diel time), for training data sets (R^2= 0.77) a) AMT 4, b)AMT 5, and for testing data sets (R^2= 0.47) c) AMT 2, d)AMT 3.

Fig. 6: Comparison of residuals between multiple linear regression (MLR) and artificial neural network (ANN) models of zooplankton for AMT 4 and 5 data sets.

Fig. 7: Sensitivity analysis, showing the effect the parameters on biomass in the different regions. Bold lines denote the parameter range occuring within each region. (N. Temp 38-50°N, N. Subtrop. 18-38°N, Equatorial 8°S-18°N, S. Trop. 28-8°S, S.Subtrop. 28-38°S, S.Temp 38-50°S) a) latitude for northern regions, b) latitude for southern regions, c) temperature for northern regions, d) temperature for southern regions, e) salinity for northern regions, f) salinity for southern regions, g) chlorophyll for northern regions, h) chlorophyll for southern regions.

Fig. 8: a) Sensitivity analysis, showing the effect the diel time on biomass in the different regions, and b) time of day derived from diel time, assuming a standard day of 12 hours daylight and 12 hours darkness. Sine is a sine wave of amplitude 1 (-diel time, the input). (N. Temp 38-50°N, N. Subtrop. 18-38°N, Equatorial 8°S-18°N, S. Trop. 28-8°S, S.Subtrop. 28-38°S, S.Temp 38-50°S),

Figure 1: AMT cruise track

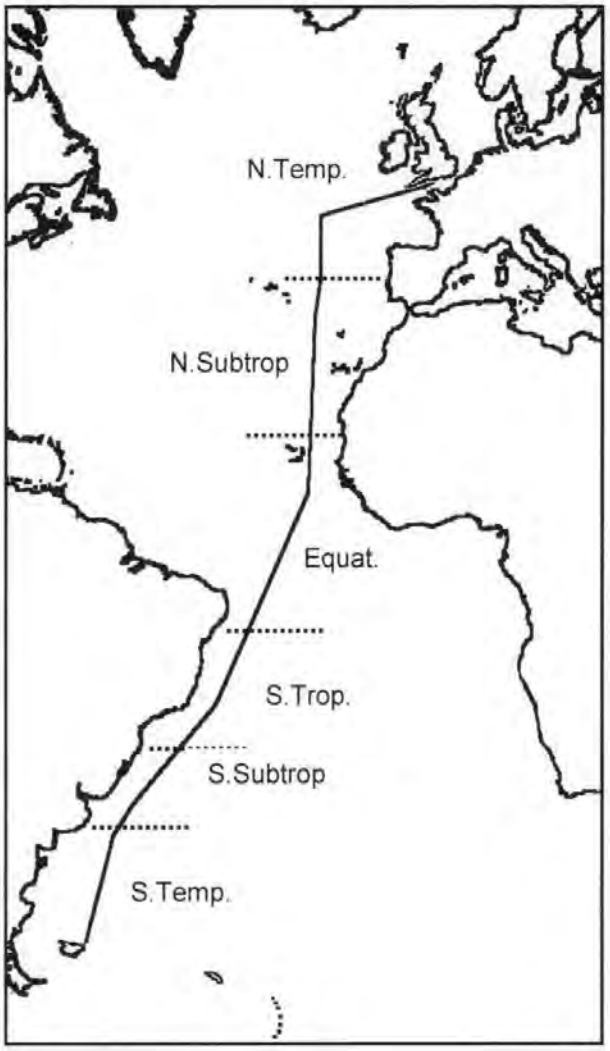

Figure 2:

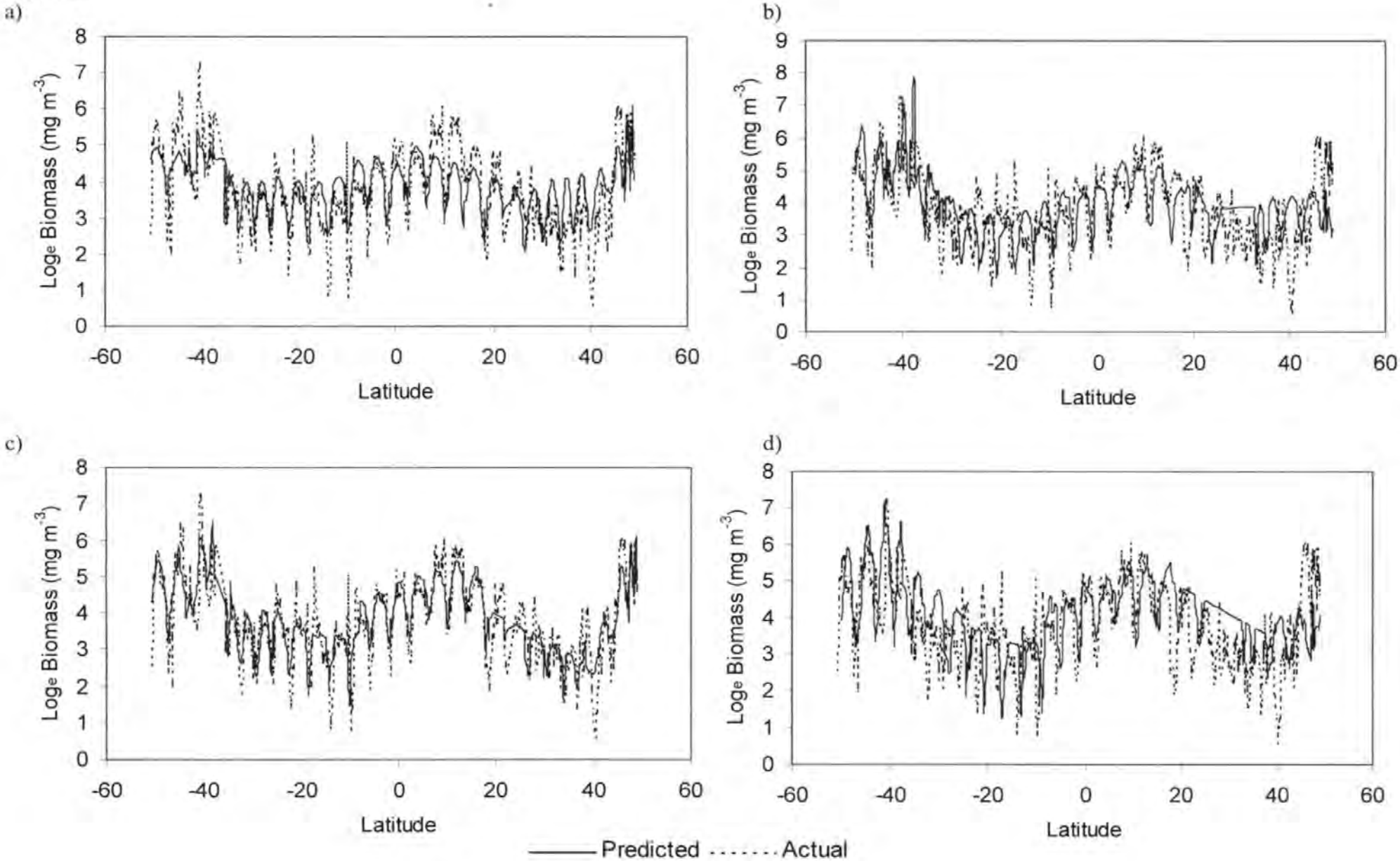
a)
b)
c)
d)
Loge Biomass (mg m-3)
Latitude
-60
-40
-20
0
20
40
60
Predicted
Actual

Figure 3 The contribution of the different components to the whole transect model of zooplankton biomass compared to the actual $\log_e$ transformed biomass (log(<2000)) for the AMT 4 transect. T&S – constant, temperature (^{o}C) and salinity, Chl – chlorophyll (mg m^{-3}), diel&TIR – diel time and total incident radiation (W m^{-2}).

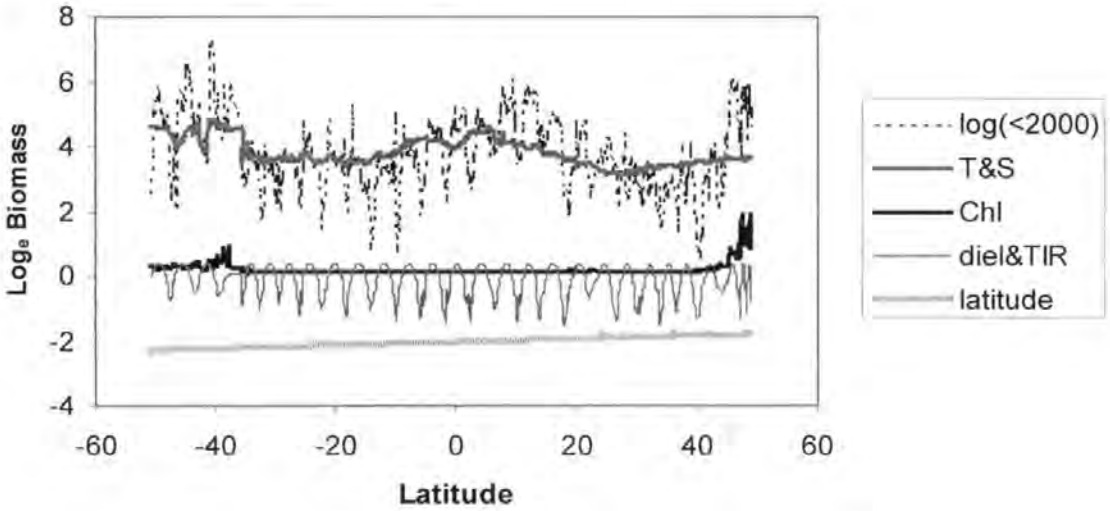

Figure 4

a)

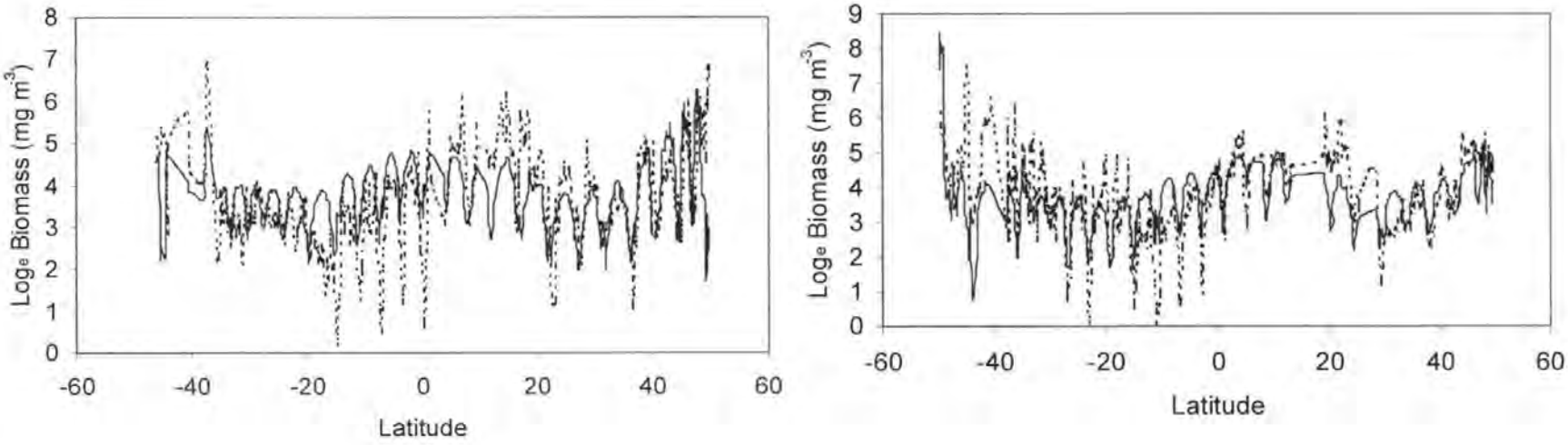
Loge Biomass (mg m-3)
Latitude
-60
-40
-20
0
20
40
60

b)

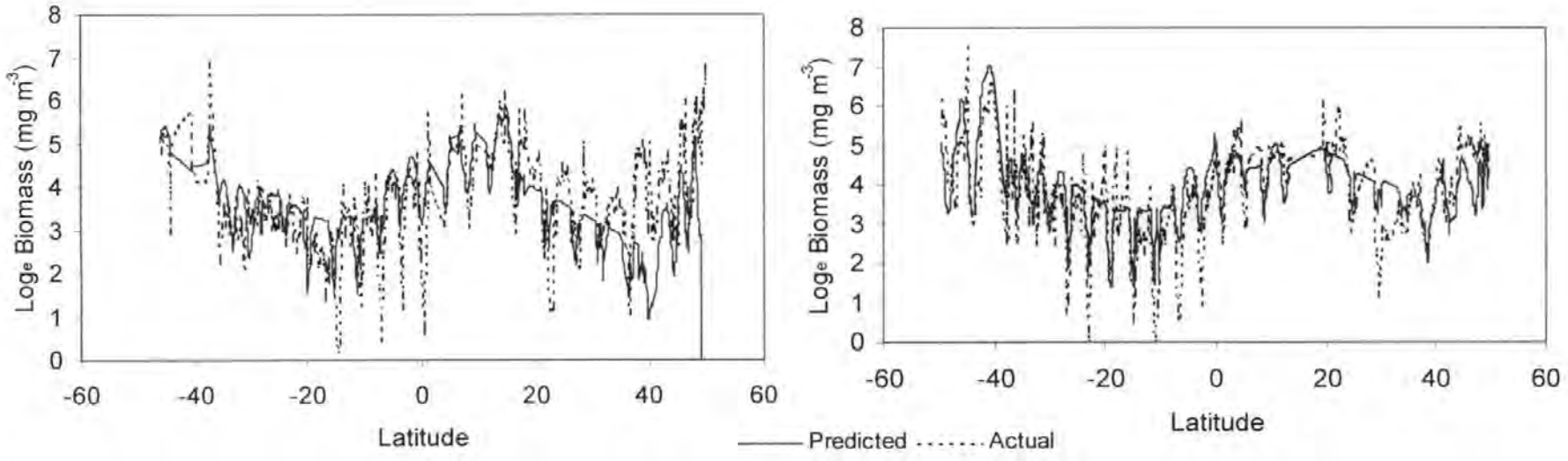
Loge Biomass (mg m-3)
Latitude
Predicted
Actual

Figure 5

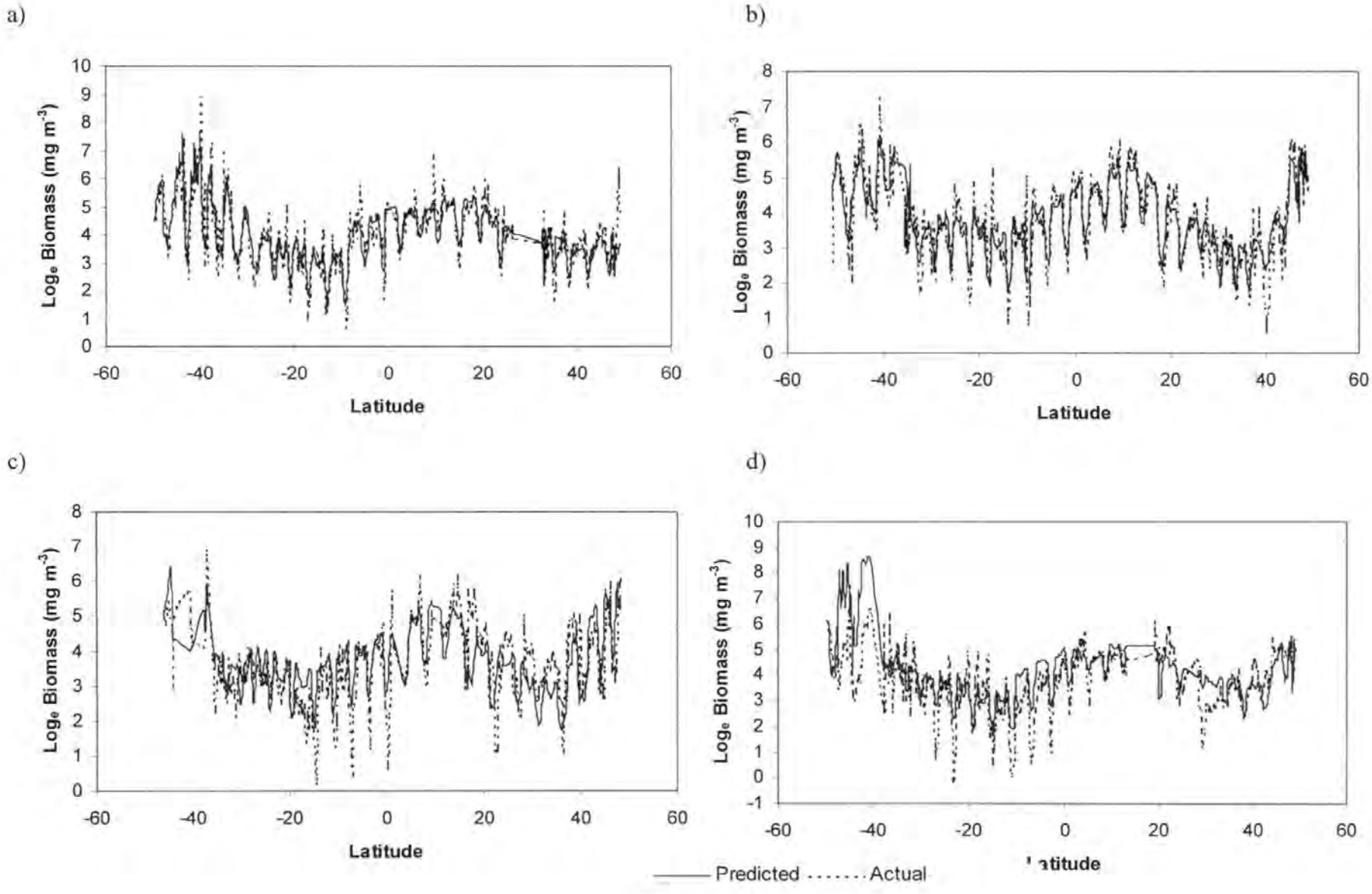

Fig 6

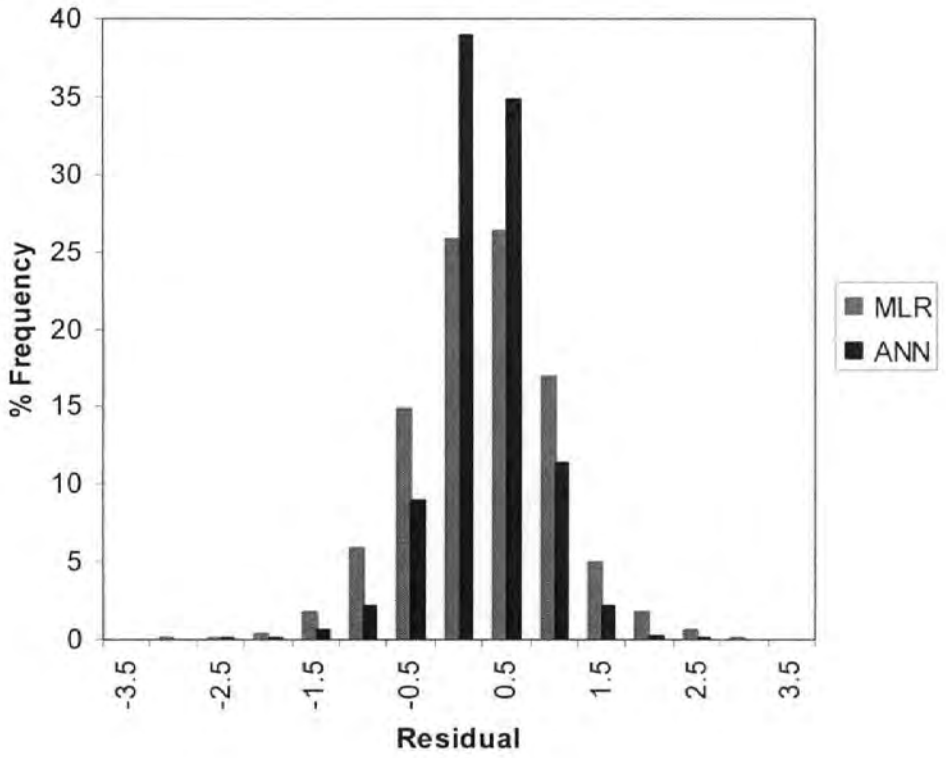
40
35
30
25
20
15
10
5
0
% Frequency
-3.5
-2.5
-1.5
-0.5
0.5
1.5
2.5
3.5
Residual
MLR
ANN

Fig7

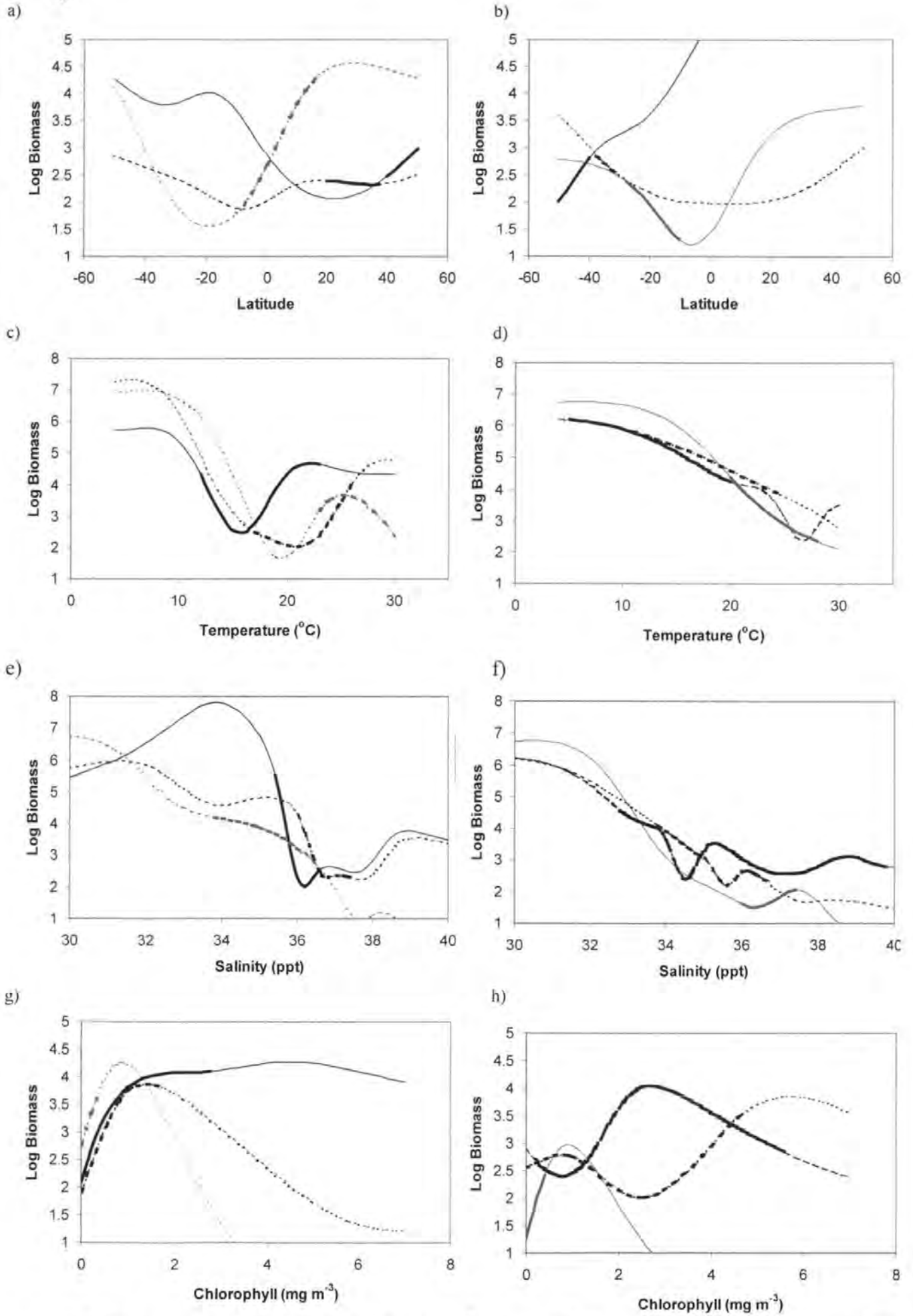
a)
b)
c)
d)
e)
f)
g)
h)
Log Biomass
Latitude
Temperature (°C)
Salinity (ppt)
Chlorophyll (mg m-3)
N. Temp.
N. Subtrop.
Equatorial
S.Trop.
S.Subtrop.
S.Temp.

Figure 8

a)

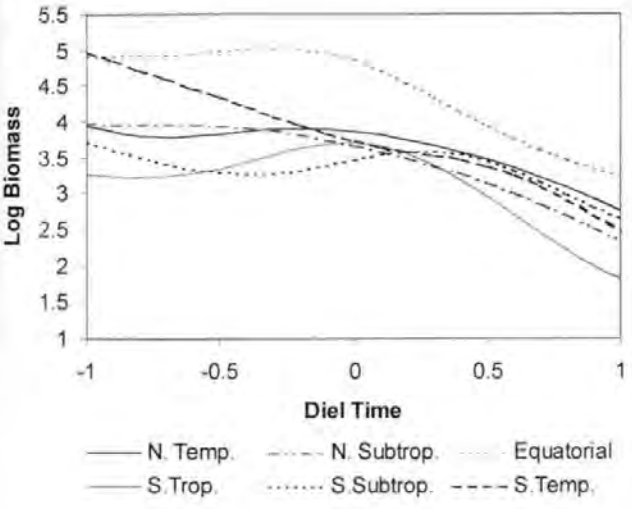
5.5
5
4.5
4
3.5
3
2.5
2
1.5
1
Log Biomass
-1
-0.5
0
0.5
1
Diel Time
N. Temp.
N. Subtrop.
Equatorial
S.Trop.
S.Subtrop.
S.Temp.

b)

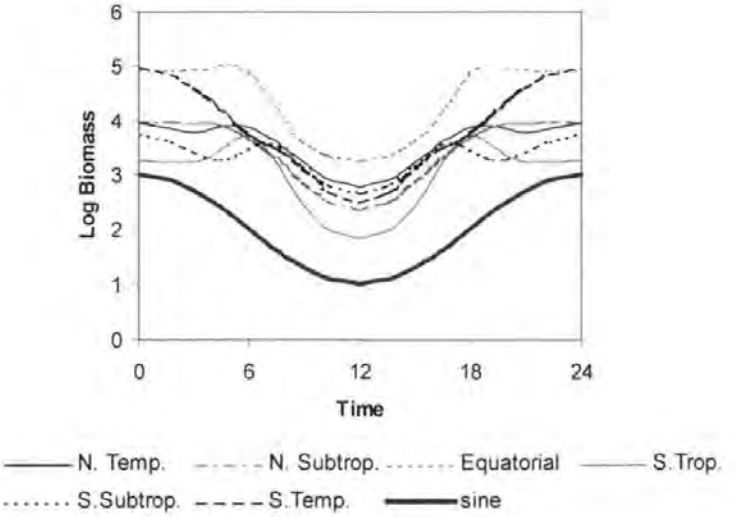
6
5
4
3
2
1
0
Log Biomass
0
6
12
18
24
Time
N. Temp.
N. Subtrop.
Equatorial
S.Trop.
S.Subtrop.
S.Temp.
sine